THE 16TH ASIAN CONFERENCE ON REMOTE SENSING

ORGANIZED BY

Organizing Committee of WORLD TECH'95 THAILAND

Asian Association on Remote Sensing (AARS)

National Research Council of Thailand (NRCT)

Suranaree University of Technology(SUT)

PROGRAM

Program for The 16th Asian Conference on Remote Sensing

20-24 November 1995
Suranaree University of Technology, Nakhon Ratchasima, Thailand

November 20, Monday 1995

8:00- 9:00 **Registration**

9:00-10:00 **Opening Ceremony (Education Complex Hall; B Building)**
Welcome Address; Prof. Wichit Srisa-an, Rector, Suranaree Univ. of Technology
Opening Address; Dr. Suvit Vibulsresth, Secretary General,NRCT
Inaugulation Address;
Her Royal Highness The Princess Maha Chakri Sirindhorn
Main Guest Speech; Representative from UN/ESCAP
General Secretary's Remarks; Prof. Shunji Murai, AARS

10:00-10:30 **Keynote Speech; Prof. Armin Gruen, ETH, Switzerland**
"Advanced Technologies in Photogrammetry and Remote Sensing"

10:30-11:00 **Coffee Break**

11:00-12:30 **Panel Discussion : How to Operationalize Remote Sensing?**
Chairperson: Prof. Shunji Murai, AIT

12:30-14:00 **Lunch**

14:00-15:00 **Tape Cut Ceremony : Commercial Exhibits start**

14:00-16:30 **EC-ASEAN Seminar (Room A)**

15:30-17:30 **Plenary Session on New Technical Information**
(Surasammanakhan Seminar Hall)
Co-chairpersons: Prof. Shunji Murai, AIT
Dr. Suvit Vibulsresth, NRCT

PS-1 Operationalization an Emphasis on RADARSAT
Robert Tack; RADARSAT (Canada)

PS-2 Outlook on Availability of Satellite Data and Thai Remote Sensing Satellite Program
Suvit Vibulsresth, Praneet Ditsariyakul, Niramon Limlamai, Leelawan Sutheparuks; NRCT(Thailand)

PS-3 SPOT An Overview on Systems and Applications
Yves Bechacq; SPOT ASIA (France)

PS-4 Indian Remote Sensing Satellites - Future trends and perspectives
Mukund Rao, V.Jayaraman and M.G. Chandrasekhar ; ISRO (India)

PS-5 Japanese Remote Sensing Activities
Kimihiko Nakayama; NASDA (Japan)

PS-6 Mission Analysis for Enginneering Test Satellite, KITSAT-3
Sungdong Park, S.Kim, D,K.Sung, S.D.Choi; KAIST (Korea)

PS-7 The Centre for Earth Observation (CEO): An Initiative of the European Commission to Promote the Use and Availability of Earth Observation Data
P. N. Churchill*,M. Sharman**, G. Schreier* and J. Aschbacher*; *European Commission(Italy) , **Directorate Gencral XII (Belgium)

PS-8 Data Distribution
Kyoichi Ito : RESTEC (Japan)

19:00-21:00 **Welcome Party**

November 21, Tuesday 1995

8:00-10:00 Session A : Forest / Vegetation Mapping
Chairperson: Mr. Thongchai Charuppat, Royal Forest Dept. (Thailand)

A-1 Monitoring of Wetland Vegetation Distribution and its Change by using Microwave Sensor Data
Y. Yasuoka*, Y. Yamagata*, M.Tamura*, M.Sugita* , Jatuporn Pornprasertchai**, Supapis Polngam**, Rachen Sripumin**, H.Oguma***, Xidong Li****; *National Institute for Environmental Studies (Japan), **NRCT (Thailand), ***NSDA , ****PASCO (Japan)

A-2 Synergism of JERS-1 SAR and Landsat TM Imagery for Forest Types Discrimination
Khali Aziz Hamzah; Forest Research Inst. Malaysia (Malaysia)

A-3 Integration of Geographic Information System and Area Production Model (APM) in the Prediction of Forest Degradation at Phrao District, Thailand
Yousif Ali Hussin , Vicente Ato and Alfred De Gier ; ITC (The Netherlands)

A-4 Monitoring of Forest Stand Condition in Thailand
H.Sawada*, H. Saito*, Thongchai Charuppat**, Jirawan Charuppat**, Suwit Ongsomwant**, Surachai Ratanasermpong***, Chaowalit Silapathong*** ; *Forestry & Forest Products Research Inst. (Japan), **Royal Forestry Dept., ***NRCT (Thailand)

A-5 Evaluation of Asian Elephant Habitat
Li Zhixi, Li Hongga and Lu. Feng; Inst. of Remote Sensing & GIS(China)

A-6 Estimating Vegetation Function from Satellite Data in Seasonal Tropical Environments
Kazue Fujiwara* and E.O.Box** ; *Yokohama National Univ. (Japan), **Univ. of Georgia (USA)

A-7 The Application of Satellite Data and GIS for Ecological Restoration
Sirin Kawla-Ierd*,K. Fujiwara*, S. Murai**, Kitti Khanthamit*** and Suvit Vibulsresth****; *Yokohama National Uni., **Univ. of Tokyo, ***Bureau of the Royal Household, ****NRCT (Thailand)

8:30-16:30 EC-ASEAN Seminar (Room A)

10:30-12:00 Poster Session P: Forest/Vegetation Resources
Chairperson: Dr. Surachai Ratanasernpong, NRCT (Thailand)

P-1 National-Wide Environmental Unit Classification using Remote Sensing & GIS - a case study in Zambia
R. Nagasawa, K. Endo, Y.Takahashi and Y.Kojima ; PASCO International Inc. (Japan)

P-2 Spectroradiometric and Digital Data Analyses of Seven Varieties of Cinchona Species in the Denr Cinchona Reforestation Project -Mt.Kaatoan, Lantapan Bukidnon, Philippines
Jose Edgardo L. Aban; Univ. of Philippines (Philippines)

P-3 Classification of Forest in Malaysia using JERS-1 SAR and Landsat TM Data
Hideki Saito*, Khali Aziz Hamzah**, and Haruo Sawada*; *Forestry and Forest Products Research Institute (Japan), **Forest Research Inst. of Malaysia (Malaysia)

P-4 Application of RS and GIS for Forest-steppe and Dry-steppe Geosystem Study
M.Ganzorig, H.Tulgaa, D.Amarsaikhan, B.Enkhtuvshin ;Informatics & RS Center (Mongolia)

P-5 Satellite Remote Sensing for Artificial Grassland in Japan
Nobuyuki Mino, Genya Saito and Akira Hirano; National Inst. of Agro-Environmental Sciences (Japan)

P-6 Monitoring Deforestation in Luzon Island, the Philippines using Satellite Data
Akira Hirano, Genya Saito, Nobuyuki Mino; National Inst. of Agro-Environmental Science (Japan)

P-7 Mask Procedure for Effective Classification and Expression on Mangrove Area with TM Dat of Landsat 5
K. Sato*, K.Takezaki**, Dwi Setyono* ; *Univ. of the Ryukyus,**Kankuu (Japan)

P-8 Relationship between Stand Factors of Mangrove Forest and TM Data of Landsat 5
Dwi Setyono and Kazuhiro Sato ; Univ. of the Ryukyus (Japan)

P-9 Relationship between Landcover and NOAA GVI in Thailand
Eiji Kodani* and H. Sawada** ; *Forestry and Forest Products Research Institute, **Forestry and Forest Products Research Inst. (Japan)

P-10 Forest Cover Change Analysis: Retrospective and Perspective; A Case of Selected Countries in South and South East Asia
Chandra P. Giri and Surendra Shrestha ; UNEP (Thailand)

P-11 Differences of SAR Image between JERS-1 and ERS-1 to Land Use/Land Cover Investigation
Anusorn Chantanaroj*, Kenji Otsuka** and Keisuke Katsuta** ; *Dept. of Land Development, (Thailand) **GSI (Japan)

P-12 Change Detection in Coastal Zone by Remote Sensing Technique
Valairat Wanpiyarat, Promchit Trakuldist, Boonrak Pattanakanok ; Dept. of Land Development (Thailand)

P-13 The Integration of Remote Sensing System and GIS for Forest Land Use Planning
Suwit Ongsomwang; Royal Forest Department (Thailand)

10:30-12:30 Expert Group Meeting on Remote Sensing 2000 by NRCT (Room B)
12:00-13:30 Lunch

13:30-15:30 Session B: Agriculture / Soil
Chairperson: Dr. Charat Mongkolsawat, Khon Kaen Univ. (Thailand)

B-1 Modelling RADARSAT Coverage in the Mekong Delta to Optimize Separability of Rice base Cropping Systems
Gordon C. Staples*, S.P.Kam** and Dennis Nazarenko* ; *RADARSAT (Canada) and **Int. Rice Research Inst. (Philippines)

B-2 Towards Sustainable uses through Land Evaluation: A case study of Muaklek, Thailand
Rajendra Prasad Shrestha and Apisit Eiumnoh ; AIT (Nepal)

B-3 A Knowledge-based Approach to Predicting Salinty in the South-West of Western Australia
Peter Caccetta*, H.T.Kiiveri** and F.H.Evans**, R.Ferdowsian ; *Curtin Univ. of Technology, **CSIRO, ***Dept. of Agriculture Western Australia (Australia)

B-4 Assessment of ERS-1 SAR Data for Rice Crop Mapping and Monitoring
Supan Kanchanasutham*, Apichart Pongsrihadulchai* and Chockchai Rodprom** ; *Office of Agricultural Economic and **NRCT (Thailand)

B-5 Multi-Seasonal Analysis of SAR Data for Agriculture
Genya Saito, Nobuyuki Mino and Akira Hirano ; National Inst. of Agro-Environmental Science (Japan)

B-6 Utilization of Satellite Remotely Sensed Data as an Information Source for a GIS in Agricultural Resource Management
Farhad Jenabfar; Agricultural Statistics & Information Dept.(ASID) (Iran)

B-7 Assessment of ERS SAR Data for Tropical Agricultural Crop Monitoring
Josef Aschbacher*, A.Pongsrihadulchai**, S.Karnchanasutham**, D.R. Paudyal*** E.Nezry* and M. Wooding****; *European Commission (Italy) , **OAE (Thailand), ***Forestry Building(Australia), ****RSAC (U.K.)

16:00-17:30 Poster Session Q: Bio/Agricultural Resources
Chairperson: Mr. Pongpit Piyapongse, NRCT Advisor (Thailand)

Q-1 Remote Sensing Data in relation to the Ecological Indices of Tropical Monsoon Forest
Moe Myint and Tri B. Suselo; AIT (Thailand)

Q-2 Computer Assisted Monitoring of Vegetation Using Multi-resolution Satellite and Geospatial Data
Surat Lertlum* and Shunji Murai**; AIT *(Thailand) and **(Japan)

Q-3 Simulating Agricultural Land Use Changes in Thailand
K.S. Rajan, Ryosuke Shibasaki and Masataka Takagi ; University of Tokyo (India)

Q-4 Application of Remote Sensing and GIS Techniques for Wildlife Habitat Research at Thang Yai Naresuen Wildlife Sancterauy
Pantip Uthanavanit, Boonchai Chertsurakul, Supoj Poonnoi; Ram Kam Haeng Univ.(Thailand)

Q-5 Capability of Remote Sensing Application in Landuse, Land Resources with using TM Data -GIS Facilities in Part of Iran
Majid Ghiassi and Mehrdad Nematzadeh ; Agric. Info. Dept. (Iran)

Q-6 Simulating Forest Degradation: Applying the Area Production Model in the Kali Konto Area in East Java, Indonesia
Alfred de Gier and Yousif Ali Hussin ; ITC (The Netherlands)

Q-7 Simulating Forest Degradation : The Application of a GIS-based Area Production Model in Kali Konto, East Java, Indonesia
Alfred de Gier , Jan Bode and Yousif Ali Hussin ; ITC (The Netherlands)

Q-8 The Crystal Globe: A GIS-Based Operational Area Production Model
Yousif Ali Hussin, Johan Bode, Alfred De Gier ; ITC (The Netherlands)

Q-9 Identification and Mapping of Irrigated Vegetation using NDVI-Climatological Modelling
Ramesh S. Hooda* and Dennis G.Dye** ; University of Tokyo *(India) and **(USA)

Q-10 Field Prediction and Potential Monitoring of Cassava Production in Nakhon Ratchasima
A. Eiumnoh*, R.P.Shrestha*, S.Baimoung** and P.Kesawapitak*** and
A. Noomhorm* ; *AIT, **Dept. of Meteorology, ***Dept. of Agriculture (Tha

Q-11 Air and Water Pollution Study in Ulaanbaatar using RS and GIS Techniques
P. Galsan, D. Amarsaikhan;Informatics & RS Centre(Mongolia)

Q-12 Identification of Agriculture in Songkla Basin from the GLOBESAR Data
Supapis Polngam; NRCT (Thailand)

Q-13 Natural Resources and Land Use Change of Phuket using Remote Sensing
Surachai Rathanacermphong, Jatuporn Pornprasertchai, Dararat Disbunchang; NRCT (Thailand)

16:00-17:30 Room B: WG: 1 km Land Cover Data Base in Asia
Chaired by Dr. Ryutaro Tateishi (Japan)

19:00-21:30 General Conference (1) (Only National Delegates are invited)

November 22, Wednesday 1995

8:00-10:00 Session C : Mapping from Space
Chairperson: Dr. Paibul Ruangsiri, NRCT (Thailand)

C-1 Monitoring Land Use/Land Cover Changes in Phuket Island
Suthep Chutiratanaphan*, A.Chanthanaroj*, K.Otsuka** and K.Katsuta**; *Dept. of Land Development, (Thailand) **GSI (Japan)

C-2 Measurement of Topographical Variation by Hyogo-Nanbu Earthquake with JERS-1 SAR Interferometry
Yuichi Maruyama and Hiroji Tsu; Earth Remote Sensing Data Analysis Center (Japan)

C-3 Land-cover Change Detection on Korean Peninsula using NOAA AVHRR Data (session H)
Kim Eui-hong; KIST (Korea)

C-4 DEM Generation by Satellite Imagery and Its Accuracy
Tsuneaki Shimoji; Geographical Survey Institute (Japan)

C-5 A Multipurpose Ecological Mapping and Evaluation of Mongolian Nature Based on Remote Sensing and Ground Data
M. Saandar and D.Gunin; Monmap Engineering Services(Mongolia)

C-6 Small-Format Airborne Remote Sensing an Effective Tool in Building Spatial Information for Urban Land Use Planning
Randolf S. Vicente; National Mapping and Resource Information Authority (Philippines)

C-7 An Archaeological Application of Synthetic Aperture Radar (SAR) in Thailand
Punnee Wara-Aswapati; Suranaree University of Technology (Thailand)

10:30-12:00 Poster Session R: Natural Resources Monitoring/Mapping
Chairperson: Dr. Prasat Witayarat, Geographical Association of Thailand

R-1 Use of Satellite Imagery for Updating Terrain Information in Topographic Databases
K.D. Parakum Shantha; Inst. of Surveying and Mapping (Sri Lanka)

R-2 Integration of Remote Sensing Data with GIS Technology for the Acceleration of the Activiti in National Mapping Agencies
Shyamali Chithraleka Perera*,K.D. Parakum Shantha**; * Survey Dept., **Inst. of Surveying and Mapping (Sri Lanka)

R-3 Block Adjustment Method for Mosaicing Large Number of Satellite Data
Koki Iwao, Ryosuke Shibasaki and Masataka Takagi ; University of Tokyo (Japan)

R-4 A Focused Approach to the Use of Space Based Remote Sensing technology for Resource Management in Equatorial Asia
Richard Marcoux and Gareth Richardson ; Spar Aerospace Limited (Canada)

R-5 Airborne Multispectral Data Including Thermal IR from a Learjet Platform (DAEDALUS 1268)
Donald H. de Vries; CSIRO COSSA (Australia)

R-6 A Study of Ecosystem Development along Coramantal Coast of Tamil Nadu using Remote Sensing Techniques
M. Manivel*, B. Manikiam**, D.Kumaran Raju*, J.Moses Edwin* ; *Bharathidasan University, **ISRO HQ. (India)

R-7 An assessment of Sedimentary Environment using IRS-1A Data: A case study in the lower hooghly estuary, East Coast of India
Syriac Seeastian and Amitava Ghosal ; Society of Management Science and Applied Cybernetics (India)

R-8 Assessment of Logged-over Forest Lands using Landsat TM in Jerangau F.R.Malaysia
Kamaruzaman Jusoff and Zulhazman Hamzah ; Universiti Pertanian Malaysia (Malaysia)

R-9 The Effective Use of Thermal Images for the Preservation of Weathered Relics
Yoshiki Yamano and Kazuya Saito ; Asia Air Survey Co.,Ltd. (Japan)

R-10 Tropical Forest Mapping using Low Resolution Remote Sensing Data Set
Surat Lertlum* and Shunji Murai**; AIT *(Thailand) and **(Japan)

R-11 Modelling for Global Land Degradation using Remote Sensing and GIS
Krishna Pahari and Shunji Murai ; AIT (Nepal)

R-12 Variation of Surface Current Offshore from Rayong Rivermouth from NRCT Buoy Data in 1994
Absornsuda Siripong, Supichai Tangjaitrong, Sirichai Dharmvanij and Chaiyong Yuangthong ; Chulalongkorn Univ.(Thailand)

R-13 Digital Classification of LANDSAT TM for Land Cover Mapping of the Pa Wang Phloeng-Muang Khom Lam Narai National Forest Reserve, Lop Buri Province, Thailand
Kaew Nualchawee and Lilita Bacareza; AIT (Thailand)

R-14 Comparison of Different Sensors and Analysis Techniques for Tropical Mangrove Forest Mapping
J. Aschbacher*, P.Tiangco**, C.P.Giri***, R.S.Ofren***, D.R. Paudyal**, Y.K. Ang** ; *European Commission (Italy) , **AIT, ***UNEP/EAP-AP

12:00-13:30 Lunch

13:30-15:30 Session D: Water / Marine Resources
Chairperson: Dr. Darasri Downreang, NRCT (Thailand)

D-1 Use of Multi-Temporal Data for the Study of Glacier Lakes and Glacier Lake Outburst Flood in Nepal Himalaya
P.K. Mool; Water & Energy Commission Secretariat (Nepal)

D-2 Optimal Cropping Pattern for an Irrigation Command Considering Sustainability of the Available Water Resources
M. Sebastian, V.Jayaraman and M.G. Chandrasekhar ; ISRO (India)

D-3 Ovservation of Western Siberian Wetlands by using Remote Sensing Techniques : Estimationof Methane Emission
M. Tamura* ,Y. Yasuoka* and K.Tokumura** ; *National Inst. for Environmental Studies, **Nakanihon Air Service (Japan)

D-4 Estimation of Chlorophyll Concentration in Lakes and Inland Seas from Near-infrared and Red Spectral Signature
Kazuo Oki* andY. Yasuoka** ; *Univ. of Tsukuba, **National Institute for Environmental Studies (Japan)

D-5 Evaluation of Selected Filters Applied on Synthetic Aperture Radar (SAR) Data for General Coastal Land Cover Mapping (**cancelled**)
Ma. Consuelo D. Garcia; National Mapping & Resource Information Authority (Philippines)

D-6 Disasters Mitigation Stratigies in Bangladesh (session C)
M. A.H. Pramanik; Bangladesh Centre for Advanced Studies (Bangladesh)

D-7 Thailand Sea Watch Program
Darasri Dowreang and Pithan Singsaneh; NRCT (Thailand)

16:00-17:30 Poster Session S : Data Processing and Application
Chairperson: Dr. Kaew Nualchewee, AIT (Thailand)

S-1 A Sobel Edge Detector Digital Filter Structure and Its Distributed Arithmetic Implementation
Kobchai Dejhan*, Fusak Cheevasuvit*, Somjin Thongplew*, Soontorn Oraintara*, Narong Arjrith** and Ekachai Prommas*** ; *King Mongkut's Inst. of Technology Ladkrabang **Srinakharinwirot Univ. , ***Kasembundit Univ. (Thailand)

S-2 Digital Image Data Recovery from Printed Image
Fusak Cheevasuvit*, K.Dejhan* , V. Tipsuwanporn*,S. Wongkharn* and A.Somboonkaew** ; *King Mongkut's Inst. of Technology Ladkrabang, **Mahanakorn Univ. (Thailand)

S-3 A New and Efficient Transform for Signal Processing - based on Gabor Discrete Cosine Transform
V.K.Singh and A.S.Manjunath; NRSA (India)

S-4 Effect of Atmospheric Correction on Satellite Image Data by Lowtran Model
Kiyoshi Torii*, Tomoyuki Mase** and Takashi Hoshi*** ; *Kyoto University , **Ministry of Agriculture, ***Ibaragi University (Japan)

S-5 A Massively Parallel Implementation of an Image Classifier
Peter Caccetta*, Norm Campbell** and Geoff West* ; *Curtin Univ. of Technology, **CSIRO (Australia)

S-6 Development of a Stereoscopic Image Processing Software
Nobuhiko Mori; ERSDAC (Japan)

S-7 Classification Methodology for Land Cover Mapping Using Global Monthly 8-km AVHRR Data
Wen Cheng-gang and Ryutaro Tateishi ; Chiba Univ. (China)

S-8 Application of Landsat TM Data in Distribution of Mangrove Forest in Southern Iran
Zahra Zanjanian; Iranian Remote Sensing Center (Iran)

S-9 Land Use/Land Cover Change Detection in the Chiang Mai Area using Landsat TM
Somporn Sangawongse; Chiang Mai University (Thailand)

S-10 A Development of DEM Generation System
Jaeyeon Lee, K. Fukue, H. Shimoda and T. Sakata: Tokai Univ. (China)

S-11 Development of Highspeed Programmable Formatter for Earth Observation Satellite Downlink Data Formatting
Hideyo Yokotsuka*, T. Sakata*, H. Shimoda*,S. Sobue**, M. Sekiguchi***: *Tokai Univ. , **NASDA, ***RESTEC (Japan)

S-12 Thai Remote Sensing Satellite System
Suvit Vibulsresth, Waraporn Suchaichit, NRCT (Thailand)

S-13 Analysis of Multi-temporal SAR Images
Rasamee Suwanwerakamtorn*, Shoji Takeuchi**; *NRCT(Thailand), **RESTEC (Japan)

S-14 The use of highly Discriminating Spectral Information for Mapping and Measuring Optical Water Quality and Shallow Benthic Cover
DLB Jupp, G.P.Harris, G.T. Byrne, M.Anstee, T.R.McVicar, E.R. McDonald, D.A. Parkin and J.L.Smith; CSIRO (Australia)

16:00-17:30 Room A: WG: ITC related workshop
Chaired by Dr. Ir. Alfred (The Netherlands)

16:00-17:30 Room B: WG: Earth Observation Information System
Organized by NASDA/RESTEC (Japan)

19:00-22:00 Dinner Party

November 23, Thursday 1995

8:00-10:00 Session E : Digital Image Processing
Chairperson: Dr. Chawalit Thisyakorn, Siamtec International (Thailand)

E-1 Data Compression using Vector Quantization and Huffman Coding for Satellite Imagery
Fusak Cheevasuvit, K.Dejhan , S.Mitatha and S. Wongkharn ; King Mongkut's Inst. of Technology Ladkrabang (Thailand)

E-2 Color Correction of Fused Images using Color Space Transformation **(cancelled)**
Tsukasa Hosomura; Kanazawa Inst. of Technology (Japan)

E-3 Automation of Road Extraction from Space and Aerial Images
Armin Gruen and Haihong Li ; ETH (Switzerland)

E-4 Verification of Atmospheric Correction for AVHRR data by Radiometric Simulation Software 6S
Takayuki Satoh*, Shoji Takeuchi**, Koji Kajiwara* and Ryutaro Tateishi*; *Chiba Univ.,**RESTEC (Japan)

E-5 Adaptive cubic convolution of high resolution remotely sensed image data
Raveentheran Suntheralingam; Sime Darby Systems (Malaysia)

E-6 Geometric Correction of NOAA AVHRR GAC Data
Kimiaki Saitoh*, Toshiaki Hashimoto**, Koji Kajiwara*, Ryutaro Tateishi*; *Chiba Univ., **Basic Engineering (Japan)

E-7 A Technique for 3D Modelling of Building
Taejung Kim, Soon Dal Choi; KAIST (Korea)

10:30-12:00 Workshop on Education and Training
Chairperson: Dr.Punnee Wara-Aswapati, Suranaree Univ.of Tech. (Thailand)

WE-1 The Importance of Training and Institution Strengthening for Remote Sensing in S.E Asia
J.W. Trevett; ISMARSC Ltd.(U.K.)

WE-2 Remote Sensing Education: The Philippines Experience
Epifanio D. Lopez ; Univ. of the Philippines (Philippines)

WE-3 A New Program in AIT: Space Technology: Applications and Research
Jean-Pierre Delsol ; AIT (France)

WE-4 Remote Sensing and GIS Education in Iran
Ramin Rahimi Djafari ; National Cartographic Center(Iran)

WE-5 Geographic Information Analysis : A case study as an AID to teaching
R. Sudarshana*, S. Seeastian** and S.K.Bhan* ; *Indian Institute of Remote Sensing, **Society of Management Science and Applied Cybernetics (India)

10:30-12:00 Workshop on Spatial Information Processing
Chairperson: Dr.Sukit Viseshsin, Chulalongkorn Univ. (Thailand)

WS-1 GA Optimization Technique on Spatio-Temporal Interpolation for Dynamic GIS
Shaobo Huang* and Ryosuke Shibasaki**; *Chiba Univ.(China) , **Univ. of Tokyo (Japan)

WS-2 The Management of Errors within the GIS Environment
K.D. Parakum Shantha; Inst. of Surveying and Mapping (Sri Lanka)

WS-3 Contour Line Interpolation by using Buffering Method
Masataka Takagi and Ryosuke Shibasaki ; Univ. of Tokyo (Japan)

WS-4 Comparison of the Certainties in a GIS
D. Amarsaikhan, M. Ganzorig;Informatics & RS Centre (Mongolia)

WS-5 Plan of the Construction of GIS for Northeast Thailand
Yasuharu Yamada*, Mitsuo Suzuki*, Wapakom Amorndham**, Somsak Sukjarn***; *Japan International Research Center for Agricultural Science(Japan), **ADRC, ***LDD (Thailand)

12:00-13:30 Lunch

13:30-15:30 Session F: Global/Regional Change Study
Chairperson: Mr. Supan Karnchanasutham, Office of Agricultural Economic (Thailand)

F-1 Nakhon Ratchasima, Resources Atlas
Charat Mongkolsawat* and NRCT Sub-committee on Landuse**; *Khon Kaen Univ., **NRCT (Thailand)

F-2 The EC-ASEAN ERS-1 Project: National Evaluation Projects into Regional Implementation Opportunities
Mike G. Wooding, PA Fletcher and IL Thomas; Remote Sensing Applications Consultants (U.K.)

F-3 Land Cover Classification System for Continental/Global Applications
Ryutaro Tateishi*, Wen Cheng Gang* and L.Kithsiri Perera**; *Chiba Univ., **Weathernews ,*(Japan), *(China) and **(Sri Lanka)

F-4 Developing Land Cover Classification System for Remote Sensing Applications in Asia
Chandra P. Giri and Surendra Shrestha ; UNEP (Thailand)

F-5 Satellite Estimation of Environmental Variables by the Contextual Analysis Method: Validatio in a Seasonal Tropical Environment
T. Saravanapavan and Dennis G.Dye ; Univ. of Tokyo (Sri Lanka)

F-6 On the characteristics of the 1993/1994 Geostationary Meteorological Satellite High Cloud Amount
Ae-Sook Suh, Kyung-Ja Ha & Seung-Hee Sohn ; Meteorological Res. Inst. (Korea)

16:00-17:30 Room A: WG: GIS for Education
Co-chaired by Dr. R.Shibasaki and Dr. K. Cho (Japan)

16:00-17:30 Room B: WG: 1 km Land Cover Data Base in Asia
Chaired by Dr. Ryutaro Tateishi (Japan)

19:00-21:30 General Conference (2) (Only National Delegates are invited)

November 24, Friday 1995

8:00-10:00 Session G : Land Degradation
Chairperson: Mr. Manu Omakupt, Suranaree Univ. of Tech. (Thailand)

G-1 Land Degradation Monitoring using Multi-Temporal Satellite Data over the Southwestern Flank of Mount Pinatubo in Luzon Island, Philippines
Jerry Hervacto G. Salvador, T.M. Santos, E.G. Domingo; Univ. of Philippines (Philippines)

G-2 Diagnosis of Land Degradation in the Semi Arid Area of Asia and Pacific Region using Remote Sensing Data -JIRCAS's Case Study -
Satoshi Uchida; JIRCAS/ ICRISAT (Japan)

G-3 Mapping of Salt-affected Soils using Remote sensing and Geographic Information Systems: A case study of Nakhon Ratchasima, Thailand
Awadh K. Sah, Apisit Eiumnoh, S.Murai and Preeda Parkpian; AIT (Nepal)

G-4 Maximizing the Potential of ERS-1 Synthetic Aperture Radar Data for Lahar Damage Assessment
Epifanio D. Lopez, Jean Chorowicz, Jean-Francois Parrot, Ernesto Corpuz, Fredy Garcia and Randy John Vinluan ; Univ. of the Philippines (Philippines)

G-5 Monitoring Global Vegetation Degradation using NOAA NDVI Data
Shiro Ochi* and Shunji Murai**; *Utsunomiya University and **AIT (Japan)

G-6 A Knowledge-based Approach for Land Evaluation using RS and GIS Techniques
D. Amarsaikhan, M. Ganzorig ; Informatics & RS Centre (Mongolia)

10:30-12:00 Closing Ceremony

12:00-13:30 Lunch

13:30-16:00 Technical Visit

PLENARY SESSION

Outlook on Availability of Satellite Data and Thai Remote Sensing Satellite Program

Dr.Suvit Vibulsresth
Ms.Praneet Ditsariyakul
Thailand Remote Sensing Center
National Research Council of Thailand

Abstract

After 1987, not only has Thailand Remote Sensing Center (TRSC) provided the high resolution satellite data worldwide but the development of remote sensing technology has also been greatly enhanced. The variety of products with different correction levels is available to fulfill the users' requirement. The Synthetic Aperture Radar (SAR) data has also been introduced under the cooperation with Japan for JERS-1 SAR reception, the EC-ASEAN Regional Radar Remote Sensing ERS-1 Project and the GlobeSAR Canada-Thailand Project in order that the users in this region can make use of the information that the present and future radar satellites can provide. Besides, it is gratifying that Thai government has realized the significance of space technology development and applications. The Thai Remote Sensing Small Satellite Program was recently approved by the cabinet. The Ministry of Science, Technology and Environment through its technical authority in the National Research Council of Thailand will own and operate the small satellite system. This paper will present an outlook on satellite data presently received by NRCT and the system to be operated by NRCT.

Paper presented at the 16th Asian Conference on Remote Senisng, 20-24 November 1995, Nakhon Ratchasima, Thailand

1. Introduction

With the capabilities of acquiring and processing multi-sensor data, NRCT has been able to develop remote sensing market sucessfully. Considering data revenue trends for the past five years starting from calendar year 1990 to 1994, the value of products sold has progressively grown from US $ 800,000 in 1990 to US $ 1.6 million in 1994. This is due to the fact that satellite imagery was no longer just used for R & D. It is now a valuable and cost effective solution. However, the existing optical sensor could not provide cloud free imagery especially in the rainy season, therefore SAR data has been introduced to overcome the said limitation. SAR data is appropriate to be used as complementary to optical sensor data of Landsat, SPOT and MOS, etc. NRCT also plans to acquire the Indian IRS data and to own and operate Thai Remote Sensing Satellite System (Smallsat Program), an optical sensor satellite to be launched in the next few years.

2. Present and Future Availability of Satellite data

Thailand ground receiving station currently acquires data from both optical sensors of Landsat, SPOT, MOS, NOAA and SAR sensor of the Japanese JERS-1 and ERS-1 of the European Space Agency. With the extensive archive of multi-level data, NRCT through the User Services Center presently offers to the users various scales, formats and correction levels of the photographic and digital products comprising:

a) Photographic product, both in film and paper prints in black & white or color at various scales and correction level: bulk, georeferenced and geocoded.
b) Digital product in the media of both computer compatible tape (CCT) and 8 mm. cartridge tape with the options of BIL/BSQ format for TM & SPOT and CEOS for ERS-1 and density of 1600/6250 bpi for CCT and 2.3/5.0 GB for cartridge tape.

Users who are interested in the data over particular area under Thai station's coverage, could access the catalog locally or remotely. In recognition of the users' need for easy query of the station's data archive, NRCT also plans to develop a capability to allow querying of the station's archive through Internet with World-Wide-Web by mid 1996.

Apart from the existing facilities, NRCT will upgrade the equipment to receive the Indian IRS-1C and, Thai station for receiving the Canadian Radarsat satellite data, in 1996.

3. Thai Remote Sensing Satellite Program

In October 1994, the Ministry of Science, Technology and Environment (MOSTE) concluded MOU with the Canadian Space Agency for cooperation in space technology and applications. Consequently, Thai Government recently gave the provisional approval to NRCT to proceed with the Thai Remote Sensing Satellite Program.

MOSTE through the National Research Council of Thailand will own and operate the satellite system. It will be the first satellite to operate in an orbit dedicated to the equatorial regions. The unique feature of this system design will give Thailand a leadership position in Southeast Asia and the global equatorial belt in general. Thailand will be able to assume a role in the international effort to use space to monitor the earth's resources and environment and to assist sustainable development. It is also good opportunity to provide significant human resource development and could be the first step in developing a space related industry in Thailand.

(I) Overall Description

The performance parameters of the Thai Remote Sensing Satellite System are summarized in the following tables :

TABLE 1 Mission Performance

Parameter	Value
Mission Life	5 years
Orbit Type	73 orbits / 5 days Multi-sun-synchronous
Orbital Period	97 minutes
Orbit Inclination	28 degrees
Orbital Altitude	600 km
Coverage Repeat	Every 5 days
Illumination Repeat	49 days
Command Uplink	S-Band : 2 kbps
Telemetry Downlink	S-Band : Direct 2/4 kbps Playback 32/128 kbps
Data Downlink	X-Band : <85 Mbps

TABLE 2 Temporal Performance

Parameter	Value
Revisit Time	Twice every 5 days
Accessibility Region	29.6° N to 29.6° S
Maximum Imaging Capability	10 minutes/orbit
Usable opportunities per year	63

TABLE 3 Spatial Performance

Parameter	Value
Swath Width	185 km imaged swath which is selectable within a 275 km
Across Track Resolution	30 m (nadir)
Along Track Resolution	30 m (nadir)
Geometric Distortion	<1/2 pixel
Band to Band Registration	<1 pixel
Image Locations	<5 km

TABLE 4 Spectral Performance

Parameter	Value
Spectral Bandwidths :	
Blue	0.45 to 0.52 μm ±0.1
Green	0.52 to 0.60 μm ±0.1
Red	0.63 to 0.69 μm ±0.1
NIR	0.76 to 0.90 μm ±0.1

4. Conclusion

As NRCT has over fifteen years equipped with remote sensing capabilities both for data reception and extensive applications, now Thailand is embarking on a new direction through Thai Remote Sensing Satellite System. This will not only benefit Thailand but would also provide new opportunity for international collaboration.

Mission Analysis for Engineering Test Satellite, KITSAT-3

Sungdong Park, Sungheon Kim, Dan Keun Sung, Soon Dal Choi
Satellite Technology Research Center (SaTReC)
Korea Advanced Institute of Science and Technology (KAIST)
373-1 Kusung-Dong, Yusung-Ku, Taejon, 305-701
Korea

ABSTRACT

The SaTReC has developed and been operating two micro-satellites, KITSAT-1 and 2, and is now developing the third satellite system, KITSAT-3. The KITSAT-3 is designed and operated from the basis of engineering test purposes. The KITSAT-3 system is a small satellite with a mass of approximately 100 kg, however, 3-axis stabilized. Each subsystem has been designed from similar concept to the KITSAT-1/2, however system architecture is so unique and modular that can be easily modified and expanded for future missions.

This paper presents how the KITSAT-3 system has been designed at system level. It will also include critical mission analyses such as power budget, mass budget, thermal analysis, link budget, operational scenarios and attitude maneuvering under given constraints. The results of mission analyses will generate a baseline system for preliminary design.

1. INTRODUCTION OF KITSAT-3 SYSTEM

The Satellite Technology Research Center (SaTReC) has launched two of micro-satellites, KITSAT-1 and KITSAT-2, in 1992 and 1993, respectively. The KITSAT-1 was the first Korean satellite and has been developed as a collaborative project with University of Surrey in UK. The KITSAT-2 has been completely newly developed and test in Korea by Korean engineers with major changes on payloads and corresponding bus systems.

The SaTReC is now aiming to design, develop, and operate the third KITSAT using experience and well trained engineers obtained from KITSAT-1/2. The KITSAT-3 system will be SaTReC's unique small satellite and will be used as bus platform for SaTReC's future space missions. The primary mission objectives are development and in-orbit test of newly designed small satellite system especially demonstrating new techniques such as 3-axis stabilized attitude control system, solar panel deployment mechanism, common bus networked architecture, high resolution and multi-spectral camera system, and payload data transmission system in high data rate.

The mission payloads on board KITSAT-3 are a remote sensing payload with 15m resolution and pushbroom type CCD camera in three spectral bands, a space science payload with a high energy particle telescope and a radiation monitor which can measure radiation environment around mission orbit and can also distinguish what types of particles and in which levels, and a data collection payload collecting data measured from buoys floating on ocean.

The KITSAT-3 is supposed to be launch ready at the end of 1996 and designed to be launched by Chinese Long March IV as a secondary launch. The weight of KITSAT-3 system shall be less than 100 kg and the dimension of satellite shall be within 45 × 45 × 60 (cm).

2. MISSION ANALYSES

In order to configure the satellite systems, it is necessary to allocate performance to the satellite elements and to specify corresponding subsystems. The process to allocate performance and to evaluate them is generally called mission analysis. It requires iterations and provides overall system configuration for preliminary design. It begins with analyzing the requirements and allocating performance parameters by establishing budgets for power, mass, and propellant. For KITSAT-3 system, the propellant budget is not considered, as there is no propellant system. The budgeting must be based upon the mission orbit and operational view point. In this paper, power budget, mass budget, and initial thermal analysis will be mainly presented.

2.1 Orbital Analysis

Prior to analyze requirements and allocate performance parameters, the mission orbit should be defined clearly and analyzed first. The mission orbit would be one of the most important constraints to design satellite systems. Once satellite system has been designed to be operated in a mission orbit, it needs significant

modifications to be operated in others. Different orbital characteristics give different solutions for available power, battery's charge and discharge characteristics, and thermal control which is the most significantly affected.
The mission orbit of the KITSAT-3 is approximately 800 km of altitude and sun-synchronous orbit. The descending node will be about 10:30 AM, therefore the sun incident angle toward orbital plane is constant and 22.5 deg. Even though there is no propellant system for station-keeping at desired orbit, it is assumed that the satellite is positioned at the initial position and the orbital properties are not significantly changed during mission life.

Sun-synchronousity gives a lot of benefit to satellite system designers. It will give nearly constant sun illumination to satellite, therefore available power and depth of discharge is constant at every mission orbit. Thermal environment is also moderate to adopt passive thermal control. For the remote sensing payload, as the areas taken by camera system are illuminated at well constant level, it helps to control gain and integration time.

At 800 km altitude, the nodal spacings between successive orbits are calculated as 25.22 deg for a day, 6.92 deg for 4 days, and 2.46 deg for 16 days. As the field of view of KITSAT-3 camera system is 5 deg, the KITSAT-3 can achieve complete coverage and take image at any area at least every 16 days. If the attitude control system is well qualified, the revisit period can be reduced to 4 days with small attitude adjustment using reaction wheels.

Through the detailed analysis on orbital property, it can be calculated that the mission control center at the SaTReC has the contact time of approximately 48 minutes over 5 deg and 17 minutes over 20 deg per day.

2.2 Power Budget

The power budget is estimated by adding the payloads' power requirements to power estimates for the spacecraft system. If the satellite system has several different operation modes that differ in power requirements, it is necessary to estimate power requirement separately for each operation mode, paying particular attention to peak power need for each subsystem. Once defined power requirements and their duty cycle, the required power from energy source can be calculated. From this result, we can size the solar panel and the battery capacities to supply enough power for operations and recharging batteries until the end of mission life. During this process, the degradation on power subsystem over the mission life should be taken into account. Radiation damage to the solar panels and depth of discharge and number of charge and discharge cycles of the battery are main factors for degradation.

Subsystems	Estimated Power (Watt)	Duty Cycle (%)
Spacecraft		
Electrical Power System	20.0	100
Attitude Control System	17.2	† [1]
C&DH System	2.5	100
Transmitters/Receivers	10.0	100
Structure/Thermal	0	
GPS Receiver/Processor	7.0	† [2]
Sub-Total	56.7	
Payloads		
Remote Sensing Payload with Data Transmitter	60.0	10
Space Science Payload	0.9/2.2	100/10, ‡ [1]
Data Collection Payload	2.0	50
Sub-Total	8.03	
Total	64.73	

Table 1. Power requirements at subsystems

where † [1], † [2] are variable to operational modes and ‡ [1] corresponds to radiation monitoring mode and pitch angle rotation modes. Pitch angle rotation mode will be activated only after solar flare precaution for about 48 hours.

Remote sensing payload will be operated once a day basis, therefore 10 % of duty cycle will be enough for estimation.

From the power budget estimation, the required power from solar panels and their area are roughly calculated as 100 Watt and 0.362 m^2, when GaAs solar cells (18 % of efficiency) are used. With the consideration of solar panels' degradation during 3 years mission life, which is about 20 % at 800 km's polar orbit and oblique

sun incident angle, which is about 22.5 deg, if the area of solar panel is over 0.56 m^2, then it will be sufficient to supply enough power until the end of mission life.

2.3 Mass Budget

To derive the first mass budget for the satellite system, the payloads' masses should be defined first. Generally payloads are developed before the spacecraft, therefore the spacecraft's mass can be roughly obtained from similarity with previously built spacecraft systems. For the KITSAT-3 system, the KITSAT-1 and 2 system were used to estimate the mass with reasonable multiplication factors from the change of complexity. The mass allocation for payload systems are as follow;

Payloads	Mass Estimated (kg)
Remote Sensing Payload	20.5
Space Science Payload	10.0
Data Collection Payload	5.0
Sub-Total	35.5

Table 2. Estimation of payloads mass

The masses of the spacecraft subsystems are estimated from the degree of complexity changed and they are as follow;

Subsystems	Pre-Mass (kg)	Complexity Factor	Mass (kg)
EPS	11.0	1.5	17.4
ADCS	6.5	2.1	13.65
C&DH	3.5	1.4	4.9
TRx	3.5	2.0	7.05
Structures/ Thermal	25.0	1.2	30.0
GPS	5.0		5.0
Sub-Total			78.0

Table 3. Estimation of spacecraft mass

where pre-mass is the mass flown on KITSAT-1/2 and complexity factor is the degree of complexity changed from KITSAT-1/2. If no value given to complexity factor, it is new subsystem.

From the Table 2 and 3, total weight estimation was found as 113.5 kg. This value is a little bit higher than design value, however, from the point of system engineer's view, all the mass estimations are over-estimated and these values are concluded to be acceptable.

2.4 Thermal Control

The thermal control for the KITSAT-3 is mainly based upon passive thermal control using thermo-optical properties of satellite structures and thermal coating materials as similar to KITSAT-1/2. As the mission orbit is sun-synchronous, heat inputs from the Sun and the Earth is constant during a orbit period. However as the KITSAT-3 system is operated in 3-Axis stabilized control mode, the thermal environment shall be severer than before.

The solar panels always pointing toward the Sun may cause them to be heated up extremely high. Therefore it is main task to decrease the temperature on the solar panels in KITSAT-3 thermal control system design.

In order to estimate maximum and minimum temperatures on a solar panel, initial thermal modeling on the solar panel has been performed using lumped model and transient state analysis method. Fig. 1 shows the temperature profile when GaAs solar cells and epoxy white paint were used on illuminated side and the other side, respectively and it tells the solar panel will be operated at the range of 255 K and 329 K (-18 C and 56 C, respectively). The other properties of the solar panels were quoted from the KITSAT-2 solar panel.

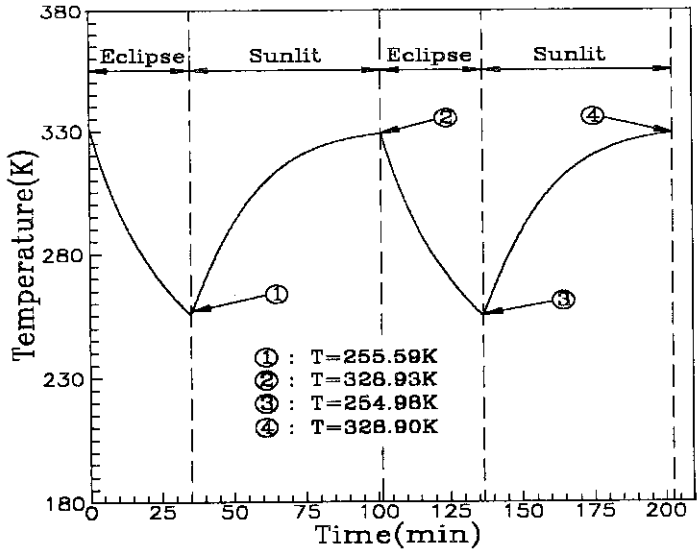

Fig 1. Temperature profile for solar panels

It predicts that the solar panel will be within sufficient temperature range. However as the solar cell generates higher power at lower temperature and there can be thermal shock during heating up and cooling down, the ratio of absorptivity over emissivity shall be reduced in order to decrease average working temperature and the specific heat capacitance or the mass of the solar panel shall be enlarged in order to decrease temperature change rate.

During the detailed analysis, if any part of the satellite cannot be operated within desired operation temperature by passive thermal control, heaters or radiators shall be used to increase or decrease temperature at some areas.

2.5 Link Budget

The KITSAT-3 system uses similar transmitters and receivers for telemetry broadcasting and command receiving. As it has been proved, it is not necessary to analyze the link budget for TT&C function again. In this paper, the link budget calculation on image data transmission (IDT) link is presented as Table 4.

Items	Unit	0 Deg	20 Deg	30 Deg
Carrier Frequency	MHz	8200	8200	8200
Data Rate	Mbps	10	10	10
RF BW Occupied (QPSK)	MHz	5	5	5
Transmitter Output Power	Watt	5	5	5
Transmit Antenna Gain	dBi	0	3	3
EIRP	dBW	6.99	9.99	9.99
Range at given El. Angle	km	3293	1769	1395
Free Space Loss	dB	-181.1	-175.7	-173.6
Polarization Loss	dB	-3	-3	-3
Implementation & Additional Loss	dB	-2	-2	-2
Receive Antenna Diameter	m	5	5	5
Receive Antenna Gain	dBi	50.06	50.06	50.06
Antenna Pointing Loss	dB	-0.1	-0.1	-0.1
Receive System Noise Temperature	K	300	300	300
Receive System G/T	dB/K	25.29	25.29	25.29
Boltzmann's Constant	dBW/Hz/K	-228.60	-228.60	-228.60
C/No	dBW/K	74.81	83.21	85.27
C/N	dBW/K	7.82	16.22	18.28
Eb/No	dB	4.81	13.21	15.27
Required Eb/No	dB	9.60	9.60	9.60
Link Margin	dB	-4.79	3.61	5.67

under the following conditions;
Carrier Frequency : 8200 MHz

Transmitter Power	: 5 Watt
Transmitter Antenna Gain	:
0 dBi at Horizon	
3 dBi over 10° of Elevation Angle	
Modulation Scheme	: QPSK
Data Rate	: 10 Mbps
Bit Error Rate	: E-5
Rx System Noise Temp	: 300°K
Rx Antenna Diameter	: 5 meter
Rx Antenna Efficiency	: 0.55

Table 4. Link Budget Calculation for IDT Link

Table 4 shows that the communication link is feasible over 20 deg of elevation angle with 5 m's receiving antenna. This result implies that the operation will be limited but still acceptable for engineering test purpose and the operational boundary can be enlarged using bigger antenna system.

4. ATTITUDE MANEUVERING AND OPERATIONAL MODES

4.1 Post Launch Operation

The post launch operation mode is the processes from lift-off to first commanding. As soon as the satellite is separated, all the program necessary are automatically loaded and then the On-Board Computer (OBC) is booted. The OBC performs Built-In-Test. If all the processes are going well, the attitude determination and control system lets the satellite come into detumbling mode. All the telemetries gathered during these processes will be saved in main memory and will be dumped at the first acquisition.

If the health-checking is completed, the mission control center will monitor the attitude in order to deploy solar panels. All the processes above will be completed within one week.

4.2 Normal Operation

This process is mainly for mission payloads. The system design and the operation are based upon this process. The normal operation process is defined as comprehensive operation on spacecraft with the operation of at least one payload. For successful operation, all the subsystem should be able to provide power supply, attitude maneuvering and keeping, and data processing with respect to the missions and their requirements.

The normal operation consists of three operation modes corresponding to different payloads. The detailed modes will not to be mentioned.

4.3 Abnormal Operation

If the satellite system detects any abnormal symptom at any subsystem, it enters fault isolation and recovery mode. If the fault was one of expected faults, then it will be automatically recovered. However if not, it enters safety mode. During the safety mode, the attitude of satellite is changed to get maximum power and performs minimum functions for telemetry and command.

4.4 Attitude Maneuvering

During the normal operation, the attitude of the KITSAT-3 is controlled to generate maximum power from the solar panels. During eclipse period, the satellite is maneuvered to keep contact with ground control.

For the operation of camera system, the attitude maneuvering is performed to let the camera point the desired area prior to initiate a series of actions.

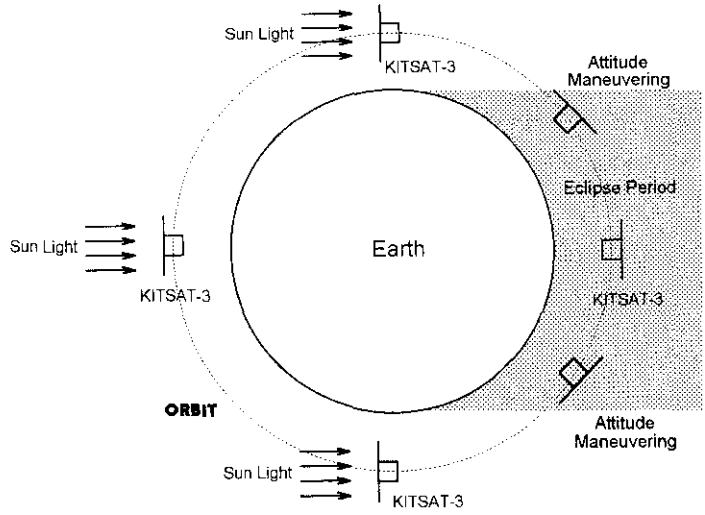

Fig. 2. Attitude control for normal operation

The other attitude control mode for payload operation is pitch angle rotation mode for the space science payload. This mode is only used after solar flare precaution for about 48 hours. During this mode, the high energy particle telescope distinguishes the kinds of particles and their energy levels and measures the directivity as well.

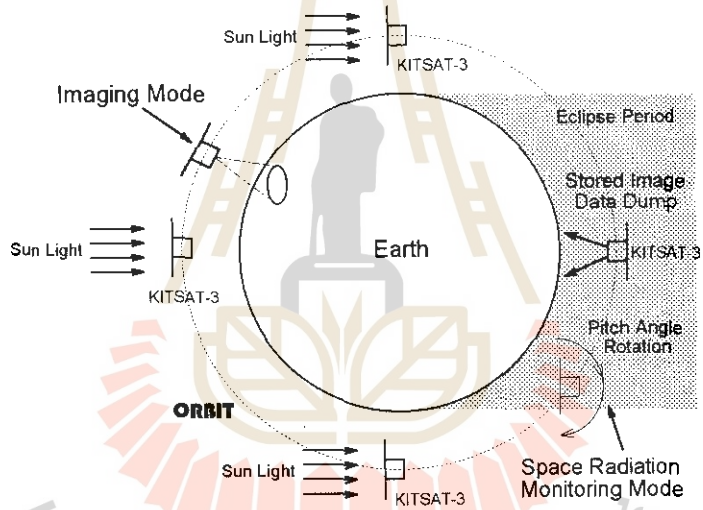

Fig. 3. Attitude control for payloads operations

5. BASELINE SYSTEM ARCHITECTURE

The KITSAT-3 system is based upon modular architecture. The system diagram is shown at Fig. 4.

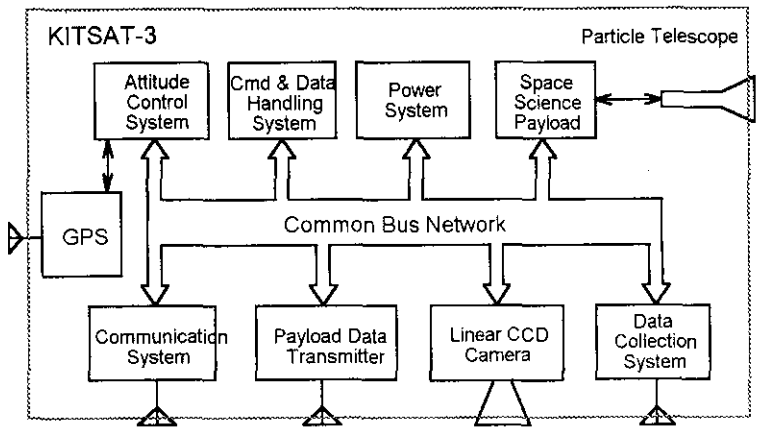

Fig. 4. KITSAT-3 System Architecture

All the subsystems are connected to others through common bus network. The network provides 38.4 kbps data communication with fault free data communication protocol. Each subsystem has its own telemetry and telecommand functions, though C&DH is primary. This configuration gives a lot of freedom to expand functions for future missions and simplicity to interconnect.

6. MISSION TIMELINES

The KITSAT-3 program has been initiated in August, 1994 as 2.5 years' time span. Until the end of 1995, the SaTReC will complete the manufacturing and test of KITSAT-3 engineering model. It also includes qualification test for new launcher. The KITSAT-3 flight model will be flight ready at the end of 1996.

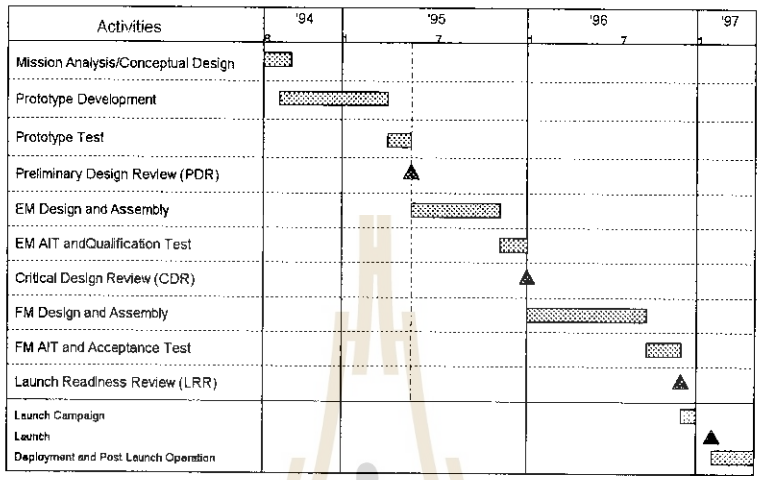

Fig. 5. KITSAT-3 Mission Timelines

The flight schedule is under negotiation, but it will not be later than the middle of 1997. The Fig. 4 shows detailed project timelines.

7. Conclusion

Through the in-orbit test, the KITSAT-3 satellite system will be thoroughly tested and proved. From the engineering test using KITSAT-3 system, the SaTReC will expand its capability to design next generation small satellite carrying a high resolution CCD camera and a SAR demonstrator.

The KITSAT-3 system will demonstrate state-of-art technology of small satellite with low cost but competitive quality with commercial remote sensing satellites or highly expensive scientific satellites.

8. References

[1]. S. Park and S. Choi, "**Space Activity at SaTReC**", *2nd APC-MCSTA,* 1995.
[2]. "**Operations Concept Document for KITSAT-3**", *SaTReC Doc.,* 1995.
[3]. "**KITSAT-3 General System Specifications**", *SaTReC Doc.,* 1995.
[4]. I. Lee, D. Sung, and S. Choi, "**Experimental Multimission Microsatellites - KITSAT Series**", *7th AIAA/USU Conference on Small Satellite,* 1993.
[5]. S. Kim, D. Sung, and S. Choi, "**A Korean Experimental Microsatellite - KITSAT-1 System**", *AP-MCSTA Workshop,* 1992.

THE CENTRE FOR EARTH OBSERVATION (CEO): AN INITIATIVE OF THE EUROPEAN COMMISSION TO PROMOTE THE USE AND AVAILABILITY OF EARTH OBSERVATION DATA

P. N. Churchill[1], M. J. Sharman[2], G. Schreier[1], J. Aschbacher[1]

[1]European Commission, Joint Research Centre, Institute for Remote Sensing Applications
I-21020 Ispra (VA), Italy, Tel: +39-332-78 5425, Fax: +39-332-78-5461
e-mail: peter.churchill@jrc.it; gunter.schreier@jrc.it; josef.aschbacher@jrc.it

[2]European Commission, Directorate General XII-D4, Space Unit
Rue de la Loi 200, B-1049 Brussels, Belgium, Tel: +32-2-29-59798, Fax: +32-2-29-60588
e-mail: martin.sharman@mhsg.cec.rtt.be

ABSTRACT

The European Commission (EC) and the European Space Agency (ESA) have agreed with their Member states to establish a co-ordinated, decentralised Earth observation network, the European Earth Observation System (EEOS). The EC contribution to this is the Centre for Earth Observation (CEO) programme. The objective of the CEO is to promote the use of Earth observation data and services and to facilitate interaction between providers of these data and services and their customers. The CEO will be driven by user requirements. It will be decentralised in its approach. It will pay due regard to and take advantage of existing and planned institutions, infrastructure and projects. It will also be designed to evolve and adopt flexibility. This paper outlines the status and objectives of the CEO Programme, and proposes a concept for the CEO.

CEO BACKGROUND

The European Space Agency (ESA) and the European Commission (EC) have agreed to work towards a more efficient and cost-effective use of Earth observation data, by combining their expertise with that of their Member States and other relevant European organisations such as EUMETSAT to establish a co-ordinated, decentralised Earth observation network called the European Earth Observation System (EEOS).

EEOS will link with international initiatives such as NASA's Earth Observation System Data and Information System (EOSDIS) and Japan's international satellite data management and information system (EOIS).

In this collaboration ESA and the national space agencies shall take responsibility for receiving data from satellites, and for the pre-processing and supply of these space data.

The EC contribution to EEOS is the Centre for Earth Observation (CEO). The CEO will foster the development of applications of Earth observation data that fulfil the specified information requirements of scientific, operational and commercial users. This will help to ensure that relevant higher level products and information are generated and made available. Associated with the application development are various services. These will include services that permit access to data and information, and help preserve the data and information.

PROJECT ORGANISATION AND STATUS

Project Status

The CEO project is divided into 3 phases:

- Feasibility Study 1992-1993
- Pathfinder Phase 1993-1995
- Design and Implementation Phase 1996-1998

The CEO programme is now at the end of the Pathfinder Phase. The goal of the Pathfinder Phase is to produce a project plan for the Design and Implementation Phase containing sufficient information and understanding of the system to bring the CEO successfully into being. The work of the Pathfinder Phase is described in a Project Plan that has been presented to and discussed with the Pathfinder Phase Steering Committee (PPSC).

The Pathfinder Phase is organised by Activities each with contributory deliverables. There are 5 Activities, of which the first two (Activity 1: Survey and understand the present infrastructure status, and Activity 2: Capture user requirements) take place simultaneously at the start of the Pathfinder Phase. The third Activity (Synthesis) starts during Activities 1 and 2, and ends when the implications of those Activities are fully assimilated. The fourth Activity (Plan the Design and Implementation phase) then starts. Throughout the Pathfinder Phase, the fifth Activity (Cost and Benefits of the CEO elements of the system) maintains an up-to-date estimate of the probable cost of the programme. This work is being supported by practical tests of potential elements of the CEO. These 'Proof of Concept' studies will aid in the definition of the plan for the Design and Implementation Phase.

Project Organisation

The Pathfinder phase is overseen by a Steering Committee (PPSC) composed of delegates of the Member States of the European Union (EU) and the European Economic Area (EEA). The PPSC is also observed by the European Environmental Agency (EEA), EUMETSAT, the European Space Agency (ESA) and relevant organisations of the EC such as EUROSTAT, plus other space data providers such as EURIMAGE and SPOT Image.

The Pathfinder Phase is managed and co-ordinated by a Project Team based in the JRC Institute for Remote Sensing Applications (IRSA). The Commission's DG XII provides strategic and policy support through its D4 Unit (Space).

Further information is available via a prototype World Wide Web (WWW) information server at the following address:

http://ceo-www.jrc.it/

CEO OBJECTIVES AND ASSUMPTIONS

The PPSC and the CEO team have established the following high level objectives for the CEO:

The CEO shall promote the application of Earth observation in the EU and Member States by:

- encouraging communication and exchange of services between individual users and between user communities;
- stimulating the creation of high level products, where and when necessary;
- promoting improved data standardisation and quality assurance;

- co-ordinating the design and operation of existing and future decentralised data archives and data bases and data delivery services;
- improving the accessibility and availability of Earth observation data, services and expertise.

Two main design constraints apply to the CEO:

- the CEO shall pay due regard to, and take advantage of, established institutions and existing and planned networks and projects.
- the CEO shall be designed to evolve and adapt flexibly to future needs of the users and to changes in data sources.

These objectives, and discussions with the PPSC, have lead to the following reflections about the CEO:

Participating Entities

The entities that should benefit from the existence of the CEO include all organisations or individuals with a professional objective that may be approached by using information obtained from Earth observation. Such entities will include the Services of the Commission, National government organisations, regional, local and city government, universities and research centres, commercial companies and international consortia.

It is therefore expected that users of and providers to the CEO will be drawn from all these entities.

Organisation Autonomy

Organisations across Europe and outside Europe will participate in the CEO programme. The CEO team and the PPSC will ensure that the CEO is implemented according to the design criteria. There is no reason for the CEO faculty to interfere with the autonomy of organisations using its facilities, but rather the CEO faculty should leave users free to expand their expertise and infrastructure by using services and resources made available through the CEO programme.

Decentralised Approach

The CEO should be decentralised, and rely on as few central services as possible. In the early stages of the CEO project a central co-ordinating facility will certainly be necessary, although its role and responsibilities remain to be determined.

Standards

The CEO programme should ensure accessibility to data, information and services. To achieve this the CEO programme should sometimes recommend or promote (but not impose) standards, formats or software.

Formats

The CEO should help users to access data and services across the full range of formats and standards available on the system. This may require the creation of specialised software, but there is no assumption about who should provide that software.

Earth Observation Expertise

Earth observation expertise and data are distributed over many organisations. The CEO should establish mechanisms to make them more easily available to potential users.

Flexibility

User requirements for the CEO programme will change as new applications are introduced, as users become more expert in the analysis of Earth observation data, and as their understanding of the capabilities and potentialities of the CEO increases. The CEO should therefore keep track of and be responsive to changing user requirements.

New Technology

New technology and its consequences must be continuously incorporated into or accommodated by the CEO programme.

SUGGESTED CONCEPT FOR THE CEO

The architecture of the CEO will only become apparent once the results of the Pathfinder Phase are available and analysed. Nevertheless, it is possible to suggest a concept that conforms to the objectives listed above, and which does not impose or imply any particular architecture.

The Present Situation

Earth observation data is rather under-exploited in Europe and world-wide. Data from different sources are typically held in separate depositories in diverse and sometimes obscure formats, and objective information about remote sensing and its possible applications is dispersed and not always easy to find. The market is fragmented, and potential users are not always aware of the possibilities. Some customers are better informed and have found suppliers of products, information or data, but in general the level of connectivity between potential customers and suppliers could be improved.

The Potential CEO Concept

The CEO concept will be user driven, and thus the exisiting and potential users of Earth Observation data and services are supported in various ways. Among these are the demonstration of the potentials of Earth Observation through application examples, education, training and promotion of remote sensing and support in Earth Observation data handling and management.

The easiest way of putting customers and suppliers in contact is to provide a clearing house in which requests can be advertised, either over a computer network or by less sophisticated means. In what follows we will discuss a computer-based solution, but this does not prejudice other means of access. This central clearing house is termed the European Wide Service Exchange (EWSE). A prototype of the EWSE is currently on-line and can be accesssed via Internet **(http://ewse.ceo.org/.).** It may contain separate sections that operate as an electronic bulletin board (exchange information in a sequential way), or as a telephone yellow pages (organised by theme) or as a dating agency (where the system aims to find a perfect match of customer requirement and service provision).

The user of the European Wide Service Exchange must find it simple and intuitive to use. It should certainly provide context-sensitive help. The customer advertising his need or the provider advertising a service should be able to use the facilities provided by the exchange to define precisely the service required or offered.

New services will appear on the market as a response to the demand from the users. Popular services will tend to be offered by several providers, thus stimulating competition and improvement in the services. Such a system adapts naturally and without outside control to changing user requirements.

Projects and Services

The critical phase in the life of the CEO will be the initial one, in which it has too few users to make it an attractive means for customers and service providers to find one another. The most direct mechanism to stimulate the use of the CEO, and to populate both its data bases and its complement of users, is for the EC to support application projects that make use of the CEO. These projects would be proposed and organised by entities that wished to examine the contribution of Earth observation to some decision making process. These projects would have clients with well defined information needs, that might in some cases be currently met using conventional data sources, but to which remote sensing might bring added benefit.

A project is intended to stimulate the Earth observation market, in its broadest sense, by injecting money and energy into the system without unbalancing the value-added market. Any project launched in the context of the CEO would have certain responsibilities. Among these responsibilities would be to ensure that the data sets and products generated by its activities were properly archived, catalogued and interfaced to the European Wide Service Exchange.

The idea of a service is a key element for the CEO. A service is defined as any activity that is carried out for a customer. Providing a list of services is a service, as is publishing the request of a customer for a certain service. Services may be provided by anyone; Earth observation data suppliers, value-added companies, university departments, or various individual users of the system. Suppliers are free to offer their service under whatever conditions they wish, as is presently the case in the absence of the CEO. Some of the services may be provided by the CEO programme or by the (hypothetical) Co-ordinating Facility (see next section).

In this manner the CEO provides a "shop window" for service providers which they are free to use or not use as they wish. The CEO may initially provide some limited funding to give an impetus to attracting service providers to establish the system. In general, though, service providers will be drawn in by the attraction of the ready access to a growing market.

Co-ordination of the CEO: User Committees and Central Facility

In this concept of the CEO, the functioning of the programme remains largely in the hands of the users. Users (either or both customers and suppliers, as appropriate) may decide to form committees to co-ordinate the behaviour of users (including suppliers) in any given domain of the CEO. The terms of reference, method of operation and method of funding of these committees is still to be determined.

Certain functions of the CEO system may have to be co-ordinated centrally. This leads to the idea of a CEO Co-ordinating Facility (CCF). The functions, responsibilities, staffing and financing of this hypothesised CCF are not yet determined and will probably change over time as the requirements of the system change. In the initial stages of the CEO most or all of the functions of the CCF shall probably be provided by the team responsible for the CEO Pathfinder phase or subsequent phases.

CONCLUSIONS

The CEO is now in its definition phase. Data are being collected on user requirements and current and planned infrastructure to help this definition. On the basis of what has already been collected a preliminary concept for the CEO suggests a distributed, decentralised approach conforming to the requirements of clients for information derived from Earth observation data, and driven by application oriented projects that produce the information that customers want and provide some of the necessary services that will make the CEO an attractive environment in which the Earth observation profession will flourish.

SELECTED BIOBLIOGRAPHY

1. CEO Pathfinder Phase Project Plan, Doc. No. CEO/074/1994 (Issue 5, July 1995), JRC Ispra
2. Preliminary Assessment of CEO User Requirements, Doc. No. CEO/155/1995, JRC Ispra
3. CEO Status Report for the 6th Pathfinder Phase Steering Committee Meeting, Doc. No. CEO/153/1995, JRC Ispra

TECHNICAL SESSION A

FOREST / VEGETATION MAPPING

MONITORING OF WETLAND VEGETATION DISTRIBUTION AND ITS CHANGE BY USING MICROWAVE SENSOR DATA

Yoshifumi YASUOKA[1], Yoshiki YAMAGATA[1], Masayuki TAMURA[1], Mikio SUGITA[1]
Jatuporn PORNPRASERTCHAI[2], Supapis POLNGAM[2], Rachen SRIPUMIN[2]
Hiroyuki OGUMA[3]and Xidong LI[4]

1 National Institute for Environmental Studies
16-2 Onogawa, Tsukuba, Ibaraki 305 Japan

2 National Research Council
196 Phaholyortin Rd., Bangkhen, Bangkok 10900, Thailand

3 National Space Development Agency, EORC
7-15-17 Roppongi, Minato, Tokyo 106 Japan

4 Pasco Corporation
1-1-2 Higahiyama, Meguro, Tokyo, Japan

ABSTRACT

The purpose of the study is to investigate remote sensing methodologies for monitoring actual vegetation distribution and its change in wetland by utilizing microwave sensor (SAR) data from ERS-1 and JERS-1 together with optical sensor data from LANDSAT TM, JERS-1 OPS and SPOT HRV.

The study includes the investigation on the microwave/landcover interaction mechanism in vegetated areas and also the development of the algorithms for vegetation classification by using SAR data. First, the relation between SAR image intensities and vegetation types and conditions has been investigated based on a set of ground survey data and overlayed satellite imageries from L-band SAR (JERS-1), C-band SAR (ERS-1), JERS-1 OPS, LANDSAT TM and SPOT HRV. Next several SAR data processing methods for vegetation classification have been investigated. Vegetation classification methods include both of the statistical approaches and texture analysis approaches. The methods were applied to the data at Kushiro Mire in Hokkaido, Japan and Prachuap Khirikhan Wetland in Thailand.

It was found that there is no clear relation between vegetation types and single SAR data in both of JERS-1 and ERS-1 SAR whereas combination of multi-seasonal SAR data is very effective for actual vegetation classification in wetland areas. The difference between JERS-1 and ERS-1 SAR data for wetland vegetation classification has been also investigated.

1. Introduction

Wetland is one the most valuable ecosystems on the earth. It abounds biological diversity and are treasure houses of living things. Also today the importance of wetland is pointed out as a major emission source of methane which is one of the green house gases. As changes in wetlands are rapid and serious due to various human activities, it is urgent to monitor wetlands and their surrounding environment from

---

This study has been conducted as a part of the Joint Research between National Institute for Environmental Studies (NIES), Japan and National Research Council of Thailand (NRCT) sponsored by the Special Coordination Funds of Science and Technology Agency of Japan, and also as a part of the JERS-1 Research Announcement (RA) program by National Space Development Agency (NASDA) of Japan.

physical, biological or social viewpoints. Ground survey of wetland is, however, not easy because of its difficulty to approach there [1]. Remote sensing is expected to provide us an efficient tool for monitoring wetland environment. In particular, as wetland is characterized by a mixture of vegetation, soil and water, microwave remote sensing is expected to delineate the relation between them. This paper describes remote sensing methodologies for monitoring wetland environment with special emphasis on the application of SAR data to vegetation classification.

First, the relation between SAR image intensities and vegetation types and conditions has been investigated based on a set of ground survey data and overlayed imageries from ERS-1 SAR, JERS-1 SAR and OPS, LANDSAT TM and SPOT HRV. And next several data processing methods have been developed for the classification of SAR data. Vegetation classification methods include both of the statistical approaches and texture analysis approaches, and they have been applied to a single SAR image and also to a set of multi-seasonal SAR images.

Two test sites, Kushiro Mire in Hokkaido, Japan and Prachuap Khirikhan Wetland in Thailand were selected as test sites for the study. In this paper the results at Kushiro Mire are primarily described. Kushiro Mire is the biggest wetland in Japan and its extent is around 29,000 ha. The dominant species in vegetation are Sphagnum, Sedge, Reed and Alder. Kushiro Mire has been facing serious environmental problems due to regional developments.

It was found that there is no distinctive relation between vegetation types and single SAR data in both of JERS-1 and ERS-1 SAR whereas combination of multi-seasonal SAR data is very effective for actual vegetation classification in wetland areas. One of the reasons for it is that SAR data reflects land surface conditions including water inundation or soil moisture condition as well as vegetation conditions. The difference between JERS-1 and ERS-1 SAR data for wetland vegetation classification has been also clarified.

2. Overlay Analysis between Vegetation and SAR images

Satellite imageries from JERS-1 SAR, ERS-1 SAR, LANDSAT TM and SPOT OPS, and other landcover data including vegetation maps were registered each other, and relations between them were analyzed . At Kushiro Mire, first, in order to get base data for wetland vegetation distribution, vegetation were classified into seven categories including Sphagnum, Sedge, Reed, Alder, open water, forest and others by using three season LANDSAT TM imageries from spring, summer and autumn in 1991 which represent the seasonal variations of vegetation conditions (Fig. 1). Three dates images were registered each other and combined into eighteen bands images. Here, for each date image, six bands (Band 1-5 and 7) from visible and near-infrared were used for classification. The maximum likelihood classification (MLC) scheme was applied to the combined eighteen bands images with more than ninety training areas. Ground survey data was used for selecting the training areas for the classification.

(1) Relation between vegetation categories and SAR image densities

For each vegetation categories SAR image densities from JERS-1 and ERS-1 were extracted and their image density distributions were compared. There were no distinctive differences between the image density distributions for each vegetation categories except the difference between the forested areas and paddy fields and between the vegetated areas and the residential areas. And also there was no clear and stable relations between the single SAR image densities and the vegetation types and conditions in both of JERS-1 SAR and ERS-1 SAR data.

(2) Difference between JERS-1 SAR and ERS-1 SAR data

Principal Component Analysis (PCA) was applied to the two band images of a JERS-1 SAR image and a ERS-1 SAR image from the same season, and the difference component (the second Principal Component) was examined to see the difference between them. It shows clear difference, however, at the same time it depends on the seasons and conditions and there is no clear relations between the vegetation types and the differences.

PCA was also applied to the combined set of SAR images from different seasons for JERS-1 and ERS-1. Figure 2 shows the PCA image for three seasons SAR images from JERS-1 SAR and ERS-1 SAR at Kushiro Mire. The first , second and third components of PCA are assigned to the red, green and blue color respectively. The results shows the multi-seasonal SAR data clearly reflect the vegetation distribution and indicates the possibility of applying multi-seasonal SAR data to vegetation classification. Figure 3(a) and (b) demonstrate the PCA images for individual three seasons JERS-1 SAR and ERS-1 SAR data respectively, and it clearly shows that the PCA image for JERS-1 SAR has the more distinctive relation with the vegetation types than that for ERS-1 SAR.

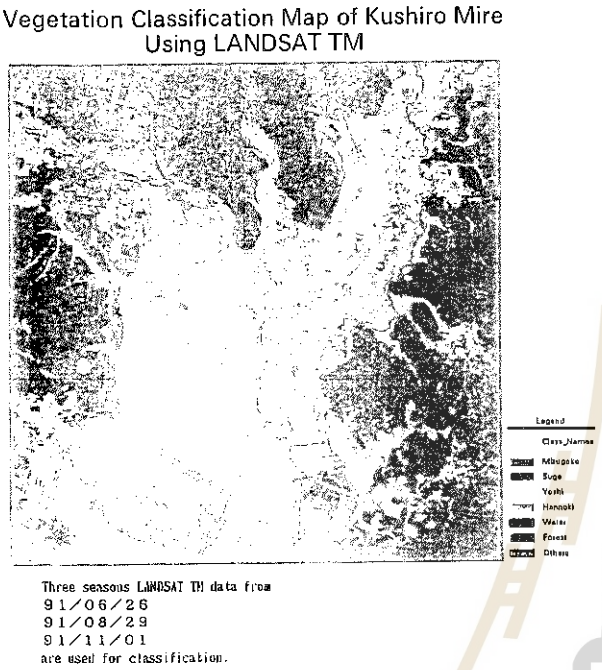

Fig.1 Vegetation map of Kushiro Mire obtained from three seasons LANDSAT TM data.

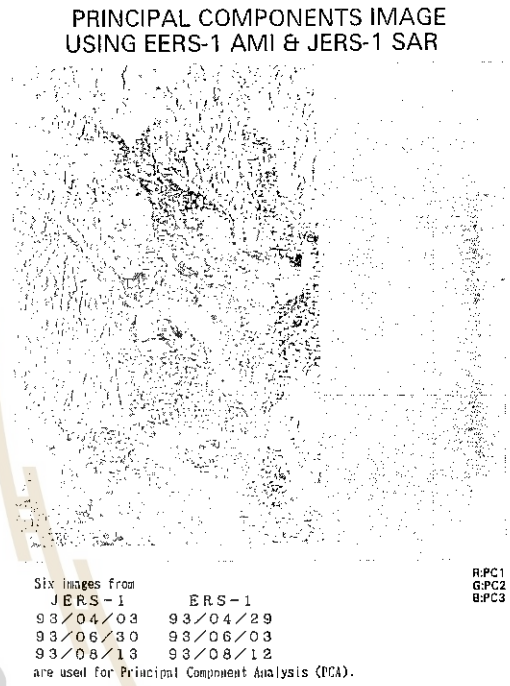

Fig.2 PCA image of three seasons JERS-1 and ERS-1 SAR images (6bands).

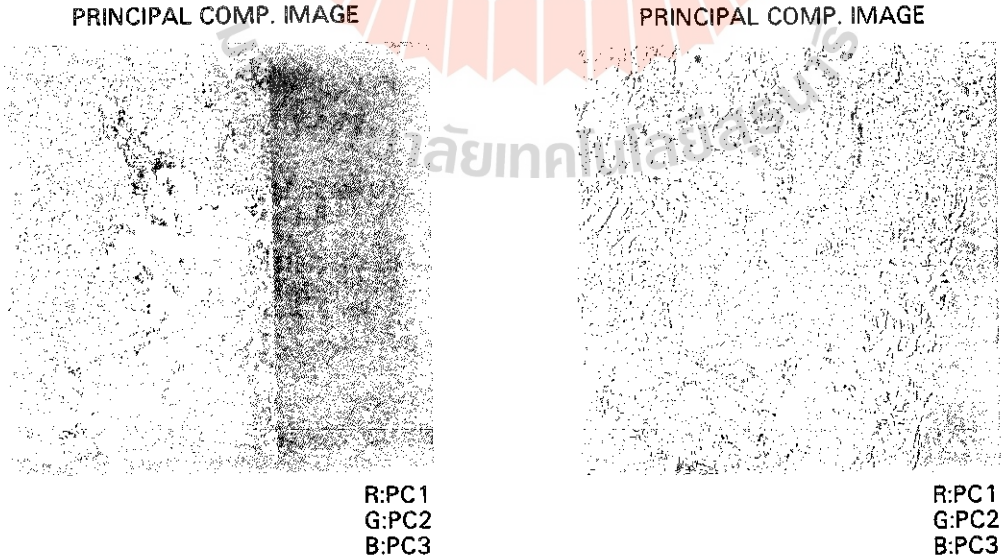

(a) (b)

Fig.3 PCA image for three seasons SAR data. (a) JERS-1 SAR , (b) ERS-1 SAR.

3. Vegetation Classification using SAR images

(1) Classification with statistical analysis and texture analysis
Conventional statistical classification scheme and texture analysis scheme were applied to JERS-1 and ERS-1 SAR data to investigate the difference between L-band SAR and C-band SAR in vegetation classification. First, maximum likelihood classification (MLC) was applied to the registered two band images of JERS-1 and ERS-1 SAR (Fig.4(a)). Texture analysis (TA) based on the co-occurrence matrix was also applied to both of the JERS-1 SAR and the ERS-1 SAR data, and to the combined two bands images of JERS-1 SAR and ERS-1 SAR data (Fig.4(b)) [2]. The result from TA shows less noisy classification than that from MLC, however, both of them show the noisy classification than LANDSAT TM based classification due to the speckle noise of SAR data.

(2) Comparison of vegetation category separability between ERS-1 SAR and JERS-1 SAR
Further, using the co-occurrence texture features [3], the separability between each vegetation categories was compared between JERS-1 SAR and ERS-1 SAR to investigate the difference in the classification efficiency between them. As a separability index Jeffrey-Matsushita distance (J-M distance) in texture feature domain among different vegetation categories were calculated with respect to different textures combination. Figure 5 shows the J-M distance increase curve for JERS-1 SAR and ERS-1 SAR data with respect to the increase of the number of texture features in the classification. Mean values and the minimum values of the J-M distance among the vegetation categories are shown in the figure. In both of the mean and the minimum values of the J-M distances, JERS-1 SAR data shows the higher separability index than ERS-1 data, and indicates higher efficiency in vegetation classification than ERS-1 data.

(3) Vegetation classification with multi-seasonal SAR images
JERS-1 and ERS-1 multi-seasonal SAR images were also used for the vegetation classification and to the measurement of other land surface conditions including soil moisture or water content. Vegetation classification using three seasons SAR imageries from spring, summer and autumn shows that SAR data, in particular L-band SAR (JERS SAR), may reflect not only vegetation conditions but also surface water conditions under vegetations. The results of the landcover classification of Kushiro Mire with maximum likelihood classification are shown in Fig.6. Figure 6(a) and (b) shows the vegetation map produced by JERS-1 SAR images and by ERS-1 SAR images respectively .

4. Conclusions

The study investigated the possibility of applying the SAR data to vegetation classification. In particular, wetland vegetation was focused as a case study. The results are summarized as follows;

(1) It is difficult to extract effective information on the vegetation types and the conditions from a single season SAR data.
(2) Combination of multi-seasonal SAR data is efficient for vegetation classification.
(3) JERS-1 SAR (L-band) data is more effective than ERS-1 SAR (C-band) data in vegetation classification.

Monitoring vegetation distribution over wetland areas has now urgent necessity from various viewpoints such as the habitats of wild animals (biodiversity), the emission source of methane or the index for environmental soundness. Usually wetland is covered by vegetation, soil and water in mixed conditions, and it is not easy to apply only optical remote sensing for monitoring of wetland conditions. Combination of different types of sensors including optical sensors and microwave sensors from different wavelengths may provide the effective tool for it.

Acknowledgment
The study was partially conducted based on the Special Coordination Funds by Science and Technology Agency of Japan, and also partially conducted as a JERS-1 RA program with NASDA on wetland monitoring. We are grateful to Mr. T. Moriyama of NASDA for his kind support for the joint research.

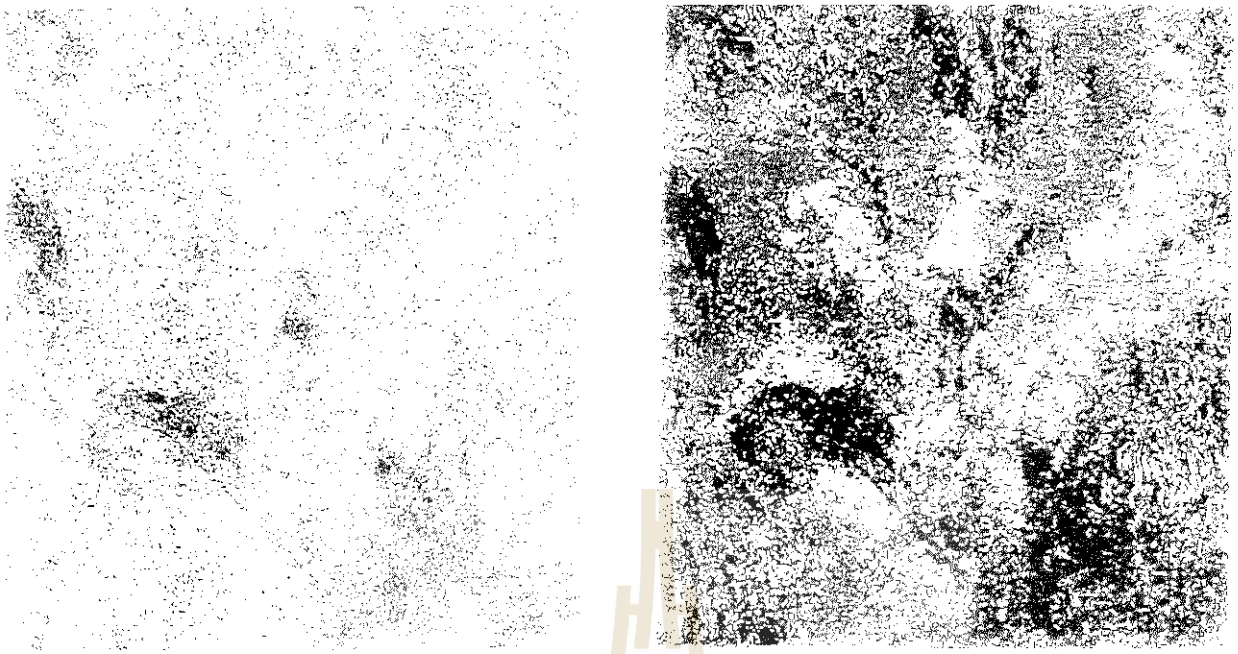

(a) (b)

Fig.4 Vegetation classification map of Kushiro Mire obtained from of two band images of JERS-1 and ERS-1 SAR data from one season. (a) Maximum likelihood classification. (b) Texture analysis by co-occurrence matrix.

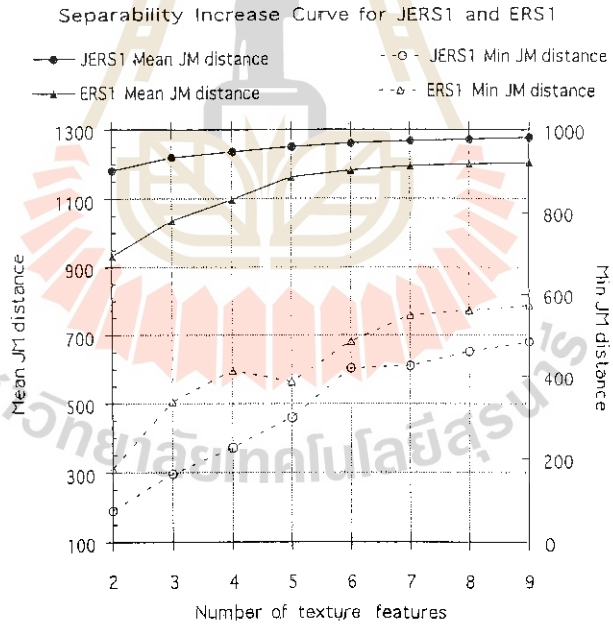

Fig.5 Comparison of separability index based on texture features of vegetation categories between JERS-1 SAR and ERS-1 SAR with respect to the number of texture features.

References

(1) Federal Geographic Data Committee (1992): Application of satellite data for mapping and monitoring wetlands - fact finding report. Wetland Subcommittee. U.S. Fish and Wildlife Service.

(2) Yoshiki Yamagata and Yoshifumi Yasuoka (1993): Classification of Wetland Vegetation by Texture Analysis Methods Using ERS-1 and JERS-1 Images. Proceedings of IGARSS'93, pp1614-1616.

(3) R.M. Haralick(1973): Textural features for image classification. IEEE Trans., vol.SMC-3, Nov., pp610-621.

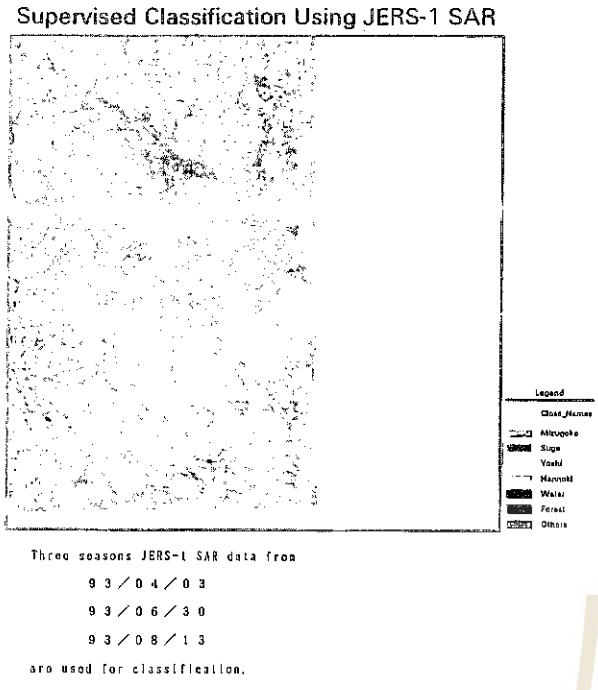

(a)

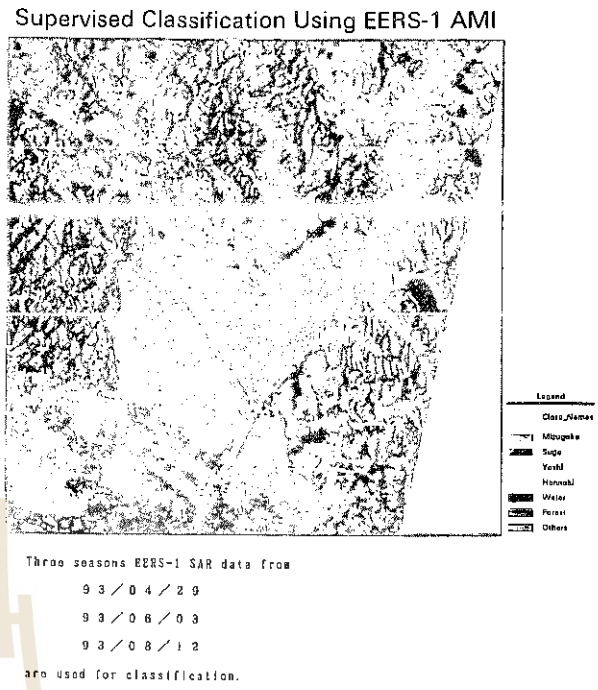

(b)

Fig. 6 Maximum likelihood classification of three seasons SAR images. (a) JERS-1 SAR, (b) ERS-1 SAR images.

INTEGRATION OF GEOGRAPHIC INFORMATION SYSTEM AND AREA PRODUCTION MODEL (APM) IN THE PREDICTION OF FOREST DEGRADATION AT PHRAO DISTRICT, THAILAND[1]

Yousif Ali Hussin Vicente Ato Alfred De Gier
The International Institute for Aerospace Survey and Earth Sciences (ITC)
7500 AA Enschede, The Netherlands
E-mail: HUSSIN@ITC.NL, DEGIER@ITC.NL
Fax: (31)(53)874-399

ABSTRACT

Recent decades have brought profound changes in the patter of land use in many developing countries. One of the clearest indicator of this changing to the land use pattern is the dramatic decline of natural forest cover, especially in the tropics. The increasingly rapid destruction of tropical rainforests is now at the centre of world attention, prompting professional foresters and politicians alike to find ways to control, stop, and even reverse this process. Given the speed of the process, two issues are clear: actions are needed without undue delay, and a sustainable effect of such actions can be expected only if the causes are tackled. The problem thus needs to be examined from a cause-effect point of view.
The objective of this research was to explore the possibility of linking the results of remotely sensed data classification with numerical output of the area production model in a GIS environment in order to validate and predict forest degradation in Phrao district, Chiang Mai province, Thailand.

INTRODUCTION

A major cause of forest destruction is the need for more agricultural land, which in turn is a consequence of rapid population growth. The need for timber, fuelwood and cash also influence deforestation. Recognizing the important role of natural resources in their national development, governments in many developing countries have shown great concern to save their remaining forest. Solutions are urgently needed. Controlling the continued degradation of the tropical forest can only be successful when detailed knowledge is obtained about the expected trend of degradation. There is a need for effective monitoring of these changes in time so that effective measures can be taken to counteract the situation. Timely and appropriate information is thus required to provide decision makers and forest managers as basis for action in order to abate the current deterioration of the forest. Remote sensing and GIS can help government planners and policy makers to decide on what step they can adopt which will best stop the degradation and meet the demand of the population for food and fiber. Prediction model can effectively provide bases for possible future scenarios about the status of forest.

Aside from unsustainable logging, the main cause of the contraction of most tropical forest lands in the world is the gradual expansion of agricultural frontier into areas which were formerly reserved or classified as forests (Cernea, 1993). Among others, expansion of agricultural lands is driven by the increasing population and the socio-economic policy of a nation.

While population growth is but one of the many factors, it is exceptionally a significant factor. The rapid increase of human number imposes unsustainable burden to the forest resource base in two ways; there is a growing demand for forest products (i.e. timber, fuelwood, etc.), and the need to feed a larger population will increase the pressure to clear forest areas and convert them to crop farming. Moreover, the scarcity of land in the lowlands triggers marginalized farmers to migrate to the uplands, bringing with them their lowland farming technology that may aggravate to the destruction of the forest. Expansion of farmland has been the primary means through which agricultural production has been increased to meet both the subsistence needs of a growing

---

[1]To be presented at the 16th Asian Conference on Remote Sensing, Suranaree University of Technology, Nakhon Ratchasima, Thailand, 20-24 November 1995.

population and the demand of domestic and agricultural commodity export markets. The increasing area of farmland per capita of agricultural population however, reflects increasing farm area allocated to upland field crops, tree crops, other agriculture related activities, and farmland allocated for grazing or fallow and non-agricultural uses.

Likewise, most analysts agree that it is the factor associated with the economic development of the country that has been the most important driving force underlying the land conversion process. These forces have contributed to both depletion and displacement of forest resources. Government policies in many developing countries are biased towards production rather than conservation. As a result, natural resources are over exploited in favour of the much needed foreign exchange. Moreover, the construction of roads and other infrastructures to facilitate economic development has played an important role in opening remote forest areas. Once access is available, a cascade of events towards forest destruction is inevitable.

Recognizing the important role of natural resources for national development, governments in many developing countries have shown great concern to save their remaining forest. Solutions are urgently needed. Mitigation of the continued degradation of the tropical forest can only be successful when detailed knowledge is obtained about the expected trend of degradation. There is a need for effective monitoring of these changes in time so that effective measures could be taken to counteract the situation. Timely and appropriate information is thus required to provide makers and forest managers as basis for action in order to abate the current deterioration of the forest. These information also help government planners and policy makers what step to adopt that will best meet the demand of the population and balance the need to protect the environment. Simulation models can effectively provide bases for possible future scenarios about the status of the forest. These help decision makers at the policy level and enable them to examine possible alternatives through identifying consequences of various strategies under given conditions (Shimada, 1986). Information about forest area changes is necessary to monitor effective forest management.

The use of remotely sensed data and geographic information system (GIS) are now gaining more and more importance as tools in natural resource management. Satellite observation provides timely, precise and quantitative data for the measurement of deforestation and monitoring land cover change. They permit observations about the proximate sources of land cover change. Under GIS, data obtained from satellite observation can be easily integrated and analysis is facilitated. Information produce from GIS can be stored and retrieve easily in forms that are more useful and understandable by the users like policy and decision maker or project implementors.

The development of the Area Production Model (APM) has been an important step in predicting land use changes. The APM is intended for simulation of long-term land use changes and the prediction of primary and secondary yields from agricultural and forest lands. Among other things, the model simulates the future need for agricultural land. The model's demand and supply scenarios for agricultural products and land are generated primarily by the growth rates of population and GDP, and by changes in land productivity. The model is comprehen-sive, but does not have excessive data requirements.

De Gier and Hussin (1993), Hussin et al., (1994) and De Gier et al. (1995), have resolved the model spatially, automatically operate the model in ILWIS GIS and apply it to an area in East Java, Indonesia. This implementation include the land transfer part of the model.

The objective of this research was to explore the possibility of linking the results of remotely sensed data classification with numerical output of the area production model in a GIS environment in order to predict forest degradation in Phrao district, Chiang Mai province, Thailand.

METHODOLOGY

The research method shall be based on five main steps. The outline of the general methodology is shown in Figure 1. These five steps are:

1. Mapping the land use/covers for different years (1975-1995). These maps will be produced from satellite images, aerial photographs and/or ortho-photos.

Existing forest cover maps will be gathered from relevant offices during the field work. Base on the multi-temporal land cover land use maps, the trend of deforestation and forest degradation will be assessed.

2. Simulating of agricultural development using APM. Data required to run the APM will be gathered during the fieldwork. Results of APM simulation will be analyzed and interpreted.

3. Regression analysis between agricultural expansion and deforestation will be achieved. The results of steps A and B will be compared. Correlation and regression analysis will be conducted in order to calibrate the model's prediction of expansion of agricultural land with the decreasing trend of forest. The regression model will be the basis of developing a spatial model to predict forest degradation.

4. Analysis of factors affecting deforestation. Environmental factors such as soil type and fertility, slope, topography, aspect, etc., as well as accessibility factors and population and market concentrations will be analyze in relation to the spatial concentration of deforestation in the study area through GIS operations.

5. Development of spatial model to predict forest degradation. The results of steps 3 and 4 will be combined as input to develop a spatial model to predict future location of forest degradation.

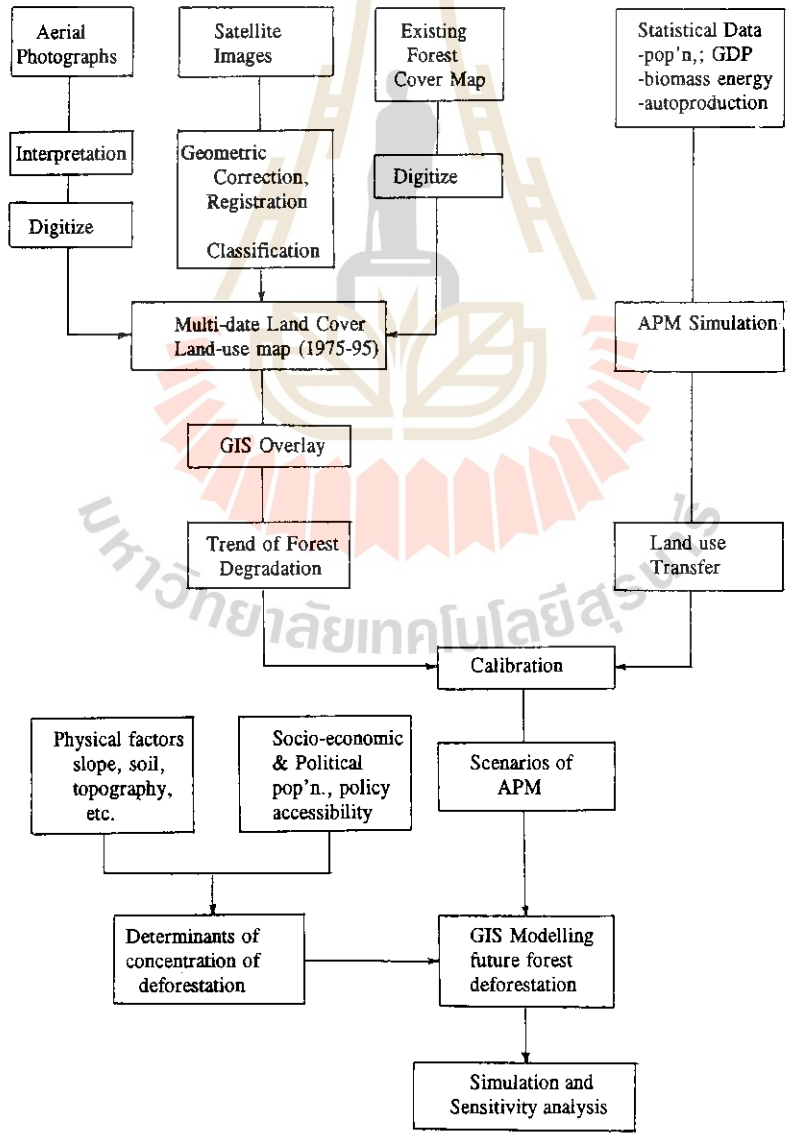

Figure 1. The general research methodology.

RESULTS

Because the authors just came back from the field work and still running the analysis, given the due date of submitting this manuscript, it was difficult to present results in this paper. However, hopefully during the conference, the authors will presents the results and a handouts to the conference attenders.

REFERENCES

CERNEA, M.M. 1993. "Strategy options for participatory reforestation. development dialogue". Vol 14, No. 2; UN Centre for Regional Development, Nagoya, Japan.

De Gier A. and Y. A. Hussin. 1993. "Spatially Resolved Area Production Model in Kali Konto, Indonesia". GIS/LIS '93 Proceedings. 31 October - 4 November, 1993, Minneapolis, Minn., USA. Vol 1. 157-169 pp.

De Gier, A., Bode J. and Y. A. Hussin. 1995. " Simulating forest degradation: the application of a GIS-based area production model in Kali Konto, East Java, Indonesia." Proceedings 16th Asian Conference on Remote Sensing, Suranaree University of Technology, Nakhon Ratchasima, Thailand, 20-24 November 1995. (In press).

Hussin, Y. A., A. de Gier, and Hargyono. 1994. "Forest cover change detection analysis using remote sensing: A Test for the spatially resolved area production model". Fifth European Conference and Exhibition on Geographic Information Systems EGIS '94 Proceedings. Paris, France. Vol. II, 1825 - 1834 pp.

SHIMADA, T. 1986. "APM case study: East Java Province, Indonesia. Manual for Using the Area Production Model. Field Document 12:2. FAO, Bangkok. 99 pp.

EVALUATION OF ASIAN ELEPHANT HABITAT

Li Zhixi Li Hongga Lu Feng
Institute of Remote Sensing & GIS, Southwest Forestry College,
Kunming, 650224, P. R. China

ABSTRACT

In this paper, in view of complicated topography and ecological environment in Xishuangbanna, we offer an approach to quantitatively analyse the spatial features of Asian elephant habitat, in which forest sampling, interpretation of TM data and aerophotos, as well as GIS techniques are mutual complementary. The results demonstrate the potential for integrating RS, GIS and sampling into accurate spatial habitat assessment.

KEYWORDS

Asian Elephant (*Elephas maximus Linnaeus*), Habitat, Sampling, Remote Sensing, Geographic Information System (GIS)

1. INTRODUCTION

The United Nations Conference on Environment and Development (UNCED) which took place in Rio de Janeiro, Brazil, 3—14 June 1992, represented the threshold of a fundamental change in the attitudes towards environment and sustainable development, signed the 21 Century Agenda and Biodiversity Convention, which put forward that the protection of biodiversity is important and imperative to safeguard the basic heritage of mankind, the quality of the earth environment, for future generations. Asian elephant (Elephas maximus Linnaeus) belongs to large proboscidean herbivorous mammal, which survives only in Asia. Due to stern reliance on suitable environment, its distributions becomes more and more narrow. According to the historical records, Asian elephants were scattered over China. In Shang Dynasty (1000 B. C.), elephants even reached the range of the Yellow River, but in Epoch of Division Between North and South (500 A. D.) shrank back to the range of the Yangtze River. Closely following destruction of forest, so far, elephants mainly survive in Xishuangbanna primitive tropic forest, and become rarer. Remote Sensing and Geographic Information System, as parts of the information technology, take important roles in assessing natural resources. So far, people are gradually introducing the two techniques into evaluating wild animal habitat, such as using Landsat Data to interpret aquatic animal habitat in the eastern South Dakota (R. G. Best 1978)[1], using Landsat digital data to analyse Cygnets habitat along thecoast of British Columbia (Y. Jim, Lee, 1987), using GIS and digital elevation model to analyse the Chequered skipper and Curlew habit patches in Scotland (R. Asp in all, 1992)[2], using GIS to manage natural reserves in Thailand (Youngynt Trisurat, 1992)[3] and using Landsat TM to identify the Amblyomma variegatum habitats in Guadeloop (M. hugh Jones et al. 1992)[4] etc. In addition, we applied Landsat to evaluate the Giant Panda habitat[5]

2. STUDY AREA

The Xishuangbanna Dai Autonomous Prefecture is situated in the south front of Yunnan Province, a transition from Himalayas to Malaysia, N 21° 08′—22° 35′, E 99° 53′—101° 50′. The special situation of low center surrounding high mountains shapes a largescale tropic climate. Because of the distinctive position, topography as well as climate, tropic rain forest with massive flora and fauna scatter on the lowland. In Xishuangbanna, from 1965 to 1988, forest coverage decreases from 46. 46% to 33. 72%, with an average of 0. 55% annually[6]. With the lessening of living spaces, shortage of foods, degrading of habitat qualities as well as the illicit hunting for elephants, elephants are confronted with the danger of extinction. So it is imperative to monitor and

Note: It is a cooperative project of Southwest Forestry College, World Wide Fund for Nature and Xishuangbanna Administrate Bureau of National Nature Reserves.

assess the habitat, furthermore, to put forward the measures to protect elephants. In this study, the study area lies in Mengyang Nature Reserve, the largest one of the five reserves in Xishuangbanna, between the XiaoHei stream and the Mekong River. Its total area is 118,410 ha and the elevation varies from 600 meters to 1600 meters. The forest vegetation types mainly comprise seasonal rain forest, mountain rain forest, monsoon forest and evergreen broad-leaf forest, etc.

3. METHOD

In this study, we took ecological and biological factors as the guide, aerophotos and satellate images as the media, GIS as an analysis tool to establish a GIS of assessing and monitoring Asian Elephant habitat. The framework includes the habitat analysis, interpretation and assessment.

3.1 The habitat analysis

3.1.1 Field sampling survey

According to ecological and biological features, we divide the habitat factors into aliment, water, shelter and living space. In view of the interpretation, we select the following factors to survey: forest vegetation type, crown degree, dsitance from water source, slope, aspect, location and elevation. Considering the socio-economic situation, we add human activity intensity. The field work mainly surveys the number of elephants trails under different factors. In order to ensure the typicalness of samples, we take the systematic sampling. Samples are arranged with 100 meter in length, 2 meter in breadth. 71 samples are set up in order that there are no less than 5 samples in each factor. In field survey, it is necessary to record elephants trails and the relevent ecological, biological and human activity intensity, besides marking the site.

3.1.2 Quantitative analysis

The number of elephants trails under various situation of eight factors is refered to table 1. The table 1 is only single—factor analysis. In view of interaction among factors, we take multi—factor composite analysis, i.e., multivariate regression to quantitatively analyse habitat factors. The formula is following:

$$Y=b_0+b_1X_1+b_2X_2+b_3X_3+b_4X_4+b_5X_5+b_6X_6+b_7X_7+b_8X_8$$

where, Y is the frequency of elephants activity (unit is trails per ha). b_0 is regression constant.

$b_1, b_2, b_3, b_4, b_5, b_6, b_7, b_8$ are regression coefficients.

$X_1, X_2, X_3, X_4, X_5, X_6, X_7, X_8$ represent correlative factors (see table 1), respectively.

Some factors in table 1 are qualitative, which cannot be directly inputed to the equation, in addition, the relation between different conditions of each factor and elephant trails is often nonlinear. In order to ensure the regression precise, we transform data from qualitative to quantitative.

Table 1.

factor (x_i)	conditions (x_{ij})		trails (y_i/ha)	relation
vegetation (x_1)	ever green broad—leaf	(x_{1-1})	1120	2
	bamboo forest	(x_{1-2})	1380	1
	shurb	(x_{1-3})	300	3
	dry farmland	(x_{1-4})	230	4
crown density (x_2)	median 0.2—0.5 D	(x_{2-2})	620	2
	median 0.2—0.5	(x_{2-2})	620	2
	dense $>$ 0.5	(x_{3-3})	990	1
distance from water (x_3)	near $<$ 100m	(x_{3-1})	1270	1
	median 100m—500m	(x_{3-2})	780	2
	far $>$ 500m	(x_{3-3})	440	3
slope (x_4)	$<$ 10°—	(x_{4-1})	440	5
	10—20°—	(x_{4-2})	650	4
	21—30°—	(x_{4-3})	1550	1
	31—40°—	(x_{4-4})	950	2
	$>$ 41°—	(x_{4-5})	760	3

factor (x_i)	conditions (x_{ij})		trails (y_i/ha)	relation
aspect (x_5)	north—east	(x_{5-1})	1350	1
	west or east	(x_{5-2})	760	2
	south—west	(x_{5-3})	270	3
location (x_6)	high	(x_{6-1})	640	3
	median	(x_{6-2})	1050	1
	low	(x_{6-3})	830	2
elevation (x_7)	< 800m	(x_{7-1})	660	3
	800—1000m	(x_{7-2})	800	2
	> 1000m	(x_{7-3})	970	1
human activity (x_8)	force	(x_{8-1})	220	3
	median	(x_{8-2})	530	2
	weak	(x_{8-3})	1540	1

In the transformation, the minimum trails of each factor under different conditions are defined as 1.0, and the others are proportional vested, e.g. the vegetation type (see table 2).
The computed coefficients are as table 3.
The precision is evaluated as following:

Lyy(the total square error of a sampling)=64889577
U(the regression sum of squares)=35931762
Q(the residual sum of squares)=28957815
F(8,62)(the test of significance of regression equation)=9.62
F0.01(8,62)=2.80 F > F0.01 R=0.76

Table 2.

conditions	trails /ha	numerical value
evergreen broad—leaf forest	1120	4.9
bamboo forest	1380	6.1
shrub	300	1.3
dry farmland	230	1.0

table 3.

factor	vegetation	crown	water	slope	aspect	location	elevation	human activity
coefficient b_j	156.40	-196.90	101.44	142.80	157.95	12.17	115.29	132.99
constant b_0	-1705.03							

The test of significance of each regression coefficient is in table 4.
table 4.

factor	F	priority
vegetation	4.973	4
crown density	1.504	5
water	5.731	3
slope	0.800	6
aspect	10.519	2
location	0.009	8
elevation	0.364	7
human activity	12.819	1

In the study, we get the precision of 82% under the reliability of 95%.

3.2 Interpretation of the habitat

Among factors, topographic factors ,i.e. , slope, aspect, location, elevation and distance from water, can be directly obtained from the topographic map. The human activity intensity, e.g. density of population, can be obtained from the statistics of late villages situation. And we gain vegetation type and crown density from interpret action of images. Athough vegetation only take the forth place, the first place human activity intensity, the second aspect are directly or indirectly reflected by vegetation. And we regard the vegetation as the foundation of the habitat. In the interpretation, vegetation is considered as the main object.

3.2.1 Image processing[6]

Data available for analysis are following: the black and white panchromatic aerophotos with scale of 1:20,000 taken in March 1989; Landsat TM data respectively recorded on 2-Feb 1988 and 28—May 1992; Spot XS data recorded on 16 Feb 1988, etc. Firstly, we carry out the image processing e.g. contrast enhancement, color synthesis. The correlation coefficient matrix of TM bands in Mengyang, illuminates that minor correlation are respectively between TM_2 and TM_4, TM_3 and TM_4, TM_4 and TM_7. Only considering correlation, TM_{346} is the best, and TM_{234} takes second place. But, when we take further steps to consider functions of each band, the synthesis of TM_{234} is prior to others, for its susceptibility to vegetation type and partly eliminating hill shadows. Secondly, we use maximum likehood for image classification. By virtue of actual situation in Mengyang nature reserve, we set up training units of 11 types, including forest, bamboo, tea plantation, farmland, rubber woods, meadow, shrub, water and the various tansitions, e.g. from forest to farmland, from farmland to forest, from meadow to shrub. The results possess 79% precision with the reliability of 95%. When 11 types are composed to 6 types, the precision increases to 86%.

3.2.2 Interpretation

The objection of interpertation training is to establish marks and to set up units for computer automatic classification. In addition, the ecological law of vegetation and the vertical vegetation distribution which are formed by difference of heat and precipitation, are also applied in the interpretation. By cartological choise, boundary lines of status quo are demarcated and transformed to topographical maps one by one to form the base maps.

3.3 **Habitat Assessment**

3.3.1 Software and Hardware

The habitat is assessed with ARC/INFO version 7.03 on SUN SPARC LX workstation, Calcomp 9500 digitizer and Calcomp 3036 plotter.

table 5.

layers	geographic data	attribution data
topography	line	contour
hydrology	line	river type, name
vegetation	polygon	vegetation type
road	line	road,path,trail
village	point	name, population,income etc.
administative bounds	line	county, village, reserve etc.

3.3.2 The Database Design

Based on factors analysis and interpretation, topography, hydrology, forest vegetation, density of population, road, village and administative boundary are used as layers to establish GIS. The organization of layers sees table 5. In the design, we use the special dictionary[7]to establish Mengyang nature reserve GIS.

3.3.3 The Database Establishment

The data are generally divided into two parts, geographic data and associated attributes. To establish geographic database, we capture geographic features with Calcomp 9500 digitizer (1000

lpi). Well-distributed 17 control points in Mengyang reserve are selected to ensure the accuracy. Meanwhile, the input error of points is under 0.2mm on maps (scale 1:50,000). The graphics are transformed and compiled to form the topology. Based on geographic database, the associated attributes such as vegetation, elevation, hydrology, road, landuse, annotion, text, etc., are defined and inputed by users, besides the automatically produced items such as area, length, perimeter. Once the input of attributes is completed, we can identify, operate and analyse the relation between geographic data and attribution and the relation among layers.

3.3.4 Analysis

According to units divided for management, and using 8 factors (see table 1), through regression equation, we estimate trails. We take the second unit as a example, vegetation(X_1) is bamboo, vested to 6.1(see table 2);according to this reason, crown density(X_2) is 1.9; distance from water(X_3) is 400 meters, 5.4; slope(X_4) between 20.-30., 2.6; aspect(X_5) is west, 2.9; location (X_6) is median, 4.9; elevation(X_7) is less than 800 meters, 3.0; human activity intensity(X_8) is weak, 7.0. According to table 3, the result is following:

$Y = -1705.03 + 156.40 * 6.1 - 196.90 * 1.9 + 101.44 * 5.4 + 142.80 * 2.6 + 157.95 * 2.9 + 12.17 * 4.9 + 115.29 * 3.0 + 132.99 * 7.0$

$= 1766$ trails/ha.

In the light of trails per ha and management levels of status quo, we classify Asian elephant habitat(see table 6).

Table 6.

trails / ha	class
< 600	bad
601 — 1200	moderate
1201 — 1800	good
> 1801	excellent

At above example, the unit belongs to good class. According to the method, by evaluating every unit, we obtain digital theme map of Asian Elephant habitat in Mengyang.

4. RESULTS AND DISCUSSIONS

4.1 RESULTS

4.1.1 Firstly, we establish an assessment system of Asian elephant habitat for protecting elephants in Mengyang. Meanwhile, we ouput the forest vegetation map (see map 1) and Asian Elephant assessment map (see map 2) , obtain present spatial information of elephant habitat, provide the foundament of protection and manag ement work.

Table 7.

class	frequency	area(ha)	rate %
excellent	101	2930	3.5
good	171	31674	28.0
moderate	225	44097	39.0
bad	181	33302	29.5

4.1.2 Through analysis, we get areas and rates of different classes (see table 7). The main features of four habitat classes are as follows:

The excellent: weak human activity impact, elevation between 1000 meters and 1300 meters, slope from 20° to 30°, aspect east-north, lower location e.g. valleys or at the foot of hills, range within 100 meters from water, bamboo forest with no more crown rate. These are best, and are generally located in core parts of reserve.

The good: little impact of human, aspect north or east, west, distance from water within 500 meters, ever green broad-leaf forest or bamboo forest.

The moderate: the normal impact of human, aspect east, west, distance from waterwithin from 500 to 700 meters, shrub or broad-leaf ever green forest.
The bad: force impact of human, aspect west-south, distance from water more than 700 meter, shrub, meadow, farmland or bare land. These are bad for elephant survival, and generally out of the core.

4.1.3 According to habitat features, in view of actual situation, correlative measures are put forward for protecting Asian elephant habitat. In excellent regions, it is urgent to strictly control and reduce villagers activity, emigrate the inner villages, prohibit the activities such as hunting, cutting, plucking bamboo shoots and destroying wild banana, etc. The inner water i.e. pools, streams are periodly casted the salt and iodine to board elephants. In moderate, bad regions, it is important to inhibit farm cultivation of slashing and burning, advocate agroforestry, set up ecological villages, reforest vegetation cover, enhance soil fertilization and water soil retention, increase villagers income and etc. Above all, it is imperative to reinforce education and promulgation of the law, punish illegal hunters for wild animals. Meanwhile, the electric fences and other defensive fences are set up to prevent elephants from destroying crops.

4.2 DISCUSSIONS

4.2.1 In this study, considering the reliability of factors, we mainly lay on physical factors. The human factor is limited in the density of population, farm cultivation and roads. On the other hand, social factor has intricate and important influence on habitat, which includes many complicated aspects such as the masses interference and protection etc. For example, illegal hunters killed sixteen elephants, injured three, from May to June 1994. On the contrary, villagers preserve wild animals. Peasant in Mengla nature reserve protected an abondoned elephant infant, and sent it to reserve station. In addition, national factor and religion factor have influence on elephants.

4.2.2 In this study, Forest Sampling, Remote Sensing and Geographic Information System are efficiently integrated. According to Remote Sensing and Permanent PlotTechniques for World Forest Monitoring Conference (IUFORO, Thailand, 1992)[8] and International Guidelines for Forest Monitoring[9] (IUFRO, 1994), the integration of FS, RS and GIS is the developing trendency for natural resources monitoring. So, the paper may be regarded as a test of integration of FS, RS and GIS.

REFERENCE

[1] R. G. Best. 1983, Remote Sensing Approaches for Wildlife Management. Proceeding of the RNRF Symposium on the Application of Remote Sensing to Resource Management, Seattle, Washington, P55—96.

[2] Richard Aspinall, 1992. Spatial Pattern Analysis Tools in GIS for Environmental Planning. Proceedings of the IUFRO Centennial Meeting, Berlin, P 223 —233.

[3] Youngyut Trisurat, 1992. Applicatian of GIS in Protected Area Management. Pemote Sensing and Permanent Plot Techniques for World Forest Monitoring. Proceeding of the IUFRO S4. 02. 05 Pattaya, Thailand. P 215—225.

[4] M. Hugh-jones, N Barre, 1992. Landsat-TM Identification of Amblyomma Variegatum (Acari: Ixodidae) Habitats in Guadeloup. Remote Sensing of Environment. Vol, 40 N0, 1 P43—54

[5] Li Zhixi 1990, Investigation for the Giant Panda habitat Using Remote Sensing, Remote Sensing of Environment, PRC. Vol 5, No 2, P 94—101.

[6] Li Zhixi et al. 1993, The tropical Forest Vegetation Mapping Using Multisensor Information. Remote Sensing of Environment, PRC. Vol 8, No 3, P 180—189.

[7] ESRI, SWFC, 1994. Datebase Design, Xishuangbanna Agroforestry Development Project.

[8] R. H. Cydelund Songkram. Risto Paivinen Thammmincha, 1992. Remete Sensing and Permenent Plot Techniques for World Forest Monitoring. Proceeding of the IUFRO S4. 02. 05, Pattaya, Thailand.

[9] Risto Paivinen, 1994. International Guidelines for Forest Monitoring. IUFRO world series Vol, 5 P 6—34.

ESTIMATING VEGETATION FUNCTION FROM SATELLITE DATA IN SEASONAL TROPICAL ENVIRONMENTS

Kazue Fujiwara
Yokohama National University
Institute for Environmental Science and Technology
Hodogaya-ku, Tokiwadai 156, Yokohama 240, Japan

and

Elgene O. Box
Tokyo University, Institute of Industrial Science
Minato-ku, Roppongi 7-22-1, Tokyo 106, Japan
(permanently: University of Georgia, Geography Department,
Athens, Georgia 30602-2502, USA)

Abstract

Highly seasonal tropical environments have provided convenient situations for demonstrating the capabilities of satellite sensors to detect changes in the landscape, based on clear seasonal changes in the foliation status of the vegetation. Foliation status does not always vary so obviously, however, and even when it does, such changes do not necessarily translate directly into high or low levels of functional activity, such as net primary production or net carbon flux (net ecosystem production). Southeast Asia is an especially good place to study this problem, due to its full range of deciduous to largely evergreen vegetation, all in a highly seasonal monsoon climate. Production, water budget, and overall net carbon flux of different vegetation types are simulated using a climate-based model of vegetation and detrital metabolism. Parallel monthly results are shown for vegetation phenology, satellite data (NDVI) and simulated carbon balance. Such models of vegetation function can and should be used for better calibration of satellite data in various parts of the world.

Introduction

When rainfall falls to near zero for several months each year and defoliation is relatively complete, satellite data can infer changes in ecosystem function quite effectively (e.g. Tucker et al. 1985). The main processes of interest include primary production (photosynthesis plus assimilation of its products into new biomass), autotrophic respiration (energy use for maintenance and growth), detrital decomposition, and the resulting net biosphere-atmosphere CO_2 flux. This overall net metabolic balance of the landscape (vegetation-detritus system) and sometimes even of the living vegetation (net production) normally becomes negative during defoliation (dry season). It can also become negative, however, in green landscapes, during their growing season, if respiration is higher than photosynthetic gains (Box et al. 1989). As a result, in using satellite data

to estimate biotic function, it seems wise to look at parallel estimates of vegetation metabolism, as are provided by simulation models based on field-measured metabolism and climatic data. Southeast Asia is a good place to study this problem, due to its full range of deciduous to evergreen but seasonal vegetation.

Data and Methods

Thailand has remaining areas of moderately natural forest as well as larger areas of substitute landscapes covering the full range from evergreen to deciduous and from forest to open savanna (e.g. Ogawa et al. 1961, Santisuk 1988). The composition, structure and productivity of the relatively natural vegetation have been studied in the field for some time (e.g. Kira et al.1967, Smitinand 1980). The main natural landscapes and their phenology are shown schematically in Figure 1 (from Fujiwara 1993).

Net primary production (NPP) is gross primary production (GPP, essentially photosynthesis) minus respiration (R). GPP increases with warmth and water availability (other factors not limiting, Lieth & Box 1977), while respiration increases at least quasi-exponentially (per unit biomass) with increasing temperature (e.g. Kira 1975). NPP thus also increases with warmth and wetness (Lieth & Box 1972) but becomes a smaller fraction of GPP under warmer conditions (high respiration losses) and can become negative if GPP is low or zero, as in an extreme dry season. Litterfall (dead leaves and other detritus) is also related to climatic conditions (Meentemeyer et al. 1982); detrital decomposition (D) also increases with warmth and wetness (Meentemeyer 1985), and completes

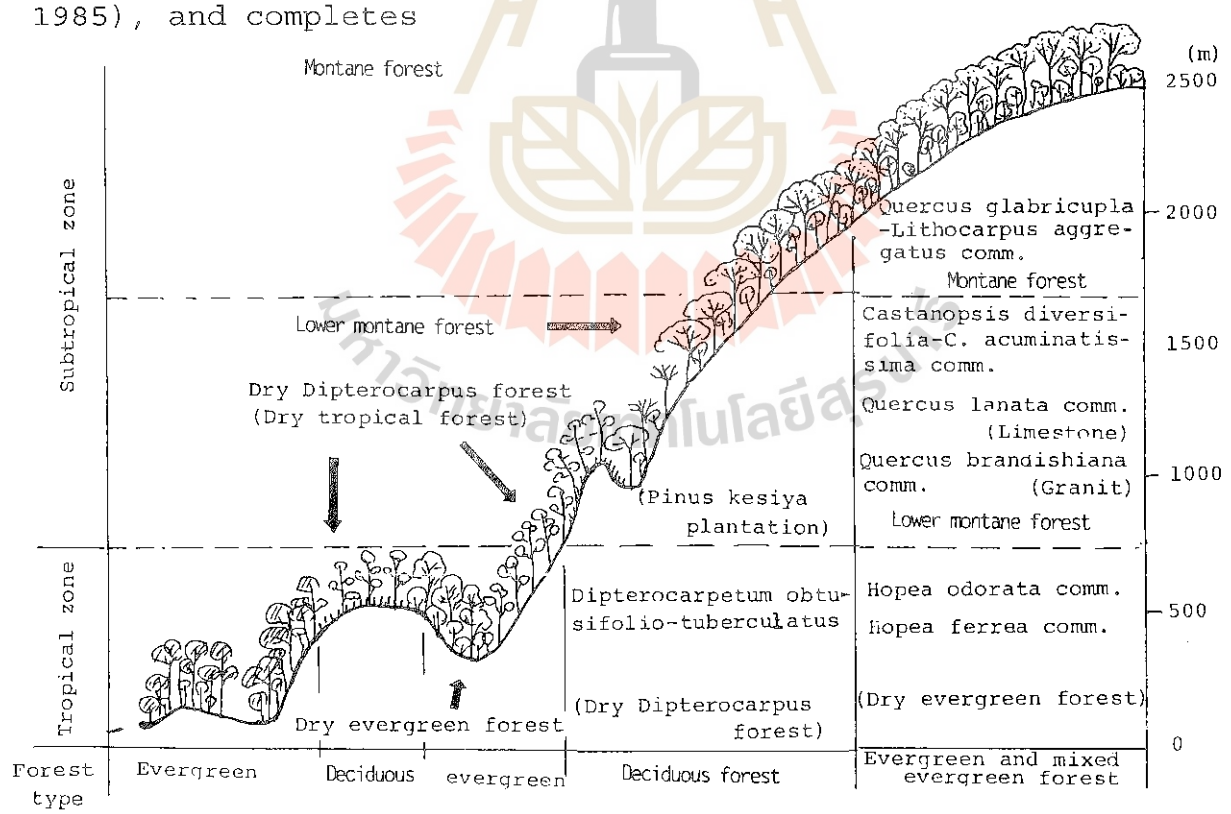

Figure 1. Schematic Zonation of Natural and some Substitute Landscapes (Vegetation) of Thailand.

the equation for overall net ecosystem production:

$$\text{net } CO_2 \text{ flux} = GPP - R - D \quad (1)$$

each component of which can be expressed in units of dry biomass or carbon equivalent. All components of this vegetation-detritus energy budget, as well as atmosphere-biosphere water fluxes, can be simulated at monthly intervals by the model MONTHLYC (Box 1988), which is based on individual process models calibrated globally to climatic data and now NDVI from field-measured annual metabolic data. In the absence of field data for monthly metabolism, monthly climatic GPP is driven by AET (actual evapotranspiration), its closest apparent correlate (cf. Box et al. 1989). Respiration is a function of temperature and is simulated therefrom using the usual Q_{10} value of two. For comparison purposes, field-measured values for natural and artificial primary production in Southeast Asia are shown in Table 1.

Satellite data for Southeast Asia, especially NDVI data, have been received, converted into imagery, and interpreted by various groups, including the Asian Institute of Technology in Bangkok, the Institute of Industrial Science at Tokyo University, and the NASA Goddard Space Flight Center in Washington. For this study, however, individual NDVI pixel values are used, since it is at pixels corresponding to field measurement sites that comparisons, calibrations and validations must ultimately be done.

Table 1. Field-Measured Primary Production in Tropical Asia.

Location	Vegetation	Standing Biomass	Production Gross	Production Net	Source
Khao Chong	rainforest	32.6	12320	2860	(4)
Ping Kong	monsoon forest	29.1	7000	1190	(6)
	savanna woodland	7.8	3200	760	(6)
Pasoh	rainforest	52.5	8190	2740	(5)
Cheko	rainforest	41.5	11700	--	(3)
Substitute/successional vegetation:					
Gorakhpur	teak plantation	74.3	--	2665	(1)
Varanasi	succ. dry forest	3.5	--	301	(1)
	subst. grassland	1.0	2166	1177	(2)

Biomass values are in units of kg/m^2, production values in units of $g/m^2/year$, each for dried biomass. Net production was generally estimated by harvest methods, whereas gross production involved gas-exchange, micrometeorological and other methods. Sources: 1 = Cannell 1982, 2 = Dwivedi 1971, 3 = Hozumi et al. 1969, 4 = Kira et al. 1967, 5 = Kira 1978, 6 = Yoda 1967.

Table 2. Monthly Climatic and NDVI-Simulated Metabolic Activity of Vegetation at Ping Kong, Thailand.

	Jan	Feb	Mar	Apr	May	June	July	Aug	Sept	Oct	Nov	Dec	Year
Climate-driven metabolism (natural vegetation):													
AET	34	30	45	72	169	172	163	155	146	125	87	43	1242
GPP	169	151	225	363	849	861	819	778	734	626	438	217	6231
Respiration	247	288	352	399	430	419	399	391	385	362	317	260	4249
NPP (GPP-Rd)	-78	-137	-127	-35	418	442	420	387	349	264	121	-43	1982
NDVI-driven metabolism (actual landscape):													
NDVI	276	268	206	176	284	318	286	332	334	310	292	280	2238
GPP	512	497	382	327	527	590	531	614	620	573	540	518	6231
Respiration	247	288	352	399	430	419	399	391	385	362	317	260	4249
NPP (GPP-Rd)	265	209	30	-72	96	171	132	224	234	211	223	258	1982
Net ecosystem production (GPP-Rd-D):													
Climatic	-141	-218	-275	-278	-79	131	226	250	243	186	56	-99	0
NDVI-based	215	136	-118	-325	-421	-151	-68	84	129	136	168	216	0
Detrital budget (NDVI-driven):													
Litterfall	181	143	21	0	66	117	90	153	160	145	152	177	1406
Surface pool	569	911	1122	1103	905	498	280	173	117	86	117	316	516
Decomp (total)	50	73	148	252	517	322	199	140	106	75	54	43	1980
Other climatic values:													
Temperature	20.4	22.6	25.5	27.3	28.4	28.0	27.3	27.0	26.8	25.9	24.0	21.1	25.4
Precipitation	15	5	26	63	169	197	228	281	321	209	49	14	1577
PET	53	78	123	156	172	172	163	155	146	125	93	59	1495
P/PET	.28	.06	.21	.40	.98	1.15	1.40	1.81	2.19	1.67	.53	.24	1.05

Monthly metabolic estimates are shown for natural monsoon forest (climate-driven simulation) and an "actual" landscape (NDVI-driven simulation), with NDVI-based values used for annual metabolism in both scenarios. GPP and NPP are much more seasonal in the natural deciduous forest, with wider extremes and longer periods of negative NPP and negative overall carbon balance (GPP-R-D). Even with green foliage remaining and a much higher dry-season GPP, however, the NDVI-based scenario also shows one month with negative NPP and a five-month period with significant negative overall carbon balance. All metabolic values are in units of grams of dry biomass per square meter (= 2 x carbon equivalents). Water-balance values are in millimeters, and temperature is in degrees Celsius.

Results

Parallel monthly values of NDVI, climate and correspondingly driven simulated landscape metabolism are compared in Table 2 for Ping Kong, a site in northern Thailand (near Chiang Rai) where vegetation metabolism has been field-measured (Yoda 1967). The potential natural vegetation at Ping Kong is mixed deciduous "monsoon" forest, but the actual landscape is evidently partly evergreen, as seen from the NDVI values, which never drop near zero. NDVI does parallel to some extent the seasonal course of precipitation and AET, all rising sharply in May. The monthly patterns of climate-driven and NDVI-driven GPP are quite different, however, and thus also the resulting monthly patterns of NPP and overall metabolic balance (equation 1). Even with significant NDVI values and NDVI-simulated GPP during the dry season, however, the corresponding NPP still falls negative in April and the overall CO_2 balance is negative for five months (with a time lag due to the smaller amplitude of the GPP curve for the more evergreen actual landscape).

Conclusion

Although time-consuming and difficult to measure, some field measurements of vegetation metabolism are available, in Southeast Asia and elsewhere. Based on these, it is possible to estimate seasonal patterns of vegetation function by simulation modeling. It is often especially difficult to interpret satellite data in humid/seasonally humid tropical areas, due to persistent cloud cover, a narrow range of NDVI variation, light-trapping effects of tall forests with dark green leaves, etc. NDVI data cannot directly estimate phenomena which become seasonally negative, including net primary production and overall CO_2 flux, since there is no way to calibrate the zero-point against NDVI values which are always positive. NDVI can be used to estimate gross production, but in order to get net production, a metabolic simulation model is still needed to estimate respiration. Such models of vegetation function can and should be used for better calibration of satellite data in various parts of the world.

References

Box, E. O. 1988. Estimating the seasonal carbon source-sink geography of a natural steady-state terrestrial biosphere. *J. Appl. Meteorol.*, 27:1109-1124.

Box, E. O., B. N. Holben, and V. Kalb 1989. Accuracy of the AVHRR Vegetation Index as a predictor of biomass, primary productivity, and net CO_2 flux. *Vegetatio*, 80:71-89.

Cannell, M. G. R. 1982. *World Forest Biomass and Primary Production Data*. London: Academic Press. 391 pp.

Dwivedi, R. 1971. Suitability of measuring carbon assimilation rates for evaluation of solar energy conservation and dry-matter production in plants. *Trop. Ecology*, 12:123-132.

Fujiwara, K. 1993. Rehabilitation of Tropical Forests from Countryside to Urban Areas. In: *Rehabilitation of Tropical Forest Ecosystems* (H. Lieth & M. Lohman, eds.), pp. 119-131. Amsterdam: Kluwer Acad. Publishers.

Hozumi, K., K. Yoda, Sh. Kokawa and T. Kira 1969. Production ecology of tropical rainforests in southwestern Cambodia. I and II. *Nat. Life SE Asia* (Kyoto), 6:1-57, 57-81.

Kira, T., H. Ogawa, K. Yoda and K. Ogino 1967. Comparative ecological studies on three main types of forest vegetation in Thailand. Part IV: Dry-matter production, with special reference to the Khao Chong rainforest. *Nat. Life SE Asia* (Kyoto), 6:149-174.

Kira, T. 1975. Primary production of forests. In: *Photosynthesis and Productivity in Different Environments* (J. P. Cooper, ed.), pp. 5-40. IBM series, vol. 3. Cambridge University Press.

Kira, T. 1978. Primary productivity of Pasoh forest -- a synthesis. *Malay. Nat. J.*, 30:291-297.

Lieth, H. and E. O. Box 1972. Evapotranspiration and primary productivity; C. W. Thornthwaite Memorial Model. Publ. in Climatology (Univ. of Delaware), 25(3):37-46.

Lieth, H., and E. O. Box 1977. The gross primary productivity pattern of the land vegetation: a first attempt. *Tropical Ecology*, 18:109-115.

Meentemeyer, V. 1985. Climatic control of litter dynamics in tropical forest. In: *Ecology and Resource Management in Tropics* (K. Misra, ed.), pp. 302-310. Varanasi: Bhargava.

Meentemeyer, V., E. O. Box, and R. Thompson 1982. World patterns and amounts of terrestrial plant litter production. *BioScience*, 32:125-128.

Ogawa, H., K. Yoda, and T. Kira 1961. A preliminary survey on the vegetation of Thailand. *Nat. Life SE Asia* (Kyoto), 1:22-157.

Santisuk, T., 1988. *An Account of the Vegetation of Northern Thailand*. Wiesbaden: Franz-Steiner-Verlag. 101 pp.

Smitinand, T. 1980. *Thai Plant Names*. Bangkok: Royal Forest Department. 379 pp.

Tucker, C. J., J. R. G. Townshend, and T. E. Goff 1985. African land-cover classification using satellite data. *Science*, 227:369-375.

Yoda, K. 1967. Comparative ecological studies on three main types of forest vegetation in Thailand. III. Community respiration. *Nat. Life SE Asia* (Kyoto), 5:83-148.

TECHNICAL SESSION B

AGRICULTURE / SOIL

TOWARDS SUSTAINABLE LAND USES THROUGH LAND EVALUATION: A CASE STUDY OF MUAKLEK, THAILAND[1]

Rajendra Prasad Shrestha and Apisit Eiumnoh

STAR/SERD, Asian Institute of Technology
G.P.O. Box 2754, Bangkok 10501, Thailand

ABSTRACT

The suitability of land for four major crops, viz., maize, cassava, fruit orchards and pasture was assessed in the Muaklek area of Thailand. The procedure followed was in accordance with Food and Agriculture Organization (FAO) Framework for Land Evaluation. Field surveys were also conducted to supplement with the socio-economic information and ground truthing. Vector based GIS (ARC/INFO) was used to analyze the spatial data. Simple benefit/ cost ratio analysis was performed to appraise the economic returns of the selected crops. The study exhibited that the present land uses are not in accordance with the land qualities, i.e. land are put under cultivation despite its unsuitability. The study demonstrates the need of conducting land evaluation in which socio-economic elements are to be considered in particular and also the application of Remote Sensing and GIS as useful planning tools.

1.0 INTRODUCTION

Thai agricultural production has been experienced to have fast growth in the past. But in the recent past (1983-93), it has been reported that the annual growth of paddy and maize production is negative, -0.2 and -2.1% , respectively, however, annual growth of cassava and total milk production has increased by 1 and 15% respectively (FAO, 1994). Share of agriculture in GDP has fall down from 26% in 1970 to 12% in 1992. The increase in agricultural imports (16.5%) is more than double of the export increase (7%) between 1982 and 1992. Despite this declining situation of agricultural production, total agricultural land in the country is reported to increase from 37.4% in 1982 to 39.4% in 1992. This articulates the situation of lower land utilization. Subsistence crop farming dominates agriculture in Thailand. Since the cropping system utilized by the people reflects short term economic goals, such systems are not necessarily environmentally sound (McGregor and Barker, 1991). 33.7 percent of the total agriculture land in Thailand are degraded due to improper utilization of marginal land and poor management practices (Dent, 1989).

Emphasis on "sustainability" has arisen because of increasing worldwide concern about environmental degradation and various related processes, such as, soil erosion and degradation, and loss in genetic biodiversity, which are known to have adverse effects on agricultural productivity. Land, being the scarce resource and basis of production, raising land productivity in stock terms is more important than flow terms for the fuller utilization of land. Land be best conserved if utilized it based on its supporting capacity for cultivation. Hence, there is the need of agronomically sensible and technically appropriate solutions to revitalize these degraded pieces of land and the eventual environmental conservation. It is on this premise that this study was carried out to determine the potentials of the land for cultivation of four important crops assessing land qualities, social and economic parameters with the purposes of both rehabilitating the land quality and conserve the environment.

2.0 THE STUDY AREA

The study area, Muaklek, situated in the central highlands of Thailand, is characterized by a rolling and sloppy terrain. The climate of the area is tropical Savannah with an annual mean maximum temperature of 32.7° C, mean minimum of 20.4° C, average humidity of 79.45% and an annual rainfall of 1,050 mm. There is a sharp decline in the crop area since 1992 for all major crops (Figure 1). The study area is the largest production area of modern dairy farming in the country (Hirunruk, 1973), but shortage of livestock fodder is the most pressing problem.

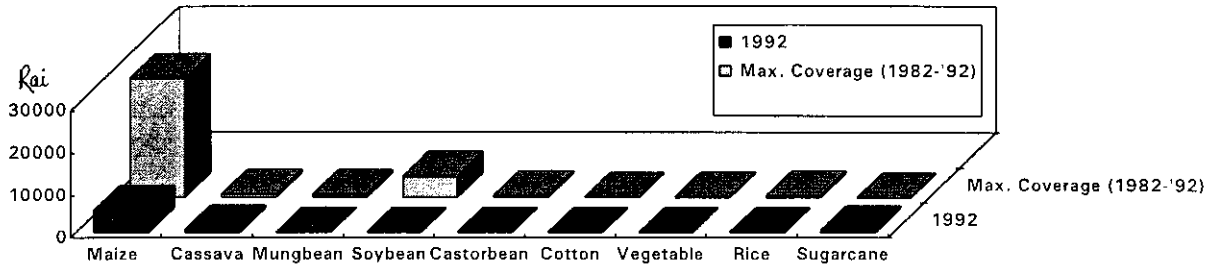

Figure 1. Change in Area Coverage for Different Crops in Muaklek.

[1] Paper presented at the 16th Asian Conference on Remote Sensing, 20-24 November 1995, Thailand

Population density accounts to 48.4 and 93.3 persons/ sq. km. of the total and cultivated area, respectively. A significant majority (88.5%) of the working population are engaged in agriculture. On the basis of land holding, the proportion of marginal farmers (land holding < 4 ha), small (4-8 ha), medium (8-16 ha) and large (>16ha) were 35.2, 24.1, 16.6 and 24.1%, respectively (Shrestha, 1993). The majority of the area is under crop farming and maize is the principle crop (Figure 2). Orchard and livestock production are important farming businesses which are gradually replacing the crop farming. Water is a scarce resource in the area. The major sources of water for drinking and household uses are underground water and collected rain water. *Dipterocarpus sp.* is the dominant forest species. Besides, *Leucaena leucocephala* as fodder species, it has also been extensively used in the new forest plantation area.

3.0 METHODOLOGY

The *FAO Framework for Land Evaluation* was adopted to conduct this study. The basic source materials used for spatial analysis of suitability classification were: soil map (scale, 1:100,000), topographic map (1:50,000), geological map (1:250,000) and meteorological data. Land use were interpreted from Landsat TM film (1:500,000) of 14 December 1989 using Procom II. The principal process involved in land suitability classification is matching the land use requirements and limitations with land qualities. The main physical parameters considered for the spatial analysis were *soil texture, effective soil depth, surface runoff, permeability, soil pH, organic matter, cation exchange capacity, available phosphorus and potassium, slope, bedrock type and rainfall.* Slope classes were generated from the topo map. Similarly, bedrock types were generated from the geological map. Information on other parameters were acquired from the existing secondary sources. Limitation concept combined with parametric classification approach was employed for performing physical suitability analysis. Proper weightage as per the land use requirement (LDD, 1992) for the selected crops were given to the different classes of individual parameter considered which were encoded into a digitized GIS coverage. Similarly, after proper rating of the every attribute of other maps, *viz.*, land use, slope and geological, their respective weightage were also encoded in their individual GIS coverages. Suitability analysis was performed following a linear combination approach by overlaying all the coverages in vector-based GIS (ARC/INFO). A field survey was also conducted to collect socio-economic information and for ground truthing. Besides evaluating the soil suitability for the selected crops, the cost and return for each crop was also appraised through Benefit/ Cost analysis to see their economic feasibility.

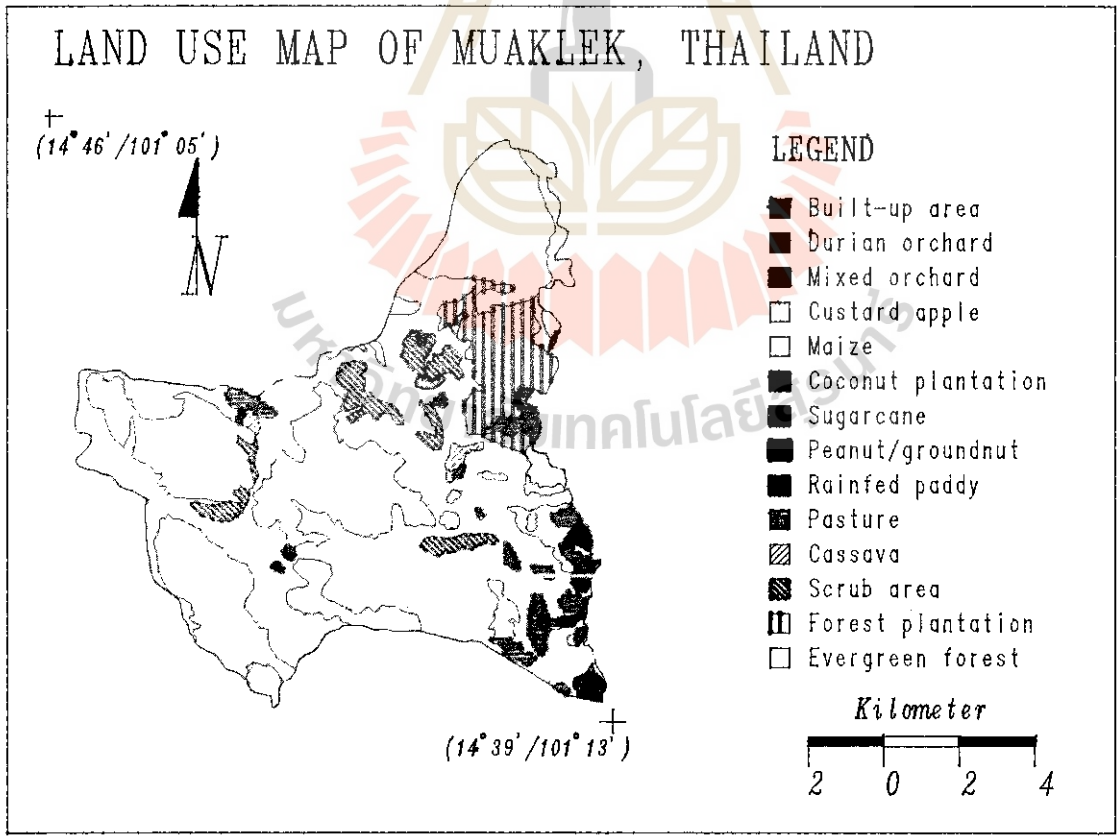

Figure 2. Land Use of Muaklek , Thailand.

4.0 RESULTS AND DISCUSSION

4.1 Land Suitability Classification

The process of land suitability classification involves appraising and grouping of specific types of land in terms of their absolute or relative suitability for a specified kind of use (FAO, 1976). The suitability map produced distinguishes four different classes for the crop production, *viz.*, highly suitable (S_1), moderately suitable (S_2), marginally suitable (S_3), and not suitable (N) on the basis of level of limitations associated. In the "not suitable" (N) class, no further distinction between "currently not suitable" (N_1) and "permanently not suitable" (N_2) was made, because this group constitutes natural vegetation and built-up areas. It was also observed during the field survey that some of the area with greater slope gradient are heavily eroded resulting into unsuitable for the crop cultivation. Since it is neither feasible to correct soil limitations nor is it economically feasible, these area can only be rehabilitated by protecting the top soil with vegetation cover. Based on the physical parameters, the study area have been delineated according to suitability classes for maize, cassava, orchard growing and pasture production. Such land suitability classes which are basically physical suitability are presented in Table 1.

Table 1. Soil Suitability for Maize, Cassava, Orchard and Pasture.

Suitability class	Maize		Cassava		Orchard		Pasture	
	Area (ha)	%	Area (ha)	%	Area (ha)	%	Area (ha)	%
Highly suitable	1,226.6	11.3	2,101.6	19.4	3,320.0	30.6	3,496.2	32.2
Moderately suitable	3,139.6	28.9	2,033.2	18.7	2,592.8	23.8	2,359.2	21.7
Marginally suitable	1,472.8	13.5	1,083.7	10.0	203.0	1.9	479.1	4.4
Not suitable	5,011.0	46.3	5,631.5	51.9	4,734.0	43.6	4,515.5	41.7
Total	10,850.0	100.0						
Existing landuse (% of total)	4,991.0	46.0	54.3	0.5	434.0	4.0	119.4	1.1

Land suitability for maize: Compared to existing land use under maize (46%), spatial analysis showed that as much as 11.3% of the total area are highly suitable for maize production. Likewise, 28.9 and 13.5% are of moderate and marginal suitability, respectively and the area under not suitable category is 46.3%.

Land suitability for cassava: Land suitability for cassava was evaluated because of the fact that the cassava was found to be the second crop after maize in terms of area coverage for the interviewed farmers. However, the cassava land use during 1989 was very insignificant (0.5%), it implies that the cultivation of cassava is increasing over time. As it is generally believed that cassava is usually grown in rather less fertile soils, it indicates that the soil fertility is decreasing over time and maize is being replaced due to loss of soil fertility. The S_1, S_2 and S_3 category for cassava production accounted 19.4, 18.7 and 10%, respectively.

Land suitability for orchard: Nearly one third (30.6%) area was found highly suitable for orchard growing where as 23.8 and 1.9% area were classified as moderate and marginal suitability.

Land suitability for pasture: For the pasture suitability, the proportion of the area under S_1, S_2 and S_3 category accounted to 32.2, 21.7 and 4.4%, respectively.

Looking at the spatial representation of the suitability classes for the selected crops (Figure 3), it is understood that the S_1 class is shared for all the crops in particular location with better land quality.

4.2 Agricultural Land Use and Management Practices

Although maize and cassava are the major crops grown in the area, their productivity of 2.05 and 5.18 ton per ha., respectively were very low compared to the average productivity of Muaklek district. The Multiple Cropping Index (MCI) of 2.4, 2.1, 1.2 and 1.1 were found for marginal, small, medium and large category farmers, respectively with an average MCI of 1.5. Majority of the farmers have adopted the monoculture/ monocropping system due to insufficient soil moisture and poor soil status. Level of management differs according to the resources affordability of the farm categories.

4.3 Farm Income and Expenditure

18.5% of the households were found having an annual income of less than 50,000 Baht (1 US$ = 25 Baht) , whereas, 13% were found having more than 400,000 Baht per annum, nevertheless, the earning from livestock was the major source of income (60% of the total income) for all farm categories. Second major source of income (25% of annual total income) was non-farm activities. The share in income from the crop constituted the least (15%) for all farm categories (Shrestha, 1993). In relation to household expenditure, expenses on livestock farming accounted a major share (60%) of total annual expenditure of a

farm household followed by expenditure on household consumption and domestic use (28%) and crop farming (12%) (Shrestha, 1993).

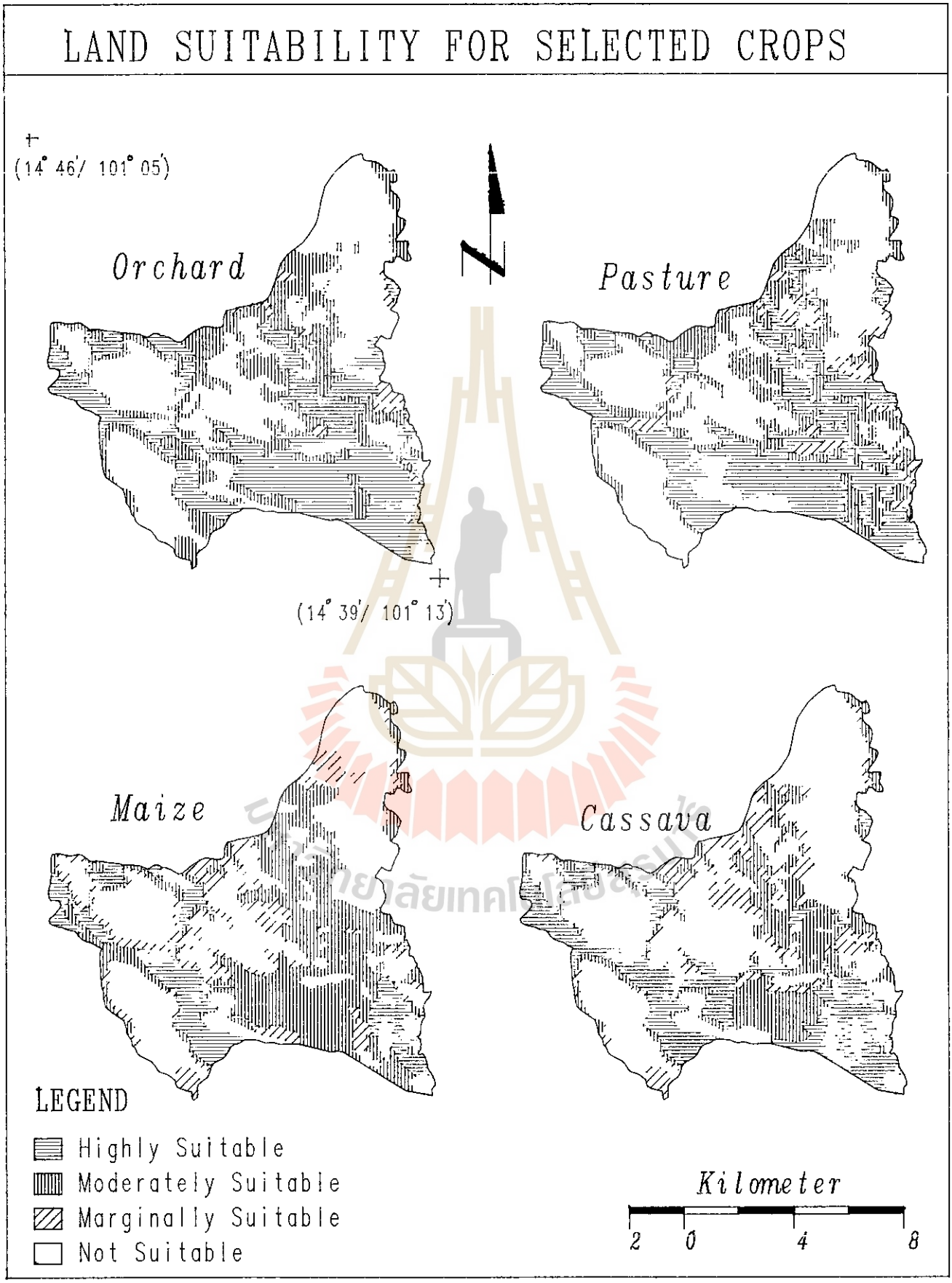

Figure 3. Land Suitability for the Selected Crops.

At this point, it is clear that the livestock production system is an important subsystem in the area. Considering this along with the area to be the largest dairy production area, it will be desirable to discuss this aspect in rather detail.

4.4 Livestock Production System and Condition of Grazing Lands

The average livestock holding is 21.3 Tropical Livestock Unit (TLU). Cattle is the major species, however, buffalo, goat and pig are also being raised by the farmers relatively in small number. Livestock holding, however, is positively correlated with land holding size, livestock unit per unit of land holding is found in the same fashion as cropping index which articulates that the smaller category farmers are more dependent on the public natural resources, such as grazing lands, waste land, roadside and fallow fields to graze their livestock. Outside source of paddy straw serves as the major livestock feed. The assessment of grazing capacity is important for assigning an optimal animal stocking rate to pastureland as well as regulating the conservation efforts. The grazing practices existing in the area are uncontrolled, particularly in the communal land. Private fallowland and community owned land are accessed to anyone for livestock grazing. In general speaking, the average condition of the grazing lands was observed to have 50 to 60% grass cover and above 60% utilization closely grazed under 1 cm. The legumes composition is less than 15%.

4.5 Environmental Impact

It was observed that people are enough cognizant of the environmental degradation and the various factors responsible for degradation. Even then, the continuous exploitation of the resources is not yet stopped, it may be because of the fact that there are no alternative resources available and people are forced to make use of it for their survival. It was revealed that there were negative impacts on all attributes, both on farmland and non-farm land. An index value of -0.76 indicated that the impact was most intense on soil moisture and water availability followed by soil erosion (-0.57) and soil fertility (-0.52), and least intense on vegetation change (-0.11).

4.6 Gross Margin Analysis

Gross Margin Analysis (GMA) was performed to appraise the economic feasibility of maize, cassava, orchards and pasture. Unlike other crops, it was difficult to calculate the return from pasture since there were no detail production statistics available. Herein, the productivity was estimated to be 25.0 tons of green matter per ha. (Tumwasorn et al, 1992). Beside the price of forage, the market value for all other crops was taken into account to calculate the gross return. Since there was no market price available per unit of cut forage, the price of one kilogram was estimated based on the price of paddy straw valuing its Dry Matter (DM) content. None of the respondents were paying any type of rent or tax for the land they cultivate. However, renting a ha. of land can cost equivalent to US $ 31.25 to 45, an additional cost US$ 31.25 per ha., as an opportunity cost, was included to calculate the total cost of production for pasture.

The analysis considered the total cost and return per crop. The maximum net return per ha. was from orchard with US$ 157.62 (Table 2). Other important crops were pasture, maize and cassava with a net return of US$ 91.25, 47.35, and 16.38, respectively. In the case of orchard farming, only the operating cost was considered. In the long run, the return could be lower when the fixed cost is taken into consideration. Similarly, except for fruit crops, the benefit-cost ratio for pasture (1.45:1) was higher than that for maize (1.25:1) and cassava (1.04:1), which are the dominant crops of the study area.

Table 2: Cost and Return of Selected Crops.

Crop	Cost/ ha			Return/ ha		B/C ratio
	TVC	FC	TC	Gross	Net	
Cassava	360.94	4.46	365.40	381.45	16.38	1.04
Maize	175.92	4.95	180.87	227.28	47.35	1.25
Pasture	169.33	35.54	204.87	296.12	91.25	1.45
Orchard	116.60	1.09	117.69	272.21	157.62	2.31

Note: Cost and Return in US $. TVC= Total Variable Cost, FC= Fixed Cost, TC= Total Cost (TVC+FC)
B/C ratio = (Gross return - TC)

5.0 CONCLUSIONS AND RECOMMENDATIONS

The crop production systems of the study area is basically a "low input-low output" system which obviously may not be sustainable from both economic and ecological perspectives because the production is decreasing over time due to reduced soil fertility and soil moisture. On the other hand, the area is the largest dairy farming producer in Thailand. However, the acute shortage of feed results in the high cost of milk production because the majority of livestock feed, especially paddy straw, has to

be purchased from other parts of the country. The overall pasture condition of the existing grazing lands is also not satisfactory in terms of grazing capacity. The area also has great potential for orchard farming because of its suitable physiography. Since, the area with better land quality for crop production is very limited, with due consideration of these fundamental factors, various land use alternatives are proposed in the process of appraising alternatives (Figure 4) which will be viable in terms of rehabilitating the land and environmental quality and best economic use as well.

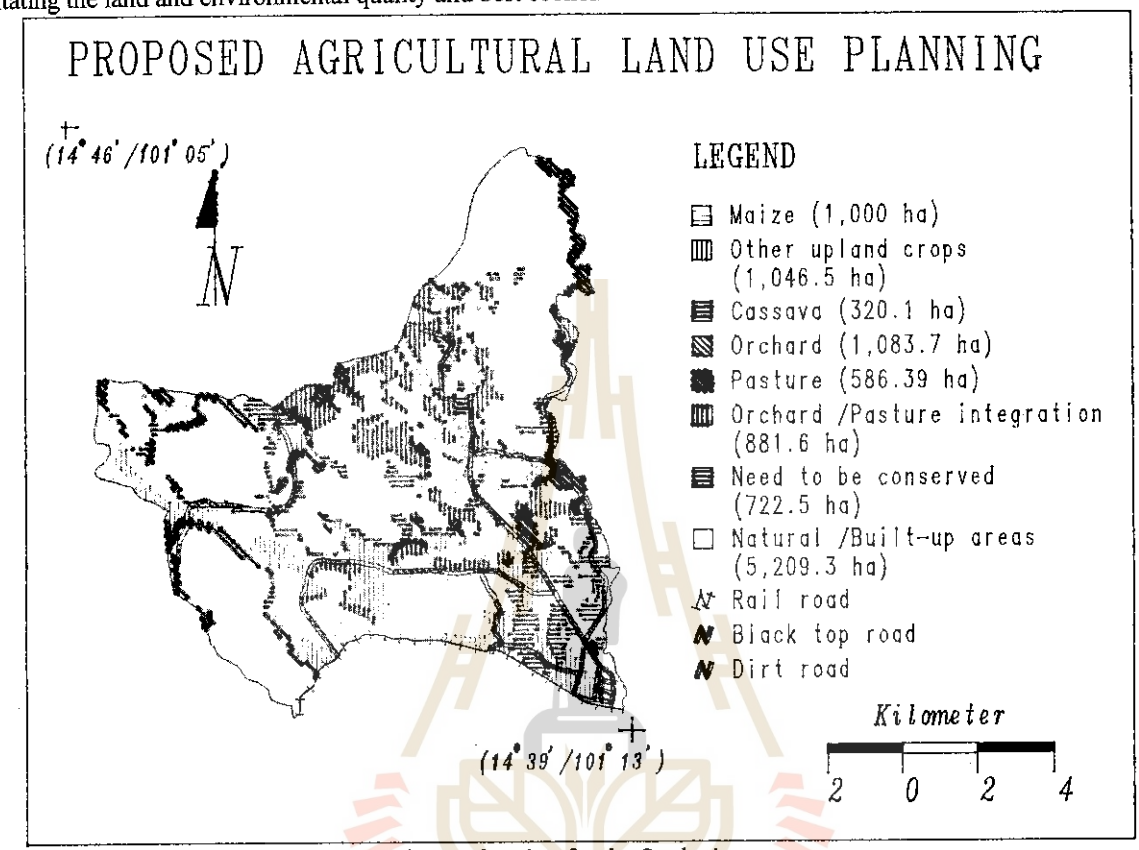

Figure 4. Proposed Agricultural Land Use Planning for the Study Area.

Nearly half of the area are to be left untouched in its natural state. Maize, other upland crops and orchard are recommended on about 10% area for each. Orchard/pasture integration, pasture alone and cassava are recommended on 8.1, 5.4 and 2.8% area, respectively. 6.6% of the area which are heavily eroded needs immediate conservation measures. Such scheme would not only solve the problem of shrinking land availability but also assist maintain the productivity of the ecosystem.

REFERENCES

Dent, F.J. 1989. Land Degradation in Asia and the Pacific. In *Environment and Agriculture*, FAO/RAPA, Bangkok.

FAO. 1976. *A Framework for Land Evaluation*. International Institute for Land Reclamation and Improvement, The Netherlands.

FAO. 1983. *Guidelines : Land Evaluation for Rainfed Agriculture*. FAO Soils Bulletin, No. 52, Rome.

FAO/RAPA. 1994. *Selected Indicators of Food & Agriculture Development in Asia-Pacific Region, 1983-93,* Bangkok.

Hirunruk, V. 1973. *A Case Study of Twenty Dairy Farms in Muaklek, Thailand.* Master's Thesis, Faculty of Economics, Thammasat University, Bangkok.

LDD. 1987. *Soil Survey Report of Changwat Saraburi.* Soil Survey Division, Department of Land Development, Bangkok.

LDD. 1992. *Quantitative Land Evaluation Manual for Economic Crops,* No. 2, Land Development Department, Bangkok.

McGregor D.F.M and Barker D. 1991. *Land Degradation and Hill Side Farming in the Fall River Basin, Jamaica*, 11, 143-156.

Shrestha, R. P. 1993. *Land Suitability Analysis for Pasture Development at Muaklek Thailand: A GIS Application*, Master's degree Research, Asian Institute of Technology, Bangkok.

Tumwasorn, S. and Luangwatanawilai, M. 1992. *Cost and Return from Sahiwal x Frisian Dairy Crossbred in Pattalung Province of Thailand.* Research and Development Institute, Kasetsart University, Bangkok, (in Thai).

A KNOWLEDGE-BASED APPROACH TO PREDICTING SALINTY IN THE SOUTH-WEST OF WESTERN AUSTRALIA

[1]P.A. Caccetta, [2]H.T. Kiiveri, [2]F.H. Evans and [3]R. Ferdowsian

[1]School of Computing, Curtin University of Technology

[2]CSIRO Division of Mathematics and Statistics

[3]Department of Agriculture Western Australia

September 18, 1995

Abstract

This paper describes the construction of a knowledge-based system and its application to predicting salinity in the Kent River catchment located in the south-west of Western Australia. The system incorporates remotely sensed data, data derived from digital elevation models, maps produced by experts and data combination rules based upon expert knowledge and expert-derived training data. Bayesian networks are used as the modelling environment, allowing reasoning with uncertainty in the process of combining data. Firstly, data were obtained for three time periods spaced roughly a decade apart. A knowledge-based system was then conceived and applied to the data, with data from one decade used to predict land condition in the following decade. The resulting prediction maps were then compared with independent validation data, giving good results. The maps were used to provide estimates of the historical spread of salinity in the catchment and its likely extent in the future.

1 Introduction

In much of the Western Australian agricultural region, the clearing of land has lead to rising saline groundwater, resulting in the loss of previously productive land to salinity. Based on farmer surveys conducted in 1979 and 1989, the Australian Bureau of Statistics reported that 443000ha (2.8%) of previously arable land was lost to salinity at a rate of about 18000ha each year.

Aerial photo interpretation has been used to assess the extent of salinity in some areas [4], but this is time consuming and expensive. More recent efforts [6] [7] [8] have used Landsat TM data to estimate the extent of salinity. Typically, statistical approaches such as maximum likelihood classification are used to classify the data into different landcover classes, which are associated with the land being severely affected, slightly affected and not affected.

The above approaches provide a means of monitoring the extent of salinity but provide no insights into the likely effects that remedial actions such as tree planting will have on the problem, or given the current land status, what areas are at risk of salinisation in the longer term. The latter is imperative for the formulation of remedial measures.

To explore ways of achieving these aims, we developed a knowledge-based system for representing relationships relevent to salinisation which can then be applied to mapping and predicting salinity. The system takes various input maps in a GIS and applies rules, which have varying degrees of confidence, to produce output maps of existing and likely future salinity. The system may also be used in an interactive fashion to answer *what-if* scenarios.

The system was developed in the Upper Kent Catchment (approximately 2000 sq. km), which lies in a high rainfall (500 – 750mm) area of the agriculture region, approximately 350km south east of Perth.

The methodology of our approach was

1. consult with experts to gain knowledge of the problem
2. based on the expert knowledge, obtain data (where possible) that is relevant, possibly with further processing, to appling the knowledge over the catchment
3. based on expert knowledge and available data sets, construct the knowledge-based system
4. use the resulting model to interpret the data, ie produce salinity risk maps more the region
5. validate the results by comparing the system output to independent validation data, and if acceptable, form a catchment salinity summary

These points are discussed in this paper.

2 Knowledge Elicitation and Relevant Data Sets

A workshop was held to provide a forum to quantify current knowledge on factors relevant to dryland salinisation in the south-west of Western Australia. The workshop was attended by 21 people, including experts on salinisation from the Department of Agriculture, the CSIRO and the West Australian Water Authority. The factors identified include time since clearing, depth to ground water, rate of ground water rise, distance to existing salinity, climate, degree of waterlogging, geology, salt storage, landform, position in flow path, historical and existing vegetation cover, depth to basement, hydrology (such as influenced by shear zones, faults and dykes) and land management.

Clearly, relevant data for some factors could not be obtained in a cost effective manner on a catchment scale; for instance, data relating to *depth to ground water* and *rate of ground water rise* typically are obtained from monitoring bore holes.

A time period of approximately one decade was chosen as the monitoring interval. Features derived from a digital elevation model (dem), satellite Landsat MSS and Landsat TM and historical aerial photographs were the primary sources of data.

Historical estimates of landuse, and in particular clearing, were obtained for the years 1977, 1988 and 1994 from classification of Landsat MSS (September 1977) and Landsat TM (August 1988 and August 1994) data. A maximum likelihood classifier was used.

Elevation data were in the form of contours derived from stereo photo interpretation. This is the most common source of elevation data presently available in the Western Australia. For the area considered, 5-metre contour data were available. These data were interpolated using cubic spline interpolation to form a raster dem.

A slope map was produced from the dem. Using the dem and the clearing information derived from the Landsat data, maps of *upslope cleared area* and *percentage upslope cleared area* were produced for each of the periods using an algorithm based on flow path predictions [5].

Independent training and validation data were obtained from an interpretation of historical aerial photographs, with the areas classified into the classes *not saline*, *potentially saline* and *saline*. The same training areas were interpreted for the years 1973, 1985 and 1994, thus enabelling predictions to be made for the years 1985, 1994 and 2004. Unfortunately some unavoidable date mismatches occured between the available Landsat data and the aerial photgraphs used for the training and validation data, although they were considered sufficient to model the general trends.

Aerial photo interpretation was also used to partition the catchment into landform patterns [2], from which surrogates for ground water salinity were derived.

The data used were:

- Upslope cleared area (UpSlpClr): the total area of land upslope of a given location that has been cleared
- Percentage upslope cleared (PerClr): the percentage of the catchment above a given location that has been cleared;
- Flowslope (FlowSlope): the slope of the land in the direction of surface flow;
- Land cover (LandCov): land use and condition as identified using Landsat satellite imagery; and
- Ground water salinity (GndWatSal): map of the expected ground water salinity as derived from landform patterns.

Based on expert knowledge and available data, a knowledge-based system representing the process of salinisation was constructed. This is the topic of the next section.

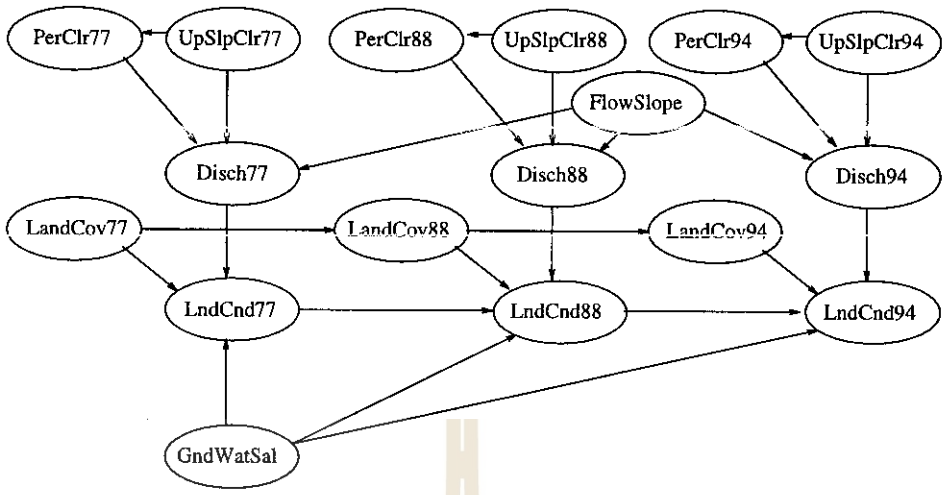

Figure 1: Graphical representation of the Bayesian network

3 Knowledge Representation

A *Bayesian network*, also referred to as a *causal network* or a *(conditional) probability network*, was used for representing knowledge and combining evidence. The network that was constructed may be represented graphically as in Figure 1. The ellipses represent variables (attributes) whose values are derived from maps, human input or inferred by the system. The directed edges represent relationships that exist between variables. For example, Disch94 is ground water discharge in 1994 and LndCov94 is land use/condition in 1994 derived from a classification of Landsat data.

The knowledge embodied in the network is represented by the joint probability distribution of the variables, i.e. beliefs (*rules*) are expressed in terms of (conditional) probabilities. The arrows in Figure 1 depict the rules that need to be specified. The probabilities for a variable are specified as the conditional probability for that variable given all variables that have an edge directed toward the variable of interest. For example, in Figure 1, one set of rules that needed to be specified was $P(Disch94|FlowSlope, PerClr94, UpSlpClr94)$.

Given evidence about the state of one or more variables, the system can be used to derive conclusions about the probable state of the remaining variables. Note that the system works with probabilities in a consistent manner, allowing probabilities to be estimated and interpreted as relative frequencies. This feature is particularly useful in remote sensing and GIS when using the system in an interactive mode, as these values relate directly to the tangible interpretation: *given the available information, it is expected that x% of the land has the characteristic in question.* For those interested, more technical details can be found in Caccetta et al [1] and Lauritzen et al [3].

The system parameters (conditional probability tables) were usually estimated using the training data, although in some instances the parameters were defined subjectively.

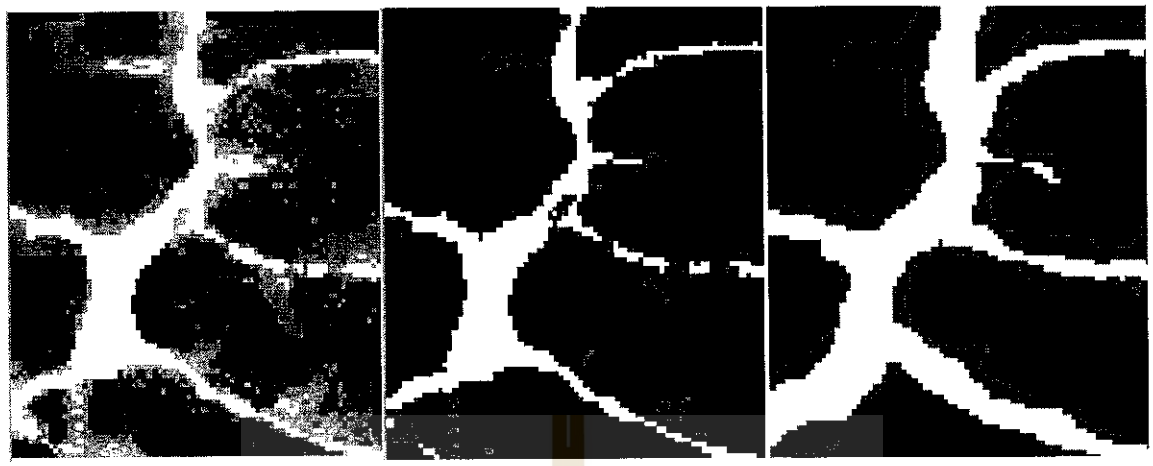

Figure 2: Risk map (left), Classification (middle), Expert's Class. (right)

	NoRisk	Risk	NoRisk	Risk	NoRisk	Risk
	1977	1977	1988	1988	1994	1994
True NoRisk	70	56	75	21	71	25
True Risk	30	44	25	79	29	75

Table 1: Network Mapping Accuracy (%), Expert vs Network

4 Results

The data for the catchment were interpreted (processed) with the Bayesian network to produce probabilistic maps of land condition for each of the three time periods. A classification may be derived from the probabilistic maps, the probabilities giving an indication of the quality of the resulting choice of label. An example of the network output is given in Figure 2, along with the expert classification for the area. The risk map is graded from black to white, with black indicating a low probability of salinisation and white a high probability of salinisation. For the classifications, black represents *not affected*, grey *potentially affected* and white *already affected.*

The classification maps were compared with the validation data and a summary of the performance of the network is given in Table 4. In the table, Risk has the interpretation *is saline or will go saline in the next time period.* For example, in 1988, 79% of the pixels predicted to be at risk by the network were also identified to be at risk by the expert.

The maps were then used to provide a summary of the historical spread and likely extent of future salinity for the catchment. According to the network, 9% of the catchment was affected in 1977; this increased to 14% in 1988, to 20% in 1994 and is predicted to increase to 27% by the year 2004 if no remedial action is undertaken.

5 Conclusions

A combination of remotely sensed data, data derived from digital elevation models and expert knowledge may be used to form cost effective estimates of historical and future salinisation in the agricultural regions of Western Australia. The strategies and methods described here are useful for integrating many different sources of data with expert knowledge, particularly when the data have an associated element of uncertainty.

Acknowledgements

The work by P.A. Caccetta was supported by a grant from the DEC External Research Programme and further funding from the CSIRO Division of Mathematics and Statistics.

This work was part of the *Predicting Salinity* project carried out with funding provided by the Land and Water Resources Research and Development Corporation.

References

[1] P.A. Caccetta, N.A. Campbell, G. West, H. Kiiveri, and M. Gahegan. Aspects of reasoning with uncertainty in an agricultural gis environment. *To appear in New Review of Applied Expert Systems*, 1995.

[2] R. Ferdowsian. Landform patterns of western forest area, on the south coast of W.A. Technical report, Department of Agriculture, Western Australia, 1993.

[3] S. L. Lauritzen and D.J. Spiegelhalter. Local computations with probabilities on graphical structures and their application to expert systems. *Journal of the Royal Statistical Society B*, 50(2):157–224, 1988.

[4] R. A. Nulsen. Salt-affected land in the shire of Wongan-Ballidu, Western Australia. *Australian Journal of Soil Research*, 19:87–91, 1981.

[5] P. Quinn, K. Beven, P. Chevallier, and O. Planchon. The prediction of hillslope flow paths for distributed hydrological modelling using digital terrain models. *Hydrological Processes*, 5:59–79, 1991.

[6] J .F. Wallace and G. A. Wheaton. Spectral discrimination and mapping of land degradation in Western Australia's agricultural region. In *5th Australasian Remote Sensing Conference, Perth, Western Australia*, pages 1066–1073, 1990.

[7] G.A. Wheaton, J.F. Wallace, D.J. McFarlane, and N.A. Campbell. Mapping salt-affected land in Western Australia. In *Proceedings of the 6th Australasian Remote Sensing Conference*, volume 2, pages 369–377, Wellington, New Zealand, 1992.

[8] G.A. Wheaton, J.F. Wallace, D.J. McFarlane, N.A. Campbell, and P. Caccetta. Mapping and monitoring salt–affected land in Western Australia. In *Proceedings of Resource Technology '94 Conference*, pages 531–543, Melbourne, Australia, 1994.

Assessment of ERS-1 SAR Data for Rice Crop Mapping and Monitoring

Supan Karnchanasutham Dr.Apichart Pongsrihadulchai

Office of Agricultural Economics, Chatuchak, Bangkok 10900, THAILAND

Chockchai Rodprom

National Research Council of Thailand, Chatuchak, Bangkok 10900, THAILAND

ABSTRACT

The objective of the study is to evaluate the capabilities of ERS-1 SAR data for monitoring of rice planting acreage and its growth. The study area was about 100 Km^2 in Tha Muang district, Kanchanaburi province. The ERS-1 PRI. acquired during 35 day repeat orbit were used in the study. These data were acquired on 20 August 1993, 29 October 1993 and 3 December 1993 respectively. The study area was divided into 10 test sites and each of which was randomly selected 6 sample areas for extensive measurements of rice plant parameters (height, density, net weight, yield etc.) as well as auxiliary information (wind, rain, and growth stage etc.). A Global Positioning System (GPS) was used to locate and register test site boundaries and calculate the area of each test site. The ERS-1 data were geometrically corrected to topographic map at scale 1:50,000. The field boundaries of all of the surveyed test site were digitised and superimposed on the geometrically corrected data which is filtered by MAP filter method.

The result of the study revealed that it was very difficult to identify the rice crop if only single data was used. The rice planted area classified from 3 date composite was found to be 20,253 hectares or about 27% of the total study area. The rice mapping accuracy was 78% while the overall accuracy was 79%. The very bright of backscattering coefficient (dB) was observed in August. This was due to the fact that the muddy broadcast rice was adopted in this area. The water level in the field for this type of planting method was very limited. The closer to the harvesting date of the rice crop is, the better classification of planted area would be obtained.

1.Introduction

Rice is the most important crop in Thailand in terms of acreage, number of farmers, and export earning. The ability to monitor and forecast its production is therefore vary crucial for short term policy determination.

One major problem in utilising satellite data for crop area estimation is due to the cloud covers of the areas on the imagery because the needed data is in the rainy season. The capability of ERS-1 satellite that can see through cloud or all-weather conditions will make the estimation of crop area possible. The combination of SAR and other satellite data such as TM and SPOT will be very useful for crop classification in the area where cloud is always present all year round.

2.Objectives

To evaluate the capabilities of ERS-1 SAR data for monitoring of rice planting acreage and its growth in Kanchanaburi province.

3.Equipment and data acquisition

3.1 Topographic map at scale1:50,000

3.2 Aerial photography at scale 1:15,000

3.3 Global Positioning System (GPS)

3.4 Field equipments i.e compass, frame, counter etc.

3.5 LANDSAT TM CCT Path 130 Row 50 acquired on 17 JAN. 1994

3.6 SPOT CCT acquired on 26 Feb.1994

29 October 1993, 3 December 1993.

4. Study area

An 10X10 square kilometers area located in Amphoe Tha Muang Kanchanaburi province , Thailand between latitude $99^{0}\ 37'\ 44.1''$E - $99^{0}\ 43'\ 17.22''$E and longitude$13^{0}\ 50'\ 58.06''$N - $13^{0}\ 56'\ 22.25''$N was used as the study area. This area is part of the Mae Klong Irrigation Project of the Mae Klong river basin which is one of the largest river basins in Thailand.

5.Methodology

5.1 Site selection and ground data collection

The study area was divided in to 10 sites and for each site 6 samples were randomly selected. Thus, in all there are 60 samples which were used for ground data parameters collection. For each time of satellite overpass (20 August 1993, 29 October 1993 and 3 December 1993) the same data parameters were collected as follows :

1. Number of stalk density per 50 CM^{2}
2. Length of leaf.
3. Width of leaf.
4. Diameter of stem.
5. Plant height above water.
6. Net weight.
7 .Dry weight.
8. Yields.

The site acreage was measured by using the Global Positioning System (GPS).

5.2 Image rectification

Rectification is the process of projecting the data onto the plane making it conform to a map projection system. Assigning map coordinates to the image data is georeferencing. Since all map projection systems are associated with map coordinates. Five Ground Control Points (GCP) are specific pixels in the image data for which the output map coordinates are

known. GCP consists of two x,y pairs of coordinates : source coordinates and reference coordinates. The resampling method used in this study is the nearest neighbor method.

5.3 Speckle filtering

The Map filter method was applied in all 3 different dates on SAR data.

5.4 Calibration of backscatter coefficient

The calibration of backscatter coefficient (σ^0) in this study used the following calibration equations below.

$$\sigma^0_{(db)} = 10 \log_{10}\langle I\rangle - 58.24$$

$$\langle I\rangle_{(16\ bits)} = DN^2_{(8bits)} \times 6$$

5.5 Image processing

Supervise classification with Maximum Likelihood method was performed on 3 different dates ERS-1 SAR data and classified into 7 classes. namely : rice, sugarcanee, bushed, water, city, mountain1 (bright) and mountain2 (dark).

5 6 Accuracy assessment

An error matrix which compares the classified data with the reference data (aerial photography) was computed. It contains parameters such as error of omission, error of commision, map accuracies and overall (global) accuracy.

6.Results and discussion

6.1 Site acrage and general information

The minimum and maximum site acreage in the study area measured by using GPS were 6.57 hectares and 11.43 hectares respectively. The rice varieties planted in this area were SP60 (Suphan 60) and RD23 (Rice Department No.23). This rice crop was planted in August and harvested in December.

6.2 Image rectifcation

Five ground control points (GCP) were used for geometric collection by map (1:50,000) to image (ERS-1 SAR images). The resampling method used is the nearest neighbor and the pixel size is 30x30 M^2.

6.3 Speckle filtering

Map filtering tehnique was performed on 3 ERS-1 SAR data.

6.4 Backscattering coefficient (dB)

Due to Earth View (EV) software which was originally planned to be used for this project can not operate on 16 bits and thus can not draw field boundaries and overlay on the image . To solve this problem the ERS-1 SAR data were converted to 8 bits and the IDRISI software was used instead to find backscattering coefficient using equation in item 5.4. The average of rice backscattering coefficients of 20 August, 29 October and 8 December 1993 a were -7.4, -9.8 and -8.5 respectively.

6.5 Image classification

Supervise classification technique was performed on 3 different ERS-1 SAR data : 20 Aug. 1993, 29 Oct. 1993, and 3 Dec.1993 and divided into 7 classes as already mentioned. Since it is very difficult to classify the rice crop if only single date data is used. Therefore, these 3 dates data were combined and used as a basis for classification.

6.6 Accuracy assessment

It was found that the rice mapping accuracy was 78% while the over all accuracy was 79%.

7.Conclusion

(1) The objective of the study is to evalate the capabilities of ERS-1 SAR data for monitoring of rice planting acreage and it growth. The study area was about 100 Km^2 located in Tha Muang district, Kanchanaburi province.

(2) The ERS-1 PRI acquired during 35 day repeat orbit were used in the study. These data were acquired on 20 August 1993, 29 October 1993 and 3 December 1993 respectively.

(3) The study area was divided into 10 test sites and each of which was randomly selected 6 samples areas for extensive measurements of rice plant parameters (height, density, net weight, yield etc.) as well as auxiliary information (wind, rain, and growth stage etc.)were gathered. A global Positioning System (GPS) was used to locate and register test site boundaries and calculate the area of each test site.

(4) The ERS-1 data were geometrically corrected to topographic map at scale 1:50,000. The field boundaries of all of the surveyed test site were digitised and superimposed on the geometrically corrected data which is filtered by MAP filter method.

(5) The minimum and maximum site acreage in the study area measured by using GPS were 6.57 hectares and 11.43 hectares respectively. The rice varieties planted in this area were SP60 and RD23 . This rice crop was planted in August and harvested in December.

(6) The average of rice dB in 20 August, 29 October and 8 December 1993 were -7.4, -9.8 and -8.5 respectively. The very bright if dB was observed in August due to the fact that the muddy boardcast rice was adopted in this area. The water level in the field for this type of planting method was very limited.

(7) Supervise classification technique was performed on each date and 3 different ERS-1 SAR data, which divided into 7 classes. Since it is very difficult to classify the rice crop if only single date data is used. Therefore, these 3 dates data were combined and used as a basis for classification. The total rice planted area about 20,253 Hectare or about 27.14% of the study area.

(8) The rice mapping accuracy was 78% while the over all accuracy was 79%.

8. Further recommendation

The recommendations for future work are as follows :

(1) The random selection of the sample plots for measurement of parameters were done independently for each time of survey. This method was not appropriate due to the heterogeneity in nature of the rice crop. Therefore, the sample plots should be fixed for every time so that the different in measurement will reflect the real change in parameters.

(2) There is ample opportunity for increased utilization of this methodology for rice planted area mapping especially in the region high cloud coverage is usually presented.

(3) Data fusion of remote sensing and integration with Geographic Information System (GIS) should be the standard way of rice planted area mapping.

(4) One has to be aware that the handling of radar data, in particular, is difficult. This is due to the geometric and radiometric distortion as well as the presence of speckle. Appropriate software must be developed to deal with such data.

9.References

7.1.Center for Agricultural Statistics ., (1990) Agricultural Statistics of Thailand Crop Year 1990/1991, Office of Agricultural Statistics, Bangkok, Thailand.

7.2 FAO & ESA, 1993. Radad imagery : Theory and interpretation (Lecture note), Remote Sensing Centre, Research and Technology Development Division, Agriculture Department, FAO, p. 21-27.

7.3 Japan Association on Remote sensing, 1993. Remote Sensing Note ,Nihon Printing, Tokyo, p. 200-201.

7.5 Schumann R., 1994. ED 13.07 Microwave Remote Sensing (Lecture note), AIT, Thailand.

Multi-Seasonal Analysis of SAR Data for Agriculture

Genya SAITO, Nobuyuki MINO and Akira HIRANO

Remote Sensing Laboratory,
National Institute of Agro-Environmental Sciences
Kannondai 3-1-1, Tsukuba, Ibaraki 305, JAPAN
Fax : +81-298-38-8199
e-mail : genya@niaes.affrc.go.jp
e-mail : minonobu@niaes.affrc.go.jp
e-mail : hirano@niaes.affrc.go.jp

Abstract

Multi-seasonal analyses of SAR data for agriculture were performed using JERS-1 (L-band SAR) and ERS-1 (C-band SAR) images at grassland, upland farming field and paddy area in Hokkaido, northern island in Japan.

In Konsen-plateau in the north-eastern part of Hokkaido, which is comprised mainly of grassland, images of JERS-1 data taken in April, June and August looked similar to each other except the spots where land use change occurred. In Tokachi plain, which is comprised mainly of upland farming field, the back scattering coefficients of ERS-1 data taken in August are larger than those of April. In the same area, images of JERS-1 data taken in June, August and October looked different from each other in agricultural field because of the soil-surface conditions. In Ishikari plain, which is comprised mainly of paddy, the back scattering coefficients of ERS-1 data taken in July are higher than those of May because of the biomass. In the same area, the back scattering coefficients of JERS-1 data taken in June when water fills the paddy are smaller than those of August and October when no water is in the paddy.

The JERS-1 microwaves pass through agricultural plants and then scatter at the ground surface, but ERS-1 microwaves scatter at agricultural plants. Although we cannot get direct information about agricultural plants using JERS-1 data, we can get useful information about agricultural environment from the data. The ERS-1 SAR can directly measure agricultural crops, but the data include other information such as soil surface conditions and topographical features.

1. Introduction

Many studies on agriculture using remote sensing technique have been performed in Japan since LANDSAT was launched in 1972. These studies were made using optical sensors such as LANDSAT/TM MSS, SPOT/HRV, MOS/MESSR, and NOAA/AVHRR. In Japan, crop growing period is from May to September, when temperature is relatively high and it rains much. It is very difficult to acquire optical remote sensing data during that time because of the cloud cover. Data acquisition is highly restricted in some tropical rainforest areas.

We use SAR data as the solution to the data acquisition problem, and to get other information concerning object size, form and water contents. Quantitative treatments to multi-temporal data can be performed, because same microwave energy reaches on earth every time when using same SAR instrument. While data from optical sensors are greatly influenced by atmospheric conditions, SAR data are believed to be quite independent from atmospheric effects.

ERS-1 and JERS-1 were launched in 1991 and in 1992 respectively, and both satellites have SAR instruments. In Europe and America, there are some experimental analyses concerning agricultural study

using SAR data[1],[2],whereas in Japan, there is no report on that subject. We made images from SAR data, and they were compared with LANDSAT/TM images, topographical maps and ground truth data.

2. Methods

2.1. SAR data

Table 1 shows characteristics of SAR instruments and table 2 shows the list of remote sensing data used in this study.

2.2. Analysis instruments

We used the remote sensing analysis system of National Institute of Agro-Environmental Sciences. The system has 5 EWS, 3 digitizers, a MT unit, 2 types of scanners, a color hard copy machine and a color electrostatic plotter. The system is installed with ERDAS as a image processing data analysis software and ARC/INFO as a geographic information system software.

2.3. Ground truth data

In Hokkaido district, ground truth surveys were made six times as the cooperative works with Hokkaido National Agricultural Experiment Station and Konsen Agriculture Experiment Station. We used topographical maps of 1/25,000 made by Geographical Survey of Japan.

Table 1 Characteristics of SAR instruments

	Wave length	Incident angle	Polarization	Spatial resolution		Swath
JERS-1	L-band 1.275GHz 23.5cm	38.5	HH	18 m	3 looks	75 km
ERS-1	C-band 5.3 GHz 5.66 cm	23	VV	15m	3 looks	100 km

3. Results

3.1. Konsen-plateau

This area is located in the north-eastern part of Hokkaido. The temperature in this area is low for growing crops and agricultural landuse of this area is mostly grass for livestock. JERS-1/SAR and LANDSAT/TM images acquired almost at the same time of years in April, June and August, and they are indicated as photo 1. In LANDSAT image acquired in April, bright parts represent grasses and evergreen forests, and dark parts represent urban areas, bare soils and deciduous forests. In LANDSAT images acquired in June and August, bright parts represent forest and grassland, and dark parts represent urban areas, bare soils and just after cutting grassland.

As for JERS-1/SAR images, three images of different times are almost same. In these images, bright parts are forests and urban area, and dark parts are grasses and bare soil. While it is very difficult to distinguish forests from grasses using LANDSAT/TM data, it is easy to separate the two things using JERS-1/SAR. Using JERS-1/SAR and LANDSAT/TM data, we can classify grasses, evergreen forests, deciduous forests, urban areas, bare soils and deciduous forests.

We tried to extract agricultural area containing grasses and bare soils in this region using JERS-1/SAR data. First, we performed speckle noise reduction using filter treatment, and then we picked up agricultural area as low digital number parts by level slice method. From the observation of JERS-1 data, it can be concluded that L-band microwave passes through grass body, and scatters on earth.

Back scattering coefficients in Konsen-plateau are calculated and indicated in fig. 1. Forest is the highest, second is urban area, and the lowest is grassland. We can not detect any seasonal changes.

Table 2 List of remote sensing data used in this study

Area name	Sensor	Acquisition time
Konsen-plateau (Hokkaido)	JERS-1/SAR	1992/04/15
		1993/04/02
		1993/06/30
		1993/08/31
	LANDSAT/TM	1992/04/09
		1991/04/23
		1991/06/26
		1990/08/13
Tokachi plain (Hokkaido)	JERS-1/SAR	1992/06/01
		1992/07/15
		1992/08/28
		1992/10/23
	ERS-1/AMI-IMAGE	1992/06/02
		1992/08/11
	LANDSAT/TM	1992/04/09
		1987/06/22
Ishikari plain (Hokkaido)	JERS-1/SAR	1992/06/04
		1992/08/31
		1992/10/14
	ERS-1/AMI-IMAGE	1992/05/20
		1992/07/29
	LANDSAT/TM	1987/06/22

3.2. Tokachi plain

This area is located in the eastern part of Hokkaido. The area is mostly comprised of crop field and no paddy. The crops are winter wheat, sugar beet, soy bean, kidney bean, corn, potato, etc. JERS-1/SAR data were acquired in June, July, August and October; ERS-1/SAR data were acquired in June and August.

In four JERS-1/SAR images, we can detect some differences caused by the soil surface change. Distinctive difference between the two ERS-1/SAR images can be observed. In early June, most areas appears very dark and small parts very bright, because there are very small crop plants or no crop in the agricultural field. Plowing direction that is perpendicular to that of microwave radiation was recognized as bright line. In August, most areas are bright because crops grew large. We can detect the edge of plateau in ERS-1/SAR images easily while it is difficult to do so in LANDSAT/TM image.

3.3. Ishikari plain

This area is located in the central part of Hokkaido. The area is mostly paddy fields, but recently other crops have been planted because of the surplus production of rice. The JERS-1/SAR images were taken in June, August and October and those of ERS-1/SAR were taken in May and July.

Back scattering coefficients of paddy, soybean (drained paddy field for upland crop cultivation), winter wheat and urban area were calculated and indicated in Fig.2. Back scattering coefficients of JERS-1/SAR in paddy are almost same in three different times in a year. However, the one in June is little lower than those of others because there is water in paddy in June and there is no water in the end of August and October. As for back scattering coefficients of ERS-1/SAR in paddy, values of July is higher than that of May because of biomass as a whole except one plot. The only exception was caused because of the planting direction. As for back scattering coefficients of JERS-1/SAR in winter wheat and soy bean field, there are

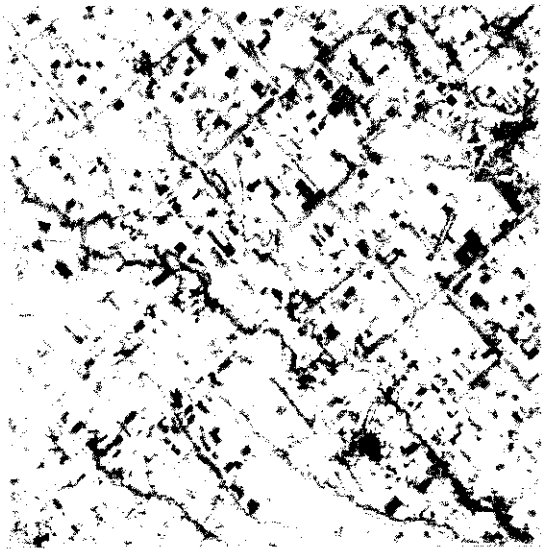

LANDSAT TM (1991.4.23)
R:BAND5 , G:BAND4 , B:BAND3

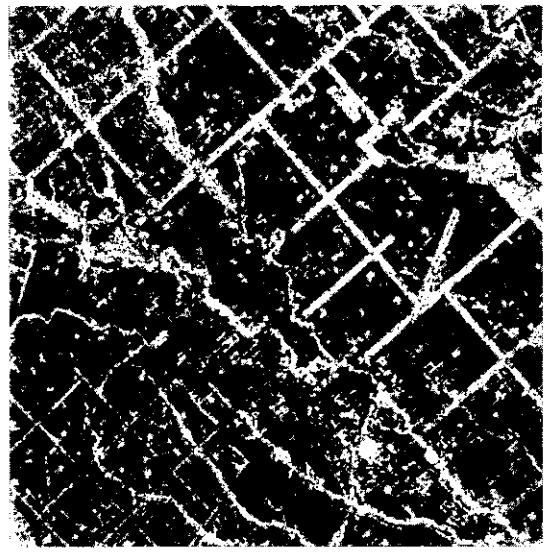

JERS-1 SAR (1992.4.15)

LANDSAT TM (1991.6.26)
R:BAND5 , G:BAND4 , B:BAND3

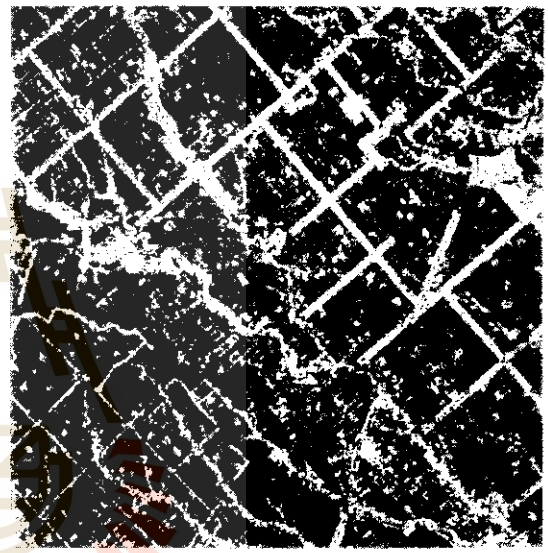

JERS-1 SAR (1993.6.30)

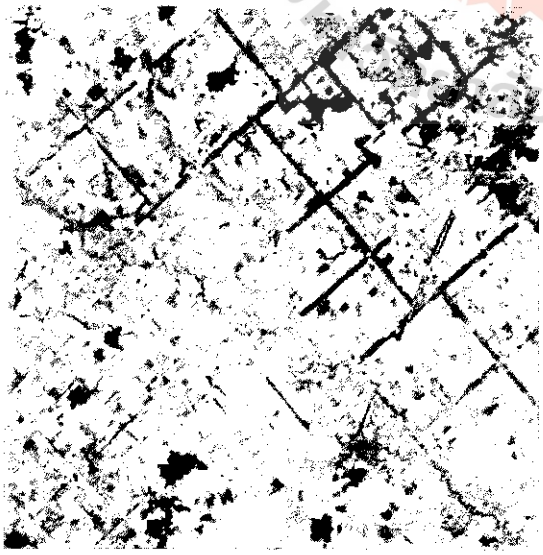

LANDSAT TM (1990.8.3)
R:BAND5 , G:BAND4 , B:BAND3

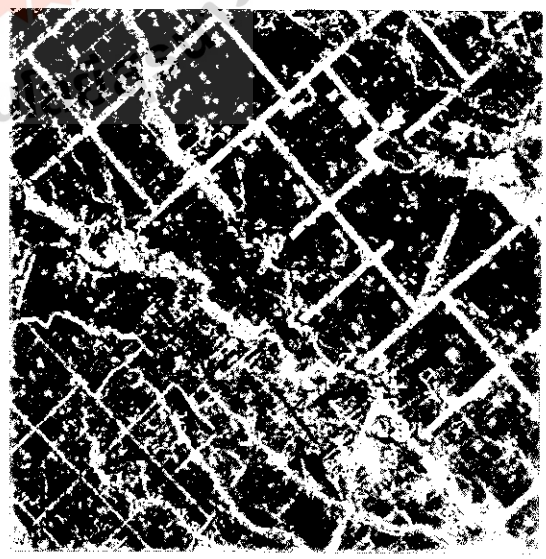

JERS-1 SAR (1993.8.13)

Photo 1. JERS-1/SAR and LANDSAT/TM images in Konsen-plateau

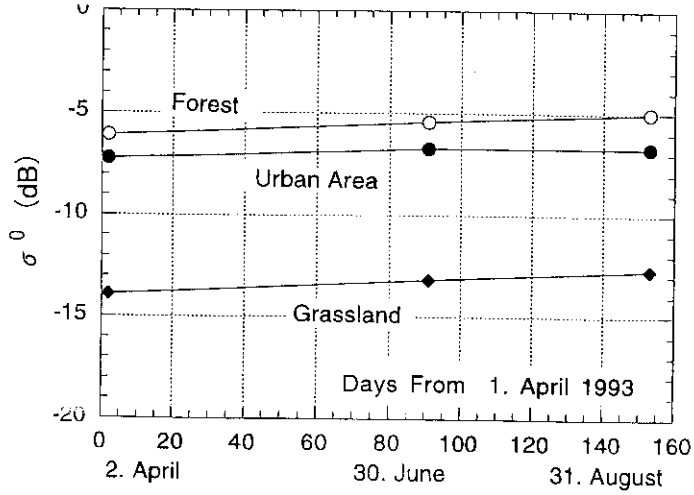

Fig. 1 Back Scattering Coefficient of JERS/SAR on Konsen Plateau.

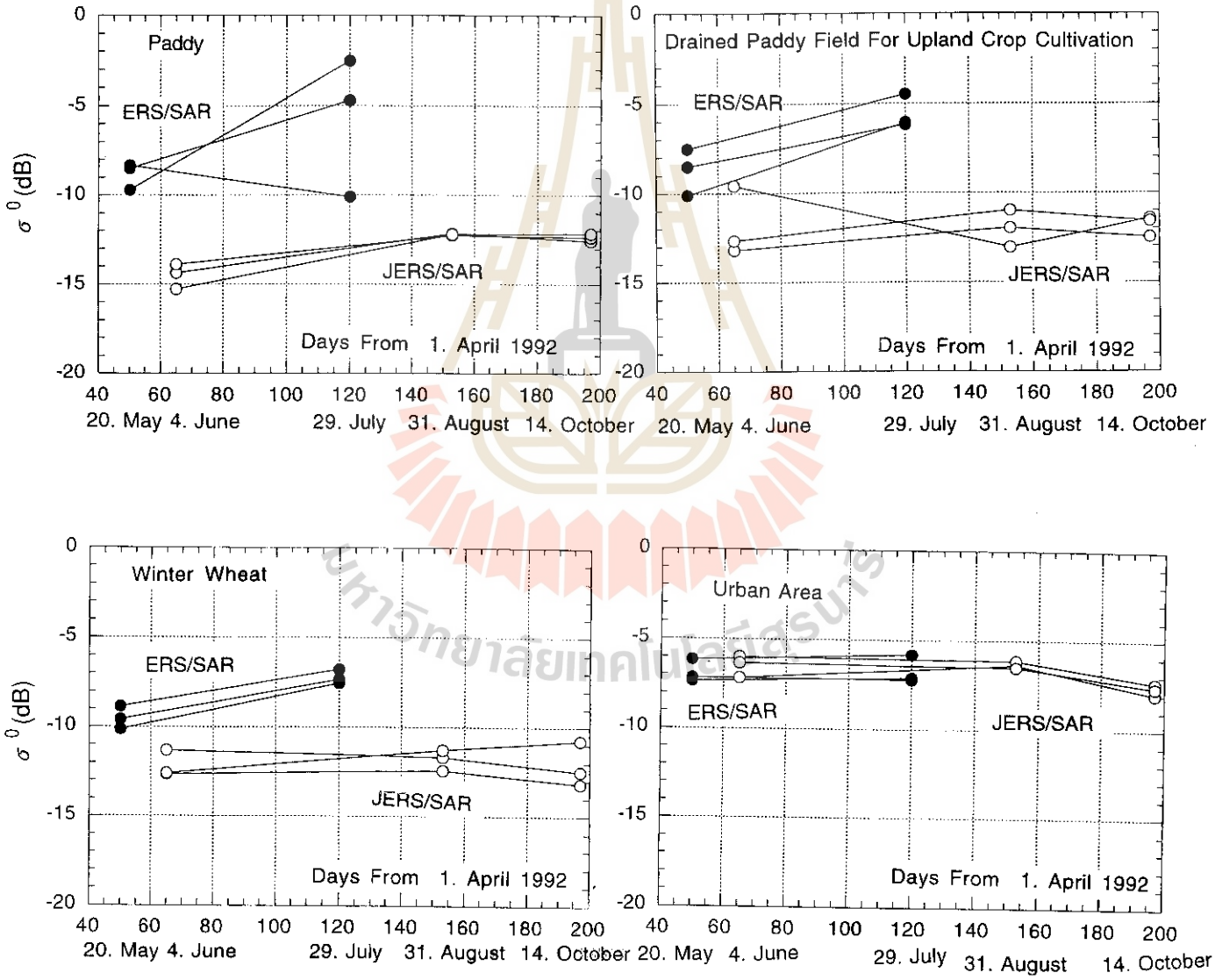

Fig. 2 Back Scattering Coefficient on Ishikari Plain.

almost no differences in the value throughout the year and they are constantly low. As for back scattering coefficients of ERS-1/SAR in winter wheat and soy bean field, values of July are higher than those of May because of biomass. For both back scattering coefficients of JERS-1/SAR and ERS-1/SAR in urban area, values are equally high in all times.

4. Conclusions

The comparison between JERS-1 and ERS-1 SAR images showed that JERS-1/SAR (L-band SAR) microwaves pass through agricultural plants and then scatter at land surface while ERS-1/SAR (C-band SAR) microwaves scatter at agricultural plants. We cannot get direct information about agricultural plants but we can get useful information about agricultural environment using JERS-1/SAR data. The ERS-1/SAR can directly measure agricultural crops, but the data include many other information about soil surface and topographical conditions.

Trees and agricultural crops (including grasses) show very similar spectral reflectance pattern. By only using data from optical sensors such as LANDSAT/TM, it is difficult to distinguish one from another. However, by using JERS-1 data, it is easy to distinguish them because trees have high back scattering coefficient by volume scattering at trunks and branches while agricultural crops have low back scattering coefficient by no volume scattering.

In urban areas, SAR data have high back scattering coefficient. On the other hand, agricultural field, bare soil and water areas have low back scattering coefficient. Using JERS-1 data, we can easily extract agricultural field because of their low back scattering coefficient. We made a distribution map of agricultural field a in Konsen Area in the north-eastern part of Hokkaido using filter treatment of speckle noise reduction in order to extract agricultural field.

A seasonal change can be observed in ERS-1 data between June and August at Tokachi plain and Ishikari plain. Agricultural field shows low back scattering coefficient in June and high value in August. In JERS-1 data, it is difficult to detect the seasonal change in Konsen-plateau.

REFERENCES

(1) NASA: Synthetic Aperture Radar, Instrument Panel Report, vol. IIf, Earth Observing System,1987
(2) CCRS: Radar Data Development Program, Gananoque Workshop, 1990

UTILIZATION OF SATELLITE REMOTELY SENSED DATA AS AN INFORMATION SOURCE FOR A GIS IN AGRICULTURAL RESOURCE MANAGEMENT

Farhad Jenabfar

Remote Sensing / GIS Division, Agricultural Statistics & Information Department (ASID)
Ministry of Agriculture, 14155 Tehran, Iran
Tel: (+98) 21 6122102 Fax: (+98) 21 650377

ABSTRACT

Landuse/Landcover data is one of the most important data layers in any Geographic information System for agricultural resource management. The lack of recent, reliable and up-to-date data for prepration of Landuse/Landcover maps has made satellite imagery, the only practical source of up-to-date data for such studies. The study area located in north of Iran, Gilan province, was selected because of its variable vegetation and economic importance. Three different seasonal TM data sets, acquired between 1991 - 1994, were utilized in the prepration of Landuse/Landcover maps which comprised seven major classes (24 sub-classes) and four mixed classes. In addition some specific crops like Tea and Olive were also mapped. The information derived from these maps together with other data such as Topography, Transportation network, International and Provincial boundaries, etc were compiled for use in the envisaged GIS that will eventually have more than 25 different information layers.

INTRODUCTION

Geographical Information Systems (GIS) provide an essential technology for concidering the interaction between spatial distribution of resources. GIS are now established as a common feature of both managemaent and research in areas such as; natural resource inventory; mineral exploration; primary production estimation and natural hazard evaluation.

Probably the biggest problem in a Geographic Information System is the base maps that the software uses to perform its analysis. The deficiency of these maps or updated ones is the main reason for using remotely sensed data as a consistent source of information. The results of visual image interpretation and digital processing can now fulfil a number of functions within a GIS.

This paper describes the methods used to create an agricultural GIS and problems encountered in this way.

STUDY AREA

The area selected for this project is Gilan Province, located in north of Iran, limited between long. 48°, 35′ - 50°, 35′ E and lat. 36°, 30′ - 38°, 30′ N, with the total area about 15000 km².

The role of this province in national agriculture is the main reason for its selection. More than a quarter of the Rice production and about the whole production of Tea and Olive in the country obtain from this province. On the other hand more than 40 percent of this area is covered by dense, natural forests that has a significant role in wood industry.

DATA SOURCES

The use of image data to derive geographical information has long been established in the form of both topogrphic and thematic maps produced by the interpretation of stereoscopic aerial photographs. The sources of visual image interpretation serves to emphasize the potential for furthur improving the accuracy of digital image analysis, by including information other than spectral data (Haralick 1979). Especially in the extraction of LU/LC information for the compilation of thematic maps, visual interpretation has set a formidable precedent in terms of the number of

distinguishable classes.

The application of satellite remote sensing to natural resource mapping has therefore often encountered resistance where there has been a history of mapping by photo - interpretation (Rivard 1990). This is especially so when landcover information is stored in GIS and then used to derive thematic products in combination with a number of other themes that are often of layer or unspecified accuracy.

Despite the legacy of photo-interpretation, remote sensing data from satellites (especially Landsat TM and SPOT) have nonetheless become well established as a primary source of information in many applications related to natural resources. The inherently digital format of the data, the frequency of routine coverage of large areas, the lower cost of data and the relative ease with which near - nadir imagery can be geo-referenced all offer very significant advantages over photographic coverages of the same area (Konecny 1979).

The Landsat satellite series which began in the 1970's is probably the most well known digital imagery gathering system. The Thematic Mapper (TM) is a popular data source and consists of seven bands or spectral ranges. The seven bands are blue, green, red in the visible spectrum, a near infra-red, two mid range infra-reds and a thermal infra-red.

The typical TM scene covers 185 km × 170 km of the earth surface and is repeated every 18 days. The data is organized into a matrix with each pixel covering an area of 30 by 30 meters. In each of the seven bands each pixel contains one data value representing the spectral intensity reflected from relative surface on the earth.

In this project 3 different seasonal TM data sets, acquired between 1991 to 94 and a CCT (1993) containing the whole coverage of the study area were selected to create LU / LC maps of the province.

DERIVING BASE MAPS FROM IMAGE DATA

A very important application of high spatial resolution satellite data is their use as a base map, especially in those application where no other reliable data is available (Gastella-Etchegorrg 1989).

Digital satellite data have a number of advantages over conventional photo-grametric methods in terms of providing cartographic information (Swann 1988). Satellites provide regular, repeat coverage, and the required data can often be simply extracted from an archive. The data are inherently digital, and so can be used directly in digital cartographic production systems. Data costs are often much less than for an equivalent aerial photographic coverage, and the cost of establishing ground control is very much less when using near - nadir satellite imagery.

Both visual interpretation and digital image processing softwares were used in the project. The below stages have been concerned;

* Visual image interpretation of 8 TM quadrants of three different dates, covering whole province according to the legend approved by Project Manager; containing seven major classes (Forests, Cultivated areas, Ranges, Wetlands, Bare lands, Water resources, Constructed area) divided into 24 sub-classes and four mixed classes. In addition, another features such as Roads, Rivers, International and Provincial boundaries were mapped.

* Digital image processing;
  - Mosaicking of TM quadrants, covering the whole province and masking the interested area.

- Image rectification, geometric correction of the mosaicked image, using 1:50,000 scale topomaps and ground control points (GCP) selection (image / map registration). Geometric correction of an image is necessary because in GIS applications the reference coordinate system is the foundation of the database. without a coordinate system coverages could not be accurately overlayed, compared or used for analysis. Once a coordinate system has been selected ground control points could be selected.

- Unsupervised classification of masked area to identify main agricultural regions and obtain the auxiliary information to be used in the furthur stages.

- Ground checking of unsupervised classification results to select the best areas for training sites.

- Concerning to the noticeable forest areas in the mentioned province, these areas were masked out to decrease the disk space and data processing time.

- Pre-precessing, enhancement and supervised classification of relative images. It worth to mention to raise the spectral separability, different kinds of data manipulation such as signature separability assessment, principal component analysis, filtering and the like were applied.

- Filed sample checking, using GPS facilities to determine the reliability of the classification and correct posible errors by statistical methods. In this step, the constant geodethic points were used as base stations for differential positioning with GPS.

- Plotting a hardcopy of classified image after all corrections.

By combination of the information derived from visual interpretation and digital image processing, the LU / LC maps of the province in 1:100,000 scale sheets, with 30′ by 30′ geographic coordinate were mapped.

CREATION OF THE GEOGRAPHIC INFORMATION SYSTEM

Two types of analyses that could use satellite imagery to create GIS coverages are ①when polygon boundaries are defined by another process but attributes are determined from the imagery, and ②when the polygon and their attributes are determined from the imagery. It is important to remember that the satellite data will need to be converted into an acceptable format by the Geographic Information Systems.

Satellite data generally have a raster data structure, which has considerable advantages during image processing operations. In contrast,the structure of data commonly used to represent geographical phenomena are vector based. At present, the majority of GIS use a vector data structure. Raster to vector data conversion is an essential step that can cause many problems. Other than raster to vector conversion, there remains a further and much more fundamental problem to be resolved before digital image data relating to natural resources can be incorporated automatically into GIS. This is the generalization of classified digital image data to the mapping scales commonly encountered in GIS (Ehlers at et al. 1989). The remotely sensed data that offer the most benefits for natural resource mapping currently come from the Landsat TM or SPOT satellites, whose sensors have ground resolutions of 30 and 20 meter, respectively. For the purpose of inclusion in GIS, these image data must be generalized to homogeneous polygons that cover an area, for example, of 100 or more pixel data. The generalization is well defined when each of the features being mapped can be uniquely classified, with the classified image consisting of relatively large domains - areas of the image which comprise a single class, with the possible exception of a relatively few, isolated,

pixels from other classes. Under these circumstances, an edge detection filter can be applied to define domain boundaris, a median or contextural filter used to generalize the data (e.g. Booth et al. 1989) and the intersection of the edge and median filtered data used to generate the general image prior to raster-to-vector conversion.

The operational procedure to create the GIS is outlined below;

* Input spatial data

- Digitizing basic geographic data of the province, using 1:250,000 scale topomaps.
- Digitizing contour lines layer from 1:50,000 topomaps.
- Scaning Landuse / Landcover maps derived from satellite data, raster-to-vector data conversion, create LU/LC data layers.
- Editing and create topology of the data, gathered in the previous steps.
- Building the geographic database,input attribute data of each geographic feature and any relative information.
- Data manipulation, projection, trans-formation, map-joinig, edge-matching.

APPLICATIONS

At this stage, the satellite image becomes useful to the GIS user as it is geographically referenced to other data sets. The primary application of the imagery is for base map generation and revision. This is carried out within range of feature coding of the digitised data. Completely new vector data files may be created or existing maps edited. A classified image can be used directly in raster overlay analysis, or the polygon boundaries can be vectorised and used in vector polygon analysis.

In view of the fact that this GIS was designed to be used as a tool in agricultural planning programs, by adding the information of soil, climate, geomorphology, socio-economiy, etc, it would be a very efficient and powerful database for the future plans of the Ministry.

CONCLUSION

The use of satellite data in the field of Geographic Information Systems is efficiently an important alternative in the creation of GIS coverages. In the past, three problem have prevented the use of satellite imagery within a GIS. Firstly, not enough information was visible in the data to warrant its use; secondly, specialised and expensive hardware was generally needed to process the data and thirdly, software was not available to analyse raster and vector together.

But the satellite imagery now, affords the user greater flexibilty, in determining scale, time of analysis, level of detail, and most imprtantly what information the coverage should contain. There are some standard digital carto-graphic products but for many others generating a coverage from satellite data may be the only alternative.

ACKNOWLEDGMENT

The author would like to thank the endless assistance of Mrs. E. Madanian (Senior Expert of GIS), in various steps of GIS creation.

REFERENCES

[1] S. Khan & R. Toleti, "Remote Sensing and Geographic Information System for environmental and pollution studies",Proc., International Geoscience and Remote Sensing Symposium, Tokyo, 1993

[2] C. M. Trotter, "Remotely-sensed data as an information source for Geographical information systems in natural resource management: a review", International Jour. of Geographical Information Systems, Vol. 5, No. 2, 1991

[3] G. Csornai, O. Dalia, J. Farkafalvy and G. Nadar, "Crop inventory studies using Landsat data on a large area of Hungary", Application of Remote Sensing in agriculture, London, 1990

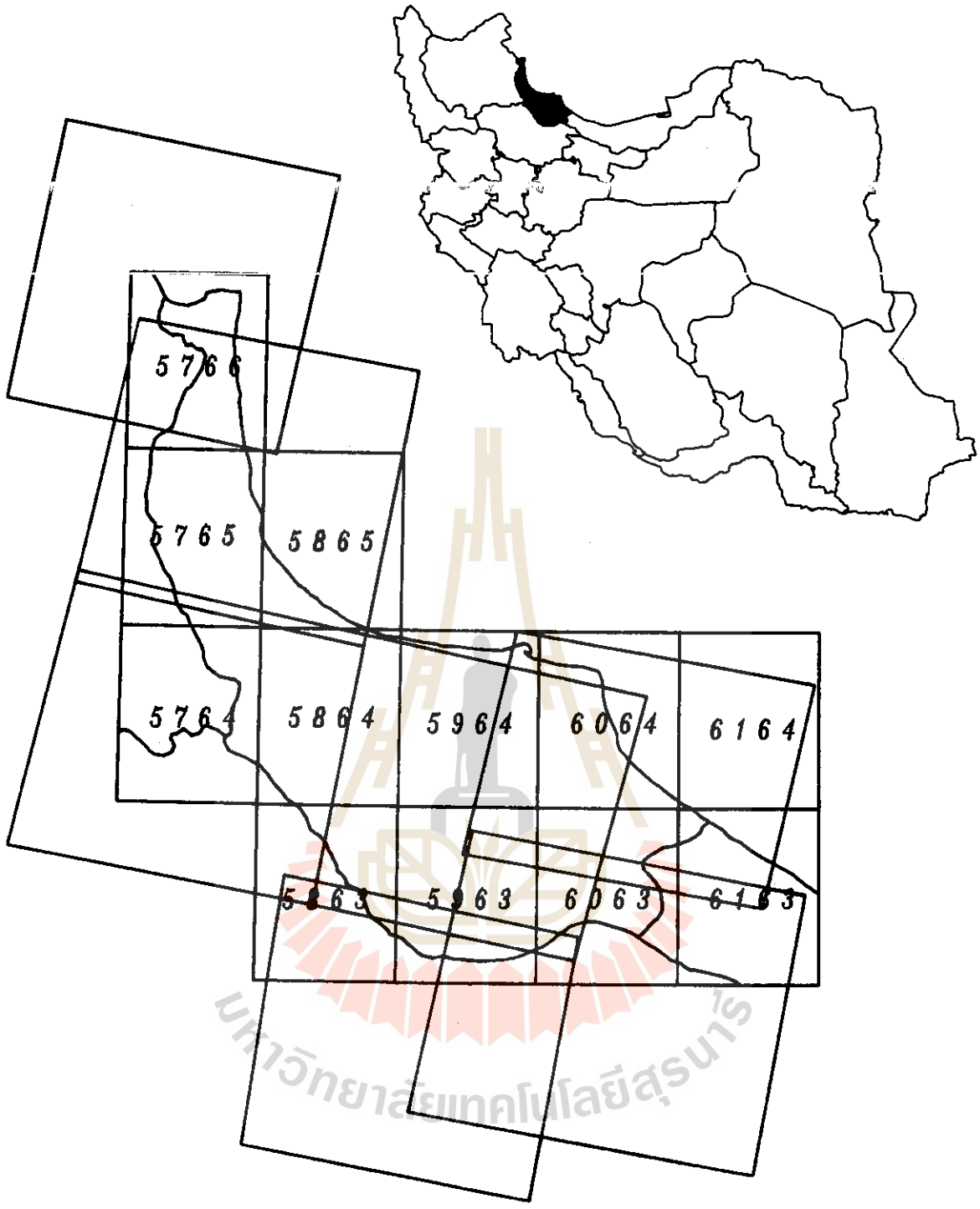

Location of the Study Area in North of Iran, Gilan Province

National Cartographic Index in 1:100000 Scale &
Coverage of TM Images were interpreted

SCALE = 1/2.000.000

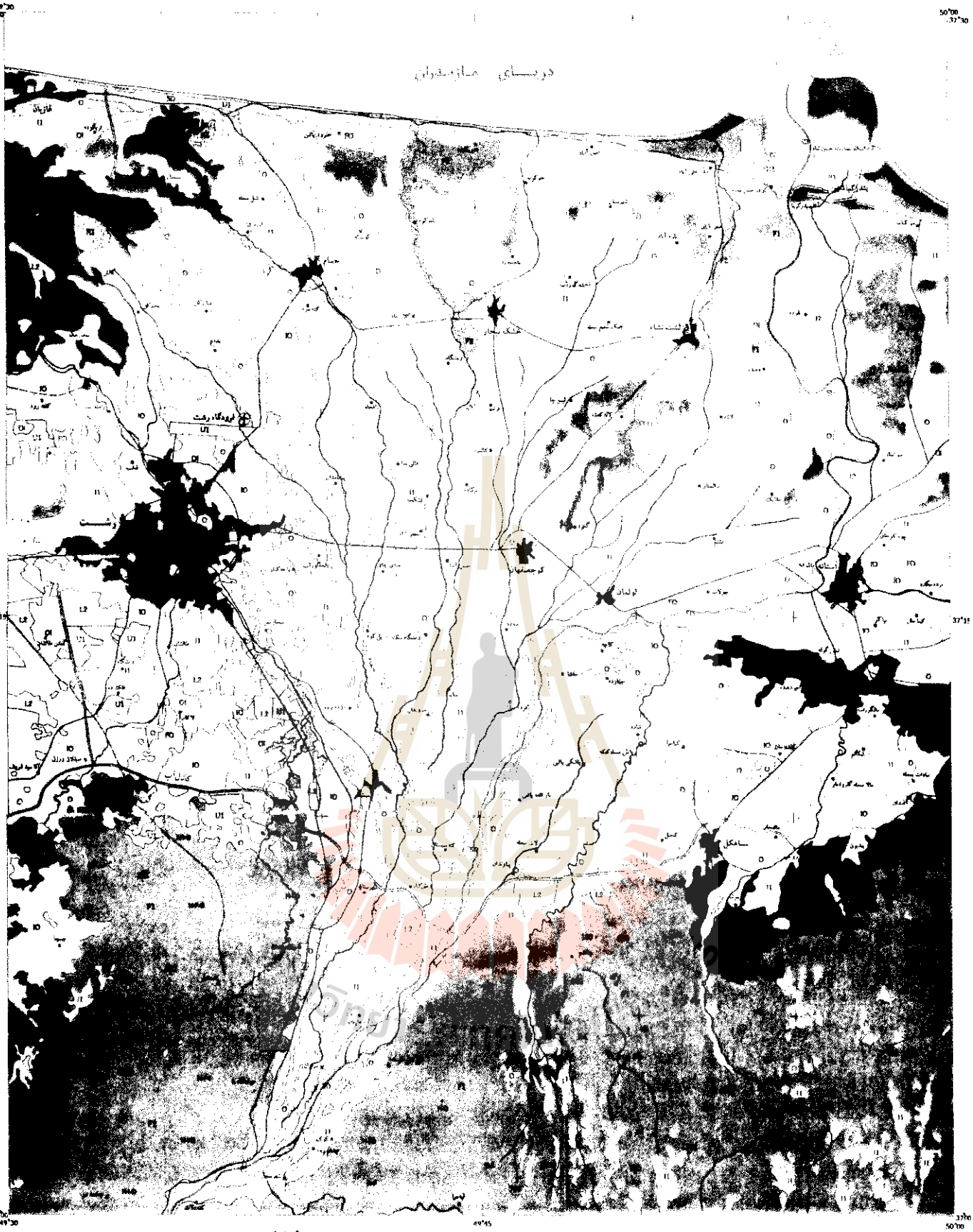

A scaled seet of Landuse/Landcovr maps; derived from satellite data

ASSESSMENT OF ERS SAR DATA FOR TROPICAL AGRICULTURAL CROP MONITORING

J. Aschbacher[1*], A. Pongsrihadulchai[2], S. Karnchanasutham[2], D.R. Paudyal[3], E. Nezry[1], M. Wooding[4]

[1]European Commission, Joint Research Centre (JRC), TP441, I-21020 Ispra (VA), Italy
Tel: Tel: +39-332-78 5425, Fax: +39-332-78-5461; e-mail: josef.aschbacher@jrc.it

[2]OAE, Phaholyothin Road, KU Campus, Bangkok 10900, Thailand

[3]Forestry Building, Indooroopilly, Brisbane QLD 4068, Australia

[4]RSAC, Mansfield Park, Medstead, Alton, Hampshire GU34 5PZ, UK

ABSTRACT

The current study discusses the potential of radar remote sensing for tropical agricultural crop monitoring. Theoretical considerations about radar backscattering of agricultural crops are presented and discussed. The theoretical considerations are complemented by actual case studies carried out on different agricultural crops such as rice, sugarcane, rubber plantations, and other crops. Temporal radar signatures are presented for different tropical crop types and compared with those of temperate crops. The presentation also compares different approaches regarding the analysis of SAR data, such as field based versus pixel based approaches, or data processing methods including speckle filtering, texture analysis and segmentation. Results obtained via different means are compared and discussed.

Among the case studies particular emphasis is given to the monitoring of rice using radar data. It can be shown that, for example, the use of radar data allows to retrieve rice area as well as accurate information about the plant's growth stage from ERS SAR data.

1. INTRODUCTION

The 1990's have seen major developments in the use of satellite remote sensing for agricultural monitoring and production forecasting. The 'Monitoring Agriculture by Remote Sensing' (MARS) project of the European Union, for example, is a major initiative using satellite-based techniques for the collection of crop statistical information. Also in tropical countries the use of remote sensing has become more important in recent years. At regional and local levels, there is increasing use of remote sensing as a source of information on changes in agricultural cropping and for production forecasting.

Agricultural applications of remote sensing are time critical. The accurate identification of crop types depends on the availability of images acquired within specific time windows through the crop growing season, when there are marked differences in the appearance of particular crop types on remote sensing images. Equally, there is a need for images acquired at particular key times for yield prediction purposes. Despite the progress which has been made towards operational applications, experience shows that high

* The work presented in this paper was carried out within the framework of the 'EC-ASEAN ERS-1 Radar Remote Sensing Project (ALA/ASN/91/28)". The project is funded by the European Commission (EC) with support from the European Space Agency (ESA) and the Association of South-East Asian Nations (ASEAN). In addition, the current project is supported by the Office of Agricultural Statistics & Economics (OAE) of the Thai Ministry of Agriculture and the National Research Council of Thailand (NRCT).

resolution visible and infra-red satellite sensors cannot always provide the desired information due to constraints related to cloud cover and revisit schedules.

Radar satellites like ERS-1 and ERS-2 overcome the problem of cloud cover. Synthetic Aperture Radar (SAR) systems transmit microwave energy down to the earth's surface and record the variable strength and phase of the 'backscattered' return signal. Images are obtained independently of cloud coverage or daylight conditions and contain information on roughness and dielectric properties of the surface. Radar is sensitive to the structure and moisture content of vegetation canopies, and to soil roughness and moisture content.

The use of radar remote sensing for tropical agricultural monitoring

There is a great variety of tropical agricultural crops, examples of which are rice, sugarcane, maize, tapioca, coffee, tea, rubber and fruit tree plantations. However, in this paper emphasis is put on rice, being the crop with the largest economic and social importance for many tropical countries. The example of rice monitoring and mapping also highlights in an exemplary manner the potential of radar remote sensing and is applicable in principle to many other crops. A short discussion on agricultural plantations and other agricultural crops (e.g. sugar cane, maize) complements the assessment of radar for rice mapping and monitoring.

2. COMPARISON OF DIFFERENT DATA ANALYSIS TECHNIQUES

Paudyal (1994) has investigated also other land cover categories at the Thailand study area, where, apart from rice fields, also large plots of sugarcane are present, intermixed with bushes, shrubs, water and urban areas.

Various classification methods were compared such as maximum likelihood with knowledge based classification methods, or unfiltered versus speckle filtered and/or texture analysed images. The latter method was developed making use of pre-assumptions about the rice growth cycle based on temporal profiles of σ^o [dB]. These results were compared with a Landsat TM image and ground measurements for accuracy assessment. A tabular overview of the classification results is given in Table 1.

Table 1: Classification accuracy for different classification methods based on five radar image dates. The observed land cover categories in the Thailand study area (Kanchanaburi) are rice, sugarcane, bush, shrubs, water and urban areas (from Paudyal, 1994).

No.	Classification method	Input data	Overall Accuracy (%)	Rice Accuracy (%)	Sugarcane Accuracy (%)
1	**Max. likelihood**	unfiltered	65.3	58.4	70.8
2	**Max. likelihood**	MAP speckle filtered	69.9	72.4	73.0
3	**Max. likelihood**	Lee speckle filtered (2 iterations)	75.2	78.0	87.5
4	**Max. likelihood**	texture (angular second moment plus contrast)	69.9	63.9	73.1
5	**Max. likelihood**	texture (ASM + IDM) plus speckle filtered (Lee)	79.7	77.8	87.7
6	**Knowledge based segmentation**	MAP filtered	79.9	91.8	71.0

The results of the supervised classification based on five dates (MAP-filtered, Nezry et al., 1991) has given an overall classification accuracy of 69.9%, while the knowledge-based method gave 79.9%, which is a clear improvement. The same accuracy was obtained when combining speckle and texture analysed images as input for a maximum likelihood classification. As an example, the classification accuracy matrix was extracted for the agricultural crops rice and sugarcane only, and compared with the overall accuracy including all six land cover categories. It is worth noting that the accuracy of rice alone has increased from 72.4% for the MAP-filtered classification to 91.8% for the knowledge-based segmentation method. For sugarcane, however, the combined speckle filtered and texture analysed images are the best input source for further classification. The accuracy reaches 87.7% in this case.

As can be seen from Table 1 there is no general method superior to another if all land-use categories are considered. However, the more sophisticated methods which combine speckle filtered and texture analysed data are clearly superior to a classification using only unfiltered or speckle filtered images. The knowledge-based method was adapted to discriminate rice fields from other categories and performs best for the category of rice. A further description of the methodology can be obtained from Paudyal (1994).

3. RICE CROP MAPPING AND MONITORING

Study area and Data Basis

A study area of approximately 10x10 km^2 size was selected in West Thailand (99.5 deg E, 14.0 deg N). The rice growing area is irrigated, flat, homogeneously managed, and has large individual fields of at least one hectare size. Multi-temporal ERS-1 SAR data were available at eight acquisition dates, namely 22-Nov-91, 7-Oct-92, 24-Feb-93, 7-May-93, 11-Jun-93, 20-Aug-93, 29-Oct-93 and 3-Dec-93. Within the whole area ten sample areas of approximately ten hectares each were selected for detailed backscattering studies of rice fields. Extensive ground measurements were taken in parallel to ERS-1 data acquisitions during the main growth period Aug-Dec 1993. Plant height, plant moisture content, plant density, number and size of leaves, stalk diameters, height of standing water were measured, together with more general observations regarding the state of the water/soil surface, state of plants, and weather at acquisition time. The analysis of ERS-1 SAR data was supported by aerial photographs and a Spot panchromatic image.

Rice plant growth and Radar signature of rice fields

Rice has three major growth phases, the *vegetative*, *reproductive* and *ripening phase*. In the selected study area the growth cycle lasts 120 days, and two harvests per year are common. The main growth period lasts from August to December, a second crop grows from April to July.

In ERS SAR images rice fields appear dark during the *vegetative phase* when the fields are flooded. During the *reproductive phase* radar backscattering increases and reaches a maximum in the *early ripening phase*. This maximum may plausibly be attributed to multiple radar reflections between vertical plant structures and the horizontal water surface at a growth stage when penetration to the surface is still possible. Later, during the *ripening phase*, the scattering from the volume of the canopy increases but penetration to the water or soil surface decreases leading to a slight darkening in the radar image.

Results - Rice area mapping

Rice acreage can be retrieved from multi-temporal radar imagery making use of the unique backscattering signature of rice fields which is significantly different from that of any other land-cover. Fig. 1 shows a multi-temporal image taken on 6-Jun-93, 29-Oct-93 and 3-Dec-93, where the rice growing area appears in dark grey and can easily be discriminated from other land covers.

A simple, pixel-based maximum likelihood classification was carried out, based on four Gamma MAP speckle filtered radar images (6-Jun-93, 20-Aug-93, 29-Oct-93, 3-Dec-93). The result of the classification is shown in Fig. 2. The classification accuracy for rice versus other land-use classes is 89% (Aschbacher et al., 1995; Aschbacher, 1995).

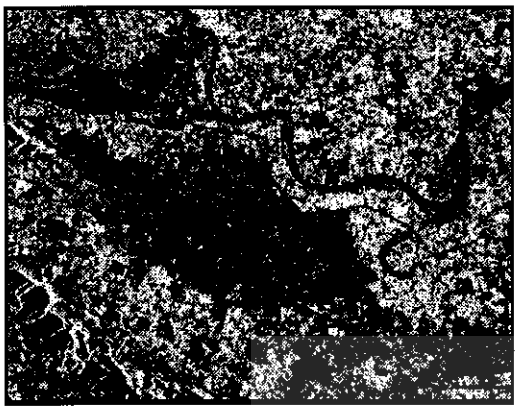

Figure 1: Multi-temporal ERS-1 SAR image of Kanchanaburi, W-Thailand. Rice fields (dark, centre) are clearly discriminated from other land-use categories.

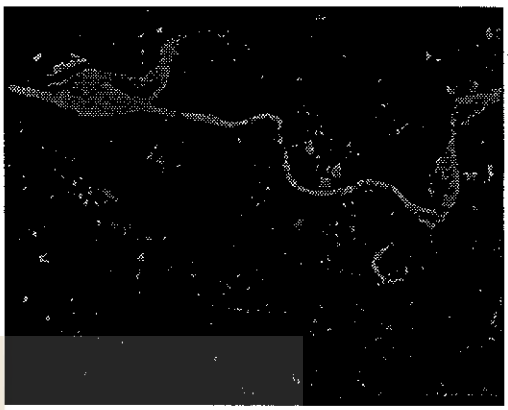

Figure 2: Rice area based on four ERS-1 SAR data acquisitions (6-Jun-93, 20-Aug-93, 29-Oct-93, 3-Dec-93). Grey scale: rice (dark), water (bright), other land-use classes (black).

Results - Rice Crop monitoring

Radar sensors have the potential to monitor rice plant growth regardless of cloud cover. An example of temporal radar signatures compared with rice plant height is shown in Fig. 3, which shows a correlation between rice plant height and radar backscattering σ^0 [dB]. The correlation coefficient is r=0.77. Also, a correlation between measured yield and σ^o values was carried out for the pre-harvest date 3-Dec-93. The fields were harvested 2-4 days later. The corresponding correlation is shown in Fig. 4. The correlation coefficient is r=0.87. It should be noted, however, that the sensitivity of radar backscattering is mainly related to the plant's total biomass, its moisture content and the plant's geometry, and therefore grain yield may only be an indirect effect of these parameters. Nevertheless, the result is interesting and worth further investigations.

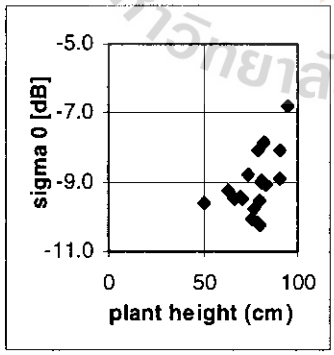

Figure 3: Correlation between plant height and radar backscattering coefficient, including data from 29-Oct-93 & 3-Dec-93.

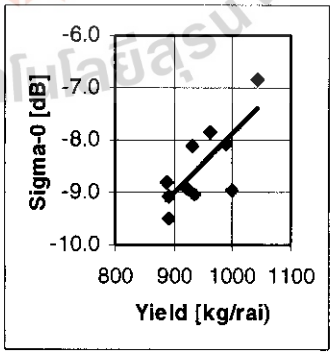

Figure 4: Correlation between measured rice yield and radar back-scattering coefficient, for the pre-harvest date 3-Dec-93.

4. CONCLUSIONS

Among all the agricultural crops the use of radar remote sensing is probably most promising for rice crops due to its significant temporal backscattering signature. The dynamic range of so [dB] is the largest among all agricultural crops, ranging from approx. -16 dB during the flooded and early growing stage to approx. -8 dB during the pre-harvest stage. The selection of appropriate acquisition times is crucial for mapping purposes. As regards yield estimates or parameters that lead to yield estimates there is a clear correlation between radar backscattering signals and plant height, which allows to determine the approximate age of rice plants and thus a prediction of the approximate harvesting time. The results available from several case studies allow to draw the following conclusions as regards the use of ERS-1 SAR data for rice mapping and monitoring (Aschbacher et al., 1995, Kurosu et al., 1993, Le Toan, 1989):

1. Multi-temporal ERS-1 SAR data can be used in an operational or quasi operational mode for mapping of rice fields, both for irrigated and rain-fed fields.

2. Multi-temporal ERS-1 SAR data can be used in a pre-operational manner for the retrieval of yield-related parameters.

3. A priori knowledge about the rice crop calendar and growing practices as well as parallel in-situ measurements largely facilitate the interpretation of radar images. However, reliable results can be obtained also without or with a very limited set of in-situ measurements. This is of particular interest in view of large scale operational rice monitoring systems.

4. For mapping purposes at least three dates should be available during the growing cycle. The optimum acquisition times are during the early flooded stage, the flowering stage and shortly before harvest. An additional post-harvest image is useful if the time of rice harvest is different from that of other agricultural crops on the same scene.

5. For the retrieval of yield-related parameters the use of 4-8 acquisitions during the growth cycle is recommended. The image dates should be equally spread throughout the growth period. An acquisition shortly before harvest is mandatory.

6. Multi-temporal ERS-1 SAR data can be used to determine field management practices, such as the timing of irrigation, time of harvest, method of water supply (irrigated or rain-fed), and the length of the growth cycle. This information can be retrieved largely without in-situ measurements.

7. As regards the optimum analysis technique applied to radar imagery for rice mapping it is recommended to speckle filter the images and apply texture and/or segmentation based algorithms before classifying the images. Depending on the characteristics of the respective scene special measures may have to be applied if field management differs within one scene.

8. If an operational rice monitoring system is developed it is strongly recommended to include multi-temporal radar imagery as a prime data source.

REFERENCES

Aschbacher, J., A. Pongsrihadulchai, S. Karnchanasutham, C. Rodprom, D. R. Paudyal, T. Le Toan; 1995: "Assessment of ERS-1 SAR data for rice crop mapping and monitoring"; Proc. IGARSS '95, Firenze/Italy, pp. 2183-2185.

J. Aschbacher, "Tropical Crops", chapter 6 in ESA-SP-xxx (The potential of ERS satellite radar in agriculture, Ed. M. Wooding et al.), ESA Publ. Div., ESTEC Noordwijk, October 1995 (in press).

T. Kurosu, T. Suitz, M. Fujita, K. Chiba and T. Moriya, "Rice crop monitoring with ERS-1 SAR: A first year result", Proc. 2nd ERS-1 Symp., Hamburg, 11-14 Oct. 1993, pp. 97-101.

T. Le Toan, H. Laur and E. Mougin, "Multi-temporal and dual-polarisation observations of agricultural vegetation covers by X-band SAR images", IEEE Trans. Geosc. Rem. Sens., Vol. 27, No. 6, 1989, pp. 709-718.

E. Nezry, A. Lopez and R. Touzi, "Detection of structural textural features for SAR image filtering", Proc. IGARSS 1991, pp. 2169-2172.

D. R. Paudyal, "An assessment of spaceborne radar remote sensing for monitoring of tropical agriculture", Doctoral thesis (unpublished), Asian Institute of Technology, Bangkok, Thailand, 1994.

ACKNOWLEDGEMENTS

The work was carried out within the "EC-ASEAN ERS-1 Project (ALA/ASN/91/28)", which is funded by the EC, ESA and ASEAN (Association of South-East Asian Nations). Additional support was provided by the Office of Agricultural Statistics & Economics (OAE) and the National Research Council of Thailand (NRCT). The author wishes also to thank their colleagues who provided valuable input to this paper, in particular Mme T. LeToan (CESBIO Toulouse) and J-P. Malingreau (EC JRC-MTV).

TECHNICAL SESSION C

MAPPING FROM SPACE

MONITORING LAND USE/LAND COVER CHANGES IN PHUKET ISLAND

by

S. Chutiratanaphan Land Development Department
A. Chanthanaroj Land Development Department
K. Otsuka Geographical Survey Institute
K. Katsuta Geographical Survey Institute

ABSTRACT

This paper outlines some major land use/land cover changes in Phuket Island, Southern Thailand. The rapid expansion of urban area has occurred both in town and along the seashore and abandoned tin mines have been changed to be golf course and luxurious resort. The changes in agricultural land are mainly the reduction of pararubber area and paddy field and the increasing of shrimp farm in the mangrove forest. All of these changes can be detected and identified by using SPOT and Landsat-TM data.

1. INTRODUCTION

The study was done in context of a combined project of the Land Development Department of Thailand (DLD) and the Geographical Survey Institute of Japan (GSI), finance was supported by The Science and Technology Agency of Japan (STA). The purpose of this paper is to monitor land use / land cover changes in Phuket Island, located in the Andaman Sea, Southern Thailand. It is the biggest island and the one of the most popular tourism land in the country. Its total area is about 539 sq.km.

During the last decade, the situation of land utilization need in this study area has been in critical stage. Due to the rapid growth of economic and population, the need of land for cultivation, human resettlement, tourism industrial and shrimp farming has drastically increased. These factors have caused a great deal of natural resource exploitation without proper planning. For instance, a large of luxuriant of mangrove forest

has been destroyed for shrimp farming, upland forest has been depleted for agricultural areas particular on the slope land and abandoned tin mines were changed to luxurious resort and some cultivation area. These changes are not only the natural resources degradation but also the deterioration of the environment. The use of remote sensing technique has proven to be a most valuable tool in monitoring land use/ land cover changes in this study.

2. THE STUDY AREA

The study area is Phuket island, which located in the Andaman Sea, Southern Thailand. It lies approximately between 7° $28'$ - 8° $13'$ N. latitudes and 98° $15'$ - 98° $28'$ E longitudes. The total area is about 539 sq.km., the population is about 162,694. The landscape of the study area is characterized by slope complex, rolling and undulating ,flat to nearly flat, mangrove back swamp forest and beach and beach ridge. The slope complex area (36.05%), rolling and undulating area(40.37%) are mainly covered by evergreen rain forest and pararubber plantation. Flat and nearly flat area(14.45%) is widely used for pararubber plantation and paddy field. The others are 9.13% of total area. Climate is defined as the tropical monsoon, mean annual rainfall about 2,227.6 mm. and the heaviest rainfall is in September and October.

3. OBJECTIVE

The main purpose is to monitor land use/land cover changes using remote sensing technology .

4. MATERIALS AND METHODOLOGY

Materials :

- Topographic maps are in the scale 1:50,000 covering the study area.
- Landsat5-TM image of path 130- row 54 (3R,4G,2B), acquired on February 15, 1993.

- SPOT image of path 26 - row 334 (2R,3G,1B), acquired on December 13, 1988.

Methodology :

- Collecting data.
- To specify changed areas from 1988 to 1993 for ground truth by using satellite data.
- Ground truth and collecting the local references data.
- Discussion and report.

5. RESULTS

The results of the study on the monitoring land use/ land cover changes in Phuket area by remote sensing technology using SPOT , Landsat-TM data and ground truth survey . The data are categorized in to 9 groups as follow, abandoned tin mines have changed to golf courses and built-up area, mangrove forest has changed to shrimp farm, rubber plantation has changed to built-up area, paddy fields has changed to built-up area and grass land and forest have changed to rubber plantation.

6. CONCLUSIONS

The main factors of land use/land cover changes in Phuket island are the rapidly increasing population, expansion of human community (including resorts and golf courses) and encroachment of mangrove forest to be shrimp farming. The remote sensing technique is appropriate tool to monitor land use/land cover changes in Phuket area. These results can establish trend in land use/land cover changes and utilized as guideline for natural resource and environment management in Phuket island.

7. ACKNOWLEDGMENT

We 'd like to express our great thanks to the staff of Science and Technology Agency of Japan for their suggestions and helps as well as the financial support for this joint project.

8. REFERENCES

B. Klankamsorn. 1992. Monitoring Mangrove Forest covered and Shrimp Farms in Thailand. Paper presented at ISY regional Seminar on Tropical Eco-System. 1992.

S. Chareonpong, *et al.*, Soil Survey in Changwat Phuket Report, Soil Survey and Classification Division, Land Development Departmaent, Bangkok, 226 p, 1984.

Y. Yasuoka, T. Miyazaki, Y. Iikura and S. Otoma (1988): Detection of land cover change from remotely sensed images using spectral signature similarity. Proc. of the 9th Asian Conference on Remote Sensing.

Y. yasuaka, T. Yokota, T. Miyazaki and Y. Iikura (1990) : Detection of Vegetation Changes from Remotely Sensed Images Using Spectral Signature Similarity. Proc. of intro. Geoscience and Remote Sensing Symposium'90.

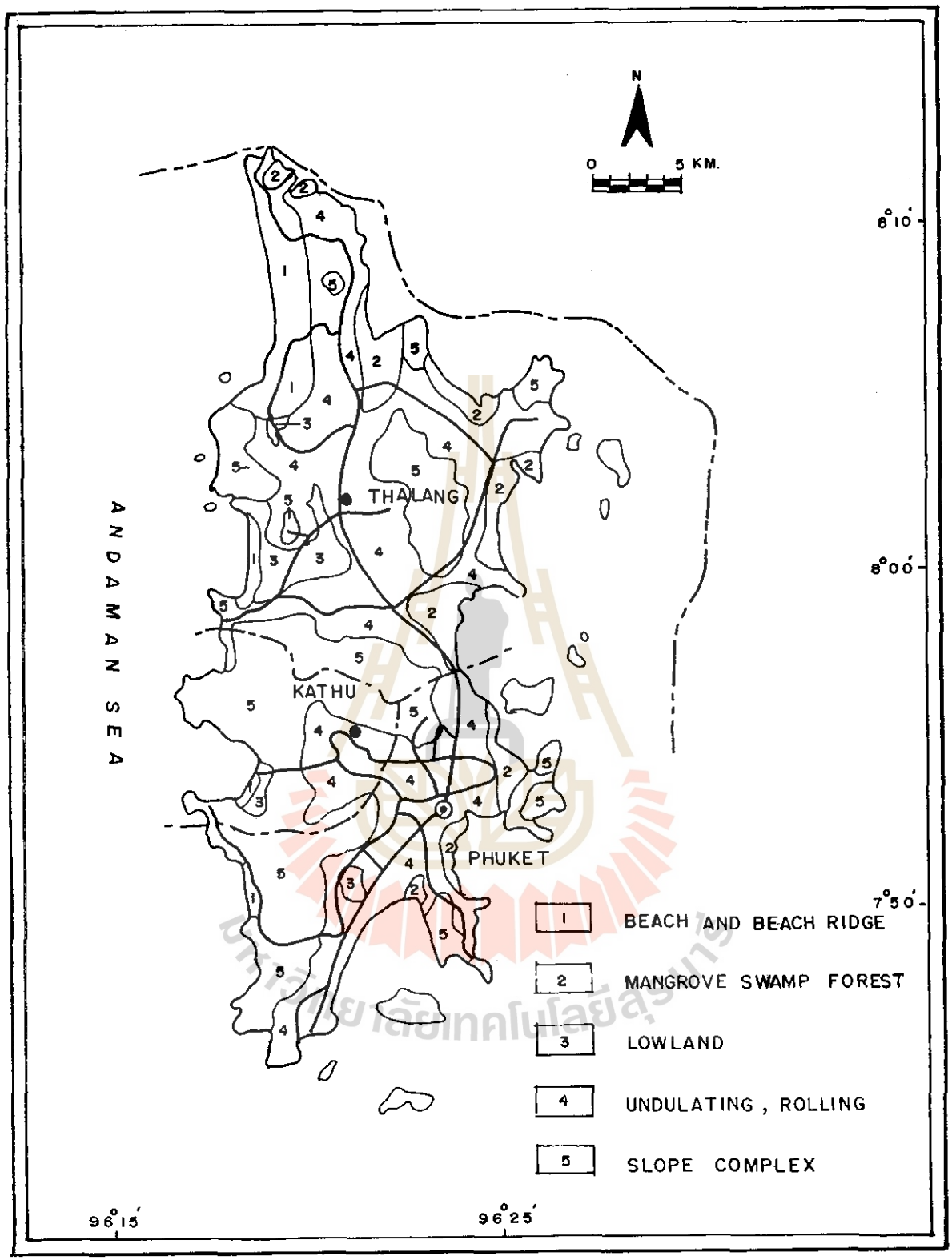

FIGURE : THE STUDY AREA

Measurement of Topographical variation by Hyogo-Nanbu Earthquake with JERS-1 SAR Interferometry

Yuichi Maruyama
Hiroji Tsu

Earth Remote Sensing Data Analysis Center (ERSDAC)
Forefront Tower, Kachidoki 3-12-1, Chuo-ku, Tokyo, JAPAN
Tel. 03-3533-9380, fax. 03-3533-9383

1. INTRODUCTION

The Hyogo-Nanbu Earthquake occurred on 17 January 1995 attacked the Kobe City and the Awaji island. More than 5,000 of human lives were lost under the collapsed houses and a fire.

The fault activity was observed on the several points in the area after the occurrence. The fault displacements were measured in many places. The deformation of the topographic surface, however, was hardly measured on the surrounded area of the fault line.

The purpose of this study is to know the availability of the interferometric SAR for the deformation of topographic surface by the earthquake with JERS-1 SAR data. Because, it can be very useful information for the study of active geological structure. In addition, it is also possible to apply for the natural disaster focusing such as landslide, volcanic hazards, etc.

For this purpose the area studied is selected in the northern part of Awaji island (Figure 1), where the Nojima fault, one of the active faults had moved to rise sever hazard.

2. METHOD

2.1 Data Used

The data employed to carry out double difference interferogram analysis are shown as followed:

(1) JERS-1 SAR data
   a. acquired on 9 September 1992
   b. acquired on 6 February 1995
(2) DEM
   It is 50m interval mesh data, that is based on 1:25,000 topographical maps.

2.2 Data Processing

The process to generate the interferogram and double difference interferogram image is shown in Figure 2. At the first step, phase preserved SAR imageries were created with the data from the 1992 and the 1995 scene, then interfered in them to create initial

interferogram. Then, reference interferogram was generated with the virtual phase and the 1992 scene data. The virtual phase was generated from the satellite position of 1995's scene to the DEM (Digital Elevation Model) surfaces.
The subtraction of these two interferogram could realize to obtain a double difference interferogram. The process and data matching are schematically shown in Figure 2 (B).

2.3 Double Difference Interferogram Imagery
The estimated phase difference was divided into three levels to assign them different colors (Figure 3), and the imagery divided into two levels is prepared additionally (Figure 4). These two kinds of imageries are prepared for the following purposes. The figure 3 is to understand total amount of topographic variation. JERS-1 SAR represent the topographic variation of 11.75 cm by single rotation. This value corresponds to a half of wavelength of JERS-1 SAR. The figure 4 is prepared as convenient imagery for the interpretation of small scale topographic deformation.

3. INTERPRETATION OF THE IMAGERIES

The double difference interferogram imagery was interpreted on the view point of geological study. The results are simply shown in Figure 5 and the following items are summarized.

1) Total variation of the area
A rotation of colors indicates the amount of topographic variation by the earthquake. The color rotation, red-green-blue-red in the double difference interferogram (Figure 3), repeats six times in this case, which means that vertical variation is recognized in 70 cm approximately in the Northern Awaji island after the earthquake.

2) Coinciding of the heavily displaced points and center of fringe pattern
The villages of Nojima-Hirabayashi and Nojima-Ohkawa are locating on the central part of the fringes (circular/oval pattern). Some of the biggest vertical displacement on the fault scarp was observed in those villages, Nojima Hirabayasi and Nojima Ohkawa. The displacement was approximately 1.8m as maximum, however such big displacement was only at the limited part of the fault.

3) The fault and related deformation
Location of the fault can be interpreted in discontinuity of the color, and they are making a lineament. The pattern of fringes does not cross the Nojima fault but there distribute many block patterns in the fault zone. Those blocks could be generated by the fault activity, right lateral strike-slip.

Most of the blocks developed along the Nojima fault have an elongated shape with axis from North to South. It seems that the ground surface was undulated by the right lateral strike-slip of the Nojima fault (Figure 4 and 5). This undulation might be in centimeter order, because the color of this area repeats in red and green, lacking blue color in most part (see Figure 3).

4. CONCLUSION

The result of image interpretation seems to be consistent to general idea of structural geology. In many cases, strike-slip structure involves en echelon folds with them.

Those folds have axis that cross the shear zone with narrow angle to moving direction. The swelling blocks in the strike-slip zone of Nojima fault are in small scale, however the direction of their axis is harmonious to en echelon folds model. It is considered that the undulation in the fault zone could be involved by the fault activity. From these view points, it can be concluded that double difference interferometry with JERS-1 SAR contain enough preciseness and useful for geological purposes in this area.

There, however, are still some problems to be solved before generalization. The topographic variation has not proved yet by field survey in a vast area. Back scatter of SAR come from ground surface, forest body by volume scatter and other artificial works. Seasonal change of forest condition affect on the phase generation. Wave length of microwave should be considered with relation to the vegetation condition. Massonnet, et al., succeeded to get topographical variation by Landers earthquake in California. This study indicates that C-band of ERS-1 SAR adapt to semi-arid zone where vegetation is sparse.

The mesh size and accuracy of the DEM data also have to be checked. JERS-1 is not designed for interferogram analysis, so data of satellite position is estimated in each time, which means there is high possibility to make mistake on the estimation.

Nevertheless, this technique is expected as a new accurate method to measure the topographical variation over the wide area in a short period.

ERSDAC/MITI is planning the next generation SAR program (SAR2), currently scheduled to launch early 2000s. As new SAR parameters, multi frequency, multi polarization and off-nadir angles are considered so far. Interferometry is also recognized as an important parameter for new SAR Mission.

REFERENCE

Boulter, C.A. ,1989, Four dimensional analysis of geological maps. Wiley
Massonnet, D., Rossel, M., Carmona, C., Adragna, F., Peltzer, G., Feigl, K., Rabaute, T., 1993, The displacement field of the Landers earthquake mapped by radar interferometry. nature, vol. 364
Lin, A., Imiya H., Uda, S., Misawa, T., 1995, Morphological characteristis of the Nojima Earthquake fault. Japan Society of Engineering Geology 36-1, P39-50
Haraguchi, T., Okamura, M., Tsuyuguchi, K., 1995, Report on the Nojima-Earthquake-Fault caused by the 1995 Hyougoken-Nanbu Earthquake. Japan Society of Engineering Geology 36-1, P51-61

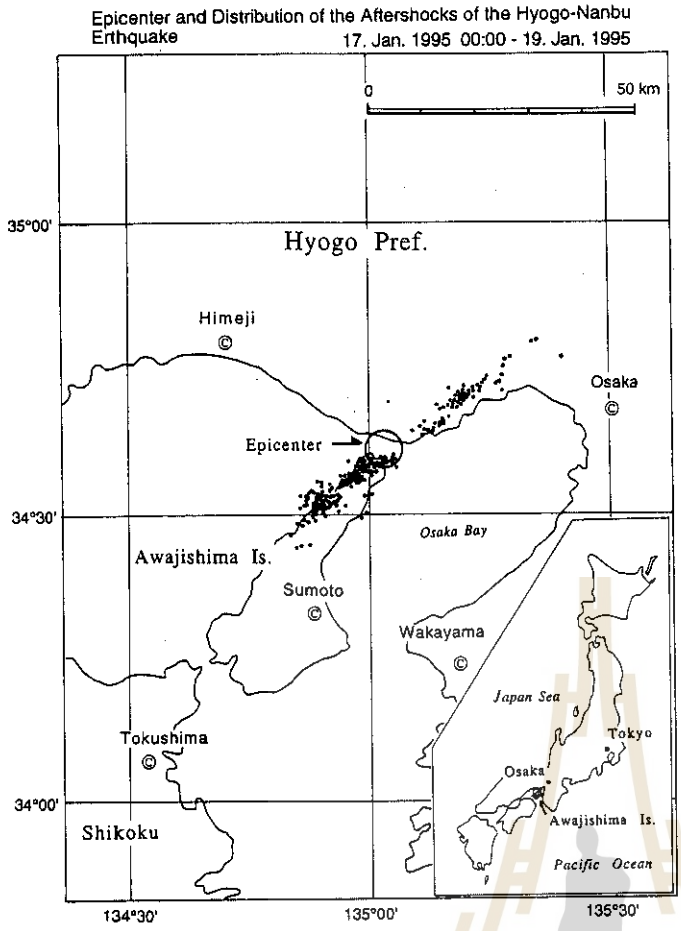

Figure 1

Location of study area

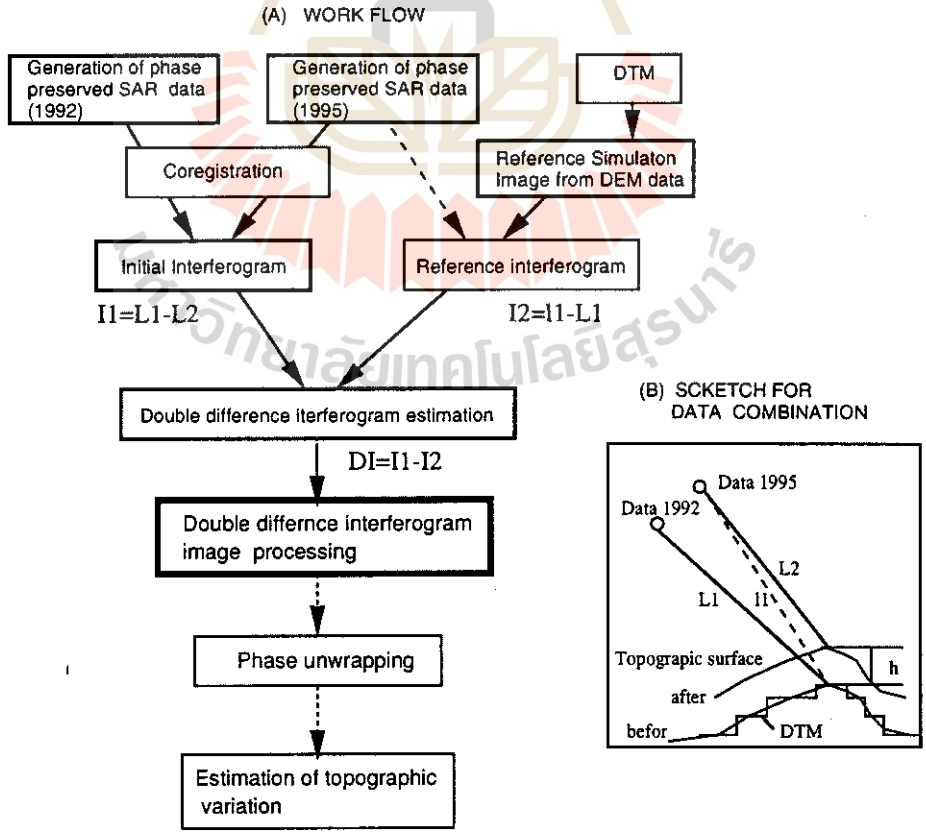

Figure 2 Flow and sketch for process of double difference interferogram image preparation

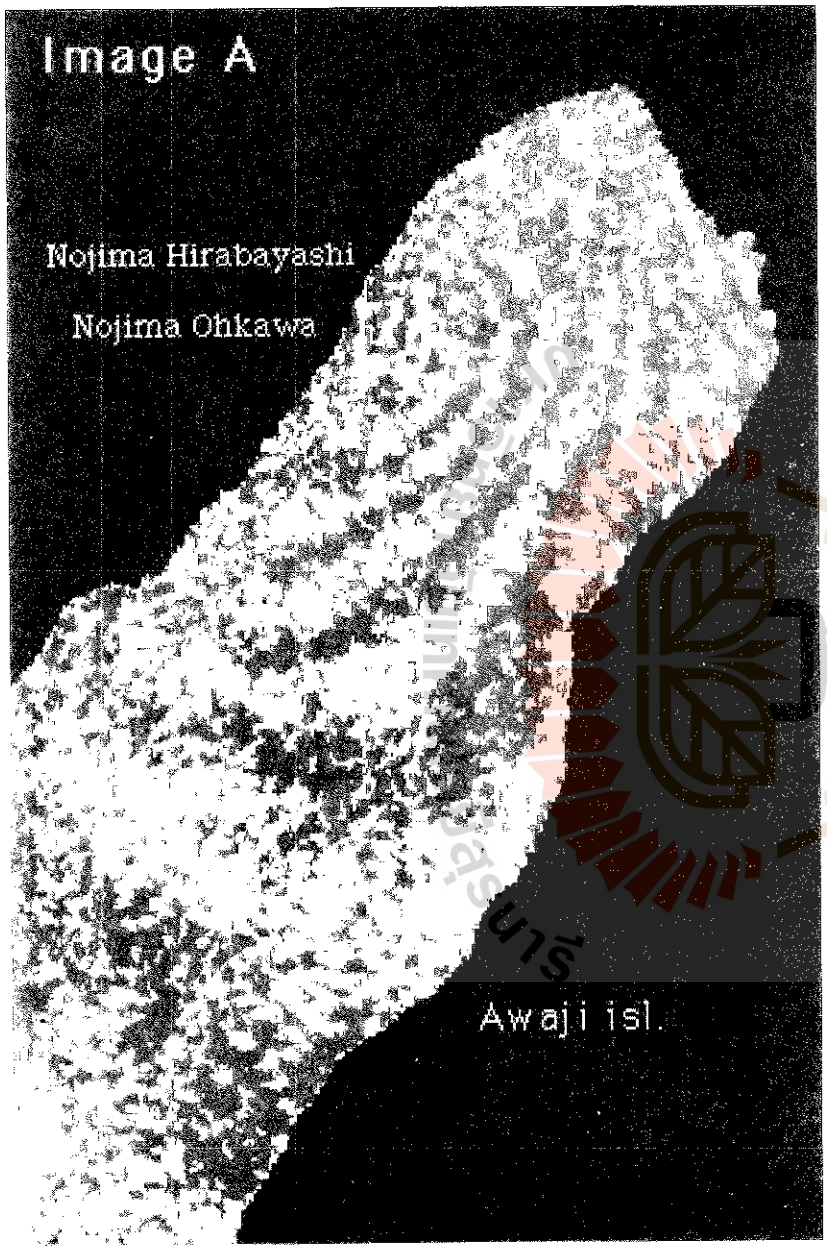

Figure 3 Double difference interferogram image (Divided into three levels)

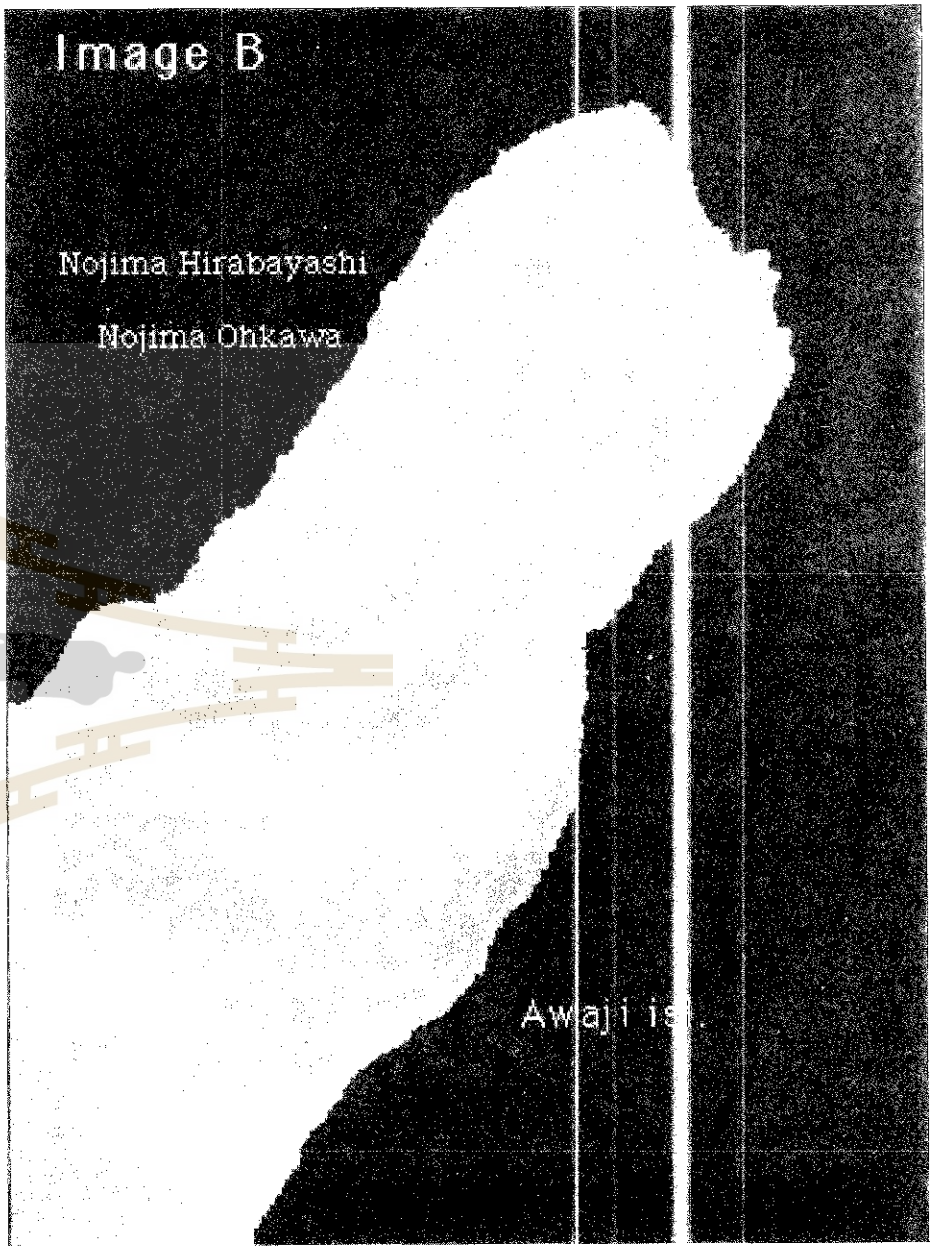

Figure 4 Double difference interferogram image (Divided into two levels)

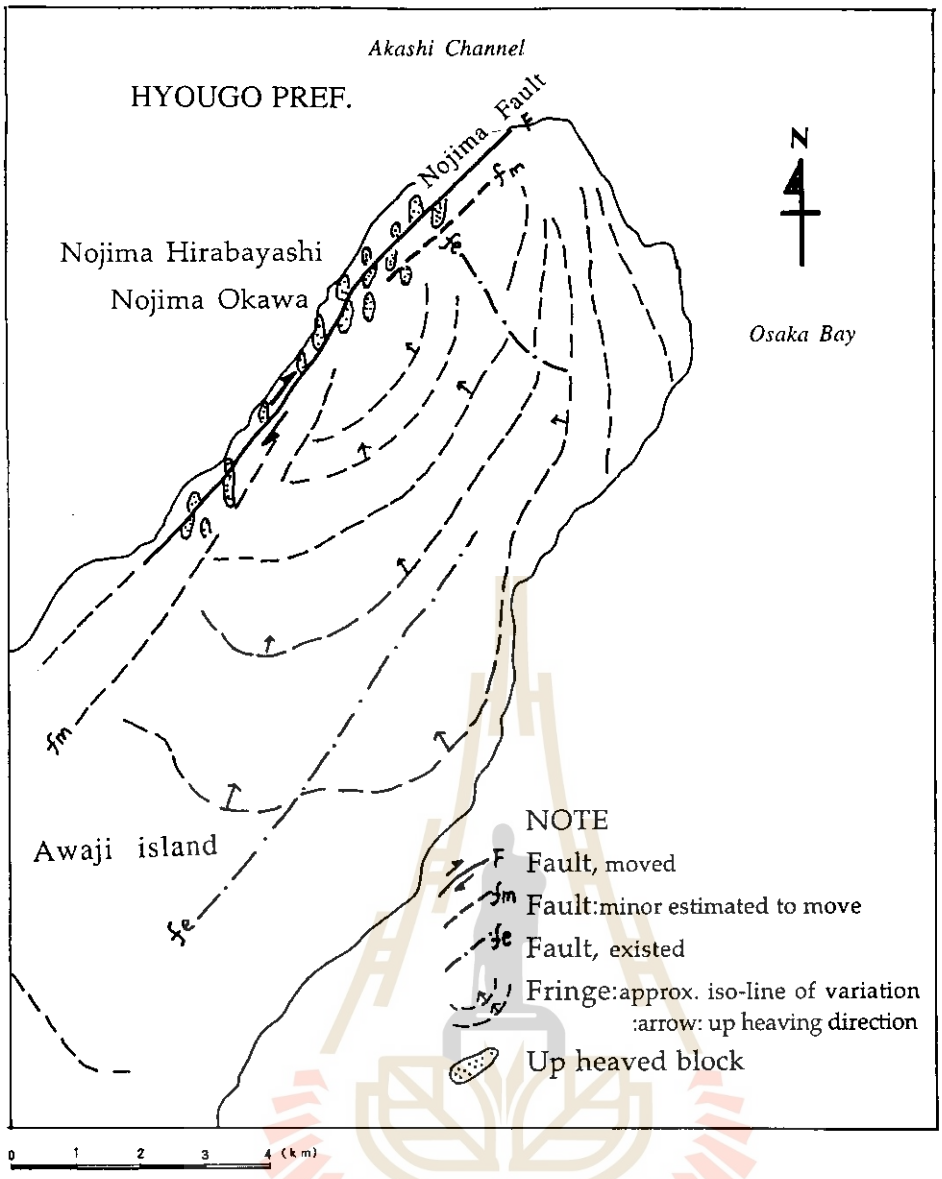

Figure 5 Geological interpretation of double difference interferogram image

DEM GENERATION BY SATELLITE IMAGERY AND ITS ACCURACY

Tsuneaki Shimoji
Geographical Survey Institute
Tsukuba-shi,Ibaraki-ken,JAPAN

ABSTRACT

DEMs were generated through stereo-matching technology by using stereo satellite imagery of JERS-1 OPS and SPOT HRV data. These data were evaluated by comparing them with existing DEMs derived from topographic maps. The accuracy was compared in the following two cases; (1) basically relying on satellite position and attitude data, (2) with many GCPs. The effect of pre-processing to original images are also tested.

No significant difference was found the accuracy of DEM in both cases. Pre-processing of images was found effective for removing large errors caused by mismatching around mountains tops.

1. INTRODUCTION

Three dimensional measurement of satellite images can be done by stereo pair images of SPOT satellite or JERS-1 satellite. Each satellite has its own characteristics. A high accuracy Digital Elevation Model (DEM) can be generated from SPOT data due to high resolution and satisfactory base-height ratio. As for JERS-1 data, stereo pair images can be obtained from the same orbit; that means time difference between stereo pair images is very small and thus the chance obtaining cloud-free stereo pairs increase.

We report in this paper the accuracy of DEMs generated by using stereo images of SPOT and JERS-1 through comparing them with existing DEMs, several cases are compared in view of target area's topography and existence of image pre-processing and so on.

2. TEST SITES

2.1 Test data

We selected test data where there are few clouds in the area so that matching accuracy is not influenced, and where are equally distributed mountains, valleys and hills. Test data used for both satellites are listed in Table 1 and 2.

Table 1. Test Data Used for SPOT Satellite

	Left Image	Right Image
Sensor	HRV-P	
Wavelength	0.51 μ m~0.73 μ m	
Path-Row	328-279 (Minobu)	
Date	1992.11.12	1992.11.16
Pointing Direction	R 17.2 degrees	L 20.9 degrees

Table 2. Test Data Used for JERS-1 Satellite

	Nadir looking image	Forward looking image
Sensor	OPS	
Scene Name	Tokyo	Nikko
Path-Row	65-241	65-239
Date	1993.3.9	
Process Level	L1	

2.2 Test sites

The following test sites were selected: A and C areas are gentle slope with plain and hills, B and D areas are severely mixed with valleys and ridges where condition of accuracy test is comparatively hard. E area was added for evaluation in JERS-1. The sizes of test areas are about 15 km in length, and figures of test areas are rectangle DEM points for accuracy verification were 90000 points for each test site.

Contour lines of test site B and D are shown in Figure 1 and 2. Respectively the data used for each test site are shown in table 3. Average and Standard deviation of table 3 were calculated from DEM of Digital Cartographic Data derived from 1:25,000 topographic map.

Table 3. Test Data Used for Test Site of Both Satellite

Satellite and Test Site		North West Corner		South East Corner			
		Latitude	Longitude	Latitude	Longitude	Average	S.D
SPOT	A	N35° 34′ 05″	E138° 24′ 35″	N35° 22′ 50″	E138° 32′ 05″	503.17	283.75
	B	N35° 21′ 08″	E138° 04′ 41″	N35° 13′ 38″	E138° 15′ 56″	1448.39	402.86
JERS-1	C	N35° 40′ 00″	E139° 07′ 30″	N35° 32′ 30″	E139° 18′ 45″	320.00	142.50
	D	N35° 40′ 45″	E138° 56′ 30″	N35° 33′ 15″	E139° 07′ 45″	537.41	205.69
	E	N35° 32′ 30″	E139° 03′ 45″	N35° 25′ 00″	E139° 15′ 00″	804.49	301.00

3. TEST METHOD

3.1 Data for evaluation

DEM of Digital Cartographic Data is used for accuracy verification of the satellite DEM. The Digital Cartographic Data DEMs are derived from 1:25,000 scale Topographic Maps published by the Geographical Survey Institute through vector-raster conversion of the scanned contour lines and height interpolation. The DEM product is published by the GSI as "Numerical Map 50m Mesh" in floppy disks. The grid interval of this DEM is 2.25 seconds in longitude and 1.5 seconds in latitude, both of which correspond to about 50 meters on ground. Because these DEMs are used for verification of the accuracy of DEMs derived from stereo matching of satellite imagery, the DEMs from satellites are also interpolated according to the same coordinate system as the existing DEM, namely grid interval of 2.25 seconds in longitude and 1.5 seconds in latitude.

For the comparison, the difference between height value obtained from stereo matching and that of the "Numerical Map 50m Mesh" is calculated. Calculated values are the mean, the mean of the absolute value, and root mean squares of the difference of the DEMs as well as relative errors by subtracting the mean of the difference.

3.2 SPOT

Eight points of GCPs were evenly obtained on the whole area. Result of the orientation of the images were within two pixels in RMS error in both pixel and line directions. Affin transformation is used for the geometric correction.

There were not any significant difference in the accuracy of DEM with or without pre-processing in both the test sites(A and B). Therefore the accuracy of the DEM was examined by the difference of topographic characteristics of the area only.

3.3 JERS-1

3.3.1 Matching method

Matching methods used are SSDA(Sequential Similarity Detection Algorithm) and area correlation method. The first search was done for only sampled points in a fixed interval with rather large searching window size by SSDA. Then the second matching was carried out by more precise area correlation method.

Correlation window size was fixed to 9x9 on each method. It was decided by the following reason. Resolution of forward looking image is a little bit worse than nadir looking image because observation distance is longer. Therefore to make matching window size too large on different resolution images may cause mismatching. The stabilest result in view of matching accuracy was obtained with window size of 9x9 from previous result of accuracy verification in Tsukuba test site.

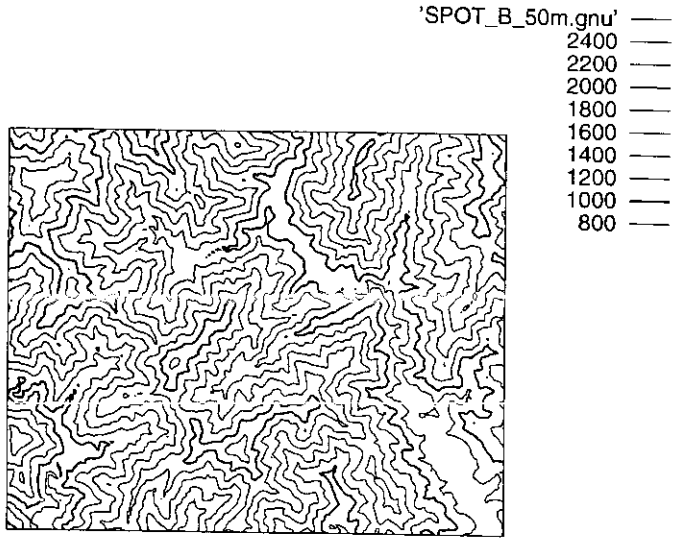

Figure 1. Contour Lines of test site B

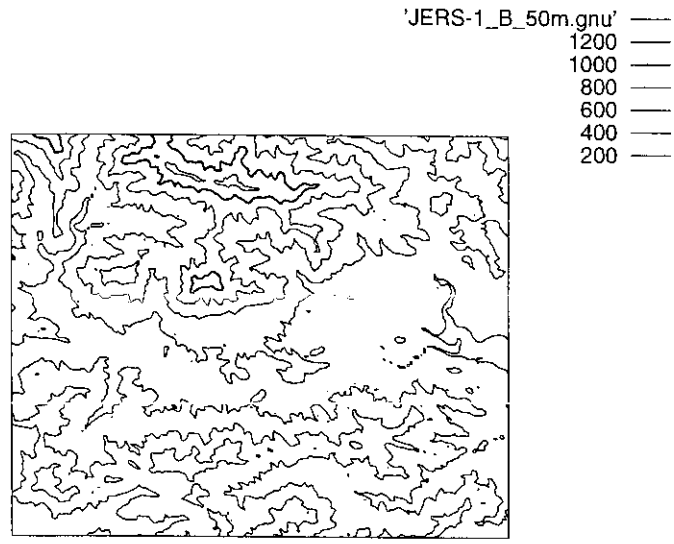

Figure 2. Contour Lines of test site D

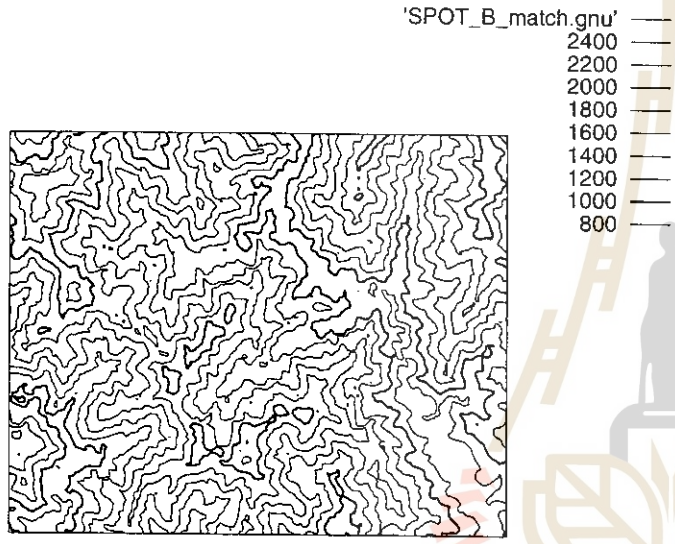

Figure 3. Contour Lines of Stereo Matching in test site B

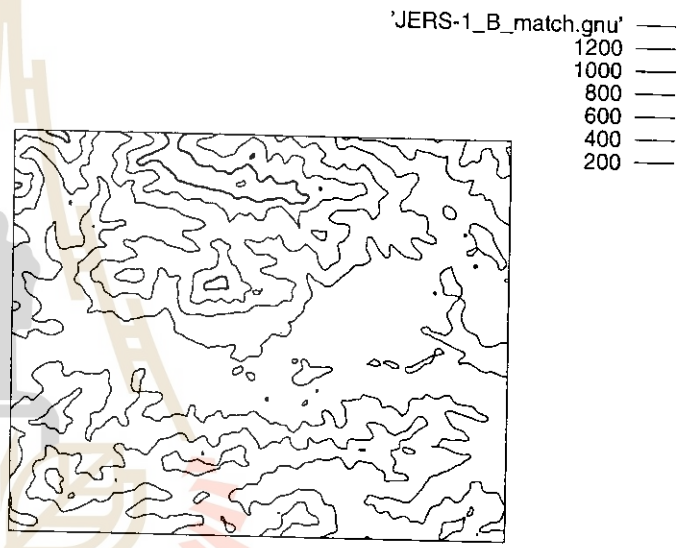

Figure 4. Contour Lines of Stereo Matching in test site D

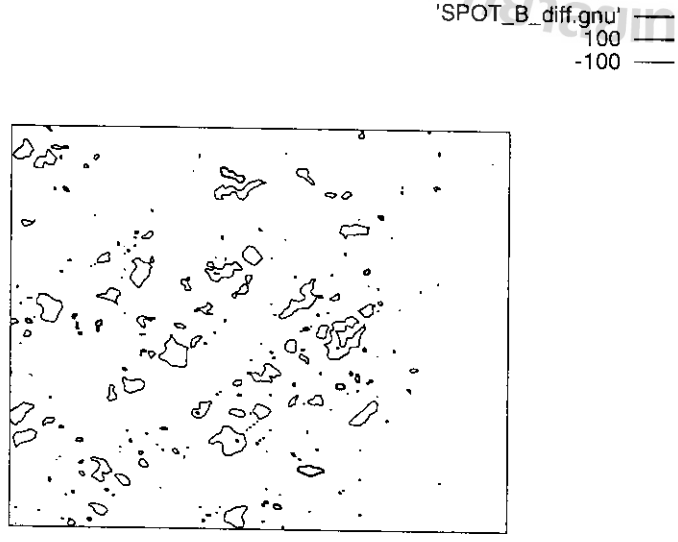

Figure 5. Contour Lines of errors in test site B

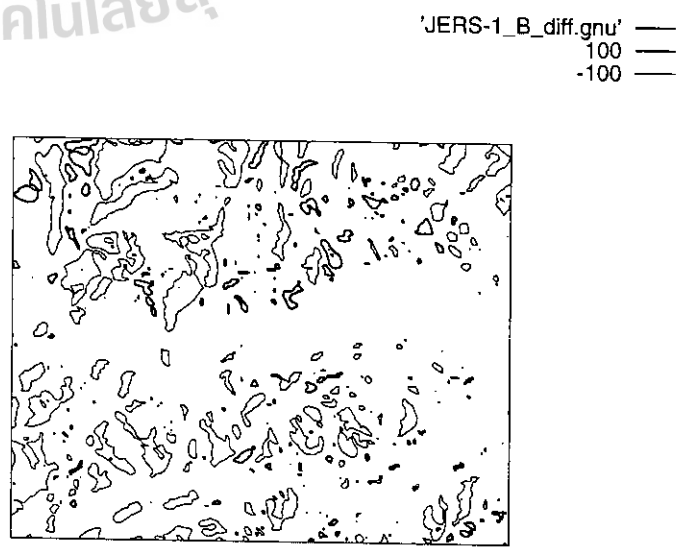

Figure 6. Contour Lines of errors in test site D

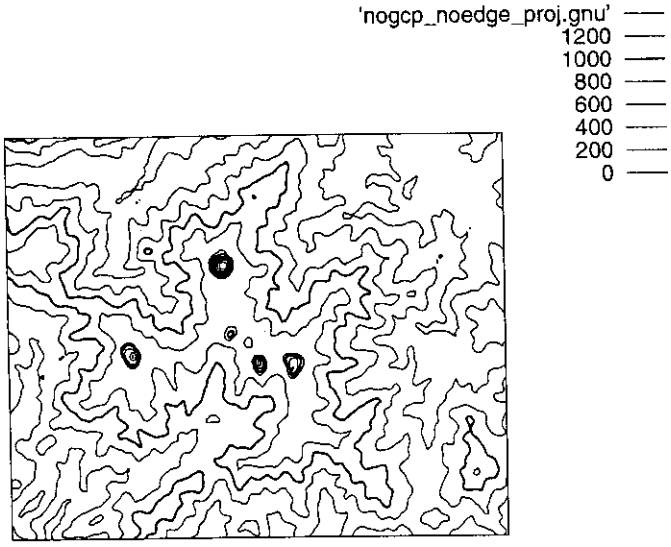

Figure 7. Contour Lines without Image Filter in test site E

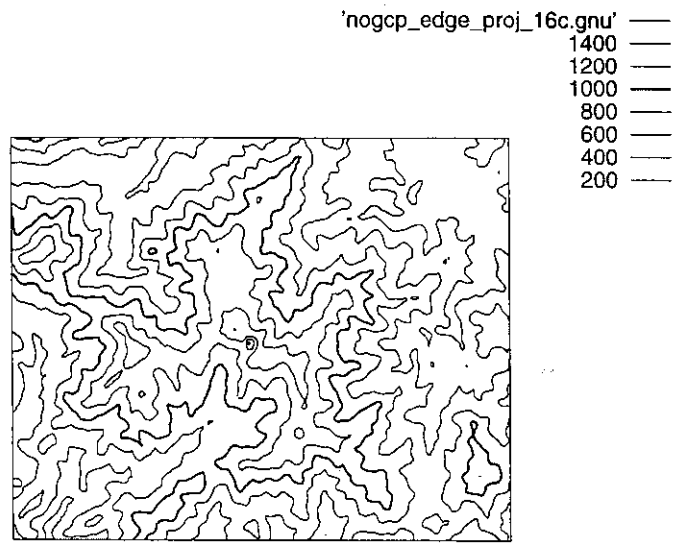

Figure 8. Contour Lines with Image Filter in test site E

3.3.2 Adoption of GCP

Accuracy was compared when many ground control points (GCPs) were used and when only one control point was used. In the former one, DEM was corrected assuming a trend surface of height error whose plane equation is calculated from GCPs. The latter method is to remove systematic error of position only at starting point in stereo image. This point is located within test site D, but the same point is used in other test sites C and D.

3.3.3 Filtering processing

High frequency component of images is enhanced so as to detect the peak of correlation in stereo matching. We employed un-sharp masking method for this enhancement. Effectiveness of this filtering pre-processing is evaluated from DEM results.

4. Test results

Test result from each test site of each satellite is listed in Table 4 and 5. Contour lines of stereo matching is shown in Figure 3 and 4. Figure 5 and 6 shows each contour lines of the difference between the DEM by stereo matching and existing DEM of Digital Cartographic Data.

Table 4. Test Result of SPOT Satellite (unit:meters)

Area	Positive Maximum Error	Negative Maximum Error	Bias	Ave.of Absolute Difference [1)]	R.M.S.E[1)]	Ave.of Absolute Difference [2)]	R.M.S.E [2)]
A	252.60	-452.10	8.13	22.34	34.97	19.80	34.02
B	266.30	-384.80	-1.01	35.55	53.20	35.78	53.19

Table 5. Test Result of JERS-1 Satellite (unit:meters)

Area and Case		Positive Maximum Error	Negative Maximum Error	Bias	Ave.of Absolute Difference [1)]	R.M.S.E [1)]	Ave.of Absolute Difference [2)]	R.M.S.E [2)]
C	Case 1	228.80	-232.00	8.14	45.55	58.93	44.17	58.37
	Case 2	233.80	-243.00	8.34	45.74	59.13	44.27	58.54
	Case 3	262.70	-206.80	19.44	46.17	59.73	42.01	56.49
D	Case 1	232.10	-291.90	-25.54	58.43	74.86	55.51	70.43
	Case 2	236.70	-323.00	-25.34	57.83	74.58	54.89	70.19
	Case 3	305.10	-223.90	33.89	62.02	77.39	54.52	69.58

Positive Maximum Error :Positive Maximum Difference with Digital Cartographic Data.
Negative Maximum Error :Negative Maximum Difference with Digital Cartographic Data.
Bias :Ave.of Difference with Digital Cartographic Data.
Ave.of Absolute Difference [1]:Ave.of Absolute Difference with Digital Cartographic Data.
R.M.S.E [1] : Root Mean Square Error with Digital Cartographic Data.
Ave.of Absolute Difference [2]:Ave.of Absolute Difference after subtracting the Bias.
R.M.S.E [2] : Root Mean Square Error after subtracting the Bias.
Case 1: with no GCP, without filter.
Case 2: with no GCP, with filter.
Case 3: with GCP, without filter.

5. CONSIDERATION

<GCP>

No difference of accuracy in both Case 1 and Case 3 was found. According to a theory, DEM with higher accuracy should be obtained by using GCPs. But Accuracy was hardly improved because test site has sharp undulation where it is very difficult to get accurate height at GCPs. Artificial objects clearly seen on images is helpful when an operator gets GCPs. But many of artificial objections in mountains are located near a steep cliff, which results in increase of errors to identify the position on a topographic map.

<Filtering Processing>

There were not large differences of accuracy in Case 1 and Case 2 from the comparison of result. But it was found that filtering processing can remove large errors caused by mismatching, particularly in test site E where there is the most hard undulation among all test sites. After this, I think so that verify accuracy of DEM by method as follows.

We plan to continue accuracy test of stereo matching using pre-processing which do not enhance the whole image but selectively enhance linear structures on using Laplacian-gaussian filters for pre-processing.

REFERENCES

Geographical Survey Institute, 1993. Report of the Study on Topography Measurement by Digital Images(in Japanese)

H. Masaharu, et. al.; Three Dimensional Measurement by JERS-1 OPS Stereo Data, ISPRS COMMISSION IV SYMPOSIUM, 1994, Jun.

M.Takagi,H.Shimada, et. al.; Handbook of Image analysis(in Japanese),Univ. of Tokyo press, 1991, pp548-558

A Multipurpose Ecological Mapping and Evaluation of Mongolian Nature Based on Remote Sensing and Ground Data

Dr. M. SAANDAR
Dr. D. GUNIN

REMOTE SENSING AND GEO-INFORMATION CENTER
ULAANBAATOR, MONGOLIA

1. SUMMARY

The growing negative tendencies changing the Mongolian nature has led to the undertaking of research works on ecological mapping and overall evaluation of the environmental situation as well as on the country's natural resources.

These studies were initially launched in 1988 and are planned to be completed in 1993. This project is aimed at the mapping of human-made degradation occurred in the Mongolian natural environment in scale 1:1,000,000 and 1:200,000 based on remote sensing data.

On the basis of the evaluations and results to be made under this project, we deem it is necessary to elaborate in cooperation with all interested foreign and national institutions a scientifically well - sounded concept on national ecologically critical situations in different regions of Mongolia and to put the resources management on an environmentally safe footing.

The remote sensing based Mongalian natural resources information system assembles available data on features of the natural environment of Mongolia and was designed to assist decisions in policies on resource use at a central Asia continental scale.

2. INTRODUCTION

The map "Modern condition of ecosystems of Mongolia" on based remote sensing data represents the fundamental cartographic work that gives an information about ecological situation in the whole country and different regions. The analyses of the map may provide obtaining representative data regarding the degree of the anthropogenic pressure on the environment.
The map shows ecological relations in the system "man-industry-environment" of the different regions and may serve as a reliable cartogtaphic source for developping regional ecological programs and plans for the separate branches of industry,for investigating of the large-scale building sites.
The map "Modern condition of ecosystems of Mongolia" is a foudation for development of the programs on the environmental protection and its execution. Also this map is a document, that is necessary for development of the regional (aimak) plans of the rational land explotation.
The map shows different kinds of the anthropogenic influence, the reaction of nature, the transformation degree of ecological situation in 1990-1991 years. Mongolia is a country with different contrast and mosaic land scapes. It is supercatena in which forest ecosystems of Siberian type are mixed with steppen and extraaring ecosystems of Central Asian type.
As a result of marked degree of gypsometric height (average altitude in Mongolia equals 1589 m), peculiar orographic estrangement from moist air streams, long season influence of formed here anticyclone and other factors, all developing ecosystems showed arid tendencies, which intensified their vulnerability, little adaptation, ecologic unstability during development.
There is world watershed between rivers of Arctic Ocean and indranaged regions of Central Asia, which cover 2/3 of the coubtry area, in Mongolian lands. Mongolia is one of a few countries, in which due to natural function. The main ecological damage in the conditions of the traditional pastorage is the vegetation violation, but there are the local areas of soils, urbanic territories and mining industry zones with intensibve anthropogenic influence.
Increase of anthropogenic pressure and

its duration is extended in areas of transformed ecosystems.
Regions with bad ecological conditions influencing on human health arise.
Space photoinformation was used for developing operative cartographic model being made up as inventory of ecosystems in diffenrent ranges increases the degree of correct interpretation of ecological data of the photographs. Selected control of obtained results was carried out inexpeditions during route inspection of areas.
The object of exploration was ecosystem, i.e. region with certain nature conditions of existing of complex parts.
The subjects of exploration were properties of ecosystems and its parts, previously vegetation and soil defining the basis of ecosystems.

The map or ecosystems of 1:1,000,000 scale means zonal and altitudal state of nature complexes. More than 300 types of ecosystems were determined on the map.
There ecosystems were classified according to distribution of soil, vegetation and forms of relief.

Ecosystems were evaluated according to pressure of various anthropogenic factors: forestry, agriculture, pasturage, settlement -industry, transport and other.
After analysis of informativiy of some characteristics and indexes of ecosystem condition about 10 main degradation process criteria was chosen and was used for inspection.
For example, the soil violation was characterized by erosion, deflation, mechanical changes of structure, increasing of salt content and others. Vegetation violation was characterized by decreasing of plant viability, phytocenonis.
Integral indexes of ecosystem transformation were laid in the foundation of the map "Anthropogenic violation degree".
Two problems were resolved during the developing of synthetic cartogrophic model "Modern conditions of Mongolia ecosystems": to show the influence of geographic characteristics on space differentiation of ecosystems and to show the depending of anthropogenic transformation degree on type of land use.
Increasing of map informativity demands combination of various cartographic methods.
Color reflects zonal and altitudinal type of the ecosystems.
To show zonal and altitudinal situation of depicted objects several color patterns were used.
The background (25 types) shows geomorphological conditions of the ecosystems. Every selected contours has received integral anthropogenic violation degree estimation in a 5-point scale: most violated ecosystems are colored lighter, less violated ecosystems have more intensive color. With the help of various indezes and colors many factors of anthropogenic violation were shown: pasturage, ploughing, transport, and others.
The key to the map, having more than 300 types of ecosystems, consistes, of tables, combined in three main parts: "Natural and natural-anthropogenic ecosystems", "Anthropogenic ecosystems" and "Anthropogenic violation degree of ecosystems". In addion to that the tendensies of natural and anthropogenic stimulated processes, geographical state are also shown by extra-scale conventional signs.
All the map are elaborated on 14 sheets of 1:1,000,000 scale and matrix key, which is a result of 20 years work of Joint Soviet-Mongolian complex biological expedition of Academy of Sciences of the USSR and Academy of Sciences of Mongolia.

The position of Mongolia in the bounds of subcontinental structures of Central Asia, South Siberia, Far East, at the interface between several subregions allows to forecast the consequences of different anthropogenic influences in these regions and consider fulfiled investigations as an example for the corresponding regions. The map "Modern condition of ecosystems of Mongolia" on based remote sensing data in the new type of work.
The method of its developing may be used for monitoring of local, regional and global environment.

3. RESULTS AND DISCUSSION

The map of modern ecosystems and evaluation of their anthropogenic violation compiled in scale 1:1,000,000 by Joint Russian -Mongolian complex Biological Expedition is intended for reflecting the condition of the soil and vegetation cover and the wild life with consideration of the degree of anthropogenic influence due to purposive land explotation,

or to unintended violation of ecological situarion.
As a whole the map provides information on natural regulations of space distribution and quality and quantity correlation of the main nature complexes.

The analyses of the map may provide obtaining representative data on the condition of ecosystems and making a forecast for their change in connection with the anthropogenic pressure.
The information presented in the map may serve a scientific foundation for making economic decisions, for wild life and soil protection planning for rational land explotation.
The quantity indexes of the violation degree of ecosystems of different administrative districts and areas (aimaks and sums) of the country, which may also be obtained with the help of the map, will be important material both for ecological and economic evaluation of the damage to nature and for correction of the socio-economics programs.
Thus, the compiled map is multipurpose in its nature with scientific and applied functions most easily forseen.

The main principle of creating the map was a system approach to the depicted objects. The peculiarity of the map is that is based on ecosystem data, i.e. the inventarization map of modern ecosystems served a basis for further estimation of the degree of their anthropogenic violation.
So, the map has two levels: the modern ecosystems are reflected on the first and estimation of the degree of anthropogenic influence at the territory occupied by certain ecosystem (or a part of it) is presented on the other.

An important feature of the present map is the naturalness of the limits of the depicted objects, which were achieved with wide utilization of space photoinformation.

As it was the first map of that kind for Mongolia the following demands were met during the work:
-Reflecting only present ecosystems and not those hypothetically existing before (the intensive anthropogenic influence);
-reflecting main peculiarities of distrubution of soil and vegetation in accordance with the principal forms of relief the character of the surface deposits, their water provision and drianage,as well as the altutude and zonal situation taken in accordance with meridional sectority; -reflecting water ecosystems in accordancewith the prophity of the water body, its regime and degree of mineralizaion of the water; -reflecting artificial anthropogenic ecosystems (economic and cultural ones) as well as territories affected by negative exogenic processes both of natural and artificial origin.

The level of depicted ecosystems was determined from the scale of the map compiled.
The ecosystems were mainly selected as corresponding to a certain type of landscape or as a group of typical landscapes. Thus, the main cartographical units were ecosystems as an aggregate of simplier ecosystems identic with biogeocenosis of Sukatchev.
The depicted ecosystems reflect regularities of space correlation of soil vegetaion cover and its links with physical and geographical condition, chiefly with the relief and indirectly, with the water provision.

The smallest contours selected on the map equals to 4mm, which corresponds to 4 space kilometers in nature.

The main criterian was the selection of correlated systems of mesorelief and ecologically close plant communities (Table 1).
The utilization of space photographs and photoplanes of the scale 1:1,000,000 helped to reliabily frame such elementary (for map of such scale) ecosystems in their modern conditions. The analyses of the selected ecosystems in their modern conditions. The analyses of the selected ecosystems has shown that the majority of them is of natural or anthropogenic-natural origin, which did not suffer any irriwersible damage along with natural and anthropogenic-natural ecosystems there are natural-anthropogenic and anthropogenic (technogenic) systems, which differ by the degree of violation of the initial natural ecosystems.

Table 1

Criterian of modern ecosystem selection

Modern ecosystems	Criteria of selection
Natural (anthropogenic-natural)	
Automorphic (eluvial, -transitive accumulative -transitive	Character of relief mesoforms, altitudinal or zonal situation, content of plant communities, ecobiotic forms of vegetation in consideration with the content of surface deposits and soils
Hydromorphic (transitive, transitive-acumulative, accumulative)	Relief mesoforms, altitudinal and zonal situation, ecogenetic plant successions with dominant phreatophytes and hydro- and hydrophytes
Water (transitive: rivers, acumulative-transitive: lakes with flowing water, accumulative: lakes)	Flowability of water body and its trophity, general mineralization of water, character of water regime (temporary, drying up)
Anthropogenic (natural-anthropogenic, technogenic)	Type of natural resource use (land, vegetation, water), intensity and duration of influence, character of inter and intra-landscape violation (reversible or irreversible), supposed duration of relaxation

When selecting natural and anthropogenic-natural, i.e. anthropogenic modifications of natural ecosystems the main distinguishing character was the figure of photoreflection of relief mesoforms on space photographs. Further classification was made taking into consideration the dominant plant communities, reflecting the altitudinal situation in the mountains, and zonal situation in the plains.

The selected types of ecosystems are divided into two unequal groups: natural and anthropogehic-natural, on one hand, and natural -anthropogenic and anthropogenic (including technogenic), on the other hand. In the cartographical part of tne Mongolian territory the natural and anthropogenic natural ecosystems occupy the dominant position. Among these unequal groups are to be distinguised according to the type of water regime, the dominant role of certain ecological groups of plants and animals, the types geochemical flows of substance: 1) automorphic and semihydromorphic ecosystems (eluvial, transitive -eluvial, accumulative-transitive); 2) hydeomorphic (transitive, accumulative-transitive, accumulative) ; 3) hydroecosystems of rivers and lakes (transitive and acumulative). The greatest diversity is characteristic the first group of ecosystems.

Automorphic ecosystems occupy both mountains and plains.
In the mountains all ecosystems are divided in accordance with their location in certain altitudianl levels: whereas in the plains their type depends on altitudinal, zonal location, which is also appliable for low lands and hilly areas.
About 400 ecosystems are determined on the map, with highest diversity stated for steppes and semideserts (nothern deserts). If all the variants of ecosystems reflecting peculiarities of the vegetation cover are to be considered their number will be over 900 (Tabel 2).
In the steppes and arid ecosystems the biological component (soil and vegetation cover) was classified in accordance with the content of surface deposits. This may loamy sandy, loamy, stony, sandy and solonchakous biotopes were determined.

Table 2

Number of automorphic and semihydromorphic ecosystems in different altitudes and zones

Groupes of ecosystems in accordance with their zonal and altitudal state	Number of units in the mountains	in the plains	Total
Natural mountain nival	1		1
Tundra	9		9
Cryophyte-meadow-steppe (mountain meadow)	19		19
Forest: high mountain taiga	4		4
mountain taiga and subtaiga	15		15
Forest-steppe	9		9
Meadow-steppe	8	9	17
Steppe: moderately dry	24	20	44
dry	19	21	40
semidesert steppe	24	29	53
Desert: semidesert (north desert)	21	23	44
steppeficated (medial desert)	12	10	22
real desert (south desert)	6	22	28
extra arid	5	12	17

For each type of automorphic ecosystem a list of the main ecologically similar plant communities often substituting each other due to meridional position is presented.

Hydeomorphic ecosystems were classified in accordance with altitudional and zonal principle more generally owing to the smoothing of the hydrosphere.

Hydroecosystems are classified according to the main ecological factors of their existance, i.e. the character of water. That is why these ecosystems are divided into groups in accordance with flowability of the water body and its trophity.

The results of such classification of natural and anthropogenic-natural ecosystems are reflected in the key.

The classification of natural -anthropogenic and anthropogenic ecosystems was based on determination of the dominant factor that influences the natural ecosystem, i.e. the type of land use. In the main types of natural resources utilization are fixed as folws: Agliculture, forestry, settlement-industry, including mining, transport. These

different in the intensity and the character influences lead to formation of agriecosystems, ruderal, cultural -ruderal and cultural ecosystems.

To estimate the degree of anthropogenic violation of ecosystem specisl criteria were elaborated that can evaluate the modern condition of an ecosystem (i.e. unchanged of very febly changed) its condition in places, where no traces of mechanical violation of micro-and mesorelief were found in the process of field examination and especially no traces of violation of vegetation cover, no traces of man's activity (roads, wells, felling, etc.) were accepted. And these places were chosen at a distance from undisputally anthropogenic objects populated localities, mining or industrial complexes, etc.

The estimation of anthropogenic violation of ecosystems and their components (elements) were performed by 5 point scale (Table 3).

Table 3

Approximate scale of evaluation of anthropogenic violation degree of ecosystems

Integral evaluation	Evaluation of anthropogenic violation of ecosystems		
	of wild life	of vegetation	of soil
1. Natural or very weak	natural weak	natural weak	natural weak
2. Weak	weak, moderate	very weak, weak	natural very weak
3. Moderate	moderate	moderate	weak
. Strong	strong	strong	moderate
5. Very strong sometimes irreversible	very strong often irreversible	very strong	strong and very strong

Table 4

Evaluation of anthropogenic violation degree of components and elements of ecosystems

Indexes of violation	Criteria of violation in 5-point scale				
	natural or very weak	weak	moderate	strong	very strong
SOIL					
Decrease of humus reserves,%	to 5	5-10	10-25	25-50	over 50
Decrease of humus horizon depth,%	to 15	to 25	25-50	50-75	over 75
Increase of sand content in plough horizon,%.	to 3	to 5	5-10	10-20	over 20
Increase of water soluble salts content,%	to 10	10-20	20-50	over 50	
Increase of gypsum and carbonats content,%	to 10	10-20	20-50	50-80	over 80
Decrease of soil profile depth, cm	to 0.5	0.5-1	1-2	over 2	
RELIEF MICROFORMS					
Water erosion dully					
(quantity for 100 cm2)					
in plough areas		to 1	1-10	over 10	
in clearings amd pastures		1-2	2-10	over 10	
(depth, cm)					
in plough areas		to 5	5-10	over 10	
in clearings		to 50	50-100	over 100	
in pastures		to 15	15-30	over 30	
Microterracing of slopes					
(quantity of paths in 100m2)		to 25	25-50	over 50	
Wind erosion forms					
quantity of microflowerings in 100 m2		10-25	25-50	over 50	
deflation ulcers depth		to 10	10-50	over 50	
quantity of positive micro-forms (siple, spits, mounds) in 100 m2,%		to 10	10-50	over 50	
sand horizon depth, cm		to 10	10-50	over 50	
hummock areas (hummocks in 100 m2,%)		to 25	25-50	over 50	
RELIEF MESOFORMS					
Quarry, sand-pit heap formatios, in 100m2				1-2	over 2
VEGETATION					
trees extermination,%					
by cutting	to 15	15-30	30-60	over 60	
by upper level fires		to 30	30-60	over 60	
by lower level fires		to 30	30-60	over 60	
graze changes of field layer and shrubs		life cycle viola-tion	substitu-tion of dominants, weeds	weeds growth, shrub distri-bution	substitu-tion of native plants cenosis extermi-nation
			appearance		
Sod violation,%		5-30	10-15	over 20	
decrease in proective cover,%		to 10	10-30	30-50	to 100
Pasture degression indexes growth.		to 1	2-3	3-5	over 5
Increase of their proective cover,%			to 30	to 50	over 50

The integral estimate of anthropogenic violation of ecosystems was calculated in accordance with estimates of deterioration of its components: soil, vegetation, relief (formation of microforms and changes in mesoforms) for which easily determined in the field quantity indexes general recommendations concerning the evaluation of soil degradation due to anthropogenic influence were taken into consideration (GLASOD.1988).

It was accepted that even under weak violation of soil, for instance, in newly ploughed virgin land, strong anthropogenic extermination of vegetation leads to very strong anthropogenic violation of the ecosystem. The tillages in their turn can be strongly modified in accordance with the condition of their soil cover.
The estimation of soil modification in the tillages was performed by components with the help of acceptabl ariteria.
As a rule, the violation degree of wild life was higher than that of vegetation, and that of soil condition reactively lower (with certain exclusions). In connention with this during the field examination and the deciphering of space photo data the basic criterian of anthropogenic violation degree of ecosystems was the condition of vegetation. Thus the vegetation was regarded as an indicator of anthropogenic violation degree of ecosystems as a whole.

When estimating anthropogenic violation degree of forest ecosystems the direction of changes was taken into consideration,

because undergeneral negative tendency cases are possible when anthropogenic influence can lead to positive changes in certain components. For instance, forest fires, having considerably changed native ecosystem, can often provide favourable conditions for distrubution of certain animals, and the soil is also enriched in the first year after the fire.
To determine the general negative tendency of the ecosystems' development due to anthropogenic influence one must examine the stages of exogenic processes stimulated by economic activity.
Criteria for estimation of such processes may serve the indexes of relief microform changes (table 4)

Using in practice the mentioned quantity criteria of violation estimation for separate components of the ecosystems we took into consideration the fact that their role in different altitudianl and geographical zones in inadequate.
Thus, the humus content in soil index is used to estimate steppe ecosystems violation, while the gypsus and easily soluble salts-in deserts.

While compiling the map a creative compilation of all the priority data received by traditional investigations during many years by different specialist -biologists, soil scientists, geographists as well as the information obtainable from different kinds of maps and distance materials were performed.

The reflection of modern ecosystems and their evaluation the anthropogenic violation point of view was performed in two variants: 1) Two separate cartographic creations: an inventory map of modern ecosystems and an estimation map of their anthropogenic violation; 2) Unified map containing both modern ecosystems and their violation information .

The key to the map of modern ecosystems consits of tables insists of tables and a textual part. In the 4 tables the main automorphic, hydromorphic and hydroecosystems are included in connection with their altitudional and zonal state as well as the selected anthropogenic ecosystems. This map's lay out is performed with the aim to show the main regularities of ecosystem is triubution in accordance with the climate, geopogic-geomorphologic and hydrologic conditions.
This inventory map reliably enough reflects the distribution of modern Mongolian ecosystems. Every contours of the map is characterized with a double index explaining the geologic-geomorphologic conditions (roman number) and the soil and vegetation cover (arabic number with a letter addition explaining the content of plant societies-the key to letter indexes is given in the textual part) of the ecosystems. The map of estimation anthropogenic violation degree is built on the basis of the modern ecosystems map and repeats its skeletion and indexation.
But every selected contours (or a part of it) has received integral anthropogenic violation degree estimation in a 5-point scale. Additionally, the main factors causing ecosystem violations were reflected, and places of exogenic negative processes localization were shown.
The key to this map included tables, which show the main types of anthropogenic influence on ecosystem. The cartographic lay-out of the map is subordinated to the table of showing estimates: the less violated ecosystems are coloured green or yellow, the most-red.

A considerable amount of information is included in extra-scale conventional signs. These signs are used to show negative exogenic processes and their direction, some types of natural resources utilization causing natural balance violation (quarries, mines, etc.)

To show all the information available on the distibution of ecosystems and the estimations of their anthropogenic violation a unmified map was elaborated.

The key to unified map of modern ecosystems of Mongolia and estimation of their anthropogenic violation is prepared in 3 tables.
In the first modern automorphic and hydromorphic ecosystems are presented: in the second types of anthropogenic influence and estimation of violation degrees. Additionally, a table of water ecosystems and their condition is presented.
In the textual part of the key details of vegetation cover are given, which are considered an integral index of ecosystem condition, on one hand, and reflected a bit more generally the peculiarities of ecological donditions of a biotope, including its soil, climate, condition, etc., on the other.

A complex content of the map demanded special attention to its lay-out.

To show the zonal and altitudinal situation of depicted objects several colour patterns were used. The tone of copour reflects the degree of anthropogenic violation: the lighter the tone the more intensive the amthropogenic violation.
Brown shading indicates relief forms characteristics of ecosystems.
In addition to that extra scale forms characteristics of ecosystems. In addition to that extra scale conventional signs are used indicating several exogenic processes and factors causing environmet violation (fires, graze, etc.).

In addition to that in forest ecosystems the tendencies of soil and vegetaion development of violated ecosystems are also shown by extra-scale conventional signs.

Every selected contours has a complex index reflecting both the biological component and relief peciluarities as well a poing estimation of anthropogenic violation. Exploration of letter signs is in the textual part of the key.

All the maps are elaborated on 14 pages each in projection and enumeration corresponding to topographical maps of 1:1,000,000 scale.
For convinience aimak and sums limits are also shown.

The reflexion of modern condition of ecosystem on the map mas an outstanding significance for further control on environmental changes, of effectiveness of economic and nature protection programs. This map can serve a basis for further cartographic and space monitoring of environment both in the borders of the whole country and separate regions (aimaks and sums), as well as separate ecosystems purposively utilized in economy.
For example, forest ecosystems utilised in both forestry and agriculture as pastures: steppe ecosystems utilized in remote stock -breedong as all-year pastures.
In addition to that these maps may serve for selecting natural reserve territories and areas of stationary observations of ecosystems reaction of different anthropogenic influence in extreme circumtances: for elaboration of regional and typological nature protection measure.

Such monitoring can be achieved by consecutive: performance for elaboration of regional typological nature protection measures.

Such monitoring can be achieved by consecutive performance ofcartographic observations in a certain period of time based on fresh air and space photography. In air and space monitoring automatic determination of changes in ecosystems condition is possible. The analysis of the determined changes will serve a basis for estimation of the effectiveness of the undertaken measures.
The estimation of anthropogenic violation (changes) degree of ecosystems presented in points and based on quality evaluation of a modern anthropogenic violation, has more restricted in time significance. It is aimak supposed to be quickly utilized by planning organs, as it points out first of all the most critical areas of ecosystems that demand urgent measures to improve the environment and eliminate the main factor of violation, or to decrease its negative effect.

Improvement of estimation criteria may help creation of more objective aontents of such a map (with a transition from point to quantity indexes).

In other words, if the map reflection of modern ecosystems is one of the basic components of all sets of natural conditions and resources maps intended to be used repeatedlly, the estimation of anthropogenic violation degree has but operative significance. They are intended exclusively for rapid reacting at extremal situations on the basis of relative estimates in points.

In Mongolia due to peculiarities of its ecologic and geographic conditions of the country the negative consequences of anthropogenic influence of nature may develop even at unconsiderable level of the latter -therefore the maps of ecosystems may serve an important initial material for inventarization of degradation (desertification) processes in ecosystems located in extreme natural conditions.

The elaborated methodics of compiling maps on the basis of wide utilization of air and space information, precise elaboration of all components of the maps, compiling separate maps and a unified map-all these allow to state that this unique experience may have great importance for surveying not only adjacent territories of InnerMongolia, China, Siberia, but also for practically all countries were exists a combination of natural, anthropogenic-natural and anthropogenic ecosystems, subject to influence of economic activity.

By now the main principles of the methodics of ecosystem's ecological estimation and peculiarities of the approaches to the analyses of regional aspects of compiling and utilization of a map of Modern ecosystems are summarized and rendered in a monograph "Methodics of estimation of condition and cartographical survey of ecosystems in extreme circumstances", prepared by a group of authors from the Russian-Mongolian complex biological Expedition.

An Archaeological Application of Synthetic Aperture Radar (SAR) in Thailand

Assistant Professor Dr.Punnee Wara-Aswapati,
Chair of School of Remote Sensing,
Suranaree University of Technology
Nakhon Ratchasima 30000, Thailand
E-mail:punnee@sura1.sut.ac.th
Tel./Fax: 66-44-216101

Abstact

An archaeological site has been identified in Northeastern Thailand using airborne Synthetic Aperture Radar (SAR). The site consists of a pair of concentric ancient moats or canals which once surrounded an ancient town called "Muang Ham Hork" near Ban Rai ,Tambol Ban Khwao, Amphoe Ban Khwao, Changwat Chaiyaphum. The site enclosed by the moat is approximately 1.6 km. in diameter. It is estimated that the site dates from the Dvaravati period (1,200-1,600 BP). Today, the site is covered by cultivated land, and now only a few earth walls and moats remain in the easthern part of the town. A part of a high wall or gate appears in the south, where a red sandstone Buddhist altar with the size of 2 m. x 0.60 m. x 0.30 m. was found on the top of the remaining wall, and broken pottery was also found at the area of the site.

The SAR data was collected by the Canada Centre for Remote Sensing Convair 580, as part of the joint Canada-Thailand GlobeSAR Program. GlobeSAR is designed to develop SAR expertise in a number of countries around the world, prior to the launch of Canada's Radarsat in 1995. Due to the characteristics of radar, in particular its capability to distinguish between adjacent areas with slightly different levels of soil moisture, it is a most effective in identifying sites such as this one, in tropical or sub-tropical environments. While archaeology was not the prime objective of the GlobeSAR program in this region, the unexpected results will add considerably to Thailand's archeaological inventory. It is planned to review the SAR data from all eight sites in Thailand to determine whether or not other sites or features can be identified.

1. Introduction

Changwat Chaiyaphum, has been a land of civilization since prehistoric times, and more recently since about the 12th Buddhist century, as seen from various Dvaravati type evidences. Most of these traces consist of the "sema" leaves found usually in groups, such as the sema group at Ban Kut Ngong, Tambol Kut Tum, Amphoe Muang , Changwat Chaiyaphum. Later times saw the spread of Khmer civillization, as Khmer type architecture such as Prang Ku, Amphoe Muang, Chaiyaphum, attest [1].

Among the ancient towns of Chaiyaphum, there is one obvious circular shape of an archaeological site, about 20 km. southwest of Changwat Chaiyaphum, in Amphoe Ban Khwao, Tambol Ban Khwao near Ban Rai, where the ancient town situates, it was named Muang Ham Hork.

2. Objective

The objective of this research are:

2.1 To study the ability of synthetic aperture radar (SAR) to detect an archaeological site and it's present landuse for the purpose of management and planning.

2.2 To develop and transfer the technology acquired from joint research at the national institutions and CCRS, involving the use of airborne and spaceborne C-Band SAR data to those engaged in land use management

2.3 To develop training materials in cooperation with national and regional institutions to promote "SAR Literacy" among professionals and technical staff, both those participating in GlobeSAR and others in the region.

3. Study Area

The study area is the test site TH-1 Chaiyaphum. Changwat Chaiyaphum is a land of ancient cities and towns in Korat Plateau, Northeastern Thailand. It situates in 15° 48' 17.5" latitude North and 102° 02' 17.5" Longitude East, with the area of 11,778.287 km2 and 342 km from Bangkok is shown in figure 1.

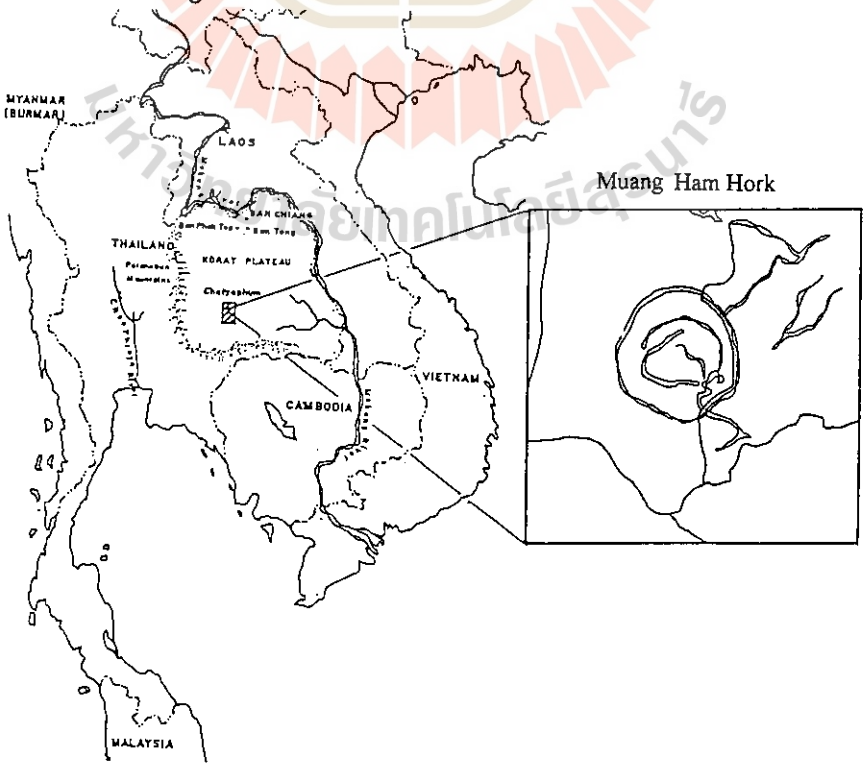

Figure 1 The study urea: Test site TH-1: Chaiyaphum.

4. Materials and Methods

4.1 Materials and Data

The following materials and data were used in this research: Topographic maps scale 1:250,000 and 1:50,000 (1-RTSD). CCT of airborne SAR (C-Band, HH) in nardir mode with resolution of 6 m. x 6 m. of 4 November 1993 (CCRS.). Aerial photographs (black and white) scale 1:50,000 of 11 November 1992 (RTSD.). CCT of Landsat-5 TM of 4 March 1994 (TRCT.). Intergraph System (UNIX.) Microstation MGE and ISI2 are hardware and software were used to create GIS and to process digital image and analysis. Hewlett Packard Scan Jet 3C. (resolution 2,400 dpi) is used to scan aerial photograps and field pictures.

4.2 The methods of the study

4.2.1 Image Processing

Digitize topographic map scale 1:50,000 of the study area to create geographic information system useful for geometric correction and geocoding for all kinds of data used. Aerial photographs were scanned in purpose of transforming hard copy data to digital form (raster file).
Landsat-5 TM's CCT was processed geometric correction, enhancement and color composite were made for comparing with SAR image.
SAR's CCT was processed, speckle remaved technique was applied to get a good result of SAR imagery of a single band data [2].

4.2.2 Extract Data

Extract data from SAR, TM and scanned aerial photograph of the same area to process digital image, as well as, to process color composite from various combination of those extracted data. In order to achieve the best digital image for analysis and interpretation.

4.2.3 Analysis and Interpretation

Analysis and interpretation were made on a single band of airborne SAR (black and white) base on microwave properties and backscattering properties of the surface, roughness, dielectric properties and local slope [2,3,4]. Comparing with aerial photograph (black and white panchromatic) and four different color composite imageries, of TM.

4.2.4 Field Check

Field check was done on 17-18 June 1995 in order to verify the first analysis an interpretation. Photographs were taken, where the important evidences were found in the area of the site.

5. Result

Archaeological site can be easily identified by man made shape of circular form which is ones of the ancient town or city pattern in Northeastern Thailand [1]. Remaining earth wall in the east, facing to the radar beam, appear in white tone and the back side is shadow. Some part of the moat where, water still remain, appare in very dark tone. The ancient town covers by cultivated land, rice is the major crop, the second is jute and the rest are vagetable mango, coconut and banana. Early dry season of November, is the begining of the harvesting season. Some rice fields were harvested, but some were not, it shows different tone in the cultived land, depends on the stage of growing, mature rice standing as the same height and smooth texture appear in gray tone, where white tone shows the area with some moisture, and dark linear

appear in gray tone, where white tone shows the area with some moisture, and dark linear irregurlar shape is stream channel and ox-bow lake. A Buddhist altar was found on the remaning acient wall in the South, where there was the trace of hard construction material (broken laterite) was found. The red sendstone alter is 2 m. long, 0.60 m. wide and 0.30 m. high. Doubt, it used to be an ancient gate. Broken potteries were also found in the ancient town. The result identification can be summarized as table below.

Table 1 Summary of Some Important Identification.

Feature	SAR C-B and HH	Color Composit Airphoto+SAR+SAR	Color Composite TM+SAR+SAR
Archaeological site(circular shape)	very clear shape	very clear shape	Clear shape
Water body	very dark	dark, red, blue	red
Culivated area	white to gray	white,light blue-blue	white, red,light blue-blue

An archaeological site, detected by SAR imagery, consists of a pair of conentric ancient moats which once surrounded an ancient town called "Muang Ham Hork". Geographical location, diameter and area of the ancient town were determined by MGE software, the result is presented as below.

Location (center of the town): 15° 43' 17" Latitute North and 101° 56' 57" Longitude East.
Diameter: 1,625 meters
Radius: 814.5 meters
Area (πr^2) : 2,085,003.64 sq.meters
Area approximately: 20.85003 hectare or 1,303.1 rai (Thai area unit)

6. Conclusion and Discussion

The result of the study shows the ability of synthetic aperture radar (SAR) to detect an archaeological site and it's present landuse. Even the ancient town of "Muang Ham Hork" has been registered to the Department of Fine Arts since 1936 [5]. The town is still using for agriÛ¥-ture. It seem to be the villagers ignore this valuable archaeological site of the ancient town.

There are important evidences were found in the present land use of the site are showed in figure 2.

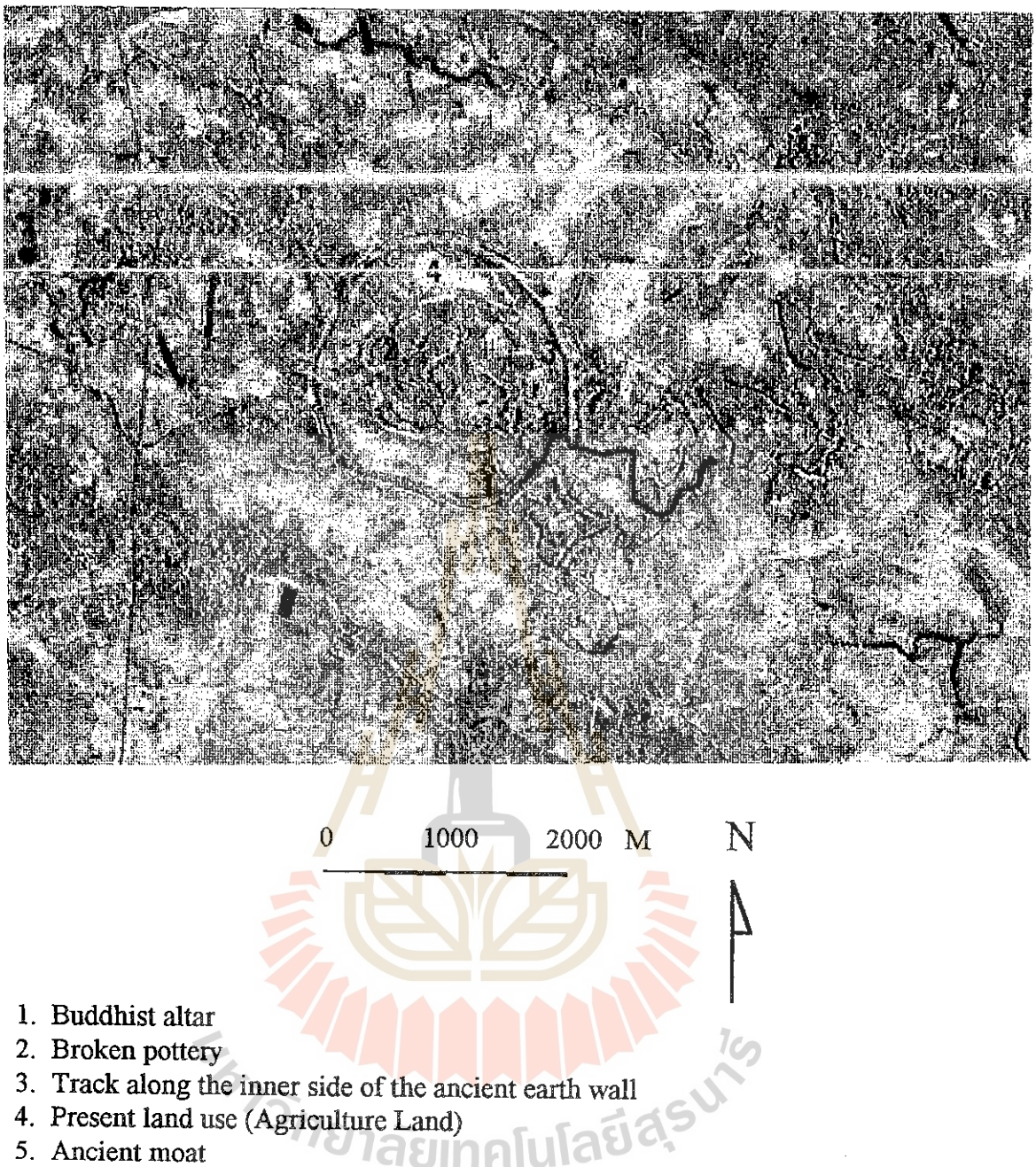

Figure 2 SAR image: Archaeological site "Muang Ham Hork", shows the location of the archaeological evidences.

7. Reference

1. Praphattong, K., *Historical Archaeology.* Department of Fine Arts. Bangkok, Thailand, p.p. 87-94, 1986.

2. Remote Sensing Center Research and Technology Development, *Radar Imagery: Theory and Lecture Note,* RSC Series No. 67. Food and Agriculture Organization of the United Nation Rome, p.p. 19-25, 1993.

3. Natural Resources Canada, *Radar Basics: Introduction to Synthetic Aperture Radar Remote Sensing.* Technology Transfer, Training & Development Section, 76 pages, 1994.

4. RadarSAT International, *Introduction to RadarSAT and it's use in project planning and execution.* GlobeSAR Regional Workshop Bangkok, Thailand, November 28- December 2, 1994.

5. Suppajanya, T., *Study of ancient cities from aerial photograph.* Chularong khorn University 1 sheet, 19.....

TECHNICAL SESSION D

WATER / MARINE RESOURCES

Observation of western Siberian wetlands by using remote sensing techniques: Estimation of methane emission

M. Tamura and Y. Yasuoka
National Institute for Environmental Studies, 16-2 Onogawa, Tsukuba, Ibaraki, 305 Japan

K. Tokumura
Nakanihon Air Service, 2-3-15 Kyobashi, Chuou, Tokyo, 104 Japan

Phone: +81-298-50-2479; Fax: +81-298-51-4732; E-mail: m-tamura@nies.go.jp

Abstract

A SPOT/HRV image was obtained at Plotnikovo test site in western Siberian wetlands. The image area was classified into eight categories of ecosystems (birch forest, conifer forest, bog_1, bog_2, bog_3, water, grass and bare soil) using ground truth data and aerial photographs. Methane emission from the image area was estimated by combining the result of ecosystem classification and the methane flux data measured on the ground. This estimate of methane emission was in good agreement with the average estimate obtained from airborne methane measurements. The agreement shows the usefulness of remote sensing techniques in extrapolating ground methane flux measurements to a regional or global scale estimate of methane emissions.

I. Introduction

Western Siberian wetlands are presumed to be large sources of atmospheric methane, which is one of the most significant greenhouse gases. Recent Japan-Russia joint research project conducted by our research institute and Russian co-workers is yielding the results supporting this presumption (Panikov, 1994). To evaluate the role of the western Siberian wetlands as sources of atmospheric methane, it is necessary to classify wetland ecosystems and to measure mean methane flux for each ecosystem type. In this research we investigate the vegetation in western Siberian wetlands by using remote sensing techniques and estimate regional methane emissions by combining the results of satellite observations with ground methane measurements. We use two categories of satellite sensors: a wide-coverage coarse-spatial-resolution sensor like NOAA/AVHRR and high-spatial-resolution sensors like SPOT/HRV and JERS-1/OPS & SAR. The former is used to estimate overall wetland distributions and to monitor the seasonal change of vegetation in the whole western Siberian wetlands. The latter is used to classify wetland ecosystems in selected test sites.

In this paper we analyze a SPOT/HRV image at Plotnikovo test site in west Siberia to classify wetland ecosystems. Methane emission from the image area is estimated by combining the result of ecosystem classification with the ground methane measurements. We then compare this methane emission estimate with those obtained from airborne methane measurements.

II. SPOT/HRV image at Plotnikovo in western Siberian wetlands

A SPOT/HRV image was obtained at Plotnikovo test site on 8 July 1995. Plotnikovo settlement is located at the map coordinates (85°05'E, 56°51'N) in the basin of Ob' river and belong to the south east part of the western Siberian wetlands (see Figure 1). The SPOT/HRV is a high resolution imaging system with a ground resolution of 20 m and has three spectral bands of green, red and near infrared wavelengths (0.50-0.59, 0.61-0.68 and 0.79-0.89 μm). Figure 2 shows the SPOT/HRV image in the near infrared band. We selected this place as one of our test sites because ground observations of vegetation and atmospheric gasses have been made since 1993 by the Moscow Institute of Microbiology. Circle symbols in Figure 2 shows the locations of methane flux measurements.

Based on the ground truth data and aerial photographs obtained in 1994 and 1995, we classified the land cover types in the image area into eight categories (birch forest, conifer forest, bog_1, bog_2, bog_3, water, grass and bare soil) using the supervised maximum likelihood classification technique. Figure 3 shows the result of land cover classification. Birch trees are dominant in forested areas and coniferous

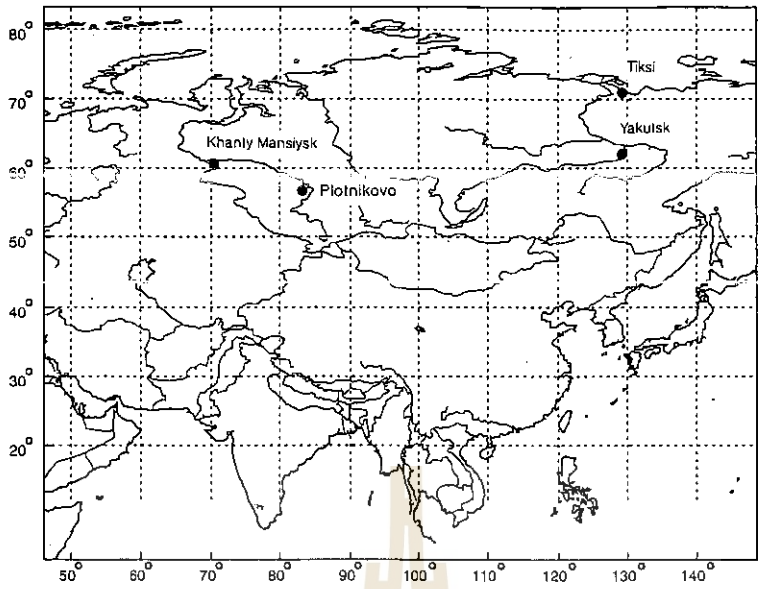

Figure 1. Location of Platnikovo .

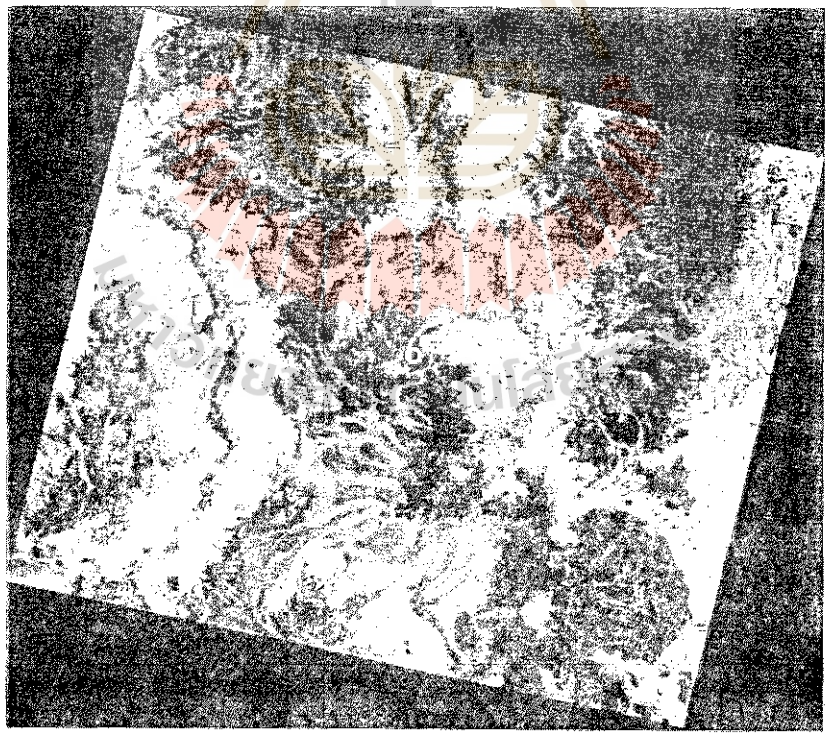

Figure 2. SPOT/HRV image at Plotnikovo. Circle symbols show ground measurement points of methane fluxes.

forests are found along rivers because soils have richer nutrients there. Bog_1 is identified as peat land with low pine trees and shrubs, bog_2 as peat land with sparse dwarf trees and shrubs, and bog_3 as peat land mainly with grasses such as sedges and cotton-grasses.

III. Estimation of methane emission from the SPOT image area

To estimate the methane emission from the SPOT image area, we used the methane flux data measured on the ground by the Moscow Institute of Microbiology (Panikov, 1994). Table 1 shows the mean methane fluxes for the period from July to August in 1993 and 1994. The measurements for open bogs were made at three points indicated by circle symbols in Figure 2. The measurements for forested bogs were made outside of the SPOT image area.

Table 1. Mean methane fluxes measured on the ground from July to August in 1993 and 1994. Flux unit is mg CH_4 m^{-2} day^{-1}.

site	No. of measurements	Mean	Standard dev.
Forested bogs	23	21.1	43.8
Open bogs	56	233.9	326.1

Table 2 shows the area size and areal ratio of each land cover type and the estimated methane emission. We calculated the methane emission by multiplying the mean methane flux with area size for each land cover type. We assumed that the mean methane flux is the same for birch and conifer forests, i.e. 21.1 mg CH_4 m^{-2} day^{-1} and also that the mean methane flux is the same for three types of bogs, i.e. 233.9 mg CH_4 m^{-2} day^{-1}. We neglected the contributions from water, grass and bare soil areas, because methane flux data are not available for these land cover types and their areal ratio is small (7 % in total). The total methane emission from the SPOT image area was estimated as 432.7×10^6 g CH_4 day^{-1} and the mean methane flux in the SPOT image area was 102 mg CH_4 m^{-2} day^{-1}.

Table 2. Estimated methane emission from the SPOT image area. (Mean methane flux in the image area: 102 mg CH_4 m^{-2} day^{-1}).

Land cover types	Area (km^2)	Areal Ratio (%)	Methane flux (10^6 g CH^4 day^{-1})
Birch forest	515.0	35.7	32.0
Conifer forest	788.6	18.6	16.6
Bog_1	818.8	19.3	191.5
Bog_2	417.2	9.8	97.6
Bog_3	406.3	9.6	95.0
Water	28.5	0.7	-
Grass	251.1	5.9	-
Bare soil	15.1	0.4	-
Total	240.6	100.0	432.7

IV. Comparison with airborne methane measurements

The atmospheric team of the Japan Russia join research project measured vertical profiles of methane concentration above Plotnikovo test site on 3, 5 and 6 August 1994 using an observation aircraft (Tohjima et al., 1995). Figure 4 shows the flight path of the aircraft on 5 August. The rectangle is the SPOT image area. From the vertical profiles of methane concentration, we can calculate the amount of methane accumulated in a vertical column of air. We can also determine the accumulation period of methane, because the accumulation of methane starts in night time at around 9 o'clock when a temperature inversion layer begins to develop. Hence we can estimate regional methane fluxes by dividing the amount of accumulated methane by the accumulation period. Table 3 shows accumulated methane, accumulation period and estimated regional methane fluxes for three measurement days. The values of the regional methane flux varies from 40 to 146 mg CH_4 m^{-2} day^{-1}. This large variation would be ascribed to spatial and temporal variability of methane concentration. The average methane flux for

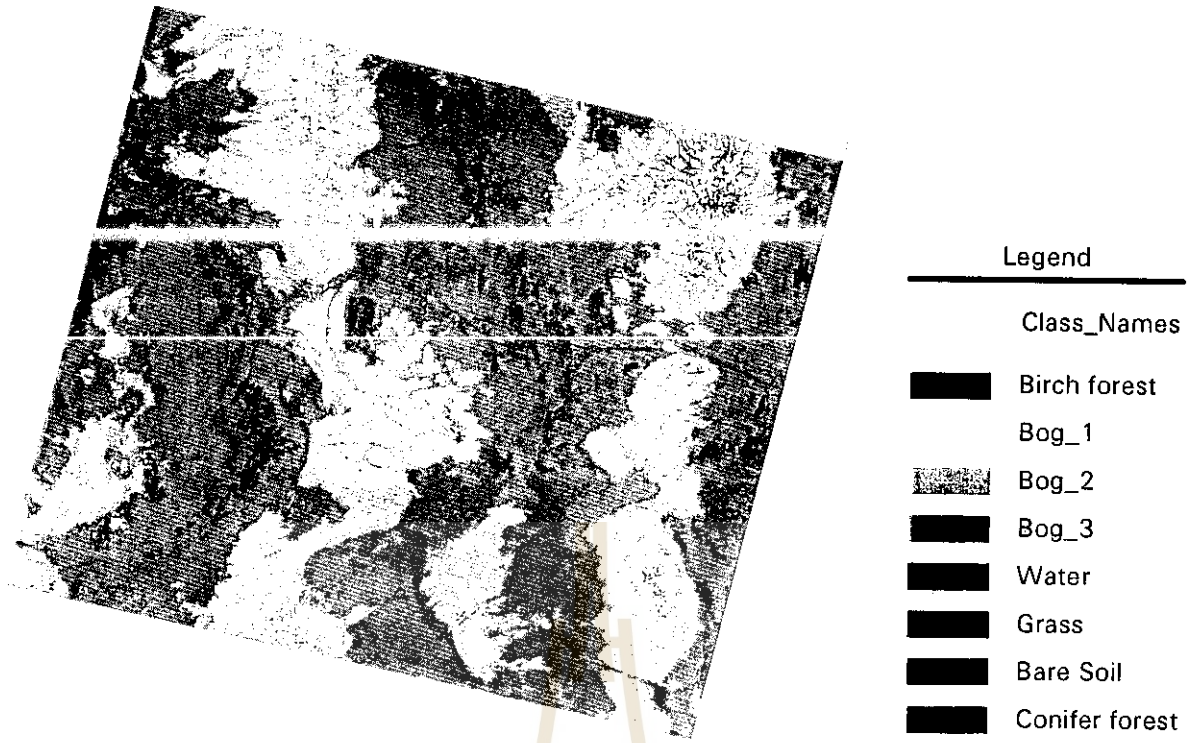

Figure 3. Result of land cover classification.

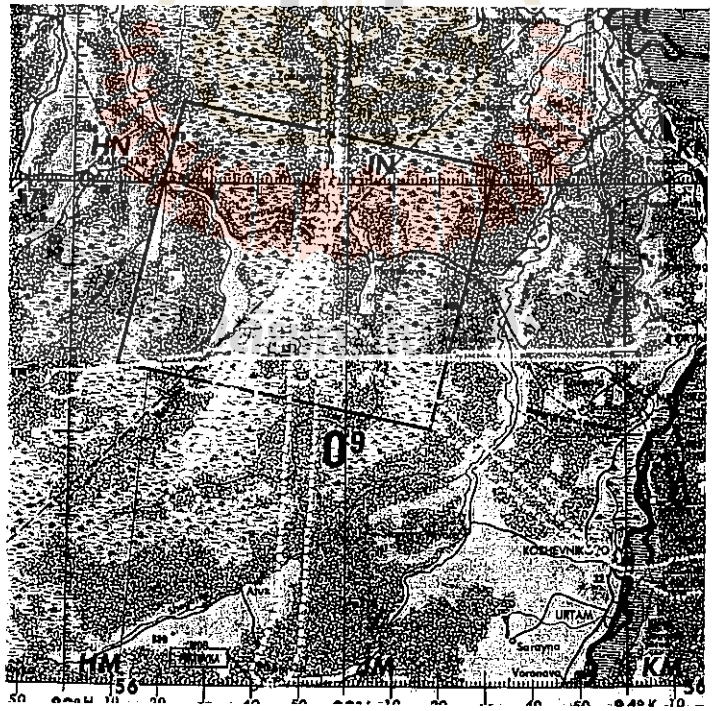

5 August 1994

Figure 4. Flight path of the observation aircraft on 5 August 1994. The rectangle shows the SPOT image area.

three days observations was 96 mg CH_4 m^{-2} day^{-1}, which almost agrees with the methane flux estimate of 102 mg CH_4 m^{-2} day^{-1} obtained from the combination of satellite and ground data.

Table 3. Regional methane fluxes estimated from the methane vertical profiles (Tohjima et al., 1994).

Date	Accumulated methane (mg m^{-2})	Accumulation period (hour)	Methane flux (mg CH_4 m^{-2} day^{-1})
3 Aug. 1994	55	13	102
5 Aug. 1994	20	12	40
6 Aug. 1994	79	13	146
Average	-	-	96

V. Summary

A SPOT/HRV image was used to classify wetland ecosystems at Plotnikovo test site. Methane emission from the image area was estimated by combining the result of ecosystem classification with ground methane flux data. This methane emission estimate was in good agreement with the average estimate obtained from airborne methane measurements. This demonstrates that ecosystem classification by remote sensing techniques would be useful in extrapolating ground methane flux measurements to regional or global scale estimates of methane emissions .

References

Panikov, N. S., CH_4 and CO_2 emission from northern wetlands of Russia: Source strength and controlling mechanisms, *Proceedings of the International Symposium on Global Cycles of Atmospheric Greenhouse Gases*, 100-112, 1994.

Tohjima, Y., Maksyutov, S., Machida, T., and Inoue, G., Airborne measurement of atmospheric CH_4 over the west Siberian lowland during the 1994 Siberian terrestrial ecosystem-atmosphere-cryosphere Experiment (STEACE), *Proceedings of the third symposium on the joint Siberian permafrost studies between Japan and Russia*, 50-57, 1995.

Estimation of Chlorophyll Concentration in Lakes and Inland Seas from Near-infrared and Red Spectral Signature

Kazuo Oki* and Yoshifumi Yasuoka**
*Institute of Socio-Economic Planning, University of Tsukuba
**National Institute for Environmental Studies

Contact : Y.Yasuoka National Institute for Environmental Studies
16-2 Onogawa, Tsukuba, Ibaraki 305, Japan
Tel. +81-298-50-2543, Fax +81-298-51-4731, E-mail yyasuoka@nies.go.jp

Abstract

A remote sensing method to estimate distribution of rich chlorophyll concentration in lakes or inland seas is proposed. First, the basic relationship between the chlorophyll concentration and the spectral reflectance of water was investigated. As a result, chlorophyll estimation model was derived using the ratio of spectral reflectance at two different wavelengths of 675nm (red range) and 700nm (near-infrared range). It was found that the spectral signature of near-infrared range is effective in remote sensing of rich chlorophyll water area like lakes or inland seas. The improved two-flow model to investigate the behaviour of the proposed model was used in rich chlorophyll water types. Furthermore, the amount of specular reflection from the water surface was assessed based on the spectral signature data measured above and below the water surface. The percentage of speclar reflection was evaluated at least 20% of the total radiance at the surface within the range of 400nm through 850nm. Finally, a method to remove the effect of specular reflection at the water surface was investigated for the proposed model. The model for specular reflection was proposed to eliminate its effect and to improve chlorophyll estimation accuracy.

1. Introduction

Environmental degradation in lakes and inland seas has been very serious due to extensive land cultivation or urbanization around area. In particular, Eutrophication has caused massive growth of phytoplankton or zooplankton in water and gives serious physical, social and economic impacts to the area. Measuring chlorophyll contents in the plankton is of significant importance in tackling with the water pollution problem. It is, however, not easy to monitor water quality distribution over a large area periodically based on a conventional water sampling and analysis method. In this papper, a remote sensing method to estimate the distribution of chlorophyll concentration is proposed. Lake Kasumigaura is selected as a test site for the study, and spectral signatures of water, spectral reflectance below and above water surface was measured together with several water quality parameters including chlorophyll, suspended solids and transparency.

Several models has been proposed for the estimation of chlorophyll concentration of lakes and oceans, however, most of them utilized only the spectral signatures in visible range (e.g., Gordon et al. 1983; Okami et al. 1982). It was because the water body usually absorbes the near-infrared spectral radiation and there is no reflectance from water in that range. In general, their models don't operate well to estimate rich chlorophyll concentration. In this study, chlorophyll estimation model which is effective in remote sensing of rich chlorophyll water area like lakes or inland seas was proposed.

The effect of specular reflection at the water surface was also one of important problem for estimating chlorophyll concentration by remote sensing. Takashima et al. (1986) developed model in order to remove effect of specular reflection at the water surface besed on Cox and Munk model. However, the Takashima model has not been verified, if it would oerate well in rich chlorophyll water area like lakes or inland seas. In this study, the model was verified based on the spectral signature data measured above and below the water surface.

2. Chlorophyll-a Estimation Model

2.1 Radiative Transfer Model at the Water Surface

The spectral reflectance R of radiance to irradiance at the water surface is defined by

$$R = \frac{I_t}{E_a} \tag{1}$$

$$I_t = I_w + I_r \tag{2}$$

$$E_a = E_i + E_s \tag{3}$$

where I_t is the upwelling spectral radiance from the water surface. E_a is the downward irradiance onto the water surface from total solar radiation. I_w is the upwelling spectral radiance just above water surface. I_r is the upwelling spectral radiance reflected from water surface due to total solar radiance. E_i and E_s are the downward irradiance onto the water surface due to direct sun and the diffuse sky light, respectively. In this report, it is assumed that the water body is a lambertian reflector and the angular distribution of radiance in the lower hemisphere of the water surface is uniform for radiance traveling upward. Then I_w can be expressed as

$$I_w = \frac{t}{n^2} I_w(0)$$

$$= \frac{t}{n^2}\frac{1}{\pi} E_w(0) \tag{4}$$

where t and n are transmittance and refractive index from water to air, respectively. $I_w(0)$ is the upwelling spectral radiance just below the water surface. $E_w(0)$ is the upwelling spectral irradiance just below the water surface. We cannot, however, measure it directly, therefore, $E_w(0)$ was estimated from the upwelling iiradiance at the depth of Z as

$$E_w(0) = E_w(Z)\exp^{k \cdot Z} \tag{5}$$

where k is the extinction coefficient for the upwelling irradiance of the water, expressed as

$$k = \frac{1}{Z2 - Z1}\log\frac{E_w(Z1)}{E_w(Z2)} \tag{6}$$

2.2 Measurement of Spectral Reflectance at Lake Kasumigaura

The upwelling radiance of the Lake Kasumigaura was measured by using spectroradiometer at the water surface and at several depth layers at the each points(Pt1 ~ Pt18). The Pt1to Pt10, Pt11 to Pt16, and Pt17 to Pt18 were mesured on 10 September 1993, 22 April 1994 and 27 July 1994, respectively. The mesurements covers the wavelength interval 400nm to 850nm with a resolution of 2nm. At the each points, were measured as follows.

- Upwelling spectral radiance from the water surface (I_t)
- Upwelling spectral irradiance of the underwater at depths of 10 and 40cm from the water surface ($E_w(0.1)$, $E_w(0.4)$)
- Spectral irradiance of white board (E_s)
- Spectral irradiance of white board shaded (E_s)

The spectral signature of water was obtained by averaging over ten times scanning. The upwelling spectral radiance ($E_w(0.1)$, $E_w(0.4)$) of the underwater was measured one time (ten times scanning) and upwelling spectral radiance (I_t) at the water surface was measured three times (thirty times scanning). Average of I_t over three times measurements is expressed as $\bar{I}_t$. Water quality parameters such as chlorophyll-a, suspended solids and transparency were also measured at the same point.

2.3 Selection of Effective Spectral Reflectance to Estimate Chlorophyll-a concentration

We ignored specular reflection for making stable chlorophyll-a estimation model, and the Eq.(1) was given I_w instead of I_t. Fig.1 shows spectral reflectance examples calculated just above the water surface at Pt1, Pt6, Pt11 and Pt18 of Lake

Kasumigaura. It shows that the richer the chlorophyll concentration is, the stronger the absorption of radiance of 675nm is.

It was reported that the ratio of spectral reflectance at two different wavelengths was well correlated with chlorophyll concentration at Lake Kasumigaura polluted by many particles (Okami et al.1982), however, it has not been confirmed numerically. In this study, regression analysis was used to evaluate the relationship between chlorophyll-a concentration and ratio of spectral reflectance at two different wavelengths in various conditions of Pt1 to Pt18.

Fig.2 shows distribution of correlation coefficient in the three dimensional space with the denominator and numerator of ratio of spectral reflectance at two different wavelengths. It is found that the ratio of spectral reflectance of 675nm and 700nm, R_{700} / R_{675} was the best correlation of all patterns within the range of 400nm through 850nm. The correlation coefficient was 0.979 despite various conditions. It is because the chlorophyll-a usually absorbes light around 675nm and reflect light around 700nm. It was reported that upward radiance at the wavelength of around 700nm was due to fluorescence of chlorophyll-a giving an effect on the reflectance peak and the peak is shifted toward longer wavelength as the chlorophyll-a concentration increase (Kishino et al. 1986). However, the effect of fluorescence was't clearly shown in Fig.1. It may be because the water type like Lake Kasumigaura polluted by many particles reduce the effect of fluorescence. Therefore, the effect of fluorescence is ignored in this study and we propose R_{700}/ R_{67} model for estimating chlorophyll-a concentration. Fig.3 shows relationship between R_{700}/ R_{67} and chlorophyll-a concentration.

3. Verification of Chlorophyll-a Estimation Model

Ocean color spectra have been computed by means of the two-flow model by many investigators, however, the final mathematical expressions obtained by each of them differ to some degree. In this study, the following equation for irradiance reflectance given by Morel et al. (1977) is used.

$$R_\lambda = 0.33\frac{b_\lambda}{a_\lambda} \tag{7}$$

where a_λ and b_λ are the absorption coefficient and the backscattering coefficient of wavelength λ,respectively. The a_λ and b_λ can be expressed as

$$b_\lambda = b_{water\lambda} + b_{other\lambda} + b_{Chl\lambda} \tag{8}$$

$$a_\lambda = a_{water\lambda} + a_{other\lambda} + a_{Chl\lambda} \tag{9}$$

where $b_{water\lambda}$, $b_{other\lambda}$ and $b_{Chl\lambda}$ are backscattering coefficient for pure water, suspended particles except for chlorophyll-a and chlorophyll-a. $a_{water\lambda}$, $a_{other\lambda}$ and $a_{Chl\lambda}$ are absorption coefficient for pure water, suspended particles except for chlorophyll-a and chlorophyll-a.

We assumed as follows ;

Assumption 1: The water type polluted by many particles can be expressed as

$$b_{water} \langle\langle b_{other}$$

Assumption 2: Okami et al. (1977) assumed that the dependence on wavelength of backscattering coefficient is constant. We also assumed as

$$b_{other\,675} + b_{Chl\,675} = b_{other\,700} + b_{Chl\,700}$$

From assumption 1 and 2 ,the Eq.(8) can be written as

$$\begin{aligned} b_{675} &= b_{water\,675} + b_{other\,675} + b_{Chl\,675} \\ &= b_{other\,675} + b_{Chl\,675} \\ &= b_{other\,700} + b_{Chl\,700} \\ &= b_{700} \end{aligned} \tag{10}$$

The absorption coefficient for chlorophyll-a of Eq.(9) is considered to be linearly related to chlorophyll-a concentration C, that is

$$a_{Chl\lambda} = a'_{Chl\lambda} \cdot C \tag{11}$$

where $a'_{Chl\lambda}$ is the absorption coefficient per unit chlorophll-a concentration. Using Eq.(7) through (11), the proposed chlorophyll estimation model can be expressed as

$$\frac{R_{700}}{R_{675}} = \frac{a_{675}}{a_{700}} = \frac{a_{water\,675} + a_{other\,675} + a'_{Chl\,675} \cdot C}{a_{water\,700} + a_{other\,700} + a'_{Chl\,700} \cdot C} \qquad (12)$$

It is found that the Eq.(12) can consequently ignore backscattering coefficient using ratio of spectral reflectance of 675nm and 700nm.

In this study, the values of $a_{other\,675}$ and $a_{other\,700}$ reported by Okami et al. (1982) were used. The values of $a'_{Chl\,675}$, $a'_{Chl\,700}$ and $a'_{Chl\,650}$ reported by Morel et al. (1977) were used, and $a_{water\,675}$ and $a_{water\,700}$ were adopted from Smith (1981).

Fig.4 shows comparison between chlorophyll-a concentration and R_{700}/R_{675} of value calculated from Eq.(12) and value measured. It is found that the calculated R_{700}/R_{675} accord with the measured R_{700}/R_{675} when chlorophyll-a concentration is less than 60 μg/l, however, they don't accord with each other when chlorophyll-a concentration is greater than 90 μ g/l. One reason might be that the assumption 2 don't hold good. It is because the value of $b_{Chl\,675}$ decrease with the increase in chlorophyll-a concentration.

Fig.5 shows the result of R_{700}/R_{675} simulated by using Eq.(12) in varing chlorophyll-a and suspended solids concentration. It is found that the R_{700}/R_{675} depend on SS concentration when chlorophyll-a concentration is greater than 30 μg/l, however, the R_{700}/R_{675} has nothing to do with ss concentration when chlorophyll-a concentration is less than 30 μ g/l. Therefore the R_{700}/R_{675} can extract chlorophyll-a concentration which is less than 30 μ g/l.

4. Method to Remove the Effect of Specular Reflection

Fig.6 shows a part of ratio ($I_r / \bar{I}_t$) of upwelling spectral radiance ($I_r (= \bar{I}_t - I_w)$) reflected from water surface due to total solar radiance to upwelling spectral radiance ($\bar{I}_t$) measured at the water surface of Pt11. The effect of specular radiance within the range of 550nm through 700nm is the smallest within the range of 400nm through 850nm, however, the percentage is evaluated at least 20% of the total radiance at the water surface. Therefore, a method to remove the effect of specular reflection at the water surface must be investigated for the proposed chlorophyll-a estimation model.

4.1 Specular Reflection Model

Takashima et al. (1986) developed the model removing effect of specular reflection at the water surface based on Cox and Munk model. In this model, it is assumed that the wind-ruffled water surface consists of a collection of individual facets obeying an isotropical Gaussian distribution.

The $I_t(\theta_r, \phi_r)$ measured by spectroradiometer must be measured k times at the water surface for obeying an isotropical Gaussian distribution, i.e.,

$$\bar{I}_t(\theta_r, \phi_r) = \frac{1}{k} \sum_{i=1}^{k} I_{ti}(\theta_r, \phi_r) \qquad (13)$$

where $\bar{I}_t(\theta_r, \phi_r)$ is average of $I_t(\theta_r, \phi_r)$ over k times measurements. The $\bar{I}_t(\theta_r, \phi_r)$ can be written as

$$\bar{I}_t(\theta_r, \phi_r) = I_{rs}(\theta_r, \phi_r) + I_{ri}(\theta_r, \phi_r) + I_w(\theta_r, \phi_r) \qquad (14)$$

$$I_{rs}(\theta_r, \phi_r) = \frac{1}{4\pi u_r} \int_0^1 \int_0^{2\pi} r(\theta_i, \phi_i \rightarrow \theta_r, \phi_r) I_s(\theta_i, \phi_i) d\phi_i d\theta_i \qquad (15)$$

$$I_{ri}(\theta_r, \phi_r) = \frac{1}{4\pi u_r} r(\theta_i, \phi_i \rightarrow \theta_r, \phi_r) I_i(\theta_i, \phi_i) \qquad (16)$$

with

$$U_r = \cos\theta_r$$
$$r(\theta_i, \phi_i \rightarrow \theta_r, \phi_r) = \rho P(\theta_i, \phi_i \rightarrow \theta_r, \phi_r)$$

where θ and ϕ are the polar angle measured from the nadir and the azimuth of propagation relative to the solar azimuth, respectively. $I_{rs}(\theta_r, \phi_r)$ is radiance reflected from water surface due to diffuse sky light. $I_{ri}(\theta_r, \phi_r)$ is radiance reflected

from water surface due to direct sunlight. $I_w(\theta_r,\phi_r)$ is radiance just above water surface. $I_s(\theta_i,\phi_i)$ and $I_i(\theta_i,\phi_i)$ are downward radiation onto the water surface due to diffuse sky light and direct sunligh. The factor ρ is the Fresnel reflectance of water. $P(\theta_i,\phi_i \rightarrow \theta_r,\phi_r)$ is the fraction of the water surface with the required orientation to reflect light from (θ_i,ϕ_i) to (θ_r,ϕ_r) and is the probability that an individual facet is visible. $P(\theta_i,\phi_i \rightarrow \theta_r,\phi_r)$ is given by

$$P(\theta_i,\phi_i \rightarrow \theta_r,\phi_r) = \frac{a^2}{\pi\sigma^2}\exp\left((1-2a)/\sigma^2\right) \tag{17}$$

$$a = \frac{\left(1+\cos\theta_i\cos\theta_r-\sin\theta_i\sin\theta_r\cos(\phi_i-\phi_r)\right)}{\left(\cos\theta_i+\cos\theta_r\right)^2} \tag{18}$$

where σ is related to the wind speed W [m/s] measured above the water surface as

$$\sigma^2 = 0.003 + 0.00512 \cdot W \pm 0.004 \tag{19}$$

Therefore, radiance I_w just above water surface from Eq.(14) can be written as

$$I_w = \bar{I}_t - (I_{rs} + I_{ri}) \tag{20}$$

4.2 Verification of Specular Reflection Model

We used data of Pt11 to Pt18 measured wind speed at the water surface. The radiance just above water surface calculated from Eq.(20) based on specular reflection model

$$I_w\left(=\bar{I}_t-(I_{rs}+I_{ri})\right)$$

and the radiance just above water surfacecalculated from Eq.(4)

$$I_w'\left(=\frac{t}{n^2\pi}E_w(Z)\exp^{kZ}\right)$$

were compared. The wind speed was used average of Pt11 to Pt16 and Pt17 to Pt18, and they were 2.022 [m/s] and 1.283 [m/s], respectively.

Fig.7 shows a part of spectral radiance distribution of I_t, I_w and I_w' at the Pt11. Furthermore, fig.8 shows relationship between I_w and I_w' of all data. It is found that the radiance just above water surface calculated from Eq.(20) and Eq.(4) accord with each other ($I_w \approx I_w'$), and the specular reflection model can remove the effect of specular reflection at the water surface.

5. Conclusions

The followings have been shown in this study.

1. Chlorophyll estimation model was derived using the ratio of spectral reflectance at two different wavelengths of 675nm (red range) and 700nm(near-infrared range). The correlation coefficient was 0.979.
2. It was found that the calculated R_{700}/R_{675} from Eq.(12) accorded with the measured R_{700}/R_{675} when chlorophyll-a concentration is less than 60 μg/l, however, they don't accord with each other when chlorophyll-a concentration is greater than 90 μg/l.
3. The value of R_{700}/R_{675} by using Eq.(12) in varing chlorophyll-a and suspended solids concentration was simulated. It was found that the R_{700}/R_{675} depend on SS concentration when chlorophyll-a concentration is greater than 30 μg/l, however, the R_{700}/R_{675} has nothing to do with ss concentration when chlorophyll-a concentration is less than 30 μg/l. Therefore the R_{700}/R_{675} can extract chlorophyll-a concentration which is less than 30 μg/l.
4. The percentage of speclar reflection was evaluated at least 20% of the total radiance at the surface within the range of 400nm through 850nm.
5. It was found that the radiance just above water surface calculated from Eq.(24) and Eq.(4) accord with each other ($I_w \approx I_w'$), and the specular reflection model can remove the effect of specular reflection at the water surface.

References

Gordon, H.R., et al., "Phytoplankton Pigment Concentrations in the Middle Atlantic Bight : Comparison of ship Determinations and CZCS Estimates ", APPLIED OPTICS, Vol.22 , No.1 , pp.20-36, 1983.

Kishino, M.,et al., "Theoretical analysis of the in situ fluorescence of chlorophyll a on the underwater spectral i rradiance", La mer, Vol.24, pp.130-138, 1986.

Morel, A.,et al., "Analysis of variations in ocean color", Limnol. Oceanogr., Vo.22, pp.709-722,1977.

Okami, N., et al, "Studies on Ocean Color Spectrum (in Japanese)", Bull. Coast. Oceanogr., Vol.15, No.1, pp.56-66,1977.

Okami, N., et al, "Correlation Studies between Spectral Radiance Reflectance and Water Qualities in Lake Kasumiga-ura", Journal of The Remote Sensing Society of Japan, Vol.2, No.1 , pp.21-31,1982.

Smith, R.C., et al , "Optical Properties of the Clearest Natural Waters (200-800nm)", APPLIED OPTICS , Vol.20 , No.2 , pp.177-184 , 1981.

Takashima, T.,et al., "A Computational Procedure of the Upwelling Radiation Emerging from the Atmosphere-Ocean System", Journal of The Remote Sensing Society of Japan, Vol.6, No.1, pp.5-33, 1986.

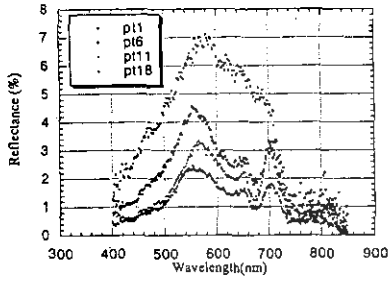

Fig.1 Spectral reflectance calculated just above the water surface at Lake Kasumigaura.

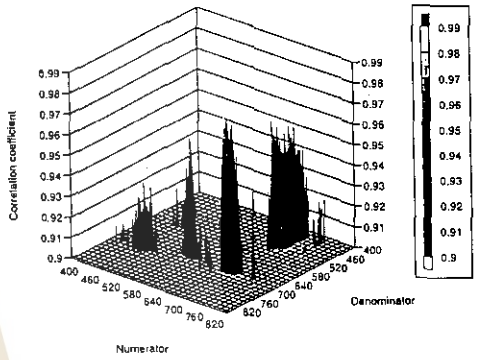

Fig.2 Distribution of correlation coefficient in the three dimensional space.

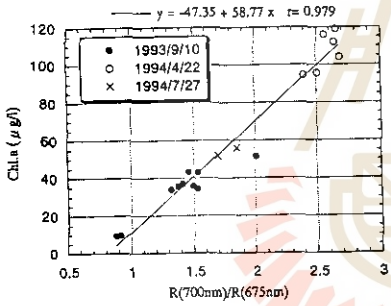

Fig.3 Relationship between Chl.a concentration and ratio of reflectance at two different wavelengths.

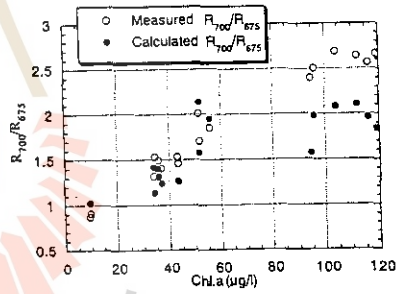

Fig.4 Comparison between measured R_{700}/R_{675} and calculated R_{700}/R_{675}.

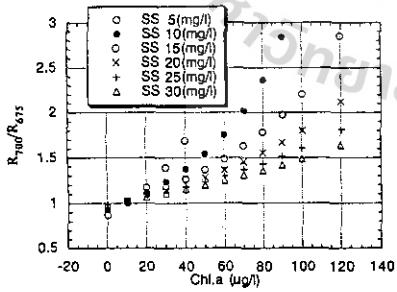

Fig.5 Simulation of R_{700}/R_{675} with varing Chl.a and SS concentration.

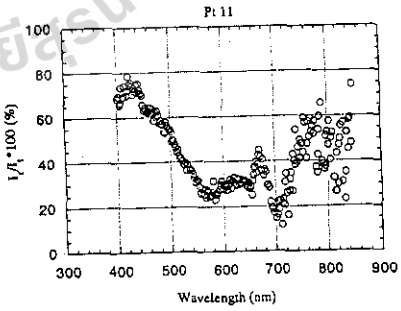

Fig.6 Relationship between $I_t/\bar{I}_t$ and wavelength at point 11.

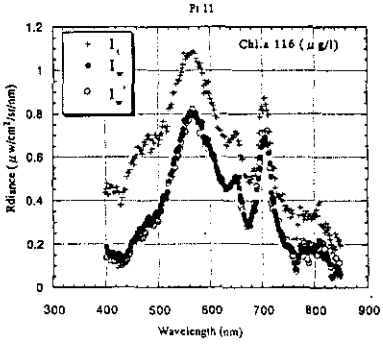

Fig.7 Spectral radiance of I_t, I_w, I_w' at Lake Kasumigaura. Wind speed is 2.022(m/s)

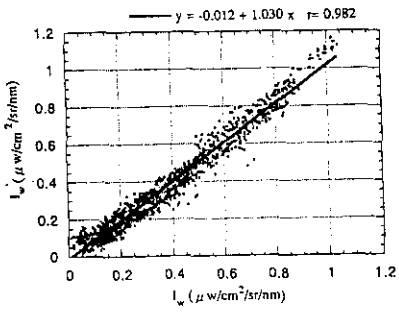

Fig.8 Relationship between I_w and I_w'.

WEATHER FORECAST AND PLANKTON BLOOM DETECTION USING OCEANOGRAPHIC BUOY IN THE GULF OF THAILAND

Dr. Pitan Singhasaneh

SEAWATCH Thailand Programme
Remote Sensing Division
National Research Council of Thailand
196 Paholyothin Road, Jatujak, Bangkok 10900, Thailand

ABSTRACT

SEAWATCH THAILAND is a complete marine environmental monitoring and forecasting system which integrates data collection, data analysis, environmental modeling and forecasting with an advanced computerized system for distribution of marine information and forecasts to interested operators and/or authorities. The data measured from the programme can be effectively used in the forecasting of weather and the detection of plankton bloom. The combination of buoy data with satellite data and air survey yields an increase of effectiveness in the weather forecast and plankton bloom detection.

1.0 INTRODUCTION

SEAWATCH THAILAND is a complete marine environmental monitoring and forecasting system which integrates data collection, data analysis, environmental modeling and forecasting with an advanced computerized system for distribution of marine information and forecasts to interested operators and/or authorities. The project is being implemented under close co-operation between the National Research Council of Thailand (NRCT), OCEANOR, the oceanographic company of Norway, and other involving parties, including the Harbour Department, the Meteorological Department, Port Authority of Thailand, Naval Hydrographic Department, Department of Fisheries, the Petroleum Authority of Thailand, Marine Police Division, Chulalongkorn University, Kasetsart University, Prince of Songkla University, Burapha University, etc.

2.0 PROGRAMME OBJECTIVES

2.1 To set up a marine database using technological integration of remote sensing, buoy network, and meteorology.

2.2 To archive and distribute marine data and information to involving agencies both in governmental and private sectors to be used in national resources development and management.

2.3 To coordinate and work with other organizations in the studies and researches in the field of oceanography and marine resources.

2.4 To coordinate and work with involving agencies in the utilization of marine data and information in national resources planning, development, preservation.

3.0 PROGRAMME ACTIVITIES

3.1 *Data Acquisition* A real time data covering is provided by a network of moored data buoys (called TOBIS buoys), which includes meteorological parameters (wind speed & direction, air temperature & pressure) and oceanographic parameters (oxygen/nutrient contents, light attenuation, waves, currents, temperature/ salinity profile, radioactivity). The buoys have also their own data logging equipment, on-board processing (for data analysis & quality control), and a transmission system. The collected data are then transmitted to a shore station through the ARGOS satellite communication system on NOAA.

3.2 *Data Storage, Analysis and Presentation* The data is processed and stored in the database in time series format. The data can be re-presented in the form of tables or graphics.

3.3 *Environmental Modeling and Forecasting* A number of numerical modeling and forecasting software have been developed under the programme, including: HYBOS, NOMAD, OILSPILL, OILSTAT.

3.4 *Data/Forecasts/Users-Relevant Information Distribution* An information system or "Thainet" allows users to have easy access to the various data collected and other derived information including the forecasts on a near real-time basis via PC terminals.

4.0 WEATHER FORECAST

Buoy data has been used by the Meteorological Department for the weather forecast. The buoy network provides valuable meteorological data (wind speed, wind direction, air pressure, air temperature) and oceanographical data (wave height & period, current, water temperature) on the near-real-time basis. The in-situ measurements from the buoy network and the data from meteorological satellite are the indispensable tools for the weather forecast in the Gulf of Thailand.

October 1994 plots of Plathong buoy are shown here to demonstrate the buoy ability to detect changes in weather and sea-state. The meteorological weather chart of the Weather Forecast Division, Meteorological Department is also included for the data comparison.

5.0 PLANKTON BLOOM DETECTION

Rate of occurrences of plankton bloom has been increasing in recent years in the Gulf of Thailand. Two species of blue-green algae; Trichodesmium erythraeum (Ehr. ex Gomont) and Trichodesmium thiebautii (Gomont ex Gomont) Geitler, and Noctiluca miliaris; are found to be the cause of sea water discoloration. Blooms are also frequently seen in the vicinity of estuarine area showing the colors of red, green, yellow, and brown.

Some of the sensors on the buoy can indicate the development of the algal bloom by the detection of changes of sea water light attenuation and dissolved oxygen. The light attenuation and dissolved oxygen values are shown in this paper together with the flight report from the Planning Divisions, Department of Industrial Work. Easily seen from the plots, the level of light attenuation increase and the dissolved oxygen values show greater fluctuations during the bloom development.

6.0 CONCLUSION

The SEAWATCH THAILAND programme is established through networking of data collection buoys. The measured parameters can be effectively used in the forecasting of weather and the detection of algal bloom. The combination of buoy data and air survey (and possibly satellite data) yields the increase of effectiveness in both areas.

Figure 1: Plots from Plathong Buoy (in the middle of the Gulf of Thailand) in October 1994, consisting of Air Temperature, Air Pressure, Wind Speed, Wind Direction, Water Temperature, Wave Height, and Wave Period.

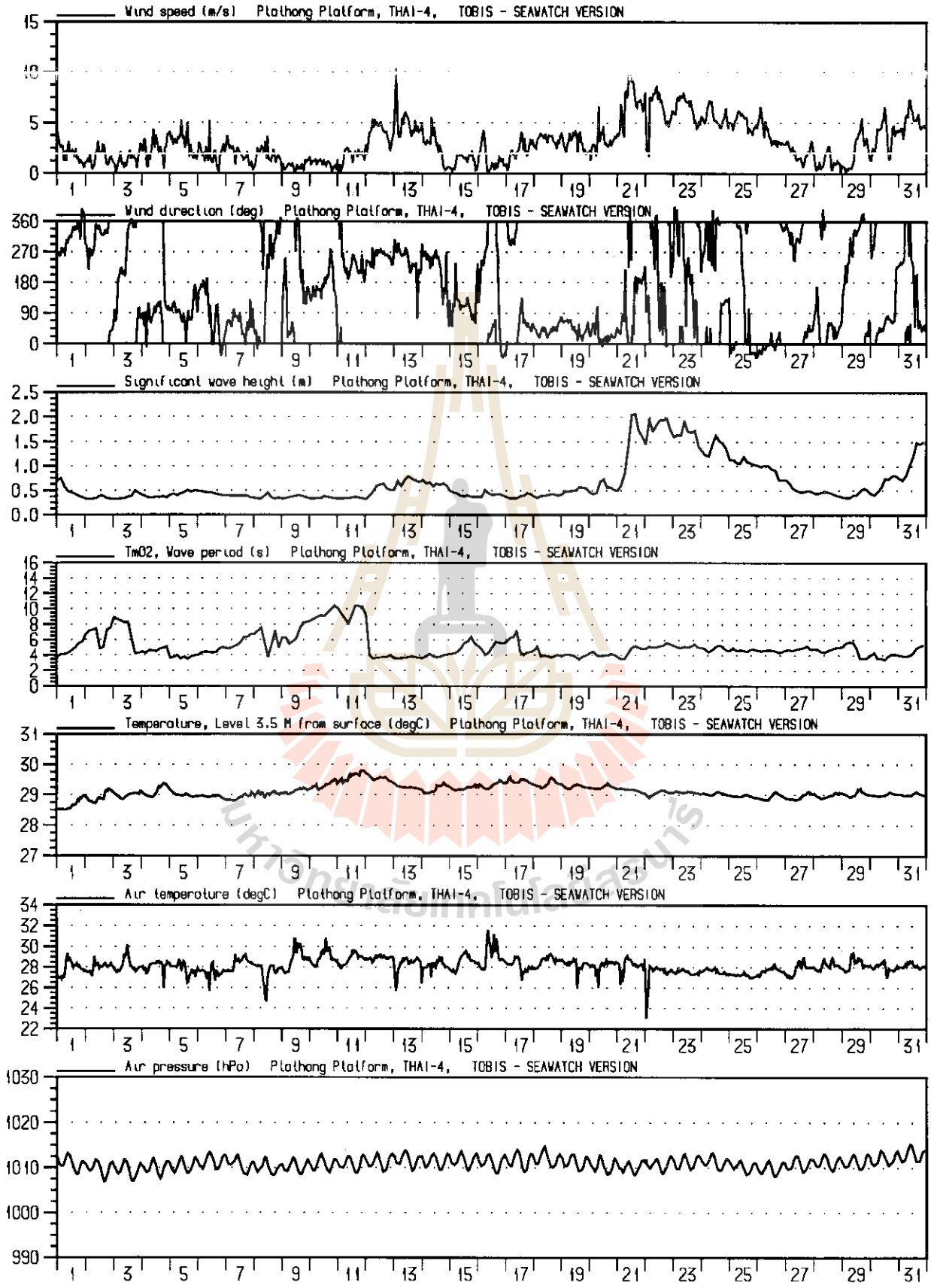

Figure 2: Weather Chart, obtained from Meteorological Department, Ministry of Transport and Communications, Thailand. The first chart is dated Tuesday 25 October 1994 at 0700 local time. The second chart was dated Wednesday 26 October 1995 at 0700 local time.

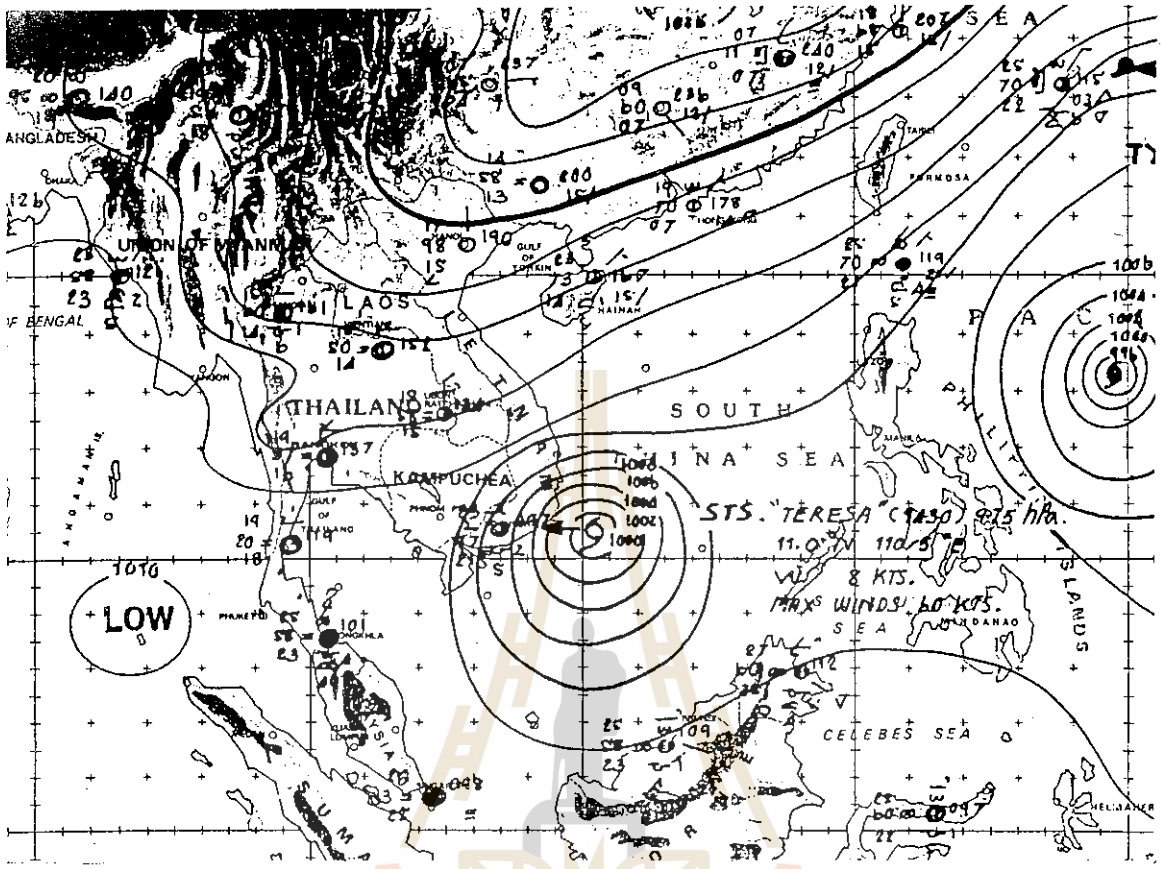

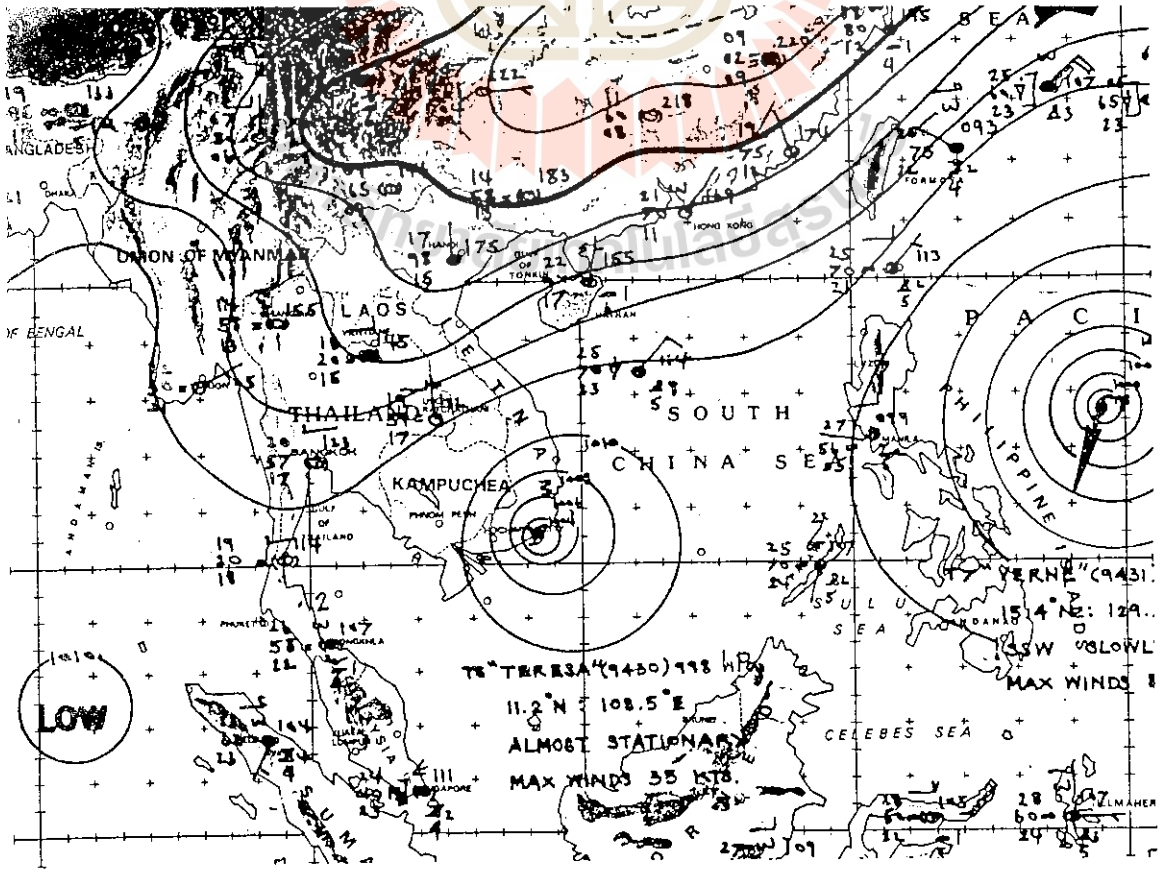

Figure 3: Plot of Sichang Buoy (near Sichang Island) showing Blue, Green, and Red Attenuation, and Dissolved Oxygen Content. The plot was taken from the period of 27 August 1994 to 10 September 1994.

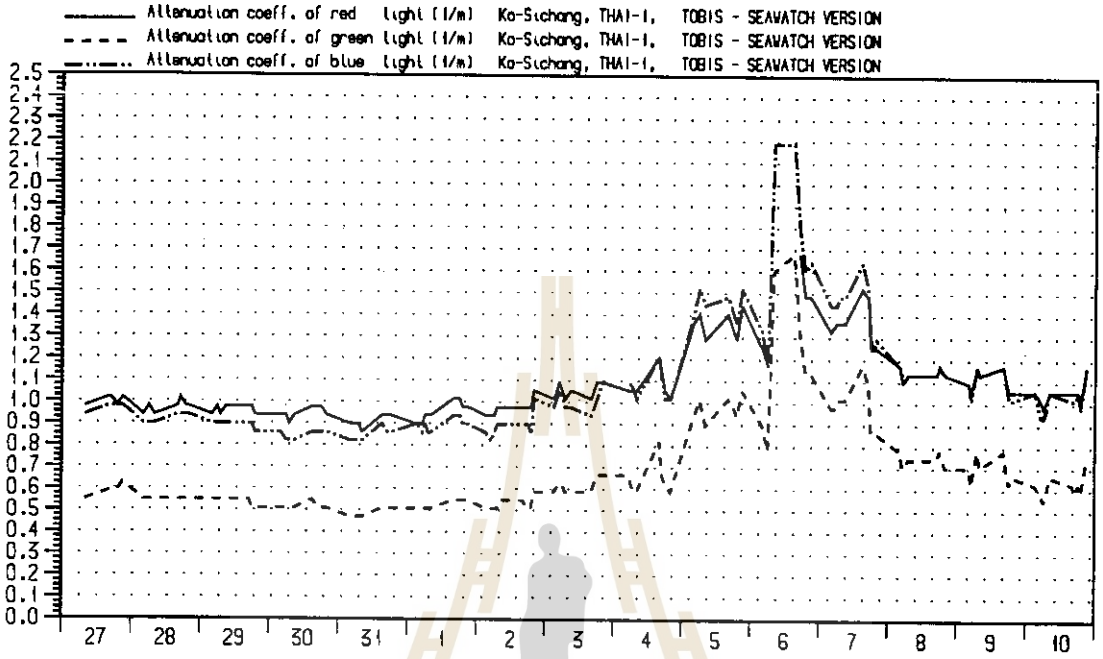

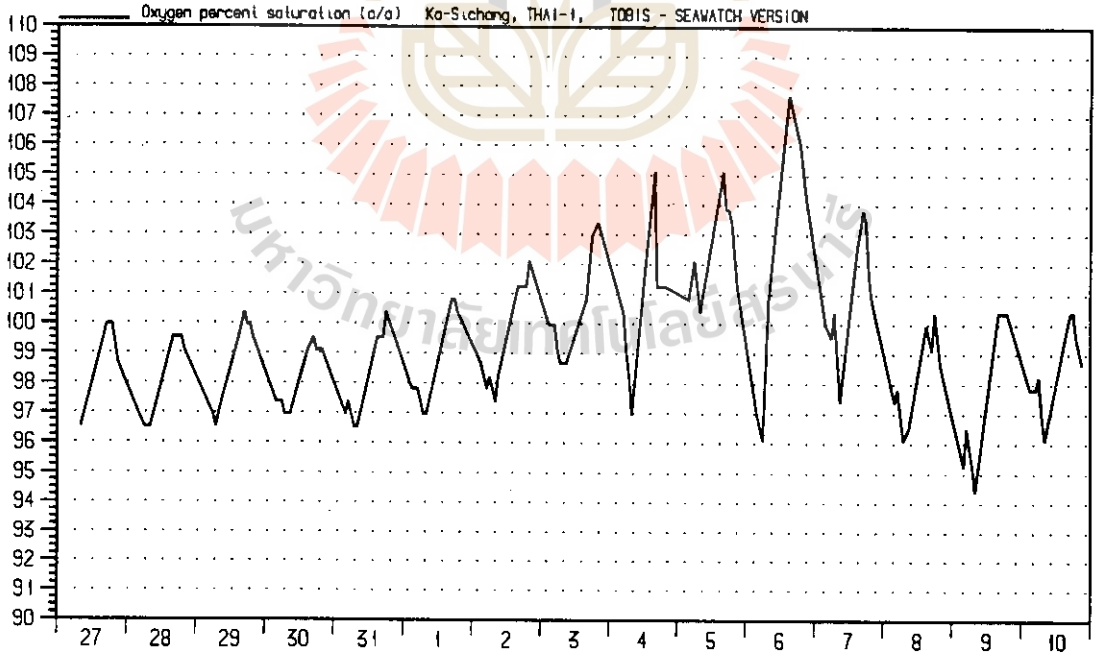

SEAWATCH THAILAND				INSTRUMENT ARGOS DATA
LOCATION Ko-Sichang, THAI-1	STATION 1	WATER DEPTH 25 m	INSTRUMENT DEPTH 3 m	OBSERVATION PERIOD 1994.08.27-1994.09.10 LT
NRCT National Research Council of Thailand			PROJECT 1	FIGURE 3

orkan33/app

Figure 4: Air Survey map of 4 September 1994 at 1050 and 1410 from Planning Division, Department of Industrial Works, showing the area which was affected by algae bloom. The survey was performed from the aircraft. The bloom was green/black in color, covering approximately 300 square kilometer from the mouth of Chophaya river to the North of Sichang Island.

TECHNICAL SESSION E

DIGITAL IMAGE PROCESSING

Data Compression using Vector Quantization and Huffman Coding for Satellite Imagery

by

F. Cheevasuvit, K. Dejhan, S. Mitatha and S. Wongkharn

Faculty of Engineering, King Mongkut's Institue of Technology Ladkrabang,

Bangkok 10520, Thailand

Abstract

The transmission of satellite image data from an organization to another through public communication network is used for change detection task such as a detection of illegal deforestation. It is necessary to transmit frequently an enormous amount of data. This will cause a high cost and need a huge transmission bandwidth. This paper presents a satellite image data compression technique via vector quantization and Huffman coding before transmission. The proposed technique will give a high compression rate so the cost and transmission bandwidth will be reduced.

1) Introduction

An important problem in satellite imagery data communication system of an organization is transmission an enormous amount of data. Although there are many techniques in data compression [1,2] to slove this problem, it is difficult for a small organization to perform. At present, a microcomputer trends to be decreased in price because of the higher micro-electronics technology. So a small organization possibly provides a microcomputer to use itselve. An image compression using vector quantization is an efficiency technique which results a high compression rate. It can easily perform on a microcomputer. However, this technique will give some distortions. So it is proposed for change detection task which does not need high quality in detail. A Huffman coding will also be applied to this vector quantized imagery to increase compression rate with preserved distortion. The advantage in this high comprssion rate reduces expenditure of a small orgaization.

2) Image compression using vector quantization

Image compression using vector quantization (VQ) [3] is a lossy compression technique. It is defined as a mapping Q of K-dimentional Euclidean space R^K into a finite subset Y of R^K. Thus

$$Q: R^K \rightarrow Y \tag{1}$$

where $Y = (\hat{x}_i; i = 1,2,...,N)$ is the set of reproduction vectors and N is the number of vectors in Y.

A vector quantizer is composed of two parts, encoder and decoder. An encoder will compare each input vector with every codevector in the codebook and generate index which represent the minimum distortion codevector from the input vector. A decoder takes the indexs to locate the codevector in the codebook and generate the output vectors.

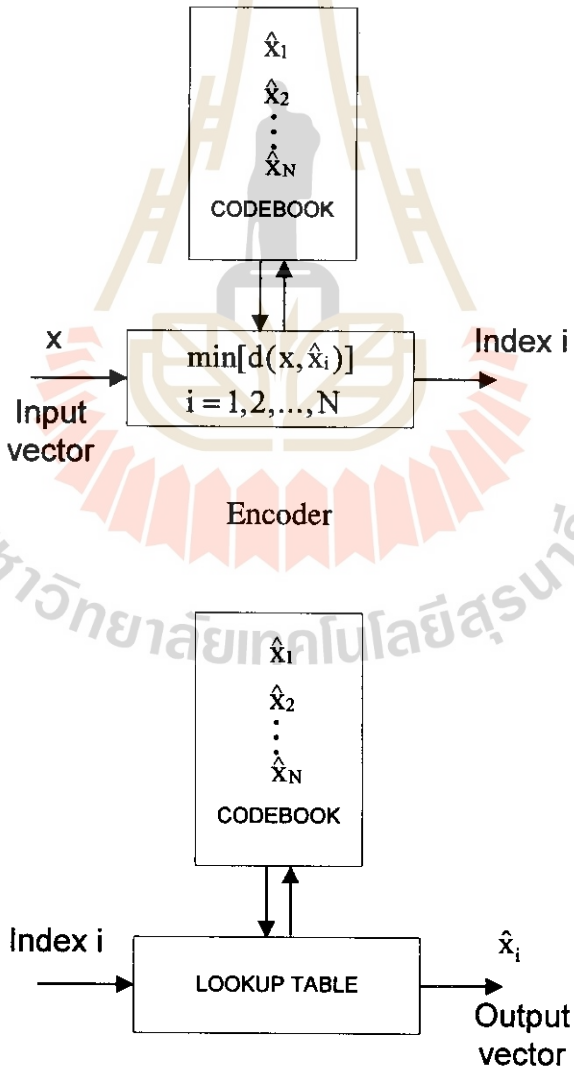

Fig.1 Block diagram of VQ

A codebook is the set of finite codevector for representing the input vector. The popular technique in codebook design is the Linde-Buzo-Gray (LBG) algorithm[4]. The whole image is partitioned into subblocks and all subblocks are used for training this codebook.

3) Huffman coding

A Huffman coding [1,2] is an error free (lossless) compression technique. The principle method of this technique is to encode the more probability data by the less bit code. It can be summarized as following algorithm.

(1) Find the probability of each data and sort them.

(2) Generate new node by combination the two smallest probability together then sort the probability of new node with the remainder probabilities.

(3) Define 1 for a branch of new node and 0 for another.

(4) Repeat (2) and (3) untill the final probability is 1.0.

An example of Huffman coding can be shown as follows :

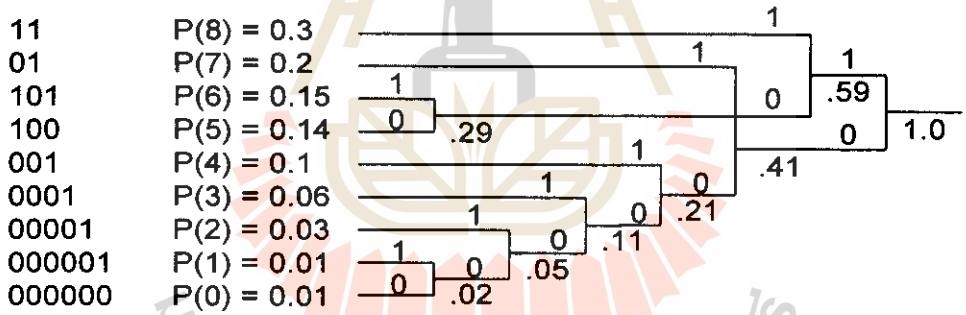

Fig.2 An example of Huffman coding

4) Experiment result

The two days , 256 x 256 pixels, Landsat MOS-I MESSR imageries were used for this experiment. The block diagram of this experiment is shown in Fig.3. The 256 codevectors in the codebook were generated by using LBG algorithm. The training sequence was the sequence of 4 x 4 subblocks of the first day imagery (Fig.4). A vector quantization and Huffman coding were applied to the first day imagery. The result of decoded imagery is shown in Fig.5. Then the same processing and codebook were applied to the second day imagery (Fig.6). The result of decoded imagery is shown in Fig.7.

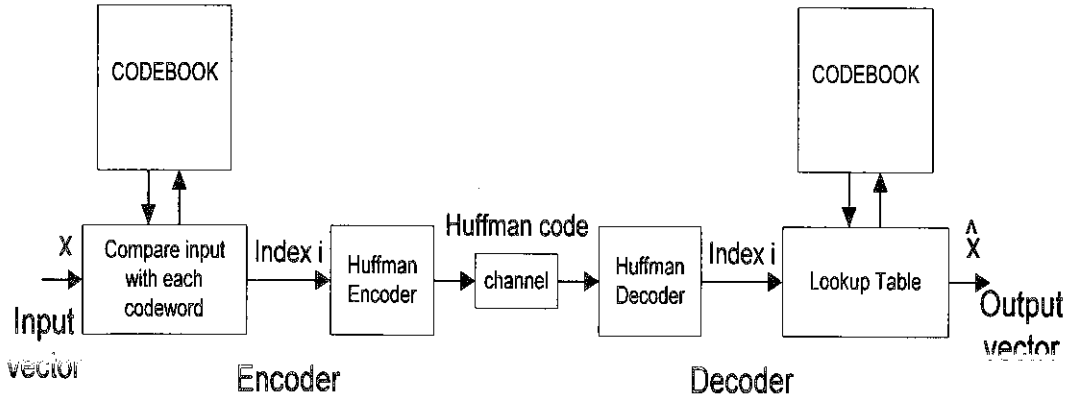

Fig.3 Block diagram of the experiment

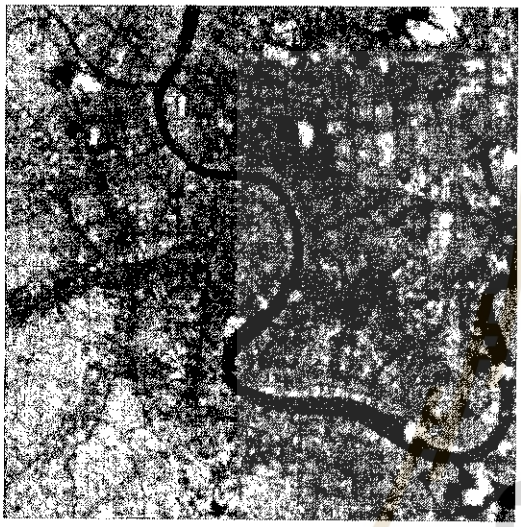

Fig.4 Landsat MOS-I MESSR imagery on the first day (8 bpp)

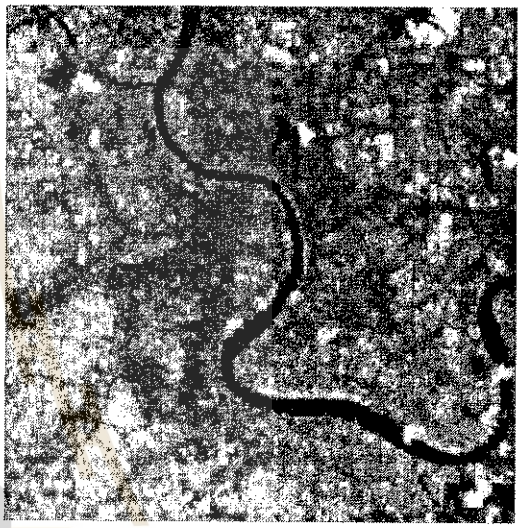

Fig.5 Decoded imagery (MSE = 89.43, Rate = 0.5 bpp)

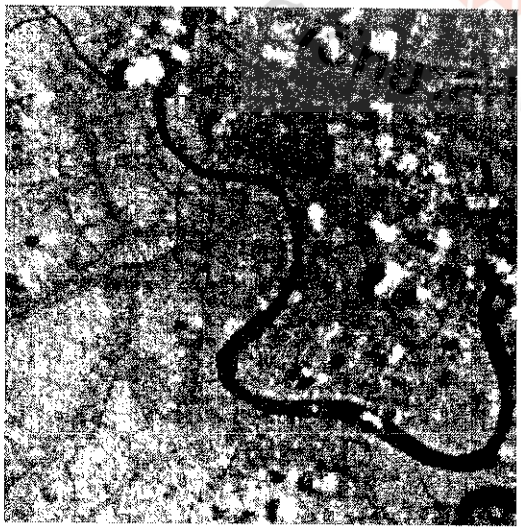

Fig.6 Landsat MOS-I MESSR imagery on the second day (8 bpp)

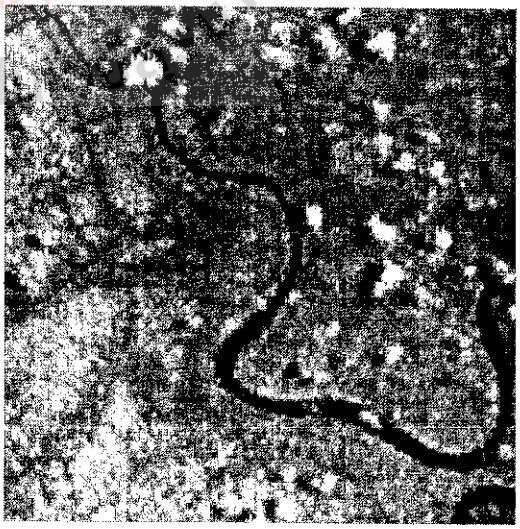

Fig.7 Decoded imagery (MSE = 130.66, Rate = 0.5 bpp)

5) Conclusion

The compressed image using vector quantization and Huffman coding in Fig.5 has mean square error (MSE) = 89.43 with rate = 0.5 bits per pixels (bpp). Another one in Fig.7 has MSE = 130.66 with rate = 0.5 bpp. These images can be detected the change of cloud in two days. This is an example of change detection task. Because of the distortion of this technique, the detection should be used with big regions of an imagery such as forest, big river, cloud etc.. The high compression rate of this technique is a benefit. Hence, the small organization can easily and economically perform this task by only using a microcomputer.

Reference

[1] R. C. Gonzalez and R. E. Woods, "Digital Image Processing," Addison-Wesley Publishing Commpany, Inc.,1992.

[2] M. Rabbani and P. W. Jones, "Digital Image Compression Techniques," SPIE Optical Engineering Press, 1991.

[3] N. M. Nasrabadi and R. A. King, "Image coding using vector quantization: A Review, " IEEE Trans. Commun., vol. COM-36, pp. 957-971, Aug 1980.

[4] Y. Linde, A. Buzo, and R. M. Gray, "An algorithm for vector quantizer design," IEEE Trans. Commun., vol COM-28, pp. 84-95, Jan 1980.

Verification of Atmospheric Correction for AVHRR data by Radiometric Simulation Software 6S

Takayuki Satoh*, Shoji Takeuchi**, Koji Kajiwara* and Ryutaro Tateishi*

* Center for Environmental Remote Sensing(CERES), Chiba University, JAPAN
1-33, Yayoi-cho, Inage-ku, Chiba 263 JAPAN

** Remote Sensing Technology Center of Japan(Restec)
1-9-9, Roppongi, Minato-ku, Tokyo 106 JAPAN

Abstract

Remotely sensed data is affected by absorption and scattering of the atmosphere. Second Simulation of the Satellite Signal in the Solar Spectrum(6S) is software to simulate these effect with many parameters such as geometric condition, concentration of atmosphere, component of aerosols, etc. Though the 6S is used for atmospheric correction, recently. However, there is no report which verifies corrected data by the 6S. The objective of this study is to verify the effectiveness of 6S for atmospheric correction using AVHRR data with different geometric conditions.

1. Introduction

Remote sensor, such as MSS, TM and AVHRR measures radiance reflected from the earth surface at different wavelengths. Reflectance of the earth surface can be derived from the radiance data measured by sensor. Reflectance data is used for many applications, for example classification, change detection and so on. However radiance is affected by various factors. If accurate data is required, these effects must be removed from radiance. These calibration and correction are as follows.

- Preflight calibration
- Calibration considering the sensor degradation
- Solar zenith angle correction
- Atmospheric correction

This study deals with atmospheric correction.

If there is no atmosphere on the earth, radiance which reflected the surface is not affected. But in the actual case, the signal is perturbed by the presence of atmosphere on the path sun-target-sensor. Only a fraction of the photons coming from the target reaches the satellite sensor, typically 80% at 850nm and 50% at 450nm, so that the target seems less reflecting(6S User Guide, 1994). These effects constitute two processes, absorption and scattering. Absorption cause by mainly O_3, H_2O, O_2, CO_2, CH_4 and N_2O. Scattering cause by dust like, oceanic, water soluble and soot component. These compositions and concentrations changes on account of the time and the location. And these data are not available. Therefore, it is impossible to perform atmospheric correction using atmospheric data. Therefore, atmospheric data must be assumed.

6S is radiometric simulation software which used for atmospheric correction recently. However the effectiveness of the atmospheric correction has not been verified. In this study, atmospheric correction was performed by 6S for multi-temporal AVHRR data and verified the effectiveness of 6S for atmospheric correction.

2. Radiometric Simulation Software 6S

6S is radiometric simulation software presented in 1994. This program is initially developed as 5S in 1984 and is used for radiometric simulation with combination of various parameters as follows.

- apparent reflectance
- effectiveness from absorption
- effectiveness from scattering, etc.

Input parameters are as follows.

- Geometric condition(Type of sensor, day, month, latitude, longitude)
- Concentration of H_2O and O_3 in atmosphere
- Component of aerosols
- Wavelength of observation
- Height of target
- Land cover type and reflectance of target, etc.

User can either input these parameters or select given values for each parameter.

3. AVHRR data and simulation by 6S

The used AVHRR data are three multi-temporal AVHRR data sets which have different geometric conditions and difference time within one week during which the surface can be assumed not to change. The AVHRR data is in Indo-china peninsula of the dates: 6/Feb(b9303708), 7/Feb(b9303808) and 12/Feb(b9304409) in 1993. The data are the same one used in Reference No.2. The land cover classes of the samples were forest, agricultural land and bare soil. Solar zenith angle, Azimuth angle, Satellite zenith angle, Ch.1 reflectance and Ch.2 reflectance for 16 selected areas are shown in Fig.1. Values in Fig.1 is the average of 5×5 pixels of 16 areas. Each parameter in 6S is selected as Table 1.

The input of 6S simulation in this study is surface reflectance which is an assumed true reflectance of the surface. The output is apparent reflectance which corresponds to AVHRR data. By changing various values of true reflectance, different surface reflectance are derived. The input surface reflectance which results in the closest apparent reflectance to the AVHRR data of a certain pixel is a corrected AVHRR data.

parameter	value
IGEOM(Geometric condition)	value of each sample points
IDATM(Atmospheric concentration)	Tropical
IAER(Aerosols Component)	Continental
V(Visibility)	Optical thickness 0.5 in 550nm(Visibility 8.49km)
IWAVE(Wavelength)	NOAA 11 AVHRR Ch.1 and Ch.2
IHOMO(Land cover type of target)	Homogeneous and change reflectance

Table 1. parameters for 6S in this study

4. Result

The result graphs of atmospheric correction are shown in Fig.2 which is the case for Ch.2. If atmospheric effect by the difference of geometric conditions for three different date's image is removed, three curves in Fig.2 should be closer than that of Fig.1(e). However curves of Fig.2 have almost same different as Fig.1(e). In the case of Ch.1, no result was derived because ever input surface reflectance of 0.0 gives higher surface reflectance than AVHRR data.

5. Discussion

The causes of the above result can be assumed as follows.

(1) Parameters may not be appropriate.
The parameters inputed in this study are prepared as standard condition in tropical and continental area in 6S. However, there is possibility that input parameters are not appropriate in this data. In order to examine the effect by input parameters, simulation was performed with visibility parameter changing from infinity to 3.57 km. However, the difference is less than 0.06. This means that visibility parameter does not affect the result of simulation much in this study. If the parameter which affects those simulation exists, it is another parameter expect visibility.

(2) Sample points may not be appropriate.
Sample points must be selected from areas with homogeneous and no cloud. However, thin cloud, un-homogeneous or changed surface in a short time might be selected.

(3) Simulation by 6S may contain some fundamental problems.

6. Future activity

Authors plan to simulate with other AVHRR data in order to make clear the above problem. And it is necessary to use ground truth reflectance data. If it is not possible, satellite data in a desert or a runway in airport, where the surface reflectance is stable, must be used for verification.

Reference

1) 6S User Guide Version 0, April 18, 1994

2) Shoji Takeuchi and Yasushi Mitomi, Effects of Sensor Degradation and Solar-Sensor Geometry on Land Cover Monitoring Using NOAA/AVHRR Data, Proceedings of The International Symposium on Vegetation Monitoring, 115-122, August 29-31, 1995, Chiba, Japan

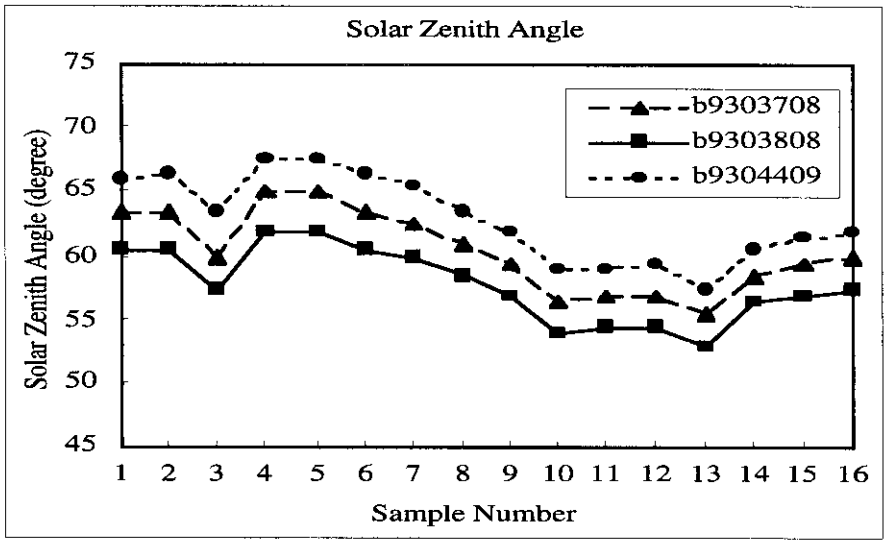

Fig.1(a) Solar zenith angle for 16 sample points

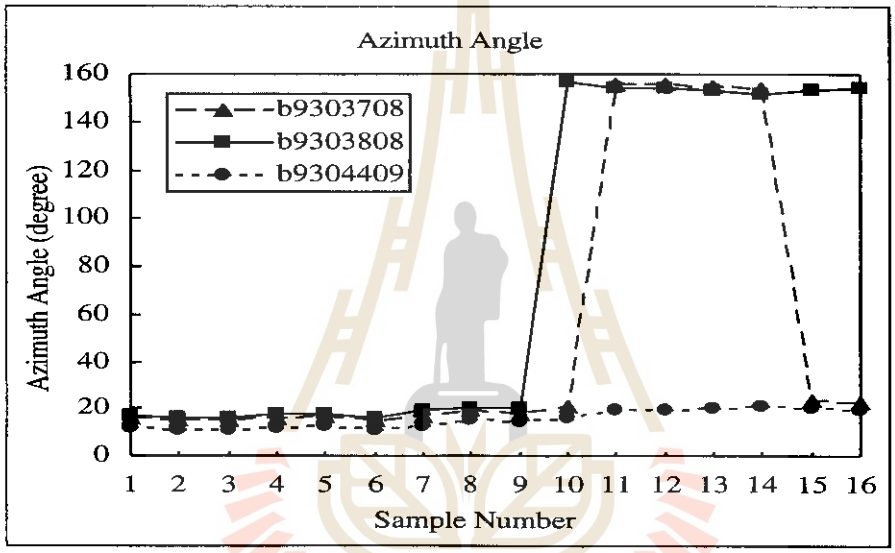

Fig.1(b) Azimuth angle

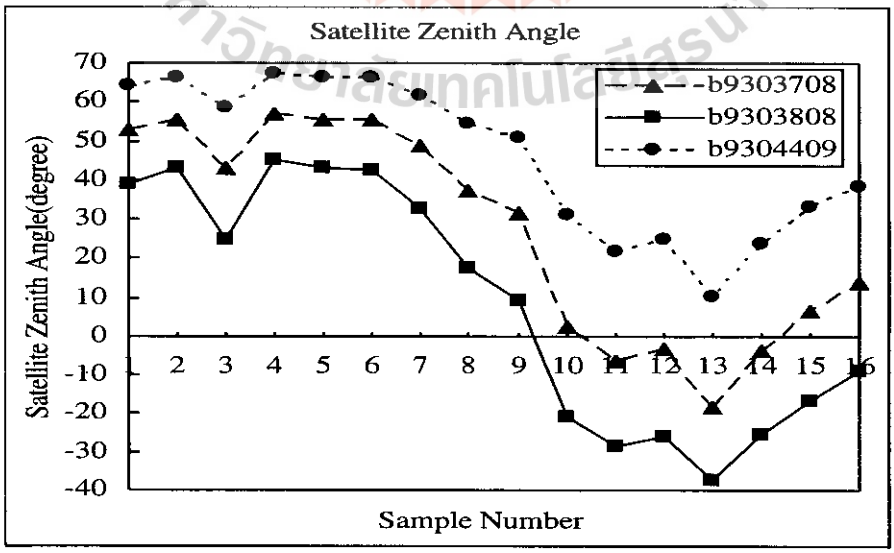

Fig.1(c) Satellite zenith angle

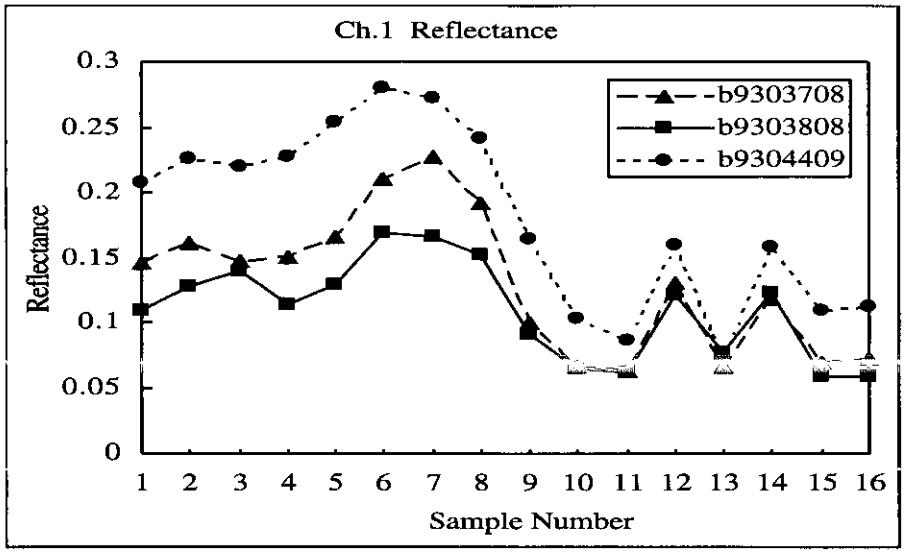

Fig.1(d) Ch.1 reflectance

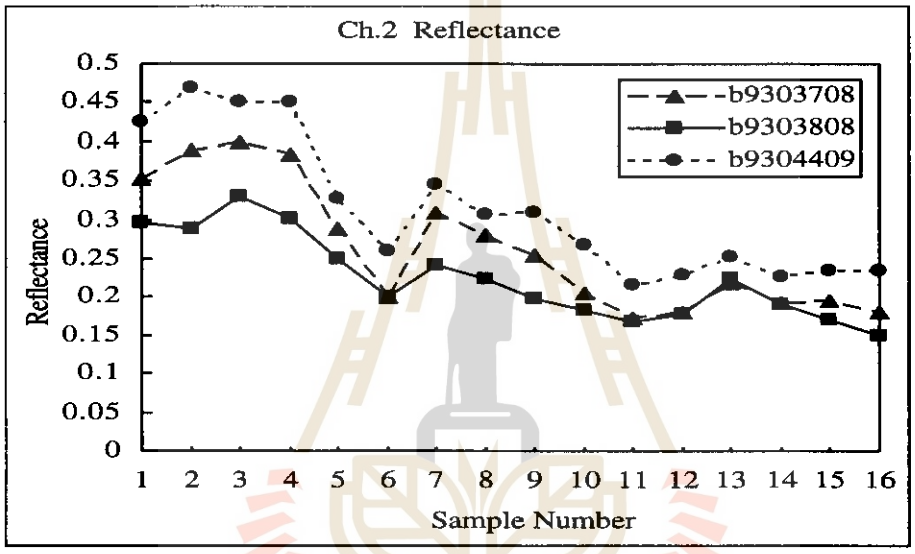

Fig.1(e) Ch.2 reflectance

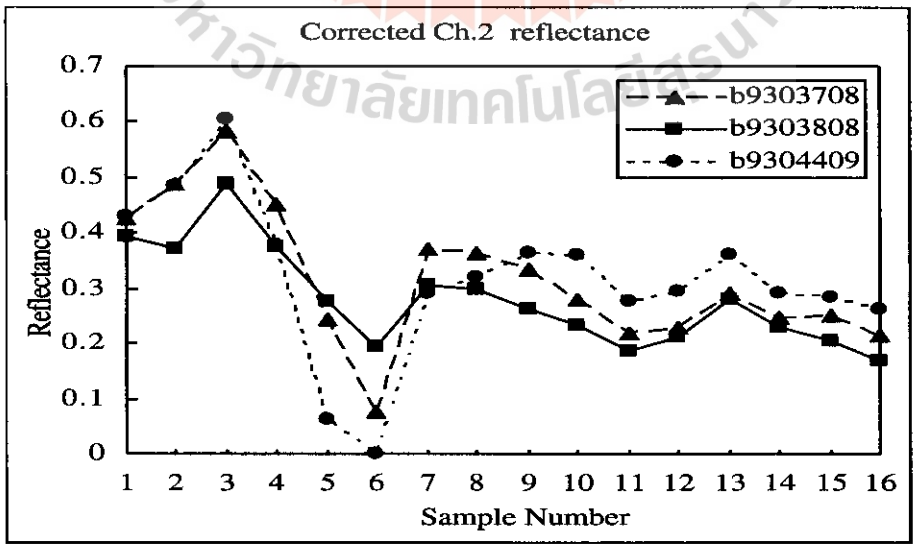

Fig.2 Ch.2 reflectance after atmospheric correction

ADAPTIVE CUBIC CONVOLUTION OF HIGH RESOLUTION REMOTELY SENSED IMAGE DATA

Raveentheran Suntheralingam
Sime Darby Systems, Wisma Sime Darby
Jalan Raja Laut, 50490 Kuala Lumpur, Malaysia
Email: rsl@sds.po.my

ABSTRACT

Cubic convolution of high resolution Airborne Thematic Mapper (ATM) images usually result in overshoot artefacts that are created on either side of boundaries or edges between spectrally different entities. The severity of these artefacts has previously been minimised by applying hybrid techniques that involve resampling by nearest neighbour assignment across edges, and cubic convolution in other regions of the image.

It is suggested that a form of cubic convolution that modifies its α and β parameters across an edge can be used to resample ATM images. In this scheme, an edge within a cross-section of an ATM image is firstly identified. Values of α and β that generate resampled grey level values obtained by nearest neighbour assignment are evaluated for each pixel across the edge. Experimental results are used to show that linear relationships exist between α and β for each pixel across the selected edge, suggesting that this adaptive cubic convolution scheme can be used to resample edges in ATM images.

1. INTRODUCTION

In most remote sensing applications, images are frequently resampled and subsequently interpolated by the nearest neighbour assignment, bilinear interpolation or cubic convolution resampling techniques. Each of these resampling schemes generate artefacts and introduce a characteristic corruption into the resampled image. Nearest neighbour assignment, for example, tends to degrade the structure of the image, but is particularly useful for resampling edges. Cubic convolution introduces overshoots at image edges, but depending on its parameters, can generate acceptable resampled images.

It is desirable to resample edges in high resolution images by cubic convolution without creating any overshoots. One approach is to use different interpolators to resample across an edge [Devereux et al. 1989]. This hybrid form of resampling can, for example, use nearest neighbour assignment to resample across edges thereby eliminating overshoot artefacts, and cubic convolution to resample other regions in the image. However if the cubic convolution function can be made to preserve grey level values across edges in the same way as nearest neighbour assignment, it would not be necessary to use hybrid schemes to resample ATM images.

In this paper, it will be shown that cubic convolution parameters that do not generate overshoot can be evaluated thereby suggesting that an adaptive form of cubic convolution that uses different parameters can be used to resample across edges. This paper is organised as follows. The relationship between cubic convolution parameters, and the resulting overshoots is presented in section 2. Estimation of these parameters that generate minimal overshoot is outlined in section 3. Conclusions are drawn in section 4.

2 ANALYSIS OF OVERSHOOTS GENERATED BY CUBIC CONVOLUTION

Cubic convolution calculates resampled pixel grey level values from sets of sixteen neighbouring pixels in the original image (four along the x-direction) by using a reconstruction kernel that was expressed by Reichenbach and Park [1989] as,

$$r(x) = \begin{cases} r_1(x) & 1 \geq |x| \\ r_2(x) & 1 < |x| \leq 2 \\ 0 & 2 < |x| \end{cases} \qquad (1)$$

where

$$r_1(x) = (\alpha - 6\beta + 2)|x|^3 - (\alpha - 9\beta + 3)|x|^2 - 2\beta + 1 \quad (2)$$

$$r_2(x) = (\alpha + 2\beta)|x|^3 - (5\alpha + 9\beta)|x|^2 + (8\alpha + 12\beta)|x| - 4\alpha - 4\beta \quad (3)$$

Here, the value of the first derivative of the kernel, and the value of the kernel at $|x|$ are represented by the α and β parameters respectively. The cubic convolution function is continuous and symmetrical, and satisfies the concavity conditions of being concave upward at $x = 0$, and concave downward at $|x| = 1$ when $-3 < \alpha < 0$ (with $\beta = 0$) [Bernstein 1976]. A severe shortcoming of cubic convolution however, is its tendency to create overshoots on either side of resampled edges. Previous work on cubic convolution by Keys [1981], Park and Schowengerdt [1983], and Mitchell and Netravali [1988] showed that the magnitude of these artefacts and quality of resampled low resolution images clearly depended on the values of α and β.

It is desirable to establish the relationship between α and β, and the magnitude of overshoot that it generates in order to develop a cubic convolution scheme that minimises the severity of these artefacts. This relationship is best illustrated by uniformly resampling one-dimensional arrays of integers representing grey level values of selected cross-sections of test or real image data. Subtle changes in resampled grey level values, which would otherwise be unnoticeable in resampled images can be easily observed. Results presented in this section are based on resampling a synthetic edge comprising 24 integers with values { 50, 50, 50, 50, 50, 200, 200, 200, 200, 200, 185, 170, 155, 140, 125, 110, 95, 80, 65, 50, 50, 50, 50, 50 }. These integer values were deliberately selected to represent the steep edge and gradual variations in grey level values found in remotely sensed images. The test data set was resampled at 25 equally spaced intervals for a range of α and β values. Percentage overshoot generated at specific pixel positions around the steep edge in the resampled test data set were calculated as $\frac{100(p-q)}{q}$ where q and p denotes pixel grey level values before and after resampling respectively.

The percentage overshoot generated at pixel position 3 (with $q = 50$) for a range of values of α (with β kept constant) is illustrated in figure 1. It can be seen that percentage overshoot at pixel position 3 increases linearly with α, and that there exists several values of α and β which do not generate any overshoot. Sets of α and β values that generate zero percentage overshoot at pixel position 3 were used to resample the original test data set at 25 equally spaced intervals. Figure 2 shows the grey level values generated between pixel positions 2 and 6 for these combinations of α and β values. It can be seen that overshoots are not found at pixel position 3 for the different values of α and β that were used. However a large range of grey level values are observed at pixel position 4. Smaller variations of grey level values are noted at pixel position 5.

It has been shown that specific values of α and β can be found to minimise overshoot or undershoot at certain pixel positions. This is achieved however at the expense of excessive smoothing or poor reconstruction generated at other pixel positions. These results also suggest that cubic convolution at specific pixels on either side of edges can be achieved without generating any overshoot at the particular pixel if appropriate values of α and β can be found. Consequently, it would seem that if α and β can be appropriately modified across the edge, cubic convolution can be applied to resample edges without generating any overshoot or undershoot.

3. ESTIMATION OF CUBIC CONVOLUTION PARAMETERS

Hybrid resampling techniques by Devereux et al. [1992] involved the use of different resampling schemes at different regions within an image. The image data set that was used to generate the results presented in this section was acquired from the cross-section of an ATM image. This data set is illustrated in figure 3, and comprises 35 integers with grey level values typical of 4 meter resolution images captured at 1.55μm to 1.75μm. A steep edge between the darker forest region and lighter grassland is located at pixel position 14. Table 1 shows the differences between the grey level values obtained by applying cubic convolution to resample the entire ATM image data set, against those obtained from nearest neighbour assignment within two pixels of the edge and cubic convolution for all other pixels. Cubic convolution in both cases was achieved with $\alpha = -0.5$ and $\beta = 0.056$. It can be seen that a large difference in grey level value exists at pixel position 12.

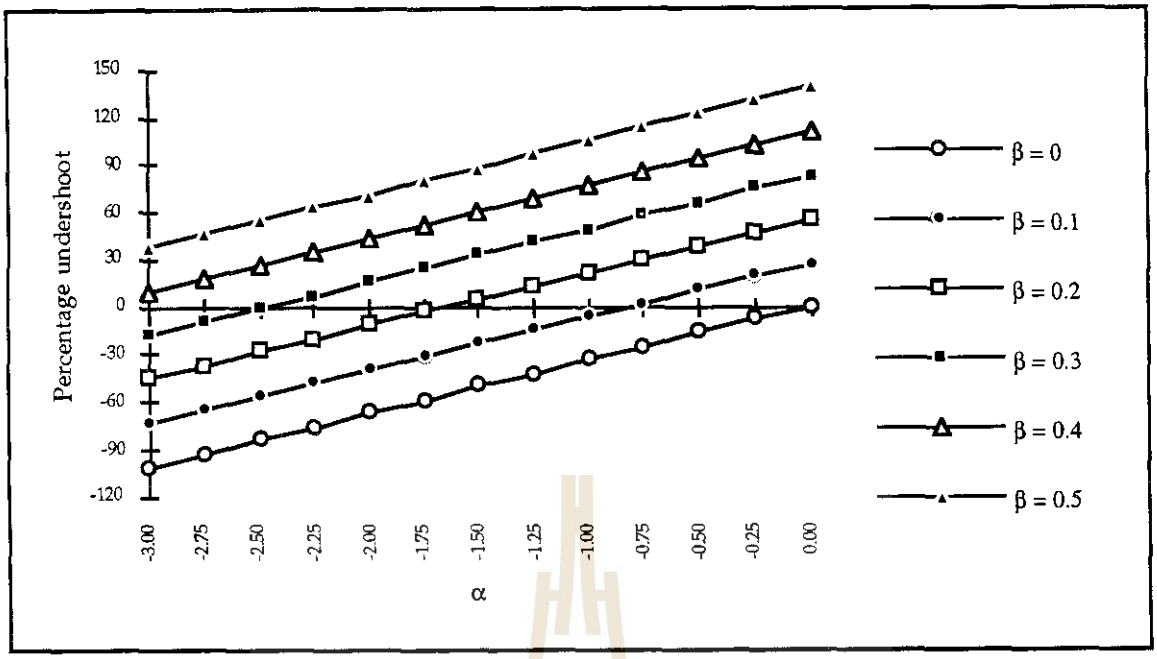

Figure 1 : Plot of percentage overshoot at pixel position 3. Values of α and β that generate zero percentage overshoot can be found.

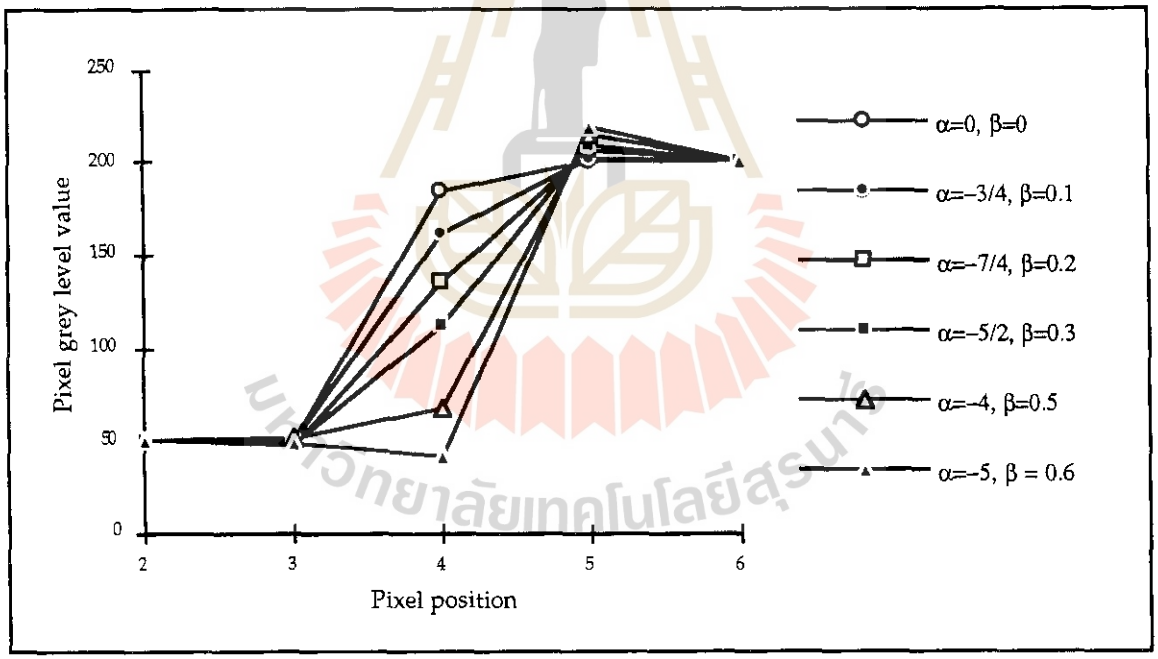

Figure 2 : Plot of grey level values for α and β that generate zero percentage overshoot at pixel position 3. A large range of grey level values are observed at pixel position 4. Smaller variations of grey level values occur at pixel position 5.

Pixel position	8	9	10	11	12	13	14	15	16	17	18
Cubic convolution of entire ATM data set	47	81	86	17	62	211	215	203	189	177	197
Hybrid resampling	47	81	86	20	195	215	205	191	189	177	197

Table 1 : Grey level values obtained by hybrid resampling and cubic convolution of the entire ATM image data set. Differences in grey level values are observed between pixel positions 11 and 16.

If P_{n-1}, P_n, P_{n+1} and P_{n+2} represent pixel values in the original data set, the resampled grey level value between pixel values P_n and P_{n+1} is estimated by cubic convolution as,

$$P_r = r_2(1+|x|)P_{n-1} + r_1(|x|)P_n + r_1(1-|x|)P_{n+1} + r_2(2-|x|)P_{n+2} \qquad (4)$$

where $|x|$ is the distance from the resampled pixel position to the nearest neighbouring pixel in the original data set. The resampled grey level values 20, 195, 215, 205 and 191 generated by the hybrid resampling scheme for pixel position 11, 12, 13, 14, and 15 respectively can be obtained by cubic convolution for appropriate values for α and β. If P_r is given the grey level value obtained by the hybrid resampling scheme, appropriate values of α and β can be evaluated by parametrically solving equation 4. Figure 4 shows the set of α and β values that generate grey level values 20, 195, 215, 205 and 191 at pixel positions 11 to 15. It can be seen that linear relationships exist between α and β. Equations of lines relating α and β are evaluated by coordinate geometry and shown in table 2. These linear relationships indicate that different combinations of α and β values can be used to generate the same grey level value. In order to select acceptable values for α and β, it is essential to ensure that the resulting cubic convolution functions for these values of α and β meet the necessary concavity conditions.

The concavity conditions, $-3 < \alpha < 0$, described by Bernstein [1976] are inadequate to establish suitable ranges of values for α and β for the adaptive cubic convolution technique since these conditions only apply to the case when $\beta = 0$. It is therefore desirable to use more appropriate concavity conditions that can be applied to select acceptable values of α and β, as shown in equation 5 [Suntheralingam 1994].

$$9\beta - 3 < \alpha < 3\beta \qquad (5)$$

Pixel	Range for α	Range for β	Relationship	α	β
11	$1.16<\alpha<-0.18$	$-0.06<\beta<0.20$	$\alpha \approx -3.7\,\beta - 0.4$	−0.4	0
12	$65.22<\alpha<5.04$	$7.58<\beta<1.68$	$\alpha \approx 10.2\,\beta - 12.1$	−0.4	1.15
13	$-1.47<\alpha<-0.22$	$-0.07<\beta<0.17$	$\alpha \approx -5.2\,\beta - 0.6$	−0.9	0.05
14	$-0.22<\alpha<0.72$	$0.24<\beta<0.31$	$\alpha \approx -14\,\beta + 4.1$	−0.1	0.3
15	$-20.41<\beta<7.89$	$-6.80<\beta<-0.54$	$\alpha \approx 2\beta - 6.8$	−8.0	−0.6

Table 2 : Relationships between α and β that generate grey levels obtained by nearest neighbour assignment.

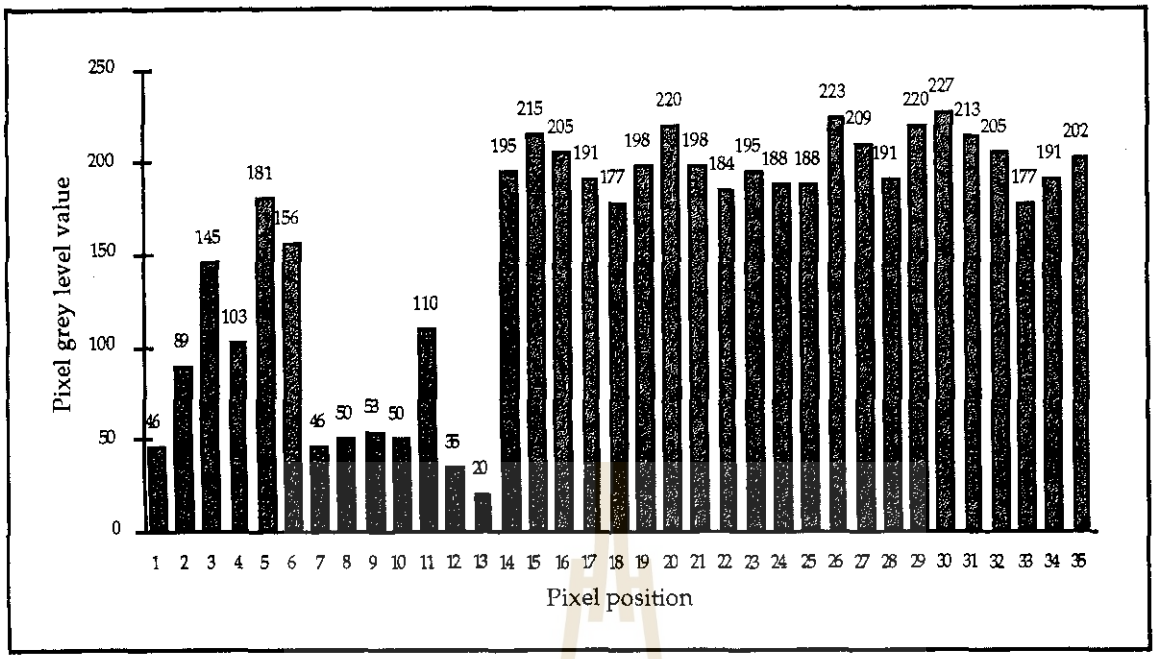

Figure 3 : Cross-section of ATM image. Pixel positions 1 to 11 represent forest. Positions 14 to 35 represent grassland. Significant variations in grey level values are typical of high resolution ATM images.

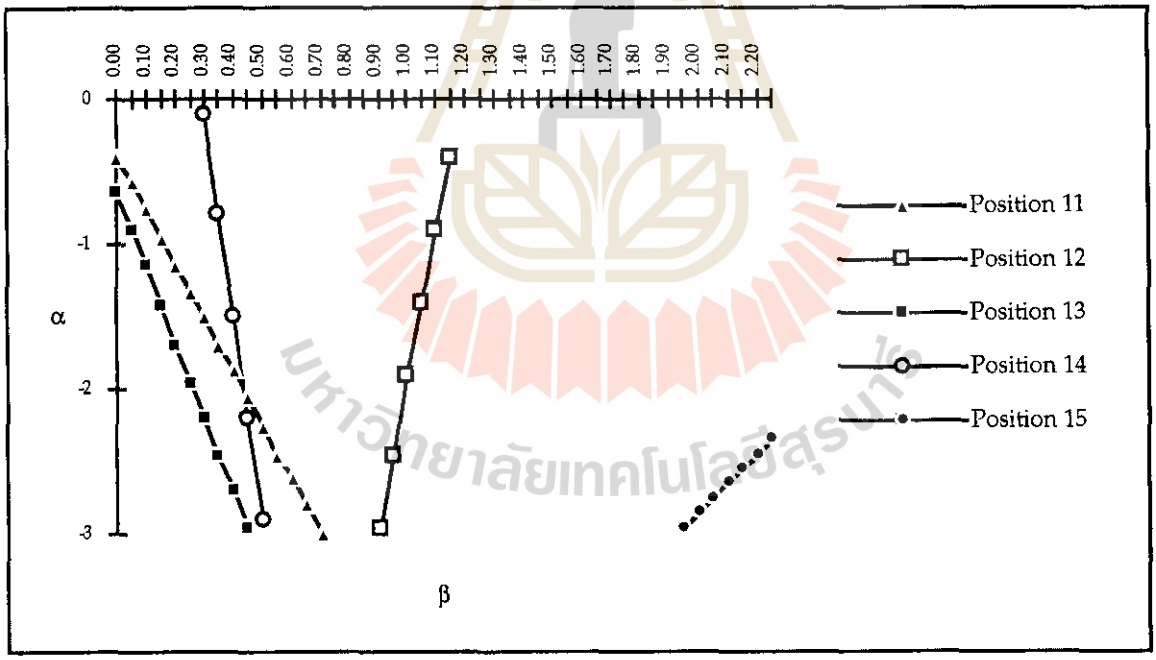

Figure 4 : Set of α and β values that generate the grey level values obtained by nearest neighbour assignment. Linear relationships are observed to exist between α and β.

These more general concavity conditions are used to evaluate appropriate ranges for α and β that generate the grey level values obtained by nearest neighbour assignment. The equations of the lines shown in figure 4 are expressed as functions of α and β, and substituted into equation 5. The resulting range of values for α and β that satisfy the necessary concavity conditions are shown in table 2. Cubic convolution of the ATM image data set using the selected α and β values also shown in table 2 were found to generate grey level values 20, 195, 215, 205 and 191 for pixel positions 11 to 15. These results demonstrate that cubic convolution is capable of generating the same grey level values that are obtained by nearest neighbour assignment.

4. SUMMARY AND CONCLUSIONS

The suitability of resampling edges in ATM image data by an adaptive form of cubic convolution that appropriately modifies its parameters across the edge has been demonstrated by experimental results presented in this paper. It has been shown that values for α and β can be evaluated to resample edges in ATM images without generating overshoots. The one-dimensional approach adopted in this paper ignored the effects of other neighbouring pixels in the image apart from those found along the recorded cross-section. In reality however, all neighbouring pixels around a resampled point within an image clearly influence the resampled grey level estimate. Further work therefore needs to be carried out to extend the adaptive cubic convolution technique to two-dimensions.

The major problem associated with adaptive cubic convolution is the difficulty in estimating suitable values of α and β for different regions in an image. Since the values of α and β are scene dependent, a simple and effective model that relates these parameters to some characteristic about the image needs to be developed. Schowengerdt et al. [1984] suggested the possibility of using local image frequency content to evaluate suitable values for the cubic convolution parameters. Visual examination shows that ATM images tend to be fairly textured. It would therefore be interesting to establish whether the local frequency content within the ATM image is related to image texture. If image texture is found to be an appropriate measure of frequency content, any texture analysis that is required to evaluate α and β is likely to impose a significant computational overhead. Adaptive cubic convolution in such a case would therefore be useful only if coupled with a very fast algorithm for estimating α and β, otherwise any increase in the image quality of the resampled image would be negated by a significant increase in computational effort.

5. REFERENCES

Bernstein R (1976) Digital image processing of earth observation sensor data. *IBM Journal of Research and Development* **20**(1):40-57.

Devereux B J, Fuller R M, Roy D P (1989) The geometric correction of Airborne Thematic Mapper imagery. *Proceedings of the NERC workshop on Airborne Remote Sensing*, Windermere, pp 19-33.

Devereux B J, Roy D P, White S J, Fuller R M, Hopper F (1992) *Cartographic Registration of Airborne Remotely Sensed Data*. NERC Research Contract Report F60/G6/28.

Keys R G (1981) Cubic convolution interpolation for digital image processing. *IEEE Transactions on Acoustics, Speech and Signal Processing* **29**(6):1153-1160.

Mitchell D P, Netravali A N (1988) Reconstruction filters in computer graphics. *Computer Graphics* **22**(4):221-228.

Park S K, Schowengerdt R A (1983) Image reconstruction by parametric cubic convolution. *Computer Vision, Graphics and Image Processing* **23**(3):258-272.

Reichenbach S E, Park S K (1989) Two-parameter cubic convolution for image reconstruction. *Proceedings of the SPIE, Visual Communications and Image Processing IV* **1199**:833-840

Schowengerdt R A, Park S K, Gray R (1984) Topics in the two-dimensional sampling and reconstruction of images. *International Journal of Remote Sensing* **5**(2):333-347.

Suntheralingam R (1994) Developments in image resampling techniques. *MPhil thesis, Cambridge University.*

Geometric Correction of NOAA AVHRR GAC Data

Kimiaki Saitoh*, Toshiaki Hashimoto** , Koji Kajiwara* and Ryutaro Tateishi*

* Center for Environmental Remote Sensing(CEReS), Chiba University, JAPAN
1-33, Yayoi-cho, Inage-ku, Chiba 263 JAPAN

** Basic Engineering Co.JAPAN
16-11, Sakae-cho, Takasaki 370 JAPAN

Abstract

The objective of this study is to estimate accuracy of geometrically corrected GAC data. The used geometric correction method requires just a small number of GCPs using ephemeris data. This method is based on photogrammetric theory. 20-30 GCPs and check points were collected from the Digital Chart of the World(DCW) for one GAC scene which goes around the earth with the width of about 3,000 Km.

1 Introduction

Images acquired by remote sensing have different distortion due to the earth's curvature and rotation, satellite parameters(for example, speed, attitude and altitude), scan skew and projection of spherical surface on a flat image. These distortions prevent meaningful comparison among multi temporal satellite images. Therefore geometric correction includes identifying the geographic coordinates corresponding to an image pixel(Direct image referencing) and locating a pixel corresponding to given geographic coordinates(Inverse image referencing), is essential in many remote sensing studies.

NOAA AVHRR data are widely used in weather, climate and environmental studies. AVHRR data, particularly GAC data(Global Area Coverage) data are adaptable for global environmental study. However its ephemeris data is not exact and geometric distortions must be removed using some GCPs. The object of this study is to correct geometric distortions using photogrammetric theory and to estimate accuracy of the geometrically corrected GAC data.

2 Geometric correction method using photogrammetry theory

If geometric correction of NOAA AVHRR is done only by using ephemeris data from National Oceanic and Atmospheric Administration, the corrected image has not enough accuracy due to ephemeris error, time error between the satellite and receiving station and satellite attitude error. Therefore it is necessary to use GCPs. The geometric correction method applied in this study is developed by Hashimoto and Murai[1] in which position and attitude of the satellite are corrected using collinearity equation of photogrammetry.

2.1 Collinearity equation

To correct the AVHRR data accurately, it is necessary to calculate the position($X_0.Y_0.Z_0$) and the attitude(ω, ϕ, κ : roll , yaw , pitch) of the satellite exactly. Therefore we regard their parameters as exterior orientation parameters in photogrammetry and calculate them from collinearity equation. The satellite position is expressed by distance from the geocentric place(R), angle from equator plane(u), inclination angle(i), right ascension of ascending node(Ω). The target earth surface is expressed by geocentric coordinate system. The Image coordinates defined the right-handed coordinate system that direction to the x is satellite trace direction and direction to the z is normal direction of satellite trace. Collinearity equation here means that center of the projection(position of the sensor) and the image point and the target earth surface is in a line.

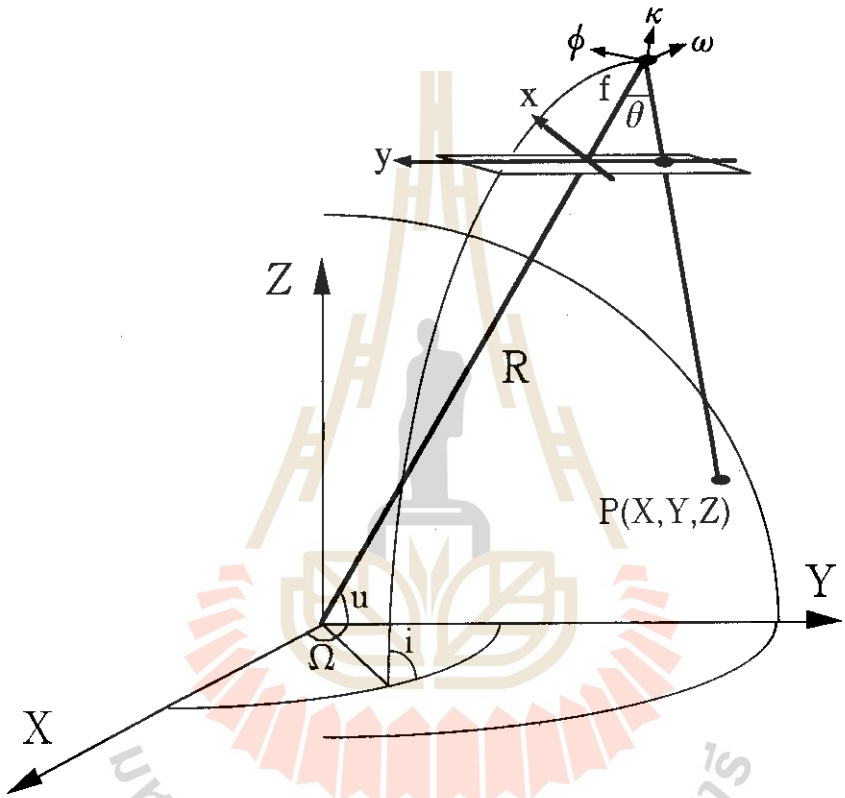

Fig.1 Collinearity equation

2.2 Parameters

Parameters(R , u , i and Ω) are expressed by ephemeris data. Ephemeris data are sent by NOAA everyday. Ephemeris data are

a : Semi-major axis e : Eccentricity of orbit i : Inclination angle

λ : Right ascension of ascending node w : Argument of perigee

M : Traverse angle of satellite position

If we consider that the motion of satellite is Keplarian motion, it obeys the Keplar's law.

$M = E - e \cos E$ (E is angle of passage of perigee)

Then the satellite position(R , v) in the orbital plain is calculated from equations bellow

$R = a (1 - e \cos E)$

$$v = 2\tan^{-1}\left(\sqrt{\frac{1+e}{1-e}}\tan\left(\frac{E}{2}\right)\right)$$

The parameters u is derived as u = w + v. Right ascension of ascending node(λ) is measured from vernal equinox. The right ascension of ascending node(λ) in geocentric coordinate system is derived as

$\Omega = \lambda + \lambda_G$ λ_G: vernal equinox longitude

If ephemeris data are enough accurate, R , u , i and Ω can be calculated accurately by the above equations and unknown parameters are only the satellite attitude(ω , ϕ , κ). Since ephemeris data are not exact, we regard R , u , i and Ω as unknown parameters too.

3 GAC data

The used data is NOAA AVHRR Global Area Coverage(GAC) Level 1b data of July 30, 1992. This data was a part ARGASS(AVHRR GAC dataset for Atmosphere and Surface Studies) which was originally produced by Dr. Compton J. Tucker of NASA Goddard Space Flight Center.

4 Collection of GCPs

GCPs are collected from DCW(Digital Chart of the world). The DCW is a comprehensive 1:1,000,000 scale vector basemap of the world. It consists of geographic, attribute and textual data that can be accessed, queried, displayed and modified with ARC/INFO software. GAC image data were compared with DCW image to collect GCPs.

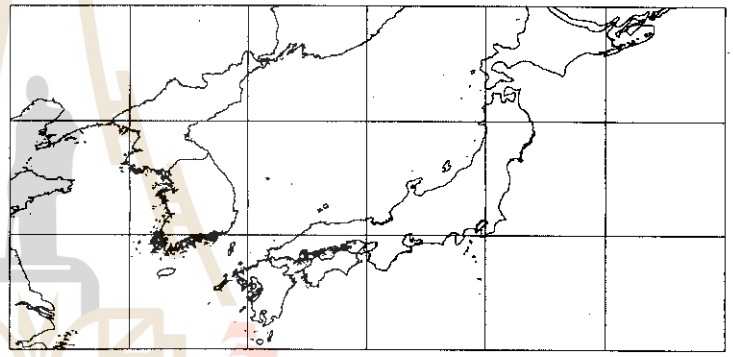

Fig.2 The DCW image nearby Japan

5 Geometric accuracy

Geometric accuracy of the corrected image is estimated by check points. The check points are a part of GCPs which are not used for correction. The advantage of GAC image is that most image include seashore lines because the image scans around the earth. The result of accuracy will be reported at the conference.

Acknowledgment

Authors would like to thank Dr. Yoshiaki Honda for providing GAC data in ARGASS.

Reference

1) Toshiaki Hashimoto and Shunji Murai, Geometric Correction of NOAA AVHRR Imagery with Few GCPs, SEISAN KENKYU, Vol. 43, No. 8, pp.44-47, 1991.
2) W. j. Emery, J. Brown, Z. P. Nowak, AVHRR Image Navigation: Summary and Review, Photogrammetric Engineering and Remote Sensing, Vol. 55, No.8, pp. 1175-1183, 1989

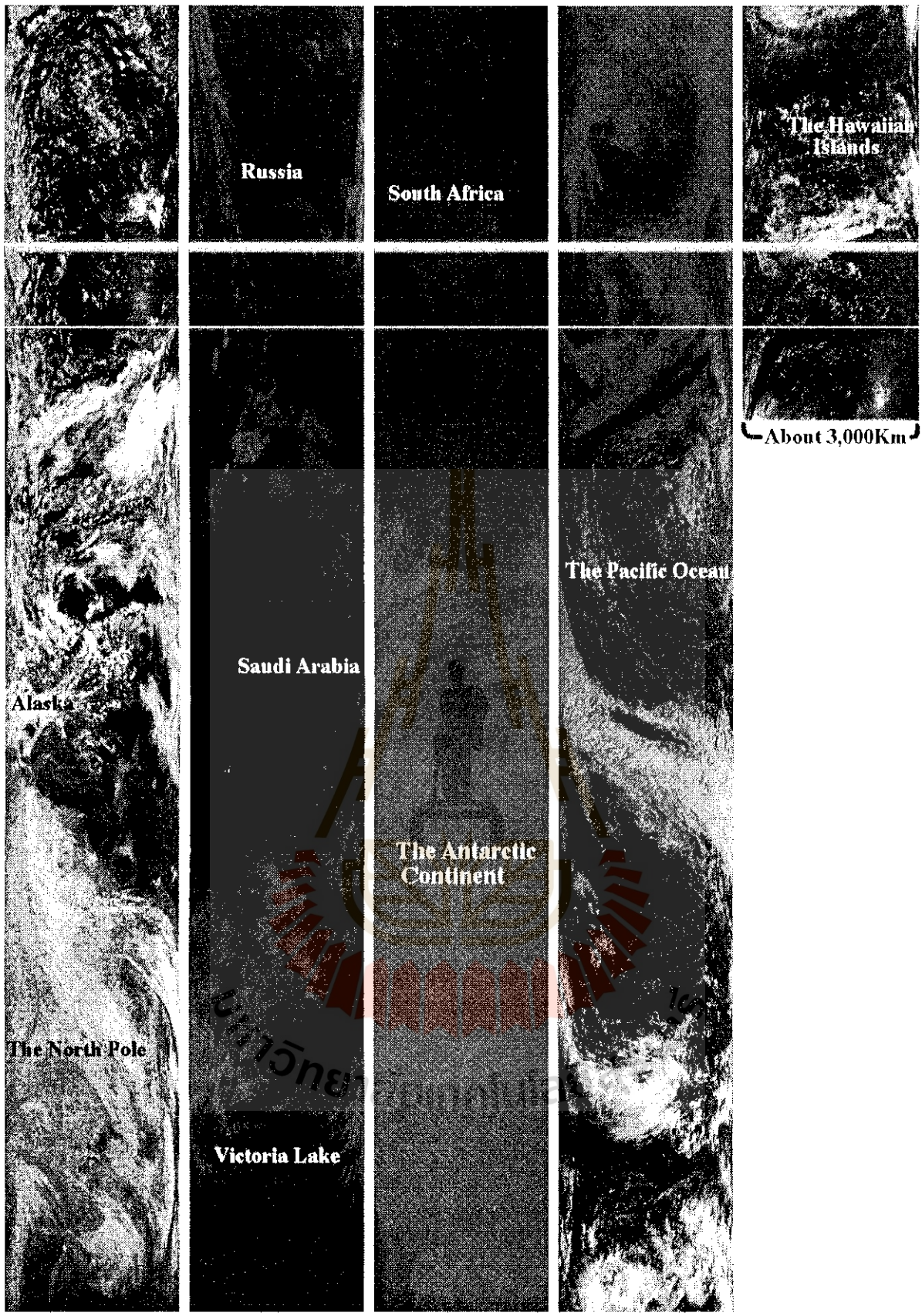

Fig.3 GAC image(July 30 1992)

A Technique for 3D Modelling of Buildings

Taejung Kim and Soon Dal Choi

Satellite Technology Research Center
Korea Advanced Institute of Science and Technology
373-1, KuSung-Dong, YuSung-Gu, Taejun
KOREA
Phone: +82-42-869-8629, Fax: +82-42-861-0064
Email: tjkim@satrec.kaist.ac.kr

Abstract

A fully automated technique has been developed for 3D mapping of buildings from high resolution aerial and space imagery. This paper will briefly describe the basic principles of the technique and present the results from various images.

The technique consists of three parts: building height extraction, building detection, and 3D modelling. For building height extraction, a pyramidal matching algorithm has been developed. This algorithm emphasises the control between levels in order to reduce the blunder propagation. For building detection, a new graph-based algorithm has been developed. This algorithm extracts lines from single image and store them and their relationships in a graph. Building hypotheses can be generated by finding closed loops in the graph.

3D modelling of buildings can be achieved by combining the results from building height extraction and building detection. Buildings are modelled as planar or apex surfaces and heights from pyramidal matching are assigned to these surfaces. Building detection output is used as interpolation boundaries. The results from various images show that the developed technique can model buildings successfully.

1. Introduction

The extraction of man-made objects from remotely-sensed imagery is one of the fundamental tasks in remote sensing as well as in image understanding. In particular, man-made objects such as roads or buildings are important features in urban areas and techniques to extract them have numerous applications in urban mapping, urban planning and Geo-Information engineering.

There have been several approaches proposed for automated building extraction. The most popular ones are perceptual grouping [1] and line analysis [2,3]. The use of shadow information and perspective geometry has also been used by many authors [4,5]. However, the nature of buildings in real world necessitate the need to include 3D analysis in building extraction: building detection performed in 2D cannot fully "understand" buildings in the scene. For such purpose, stereo matching has been used with the combination of other approaches mentioned before. However, building extraction (in 3D) remains still difficult as it requires not only good low-level vision techniques such as edge or line extraction but also good middle-level or high-level vision techniques such as cognition and interpretation.

This paper describes a new approach developed for automated 3D building extraction. The new approach uses a stereo matching technique to retrieve 3D information on buildings and a building detection technique to "recognize" buildings in 2D. These two techniques are combined for 3D building extraction. The next section will describe briefly the principles of this approach. In section 3, some results of building extraction will be presented. Conclusions and future work will be discussed in section 4.

2. A new technique

The new technique can be divided by three parts: height extraction using a pyramidal matching algorithm, building detection using a line-relation graph and 3D modelling of buildings using the results from height extraction and building detection. This section will describe each of them briefly. Interested readers should refer [3,6,7,8] for more detailed explanation.

2.1 Height extraction

For height extraction, a pyramidal matching technique was proposed and proved effective. Due to the nature of buildings, there are many abrupt discontinuities in any scene containing buildings. This violates the assumption of contiguous disparity field, which almost all stereo matching algorithms adopt. Previous experiments with a adaptive least squares correlation matching algorithm showed that buildings in a scene make blunders and isolated regions for stereo matching [6].

Pyramidal matching can partly solve these problems: it can reduce the magnitude of height discontinuities and (hence) the number of isolated regions by averaging down the image resolution; it can also enhance stereo matching by utilising the matching results of lower resolution as the initial guess for higher resolution matching; it can also enable a fully automated system by using automatically generated initial guess at the lowest resolution matching.

One of the difficulties for any pyramidal matching approaches is the problem of "blunder propagation": errors at the lowest resolution are amplified through image pyramid. In order to minimize this problem, a tile-based control strategy was developed. Tiles with a given size are defined across the image plane and only the best matched point within a tile is selected as the initial guess for the next resolution matching.

This pyramidal matching algorithm was tested with many aerial and spaceborne images and it produced successful results [9,10]. The results of experiments were reported elsewhere.

2.2 Building detection

For building detection, a graph-based algorithm was developed [3]. This algorithm generates building hypotheses by line analysis and then verifies them using shadow information and/or perspective geometry. This algorithm needs only a single image and building detection is performed in two dimension.

Firstly, lines are extracted in an image using several steps: edge elements are detected by a Canny-Petrou-Kittler filter; a connected edge labelling algorithm is applied; two end-points of a linear elements are searched for with end-point templates. A line is defined with two end-points. Small lines broken from a long line and parallel lines with a narrow gap are merged.

Secondly, the relations between lines are searched for. The line relations are classified as positive, negative, or parallel connection. The value of connection is also defined accordingly. Lines and line relations (type and value of connections) are stored in s graph. The nodes of the graph consist of lines and the arcs the relationship between lines.

Thirdly, the system generates building hypotheses by finding closed loops in the line-relation graph. To traverse a graph, a depth-first search algorithm is used. In order to make sensible building hypotheses, the search is limited by some connection rules and the maximum number of nodes it visits. However, experiments with this method revealed some limitations, the main one being unable to generate any building hypothesis where lines from one or more sides of a building are missing. To overcome this limitation, the concept of "super" building hypothesis, the building hypothesis generated from a "U"-shaped chain, is introduced.

Finally, building hypotheses are verified. Similar building hypotheses are merged and some small building hypotheses are removed. Similarity is defined when building hypotheses have all identical components but one in their search chains. Shadow analysis is performed and lines in a scene are classified into ground-level and building-level lines. False building hypotheses, which contains any ground-level line, are removed. For an oblique viewing geometry, vertical lines can be visible in a scene and perspective geometry can be used to verify building hypotheses. After detecting vertical lines, lines are also classified into building-level, middle-level, and ground-level lines. Building hypotheses which consist of alone building-level lines are verified. After the verification procedure, a building hypothesis represents a whole or part of a building.

2.3. 3D modelling of buildings

One of the weakest application areas of any monoscopic approach is the extraction of height or depth information. The building detection system described above suffers from the same drawback. Although some indication of building height may be possible by shadow analysis and perspective geometry, the system cannot provide accurate information on building height.

Stereo matching results usually give accurate height information. However, height is assigned only on grid-points and it is difficult to obtain the height of objects such as building roofs without further processing. Also there is a problem of height for urban areas. In such areas, the surface does not vary in a geo-statistical manner. Large areas of the surface are very flat or linearly varying and there are many cliffs due to building boundaries. Hence "kriging", one of the common techniques for height interpolation, cannot be applied. Height interpolation requires external guidance or, alternatively, a proper statistical model of the surface should be modelled.

The fusion of stereoscopic and monoscopic cues can potentially solve these problems [8]. Rich height information from the stereoscopic process can be used to assign height onto buildings. Building hypotheses detected by the monoscopic process can provide the external guidance of height interpolation so that interpolation only takes place within the boundary of a building hypothesis.

From the pyramidal matching technique described in section 2.1, a matching list can be generated. From the building detection system described in section 2.2, building hypotheses are generated. Each building hypothesis provides interpolation boundaries and matched points in a matching list provide height information. Using the matched points which fall in a building hypothesis, coefficients of a surface model of a building hypothesis are calculated. Interpolation is then performed using the surface model equation.

Three surface models were considered for building roofs: a planar, an apex, and a quadratic surface model. The coefficients of each model can be calculated using the matched points within a building hypothesis through least squares estimation. The estimation errors of three models are then compared and the model with the least error is chosen as a proper surface model. However, previous experiments have shown that a quadratic surface model has an unacceptable error when the number of modelling points is too small and these points are not well-distributed in a building hypothesis. Although there may be dome structures in a scene, these are rare and could be dealt with by specialised processes. The quadratic surface model was, therefore, discarded. The surface is assumed to be either planar or apex. Also, if the estimation error of a surface model is larger than some threshold value, the surface model is not accepted and a building hypothesis remains un-modelled. After choosing a proper surface model, interpolation can be done simply by calculating the corresponding height using the surface model equation.

3. Results and Discussions

Figure 1(a) and (b) show an ISPRS test stereo pair ("Flat" area) supplied by the University of Sttutgart. The resolution of images used for experiments was 24 cm. The height extraction system was applied to this stereo pair. A 5-level image pyramid was generated by reducing the images successively by the factor of 2. Pyramidal matching was applied to this pyramid and 33146 points were matched (83.6% of total matchable points). These points were converted into ground coordinates by applying camera model and a Digital Elevation Model (DEM) was generated. This DEM is shown in figure 1(c). This DEM had a RMS height error of 1.1 m compared to a ground-truth DEM. Height information was retrieved successfully using pyramidal matching. However, there are many "holes" in the DEM, in particular on the roofs of buildings. This indicates that the height discontinuities due to buildings still remain as an obstacle for height extraction. This is the current limitation of the height extraction system.

Building detection was performed to the image in figure 1(a). After line extraction, 844 lines were obtained. From these lines, 996 line relations were found. A line-relation graph was constructed using the 844 lines as nodes and the 996 line relations as arcs. A depth-first graph traversal algorithm was applied to find closed loops and "U"-shaped loops in the graph. 60 "normal" building hypotheses (closed loops) and 240 "super" building hypotheses ("U"-shaped loops) were found initially. After building hypothesis verification process, 28 "normal" and 22 "super" building hypotheses were finally obtained. Note that there has been a great reduction in the number of "super" building hypotheses after the verification process. This is because, in our implementation, every "normal" building hypothesis makes one or more "super" building hypotheses and these redundant "super" building hypotheses are removed after the verification process. Figure 1(d) shows the 28 "normal" and the 22 "super" building hypotheses. There are 19 buildings in the scene. 10 buildings are fully and 9 buildings are partly detected.

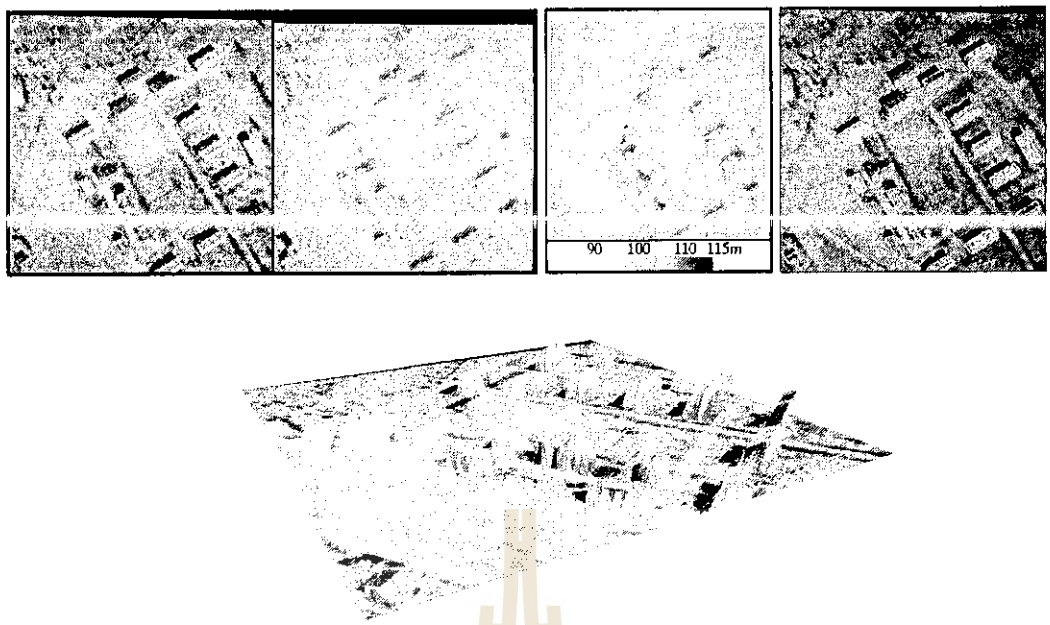

Figure 1. (a) and (b): An ISPRS test stereo pair. (c) A DEM from the height extraction system. (d) A building detection output (e) A perspective view of buildings.

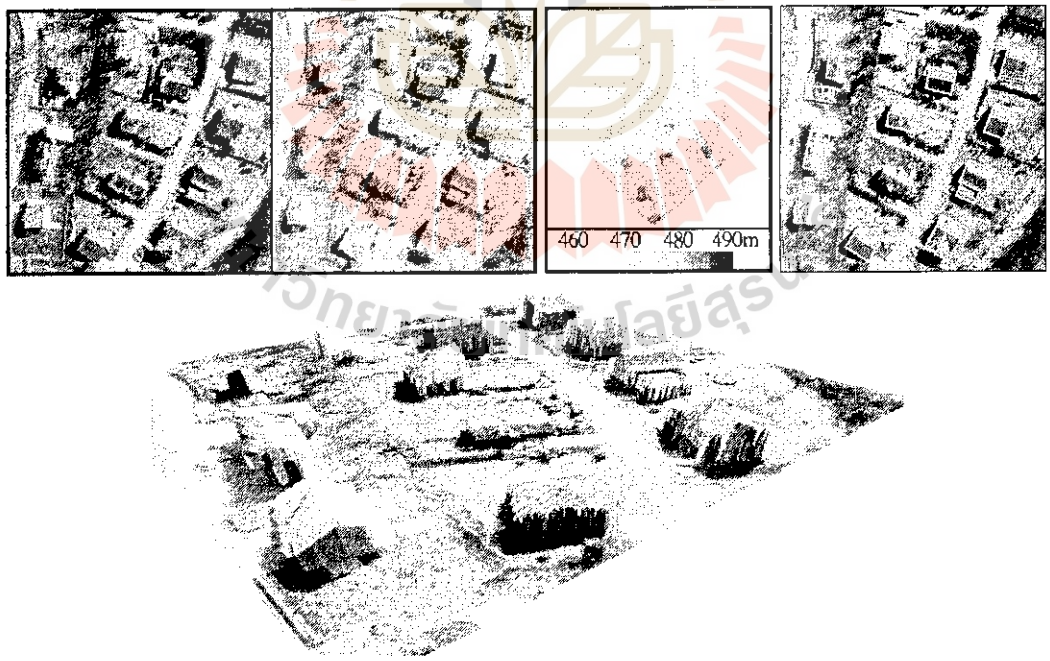

Figure 2. (a) and (b): Another test stereo pair. (c) A DEM. (d) A building detection output. (e) A perspective view of buildings

The 3D modelling of buildings was applied by fusing the pyramidal matching output and the building detection output. From the 50 ("normal" and "super") building hypotheses, 23 building hypotheses were modelled as planar surfaces and 1 building hypothesis an apex surface. However, 26 building hypotheses were not modelled due to insufficient modelling points or a large estimation error. Although all building roofs are apex in the scene, many building hypotheses were modelled as planar surface. This is valid because many building hypotheses cover only half of building roofs which are planar. Height interpolation was carried out using these surface models. Figure 1(e) shows a perspective view of buildings after the height interpolation. A constant value of 100m was assigned to the 26 un-modelled building hypotheses to distinguish them from the ground plane. The perspective view shows that 3D modelling was performed successively. Many buildings have apex-shaped roofs. Some low buildings are due to the un-modelled building hypotheses with the constant height of 100m.

Figure 2(a) and (b) show another test stereo pair supplied by ETH Zurich. The resolution of the images was 15 cm. A 5-level image pyramid was created and the height extraction system was applied to this pyramid as before. 18448 matched points (91% of the total matchable points) were matched. After converting them in ground coordinates, a DEM was generated (figure 2(c)). In the DEM, height information even on the roofs of buildings was successfully.

The building detection system was applied to the image in figure 2(b). After line extraction, 338 lines were obtained. 508 relations between these lines were found and a line-relation graph was contracted accordingly. From this graph, 50 closed loops ("normal" building hypotheses) and 210 "U"-shaped loops ("super" building hypotheses) were initially generated. After the verification process, 27 "normal" and 8 "super" building hypotheses was finally verified. These are shown in figure 2(d). There are 12 buildings in the scene. Among them, 8 buildings were detected fully and 3 partly. However, one building in the middle of the scene was completely undetected. There are three building hypotheses which are not from real buildings but from other objects (two of these do "look" like real buildings).

The 3D modelling was performed as before. The 35 building hypotheses and the height information in the DE< were combined for height interpolation. 24 building hypotheses were modelled as planar surfaces and 5 building hypotheses apex surfaces. 6 building hypotheses were not modelled. Height interpolation was carried out using these surface models. For the 6 un-modelled building hypotheses, a constant height value of 470m was assigned. Using these results, a perspective view of buildings was created (see figure 2(e)). As shown in the figure, 3D modelling was performed successfully. Many building roofs have apex-shapes. The flat building in the middle of the scene is due to the one undetected building.

4. Conclusions and future work

In this paper, a new technique developed for automated 3D modelling of buildings was briefly described. The results shown support the good performance of the technique. This section will discuss some other aspects of the technique.

There are many pyramidal matching algorithms developed and proposed so far. The major difference between the one described here and others is that the problem of blunder propagation was carefully considered. A naive pyramidal matching algorithm without considering this problem may fail to work in a extreme circumstances where, for example, there are a lot of height discontinuities in a scene.

The building detection system described here also uses the concept of perceptual grouping but emphasises the connection between lines. The use of type and value of connections between lines is a very unique approach. One of the main differences between this building detection system and others is that this system works reasonably well without any verification process (results without verification process, however, were not presented in this paper due to the limited space). Compared to other systems, the number of building hypotheses removed after the verification process in small. The reason is because building hypotheses are generated very carefully in this system. (Other systems may apply "strong" verification process for successful building detection.)

3D modelling of buildings was achieved by combining the height extraction system and building detection system. In is worth noting that this 3D modelling was done without any manual intervention. This approach can be a good example of the potential benefits due to the fusion of monoscopic and stereoscopic processes. The major contribution of the work described in this paper is the development of techniques which can be used for automated urban mapping.

There are several aspects to be considered for the future work on this technique. As the 3D modelling is achieved only after quite a number of processes, there are many parameters to be specified by operators. Although most of them can be substitute automatically, some should be carefully chosen. This can be an obstacle for a "truly" automated system. In the building detection system, the verification process may need further development. Compared to other systems, the verification process used here is one of the simplest. This is partly due to the reliability of candidate building hypotheses as mentioned earlier. However, for a more robust system, further development on the verification processes should bring some benefits.

References

[1] R. Mohan and R. Nevatia, "Using Perceptual Organization to Extract 3D Structures", *IEEE Trans. on Pattern Analysis and Machine Intelligence*, **14(6):616-635**, June 1992

[2] J. Shufelt and D.M. McKeown, "Fusion of Monocular Cues to Detect Man-Made Structures in Aerial Imagery", *Computer Vision, Graphics and Image Processing: Image Understanding*, **57(3):307-330**, 1993

[3] T. Kim and J-P. Muller, "A New Algorithm for Building Detection: A Graph-based Approach", *IEEE Trans. on Pattern Analysis and Machine Intelligence*, submitted, 1994

[4] A. Huertas and R. Nevatia, "Detecting Building in Aerial Images", *Computer Vision, Graphics, and Image Processing*, **41:131-152**, 1988

[5] M. Herman and T. Kanade, "The 3D Mosaic Scene Understanding System", *From Pixels to Predicates edited by A.P. Pentland*, **pp. 322-358**, 1986

[6] T. Kim and J-P. Muller, "Automated Urban Area Building Extraction from High Resolution Stereo Imagery", *Image and Vision Computing*, 1995, (in press)

[7] T. Kim and J-P. Muller, "Building Extraction and Verification from Spaceborne and Aerial Imagery using Image Understanding Fusion Technique", *Proc. of Ascona Workshop 95 on Automatic Extraction of Man-made Objects from Aerial and Space Images*, Ascona, Switzerland, 24-29 April 1995

[8] T. Kim and J-P. Muller, "Fusion of Stereoscopic and Monoscopic Cues for Urban Area Image Understanding", *Computer Vision and Image Understanding*, submitted, 1995

[9] T. Kim and J-P. Muller, "Automated Building Height Estimation and Object Extraction from Multi-Resolution Imagery", *Proc. of SPIE conference on "Integrating Photogrammetric Techniques with Scene Analysis and Machine Vision II"*, **SPIE Vol. 2486**, Orlando, Florida, USA, 19-21 April 1995

[10] T. Kim and J-P. Muller, "Effects of Image Resolution on an Automated Building Extraction System", *Proc. of the 21th Annual Conference of the Remote Sensing Society on Remote Sensing in Action (RSS95), Southampton*, UK, 11-14 September 1995

TECHNICAL SESSION F

GLOBAL / REGIONAL CHANGE STUDY

Nakhon Ratchasima, Resources Atlas

C. Mongkolsawat** and NRCT Sub-committee
on landuse, agriculture and forestry

Abstract

The objective of this study is to establish a spatial information system essential for provincial resources planning. Nakhon Ratchasima, a province in Northeast Thailand was selected for this study. The province covers an area of about 12,778 sq.km. and is 260 kms from Bangkok. The spatial information needed was evaluated in terms of data availability as well as its reliability and compatibility. This includes an analysis of spatial data and its associated attributes as related to system structure. Methods for efficient data conversion have been developed in consistent with the application scale. Spatial data was georeferenced, based on the Universal Transverse Mercator (UTM) used by the Royal Thai Survey Department. The spatial information established was organized by theme into layers. Those layers include administrative boundaries, infrastructure, land resources, digital terrain model, biological resources and socio-economic aspects. The system developed provides a tool to search spatial information on resources of the province. The hardcopy outputs are also carried out to provide basic spatial information to publics. In addition, with the set of themes and conditions identified as related to the problem, spatial modeling can be proformed accordingly.

1. Introduction

The 7th National Economic and Social Development plan (1992-1996) called for concommitance of natural resources management and sustainable economic growth (NESDB 1992). The plan describes development issues and problems faced by each natural resource. Natural resource and environmental concerns have been integrated into the regional development master plan. To formulate the plan, it is necessary to gather information in form best suited for management. The information to be collected should include spatial form and its associated attributes. A number of agencies in Thailand have a mandate in establishing information mostly in sectoral and specific form. With regarding spatial information, there exists paper maps with various scales and standards which have significant effect on the creation of spatial databases and ultimately on the integration and modeling. With advancement of technology (remote sensing and GIS), it is now possible to effectively establish spatial information and to formulate the integrated development plan. The National Research Council of Thailand (NRCT) then decided to make inventory of resource information to support the formulation of the provincial resource management plans. The work was assigned to a study team consisting of a number of government agencies concerned. This is to avoid duplication in setting up database and lowering the expenses. Moreover, the resultant information for each theme will be accordance with the system developed by the agency and provide consistent information to all of the users. In the same time, information can be updated and collected in form and manner suitable for modeling and integration.

---

* paper to be present at the 16th Asian Conference on Remote Sensing, November 20-24, 1995 Nakhon Ratchasima Thailand.

** Computer centre, Khon Kaen University Khon Kaen 40002, Thailand.

2. Objectives

The objectives of this study are:

1. to make inventory of resources of Nakhon Ratchasima Province using satellite data.
2. to establish spatial resource database for management strategies

3. Study area

Nakhon Ratchasima (NR) Province is situated in the Northeastern part of Thailand (Figure 1). The annual rainfall in mostpart is less than 1000 m.m. Geologically, the area is formed by a thick sequence of Mesozoic sediments, the Khorat group, ranging in age form upper Triassic to Tertiary and Tertiary igneous rock. The Mesozoic sequence has been devided into 5 formations: Phra Wihan, Sao Khua, PhuPhan, Khok Kruat and Mahasarakham. The area is drained by a number of rivers from southwest direction into the Mun River. The central parts of the province are formed by flat to gently undulating alluvial plains with prominent raised margin to the southwest. The land ecosystem of the area can be divided into 2 main systems: 1) alluvial plains with gently undulating topography and 2) dissected erosion surface and mountain with variation in vegetation density. The former mostly consists of agricultural landuse and scattered remnant tree, the later includes protected forest area, recreation land and different kind of agricultural landuse.

4. Methodology

4.1 Evaluation of existing information

The objectives of this phase are:

- to identify all existing databases produced by Governmental agencies its characteristics, format and reliagility.
- to define data layer for establishing resource atlas and its associated attributes.

This evaluation included the identification of information need. In general, the information need is defined in relation to the extent and potential of problems. The evaluation was carried out by collecting maps generated by each organization. The characteristics, forms and reliability of map were assessed and assembled. The reliability features of which was adopted in the establishment of spatial database. The classification scheme of themes follows the organizations that have mandates. The basic features in the map e.g. georeference, contour lines and water resources are in accordance with either the RTSD topographic map or satellite imagery whichever better.

4.2 Establishment of database

4.2.1 Data collection

The current informations available both in digital and paper map were assembled and collected. Data for resource atlas could be acquired from the following sources:

- Existing maps

Topographic maps (1:50,000) : Produced by the Royal Thai Survey Department is among the most important data as geo-referenced map, and basic spatial information.

Thematic maps : A number of organizations in Thailand have produced thematic maps that can be used as input to the system. These include soil, geology, forest, watershed class quality, protected forest area, water resources and etc.

- Other information

- Socio-economic data, e.g. census data from the National Office for Statistics, national rural development data (NRD2C) can be defined and converted into digital spatial form.

- Rainfall data from the Meteorological and Royal Irrigation Departments.

- Satellite data

Satellite data offer the most updated information suited to input into the system. Continued development in earth observation satellites has made it possible to collect a wide variety of spatial data. Analysis of satellite data both analog and digital forms provided information on current landuse, forest, water resource, landform and etc.

4.2.2 Data conversion

Much of data collected in the study area are available in paper maps which have various accuracies and standards. Prior to input data in the system, preprocessing was performed. The preprocessing included auditing, editing, mosaicing and recitifying. The rectification and other preprocessing related to accuracy based on the topographic map. The updating informations were also undertaken using satellite data and field survey for landuse, water resources, landform and some features concerned.

4.2.3 Data analysis

Data can be analyzed using a GIS for a number of functions : to establish and manage database, and to perform modeling. Graphic database and its associated attributes are organized in theme layers. For each layer, the system uses vectors to create line drawing of geographic elements which are rasterized for analysis. The bridging between polygon and its associated database record was performed through identification numbers. Each polygonal layer has its own database in which to store attributes. Each structure of attribute database permits the user to relate many data tables through a common item.

4.2.4 Spatial data output

A selected theme layer or combination of layers are plotted in either vector or raster form, including a related legend. Graphic and its associated attributes can be accessed from the system.

5. Results and Discussions

5.1 Theme layers organization

Spatial and attribute data in Nakhon Ratchsima can be grouped and defined in terms of themes as follows:

- Physical Resources
  - Administrative boundary
    - Amphoe & Tambon
  - Topography
    - Contour lines
    - Landform
- Climate
  - Rainfall

- Temperature
- Relative humidity

- Natural Resources
  - Geology, Soil
  - Water resources, Forest resources
  - landuse, Touristic resources
- Human Resources
  - Population
  - Education
- Infrastructure
  - Transportation networks
  - Electricity
  - Water supply
  - Telecommunication
- Economics
  - General economics
  - Land tenure
  - Industry

5.2 Presentation of the atlas output

The theme layers established can be displayed in both map and statistical forms. The method of display are hard-copy maps and its description, statistical tables, graphs and digital map. However a resource manager often need hard copy map to use as the basis of planning work and discussing program. To serve as basic needs of users the map will be published together with its detailed description. Examples of the spatial informations on sub-district (Tambon) population density and watershed quality class are illustrated in figure 2 and 3 respectively.

5.3 Application of the database

The system provides spatial data and its associated attributes. It is possible to offer either individual layer or a combination of layers. With selected theme layers, it is possible to formulate spatial model for resource strategies. To select theme layers for spatial modeling, the set of relationship should be reviewed and studied. This is to ensure that the information meets the need of parameterizing the model.

6. References

DMR Group Inc. 1989. A corporate Land Information Strategic Plan for the Government of British Columbia, Victoria.

Institute of Applied Science. 1969. Resources Atlas, Nakhon Phanom. Advanced Research Project Agence (ARPA) US. Dept. of Defence.

Institute of Applied Science. 1971. Resources Atlas, Sakhon Nakhon. ARPA. US. Dept of Defence.

McCloy Keith R. 1995. Resource Management Information Systems Talar & Francis. London

Mongkolsawat .C Thirangoon .P and Sowana .A 1995. Spatial Decision Support System for Landuse Planning within a Watershed Area. Proceedings of the GIS AM/FM ASIA'95 August 21-24, 1995 Bangkok.

Figure 1 Study area

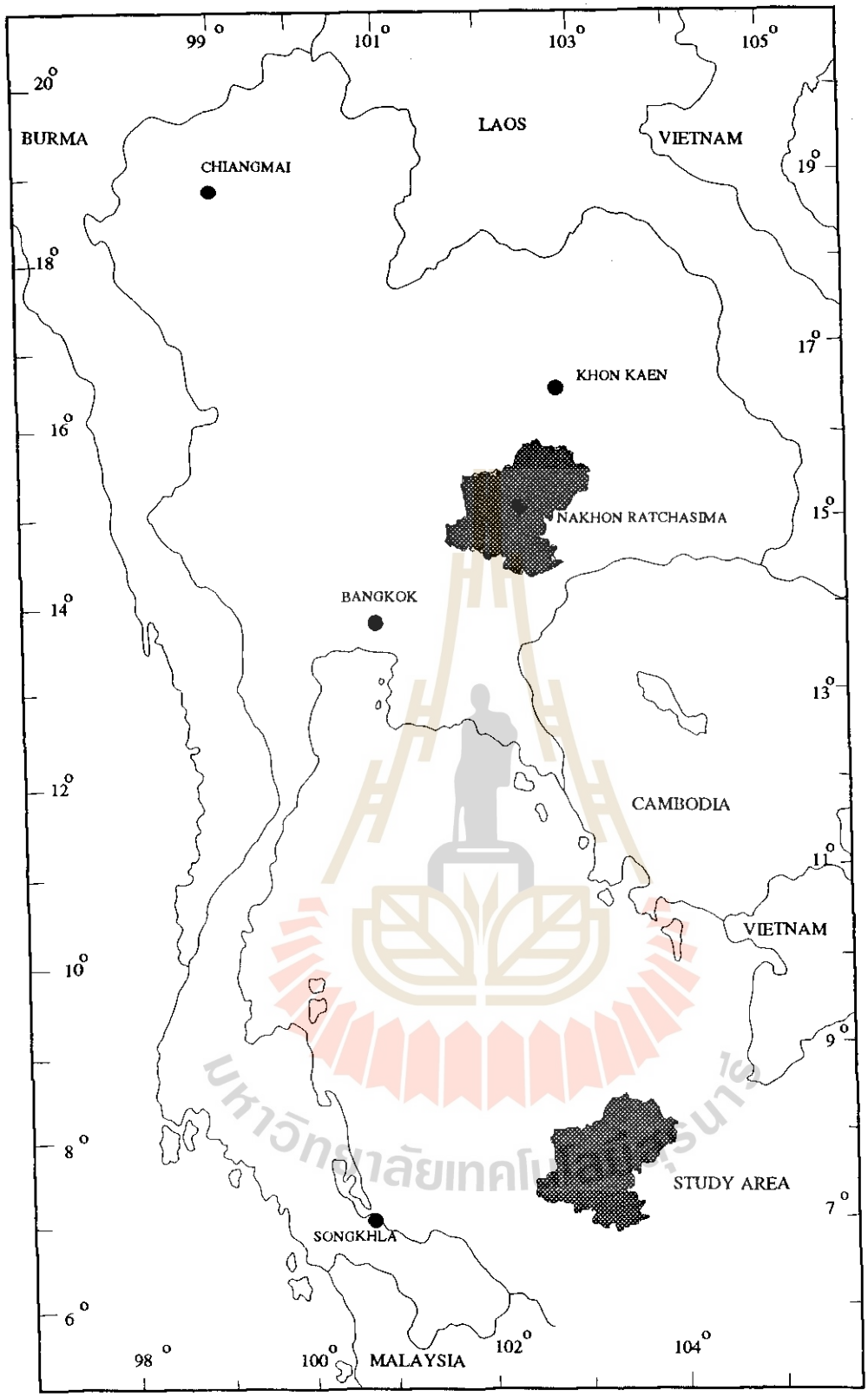

Figure 2

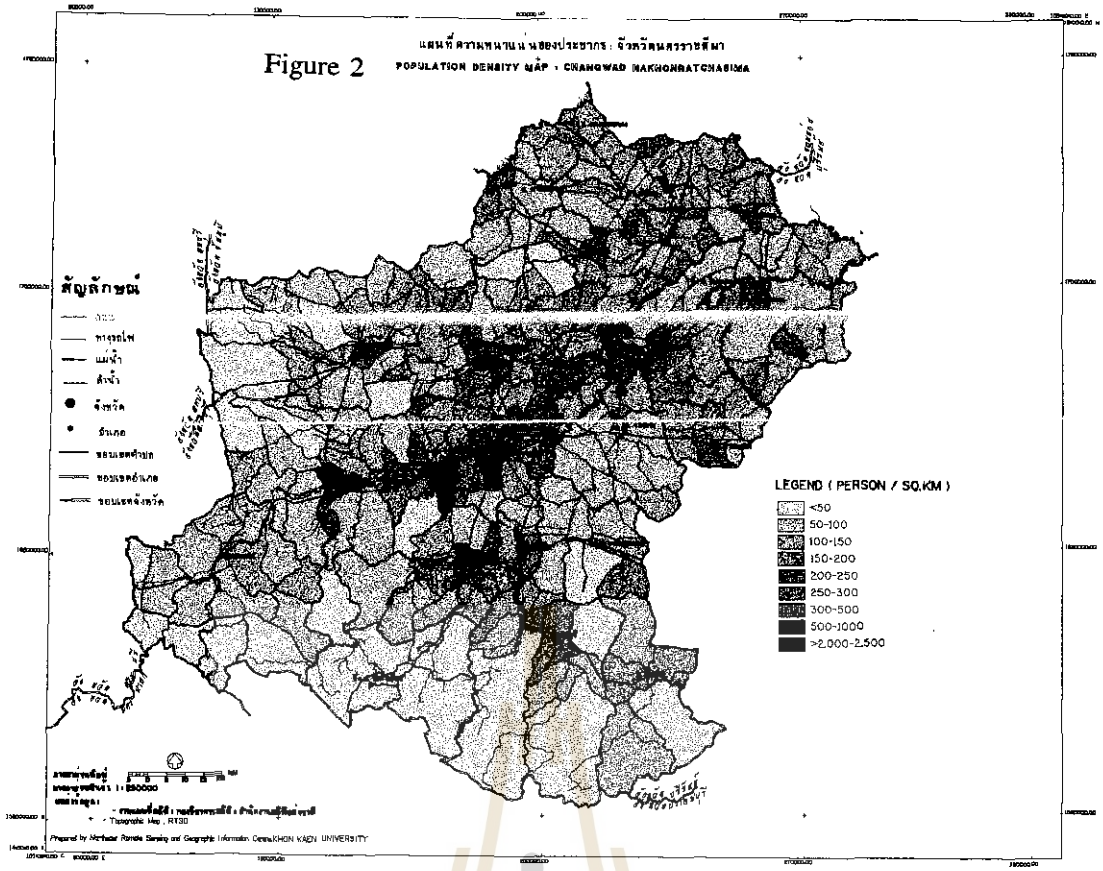

Figure 3

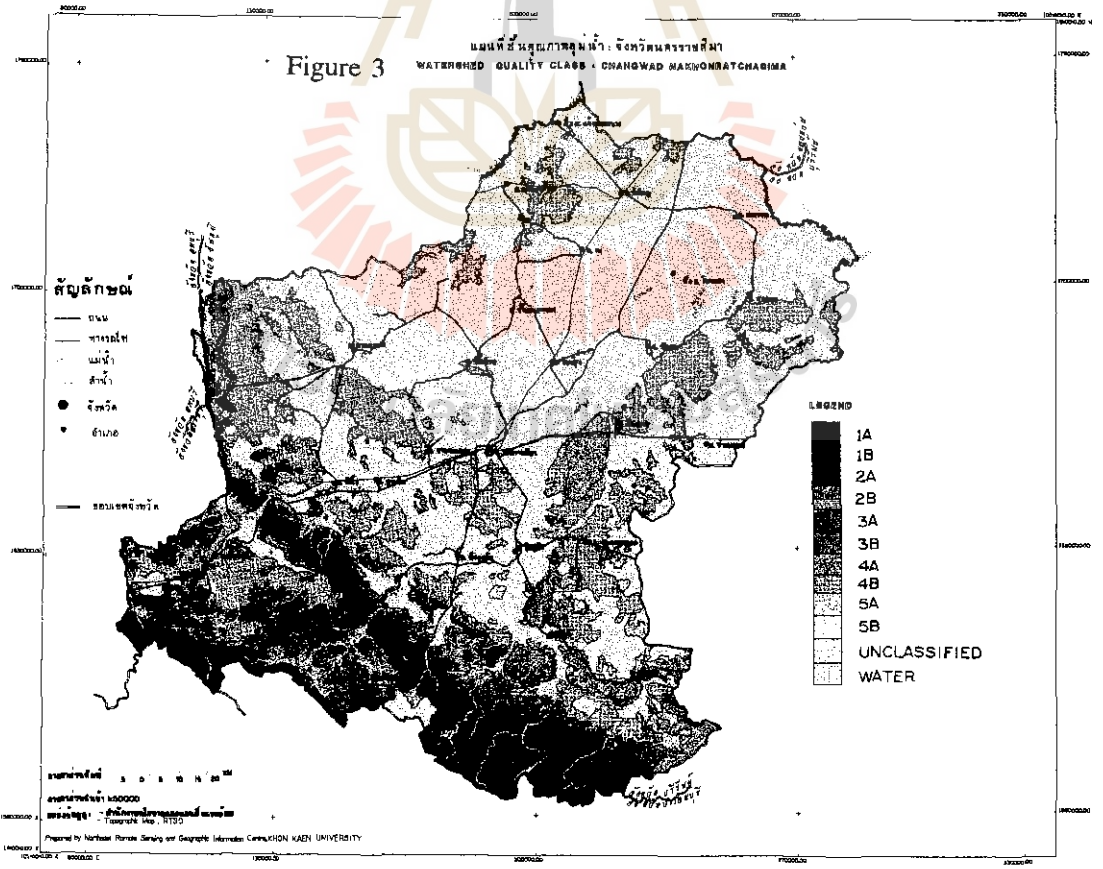

Land Cover Classification System for Continental / Global Applications

Ryutaro Tateishi*, Wen Cheng Gang*, and L. Kithsiri Perera**

* Center for Environmental Remote Sensing (CEReS), Chiba University
1-33 Yayoi-cho, Inage-ku, Chiba 263, Japan
Fax: +81-43-290-3857
Email: tateishi@rsirc.cr.chiba-u.ac.jp

** Weathernews Inc.
D21, 1-3, Nakase, Mihama-ku, Chiba 261, Japan
Fax: +81-43-274-5012

Abstract

A new land cover classification system is proposed for continental / global applications. In this study, a classification system is distinguished from a legend. A classification system is a category system for the classification work while a legend is a category system for the usage of a classified product. A legend is based on a classification system and different legends are possible from one classification system. The proposed classification system has a hierarchical structure with the possible extension of classes up to 255. The approximate resolution of satellite remote sensing image for the proposed classification system is from 250m (future GLI sensor on ADEOS-II, Japan) to 8 km (sampled AVHRR). However detail land cover categories are included in the classification system in order to correspond to other maps and ground survey. Another important feature of the system is that easily classified categories are in the higher level in the hierarchical classification system. This classification system is developed as the activity of the working group, "1-km Land Cover Database of Asia"(LCWG), in the Asian Association on Remote Sensing (AARS).

1. Introduction

One general problem of land cover legend is that there are many kinds of legends in different countries and different projects. This fact prevents data comparison, exchange and integration. This is why UNEP/FAO has a project on harmonization of land cover and land use classifications (UNEP/FAO 1993). The goal of this project is to make clear the relationships among different land cover/use classification systems both within and between countries, both within and between applications, from national to regional to global scales. In the International Workshop on Global Databases organized by the International Society for Photogrammetry and Remote Sensing (ISPRS) Working Group IV/6, the same problem was discussed (Tateishi 1995a). One question in the discussion was "Is the standard legend possible?" The answer was No because users community is diverse and there are a variety of needs for land cover. However it was suggested to develop several standards for each of the users community. The important thing here is that a legend must reflect needs of users. It must be also noted that needs are not static. They will evolve over time.

The Land Cover WG(LCWG) of AARS was established in October 1993. The objectives of the production of land cover database of Asia by the LCWG, AARS are:

- First, global change studies (from scientific needs) and
- Secondly, land use management and planning (from social needs)

In 1994, the LCWG tried to classify land cover of Asia using Global Vegetation Index (GVI) data with the nominal resolution of 16 km. A land cover classification system was developed first for this trial (Tateishi 1994). In 1995, the LCWG is carrying out land cover classification using NOAA / NASA Pathfinder

AVHRR Land Data Set with the nominal resolution of 8 km. Through this activity, the first land cover classification system was modified (Tateishi 1995b). At the working Group meeting during the International Symposium on Vegetation Monitoring held at Chiba University from August 29-31, 1995, and through letter communications, many valuable comments and opinions were received for the modified land cover classification system. The land cover classification system in this paper reflects these comments and opinions.

2. Classification system and legend

The word, "classification system", has been used as the same meaning as "legend". Land cover legend has been decided based on user needs in a country or in a project. The classified result is presented by the legend and its classification work has also been done according to the legend. When a legend has a hierarchical structure, a higher level category is not necessarily easier to be classified than a lower level category. For example, if "forest" and "shrubland" are higher categories than "evergreen" and "deciduous", higher categories are more difficult to classify by multitemporal low-resolution satellite data. For this reason, a classification system is distinguished from a legend in this study. A classification system is a category system for the classification work while a legend is a category system for the presentation of a classified result. That is, multiple legends are possible from one classification system. What authors propose here is a land cover classification system, not a legend.

3. Proposed land cover classification system

Table 1(a) and (b) shows a proposed land cover classification system which has the following characteristics.

(a) Hierarchical structure
(b) Maximum number of possible land cover classes : 255
(c) Harmonization with internationally accepted land cover classification system
(d) Inclusion of Asian main land cover types
(e) Possibility to extend globally applicable classification system
(f) Flexibility
(g) Unique classification among forest, shrubland and grassland
(h) Separated cropland into tree crops, shrub crops and grass crops

(a): There is seven levels at maximum. The highest level has three categories: Vegetation, Non vegetation, and Water. Going to the lower level, it becomes more difficult to classify by satellite remote sensing. For example, discrimination of forest and shrubland by low-resolution satellite remote sensing data is more difficult than that of evergreen and deciduous. This is why forest (code:16 or 42) and shrubland(code:72 or 92) is in lower level than evergreen (code:14) and deciduous (code:70). Though each level does not correspond to a specific resolution or a map scale, classes of only higher level can be classified by low-resolution satellite remote sensing data. The lower level classes are included for ground truth collection or comparison with detail maps.

(b): The classification system consists of 59 classes including 47 classes for vegetation, 8 classes for non vegetation, and 4 classes for water. Addition of new classes up to 255 is possible. Class code is recorded in one byte.

(c): The latest project to map global land cover by remote sensing is being done by the IGBP-DIS Land Cover Working Group which has established land cover classification system based on Running's methodology (Running 1994). In this classification system, forest are divided into four main classes such as Evergreen Broadleaf, Evergreen Needleleaf, Deciduous Broadleaf, and Deciduous Needleleaf. These four classes are introduced to the proposed classification system because discrimination of these classes are important for global change studies.

Table 1(a) Proposed land cover classification system (LCWG, AARS) September 1995

Land cover class	Class code
Vegetation	10
Forest or shrubland	12
Evergreen	14
Forest	16
Broadleaf	18
Natural	20
Tree crops	22
Oil palm	23
Coconut	24
Others	25
Needleleaf	36
Shrubland	42
Natural	44
Shrub crops	46
Tea	47
Others	48
Forest and shrubland	60
Deciduous	70
Forest	72
Broadleaf	74
Natural	76
Tree crops	78
Rubber	79
Others	80
Needleleaf	90
Shrubland	92
Natural	94
Shrub crops	96
Cotton	97
Others	98
Forest and shrubland	110
Mixed forest or shrubland	120
Grassland	130
Natural grassland / pasture	132
Grass crops	140
Paddy	141
Wheat	142
Sugarcane	143
Corn	144
Others	145
Mixed vegetation	160
Wetland	170
Mangrove	172
Swamp	174
Little vegetation	180
Tundra	182
Others	184
Non vegetation	190
Bare ground	191
Rock	192
Stones or gravel	193
Sand	194
Clay	195
Perennial snow or ice	200
Built-up area	210
Water	220
Inland water	222
Water with seasonal change	224
Tidal flat	226

Table 1(b) Explanation of land cover classes

Class code: Class name and Explanation

10: Vegetation
Vegetation but cannot be interpreted into any class from 12 to 184; hereafter the meaning of the underlined part is written like (12-184)
12: Forest or shrubland (14-120)
Forest or shrubs canopy cover is > 60%
14: Evergreen forest or shrubland (16-60)
Canopy is never without green foliage.
Evergreen canopy cover > 60%
16: Evergreen forest (18-36)
Forest canopy cover is > 60%. Tree height is exceeding 2 meters.
18: Evergreen broadleaf forest (20-25)
20: Natural evergreen broadleaf forest
22: Evergreen broadleaf tree crops (23-25)
23: Oil palm
24: Coconut
25: Others
36: Evergreen needleleaf forest
42: Evergreen shrubland (44-48)
shrubs canopy cover is > 60%. Tree height is less than 3 meters.
44: Natural evergreen needleleaf shrubland
46: Evergreen shrub crops (47-48)
47: Tea
48: Other evergreen shrub crops
60: Evergreen forest and shrubland
10% < forest canopy cover < 60%
10% < shrub canopy cover < 60%
70: Deciduous forest or shrubland (72-110)
With an annual cycle of leaf-on and leaf-off periods. Deciduous canopy cover > 60%.
72: Deciduous forest (74-90)
Forest canopy cover is > 60%. Tree height exceeding 3 meters.
74: Deciduous broadleaf forest (76-80)
76: Natural deciduous broadleaf forest
78: Deciduous broadleaf tree crops (79-80)
79: Rubber
80: Other deciduous broadleaf tree crops
90: Deciduous needleleaf forest
92: Deciduous shrubland (94-98)
Shrub canopy cover is > 60%. Tree height is less than 3 meters.
94: Natural deciduous shrubland
96: Deciduous shrub crops (97-98)
97: Cotton
98: Other deciduous shrub crops
110: Deciduous forest and shrubland
10% < forest canopy cover < 60%
10% < shrub canopy cover < 60%
120: Mixed forest or shrubland
Neither evergreen nor deciduous forest or shrubs exceeds 60% of coverage.
130: Grassland (132-145)
Tree and shrub cover is less than 10%.
132: Natural grassland / pasture
140: Grass crops (141-145)
include cereal and other grass type crop
141: Paddy
142: Wheat
143: Sugarcane
144: Corn
145: Other grass crops
160: Mixed vegetation
10% < forest or shrub canopy < 60%
10% < grass cover < 60%
include savanna and
mixed land with cropland, shrubland, forest and few houses
170: Wetland (172-174)
172: Mangrove
174: Swamp
Any type of wetland with vegetation except mangrove
180: Little vegetation (182-184)
Vegetation cover is more than 10 % at the peak season
182: Tundra
184: Others
190: Non vegetation (191-210)
Vegetation cover is less than 10 % at any time of a year
191: Bare ground (192-195)
192: Rock
193: Stones or gravel
194: Sand
195: Clay
200: Perennial snow or ice
210: Built-up area
220: Water (222-226)
222: Inland water
Lake, pond, river, reservoir
224: Water with seasonal change
Inland water with dry period
226: Tidal flat

For example, Evergreen forest and shrubland (60) is included in Evergreen forest or shrubland (14), Forest or shrubland (12) and Vegetation (10). Therefore an explanation of Evergreen forest and shrubland (60) includes the explanation of the classes, 14, 12 and 10. That is, "Evergreen canopy cover > 60%" must be added to the explanation of Evergreen forest and shrubland (60)

(d): One of the main concern in land use management and planning in Asian countries is agricultural land. Therefore main crop types are included in the classification system.

(e): Unique land cover classes in African or American continent can be added as a new class.

(f): The proposed land cover classification system is not a fixed one. It can be improved by addition of classes or modification of system. For example, once all forest and all shrubland in the global area are classified correctly, "Forest or shrubland (12)" will be removed and new classes, "Forest" and "Shrubland", will come to the second highest level of the hierarchical system. And "Evergreen forest (16)" and "Deciduous forest (70)" will be included in the "Forest".

(g): Classification of Forest, Shrubland, and Grassland
For the purpose of global change studies, the discrimination of vegetation into forest, shrubland, and grassland is important. Shrubs is small woody plants that are branched from the base. The proposed system used a threshold value of 3 meters height to distinguish shrubland from forest. As shown in Figure 1(a), there are logically seven categories in the combination of forest, shrubland and grassland such as F, S, G, FS, SG, FG, FSG in the figure. Since the category of FSG is too detail, FSG is divided into Mfs, Msg, and Mfg and these three are combined to FS, SG, and FG, respectively (see Figure 1 (b)). By this alternation, seven categories are reduced to six categories. Moreover, since the discrimination between forest and shrubland by low-resolution satellite remote sensing data is difficult, two categories, "Forest" and "Shrubland" are combined into a larger category, "Forest or shrubs". Similarly, FG and SG are combined into a larger category,"Mixed vegetation". Finally, seven categories in the figure are merged into three categories such as "Forest or shrubs (code: 12; F, S, FS, and Mfs)", "Grassland (code: 130; G)", and "Mixed vegetation (code: 160; FG, SG, Mfg, and Msg)" as shown in Figure 1(c).

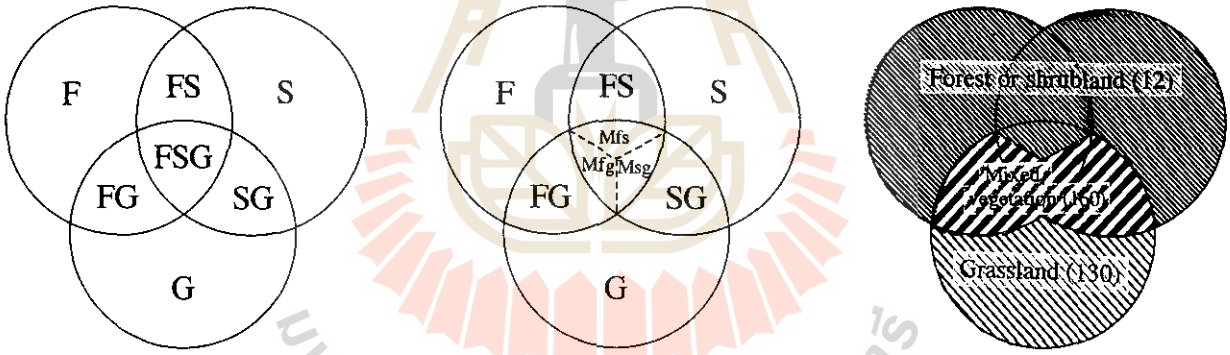

(a) (b) (c)

F: Forest
S: Shrubland
G: Grassland

FS: Forest and shrubland
FG: Forest and grassland
SG: Shrubland and grassland

FSG: Forest, shrubland and grassland

Mfs: Forest, shrubland and grassland; with the least coverage of grassland
Mfg: Forest, shrubland and grassland; with the least coverage of shrubland
Msg: Forest, shrubland and grassland; with the least coverage of forest

"Forest or shrubland" (class code 12): F + S + FS + Mfs
"Grassland" (class code 130): G
"Mixed vegetation" (class code 160): FG + SG + Mfg + Msg

Figure 1 Forest, Shrubland and Grassland

(h): Cropland is divided into tree crops (code: 22 or 78), shrub crops (code: 46 or 96) and grass crops (code: 140) because the discrimination between cropland and natural vegetation by low-resolution satellite remote sensing data is generally more difficult than the discrimination between "Forest or shrubs" and "Grassland".

4. Examples of legends

Based on the land cover classification system as shown in Table 1, some legends can be established. The following shows relationships between a category, "Forest" (and a category, "Shrubland"), in a legend and class codes in the land cover classification system.

Forest: class code 16+18+20+22+23+24+25+36+72+74+76+78+79+80+90
+ part of 120 + part of 12 + part of 10

Shrubland: class code 42+44+46+47+48+92+94+96+97+98
+ part of 120 + part of 12 + part of 10

5. Conclusion

The Land Cover Working Group of AARS proposed a new land cover classification sytem in this paper. Any comments or opinions about the proposed classification system are welcome to improve it. Based on the classification system, land cover dataset of Asia with 8 km resolution is developing.

Acknowledgements

The land cover classification system proposed in this paper has developed by the cooperation with 49 working group members from 28 countries. Authors would like to thank all working group members for their valuable cooperation. Authors would also thank Dr. Colin Mitchell of ISMARSC Limited for his detail comments to the land cover classification system.

References

Running,S.W., T.R. Loveland, and L.L. Pierce,"A Vegetation Classification Logic Based on Remote Sensing for Use in Global Biochemical Models", Ambio, Vol.23, No.1, 1994

Tateishi, R., C.Wen, and K. Perera,"Working Group Report and Land Cover Database of Asia", Proc. 15th ACRS, 17-23 Nov., 1994, pp.M-3

Tateishi,R.(Ed.), "Report of the International Workshop on Global Databases", International Archives of Photogrammetry and Remote Sensing, Vol.XXX, Part 4W1, Boulder, 30-31 May, 1995a

Tateishi,R., "Land Cover Database of Asia", Proceedings of the International Symposium on Vegetation Monitoring, Chiba, Japan, 29-31 August, 1995b

UNEP/FAO, "Report of the UNEP/FAO Expert Meeting on Harmonizing Land Cover and Land Use Classifications", Geneva, 23-25 November, 1993

DEVELOPING LAND COVER CLASSIFICATION SYSTEM FOR NOAA AVHRR APPLICATIONS IN ASIA

Chandra Giri
Surendra Shrestha
UNEP Environment Assessment Programme for Asia and the Pacific
Asian Institute of Technology
P.O. Box 2754
Bangkok 10501
Thailand
Tel: (66-2) 524-6236
Fax: (66-2) 516-2125
E-mail: grid@cs.ait.ac.th

Abstract

In this paper, a land cover classification system for use with coarse spatial resolution remotely sensed data such as NOAA AVHRR, suitable for Asian conditions has been proposed. Considerations of Users' needs and sensor's capabilities in selecting land cover classes has been discussed. The need for harmonized and consolidated efforts to come up with better classification system at different scale is noted.

1.0 Introduction

The classification system for remotely sensed data varies primarily with the kind of the satellite data used and the objective of the classification. Due to these variations, the nomenclature and definition of land cover types tend to vary considerably in the existing literature. As a result, today, comparison across time and space of land use has become very arduous (Mucher et. al., 1993). Moreover, ambiguity in the mapping and classification criteria can often causes significant differences in the results of the interpretation (Singh, 1986). Efforts in developing standard and harmonized land cover types for Advanced Very High Resolution Radiometers (AVHRR) data interpretation is necessary as land cover cut across numerous sectors of resource management and the selection of classes plays an important role in the AVHRR analysis.

2.0 NOAA AVHRR Data

AVHRR data in 1 km resolution operated by the US National Oceanic and Atmospheric Administration are available either in LAC or HRPT. The data is suitable for macro assessment and monitoring of land cover status and their change patterns in near real time basis (Giri & Shrestha, 1995). Considering the strengths and weaknesses of the data (see Table 1), it can be said that this is the only option available for large scale assessment and monitoring of resources, at least for few years until the moderate resolution satellite data will be available in the market.

Negotiations are being held with China, India, Indonesia and Iran to extend the project in these countries. Two "hot spot" (major disturbance front) areas, one in Northern Laos and another in the Mekong Delta (Vietnam) have been identified for further investigation using high resolution satellite data such as LANDSAT TM and SPOT. Methodological guidelines on the use of AVHRR data for the assessment and monitoring of major land cover types in the region is being developed. These activities are expected to continue in 1995 and beyond.

The major land cover classes of interest were selected owing to the capability of the sensor to detect features on the earth's surface and their practical significance in the real world. For the purpopse information such as variation in the phenological characteristics of the vegetation through different season and cropping system in the region were taken into consideration. Furthermore, information and experiences from previous similar exercises, guidelines prepared by UNEP/FAO on land cover/land use and experts' views on the field were also used in selecting classes. The principal aim is to harmonize the land cover classification system for regional aggregation and comparison.

The following diagram presents an overview of the land cover classification system.

Fig. 1 Land Cover Classification System

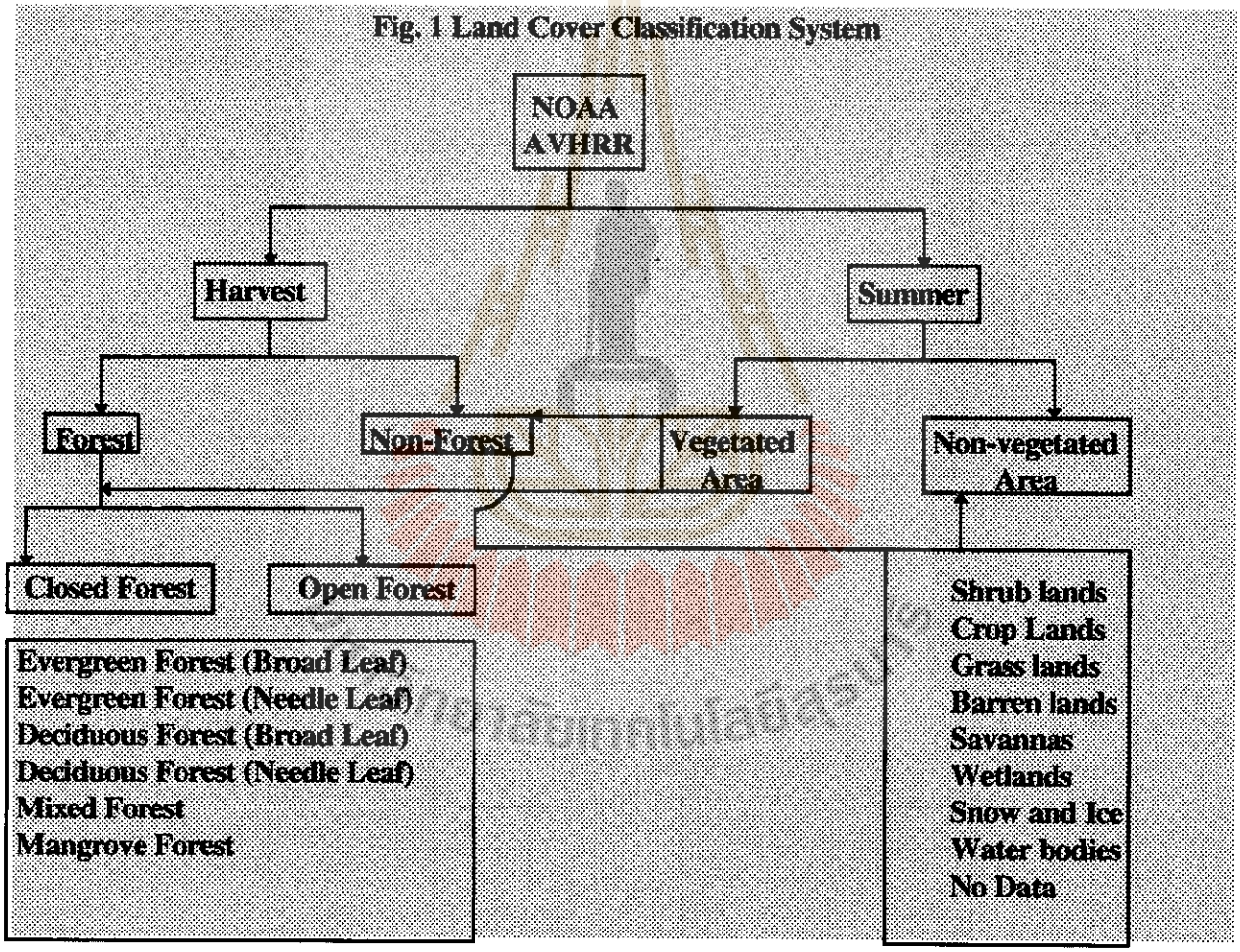

Table 1.0 Advantages and Disadvantages of NOAA AVHRR HRPT Data

Advantages	Disadvantages
1. Synoptic coverage and hence low data volume	1. Coarse resolution (1.1 km at the Nadir)
2. High radiometric resolution (10 bit)	2. Pre-processing is time consuming
3. Relatively low cost (Free!, only handling cost)	3. The methodology in handeling AVHRR data for land applications is not well developed
4. Twice daily coverage and hence high possibilities of having cloud free data.	4. LAC data has limited capability to record on-board

3.0 Classification Criteria

The underlying supposition in the analysis of remote sensing data is that each feature on the earth's surface records its unique signature in the sensor thus providing opportunities for discriminating between different objects on the earth's surface. Features on the earth's surface in-distinguishable with the satellite data should not be taken as a separate class. On the other hand, all the classes discernible by the sensor may not be of practical use to the users. A positive synergism of two is necessary in selecting land cover classes prior to the analysis of the satellite data. However, this will not overcome the possibility of incorporating secondary information with the help of GIS.

4.0 Classification Scheme

Once we have selected the classes, it is necessary to define them properly. There is a great tendency to mix two commonly used terms viz. land cover and land use, principally because these two are closely interlinked. Land cover can simply be defined as "the physical attributes of the land that can be seen readily as opposed to the land use which describes a pattern of human activities undertaken within a social and economic context". Land cover has visual effects, visible by the remote sensor, as it is what covers the land at the time of satellite observation. Examples of land cover are forest, snow, grass land etc. with an exception of barren land without any cover.

More difficult problem can be encountered in defining individual land cover classes. Forest, for example, is the most controversial one. FAO has two definitions of forest, one for developing countries and one for developed countries. Forests for developing countries have been defined as an "ecological systems with a minimum crown coverage of land surface (here assumed as 10 percent) and generally associated with wild flora, fauna and natural soil conditions; and not subject to agronomic practices". For developed countries on the other hand forest is "with tree crown cover (stand density) of more than about 20% of the area. Continuous forest with trees usually growing more than about 7 m in height and able to produce wood... " (FAO, 1993). The reason for defining forest differently for developing and developed countries is not mentioned in the report. The definition of forest in the International Geosphere Biosphere Project (IGBP), is based on the percent canopy cover and height . Land dominated by trees with a percent canopy

cover greater than 60% and height exceeding 2 meters has been considered as forest in their definition. On the other hand, agriculture is widely used as a land cover but for some, it sounds more like land use and the alternative term "crop lands" has been proposed.

Numerous land cover classification systems exists at the global level. UNESCO's International Classification and Mapping of Vegetation (1973) based solely on the ecological and physiological criteria is not much importance for use with remotely sensed data. FAO, The Forest Resources Assessment 1990 focuses more on the forest cover classification system with different methodologies in different parts of the world and fails to provide spatial distribution of forest within the territory.

The most comprehensive classification system at the global level for use with AVHRR 1 km satellite data has been proposed by the IGBP-DIS Global 1 km Land Cover Project. We felt it necessary to refine this classification system to be applicable in the Asian region. A new approach of land use and land cover classification systems for use with high resolution remote sensing data has been developed by Anderson et. al (1976) and a modified forest cover classification system in an Indian perspective has been proposed by Singh (1989). Neither of these methods provides a comprehensive means to deal with land cover classification systems for macro assessment in use with coarse resolution satellite data such as NOAA AVHRR.

The following criteria has been proposed through this paper for general use.

The classification system should have land cover classes discernible with the satellite data in use (AVHRR data in this case) taking advantage of the ground information as well as the ancillary information available.

The classes discernible should have practical meaning in terms of it's application. Grouping and regrouping of several classes according to the users' need might be necessary.

The accuracy of the analysis of satellite data should be 85% or more, however, standard means and techniques to assess accuracy of the classification results derived from AVHRR data need to be developed. The rule of thumb is "Accuracy of the classification results is inversely proportional to the number of classes used".

The same results, within the threshold accuracy, should be attainable by number of analysts using imagery of different seasons.

5.0 Parameters for Classification

Tree height and percent crown cover are two quantitative parameters of forest widely used in classifying forest and non-forest areas and different categories of forest classes. FAO categorizes forest as closed forest if the percent canopy cover is greater than 40% and open forest if the percent canopy cover is in the range of 10-40%. To be classified as forest the height of the tree should be greater than 7 meters. In IGBP

classification system, percent crown cover should be more than 60% and tree height should be more than 2 meters to be classified as forest. This definition underestimates the forest acreage in Asia. For our purpose, neither method gives an accurate representation. Forest with 10-40% canopy cover and trees greater than 3 meters in height has been classified as open forest and that of percent canopy cover greater than 40% has been classified as closed forest. More research is necessary to correlate digital count with these two quantitative parameters. Till now, these two are determined based on the subjective judgment.

The above definition of forest is in compliance with the existing forest classification system in majority of the countries in the region with some exceptions. For example the definition of forest for developed countries (20% canopy cover) has been followed in China and in Lao P.D.R.

Phenology of the vegetation and season consideration that varies across countries, might be the best parameter to be taken into account to discriminate evergreen and deciduous forest. Season and cropping patterns are vital in discriminating forest and non-forest areas and barren land and crop land. This is because barren land and harvested paddy field appear to be the same in the satellite data. Consideration should be given to the cropping systems. Special consideration is necessary to discriminate between clouds and barren land and clouds and snow.

6.0 Past Efforts

No general agreement on the global classification system exists and so is with regional and local. It is increasingly felt necessary to develop an international and well accepted system for land cover classification. However, experiences shows that by no means this broad categorization is sufficient for thematic use. A multi-level approach for defining the land cover classes need to be developed..

At the global level, efforts have been in place for standardization of land use and land cover classification system. A number of individuals and organizations have contributed their efforts in harmonizing land cover classes in the past. UNEP and FAO jointly initiated a project in collaboration with the Institute of Terrestrial Ecology in UK for standardization of land use/land cover classification systems. IGBP and UNESCO are two other actors active in this field. USGS EDC planned to map the entire globe for the land cover before 1997. Land cover working group of Asian Association of Remote Sensing (LCWG/AARS) is also working on this.

7.0 UNEP's Efforts in Asia

UNEP through its Environment Assessment Programme for Asia and the Pacific has been involved in macro scale land cover assessment and monitoring of selected countries in the region using AVHRR data and subsequently developing the land cover classification system at the regional/national level. Land cover mapping of Bangladesh, Cambodia, Lao. P.D.R., Myanmar, Nepal and Vietnam for the period of 1985/86 and 1992/93 was finalized in 1994. Data for Pakistan and Sri Lanka is being analyzed.

8.0 Definition of Land Cover Classes adopted by UNEP/EAP-AP

Forest: Land covered by trees with the percent canopy cover greater than 10%. Trees are woody plants with a single well defined stem and more than 3 meters in height. Forest with 10-40% canopy cover is classified as open forest and with 40% and above is classified as closed forest.

Evergreen Forest: Forests with green foliage throughout the year.

Deciduous Forest: Forests that sheds their leaves in certain period of the year.

Mixed Forest: Forests consisting of mosaic of evergreen and deciduous forest.

Mangrove Forest: Tidal forests found near the sea shore.

Shrub Lands: Woody plants often with multiple stems and height ranging from 50 cms to 3 meters. The percent canopy cover is greater than 10%.

Savannas: Land covered mainly with herbaceous plants in association with . Isolated trees.

Grasslands: Land covered with herbaceous plants with less than 10% tree and shrub cover

Wetlands : Land covered with mosaic of water and shrubs and woody vegetation

Croplands: Land covered with agricultural crops

Snow and Ice: Land covered with snow and/or ice at the time of satellite observation.

Barrenlands: Land without any land cover. This includes lands with shrubs and forests having less than 10% canopy cover.

Water Bodies: Land covered with rivers, lakes, estuaries.

No Data Available: Cloud covered or mountain shadowed areas.

Satellite Estimation of Environmental Variables by the Contextual Analysis Method : Validation in a Seasonal Tropical Environment

T. Saravanapavan and Dennis G. Dye
Global Engineering Laboratory
Institute of Industrial Science
University of Tokyo, Japan

Abstract

Previous research suggests that a remote sensing contextual analysis method can be successfully used for estimating and mapping air temperature, soil moisture conditions and atmospheric humidity at regional-to-global scales. Reported validations, however, have so far been limited to only mid-latitude temperate environments. We examine the robustness of the method in an application to sites in the seasonally moist tropical environment of Thailand. Our initial analysis focuses on the air temperature variable and employs 10-day composites of 1 km resolution normalized difference vegetation index (NDVI) data from the NOAA Advanced Very High Resolution Radiometer (AVHRR). For most sites our satellite estimates of air temperature agree well with surface data, confirming that the method can be successfully applied in a seasonally moist tropical environment. Because our 10-day composite NDVI data may not adequately represent daily variations in temperature, we anticipate improved results when the method is applied at the daily time scale.

1. Introduction

Spatial and temporal information on surface temperature, air temperature and soil moisture conditions is important for modeling and monitoring regional evapotranspiration and related biospheric processes, and for linking between the land surface energy budget and the hydrologic budget. Ground based measurements for these variables are commonly available for only a limited number and distribution of point locations. Interpolation techniques are often applied to generate continuous spatial data fields, but these techniques often introduce considerable uncertainty, particularly in regions where station coverage is sparse. Satellite remote sensing provides a means for estimating these variables in a direct and spatially comprehensive manner.

Research in recent years has led to the introduction of a "contextual" analysis approach that shows particular promise for estimating and mapping temperature, soil moisture conditions and atmospheric humidity (Goward et al., 1985, Nemani 1989, Goward and Hope 1989, Prihodko 1992, Goward 1994, and Prince and Goward 1995). The technique estimates temperature and soil moisture conditions based on the relationship between coincident spatial sample arrays of satellite-acquired data on the normalized difference vegetation index (NDVI) and surface temperature, and has been successfully tested in temperate mid-latitude environments. The method, however, has not yet been evaluated in tropical environments, which have energy, temperature and precipitation regimes that differ sustantially from than those of temperate latitudes. This study evaluates the robustness of the contextual analysis method through an application in the seasonally moist tropical environment of Thailand in Southeast Asia.

2. Background

The contextual analysis method takes advantage of the relation between vegetation cover (as expressed by the NDVI) and surface temperature (Nemani and Running, 1989; Goward et al., 1994). Because the amount of vegetation in a landscape tends to be spatially heterogeneous, the observed surface temperature will vary accordingly. Satellite remote sensing of surface temperature, e.g. based on thermal infrared measurements with the "split window" technique (Price, 1983, 1984), enables these spatial variations to be measured and mapped. When coincident measurements of the NDVI are plotted against corresponding surface temperature measurements, the spread of points exhibits a negative slope. The slope tends to be negative because, as the vegetation cover in an observed landscape increases, the surface temperature decreases as a result of differences in heat capacity between bare soil and vegetation canopy, and the cooling effects of transpiration. The magnitude of the slope is sensitive to changes in the moisture conditions of the surface at the time of observation, primarily because of the variations in the magnitude of latent heat exchange by evapotranspiration. A fully vegetated landscape generally exhibits temperatures close (e.g. within ±2°C) of air temperature (Goward, 1994). The air temperature may therefore be estimated by extrapolating the best-fit line through the NDVI of a full vegetation canopy (generally 0.7) and determining the surface temperature at that point. Variations in soil moisture conditions are expressed as variations in the slope of the relation between observations dates.

In this initial analysis, we focus our attention to application of the technique to estimate air temperature in the seasonally moist tropical climate that characterizes Thailand.

3. Data and Methodology

Ten-day composites of NOAA-11 Advanced Very High Resolution Radiometer (AVHRR) data for 7 periods from April 1 to June 10, 1992, were obtained from the EROS Data Center. We applied the split-window technique of Price (1984) to estimate surface temperature. Because field measurements of surface temperature were not available for validation of satellite-derived surface temperature estimates, our analysis assumes that the surface temperature measurements are reliable.

Five sample sites were selected for analysis based on the ready availability of climatic data (Table 1). The sites are Bangkok, Chiang mai, Khonkean, Ranong and Trang. Cloud cover in this tropical region is potentially interrupts the spectral measurements. We removed cloud-contaminated pixels by applying the gross cloud check and the thin cirrus test proposed by Saunders (1988). We applied the contextual analysis method for estimating air temperature by extracting surface temperature and NDVI values in coincident arrays with dimensions of 64 x 64 pixels.

Daily air temperature data for the five locations were averaged to correspond to the seven AVHRR composite periods. These measured data were compared with the satellite estimated air temperature for validation.

Table 1. Location of sample sites. Latitude and longitude are given in decimal degrees.

Site name	latitude (degrees)	longitude (degrees)
Bangkok	13.73	100.57
Chiang mai	18.78	98.98
Khonkean	16.43	102.83
Ranong	9.97	98.63
Trang	7.52	99.63

4. Results and Discussion

The observed NDVI-surface temperature relation displays the expected pattern, with increasing NDVI associated with decreasing surface temperature (e.g. Fig. 1). The satellite estimated air temperatures for the five sites and seven time periods are in general agreement with the ground-measured air temperature values (Fig. 2). The results, however, differ among the sample locations (Table 2). When data for all time periods are considered, the computed coefficient of determination (r^2) varies from a minimum of .03 at Chiang Mai to 0.81 at Khonkean. The poor results in terms of the r^2 value may be attributable to the influence of a limited number of extreme outlying values, most evident at Chiang Mai, Bangkok, and Ranong sites. The RMS differences range from a minimum of 0.7° C to 2.2 °C, suggesting that on average the method provides a reasonably high level of accuracy. The source of the variation requires additional investigation. The outliers are associated with the time of onset of the monsoonal rain period in Thailand, so they potentially reflect the effects of partially cloud contaminated satellite measurements that passed undetected by our cloud screening procedure. If we assume that the outliers do indeed represent artifacts and remove them from consideration, the results for all sites appear consistently good (Table 2). The r^2 values then range from .46 to .93, and the RMS difference ranges from 0.4°C to 0.9°C.

Our use 10-day composite NDVI images to represent the mean air temperature conditions for time period requires further consideration. Because the composite procedure selects the maximum NDVI for the 10-day period to minimize cloud effects, the resultant NDVI images may be biased toward the temperature of the clearest day (i.e. highest NDVI). If temperatures vary during the composite period, the variation may not be adequately represented by the NDVI that is retained for the composite. We therefore expect that additional improvements in accuracy would be attained if the analysis is applied at the daily time scale, together with rigorous cloud screening. We are examining this possibility in our current research.

Although additional analysis is required, our initial results suggest that the contextual analysis method for estimating air temperature can be successfully and reliably applied in the seasonal moist tropics, but may depend heavily on the success with which cloud effects can be detected and removed. In our follow-on research we are expanding our analysis to include the surface moisture and atmospheric humidity variables.

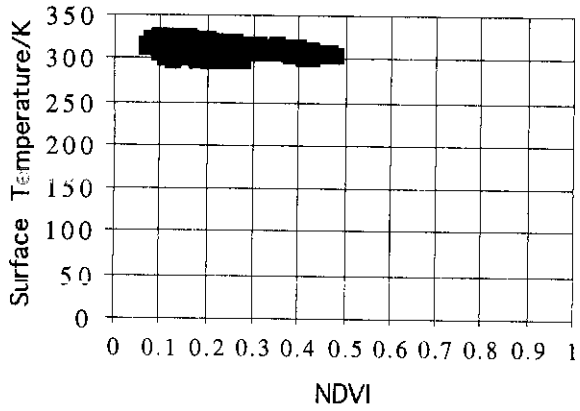

Figure 1. Observed relation between NDVI and surface temperature at Bangkok for period of April 11-20, 1992. Surface temperature decreases with increasing NDVI. Higher NDVI indicates more vegetation cover. Air temperature is estimated by extrapolation of NDVI through the NDVI value of full vegetation cover, assumed as 0.7.

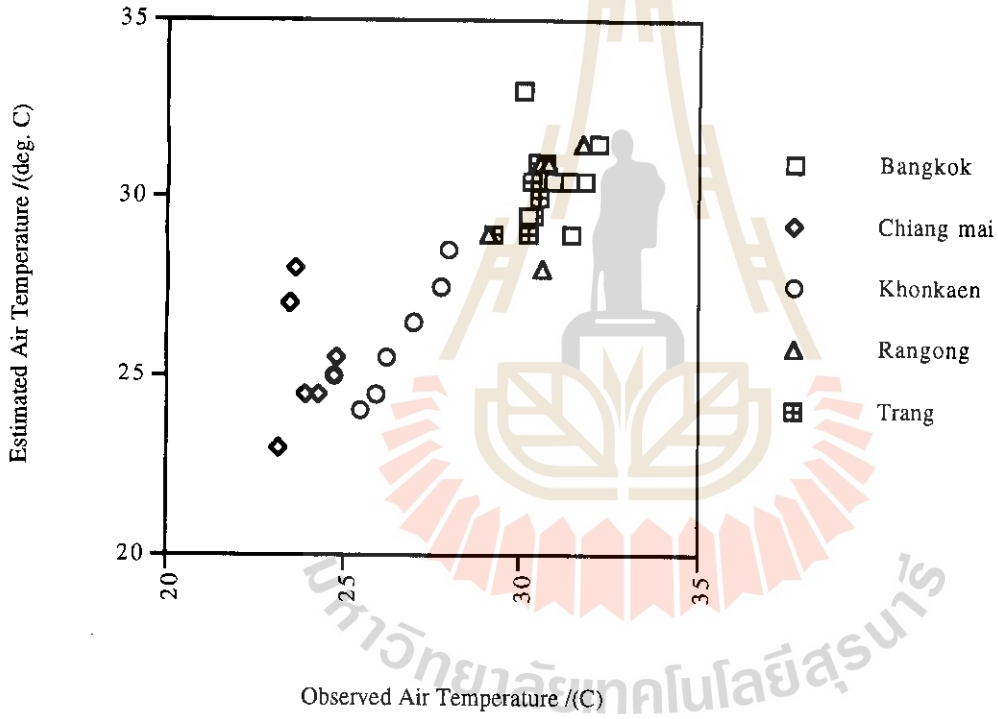

Figure. 2. Comparison of satellite estimated air temperature with the observed air temperature for the five sample locations and seven time periods.

Table 2. Validation results for satellite-estimated air temperature. Values in parentheses indicate results with outlying values removed.

Location	r^2	RMS. Diff. (°C)
Bangkok	0.04 (0.83)	1.6 (0.7)
Chiang mai	0.03 (0.93)	2.2 (0.4)
Khonkean	0.81	0.9
Ranong	0.31 (0.60)	1.1 (0.6)
Trang	0.46	0.7
All Sites	0.77 (0.95)	1.4 (0.7)

5. References

Goward, S.N., and A.S. Hope. 1989. Evapotranspiration from combined reflected solar and emitted terrestrial radiation: preliminary FIFE results from AVHRR data. Advances in Space Research 9 : 239-249.

Goward, S. N., R.H. Waring, D.G.Dye and J.Yang. 1994. Ecological remote sensing at otter: satellite macroscale observations. Ecological Applications, 4(2), pp. 322-343.

Goward, S.N., G.C. Cruickshanks, and A.S. Hope. 1985. Observed relation between thermal emissions and reflected spectral reflectance from a complex vegetable landscape. Remote Sensing of Environment 18 : 137-146.

Nemani, R.R., and S.W. Running. 1989. Estimation of resistance to evapotranspiration from NDVI and thermal-IR AVHRR data. Journal of Climate and Applied Meteorology 28:276-294.

Price, J.C. 1983. Estimating surface temperatures from satellite thermal infrared data-a simple formulation for atmospheric effect. Remote Sensing of Environment 13:353-361.

Price, J.C. 1984. Land surface temperature measurements from the split window channels of NOAA 7 advance very high resolution radiometer. Journal of Geophysical Research 89,D5:7231-7237.

Prince, S.D., and S.N. Goward, 1995. Global primary production: a remote sensing approach. Journal of Biogeography 22: 2829-2849.

Prihodko, L. 1992. Estimation of air temperature from remotely sensed observations. M.A. thesis, University of Maryland at College Park.

Saunders, R.W., K.T. Kriebel. 1988. An improved method for detecting clear sky and cloudy radiation from AVHRR data. Int. J. Remote Sensing, vol. 9, No. 1, 123-150.

On the characteristics of the 1993/1994 Geostationary Meteorological Satellite high cloud amount

Ae-Sook Suh, Kyung-Ja Ha*, Sung-Euii Moon* and Seung-Hee Sohn
Remote Sensing Lab., Meteorological Research Institute, Seoul, Korea
Dept.of Atmospheric Sciences, Pusan National University, Pusan, Korea

Abstract

The characteristics of the GMS high cloud amount have been investigated for summer monsoon period of 1993/1994, the contrasting years in view of the summer monsoon precipitation. In order to investigate the monsoon features over the eastern Asian monsoon region, the cloudiness (using derived by the geostationary meteorological satellite), the condition of underlying surface including sea-surface temperature, and the summer rainfall are analyzed and some comparisons with 1993 and 1994 are also made and the characteristic differences are discussed.

An analysis of the 2-degree latitude-longitude gridded 5-day mean high cloud amount data shows the detailed movement and persistence of the convective activities. In order to describe the spatial and time structure of the intraseasonal oscillation for the movement and evolution of the monsoon cloud, the extended empirical orthogonal function analysis with the twenty-day window size is used for the each year. Also, in order to find out the periodicity of the equatorial convective cluster, Fourier harmonic analysis is applied to the each year.

The most prevailing intraseasonal oscillations of high cloud amount are 61 day mode and 15 day mode in the equatorial and the subtropical oceans. However it was found that the most prevailing modes over the equatorial western Pacific and Indian ocean were different for each year, hence raising the possibility that the contrasting monsoon precipitation may be more fundamentally related to the interaction of intraseasonal oscillations and seasonal variation of convective activities over the lower latitude ocean.

1. Introduction

During the 1993/1994 summer over east Asia, we suffered from the contrasting climatic characteristics of precipitation such as a prolonged intense changma rainfall in 1993 and a weak changma with hot temperature in 1994. This paper, this contrasting characteristics will be analyzed from connection to the monsoonal structure of high cloud amount over east Asia and the equatorial ocean.

The intensity and duration of east Asia monsoon precipitation were thought to be connected with the onset and retreat dates of monsoon convective band, and its variabilities were characterized by sea surface temperature(SST) anomaly, the amount of snow mass over Eurasia, the equatorial flow of tropospheric low level, the process of flux convergence of moisture and the dynamic process of upper atmosphere. Specially, it has been well recognized by recent observational and theoretical studies that the summer precipitation over east Asia is largely affected by the SST and convective activity in the tropical Pacific(Nitta, 1987; Shen and

Lau,1995). This relationship between the tropical western Pacific and the summer climate over east Asia has been clarified by the interaction of annual and intraseasonal variation of convective activity in the tropical region(Li and Wang, 1994). In the key studies of this nature, the 30-60 day oscillation was analyzed by many studies(Madden and Julian, 1971; Lau and Chan, 1986), the quasi-biweekly oscillation has been recognized (Krishnamurti and Bhalme, 1976).

In a more recent study, Tanaka(1994) have used the high cloud amount derived by the geostationary meteorological satellite(GMS) to analyze the summer monsoonal convection over east Asia. Maruyama *et al* (1986) showed also that the GMS high cloud amount can be used to estimate the rainfall in the tropical Pacific. Nitta(1987) and Tanaka(1991, 1994) analyzed this data set and investigated the onset and retreat dates, and seasonal cycle in the summer monsoon clouds and its interaction with the intraseasonal oscillation. These results let it confirm that GMS high cloud amount is useful to analyze the summer monsoon activity.

In the present study, the extended empirical orthogonal function is used to obtain the evolutional structure of the principal spatial function of high cloud amount. And the intraseasonal oscillation is analyzed by the Fourier harmonic analysis, and its anomalous oscillation is established by means of the comparison of 1993 and 1994.

2. Data

The major data used in the present study is the five-day mean 2-degree latitude-longitude grid data of the GMS high cloud amount producted by the Japan meteorological satellite center. The data is constructed by time series from 1 April to 2 October in 1993 and 1994 respectively. The GMS high cloud amount is expressed as non negative integer below 10 and defined as the clouds having a cloud top temperature below the 400 hPa level climatological temperature based on observation (for example, Tanaka(1992) defined the summer monsoon cloud by the regions with more than 3 of the mean high cloud amount). This data is useful to estimate the precipitation for the reason of no missing data over land and ocean.

3. The characteristics of the 1993/1994 east Asian high cloud amount

Time-longitude sections of latitudinally averaged high cloud amounts for 32-38N and 6-12N are presented by Figure 1 and Figure 2, respectively. In case of 1993, the convective activity is situated strongly during summer monsoon period(June-July) over east Asia. Specially, one cloud branch moves to the northward toward Korea and Japan, while the inter tropical convergence zone(ITCZ) in the Northern Hemisphere appears lastingly in 5N-10N and extends northwestward in summer monsoon. However, during June and July in 1994, the northward branch is not appeared and the large cloud amount is accumulated at 15N-20N and the convective activity around Korea becomes noticeable in August.

Specially, characteristics over eastward of 120E is situated contrastly. The convective activity moves eastward in time for May-June in 1993. That is the horizontally extended convective cloud band is appeared from July to August. In 1994, this developmemt of convective activity is separated by two band with relatively small cloud area along northward movement and the strong convective cloud from 130E to 150E is lasted for July at lower latitude.

Namely, in case of 1993, the strong activity at the lower latitude is appeared for whole changma period. Whereas, in 1994, for July the convective activity exists slightly around Korea and Japan, and it is distinctly lasted at the lower latitude.

3.1 Extended empirical orthogonal function of high cloud amount

In order to investigate characteristics of time evolution of the principal spatial structure,

extended empirical orthogonal function(EEOF) analysis with the 20-day window size and 10-day window size is applied to each year. The window size is decided by judgement that the 20-day can include the synoptic scale motion and then mean structure in 20 day explains the quasi-stationary character. Now we can convert the original time-spatial function μ_{ij} of high cloud amount to new time-spatial function $\mu_{ij}^{(n)}$ reconstructed by which n is the number of windows. Then, $\mu_{ij}^{(n)}$ can be expressed by the sum of the products of the time variation function, Ψ_{jl} and the space variation functions, $\alpha_{il}^{(n)}$ as following formula. Then, $\mu_{ij}^{(n)}$ is consisted of time function by spatial function.

$$\mu_{ij}^{(n)} = \sum_{l=1}^{L} \alpha_{il}^{(n)} \Psi_{jl}$$

Where, α_{il} is the window averaged space structure with the weight being the l-th eigenfunction. Ψ_{jl} is common time structure of windows, and can be determined as the eigenfunction of covarience matrix of μ_{ij}. Eigenvector represented by common time structure for the each window represents the time variation within the window size.

The first principle mode (Figure 3) explains the most of variability over 77% of mean total variances for 1993 and 1994. This EEOF mode exhibits relatively stationary phase, while second, third and fourth mode represent wave motion as shown by Figure 3 Figure 4 and 5 represent the time evolution of the spatial structure corresponding to the first principal mode in 1993 and 1994, repectively. The period indicated in figure is from 31 May to 8 August including Changma season. We can percieve that the cloud band around 20N moves northward toward Korea and Japan during 20 June - 19 July. Whereas, in 1994 it is noticed that the cloud band near 20N exists continuously without moving northward.

In order to compare between characteristics in 1993 and 1994, we have obtained the differences(1994-1993) of the spatial structure of the first mode in time. It is characterized that the strong negative value around Korea and Japan is shown during 20 June - 29 July and the positive activity near 20N is sustained from 20 June. As a consequence, we can infer that the monsoon convective activity around Korea and Japan in 1994 is weaker than that of 1993, in contrast to the character in north region of east Asia, the convective activity in lower latitude near 20N in 1994 exists intensely and is stationary in character. One may thus conclude that the convective activity in 1994 doesn't move northward and continue to act at the lower latitude. The climatic variability which is producing this results is characterized as the contrasting features between 1993 and 1994. It may explain that this characteristics is forced by the constraint of equatorial and subtropical condition.

Unlike, the first mode, the second EOFs for 1993 and 1994 are relatively small on the contribution to total variance, however, the mode was produced by different character in 1993 and 1994. In 1993, the wave motion was concentrated on South China Sea, and in 1994 the wave motion was prominently represented at the western and northern borderline of Northern Pacific high. The second mode was not shown in the figures, but in order to find out the outstanding period of the wave motion for convective activity over east Asia, Fourier harmonic analysis was performed.

3.2 Fourier harmonic analysis

Fourier harmonic analysis is performed to determine what types of wave mode are pronounced over the analyzed area. The prevailing mode of intraseasonal oscillation in equatorial region and the different character between 1993 and 1994 are investigated.

Harmonic function which is derived from time series of high cloud amount at each grid point is represented as a function of wavenumber. Figure 6 shows the power amplitude as a function

of wavenumber obtained from Fourier harmonic analysis. The ten symbols represent the amplitude of different area separating by two degree longitude from 130E to 148E at equator. Symbol x at wavenumber 12 has higher harmonic amplitude than any other symbol in 1993. In 1994, the most dominent symbol is y at wavenumber 3.

Then, it is possible to express over the equatorial and subtopical oceans. From the Fourier analysis applied to the tropical and subtropical region, it is noteworthy that the difference between 1993 and 1994 in wave modes is recognized.

Figure 7(a) informs that 15.4 day mode is predominant also in subtropical region. The 61 day mode is dominant in 1994 as shown Figure 7(b). The 15.4 day mode of the most prevailing mode in 1993 is known as the quasi-biweekly mode. Like this, The most prevailing modes over the central equatorial Pacific and Indian ocean was obtained differently, in 1993 the 61 day mode is represent and in 1994 this mode is weak in Indian ocean. Then it is probably a judicious conjecture that the different climatic features between 1993 and 1994 may be claimed significantly in terms of the 15 day and 61 day modes at lower latitude, raising the possibility that the contrasting monsoon precipitation in 1993 and 1994 may be more fundamentally related to the interaction of intraseasonal oscillations and seasonal variation of convective activities.

4. Concluding summary

Rainfall is considered as an index for the strength of the east Asian monsoon. There are the contrast characteristics that we experienced a small amount of rainfalls in 1994 in comparison with 1993.

The evolution of high cloud amount for the period of summer monsoon amount is compared as a function of latitude.

EEOF analysis is used to investigate the principal characteristics of time evolutional structure, and Fourier harmonic analysis is applied to examine the activity of wave mode in equatorial Pacific region. The results can be summarized as following.

First, high cloud amount is compared for the each year through longitude-time cross section averaged at 32-38N and 6-12N. There are strong convective activity during June and July in 1993. The other hand, the monsoonal convective activity for July in 1994 isn't appeared at the region from 110E to 172W of east Asia.

Secondly, from the analysis of SST monthly difference, at lower latitude than near 18N, the onset time of monsoon in 1994 is represented as the faster tendency than that in 1993. And it is shown that the continuous increasing tendency is represented to the sourthward of 18N in 1994. By this result, it seems to be explained that the convective activity at lower latitude is strengthened lastingly.

Thirdly, from the difference(first mode in 1994 - first mode in 1993)analysis of the first mode obtained from EEOF analysis, a positive difference of convective activity appeared at the lower latitude than 20N, and a negative difference at the higher latitude.

Lastly, it is noteworthy that the wave activity in the equatorial Pacific is represented differently for the contrasting years, 1993 and 1994. The 15 day mode and 31 day mode in 1993 and 61 day mode in 1994 than any the other modes were relatively dominant in equatorial central Pacific and western Pacific. And the 61-day mode in 1993 was predominantly shown in the Indian ocean to the westward of 100E, and about 20 day oscillation was continuously existing over the east Asian monsoon region. From these results, we can infer that intraseasonal oscillation in equatorial Pacific, subtropical Pacific and Indian ocean plays an important role on the migration of the convective cluster to east Asia monsoon region during the monsoon period.

References

Hendon, H. H., and M. L. Salby, 1994: The life cycle of the Madden-Julian oscillation. *J. Atmos. Sci., 51,* 2225-2237.

Knutson, T. R., K. M. Wickmann and J. E. Kutzbach, 1986: Global scale intraseasonal oscillations of outgoing longwave radiation and 250mb zonal wind during northern hemisphere summer. *Mon. Wea. Rev.,114,* 605-623.

Kousky, V. E., 1995: *Climate diagnostics bulletin. Jan. 1995.* Climate Analysis Center, National Meteorological Center, 78pp

Krishnamurti, T. N. and N. H. Bhalme, 1976: Oscillations of a monsoon part I: Observational aspects. *J. Atmos. Sci., 33, 1937-1954*

Lau, K. -M. and P. -H. Chan, 1986: Aspect of the 40-50 day oscillation during the northern summer as unfered from outpoing longwave radiation. *Mon. Wea. Rev., 114, 1354-1367.*

Li, Tianming and B. Wang., 1994: The influence of sea surface temperature on the tropical intraseasonal oscillation: A numerical study. *Mon. Wea. Rev, 112,* 2349-2362.

Madden, R. A. and P. R. Julian, 1971: Detection of a 40-50 day oscillation in the zonal wind in the tropical Pacific. *J. Atmos. Sci., 28,* 702-708.

Maruyama, T., T. Nitta and Y. Tsuneoka, 1986: Estimation of monthly rainfall from satellite-observed cloud amount in the tropical western Pacific. *J. Atmos. Sci., 62,* 88-108.

Murakami, T. and J. Matsumoto, 1994: Summer monsoon over the Asian continent and western north Pacific. *J. Meteor. Soc. Japan, 72,* 719-745.

Nitta. T., 1987: Convective activities in the tropical western Pacific and their impact on the northern hemisphere summer circulation. *J. Meteor. Soc. Japan, 65,* 373-390.

Reynolds, R. W. and T. M. Smith, 1994: Improved global sea surface temperature analysis. *J. Climate, 7,* 929-948.

Shen, S. and K. -M. Lau, 1995: Biennial oscillation associated with the east Asia summer monsoon and tropical sea surface temperature. *J. Meteor. Soc. Japan, 72, 235-*253.

Tanaka, M., 1992: Intraseasonal oscillation and the onset and retreat dates of the summer monsoon east, southeast Asia and the western Pacific resion using GMS high cloud amount data. *J. Meteor. Soc. Japan, 70, 1,* 613-628.

Tanaka, M., 1994: The onset and retreat dates of the Austral summer monsoon over Indonesia, Australia and New Guinea. *J. Meteor. Soc. Japan, 72, 235-*253.

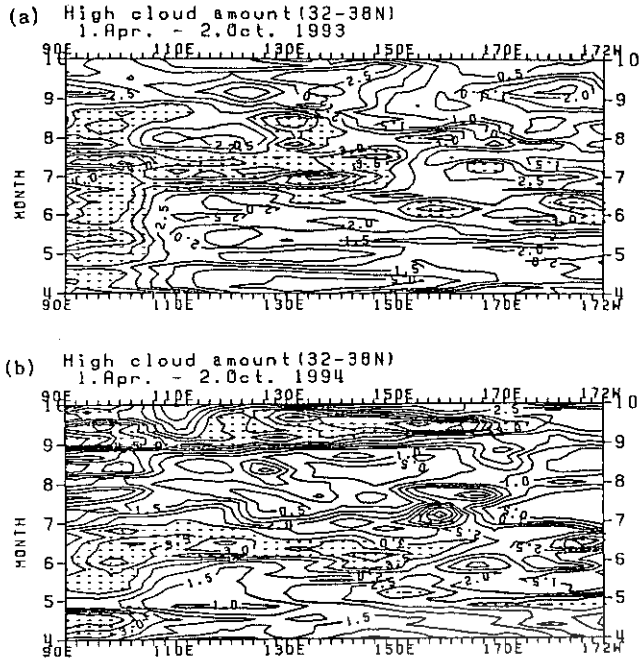

Figure 1. Time-longitude section of latitudinally(32-38N) averaged high cloud amount (a) 1993 and (b) 1994 The dotted regions indicate the area larger than 3.0 of high cloud amount fraction.

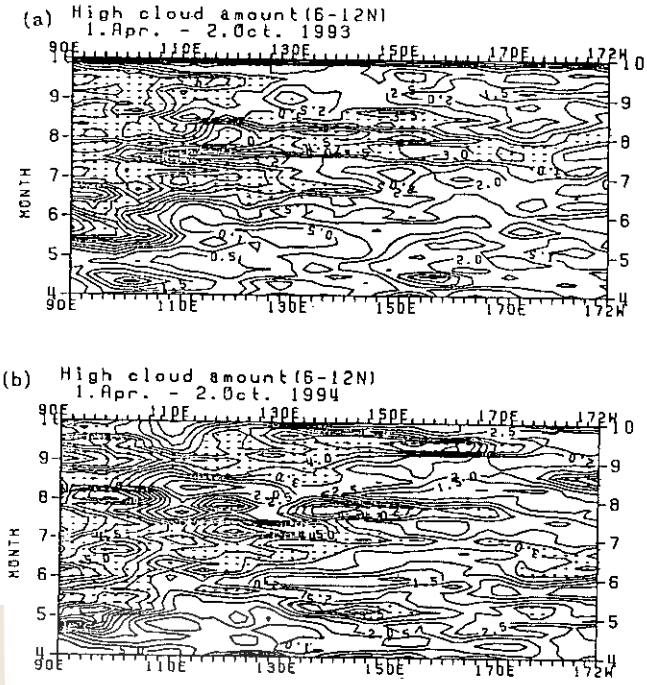

Figure 2. Same as in figure except for 6-12N.

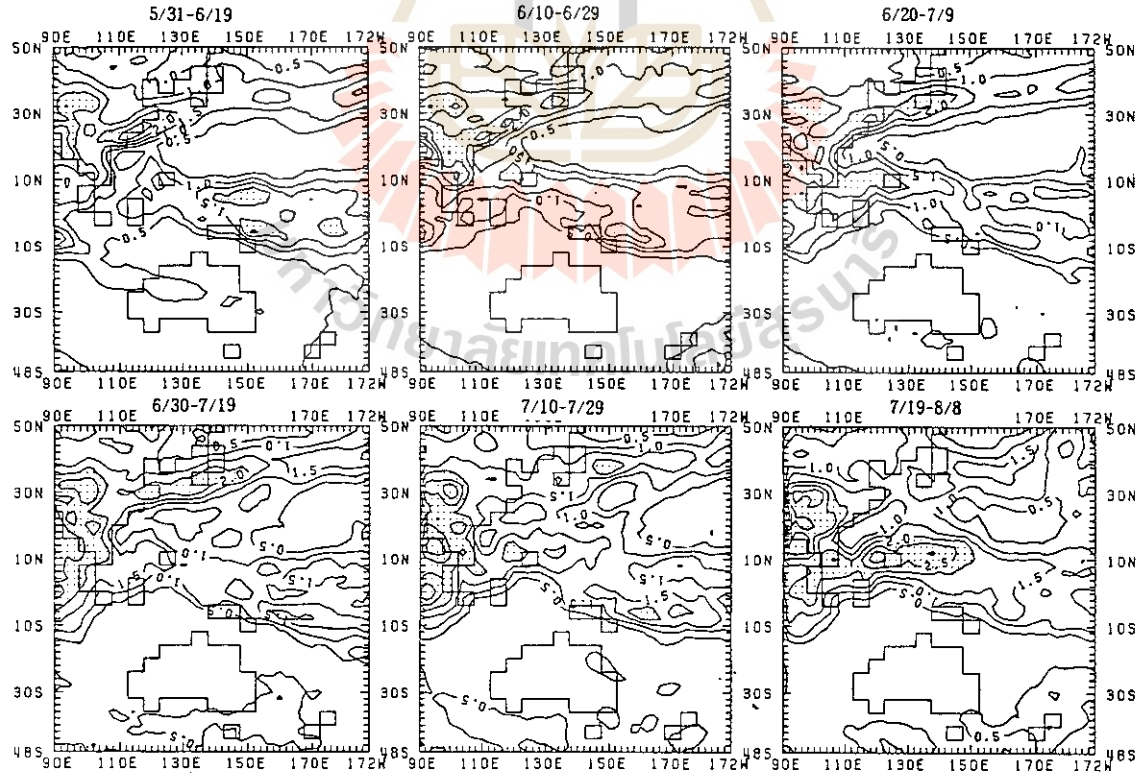

Figure 3. The spatial structure of the first extended empirical orthogonal function for the five-day mean high cloud amount in 1993.

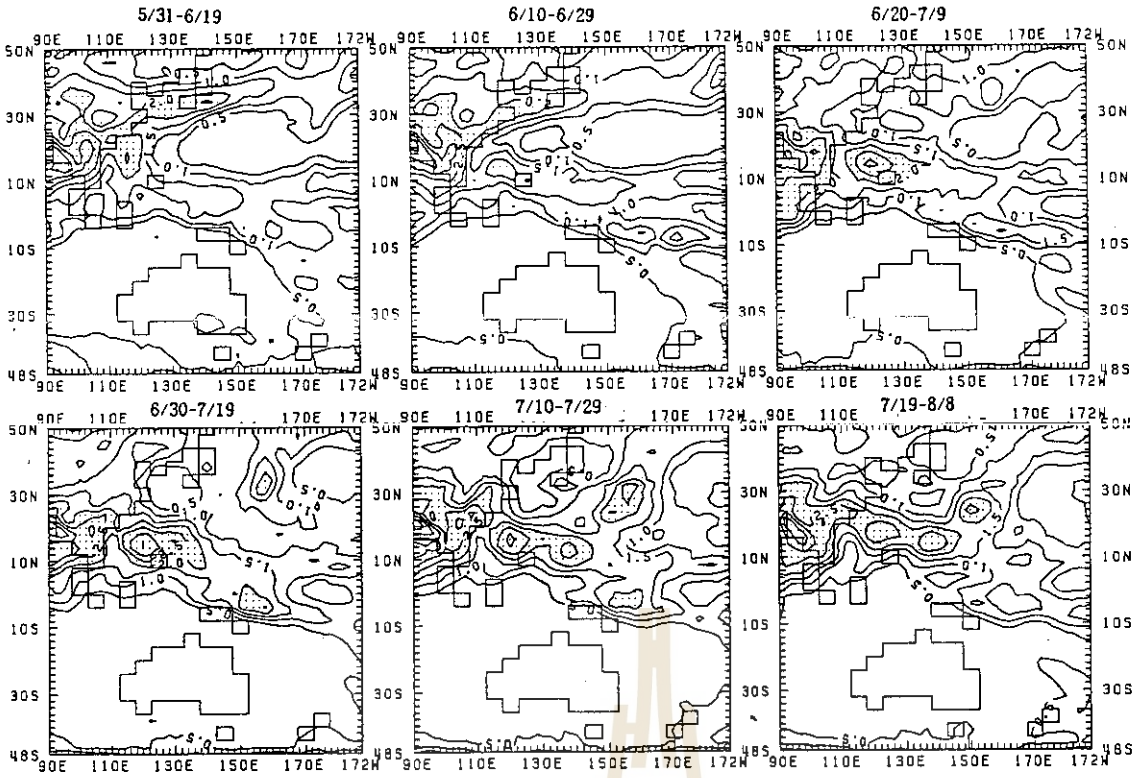

Figure 4. Same as in Figure 9 except for 1994.

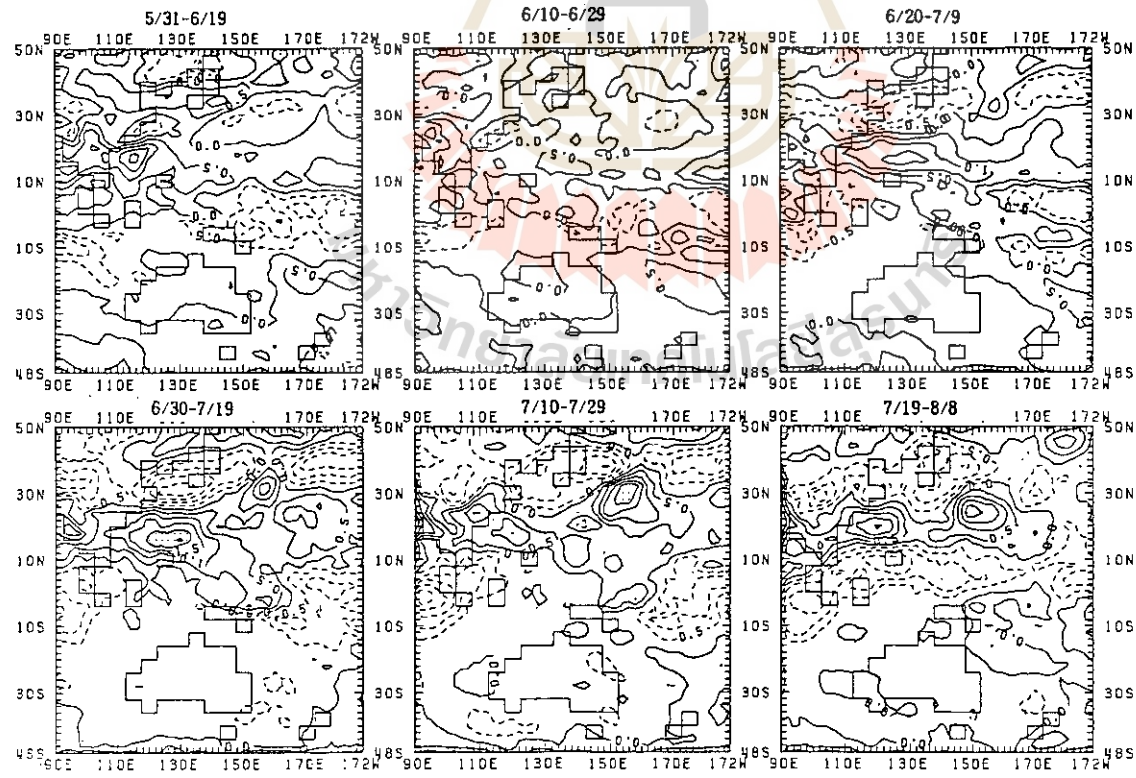

Figure 5. Plots of the spatial structure differences(1994-1993) of the first extended empirical orthogonal functions.

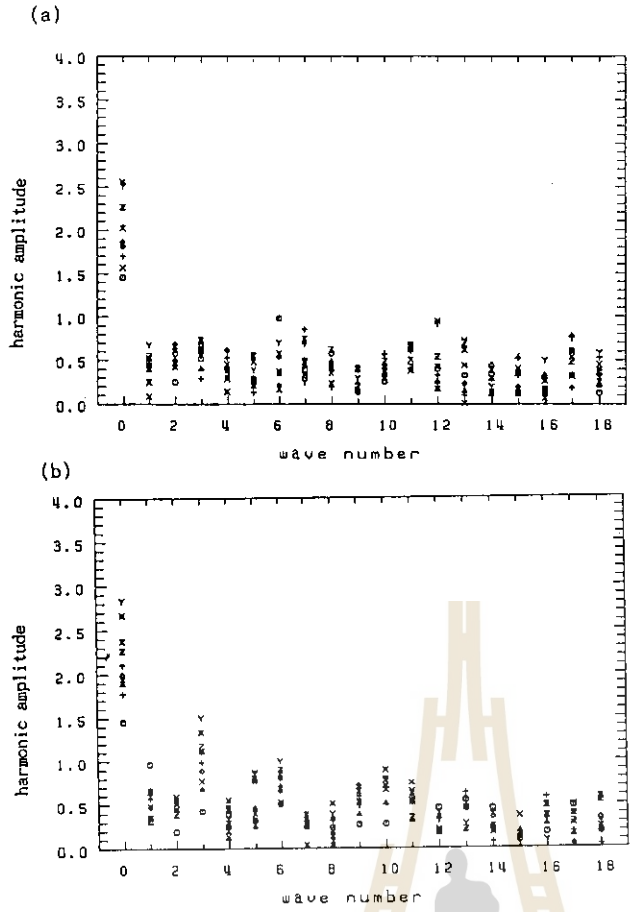

Figure 6. The plots of the power amplitude as a function of wave number obtained from Fourier harmonic analysis. The ten symbols represent the amplitude of different area separating by two degree longitude from 130E to 148E.

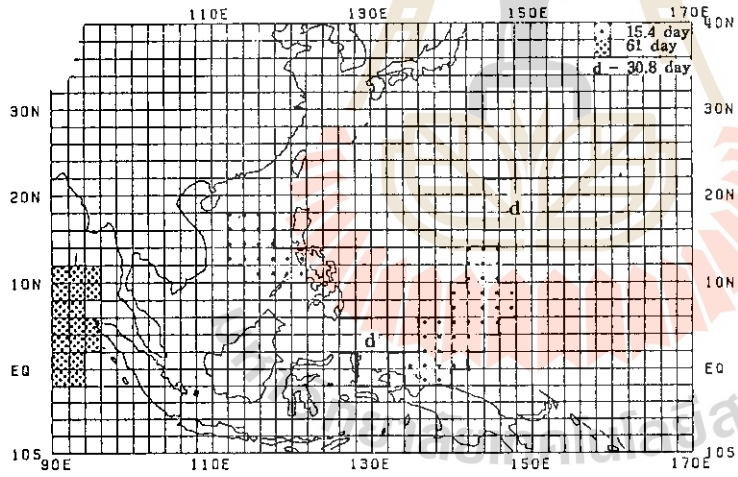

Figure 7(a) The prevailing modes of the intraseasonal oscillations over the equatorial and subtropical oceans for the period of 1 April - 2 October 1993.

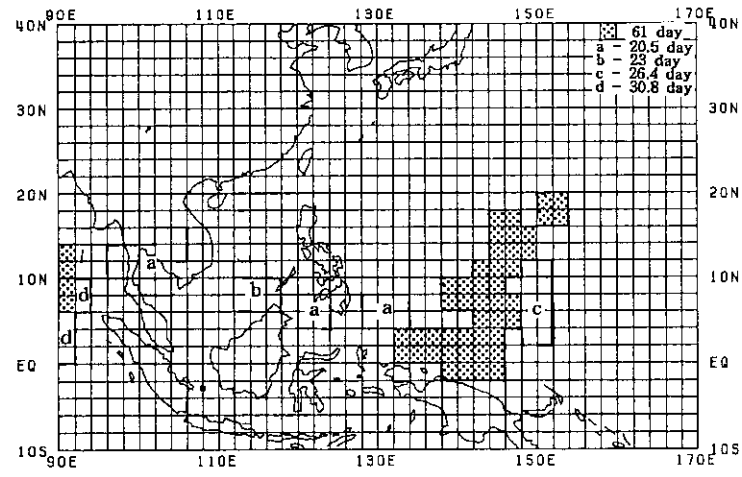

Figure 7(b) Same as in fig.13 except for 1994.

TECHNICAL SESSION G

LAND DEGRADATION

Diagnosis of Land Degradation in the Semi-Arid Area of Asia and Pacific Region Using Remote Sensing Data -JIRCAS's Case Study-

Satoshi UCHIDA

Japan International Research Center for Agricultural Sciences (JIRCAS)
1-2 Ohwashi, Tsukuba, Ibaraki 305, Japan
presently Visiting Scientist of International Crops Research Institute for the Semi-Arid Tropics (ICRISAT)
Patancheru 502324, Andhra Pradesh, India

Abstract

Land degradation which restricts the reproductivity of biomass appears at various areas in the world. In the semi-arid area the multiple types of land degradation happen to integrate to accelerate desertification. JIRCAS has implemented several research projects in collaboration with overseas institutes for the purpose of seeking sustainable land use system in the semi-arid area. This article describes the activities of case studies which have been adopted remote sensing data. This treats the physiographically specific topics in terms of land degradation appeared in the objective countries such as soil erosion in Pakistan and desertification of rangeland in Australia. The methodology to assess land degradation using remote sensing data should consist of the different stages of process, which are to identify the objective phenomenon from the image , to develop an appropriate indicator, to produce dataset and to evaluate the availability of land resources. This article also mentions about the interrelation between these stages.

1.Introduction

In recent years global environment issues have been argued in focus with quantitative measurement of objective parameters which may vary temporally and spatially. Once an estimated value is quantified and published, analyst who often utilize the secondary data may produce unreliable result. This problem is probable to occur in the estimation of global value accumulated with local data taken by nonstandardized methodology. Researchers expect to establish the methodology to assess global environment using remote sensing data as a quantitative information source. At this point it is necessary to discriminate the phenomenon whether it would be suitable as a target of remote sensing data analysis or not.

Land degradation, which is one of representative deteriorating factor of the environment, could be observed in the world wide. Land is a base to reproduce vegetation and its degradation corresponds to the restriction of vegetative activity by the change of growth conditions. Vegetative activity correlate with both agricultural productivity and environmental conservation. Land degradation tends to be an irreversible process, therefore in order to establish sustainable land use system it is important to make attempts to discover the area prone to land degradation as well as to monitor the progress of degradation .

Some typical phenomena of land degradation appear in the semi-arid area and they often cause the expansion of desert area. Desertification may be evaluated through vegetative activity on the surface but the difficulty comes from its temporal variation. Ground conditions which influence the growth of vegetation must be more suitable indicators of desertification. Representatively geomorphologic, chemical and physical degradation of soil can be identified to evaluate the state of desertification.

JIRCAS (Japan International Research Center for Agricultural Sciences) is one of the research institutes belonging to the Ministry of Agriculture, Forestry and Fisheries and has implemented collaborative research with overseas institutes. JIRCAS has introduced remote sensing and GIS techniques for the resource management of semi-arid areas. This article describes the outline of recent JIRCAS's activity adopting remote sensing data for the specific topics of semi-arid area. The author will try to explain the scheme of research projects in view of standardizing the methodology to assess environmental conditions.

2. Delineation of Land Degradation Using Remote Sensing Data

The quantification of spatial behavior at the specific moment is an initial step to monitor the progress of land degradation. The capability of wide spatial coverage of remote sensing data is its advantageous feature. On the contrary the limitation of spectral variety and spatial resolution of remote sensing data often makes it difficult to discriminate the different appearance of land degradation. It is needless to say that remote sensing data cannot apply to analyze any types of land degradation.

In the previous studies applications of remote sensing data to land degradation have been performed to delineate the state of soil erosion, soil salinization, water logging, foliage deterioration, etc. The experimental site of these examples spread over various parts of the world of which considerable percentages have treated cases in the semi-arid climatic conditions. The reason of this selection is supposed that the semi-arid area would be fragile against the environmental change in terms of its vegetative activity and land could be degraded in association with vegetation coverage over the land.

There are two types of soil erosion, one is wind erosion and the other is water erosion. Both of erosion types affect the geomorphologic feature of land as well as distribution of top soil. Remote sensing data can detect directly the geomorphologic feature if spatial resolution is small enough to discriminate the pattern of eroded topography. Another method to evaluate the strength of erodibility, which is a kind of indirect way, adopts an empirical parameter in correspondent with controlling factor by coverage of ground surface. Many examples have published to estimate C factor of USLE equation from vegetation index or other indices calculated from multispectral data of remote sensing.

The appearance of saline soil or water logging area could be interpreted from the remote sensing imagery. The problem of reproductivity of the same result by manual interpretation may become critical if quantitative analysis is necessary. The extraction of salt affected or water logging area requires the information not only spectral characteristics but its geographical location in association with the topography of objective area. It is significant to introduce GIS for the purpose of extracting and monitoring salt affected or water logging area in the digital based remote sensing data analysis.

The growth of vegetation is influenced by the factors of land management besides climatic and nutrient features of land. In case of agricultural land vegetation coverage varies with the cropping pattern therefore land degradation cannot be evaluated by only the change of vegetation. Apart from agricultural land and manmade land use, vegetation coverage may indicate the magnitude of land degradation. The rangeland in the semi-arid area is a good example to show the tendency of deteriorating vegetation associated with land degradation. The methodology to monitor vegetation coverage using remote sensing data has been developed and examined its applicability by number of researchers for these decades.

Table 1 summarizes the use of remote sensing data to delineate land degradation in the semi-arid area. This table suggests that remote sensing data would be evaluated as a useful information to monitor land degradation although the methodology of quantitative measurement has not been established. Studies on standardization of method of analysis are required primarily at this stage.

Table 1 Use of remote sensing data to delineate land degradation in the semi-arid area

Degradation Type	Delineated Feature	Methodology	Remark
Water Erosion	Gully (Topography) Coverage (Control Factor)	Interpretation, Texture Indices by multiple bands	Empirical factors would be included.
Wind Erosion	Sand move	Interpretation, Band calculation	Difficult to find position.
Soil Salinization	Soil color change	Interpretation, Band calculation	Difficult to be quantified.
Foliage Deterioration	Density (Biomass) Species change	Vegetation index etc. Classification	Seasonal change should be considered.

3.Case Studies Implemented by JIRCAS

JIRCAS has implemented collaborative research projects with overseas institutes since 25 years ago when the name of institute was Tropical Agricultural Research Center at the time. There are a number of on-going projects of which the target site is located in the semi-arid area and remote sensing technology is employed. Table 2 shows a list of projects in which the author has taken part for recent years. Every projects treat the problem in the semi-arid area and employ the remote sensing data as information sources to analyze regional characteristics. Summary of each project will be described in the following to the table.

Table 2 Projects adopting remote sensing data to land degradation study implemented by JIRCAS

Project Theme	Country	Collaborative Institute	Period
Analysis of soil erosion in rainfed agricultural land	Pakistan	National Agricultural Research Centre	1990-
Environmental changes associated with land use conversion in the semi-arid tropics	India	ICRISAT	1993-
Production of desertification dataset of rangeland	Australia	Centre for Arid Zone Research,CSIRO	1994-

(1) Analysis of soil erosion

The objective of this study is to delineate the topographic patterns appeared in the eroded area using remote sensing data and to analyze the relation between erodibility and ground surface conditions. Experimental site is the Pothwar plateau located in the northern part of Punjab province in Pakistan, where agricultural land is generally rainfed. In this area water erosion is a representative land degradation phenomenon due to the existence of erosible soil and high rainfall intensity in the rainy season. Land management which may affect the coverage of ground surface is another significant factor to extend the disaster prone area.

The procedure of analysis adopted in this study consists of two steps. One is to estimate erodibility of land by digital image processing of SPOT panchromatic mode data. The other is to examine the relation between erodibility and ground surface conditions estimated from multi-spectral information of LANDSAT-TM data.

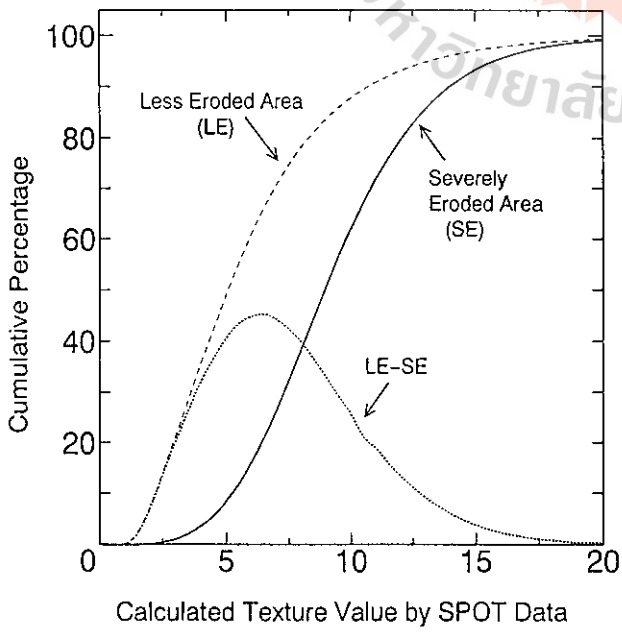

Fig.1 Erodibility estimation by SPOT data

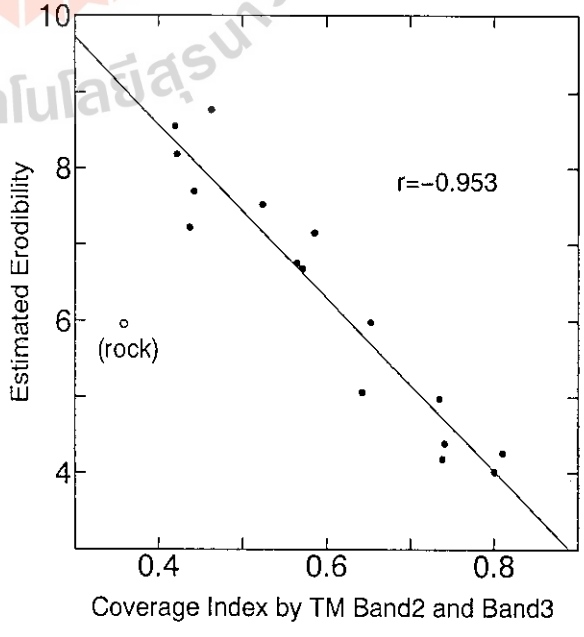

Fig.2 Relation between coverage and erodibility

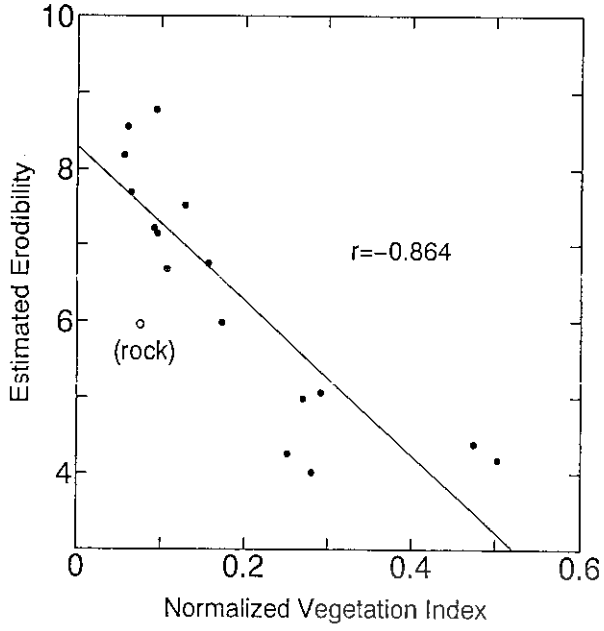

Fig.3 Relation between NDVI and erodibility

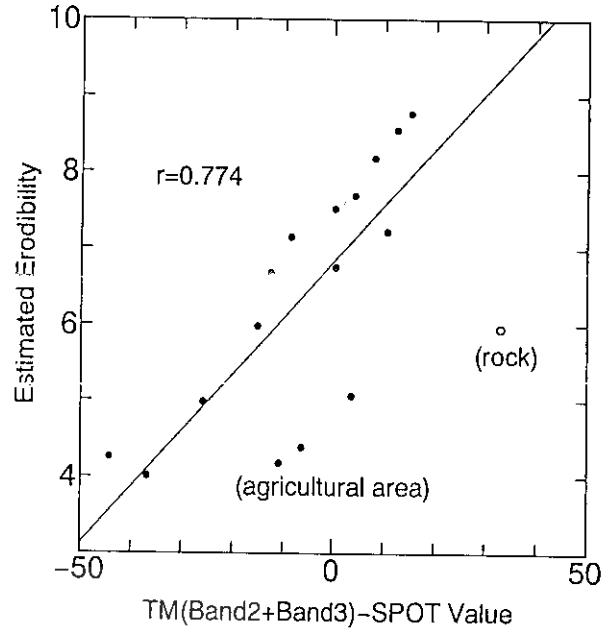

Fig.4 Relation between seasonal change and erodibility

Figure 1 shows the distribution of calculated erodibility from SPOT data in the severely and less eroded area which are manually interpreted from imagery. The method of estimating erodibility is that first the standard deviation of digital number within 3 x 3 window for high pass filtered image data is calculated and then 5 x 5 rank order filter is applied to represent the spatially extended feature. This result denotes that the method employed here could estimate the erodibility appeared in topographic feature by digital processing of remote sensing data only the improvement of method would be necessary. The discussions about spatial feature of experimental site have been described in the Proc. 15th ACRS last year (Uchida et al.(1994)).

Figure 2 to 4 show the relation between erodibility estimated by the method used in Figure 1 and ground surface characteristics, where dot represents averaged value for each unsupervised classification unit. From these figures Coverage Index calculated from band 2 and band 3 data of LANDSAT-TM, which is a modification of PD54 developed by Pickup et al.(1993), has stronger correlation compared with Normalized Vegetation Index. Another interesting feature is that seasonal difference between Rabi cropping season , represented by LANDSAT-TM taken on 9th February 1992, and hot dry season, represented by SPOT taken on 2nd April 1990, has a strong correlation with erodibility at naturally vegetated area excluding agricultural land. Although analysis has not been finished due to the limitation of available data and field survey, these results provide the direction of mapping and land management for the risk of soil erosion with spatial context.

(2) Environmental changes

This study has substantially started in this year and the author has stayed at ICRISAT since March 1995. ICRISAT is specialized its research activity to increase and stabilize the production of major six crops, which are sorghum, pearl millet, finger millet, pegeonpea, chickpea, groundnut in the semi-arid tropics. The main objective of this study is to evaluate the effect of land use conversion on physical, chemical and biological processes occurring in the production systems in the semi-arid tropics. In this study Indian remote sensing satellite (IRS) data would be employed as a major data source for depicting the ground surface conditions.

ICRISAT is located at the boundary of two major orders of soil appeared in the semi-arid part of India, which are Vertisol (black soil) and Alfisol (red soil). The fertility and capacity of water retention of these soils show different characteristics and the cropping patterns are generally different in association with these factors. These soils could be discriminated by manual interpretation of IRS imagery especially taken in hot and dry season. On the other hand it seems difficult to classify the cropping pattern accurately because a variety types of inter-cropping is commonly observed in this area.

Many Indian scientists have conducted the works to produce maps relating to land degradation using remote sensing data. This study aims at the development of the method to analyze land degradation process using remote sensing data in collaboration with scientists in the field of crop and soil sciences. The sustainability of land would be examined in association with the probability of occurrence of droughts, floods, etc. in the production systems. Project activity would be strengthened after equipment and research associate are settled at ICRISAT.

(3) Production of desertification dataset

This study is a part of one of research themes in the Global Research Network Systems (GRNS) funded by Science and Technology Agency (STA) of Japan. The title of research theme is 'Research on the production of fundamental dataset for the studies on earth science technology', which started in 1993. This theme consists of five working groups, which are hydrology, vegetation, desertification, ocean and base maps. The objective of the theme is to produce a standardized dataset applicable to environmental problems appeared on the earth.

Desertification dataset working group determined to implement the research in collaboration with Centre for Arid Zone Research, CSIRO in Australia. This institute has a long term experience on the management of rangeland, where cattle is extensively grazed, using remote sensing data. The representative land degradation of experimental site of this study is the deterioration of foliage induced by grazing and soil erosion. The rate of defoliation could have a positive correlation with the density of cattle. Grazing pattern of cattle at this area, where surrounding fence of each paddock control the moving range of animals, has been observed to show a function of distance from water supply point (e.g. Pickup and Chewings(1994)). Soil erosion is shallow but influential to vegetative activity because soil layer which provide the growing conditions of vegetation is generally thin at this area.

Table 3 shows the contents of desertification dataset which JIRCAS plans to produce. There are two types of data specification in terms of spatial resolution, one is low spatial resolution data to indicate the general physical conditions of the area and the other is higher spatial resolution data to indicate surface conditions. Desert Class may indicate generally the extent of desertification. In the arid and semi-arid area annual Normalized Vegetation Index (NDVI) of agricultural land would show the higher value than that of natural vegetaion area provided soil characteristics for vegetaion activity is similar. In order to evaluate the status of vegetation change year by yaer, remote sensing data taken at the moment of driest season would be selected. Sample dataset would cover the experimental site of CSIRO near Alice Springs in the central part of Australia.

Table 3 Contents of desertification dataset

Data Name	Methods	Spatial Resolution	Frequency
Desert Class	Aridity Index (P/PET) vs. Annual NDVI Soil Factor (physical characteristics)	30" x 30"	once
Topography	Elevation, Slope, Variance	3" x 3"	once
Grazing Intensity	Distance from Water Point	3" x 3"	once
Soil Stability Index	Soil Classification from Remote Sensing Data	3" x 3"	once
Coverage Index	Modified from PD54 (Pickup et al.(1993))	3" x 3"	annual (driest season)
Vegetation Change	Rate of Change of Vegetation Index	3" x 3"	annual (driest season)

4.Assessment of Land Degradation for Sustainable Land Use Systems

The ultimate objective of assessment of land degradation is to establish sustainable land use systems. The definition of sustainability is controversial problem because it is difficult to define the spatial and temporal ranges to be considered. From this situation the reliable information of ground surface conditions should be collected systematically using remote sensing data. This information becomes the base to discuss the sustainability of land use systems.

The methodology to assess land degradation using remote sensing data can be divided into several stages in general. First is a stage to identify the objective phenomenon from the image. If the phenomenon can be discriminated by interpretation, there is a possibility to develop an appropriate indicator by calculation of digital data. Next stage should be a process of standardization of method to calculate indicators as well as examination of its reliability. Dataset production is another important stage to recognize the regional characteristics of land degradation in comparison with other areas. The last stage is to evaluate the availability of land resources in other word the tolerance against environmental changes quantitatively.

Case studies introduced in the previous chapter have shown typical land degradation studies on selected experimental site. In some cases the methods to delineate the state of surface conditions are commonly adopted. For example a modified form of coverage index developed by CSIRO for monitoring the effect of grazing on vegetation coverage of rangeland has presented as an effective indicator to estimate erodibility of land in case of Pakistan. It seems necessary to examine the applicability of indicators, which have been developed by a number of researchers, to the various types of land degradation although most of them have not been analytically explained.

5.Conclusions

Land degradation is of significant environmental problem which could be observed at many areas in the world. Due to its variety of appearance, however, quantitatively reliable data about the extension of land degradation in regional scheme has not yet been obtained. Remote sensing data has been expected to provide quantitative information about land degradation, on the other hand it has limitation to measure the detailed characteristics of the ground surface. At this it is proposed that land degradation should be categorized into the groups of which their physiographical features could be delineated by remote sensing data. Standardization of method to obtain the appropriate indicators is significant process to discuss and compare the regional characteristics of land degradation with other areas. Although the case studies described in this article are examples to have initiated from separate background, their direction of research should point at the establishment of methodology for common use.

Acknowledgment

The author is grateful to the counterparts of collaborative research institutes, Dr.Shahid Ahmad, Dr.Rakhshan Roohi and their staffs at Water Resources Research Institute of National Agricultural Research Centre in Pakistan, Dr.K.K.Lee, Dr.S.M.Virmani and relevant staffs of Division of Soil&Agroclimatology and Agronomy at ICRISAT, and Dr.Geoff Pickup and his staff at Centre for Arid Zone Research of CSIRO, for their continuous cooperation to each project activity.

References

Pickup,G., V.H.Chewings and D.J.Nelson (1993): Estimating changes in vegetation cover over time in arid rangelands using Landsat MSS data, Remote Sens. Environ., 43, 243-263.

Pickup,G. and V.H.Chewings (1994): A grazing gradient approach to land degradation assessment in arid areas from remotely-sensed data, Int. J. Remote Sensing, 15, 597-617.

Uchida,S., R.Roohi and S.Ahmad (1994): Land degradation analysis of rainfed agricultural area in Pakistan using remote sensing data, Proc. 15th Asian Conf. Remore Sens., I, C-4, 1-5.

MAPPING OF SALT-AFFECTED SOILS USING REMOTE SENSING AND GEOGRAPHIC INFORMATION SYSTEMS: A CASE STUDY OF NAKHON RATCHASIMA, THAILAND[1]

Awadh k. sah, Apisit Eiumnoh, Shunji Murai and Preeda Parkpian
Space Technology Applications and Research Program, Asian Institute of Technology
GPO Box 2754, Bangkok 10501, Thailand

ABSTRACT

This paper is based on a research carried out to develop a methodology to classify the salt-affected soils using remote sensing and GIS. Taking salt crust as a criterion, Landsat TM with bands other than two and six was found effective, to a greater extent, in classifying the extremely and moderately saline area. Integration of GIS was found effective in classifying low and potential saline area as well as in correcting some of such area misclassified as extremely or moderately. The confirmation of resulted six salinity classes with field check, existing map and soil analysis proved it as reliable one. However, similar pattern of soil salinity was obtained from the study compared to the existing map of 1989 prepared from Landsat MSS at scale 1:250,000, the classification result was found to show more details. The study concluded that integration of GIS with digital image processing of TM was very effective for classifying and monitoring of saline soils.

1.0 INTRODUCTION

Salt-affected soils have been identified as one of the three main hurdles against crop production in northeast region of Thailand (Mitsuchi et al., 1986) where out of 3.61 million hectare of such soils in whole territory, as high as 2.58 million hectare, i.e. 17% of total regional area, is prevailing (Arunin, 1992). The widespread deforestation of past is considered as the main cause in bringing the salts from lower strata up to soil surface which despite of various control measures, has resulted in rapid expansion of salt-affected areas. Such the dynamic condition calls for up-to-date information regarding its extent and nature as pre-requisite for the sound management. Unfortunately, until present, this usually remains inadequate mainly due to lacking of efficient assessment method. However, Satellite Remote Sensing (SRS) with higher spatial resolution is now available for this purpose (Singh and Dwivedi, 1989) which in combination with Geographic information Systems (GIS) may yield more reliable result (Batlle-Sales and Abad-Franch, 1992). Under this context, the present study was carried out with the objectives (i) to develop a methodology for mapping the salt-affected soils using SRS and GIS , (ii) to assess the capability of GIS for comprehensive classification when interfaced with SRS data, and (iii) to interpret the salinity classes with respect to crop production.

2. 0 THE STUDY AREA

The study area, encompassing 469 square kilometers, lies between 14° 56' and 15° 12' North latitude and 101° 53' and 102° 08' East longitude in Nakhon Ratchasima province of northeast region of Thailand. Mean annual rainfall of the locality, as revealed from meteorological data for 34 years (1961-94), is 1060 mm out of which nearly 85% occurs within six months (May to October) while along with mean monthly maximum temperature between 29.8^0 to 37.0^0 , the mean annual evaporation is as high as 1873 mm. Lam Takong irrigation project covers 20.4% of the whole study area extending mainly in flood plain and basin. The altitude ranges from 170 to 210 m above mean sea level. 85.7% of whole study area is under cultivation while forest is covering only in 1% area. Paddy and cassava are the two major crops occupying the low and up land, respectively.

3.0 METHODOLOGY

An integrated approach of digital image processing of satellite data combined with GIS was carried out in this study.

3.1 Collection of Ancillary Data

Besides the above facts, two field surveys were conducted, the first mainly to observe the dominance and spatial relationship of salt crusts and the second to verify field and to collect soil samples. Following satellite data and source maps were used:

---

[1] Paper presented at the 16th Asian Conference on Remote Sensing, 20-24 November, 1995, Nokhon Ratchasima, Thailand.

1. Landsat-5 TM data of path/row 128-050, acquired on 10 January 1994.
2. Existing Maps:
   a) Topographic map (scale 1:50,000) of year 1969.
   b) Geology map (scale 1:250,000) of year 1976.
   c) Soil map (scale 1:100,000) of year 1978.
   d) Land use map (scale 1:250,000) of year 1987.
   e) Ground Water Quality and Well Yield map (1:100,000) of year 1988.
   f) Salinity map (scale 1:250,000) of year 1989.

3.2 Analysis of Satellite Data

Various steps involved in the analysis of satellite data are presented in Fig. 1. In brief, after geometric correction and linear contrast stretch, the image was visually interpreted in individual bands and various band combinations, and by applying filtration, Principal Component Analysis (PCA) and band ratioing. Supervised classification was employed with maximum likelihood, mahalanobis and minimum distance methods including the bands 1,3,4,5 and 7. Band six had poorer separation of features and band two was highly correlated with one. Unsupervised classification was also tried with sequential clustering including seven separable classes.

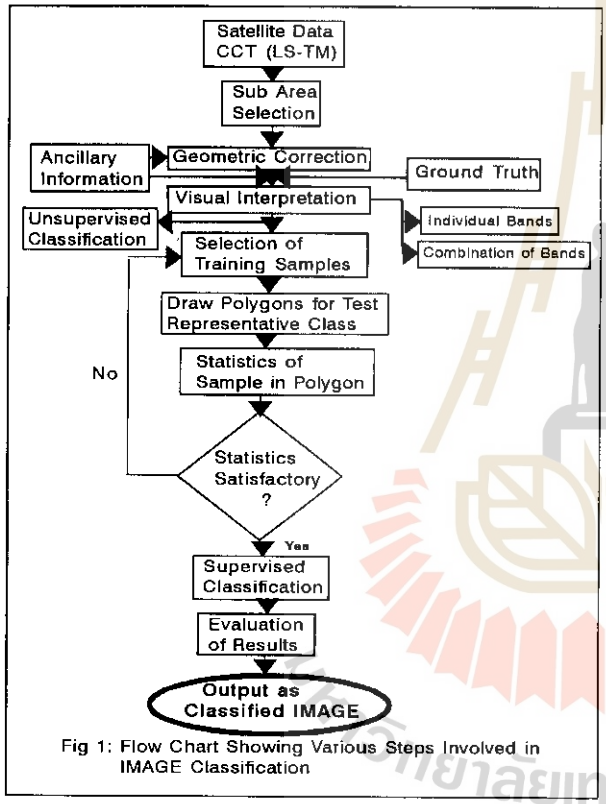

Fig 1: Flow Chart Showing Various Steps Involved in IMAGE Classification

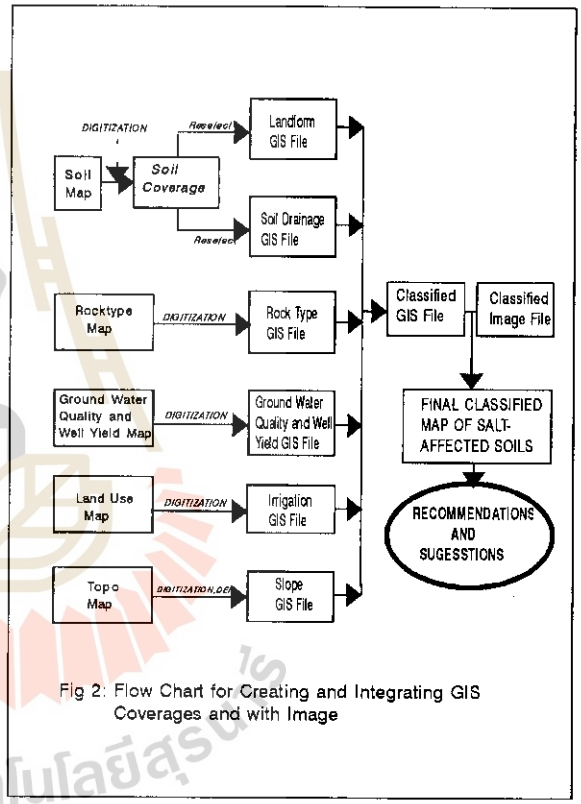

Fig 2: Flow Chart for Creating and Integrating GIS Coverages and with Image

3.3 Development of GIS Thematic Layers and Their Integration

3.3.1 Selection of Parameters

The ideology behind the selection and further classification of parameters (Table 2) were as follows:

(A) Landform: Among the five types of landform present in study area, virtually no salt crust is seen in high and middle terrace while it can be frequently seen in flood plain and basin. Lower terrace and peneplain remain somewhere in the middle.

(B) Ground Water Quality and Well Yield: Along with the quality of ground water, its extracted quantity also needs to be considered for salinity assessment. Hence, for overlaying purpose, the twelve classes of ground water quality and quantity so found in study area were grouped into four by considering the expected salt quantity (in term of kg/hr) that can come out under average condition along with same operation hour. The criteria set was <1.25, 1.25 to 6.00, 6.01 to 12.00 and >12.00 kg/hr for Good (W1), Medium (W2), Worse (W3), Worst (W4) , respectively (Table 1).

Table 1: Coverage and Grouping of Ground Water Quality and Well Yield Classes

Quantity/ Quality	< 2 m^3/hr		2-10 m^3/hr		10-20m^3/hr		>20 m^3/hr	
	% of area	Salt (kg/hr)	% of area	Salt (kg/hr)	% of area	Salt kg/hr)	% of Area	Salt (Kg/hr)
<750 mg TDS/l	0.80	0.37 (W1)	0.30	2.25 (W2)	0.40	5.12 (W2)	0.20	7.50 (W3)
750-1500 mg TDS/l	0.50	1.12 (W1)	0.60	6.75 (W3)	0.80	16.87 (W4)	1.20	22.50 (W4)
>1500 mg TDS/l	8.00	1.50 (W2)	42.10	9.00 (W3)	2.70	22.50 (W4)	2.40	30.00 (W4)

(C) Rock type: The Maha Sarakham Formation having salt layer, its area is considered as the most vulnerable to salinity while that of the Khok Kruat Formation area being free from such salts is considered as least vulnerable. Considering these two diversified Formations, however, it is difficult to assess about the vulnerability of Quaternary deposited areas where the soil parent materials are dependent upon the materials that are transported from the source place.

Table 4.2: Grouping of Parameters for GIS Analysis

Parameters	Attributes
- Landform	- High/Middle Terrace (L1), - Peneplain (L2), - Low Terrace (L3), - Flood Plain (L4), and - Basin (L5)
- Ground Water Quality & Well Yield	- Good (W1), - Medium (W2), - Worse (W3), and - Worst (W4)
- Rock Type	- Khok Kruat Formation (R1), - Quaternary deposits (R2), and - Maha Sarakham Formation(R3).
- Soil Drainage	- Well (D1), - Moderate (D2), and - Poor (D3).
- Irrigation	- Rainfed (IR1), and - Irrigated (IR2)
- Slope	- Slope > 2% (SL1), - Slope 1 to 2% (SL2), and - Slope 0 to 1% (SL3)

Table 4.3: Combination of Conditions for GIS Analysis and its Result.

S. N.	Soil Salinity Potential Classes	Combination of Conditions	Resulted Area (%)
1.	Non-saline (G1)	-L1+IR1+R1+W1	0.70
2.	Highland salt source area (G2)	-L1+IR1+R1+(W2/W3/W4) -L1+IR1+(R2/R3)	32.20
3.	Slight salinity potential (G3)	-L1+IR2 -W1+(L2/L3/L4/L5) -W2+(L2/L3)+R1 -W2+(L2/L3)+R2+SL1 -W2+(L2/L3)+R2+D1	2.00
4.	Moderate salinity potential (G4)	-W2+(L2/L3)+R2+(SL2/SL3) -W2+(L2/L3)+R2+(D2/D3) -W2+(L2/L3)+R3 -W2+(L4/L5) -W3+(L2/L3) -W3+(L4/L5)+(R1/R2)+SL1 -W3+(L4/L5)+(R1/R2)+(D1/D2) -W4+(L2/L3/L4/L5)+R1+SL1 -W4+(L2/L3/L4/L5)+R1+D1	29.20
5.	Extreme salinity potential (G5)	-W3+(L4/L5)+(R1/R2)+(SL2/SL3) -W3+(L4/L5)+(R1/R2)+D3 -W3+(L4/L5)+R3 -W4+(L2/L3/L4/L5)+R1+(SL2/SL3) -W4+(L2/L3/L4/L5)+R1+(D2/D3) -W4+(L2/L3/L4/L5)+(R2/R3)	31.20

D) Soil Drainage: Generally, poorer the soil drainage, greater the possibility of rise in the level of perched ground water especially in low-lying areas.

(E) Irrigated Area: Regular water supply to an area generally enhances the salinization by leaving the salts on soil surface and/or increasing the ground water table. This becomes more concerning factor if it contains more salt and/or ground water quality is worse.

(F) Slope: Generally, slope percent two or less has been reported as associated with the salinization and again one or less percent as the most serious one (Ratanavong, 1991).

3.3.2 Creation and Integration of GIS Layers

The digitized contour lines were further processed to create Digital Elevation Model (DEM) first which was used to derive slope GIS layer. Similarly, to create landform and drainage GIS layer, the digitized soil coverage was assigned with respective value. Rest of GIS files were obtained just by digitization (Fig. 2).

Integration of thematic layers was done using logical approach as employed by (Mongkolsawat and Thiragnoon, 1990). This involved the identification of saline areas where a specified combination of conditions occurred (Table 3). For the first two classes, main priority was given to landform type while for the rest classes, ground water quality and well yield was given highest consideration followed by landform and rock type. Area under L1, being considered as not affected by salinization themselves, were classified as G1 and G2 except the irrigated one. These were further separated by assigning R1 with W1 as G1 and rest as G2. Similarly, to separate G4 and G5, further base was taken from the slope and drainage conditions. Alluvial complex with all area as R2 and IR1 and majority as W3 and SL1, was classified as G4.

3.3.3 Integration of Classified GIS Coverage with Image

In brief, G1 and G2 classes having L1 type of landform were assigned the same class name. Rest of extremely as well as moderately saline areas so classified from image were put as such while that of slight saline area was further categorized into potential (S4) and slightly saline area (S3) (Table 5). The interpretation of salinity result with respect to crop production was based on the salt tolerance guidelines given by Mass (1984).

4.0 RESULTS AND DISCUSSIONS

4.1 Image Analysis

(A) Visual Interpretation: In contrast to others, band six showed darker tone for the area having >50% salt crust coverage which may be due to the discontinuity of pores/channels in soil that resulted into more moisture. Among the various band combinations, 5,3,1 (R, G, B) had clearest distinction of salt crust area followed by standard FCC (4,3,2) and 7,5,3. The other band combinations had similar color appearance to one of above combinations. For instance, the combinations 5,3,2; 7,3,2; 7,3,1 and 5,2,1 were similar to 5,3,1. Filtering, band ratioing and PCA were found no more helpful in this respect than as in above band combinations.

(B) Unsupervised Classification: Majority of the area (84.86%) so classified as nearly barren and vegetative, from this classification, were not interpretative from salinity point of view (Table 4).

Table 4: Result of Unsupervised Classification with all Bands (Sequential Clustering).

S.N.	Class Name	% Area
1.	Nearly barren area	54.13
2.	Vegetative area	30.73
3.	Extremely saline area	9.56
4.	Salt making area	0.03
5.	Shallow water bodies	0.26
6.	Deep water bodies	0.26
7.	Vegetation with water	5.03
	Total	100.00

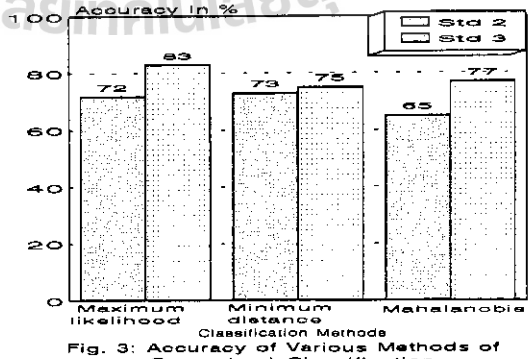

Fig. 3: Accuracy of Various Methods of Supervised Classification

(C) Supervised Classification: Four classes viz; Extremely saline (I1), Moderately saline (I2), Slightly saline (S3) and Deep water bodies could be separated from this classification. Various methods had similar coverage of each class, especially maximum likelihood and mahalanobis. However, the spatial distribution of the classes was different in these two methods, too. Also, the accuracy assessment showed that maximum likelihood with standard deviation three had the highest accuracy (Fig. 3). The result was more accurate at standard deviation three than two. It can be attributed to well

separability of different features even at three. The result of maximum likelihood at standard deviation three was used for further analysis.

4.2 Analysis of Classification Obtained by GIS

Altogether, moderately and extremely salinity potential comprised as high as in 60.4% of the total area. 32.2% area was found as high land, i.e. saline free but ability to make the other areas vulnerable (Table 3).

4.3 Analysis of Classification from Integration of Image With GIS

Among the six salinity classes, negligible area was found as non saline (Fig. 4) while extremely and moderately saline, altogether, were extending in nearly one third area, i.e. in dry season salt crust can be seen in such large portion. The accuracy assessment done with the sixty sites showed the over all mapping accuracy as 86.7%. Soil analysis result revealed that ECe was highly correlated with salinity classes while the correlation was lacking for pH (Table 5).

The interpretation of salinity classes revealed that potential and slightly saline area can be used for various crops but due attention be given against its further increment. Moderately saline area may be suited for the production of certain crops but no more in extremely saline area. Deep rooted crops or trees would be more suitable in highland salt source area.

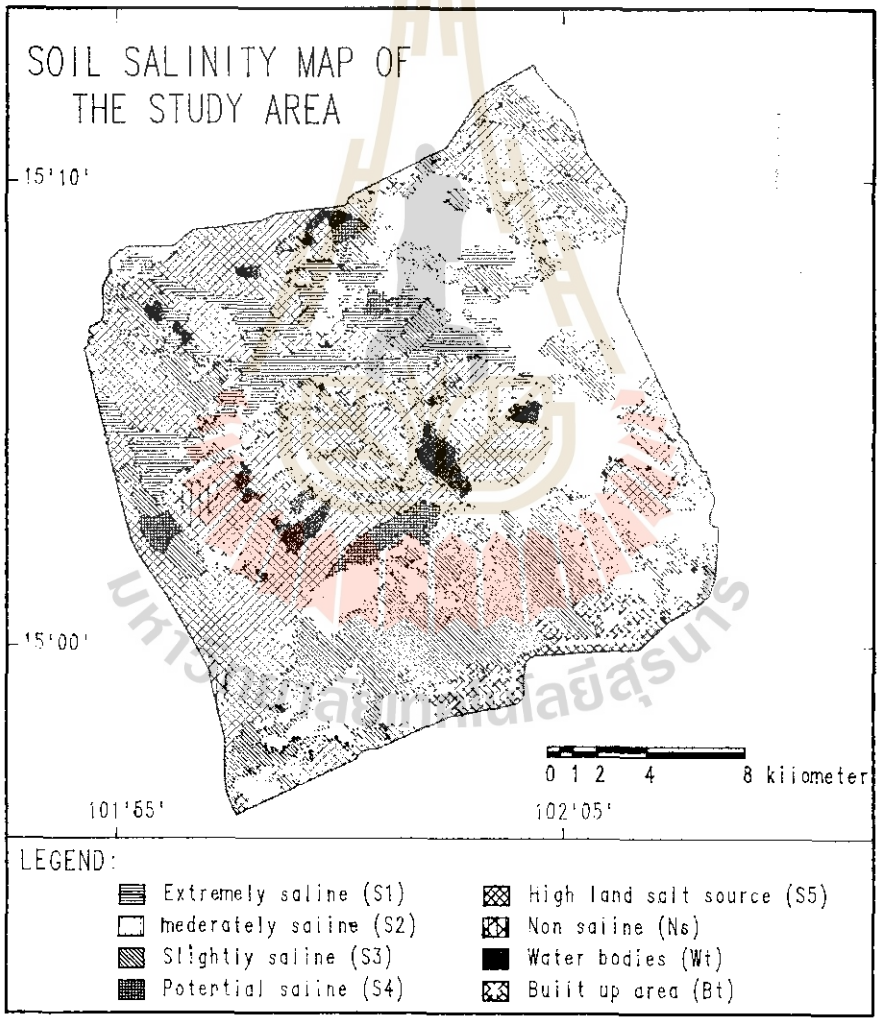

Fig. 4: Soil Salinity Map of the Study Area Resulted from Present Study with the Integration of Landsat-5 TM and GIS.

4.4 Comparison of Present Salinity Classification with Earlier One

The Comparison of present salinity classification with earlier one that classified in 1989 from Landsat MSS along with field survey, showed the difference in aerial extent of classes, however, various degrees of salinity had similar pattern of distribution. For instance, altogether the coverage salt crust area in both classification was nearly same, i.e. 34.1 and 34.8%, respectively (Table 5). Difference in class coverage from the two classification may be partly due to the use of different satellite data.

Table 5: Condition of Combinations and Results of the Present Classification and its Comparison with 1989 Classification.

Classification from Present Study					Classification from 1989	
Class Name	Condition of Combinations	ECe Range (dS/m)	pH Range (at 1:2.5)	% Area	Class Name	% Area
Extremely saline (S1) (>50% salt crusts)	I1 + (G3 or G4 or G5)	39.3-82.1	7.30-8.04	8.5	Very severely saline (>50% salt crusts)	15.5
Moderately saline (S2) (<50% salt crusts)	I2 + (G3 or G4 or G5)	5.0-13.8	5.73-7.49	26.3	Severely saline (10-50% salt crusts)	4.6
Slightly saline (S3)	I3 + (G4 or G5)	4.1-4.4	5.78-6.34	26.0	Moderately saline (1-10% salt crusts)	14.0
Potential saline (S4)	I3 + G3	1.2	6.25	1.5	Slightly saline	33.4
High land salt source (S5)	G2	0.5-2.8	5.04-6.85	32.2	Potential saline	29.5
Non saline (Ns)	G1	1.8	6.20	0.7	Non saline	1.0
Water bodies (Wt)	I4 or G6			2.1	Water bodies	2.0
Built up area (Bt)	G7			2.8		
Total area				100.0	Total area	100.0

5.0 CONCLUSIONS

This research showed that integration of Landsat TM with GIS can be used successfully in mapping saline soils. Supervised classification of TM is useful in separating extremely and moderately saline areas up to greater extent. GIS, is useful to classify lower and non saline areas and also to correct the area classified by TM.

REFERENCES

ARUNIN, S.(1992), Strategies for Utilizing Salt-affected Lands in Thailand, *Proc. of the int. Sympo. on Strategies for Utilizing Salt-affected Lands*, Bangkok, Thailand, Feb. 17-25, 1992, pp:259-268.

BATLLE-SALES, J. & ABAD-FRANCH, A.(1992), Survey and Mapping of Salt-affected Soils Using Remote Sensing and Geographical Information Systems, *Proc. of the int. Symp. on Strategies for Utilizing Salt-affected Lands*, Bangkok, Thailand , Feb. 17-25, 1992, pp:511-518.

MASS E.V.(1984), Salt Tolerance of Plants. *In: the Handbook of Plant Science in Agriculture*. B.R. Christie (ed). CRC Press, Boca, Raton, Florida.

MITSUCHI, M., WICHAIDIT, P. & JEUNGNIJNIRUND, S.(1986), Outline on Soils of the Northeast Plateau, Thailand, Their Characteristics and Constraints, Technical Paper No. 1, Agric. Dev. Res. Center in Northeast Thailand, Khon Kaen, pp:76.

MONGKOLSAWAT, C. & THIRANGOON, P.(1990), A Practical Application of Remote Sensing and GIS for Soil Salinity Potential Mapping in Korat Basin, Northeast Thailand, Tech. Rep. Series No. 8, Remote Sensing, Soil and Water Managt. in Northeast Thailand, Khonkaen.

RATANAVONG, N.(1991), Assessing Potential Salt-vulnerable Areas Through Terrain Analysis using Remote Sensing and GIS, The Vientiane Plain Case Study, M.Sc. Thesis, AIT, Bangkok, Thailand.

SINGH, A.N. & DWIVEDI, R.S.(1989), Delineation of Salt-affected Soils through Digital Analysis of Landsat MSS Data, *Int. J. Remote Sensing*, 10:83-92.

Monitoring Global Vegetation Degradation Using NOAA NDVI Data

Shiro Ochi(*), Shunji Murai(**)

* Utsunomiya University
350 Mine, Utsunomiya, 321, Japan
E-mail:ochi@cc.utsunomiya-u.ac.jp

** Asian Institute of Technology
GPO BOX 2754, Bangkok, 10501, Thailand
Fax:+66-2-524-5721

Abstract

Seasonal NDVI Data generated from NOAA AVHRR data with 8km spatial resolution show unique fluctuation patterns based on vegetation types and meteorological and topographic conditions. By analyzing the NDVI fluctuation patterns, vegetation degradation is estimated. In this study, Vegetation Degradation Index(VDI) which is proposed to figure the global vegetation degradation, is calculated using the NDVI data for a decade and several kinds of geographic information in global scale those are soil, elevation, climate, etc. VDI is applied to assess the global land degradation which is difficult to be monitored directly with only remotely sensed data.

1. Introduction

The importance for assessment of land-degradation and desertification are pointed out in Agenda-21, however, the methodology by means of Remote Sensing technology with GIS is not established . Some studies about drought and desertification in Africa using NOAA AVHRR, and the results are that long-term observation for several decades is required for the assessment of desertification and land degradation in global and continental scale. (Justice, et al, 1985, Tucker, et al, 1986). So the vegetation degradation instead of land degradation is assessed in this study, because it is more possible to assess by remotely sensed data, and it is considered to be very close relation with land degradation and desertification.

Two approach can be considered for the assessment of vegetation degradation. One is to monitor in global scale, and the other is in local scale. For the global scale, NOAA data is suitable for analysis. GVI which is 10 minutes spatial resolution(approximately 16km pixel size) NDVI data, and 8km NDVI data are available. GAC data which is 4km pixel size is going to be available in a few year. And 1km land cover monitoring project and Landsat Pathfinder Project are now going on. By using these data, the tendency of vegetation degradation can be found because these data are available for a few decades spans. In local scale, it would be impossible to find the process of land degradation and desertification by using SPOT and/or LANDSAT-TM data because such a long term observation had not been made by these sensors. However, the high spatial resolution data can show the current status of the land degradation and desertification.

In this study, long term observation to find the tendency of land degradation in global scale by using NOAA

NDVI data. The objectives of this study are:

1) To understand the characteristics of NOAA monthly data those are in scale of approximately 16km using GVI and 8km NDVI, and

2) To develop the methodology to assess the vegetation degradation in global scale.

2. Data

Data used in this study were extracted from NOAA Global View Dataset, those are;

1. Monthly GVI data, from April 1985 to December, 1988(45 months)
2. Leemans and Cramer IIASA Climate data(30 minutes pixel resolution)
   - 2.1 Average Monthly Air Temperature
   - 2.2 Average Monthly Precipitation
3. Baily Ecoregions of Continents(10 minutes pixel resolution)
4. Monthly NOAA NDVI data (8km pixel resolution)

And NOAA NDVI data with 8km spatial resolution was used.

In order to use GVI data for monitoring vegetation degradation, the quality of the GVI should be examined. Figure-1 shows the mean value of total of GVI and the number of pixels which are not zero value in the images. This means that the GVI is not standardized in the period, and it looks to be brighter year by year. However the procedure to generate the data is not clarified in our site.

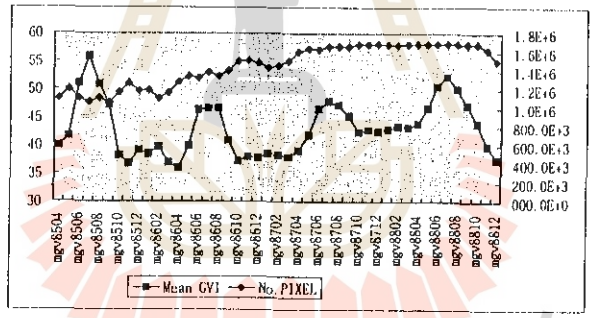

Figure-1. Mean GVI

3. Methodology

It is very hard to understand the vegetation degradation from the Figure-1. In this study, the GVI characteristics are drawn by overlaying with the above mentioned eco-regions map. By making fluctuation pattern of mean GVI for each eco-regions category, the vegetation growing and declining patterns can be found.

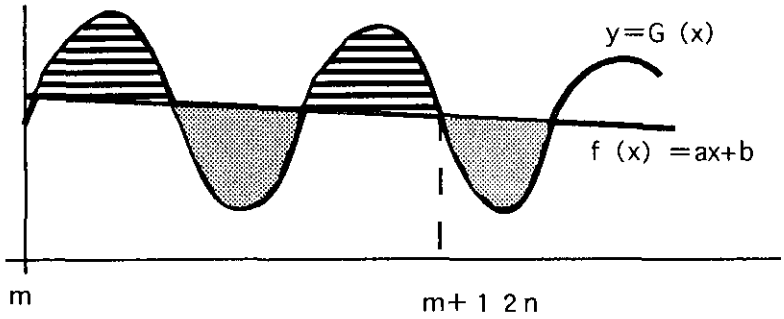

$$\int_{m}^{m+12} (G(x) - f(x)dx = 0 \cdots\cdots (1)$$

Figure - 2

After making the vegetation fluctuation pattern for each category, a vegetation degradation index is defined. In this study the index is proposed to indicated the vegetation degradation tendency. In the Figure-2, the line is define to fit the formula (1). The vegetation degradation index is define as "a" described in f(x).

4. Results

Figure-3 shows the vegetation fluctuation patterns for some ecoregion categories. The tendency of GVI dynamics can be easily known from the graphs.

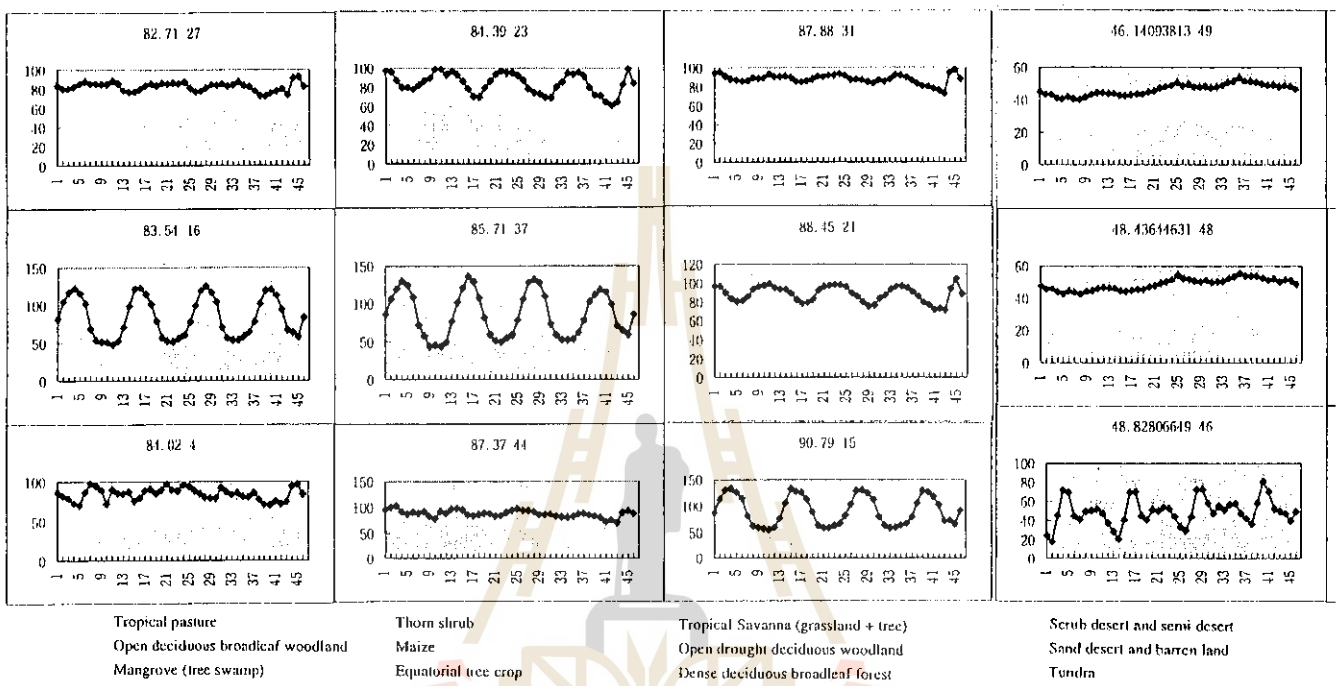

Figure-3. GVI Fluctuation Patterns by eco-regions categories

Table-1 shows the calculated vegetation degradation index. Minus value of the index means that the tendency of vegetation activity is declining. So the less the vegetation degradation index shows, the more the vegetation degradation is proceeding. Generally, the categories those average of GVI are low have the tendency to increase the vegetation activities, and the categories those average of GVI are high have that to decline the vegetation activities.

Table-1 Vegetation Degradation Index(VDI) and categories

VDI	Categories	VDI	Categories
0.33	Ice	-0.18	Urban
0.22	Semi arid rough grazing	-0.20	Tropical savanna
0.22	Sand desert and barren land	-0.21	Open drought deciduous woodland
0.21	Tundra	-0.25	Dense drought deciduous forest
0.21	Scrub desert and semi desert	-0.31	Thorn shrub
0.21	Semi desert+scattered trees	-0.34	Equatorial tree crop
0.20	Irrigated cropland	-0.37	Tea
0.20	Dwarf shrub	-0.42	Coffee
0.16	Vineyard	-0.44	Open tropical woodland
0.12	Temperate rough grazing	-0.44	Equatorial rain forest
.....	.....	-0.55	Dense evergreen broadleaf forest

Figure-4 shows the global map of the vegetation degradation index. Large area are affected by degradation in South America, especially the central Amazon, and the LaPlata River basin, middle Africa, and South East Asia. It looks strange that the low vegetation degradation index area can be seen in Japan. The output is considered to be reasonable in the tropical regions.

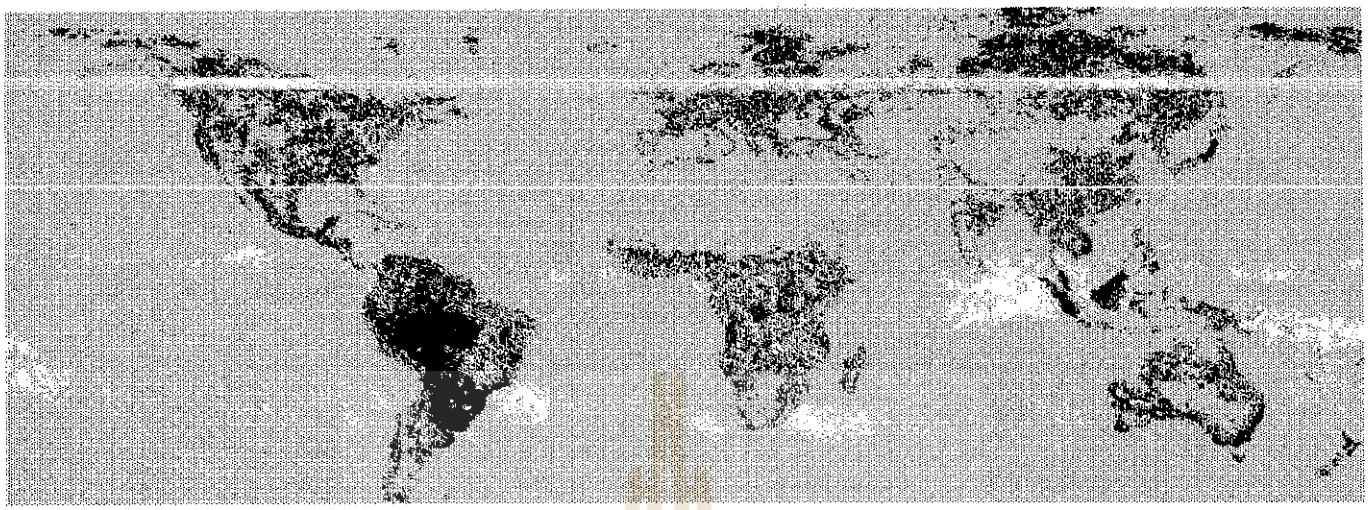

Figure-4. Vegetation Degradation Index Map by eco-regions categories

5. Conclusion and Discussion

GVI fluctuation patterns could be recognized by overlaying the long-term NOAA NDVI data and eco-regions map. By using the pattern graph, a vegetation degradation index was proposed which is showing the trend of vegetation degradation in global scale. However, the land degradation as well as vegetation degradation are considered to happen with area of several hectares to several square kilometers, depending on the types of degradation. So the s[spatial resolution is expected to be improved.

The index is showing reasonable output about the vegetation degradation in the tropical area where the mean GVI is rather high, however, some part of temperate zone such as Japan is recognized as the area where the degradation is proceeding. To correct such error, statistical modification to the original GVI is recommended to be made.

References

Justice, C.O., Townshend,J.R.D., Holden,B.N. and Tucker,C.J., Analysis of phonology of global vegetation using meteorological satellite data, INT.J. Remote Sensing, 1985, vol6, No8, 1271-1318

Tucker,C.J.,Maximum Normalized Difference Vegetation Index Images for sub-Sahara Africa for 1983-1985, INT.J. Remote Sensing, 1986, vol.7, No.11, 1383-1384

A KNOWLEDGE-BASED APPROACH FOR LAND EVALUATION USING RS AND GIS TECHNIQUES

D.Amarsaikhan, M.Ganzorig

Informatics & RS Centre, Mongolian Academy of Sciences
av.Enkhtaivan-54B, Ulaanbaatar-51, Mongolia

ABSTRACT

Application of a knowledge-based approach in the earth sciences is of great interest nowadays. The main aim of the research was to build a prototype geo expert system (GES) which can be used in decision making on the basis of the knowledge-base gathered from RS and GIS experts within GIS environment. For this purpose, land evaluation for wheat suitability was performed. In the selected area, the basic object consists of the surface elements characterized by attributes some of which are unknown. They were determined by the use of RS and GIS techniques cooperating with the experts from this field.

1. INTRODUCTION

Land evaluation is a method applied to the assessment of land suitability for a specific use. Land evaluation is itself knowledge-based and requires an extensive knowledge and different conditions to be fulfilled. This can be done automatically by the use ALES, LECS and GIS systems. At present, the use of knowledge-based (expert) systems in the geo-related sciences is not a new phenomenon. Different types of these systems have been and are being developed depending upon the structure of knowledge representation. Knowledge can be represented in the forms of semantic networks, object-attribute-value (O-A-V) triplets, frames, decision trees, production rules, etc. The characteristics of these techniques are discussed by Amarsaikhan (1994). At present, in the field of geoinformatics the widely used structures of knowledge representation are the frame-based and rule-based types. Our aim in this study is to use a knowledge engineering approach for land suitability analysis. For this purpose, land evaluation for wheat suitability was performed. The crop requirements were conditionally defined by the use of knowledge acquisition techniques.

2. THE STUDY AREA

As a test site was selected an area situated in the central part of the Orkhon-Selenge basin, Mongolia. The area is included into the mountain-forest-steppe zone and its landscape is divided into 5 zones within which the agricultural landuse is distributed (Ganzorig et al. 1995). The area has different types of relief and soil and vegetation cover changes according to the relief morphology. The relief and weather conditions in this area are very suitable for agriculture. The selected area is located on the south-facing low slope and has zonal dark chestnut soil. The main cultivated plants are wheat and luzern.

3. DATA COLLECTION AND KNOWLEDGE ACQUISITION

For the land evaluation the following materials were available:

- SPOT XS image of May 1988;
- Soil map, scale 1:50, 000;
- Topographic map, 1:50, 000;
- ground truth data.

Knowledge acquisition is the gathering of the facts and the relationships between them from any available sources. In this study we used such knowledge acquisition techniques, like the authors' own knowledge about the study area, literature review, interviews with experts in this field, ancillary datasets stored within a GIS, and RS and GIS processing due to which some new facts were generated.

4. RESEARCH PROBLEMS AND METHODS

4.1. In the selected area the basic object (landunit(LU)) consists of surface elements characterized by attributes:
LU(#, name, depth, ph, stony, rockiness, erosion class, slope, texture, moisture).
So there is a model for land evaluation and we conditionally assumed that some important values(slope and moisture) are unknown. They will be determined using RS and GIS techniques cooperating with experts from this field. To reach the goal in the study, the following basic problems should be considered:

- How to select appropriate algorithms from a subroutine library of RS/GIS software (ILWIS) ?

- How to choose parameters of the selected algorithms for optimal land evaluation using RS and GIS data?

- How much does the selection of procedures and parameters depend on context ?

4.2. In the problem solution, the unknown values will be determined in the following way:

Slope will be calculated using contour map of the area.
Moisture will be determined by statistical pattern recognition. In this case, by maximum likelihood decision rule using prior probability which will be defined from the ancillary data by experts in geoscience whose knowledge is important for the best training sample selection.
In the Hypotheses domain 4 hypotheses will be proposed (S1,S2,S3,S4 which are highly suitable, marginally suitable, moderately suitable and not suitable, respectively).

5. SYSTEM DESIGN AND IMPLEMENTATION

Based on the concepts of a KBS and a GIS a prototype GES has been

developed. The program was written in C language and linked to the ILWIS GIS software. The structure of the system is shown in Figure 1. GIS contains a specific view of a certain part of the real world which means it should contain a database and the analysis tools to be used in a given problem solution. The development of the database was done by digitizing soil and topographic maps and into which satellite image was registered.

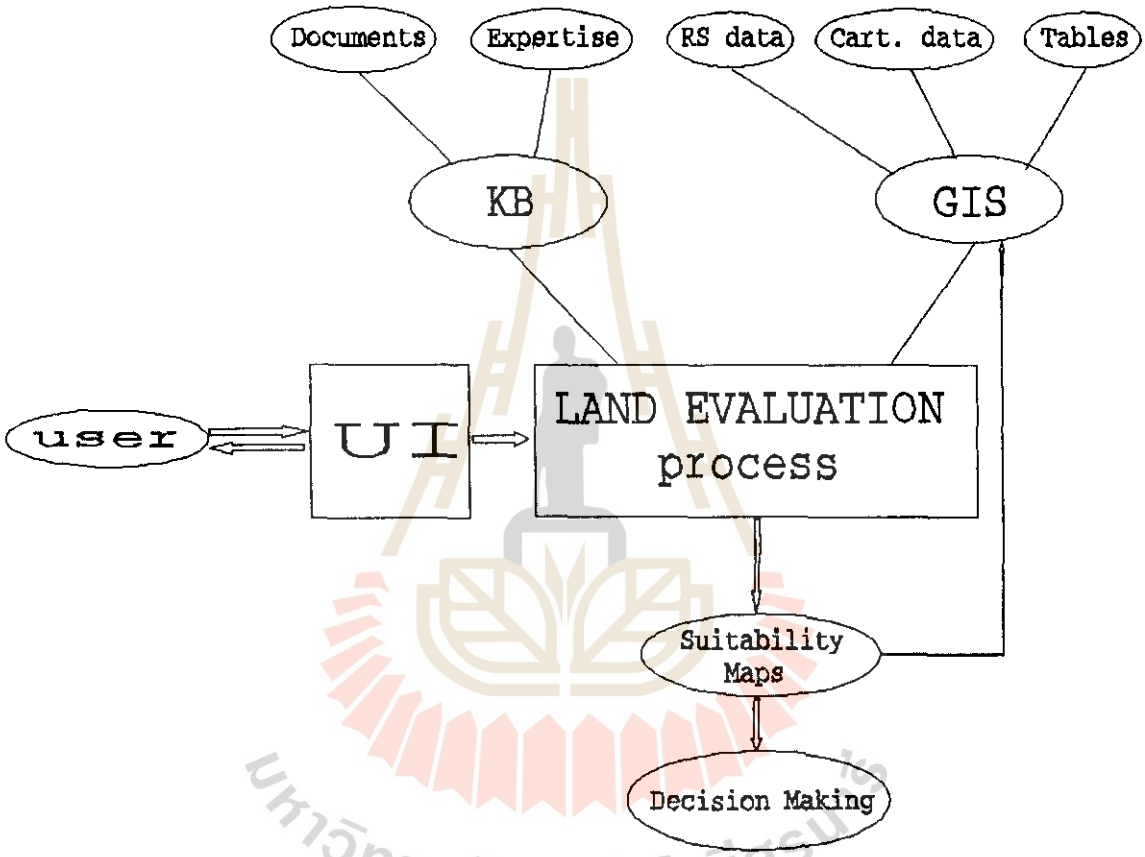

Fig.1. General Structure of the GES

In the image haze correction and enhancement techniques were applied. For the development of the GES simple frames have been used for the questions' display and the knowledge base was represented using "IF conditions THEN conclusion" statements. It is possible to manipulate all necessary procedures of the GIS from within the GES. All attribute values have been conditionally collected. Knowledge on the study area has been first represented as a O-A-V triplet and then normalized using an inference tree. From the normalized tree the rules to be used for the hypotheses evaluation were hierarchically extracted. Slope and moisture information were defined by the use of the above mentioned techniques (see section 4.2) and the related attribute values were exported to the O-A-V triplet before the normalization. During the slope and moisture determination in RS and GIS procedures the

appropriate parameters have been automatically suggested according to the context of the area.

For the hypotheses evaluation forward chaining principle has been used and the procedure is described as follows:

```
IF
depth > 40      AND
ph => 6         AND
ph <= 7         AND
texture = 6     AND
slope = 1       AND
moisture = 2
THEN Suit1.
```

The output is the map indicating the land suitability for wheat planting (Figure 2).

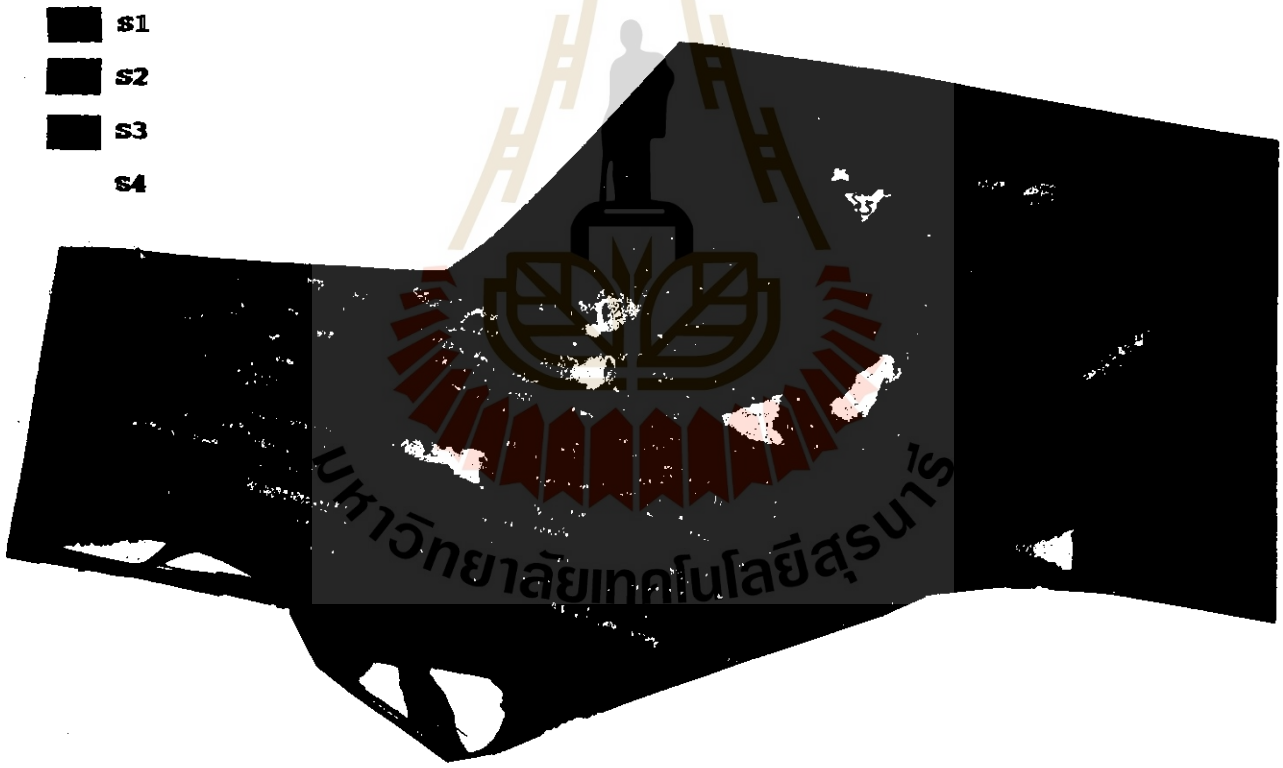

Fig.2. Suitability Map for Wheat

6. CONCLUSIONS

The research was carried out to test the role an expert system approach in geo related processing in case of missing some facts. As seen from the analysis, knowledge of the accuracy of the

information required for the decision making is very important. The developed system is an early prototype and has many limitations. Also forward chaining search has demonstrated its weakness. It stops when missing some facts. In this case, it is better to use backward chaining in the matching of the rules and forward chaining in data processing.

REFERENCES

1. Amarsaikhan, D., Gorte, B., 1992, Knowledge-based Approach to Update Landuse Layer of an Operational GIS, Proceedings of ACRS, Ulaanbaatar, Mongolia.

2. Amarsaikhan, D., 1994, Fundamentals of KBS and Artificial Intelligence Approach in RS and GIS, Journal Informatics, 82-93, Ulaanbaatar, Mongolia.

3. Ganzorig, M., Adyasuren, Ts., 1995, Application of RS and GIS for Ecosystem Monitoring and Management, Paper presented at the International Seminar on Space Informatics, Ulaanbaatar, Mongolia.

4. Jun Chen, Peng Gong, Newkirk, R.T., and Davidson, G., 1991, A Knowledge Based GIS for Zoning, Proceedings of European Conference on GIS.

5. Miller, D., and Morris, J., 1992, An ES and GIS Approach to Predicting Changes in the Upland Vegetation of Scotland, European Conference on GIS, 11-19.

6. Matsuyama, T., 1987, Knowledge-based Aerial Image Understanding Systems and Expert Systems for Image Processing. I.E.E.E. Transactions on Geoscience and Remote Sensing, 25, 317-328.

POSTER SESSION P

FOREST / VEGETATION MAPPING

National-Wide Environmental Unit Classification Using Remote Sensing and GIS - A Case Study in Zambia

Ryota Nagasawa Kazushi Endo
Yoshinori Takahashi Yukiko Kojima

PASCO International Inc.
3-7-8 Kamiuma, Setagaya-ku
Tokyo, 154, Japan
Tel : 81-3-3413-9321 Fax : 81-3-3413-9805
E-mail : 34153274@people.or.jp

Abstract

For the purpose of structurally understanding the regional ecosystems, natural environmental factors, consist of geomorphology, geology, land cover, elevation, annual precipitation and evapotranspiration, were databased and combined so as to divide the national area into environmental units or zone. Quantification theory III is applied in multivariate analysis, in which qualitative data (categorical data) relating to each environmental factor, because it was proved to be effective in graphically expressing and categorizing the samples based on the patterns of reaction of sample data categories. Mesh (grid) data, which are used for multivariate analysis, on a size of 1 km (totally numbers 7,522) were prepared through vector / raster conversion of the established database. As a result of analysis, the study area, the Republic of Zambia, can be divided into 10 environmental units reflecting the mutual interrelations between 6 environmental factors . The result almost totally matches with existing ecological viewpoints and can be said with great confidence to be proper and correct.

1. Introduction

It wasn't until the late 1980s that the world sat up and started to show concern towards global environmental issues. Problems such as global warming, destruction of the ozone layer, the depletion of forests and desertification caused by acid rain each differ in their effects, ranges and features, however, the solution to these problems can be said to be largely dependent on the actions of every individual human being and the degree of environmental management on the local and regional levels. When people come to plan and implement regional development projects in the future, they will have to pay attention to the global environment and give ample consideration to environmental plans aimed at the preservation and revitalization of regional ecosystems.

Regional environments are composed of single ecosystem that is formed from the delicate relationship of a variety of environmental factors such as topography, geology, soil, climate and flora and fauna. This means that it is necessary to spatially unify environmental factors in order to be able to understand the regional ecosystem. This report aims to give an introduction to methods for obtaining a structural understanding of regional ecosystems, seen from the regional environmental viewpoint, through the use of remote sensing and GIS technology.

2. Study Area

The whole of the Republic of Zambia, located in south-central Africa and covering an area of 752, 612㎢, is the area of study. Most of the national land area of this country is situated on geographically the Zambezi River and its tributaries, there are steep fault

escarpments and tectonic valleys that result form the tectonic structure of the rift valley.

Zambia is located within the tropical zone, however, the high altitude ensures that the climate is comparatively cool throughout the year. The vegetation land cover in Zambia is broadly classified as savanna, but within this classification, some district differences are identified due to the type of soil, gradient, altitude and climate.

3. Methodology

The methodology used here consists mainly of regional area division methods that utilize multivariate analysis. As statistical means form the basis, an overlay-like spatial analysis model enables, not only elimination of the arbitrariness (subjectiveness) that often occurs in the stage of environmental factor unification, it also allows a quantitative understanding of factor cause and effect interrelationships to be gained in those cases where numerous environmental factors exist. In this study, natural environmental factors (topography, geology, land cover information, etc.) were combined to divide the study area into environmental units or zones, and an attempt was made to gain a structural understanding of the mutual cause and effect relationships of environmental factors. Quantification III theory is utilized in multivariate analysis, in which qualitative data (categorical data) relating to Geomorphology, geology and land utilization, etc. is used.

Quantification III methodology involves the quantification of both samples and categories based on the patterns of reaction of sample data categories, and it is intended to graphically express and categorize those samples and categories. This method was originally proposed by Dr. Hayashi in 1983 and proves useful in classifying and finding out about samples and categories. In this study, the six types of map data (qualitative data) of elevation, geomorphology, geology, land cover, annual precipitation and evapotranspiration were used in carrying out regional area division in terms of environment, in order to gain an understanding of environmental units. Fig.-1 illustrates the analysis flow formed by this qualitative data.

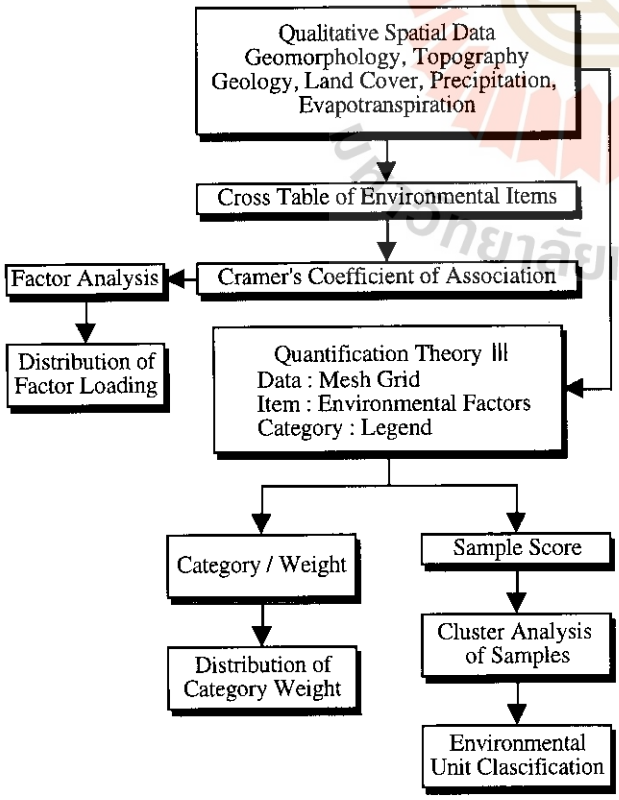

Fig.-1 Analysis Flow Chart

4. Spatial Data Preparation

In developing countries such as Zambia, it is often difficult to obtain latest national land information (geomorphology, geology, land cover, etc.) on a comprehensive scale and with a unified degree of accuracy. In the case of this study, however, remote sensing data (LANDSAT TM 41 scenes), covering the whole territory of Zambia, were obtained, and those original images were processed and interpreted in order to prepare geomorphological, geological classification and land cover maps on a scale of 1:500,000. As a result, vector based data base were established using GIS. Moreover, existing data on elevation, precipitation and evapotranspiration were also digitized to eventually construct six types of thematic map data bases (see Fig. 2).

Mesh (grid) data ,which are used for multivariate analysis, on a size of 1 km were generated through the vector / raster conversion of the thematic maps. The resulting sample mesh data numbers 7.522 units in all and consists of the aforementioned six environmental factors (items). The six items of elevation, geology, land cover, annual precipitation and evapotranspiration are each divided into 7-9 separate categories. The items, their categories and the numbers of samples are listed on Table-1.

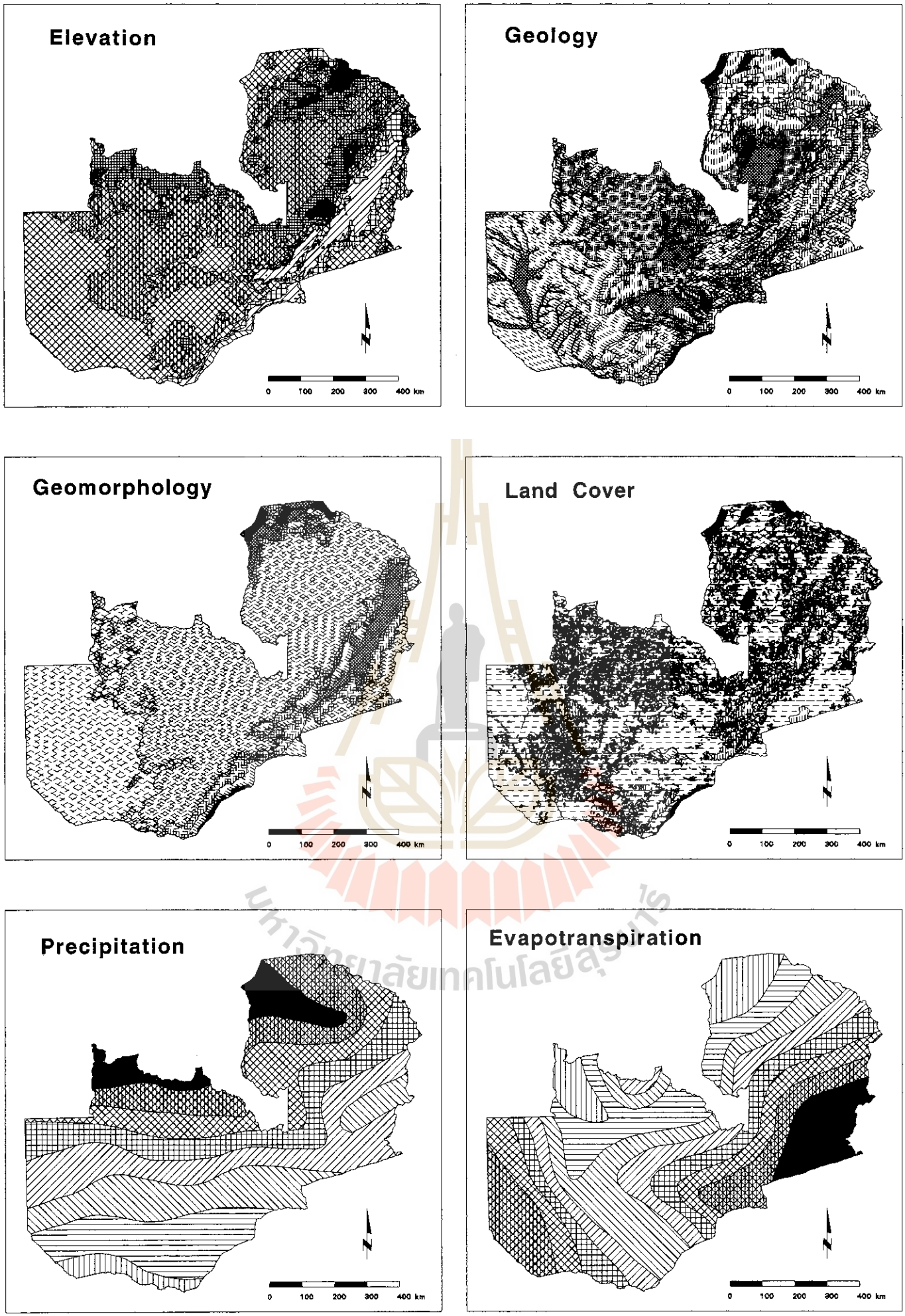

Fig.-2 Thematic Database

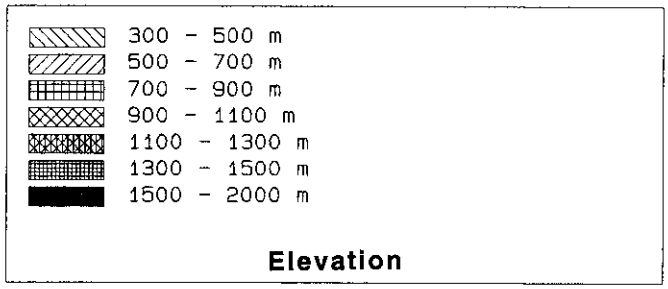

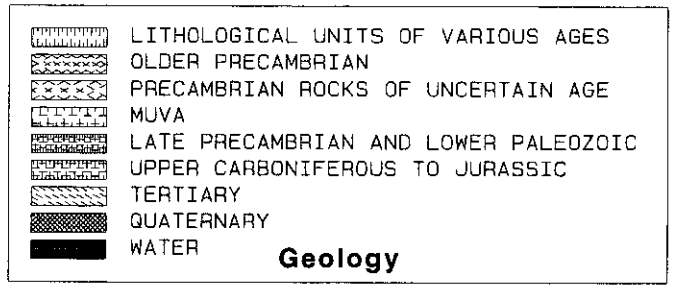

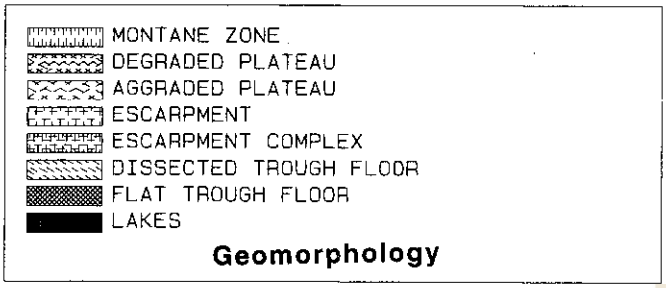

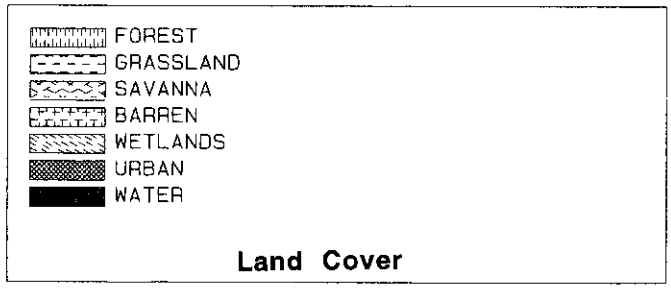

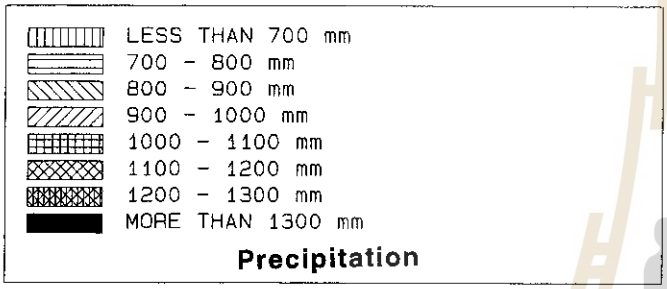

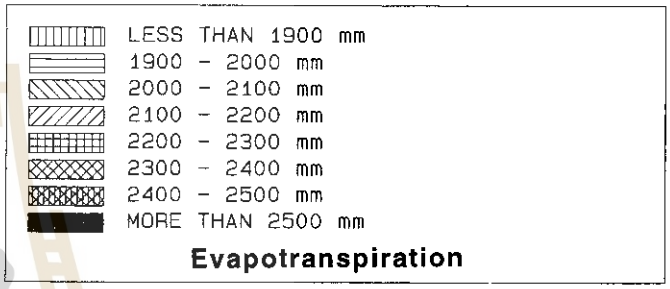

Legend of Thematic Maps

Table-1 List of Environmental Items, Categories

Environmental Item		Environmental Category	Sample	Environmental Item		Environmental Category	Sample
Geomor-phology	1	Montane zone	2	Landcover	1	Forest	923
	2	Degraded plateau	4,157		2	Grassland	4,197
	3	Aggraded Plateau	1,893		3	Savanna	2,072
	4	Escarpment	13		4	Barren	
	5	Escarpment complex	672		5	Agriculture	151
	6	Dissected trough floor	313		6	Wetland	64
	7	Flat trough floor	389		7	Urban	3
	8	Lake	83		8	Water	112
Elevation (m)	1	300～ 500	50	Annual Precipitation (mm)	1	～ 700	213
	2	500～ 700	457		2	700～ 800	1,030
	3	700～ 900	373		3	800～ 900	1,234
	4	900～1100	2,511		4	900～1000	1,399
	5	1100～1300	2,998		5	1000～1100	1,120
	6	1300～1500	949		6	1100～1200	989
	7	1500～2000	184		7	1200～1300	992
Geology	1	Lithological unit of various ages	1,142		8	1300～	545
	2	Older Precambrian	1,206	Evapo-transpiration (mm)	1	～1900	603
	3	Precambrian rocks of uncertain age	67		2	1900～2000	1,050
	4	Muva	560		3	2000～2100	1,418
	5	Late Precambrian and Lower Paleozoic	1,406		4	2100～2200	1,096
	6	Upper Carboniferous to Jurassic	602		5	2200～2300	932
	7	Tertiary	1,841		6	2300～2400	856
	8	Quaternary	585		7	2400～2500	1,020
	9	Water	113		8	2500～	547

5. Natural Environmental Factor Interrelationships

Cramer's coefficient of association between the items was obtained in accordance with the square of χ (solution), which was found through the cross tabulation of the sample data (see Table-2), in order to understand the strength of the mutual relationships (links) that exist between the environmental items. The largest value obtained is the 0.547 that exists between geomorphology and geology, and this is followed by the 0.411 that exists between geomorphology and elevation.

Table-2 Cramer's Coefficient of Association

	Precipitation	Evapotranspiration	Geology	Geomorphology	Land Cover	Elevation
Annual Precipitation	1.0000	0.3676	0.2580	0.1954	0.1027	0.3057
Evapotranspiration	0.3676	1.0000	0.2566	0.2406	0.1174	0.2897
Geology	0.2580	0.2566	1.0000	0.5499	0.3998	0.3863
Geomorphology	0.1954	0.2406	0.5470	1.0000	0.3263	0.4111
Land Cover	0.1027	0.1174	0.3998	0.3263	1.0000	0.1614
Elevation	0.3057	0.2897	0.3863	0.4111	0.1614	1.0000

Furthermore, the matrix, which is formed by Cramer's coefficient of association, became the basis for the factor analysis as a correlation matrix. The aim of the factor analysis was to find out which factors are the fundamental ones. As a result of this, as can be seen in Fig.-6, it was possible to broadly divide the environmental items into two groups; the first factor group consisting of the land-related items of geomorphology, geology and land cover, and the second factor group consisting of the climate-related items of annual precipitation, evapotranspiration and elevation (see Fig.-3).

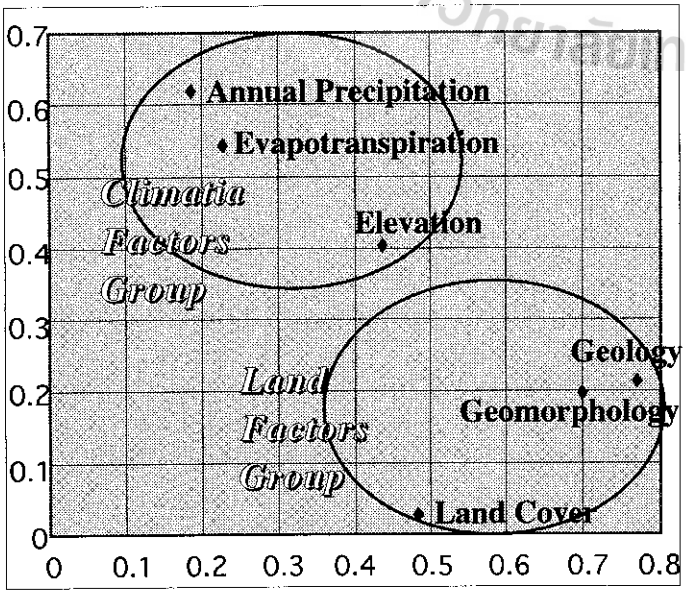

Fig.-3 Grouping of Environmental Factors based on Factor Analysis

6. Environmental Unit Classification by Cluster Method

First, Quantification theory III was applied using the sample categories as variables. Regarding the axis unique values and contribution ratios, an accumulated 21.5% is explained up to three axes, as shown in Table-3. Next, the sample weight matrix

Table-3 Result of Quantification III

Axis	Eigenvalue	Coefficient of Conrtibution	Accumulation	Correlation Coefficient
1	0.4727	7.9	7.9	0.6875
2	0.4363	7.3	15.2	0.6605
3	0.3763	6.3	21.5	0.6135
4	0.2467	4.1	25.7	0.4967
5	0.2410	4.0	29.7	0.4909

obtained in Quantification III were used in carrying out cluster analysis (Ward method). As a result of this, it was possible to classify the environmental units into 10 groups (Group A - Group J) as shown in Table-4 and Fig.-4 Looking atthese environmental unit groupings for the whole of Zambia shows that, with the focus being placed on topography, they accurately reflect the land classifications together with the geology and land cover, which are discernible in the aggradated and degraded areas of the Central African Plateau and the fault valley bottoms and escarpments that lie along rift valleys. These results almost totally match with existing ecological viewpoints and can be said with great confidence to be proper and correct.

Reference

K. Takeuchi and A. Tsunekawa (1994) : Environmental Resources and Information System (in Japanese), Kokon Shoin, 219pp.

K. Takeuchi, A. Tsunekawa and H. Ikeguchi (1990) : Numerical Classification of Natural Regions of Japan, Geogr. Rep. Tokyo Metropol. Univ,. No. 25, 269 - 287

J. Townshend (1991) : Environmental database and GIS. In : D.Maguire et al (eds) Geographic Information System : Principles and Applications, Vol.2, Longman, 201 - 216

Table-4 Characteristics of Each Environmental Unit

ENVIRONMENTAL ITEM	GROUP A	GROUP B	GROUP C	GROUP D	GROUP E
GEOMORPHOLOGY	Aggraded Plateau	Degraded Plateau	Degraded Plateau Aggraded Plaeau	Degraded Plateau	Aggraded Plateau Degraded Plateau
GEOLOGY	Tertiary	Upper Carboniferous to Jurassic	Order Precambrian	Order Precambrian	Tertiary
LAND COVER	Grassland	Grassland - Savannah	Grassland Savannah - Forerst	Savannah - Grassland	Grassland Savannah - Forest
ELEVATION	Middle	Middle	Middle	Middle	Middle
PRECIPITATION	Middle	Middle - Much	Middle	Middle	Less - Middle
EVAPO - TRANSPIRATION	Middle	Low - Middle	Low	Low	Low - Middle
ENVIRONMENTAL ITEM	GROUP F	GROUP G	GROUP H	GROUP I	GROUP J
GEOMORPHOLOGY	Aggraded Plateau Degraded Plateau	Degraded Plateau Aggraded Plateau	Desected Trough Floor Escarpment Complex	Lake	Flat Trough Floor Dissected Trough Floor
GEOLOGY	Tertiary	Upper Carboniferous to Jurassic	Upper Precambrian to Lower Paleozoic	Water Body	Upper Precambrian to Lower Paleozoic
LAND COVER	Grassland - Savannah	Grassland - Savannah Forest - Agriculture	Grassland - Saavannah	Water Body	Grassland
ELEVATION	Middle - High	Middle	Low	Middle	Low
PRECIPITATION	Less	Much	Less - Middle	Much	Middle
EVAPO - TRANSPIRATION	Low - Middle	Middle - High	High	Middle - High	Middle

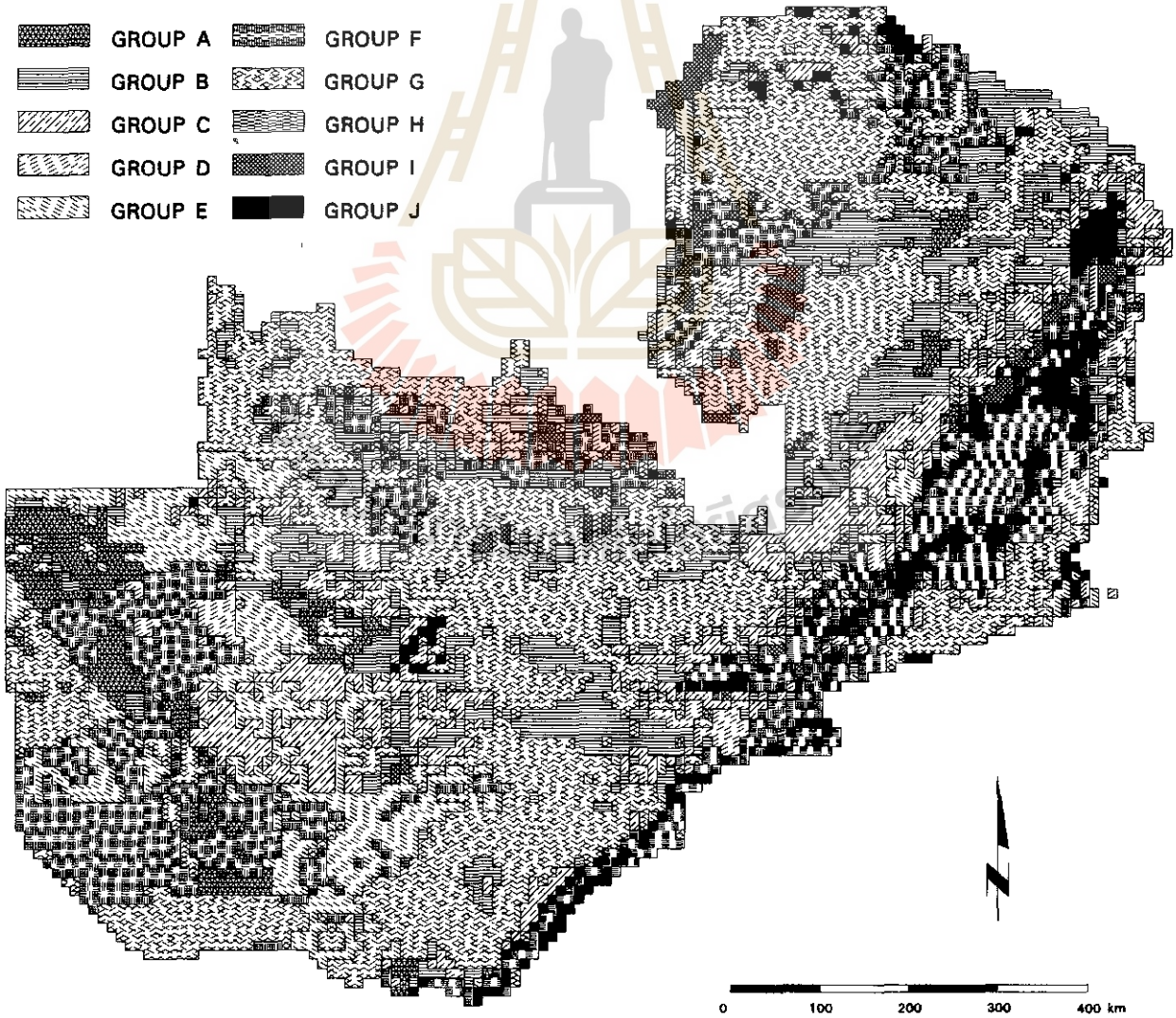

Fig.-4 Environmental Unit Classification Map

CLASSIFICATION OF FOREST IN MALAYSIA USING JERS-1 SAR AND LANDSAT TM DATA

Hideki Saito[1], Khali Aziz Hamzah[2] and Haruo Sawada[1]

[1]Forestry and Forest Products Research Institute

P.O. Box 16 Tsukuba Norin Danchi, Tsukuba Ibaraki 305, JAPAN

TEL: 0298-73-3211 ext. 636 FAX: 0298-73-3799 E-mail: rslsaito@ffpri.affrc.go.jp

[2]Forest Research Institute of Malaysia

Kepong, Kuala Lumpur 52109, MALAYSIA

TEL: 03-6342633 FAX: 603-6367753 E-mail: khali@frim.gov.my

ABSTRACT

We can get SAR images in both wet and dry seasons, as they are available in all-weather. In addition, SAR observes objects with the same energy, thus we can compare any SAR images that are acquired at different time directly. These characteristics are effective for monitoring a forest in Malaysia that is often covered by cloud and has different condition due to seasons. The purpose of this study is to improve the classification accuracy of forest area in east coast Malaysia using JERS-1 SAR data and Landsat TM data. However SAR data alone is not enough for obtaining good result on forest classification. Therefore we attempted to combine SAR and TM data for the classification. Their results are as follows; (1) The classification accuracy of peat swamp forest, hill forest and grass land are improved, (2) It is effective to use average filtered image of SAR, (3) It is also effective to use two SAR data that are acquired in different seasons. Combining TM and SAR data is quite useful for the classification of forest in Malaysia. These results indicate that SAR is closely related to the forest volume and structure of forest in Malaysia. This point must be the subject of future research.

1. Introduction

Lately, decreasing and degrading of tropical forest have become important problem at not only local or regional level but also global level. Remote sensing technology has been available for monitoring tropical forest. Spatial and spectral resolutions of Landsat TM are so high that it is suitable sensor for monitoring of tropical forest. But it is restricted to acquire the observation data, because optical sensor, such as Landsat TM and SPOT HRV, were obstructed by cloud. Compared with these sensors, SAR has some advantages in observing the forest. (1) SAR data is possible to be acquired in both dry and wet seasons, as it is available in all-weather. (2) SAR observes objects with the same

energy, thus we can directly compare SAR images that are acquired at different time. Thus these characteristics allow us to monitor tropical forest periodically. (3) L-band SAR digital number and forest volume have deep relationship, since it can penetrate the canopy layer and is reflect by forest floor and tree stem or branch (L. L. Hess, 1990). There is a study about classification using Landsat TM together with ERS-1 SAR. It says that the combination of Landsat TM and ERS-1 SAR data can potentially lead to improved land cover mapping (R.P.H.M. Schoemakers et al., 1993). It is considered to be admitted that the combination of Landsat TM and JERS-1 SAR can improve the classification accuracy.

2. Study Area and Data

A test site was selected in forest area in the south part of Pekan village (102 30'E, 3 30'N), Pahang in the east coast of Peninsular Malaysia. Peat swamp forests are major occupation in this area and oil palms are planted around peat swamp forest. The topology is flat, especially in the peat swamp forest. The weather is seasonal tropical climate, and temperature keeps high and it has small seasonal changes. Both wet and dry seasons are found in this area. Monthly temperatures and monthly mean precipitation at Kuantan, Pahang, MALAYSIA are represented in Figure 1 and 2 (NOAA, 1987-1994). Kuantan is northern part of Pekan and distance between both towns is about 50 km. The data that were used in this study are represented in Table 1.

3. Methodology

3.1 Reducing Speckle Noise

To minimize effects of speckle noise, a median filter is applied to SAR image. The median filter can remove very high or low values in its windows, so it is expected to reduce the effect of speckle noise. The window size of that filter was 5 by 5.

3.2 Overlay

Both of SAR data were overlaid to TM data and the pixel spacing of both was set to 30 m, the pixel size of TM data, using nearest neighbor interpolation as a resampling method.

3.3 Texture Analysis of SAR

The statistical values such as average and standard deviation of the gray level histogram of n by n windows can be used as a textual information (J. A. of RS, 1993). Average and Standard deviation filter of 5 by 5 windows were applied to median filtered SAR image to get textural information of SAR in this study.

3.4 Normalized Difference Vegetation Index (NDVI) of TM

NDVI are calculated by following expression;

NDVI = (TM4 - TM3) / (TM4 + TM3)

where TM4 is Near Infrared band and TM3 is Visible band.

NDVI shows as a high value for denser vegetation, while NDVI very low in desert, or non-vegetation region (J.A. of RS, 1993).

3.5 Maximum Likelihood Classification

First, Training areas were selected referencing field survey and interpretation of Landsat TM image. Then Training data sets that contain 13 classes were extracted. Second, We generate 9 sets of combination of TM, NDVI and SAR for comparing the classification accuracy. These combinations are shown on the first line of Table 2. Band 1 of TM is strongly affected by path radiance and band 6 is the thermal band. Therefore these bands were not used in this study. Third, the Maximum likelihood classification was executed for each set using above-mentioned training data sets. Finally, we evaluated the accuracy of each classification by the Mapping accuracy that was calculated from confusion matrix.

4. Results and Discussion

The results of classification of each class, which were evaluated by Mapping accuracy, are represented in Figure 3 and their improving rates are shown on Table 2. It is clear that classification of TM data alone, their improving rates are in order of the number of bands that were used in classification. In the case of the combination of TM and NDVI, classification accuracy was slightly decreased in almost classes. An improvement of classification accuracy could not find in the case of the combination of TM and median filtered SAR. These results carried out that we cannot improve the classification accuracy combining TM and original SAR or median filtered SAR images. Original SAR data are not suitable for classification, because there are many speckle noises in this image. Median filtered SAR image also cannot be used for classification, because it still has many speckle noises. Classification accuracys are improved in the case of the combination of TM and the textural data of SAR. We got textural data from applying the average and the standard deviation filter on median filtered SAR image. Average filtered image was more effective for improving of classification accuracy than standard deviation filtered image. Average filter on median filtered image has very strong effect to reduce the speckle noise, however this process has some problem such as destroying edge and line feature. Classification accuracys were improved in almost classes, especially classes of peat swamp forest, hill forest and grass land are improved more than any other classes. For class of bare soil significant improvement, could not be found, because those classes have high accuracy without SAR data. It seems that these results reflected the characteristics of SAR on the information concerned with forest volume and structure.

Combining TM and two SAR that were acquired in different seasons, classification accuracys were improved more. One SAR image was acquired in July (Dry season) and another one was acquired in October (Wet season). The changes of SAR digital numbers of each class are shown in Figure 4. This figure indicates that SAR digital number of swamp forest classes is decreased and the other classes have no change or increase. It is considered that these differences are caused by the difference of the hydrological condition between both seasons. Especially, peat swamp forest is strongly affected by flooding in wet season. L. L. Hess et al. mentioned about detection of flooding on forested floodplain by SAR remote sensing. They summarized as follows; Synthetic aperture radar remote sensing is a promising tool for detection of flooding on forested floodplain. The bright appearance of flooded forests on radar images results from double-bounce reflections between smooth water surfaces and tree trunks or branches. Enhanced backscattering at L-band has been shown to occur in a wide variety of forest types. Lack of enhancement is a function of both stand density and branching structure (Laura L. Hess et al., 1990). We can find a suggestion here that L-band can detect the flooding in the forest as a bright appearance. However it is not useful in dense forest, because L-band cannot penetrate dense canopy. In this study the relationship between differences of SAR digital number and seasonal changes of backscattering properties of peat swamp forest have not been clear. But this result indicates that SAR may observe seasonal change of peat swamp forest.

Tropical peat swamp forest accumulates a large quantity of carbons in not only terrestrial part but also subterranean part as a peat that contains a litter and methane, even though that area is not so large (Furukawa, 1985). Therefore, the mapping and monitoring of peat swamp forest are important for not only local environment but also global environment. However Field survey is difficult in peat swamp forest, because flooding and thick tangles of stems and roots prevent us from going into forest. Results of this study allow us more accurate mapping of forested area such as peat swamp forest using Landsat TM and JERS-1 SAR data and continuous monitoring all the year round using JERS-1 SAR.

References:

Furukawa Hisao and Supiandi Sabiham, Agricultural Landscape in the Lower Batang Hari, Sumatra Part 1, SOUTHEAST ASIAN STUDIES, Vol. 23, No. 1, pp. 3-37, 1985.

NOAA, MONTHLY CLIMATIC DATA FOR THE WORLD, NOAA, Vol. 40-47, 1987-1994.

Laura L. Hess, John M. Melack and David S. Simonett, Radar detection of flooding beneath the forest canopy: a review, INT. J. REMOTE SENSING, Vol. 11, No. 7, pp. 1313-1325, 1990.

Japan Association on Remote Sensing, REMOTE SENSING NOTE, Japan Association on Remote Sensing, 284pp., 1993.

R.P.H.M. Schoenmakers, G. G. Wikinson and Th. E. Schouten, Use of Landsat TM Image Segmentation for Smoothing ERS-1 SAR Imagery in Combined Multi-sensor Landscape Classification, International Geoscience and Remote Sensing Symposium (IGRSS'93), pp. 1228-1230,1993.

Table 1 Attribute of Data that are used in this study

Satellite	Sensor	Path - Row	Acquisition	Season
Landsat	TM	126-58	24 June, 1992	Dry Season
JERS-1	SAR	118-29	17 July, 1993	Dry Season
JERS-1	SAR	118-29	13 October, 1993	Beginning of Wet Season

Table 2 Improving rates of classification accuracy

	TM2 3 4 5 7	TM2 3 4 5 7 + NDVI	TM2 3 4 5 7 + SAR07	TM2 3 4 5 7 + SAR07ave	TM2 3 4 5 7 + SAR10ave	TM2 3 4 5 7 + SAR07ave + SAR10ave
Swamp Forest	0.00	-1.23	1.72	12.18	7.56	15.15
Disturbed Swamp Forest	0.00	-0.87	1.16	2.72	3.88	5.72
Swamp Forest (Bright)	0.00	-0.43	1.24	6.47	5.90	8.59
Swamp Forest (Dark)	0.00	-0.47	0.87	5.02	3.66	6.62
Oil Palm	0.00	-0.31	0.49	1.99	4.97	5.79
Oil Palm (Young)	0.00	-1.63	3.28	10.13	5.60	11.07
Oil Palm (New)	0.00	-1.01	1.19	2.74	1.19	3.99
Bush	0.00	-1.46	0.60	4.77	1.97	6.22
Hill Forest	0.00	-0.90	2.29	5.46	3.40	10.59
Disturbed Hill Forest	0.00	-2.80	1.37	5.74	3.45	6.34
Bare Soil (White)	0.00	0.39	0.20	0.54	0.17	1.23
Bare Soil (Red)	0.00	-0.37	0.11	0.08	0.04	0.25
Grass Land	0.00	0.00	0.98	4.00	4.57	8.16
Average accuracy	0.00	-0.85	1.19	4.76	3.57	6.90

"Bright", "Dark, "White" and "Red" represent colors on Landsat TM image (R:G:B = 5 4 3).

"SAR07" means median filtered SAR data acquired at 17 July,1993.

"SAR 07ave" means average filtered data on median filtered SAR data acquired at 17 July, 1993.

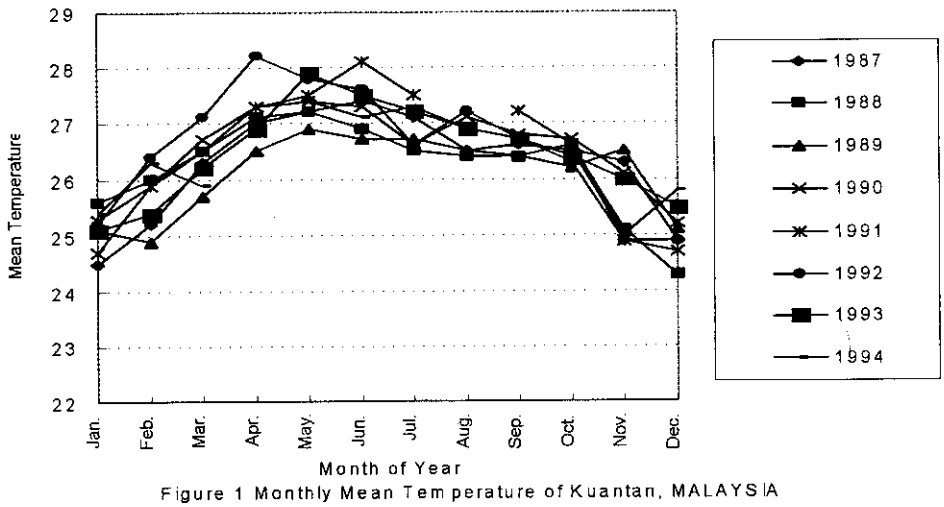

Figure 1 Monthly Mean Temperature of Kuantan, MALAYSIA

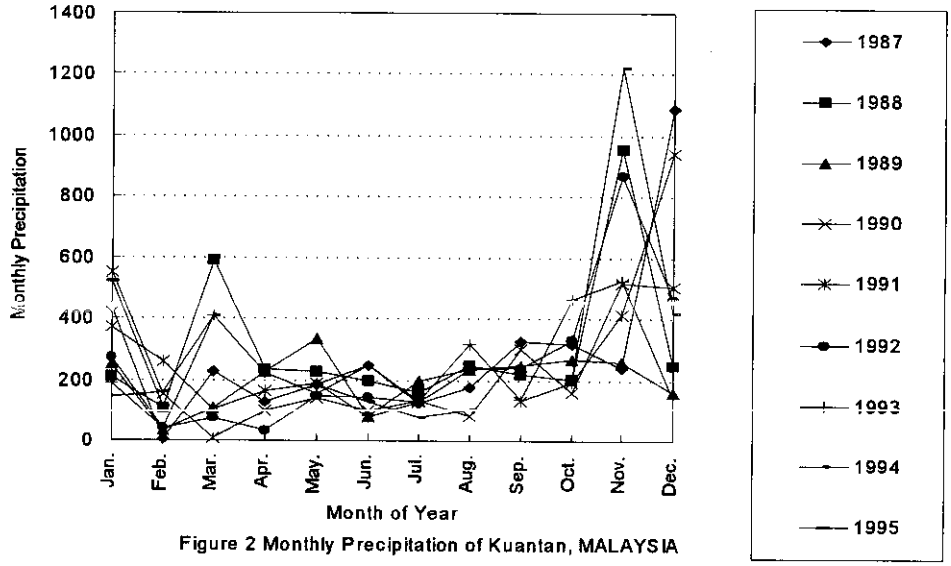

Figure 2 Monthly Precipitation of Kuantan, MALAYSIA

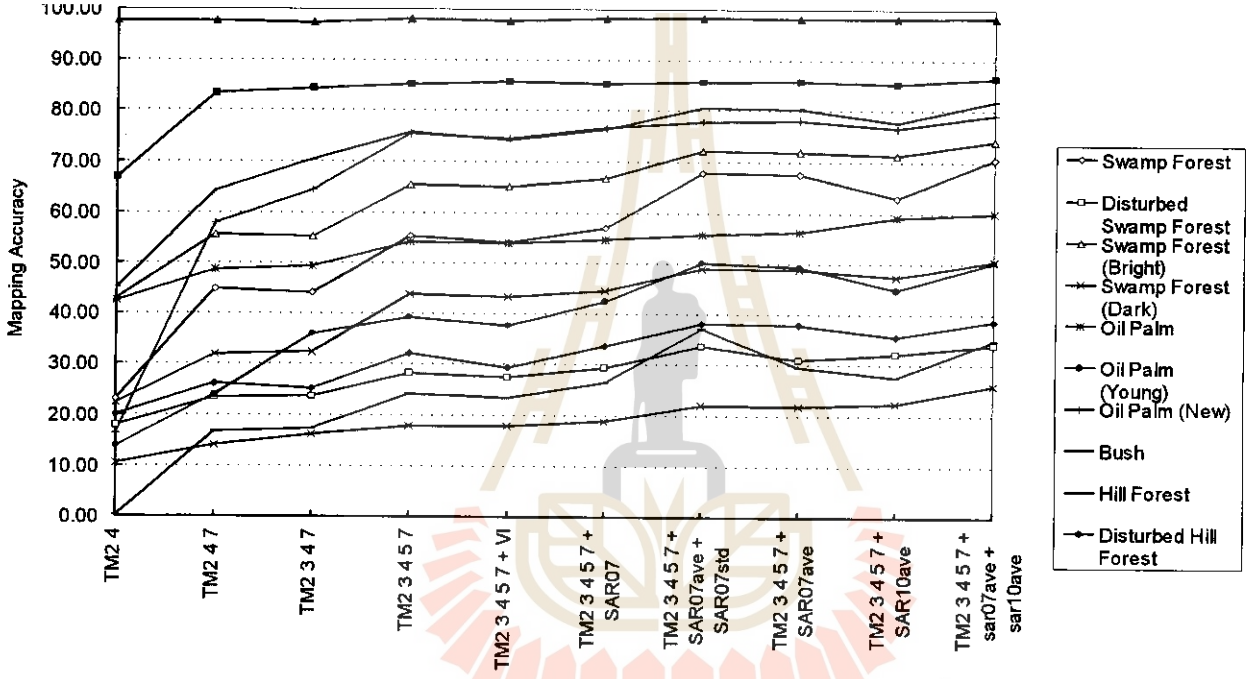

Figure 3 Relations between Mapping Accuracy and Band Conbination

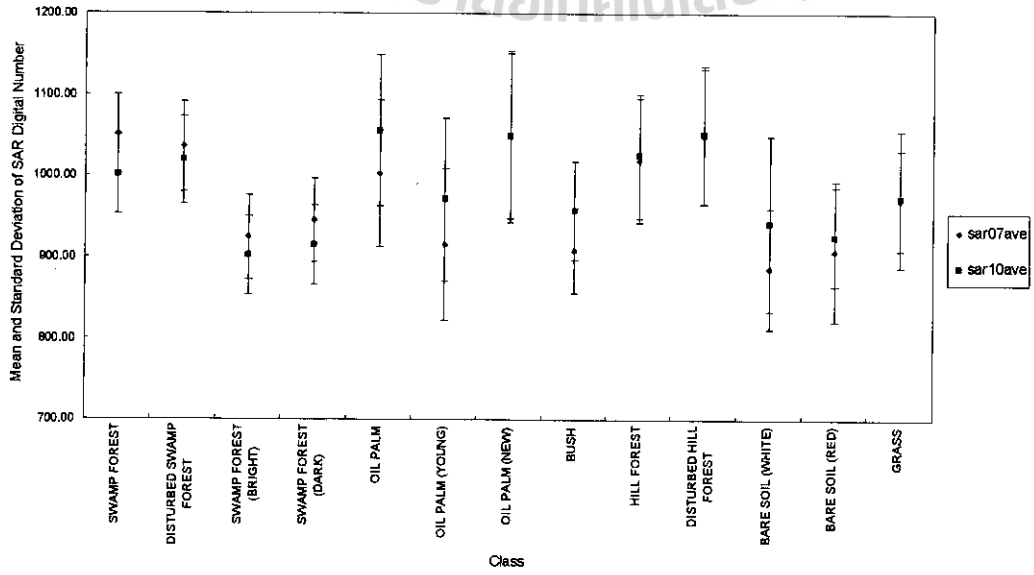

Figure 4 Mean and Standard Deviation of SAR Digital Number in Each Classes

APPLICATION OF RS AND GIS FOR FOREST-STEPPE AND DRY-STEPPE GEOSYSTEM STUDY

M.Ganzorig, H.Tulgaa, D.Amarsaikhan, B.Enkhtuvshin

Informatics and RS Centre of Academy of Sciences
av.Enkhtaivan-54B, Ulaanbaatar-51, Mongolia

ABSTRACT

Different airspace experiments for various scientific and economic purposes have been carried out in Mongolia using remotely sensed data taken from different platforms and materials of the ground measurements. The investigation of the physical condition of a geosystem in past and present time is one of the urgent tasks of many researchers dealing with earth sciences. Our aim in this study is to investigate two different geosystems in Mongolia. To reach the goal the diverse data were compiled within the ERDAS and ILWIS-systems and various RS and GIS techniques were applied.

1. INTRODUCTION

The results of the various experiments, carried out on Mongolian territory, with the aim of exploring the environment and mineral resources by methods of remote sensing indicated indeed great opportunities for the application of remotely sensed data to solve the problems, associated with the environmental protection and earth sciences within such comprehensive area (1.565 mil.sq.km) having various natural surroundings and unique geosystems (Ganzorig et al. 1994). Among the methodical problems of RS the main attention has been paid to the thematic cartography and the study of the physical condition of a geosystem. If the first is the traditional, then the latter is the new one related with the space monitoring of environment. In this case, the aim of RS is to measure different characteristics of the geosystem whose investigation should be based on a systematical approach. Such approach requires an implementation of a GIS which is a management tool of geographical and other spatial related information for some decision making process. Within the scope of our research, forest-steppe and dry-steppe geosystems have been analyzed. As a case study the following areas have been selected:

'Tsagaantolgoi', where the basic attention was paid to the investigation of the forest-steppe geosystem and estimation of its condition;

'Tumentsogt', where the aim was the study of the dry-steppe geosystem, its pasture degradation, soil erosion and soil saltiness;

To develop the GIS we have designed two types of databases (spatial and attribute) in different levels and for their implementation and final analyses different RS and GIS techniques were used.

2. DATABASES

We have designed databases in 3 different levels: satellite, air and ground. The satellite level is based on the middle scale maps (1:200,000), the air level is based on the larger scale airborne data (1:25,000). The ground level is based on the data collected through field investigation. Generally, the proper physical implementation of the conceptual model is very simple within the ERDAS domain because we need not to define topology to find spatial relationships or posted identifiers to join various attribute tables. Initially, in order to get the right georeference digital images in different levels were geometrically corrected to Gauss-Kruger map projection using topographic maps of the test areas (Ganzorig et al. 1994). All maps, except the topographic maps were converted to digital form by video scanning using a CCD camera. Then they were resampled into the geometrically corrected digital images. After that was done screen digitizing of each map using the DIGSCRN-module of the ERDAS-system. Within the GIS the entities should be uniquely identified and have a set of attributes. In our case,

the ordering numbers(#) of the classes of objects served as the identifiers or keys. Some attribute tables were designed in DBASE-IV. Saturation enhancement and 3D view were implemented within the ILWIS environment.

Source materials

Different maps for the test areas are described as follows and RS data are shown in Table1.

'Tsagaantolgoi' area

- Topographic maps, scales 1:100,000; 50,000; 1:10,000
- Soil map, scale 1:200,000
- Geological map, scale 1:200,000
- Natural landscape (geocomplex) map, scale 1:200,000
- Pasture vegetation map, scale 1:200,000
- different ground truth data and field materials.

'Tumentsogt' area

- ground spectrometrical data
- Topographic maps, scales 1:50,000; 1:25,000
- Soil map, scale 1:200,000
- Natural landscape map, scale 1:200,000

RS data	Spectral resolution	Spatial resolution	Swath width	Date
KFA-1000	panch.	5m	75km	1982
MSU-SK	panch.	240m	600km	1990
MSU-E	3 bands (vis., NIR)	40m	40km	1990
AFA	panch.	1:33,000	1962, 1963, 1975	
MSK-4	4 bands (vis., NIR)	1:25,000	(07-08).1990	
SPOT-XS	3 bands (vis.,NIR)	20m	60km	1986

Table1. Available RS data

3. TEST SITE 'TSAGAANTOLGOI'

Tsagaantolgoi area is included into the forest-steppe zone and its landscape is divided into 5 zones, like mountainous taiga or forest (1500m-2000m above sea level (asl)), mountainous forest steppe (1300m-1500m asl), mountainous steppe (1200m-1400m asl), mountainous steppe (1000m-1200m asl), dry steppe and meadow steppe in the river valley and between the mountains (Ganzorig et al. 1995). The objectivity of the separation of the natural boundaries between the natural landscape subdivisions is defined by the availability of the information extracted from various RS data. In this area a large scale photograph taken by the 'KFA-1000' photocamera from the series of the Russian satellite 'Cosmos' with a high spatial resolution was used as a basis for the differentiation between the objective contours and defining the quantitative relationships between the natural landscapes. After applying some corrections to make more clear the boundaries between the objects different gradient and high pass filtering techniques were applied. After that, on the basis of knowledge about the area and other thematic information, in the enhanced image the geocomplex features were digitized using DIGSCRN-module and was created a natural landscape map containing the relationship between the natural components (eg, relief, soil, vegetation, etc.) of the forest-steppe zone in Mongolia (Fig.1).
From the interpreted natural landscape map it is clearly seen that a set of stow combination in the western and north-western parts of the test area is significantly distingueshed from that in the eastern and southern parts. Therefore, in order to find out the reason for these differences and check how much it is real in large territory, we have used MSU-SK digital data and for its quality improvement destriping and low and high pass filterings have been applied (Fig.2).

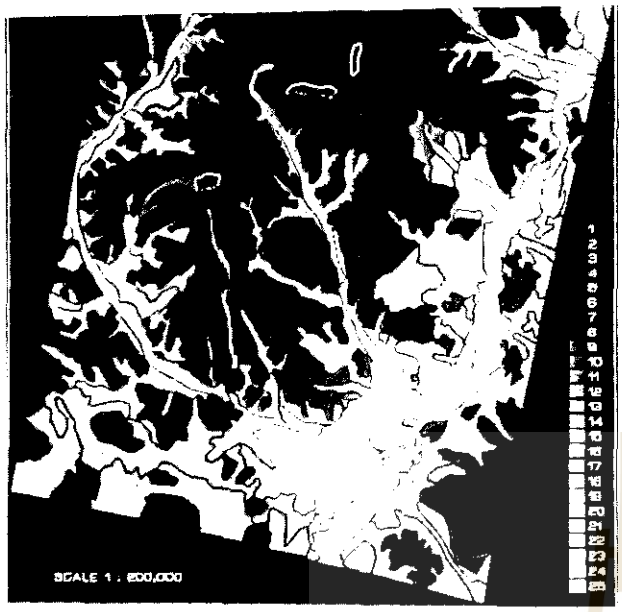

Fig.1. Natural landscape (geocomplex) map.
1. Larch-tree taiga, 2. Cedar-larch taiga, 3. Birch-larch subtaiga, 4. Forest with mezophit grasses 5-7. Forest-steppe with different stow modification, 8-10. Steppe with different stow modification, 11-21. Dry steppe with different stow modification, 22-25 Dry steppe and bottomland meadow with different stow modification.

Fig.2 Natural regionalization. I. Selenge forest-steppe middle mountain and basin subprovince with regions: I-1 Buteeliin forest and forest steppe, I-2 Selenge rivers dry steppe, I-3 Buren taigaforest, I-4 Burgaltain dry steppe.II. Orkhon-Tuula dry steppe low mountain and basin subprovince with regions: II-5 Enkhtal forest steppe, II-6 Tuula dry steppe and meadow, II-7 Orkhon-Kharaa dry steppe.

The investigation of the most general tonal and textural differences of MSU-SK image indicated that there are along the north-western parts of the territory 6 types and subtypes of the natural landscapes, consisting of dozens and hundreds of stows, whereas in the southern and eastern parts were only 2-3 types of geocomplexes from the not rich combination of stows and used for husbandry mainly in agriculture. MSU-SK data helped us to make clear the following basic natural laws:

a) to determine the above mentioned differences related with the bioclimatic and anthropogenic influences;

b) to identify in detail the morphostructure in the regional level and geologico-tectonic formation clearly appeared in the relief of the territory with large area.

On the basis of these natural laws geosystems of middle taxonomical level (natural subprovinces and regions) have been detected. The further analyses require the application of multispectral data. To get the best colour image different spectral enhancement techniques have been applied to the MSU-E data and the best result was obtained by the use of the saturation enhancement. To apply this technique, after sum normalization, 3D RGB data was mapped to the 2D colour triangle, removing the influence of the Intensity. Within the triangle, at first the data cloud was shifted to the origin, to make a colour balance and then spread throughout the feature space to use all possible colours.

Then to improve the interpretation and detection of the object boundaries high pass filtering and some normalizations have been applied. Colour differences in the enhanced image indicated the local variants of geocomplex structures and some landuse types and allow to group geocomplex types (Fig.3a). Making a querry using GISMO-module we have obtained a map of the grouped natural landscapes coincided by the basic landuse types, as pasture, agriculture, etc.(Fig.3b).

As seen from Fig.3 pasture is dominant in the forest-steppe zone of Mongolia. At the same time there are some separately existing agricultural lands and small groups of fields chaostically scattered basically in the dry-steppe pasture lands.

In this area, except pastures were considered such types of landuse, as irrigated

and non-irrigated arable lands, hay-makings, having high specific weight in the whole area.

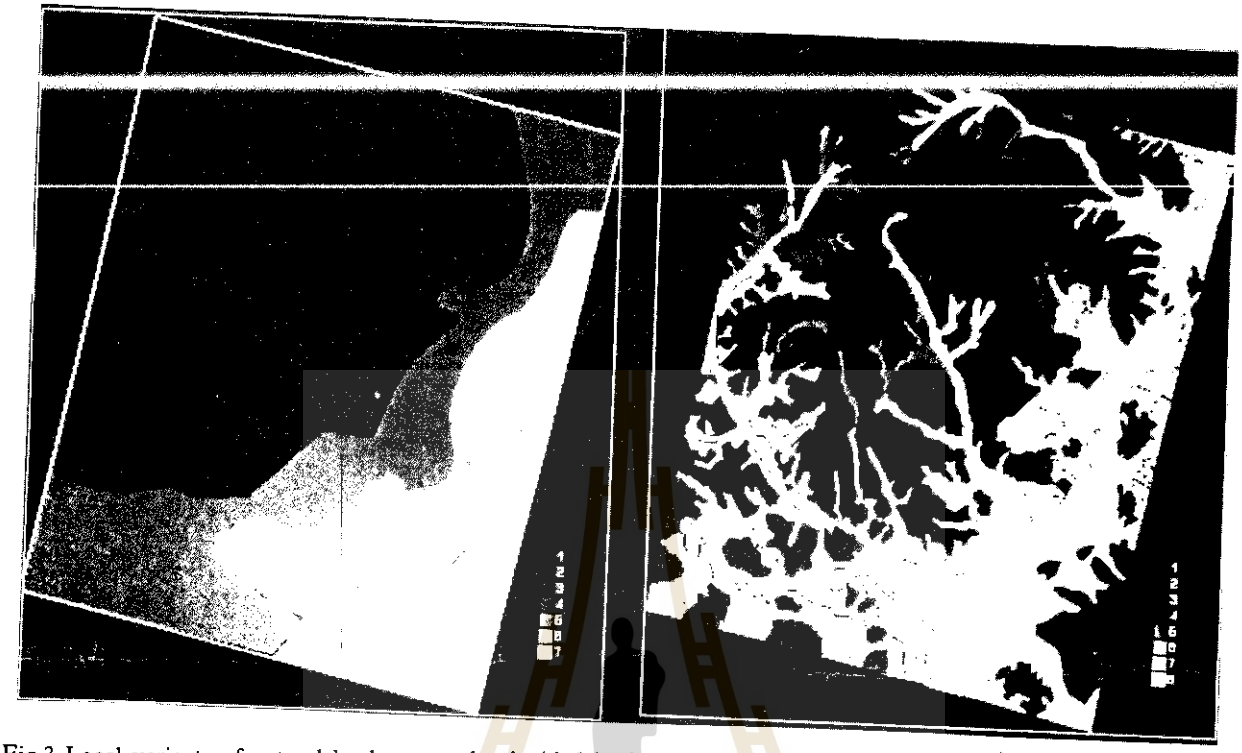

Fig.3 Local variants of natural landscape and coincided land types.A: 1. Middle mountain taiga, 2. Saddle meadow steppe, 3.low mountain forest and forest-steppe, 4. Hills low mountain steppe. 5 & 7. Oval plain dry steppe, 6.basin-valley dry steppe and bottomland meadow.B: Forest land: 1. Taiga, 2. Herbaceous forests, Natural fodder and arable land: 3. Pastures, partly used for the haymaking, 4.Summer pasture, 5. Spring-Autumn pasture, 6. Spring-Autumn-Winter pasture, 7. Summer-Autumn pasture,8. Spring-Winter pasture and partly haymaking.

For the investigation of some changes in the land resources we compared two subparts in the images taken in 1982 (Cosmos) and in 1990 (MSU-E). In result, the formation of the new landuse types which allowed to get information about the dynamics of the physical condition and usage of land resources for almost 10 years was detected (Fig.4).

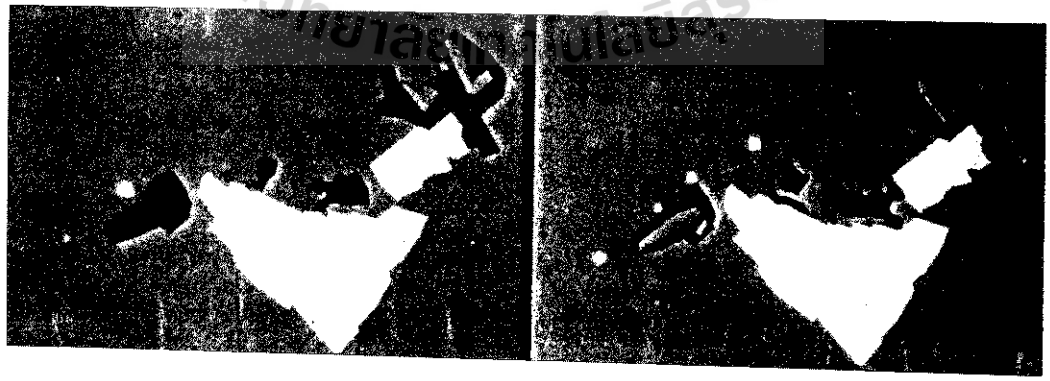

Fig.4 Land resources changes a - results of interpretation from Cosmos photoimage (1982) b - results of interpretation from MSU-E (1990) digital data

As seen from Table2, by the interpreted from the satellite image features it is possible to distinguesh not only the acting irrigated and non-irrigated fields, also to calculate the increased salty, sandy and non-irrigated fields and decreased pastures and fallows.
For this aim we used a digital elevation model(DEM) of the area. To create it, contours were digitized at 50m intervals from the topographic map, scale 1:100,000 and interpolated in every 10m. After applying masking, overlaying and enhancement techniques we have illustrated landuse changes for 10 years using Cosmos, MSU-E and MSK-4 data (Fig.5b).
In the test fields a methodology to use air data for the investigation and mapping of the landuse types was elaborated.

Table2. Illustration of landuse changes (total area = 24010 ha)

RS data	irr. land	ir.l w.f.of sd&st.	non-irr. land	n.irr.l with f. of sand.	virg.l and fallows	beat.p. around w.camp	bea.l arou. vill.	gar.	past. and hay.
COSMOS (1982)	3097.8	0	1180.3	0	1172.8	16.32	214.2	0	18382.7
MSU-E (1990)	2943.0	151.9	1293.4	36.9	1019.2	28.32	282.7	32	18276.9

For this aim MSK-4 air data have been used and different enhancement, feature extraction (principle component analyses, sum and vector normalizations, etc.) and classification (minimum distance, maximum likelihood, etc.) techniques were applied to study pasture and soil degradation.
The methodology allowed to increase in detail the accuracy of the object separation. In the air image the main attention has been paid to the investigation of the nature of the boundaries not always having homogenious expression, specially for the objects mixed with those which are naturally-anthropogenically
originated (eg, beaten land close to the inhabited places, beaten pasture around the winter camps, etc.). For the determination of the exact boundaries between different lands it is necessary to quantitatively analyze cartographic and other materials.
More changed by cattle herding, vegetation groups coincide with winter camps, wells, herdings and to settled areas. In our analysis was established that the zone of the influences of the winter camps the condition of the natural vegetation is within the distance of 1-2km. This zone is well expressed in the multispectral data.
Intensification of the developing agricultural productions influenced the ploughing in the large area, especially in the chestnut and dark chestnut soils of the valley-basins and slopes because the slope, water amd wind erosions of the soil have been increased.
Through the principle component analyses and saturation enhancement and filtering techniques we have obtained information on qualitative containt of the separate contours and detected some new objects.In the panchromatic image this zone is not detected and through the field work it was also not distingueshed from the surroundings. However, the fixation of such objects is vitally important as an indicator for the possible degradation of the pastoral vegetation and soil erosion and also as an index for the forecasting of the ecological situation in the region.
From these analyses it is seen that the investigation and mapping of the natural landscapes and their application in agriculture allow us to carry out classification of the objects by the different features with high confidence.

4. TEST SITE 'TUMENTSOGT'

Initially, digital MSK-4 photoimages were mosaicked and then radiometrically & geometrically corrected. After applying spectral enhancement techniques different low and high pass filterings were used. In comparision with the filters

used in other test areas in this polygon the bigger size kernels (7x7, 9x9 and larger) were applied.
The results of the analysis indicate that in the non-irrigated plough land of the dry-steppe zone degradation processes have been detected such as the intensification of the sandy fields related to deflation and increase of the stained (heterogenious) fields, associated with the phoughing of the carbonate horizon. Comparing the degradation processes in this area and in the mountainous forest-steppe zone one can observe that the degradation process in the Tumentsogt polygon is stronger than in the Tsagaantolgoi area.
This is related with the following factors:
1) the mechanical composition and the depth of plough horizon of the soil.
2) the strength and direction of the wind.

CONCLUSIONS

In result of the creation of the geocomplex map there was established that the limit for the natural landscape mapping by the use of the large scale RS data is within the level of the stows and further geographical differentiation until the level of facies requires an application of aerial data.

Taking into account the specification of the photoimages reflecting the pecularities of the modern distribution of the landuse types related with the local variants of the geocomplexes in each natural region it is concluded that the usage of land resources in the territory is totally submitted to the existing natural laws.

During the analyses in the 'Tsagaantolgoi' area has been established that due to the developing agricultural productions slope, water and wind erosions of different soils have been increased.

These analyses show that the investigation and mapping for the natural landscapes and their application in agriculture allow to carry out classification of the objects by the different features with the high confidence.

The analysis in the 'Tumentsogt' area indicated that the degradation processes in the mountainous forest-steppe zone are weaker than in the dry-steppe zone.

As seen from our investigation, multitemporal and multisource data with the application of RS and GIS techniques can be effectively used to study the conditions of the natural-territorial complexes in different regions.
Such analysis can be applied for the natural objects' study in the comprehensive area related global change monitoring of the Earth.

REFERENCES

1. Ehlers, M., Greenlee, D., Smith, T., and Star, J., 1991, Integration of RS and GIS, Data and Data Access, PE & RS, Vol.57, No.6, 669-677.

2. Ganzorig, M., Amarsaikhan, D., and Enkhtuvshin, B., 1992, An Application of Remote Sensing and GIS Technique in Mongolia, European 'International Space Year' Conference 1992, Munich, Germany.

3. Ganzorig, M., Amarsaikhan, D., Enkhtuvshin, B., Tulgaa, H., 1994, Design of A Multilevel Database using RS and GIS Techniques, Proceedings of the ACRS, Bangalore, India.

4. Ganzorig, M., Adyasuren, Ts, 1995, Application of RS and GIS for Ecosystem Monitoring and Management, Paper presented at the International Seminar on Space Informatics, Ulaanbaatar, Mongolia.

5. Manual of Remote Sensing, 1983, American Society of Photogrammetry Second Edition, Volume 1.

Satellite Remote Sensing for Artificial Grassland in Japan

Nobuyuki MINO, Genya SAITO, and Akira HIRANO
National Institute of Agro-Environmental Sciences
3-1-1, Kannondai, Tsukuba, Ibaraki, 305, JAPAN

TEL: (81)-298-38-8225
FAX: (81)-298-38-8199
E-mail: minonobu@niaes.affrc.go.jp

ABSTRACT

Spatilal information on grassland status is required for various grassland managements. Field survey costs much labor and time, but, satellite remote sensing can provide wide areal information of grassland efficiently. In this study, we attempt to monitor annual change of grassland and grass-renovation status using multi-temporal satellite data. As results of annual change analysis, for satellite data acquired in May, an increase trend in visible, near-infrared, middle-infrared reflectance with aging after grass-renovation was observed. We considered that the change in reflectance is due to the accumulation of dead plants on ground surface. On the other hand, for satellite data acquired in June, a sudden decrease in near-infrared, middle-infrared reflectance was observed approximately in 4 years period after grass-renovation. We considered that the change in reflectance is due to the change of grass-species composition. Then, we compile 'Grass-renovation yeras map (1985-1994) by extracting 1-year grassland and renovated grassland from each satellite data. Renovation-years from satellite data agreed with that from ground survey with high accuracy. Those results show that great ability of satellite remote sensing to monitor grassland status.

1. Introduction

In Japan, grassland is managed intensively for mowing or grazing. Grassland just after seeding has high productivity, but, to maintain it for many years is very difficult. To maintain high productivity of grassland, proper management should be conducted according to various conditions of grassland. Especially, annual change of grassland affect grass-yield seriously, so that it is a key item to be monitored for grassland management.

Once grassland productivity decreases, grass-renovation which is accompanied with plowing and seeding needs to be conducted to improve its productivity. Passed years after grass-renovation is one of indices which indicate grassland productivity. So, grass-renovation year is very important for grassland management.

Since, grassland covers wide area, field survey costs much labor and time to collect spatial information of grassland status. Satellite remote sensing can collect a wide range of spatially distributed information efficiently. If satellite remote sensing can be used for grassland monitoring, it will be an effective tool for various managements. In this study, we attempt to monitor annual change of grassland and grass-renovation status using multi-temporal satellite data.

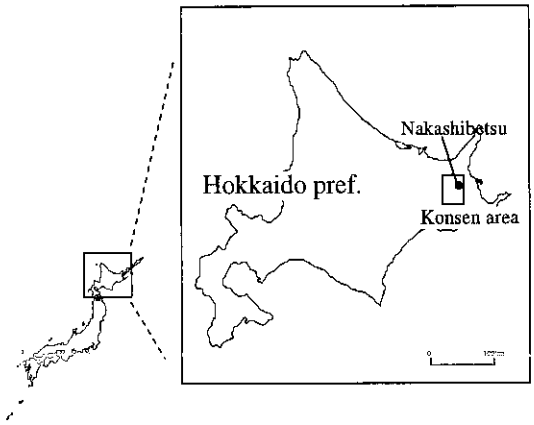

Fig. 1. Study site (Konsen area in Hokkaido pref.)

Table 1. Satellite data list in this study

Path-Row	Sensor	Date	Path-Row	Sensor	Date
106-30	TM	85.05.24.	106-30	TM	91.04.23.
106-30	TM	85.07.27.	106-30	TM	91.06.26.
			106-30	TM	91.08.29.
106-30	TM	86.06.28.			
106-30	TM	86.07.30.	105-30	TM	92.04.09.
			106-30	TM	92.06.28.
105-30	TM	87.05.07.	105-30	TM	92.08.24.
19-59E	MESSR	88.06.06.	105-30	TM	93.04.21.
			105-30	TM	93.06.08.
105-30	TM	89.05.19.			
105-30	TM	89.06.13.	105-30	TM	94.05.17.
19-59E	MESSR	89.08.22.			
106-30	TM	90.04.20			
106-30	TM	90.06.07	59-227	JERS-1/SAR	92.4.15
105-30	TM	90.07.02.	59-228	JERS-1/SAR	92.4.15
105-30	TM	90.08.03.			

2. Method

(1) Study site

Study site is Konsen area which is a major dairy farming region in northern part of Japan (Fig. 1). Due to the low temperature and insufficient sunlight in summer, agricultural lands in this area is not suitable for crop except for grass. In study site, more than 97% of agricultural lands is grassland. Usually, grasslands in study site are mowed in June and August, or are grazed from May to September.

(2) Satellite data

As for satellite data, we collected LANDSAT/TM, MOS-1/MESSR, JERS-1/SAR acquired during 1985-1994. (Table 1.) Geometric correction was applied to the original images and a pixel size of 25m by 25m was used.

(3) Extraction of grassland

Since study site contains forest, cropped area, urban area except for grassland, we produced a file to mask those using some kinds of satellite data. For masking cropped area and urban area, we used multi-temporal LANDSAT/TM data. For masking forest, we used JERS1/SAR data. In this study, we analyzed annual change of grassland and grass-renovation status on the portion except for masked area.

(4) Annual change of grassland

For the study of reflectance annual change, there is a method to compare multi-temporal satellite data directly. However, both observation dates and annual difference of grass growth may affect grassland reflectance. Therefore, direct comparison among multi-temporal satellite data can not supply the information about annual change of grassland reflectance. In this work, using the characteristics of grassland just after renovation, we study annual change of grassland reflectance.

Once grassland productivity decrease, grass-renovation which is accompanied with plowing and seeding needs to be conducted to improve its productivity. Since bare soil is appeared on grassland just after renovation in growing season, such grassland can be distinguished easily from the other grassland coverage using satellite data. (Fig. 2) Using multi-temporal satellite data, we can compile a map which contains spatial distribution of grass-renovation status. Here, we extracted grassland just after renovation according to thresholds of each data, overlaied those and call it "grass-age standard map". By overlaying this map and individual satellite image, we can compare the different age grassland with each other on one satellite image (Fig. 3).

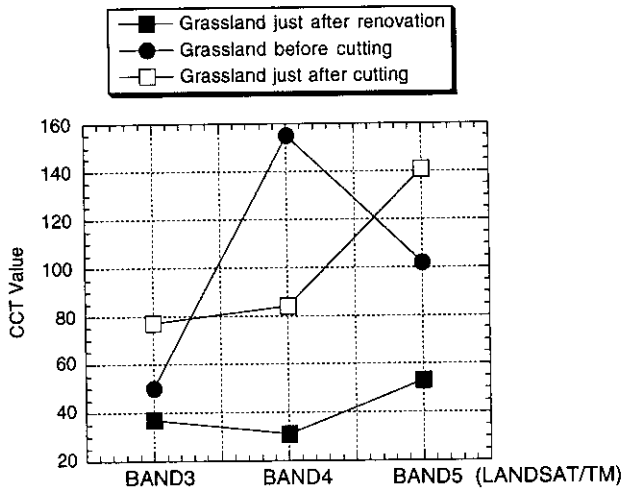

Fig. 2. Reflectance characteristics of grassland just after renovation

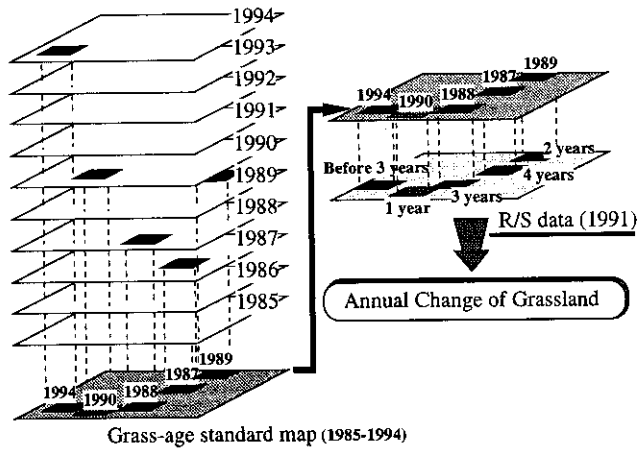

Fig. 3. Conceptual figure of annual change analysis

Suppose we have satellite data acquired from 1985 to 1994 and we are analysing the satellite data of 1991. For grassland coverage which renovated in 1990, we can extract 1-year old grassland reflectance. In the same way, for grassland coverage which renovated in 1989, we can extract 2-years old grassland reflectance. Further, using 1988, 1987, 1986, 1985 satellite data, we can extract reflectance of 1-year to 6-years old grassland. Such comparison is seemed to be annual change of grassland reflectance. Using this method, we study annual change of grassland reflectance in LANDSAT/TM data acquired in May and June respectively. The grass-age of annual change which was made clear in this study are listed in Table 2.

Table 2. The grassland age detectable in each satellite data

Satellite data	1993.6.8.	1992.6.28.	1991.6.26	1990.6.7.	1989.6.13.	1994.5.17	1989.5.19
Grassland age	1 year 2 year 3 year 4 year 5 year 6 year 7 year 8 year 1 year before renovation	1 year 2 year 3 year 4 year 5 year 6 year 7 year 1 year before renovation 2 year before renovation	1 year 2 year 3 year 4 year 5 year 6 year 1 year before renovation 2 year before renovation 3 year before renovation	1 year 2 year 3 year 4 year 5 year 1 year before renovation 2 year before renovation 3 year before renovation	1 year 2 year 3 year 4 year 1 year before renovation 2 year before renovation 3 year before renovation	1 year 2 year 3 year 4 year 5 year 6 year 7 year 8 year 9 year	1 year 2 year 3 year 4 year 1 year before renovation 2 year before renovation 3 year before renovation

(5) Grass-renovation status (1985-1994)

"Grass-age standard map" above mentioned has spatial information of grass-renovation. But, this map does not detect grass-renovation after satellite observation in the year. And, it does not detect grass-renovation 1-2 months before satellite observation in the year. So, extracting 1-year grassland from satellite data in addition to grassland just after renovation, we catch grass-renovation status of each year. Besides, we produce "grass-renovation years map (1985-1994)" by overlaing grass-renovation map of each year.

3. Results and discussions

(1) Annual grassland change in May data

For satellite data acquired in May, an increase in visible, near-infrared, middle-infrared reflectance with aging was observed. (Fig. 4.)

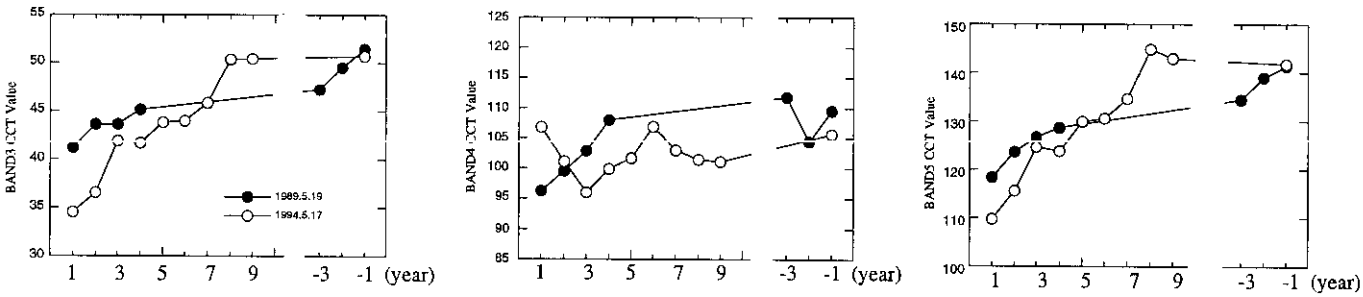

Fig. 4 Annual change of grassland reflectance in Landsat TM data acquired in May

In May, grass-field is covered with only a little vegetation. For satellite data acquired in May, reflectance of grassland is dependent on that of its background. On the ground, that is the background of grassland, an increase of dead leaves accumulation with aging was observed. Accumulation of dead leaves on the ground is a very little on the grassland just after renovation, or young grassland. Whereas, old grassland accumulation of dead leaves on the ground has a lot of amount. Dead leaves present bright color. Therefore, ground surface on which the accumulation of dead leaves exists appear to be brighter than ordinary bare soil. We considered that an increase in visible, near-infrared, middle-infrared reflectance with aging is due to the accumulation of dead leaves on ground surface. (Fig. 5)

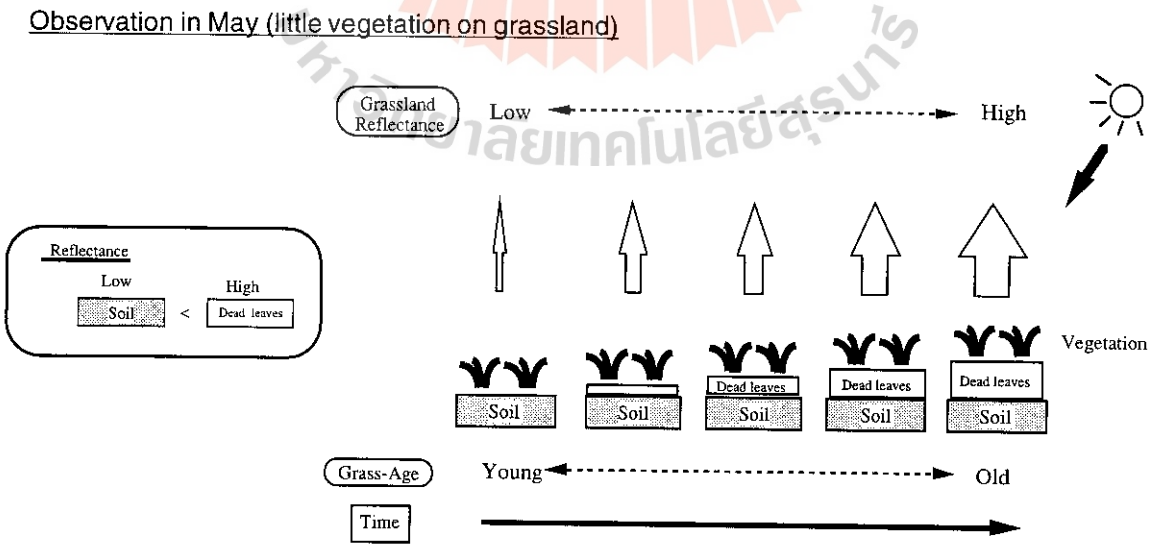

Fig. 5. Conceptual figure about annual change of grassland reflectance in data acquired in May

(2) Annual grassland change in June data

For satellite data acquired in June, a sudden decrease in near-infrared, middle-infrared reflectance was observed approximately in 4 years period after grass-renovation, while, visible reflectance maintain its constant value. (Fig. 6.)

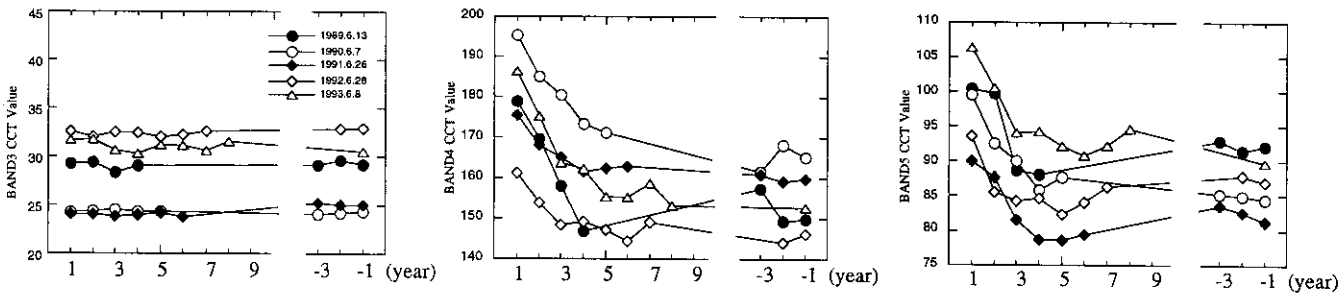

Fig 6. Annual change of grassland reflectance in Landsat TM data acquired in June

June is just before harvest season. Grass-field is covered with much vegetation. In June, grassland reflectance is considered to be dependent on its vegetation. In some previous field survey studies about annual change of grassland vegetation in Konsen area, the change of grass-species composition with aging had been reported. As a major change, it is reported that clover crown cover suddenly decreases and ordinary grass occupied mainly in approximately 4 years period after grass-renovation.

The decrease trend of near-infrared and middle-infrared reflectance and the decreasing trend of clover crown cover are similar. There is a structual difference between clover and grass, clover has a horizontal leaf angle distribution whereas grass has vertical. This means that for a given area and biomass clover may have higher reflectance than grass. Therefore, it is considered that young-age grassland with much clover crown cover has higher reflectance than old-age grassland with ordinary grass. From those, we considered that the major factor of the sudden decrease of reflectance is due to the change of grass-species composition with aging. (Fig. 7.)

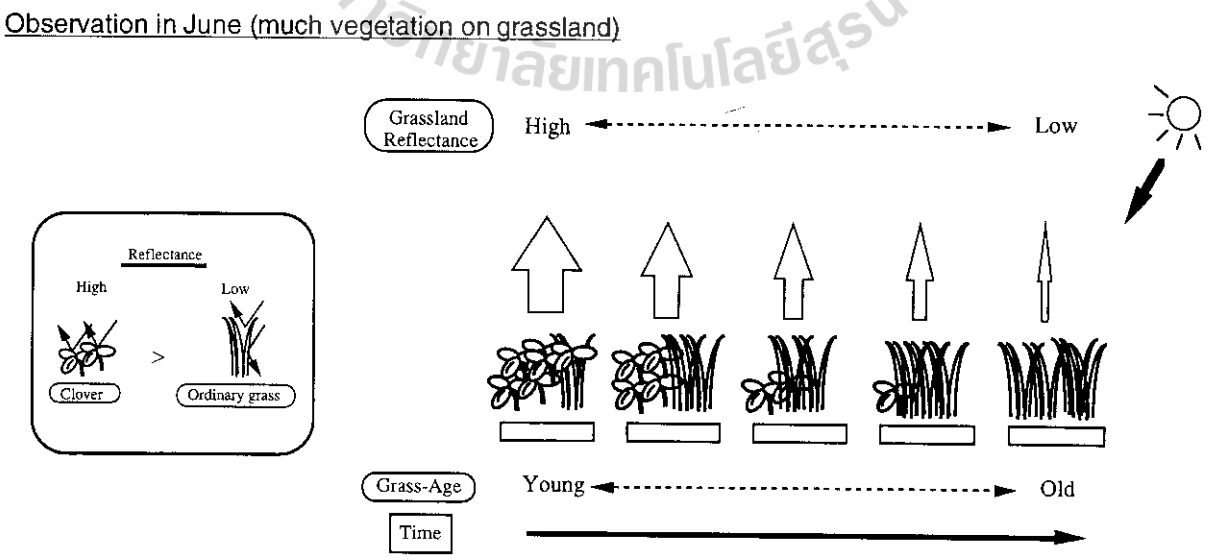

Fig 7. Conceptual figure about annual change of grassland reflectance in data acquired in June

(3) Grass-renovation status (1985-1994)

The results show that grass-renovation was conducted every year for about 7% of grassland in study site. However, on 1987, 1994, due to limitation of satellite data acquisition, we can not detect grass-renovation enough. Ground survey reported that grass-renovation percentage of total grassland in study site is 7-8%. And, grass-renovation year of the map from the satellite data agree with that of ground survey on about 80% grassland. (In some cases, plowing year and seeding year do not agree. In this accuracy assessment, we regard it as agreement that renovation year from satellite data was 1-year prior to the year from ground survey.) Those results show satellite remote sensing is very useful for survey of grass-renovation status.

Table 3. Grass-renovation status in study site

year	grass-renovation percentage of total grassland (%)
1985	7.1
1986	7.5
1987	5.5
1988	7.1
1989	8.6
1990	6.8
1991	7.0
1992	7.5
1993	7.0
1994	4.9

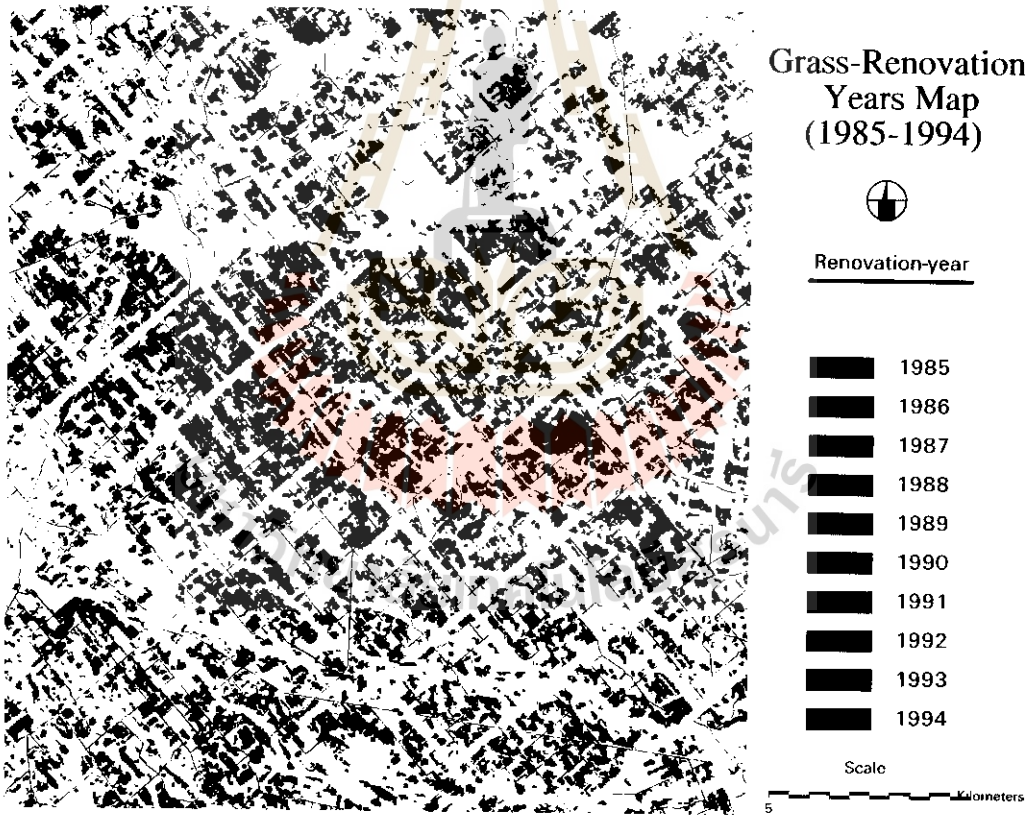

Fig 8. Grass-renovation years map (1985-1994)

4 Conclusion

In this work, we study annual change of grassland reflectance and grass-renovation status using multi-temporal satellite data. Those results show satellite remote sensing can distinguish different-age grassland, and also is so useful for grass-renovation survey. We concluded that satellite remote sensing will be an effective tool for grassland management.

MONITORING DEFORESTATION IN LUZON ISLAND, THE PHILIPPINES USING SATELLITE DATA

Akira HIRANO, Genya SAITO and Nobuyuki MINO

National Institute of Agro-Environmental Sciences (NIAES)
3-1-1 Kannondai, Tsukuba, Ibaraki 305, JAPAN
Tel : +81-298-38-8225, Fax : +81-298-38-8199

ABSTRACT

A comparison was made between a land use map derived from remote sensing data and an existing land use map. A GIS (Geographic Information System) was implemented to evaluate the land use change of Camiling district, Luzon island, the Philippines. Deforestation in the study area was evaluated. Soil/Vegetation matrix method was used to create land use map from MOS-1/MESSR data. Two satellite data taken during the dry season and the rainy season, respectively, in the study area were used to make the classification more accurate.

Following procedures were taken for both satellite images taken during the dry season and during the rainy season in 1990. Pixels of the image were classified according to their VCR (Vegetation Coverage Ratio) and SDI (Soil Dryness Index) using a matrix. Classified images derived from two different seasons were then logically related to each other to generate the satellite-derived land use map. Land use information was extracted from an existing topographic map published in 1977. The information was then input to a GIS (Geographic Information System).

Land use maps of two different times were logically overlaid onto each other to evaluated the land use change happened during the period. Clear decrease in forest area, namely deforestation was monitored. Forest area in the Camiling district was about 457 km^2 in 1977, whereas it was about 246 km^2 in 1990. It had shrunk by about 48 percent. Spatial analysis showed that 45 percent of the ex-forest area turned into paddy field.

1. INTRODUCTION

Recent deforestation in Asia has come to be one of the most pressing environmental problems. The major causes of deforestation in Asia are commercial logging, shifting cultivation, transmigration, acquiring of fuel woods, forest fire, agricultural development, resort development, mining and urbanization.

Deforestation leads such deterioration of natural conditions as follows (Murai, 1991):

1) Run off ratio increases resulting in flash flood.
2) Water level and volume of ground water decline.
3) Wild animals and species become extinct.
4) Soil is eroded or degraded.
5) The climate may change to dry weather condition; characterized by less rainfall, higher temperature and more evaporation.

Land use map is one of the most important thematic maps because it provides the present status of land use and pattern of its change. Land use change is very fast in Asia. Up-to-date land use map is required for monitoring the urban and rural environment. This is why satellite remote sensing is widely used for land use/land cover mapping.

However, current digital classification technique has not sufficient accuracy for operational utilization. Using two independent parameters derived from the information on vegetation coverage and soil dryness provides us with higher accuracy in classifying land use patterns. Cross-examinatio n of two data sets from different seasons can raise the classification accuracy.

2. STUDY AREA

Camiling district was selected as the study area to evaluate a typical deforestation in the Philippines. The study ares is located at western-central part of Luzon island. It is about 150 km northwest of Manila City. The area covers about 25 km east to west, 27 km north to south and encompasses approximately 675 km^2. The area is located at the eastern foot of Zambales mountains, land use is mainly paddy field and tropical forest. Terrain consists of relatively flat alluvial plain and steep mountain slope with elevations ranging from 20 to 1180 meters (Figure 1).

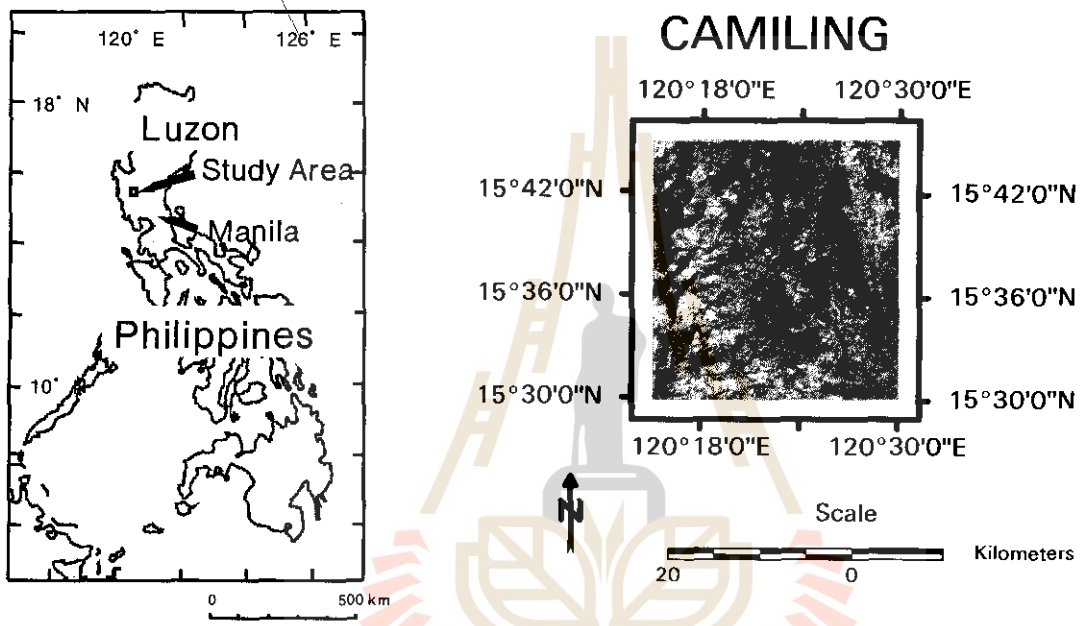

Figure 1. The study area (Camiling district, Luzon island, the Philippines).

3. DATA

3.1 Satellite data

Two MOS-1/MESSR data (Path-Row : 29-98W) that cover the western-central part of Luzon island taken during the dry season (February 1, 1990) and the rainy season (October 31, 1990) were utilized to create the land use map. These satellite images include the study area.

In order to minimize the effects of sun elevation when comparing the data obtained in different seasons, radiometric correction was applied to these multi-temporal images. Each CCT value in the image was divided by $\sin\theta$, where θ is the sun elevation at the date when the satellite data were acquired. The images were then geo-coded to UTM coordinate system. Geo-coding was performed using 1:50,000 scale topographic maps published by NAMRIA (National Mapping & Resource Information Authority) .

3.2 Existing map

As for the existing map, topographic map at a scale of 1:50,000 compiled and published by NAMRIA in 1977 was utilized.

4. ANALYSIS AND DISCUSSION

4.1 Land use classification procedures using soil/vegetation matrix method

Using soil/vegetation matrix method, pixels in the satellite image were classified according to their vegetation coverage and to their soil dryness. The procedures are described as follows.

4.1.1 Vegetation Index

To evaluate the vegetation coverage information, K-Vegetation Index (KVI) was utilized. KVI is a vegetation index based on reflectance of vegetation in near IR wavelength as shown schematically in Figure 2 (Yoshida et al. 1993). KVI is given by

$$KVI = Band3 - (a \times Band2 + b) \quad (1)$$

where a and b are constants. Here a is obtained from the slope, and b is the y-segment of the least square line fit through the data points that constitute the description of bare soil on the scatter plot of band 2 versus band 4. This regression line is conventionally called the Soil Line. Band2 and Band3 are the CCT (computer compatible tape) values of the pixel concerned at MOS-1/MESSR band 2 (Red: 610-690 nm) and band 3 (IR: 800-1100 nm), respectively. Using KVI, Vegetation Cover Ratio (VCR) was then calculated for each pixel to estimate the proportion of vegetation coverage to the area of the pixel concerned. VCR is given by

$$VCR = KVI / KVI_{max} \quad (2)$$

where KVI_{max} is the maximum value of KVI recorded in the image of the study area. VCR of any pixel on the Soil Line is equal to 0 for there is no vegetation on these pixels. Pixels in the image were classified into 5 levels according to their VCR values from high to low.

4.1.2 Vegetation Cover Ratio

To evaluate the soil dryness information, Soil Dryness Index (SDI) was utilized. SDI, referred to as Soil Index (SI) by Fukuhara et al.(1979), is sensitive to the soil brightness, which depends on soil moisture and soil organic matter conditions. SDI is given by

$$SDI = \arctan \frac{P4 - Band4}{Band2 - P2} \quad (3)$$

where P2 and P4 are the x-coordinate (Red) and the y-coordinate (NIR) of the pixel that has the maximum vegetation coverage, respectively. The higher the SDI value of a pixel, the drier the soil of the pixel is. Pixels were classified into 5 levels according to their SDI values from high to low.

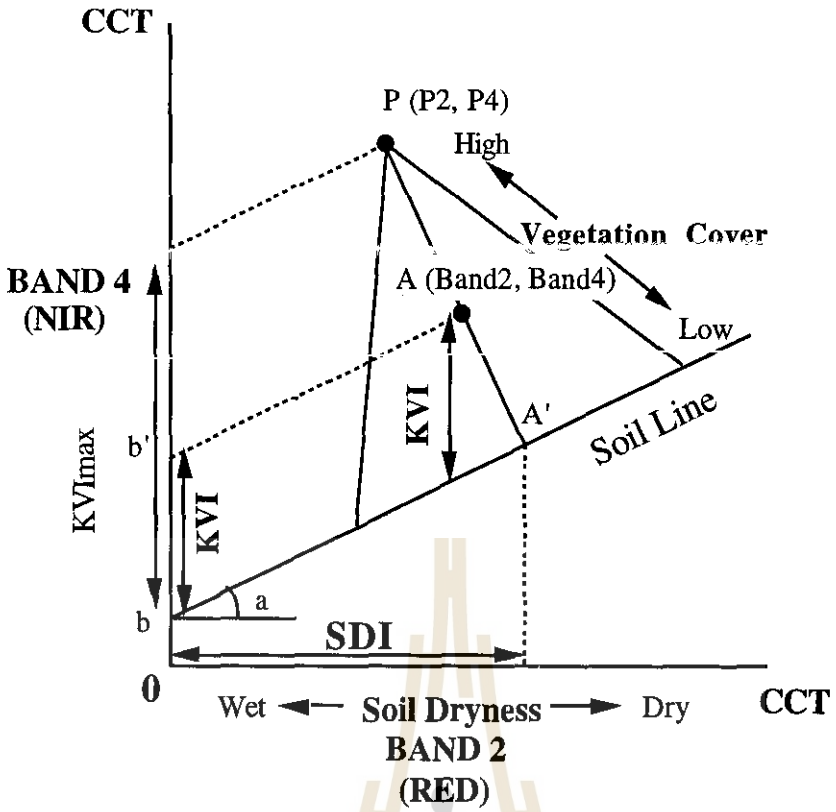

Figure 2. Conceptual figure of KVI, VCR, and SDI.

4.1.3 Soil/vegetation matrix method

Each pixel was distributed over 5×5 matrix of VCR and SDI, and they were classified into 8 classes according to their land cover conditions (Figure 3).

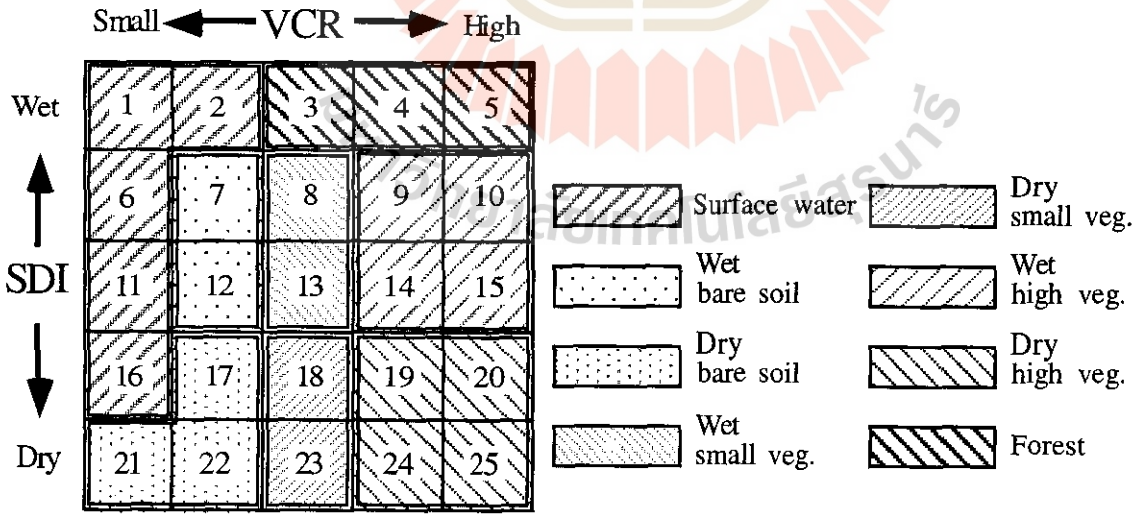

Figure 3. Soil/vegetation matrix according to VCR and SDI.

4.1.4 Re-classification

Soil/vegetation matrix method was carried out to both images taken during the dry season and the rainy season that resulted in two sets of land use/land cover classified images. Using GIS overlay function, these two images were cross-examined to generate a re-classified land use map to make the land use classification more accurate. Classification classes were determined in order to keep the consistency with the classes derived from the existing map. Those are (1) Water, (2) Fish pond, (3) Bare soil, (4) Upland farming field, (5) Paddy, and (6) Forest.

Land use information was extracted from an existing topographic map compiled and published by NAMRIA in 1977. In order to maintain the consistency with the satellite-derived land use map, land use information was digitized with the aid of GIS software so that overlay analysis can be carried out. At the same time, major roads and rivers in this area were also digitized to make the geographical registration easier.

4.3 Land use change analysis

Satellite-derived land use map and the land use map derived from the existing map were input into a GIS to perform an overlay analysis in order to detect the land use change happened between 1977 and 1990. With the help of GIS, spatial distribution of land use change was also detected. Distinct deforestation was monitored during the period. Considerable amount of forest area decreased by nearly half (Figure 4). Of 4.6×10^2 km^2 of forest area in 1977, 2.1×10^2 km^2 turned into paddy in 1990. This explains 93.9 percent of the total loss of forest area (Figure 5).

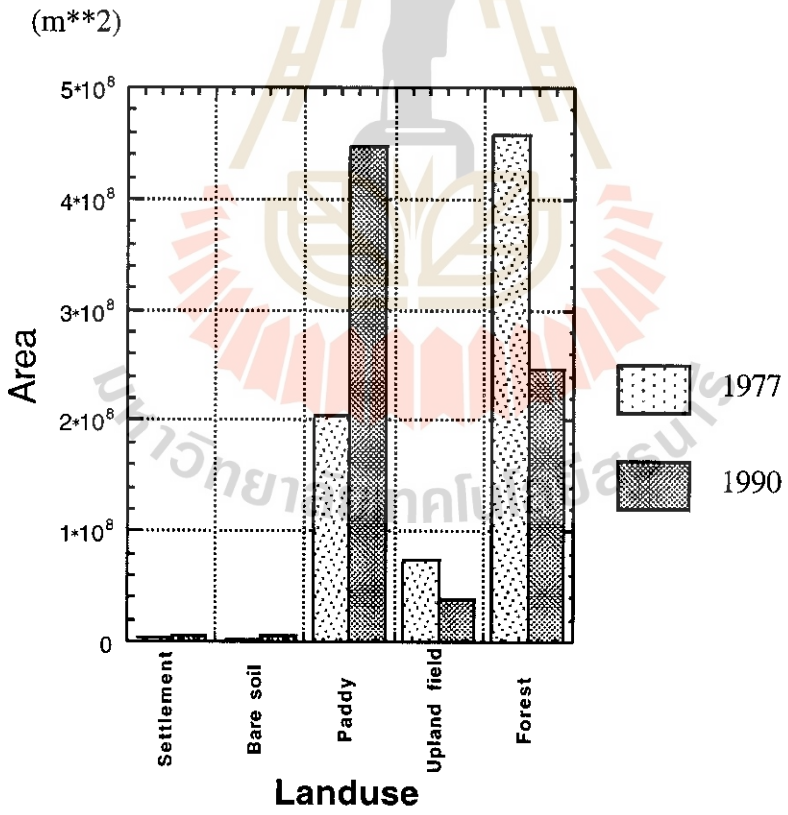

Figure 4. Land use change for settlement, bare soil, paddy, upland field, and forest : 1977 to 1990.

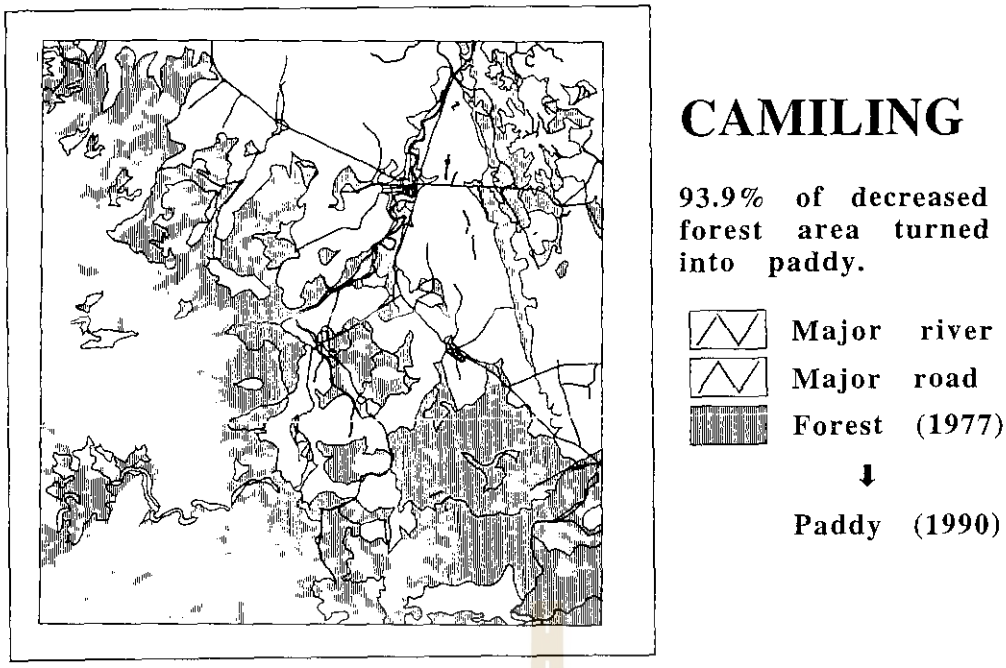

Figure 5. Spatial distribution of land use change (Forest (1977) -> Paddy (1990)).

5. CONCLUSION

Deforestation in Luzon island, the Philippines was monitored and evaluated both numerically and spatially with the help of soil/vegetation matrix method and GIS technique. From 1977 to 1990, a considerable amount of forest area turned into paddy in the study area. Soil/vegetation matrix method, a land use classification method using the information on vegetation coverage and on soil dryness is effective to generate a land use map from satellite data. Using two sets of satellite data acquired during the dry season and the rainy season, respectively, makes the classification accuracy higher.

ACKNOWLEDGMENTS

Part of this study was made as the cooperative work with National Space Development Agency (NASDA) of Japan. The authors are grateful to NASDA for providing the MOS-1/MESSR data.

REFERENCES

1. Fukuhara, M., Hayashi, H., Yasuda, Y., Asanuma, I., Emori, Y., and Iisaka, J., "Extraction of soil information from vegetated area.", Machine Processing of Remotely Sensed Data Symposium, pp.242-252., 1979.
2. Murai, S., "Application of remote sensing in Asia and Oceania. - Environmental change monitoring -", (Asian Association on Remote Sensing: Murai, S.), 1991.
3. Yoshida, M., Rondal, D.J., Evangelista, M.A.M., and Saito, G., "Land-use/Land-cover analysis by the matrix method using remote sensing", *Asian-Pac. Remote Sensing J.*, Vol.5, pp.79-84, 1993.

Mask Procedure for Effective Classification and Expression on Mangrove Area with TM Data of Landsat 5

Kazuhiro SATO*, Dwi SETYONO* and Kenshi TAKEZAKI**

*** : College of Agriculture, University of the Ryukyus,**
Senbaru 1, Nishihara, Okinawa, 903-01 Japan
Tel. 098-895-2221 (Ex.2912), Fax. 098-895-2864

****: Information System Department, Kankou Co., Ltd.,**
Higasinoda 1-6-1, Miyakojimaku, Osaka, 534 Japan
Tel. 06-351-1416, Fax. 06-351-3398

Abstract

In this paper, a mask procedure as a preprocessing, preparing two sets of secondary imagery data using respective mask, separated classification of the inside and outside of a mangrove area were proposed and tried for the effective classification and expression on a mangrove area. The product took two forms of overlaying classified result of the inside to the classified result or three bands color composed image of the outside.

For the mask and following procedures, manual designation and input of threshold values, and functions in an imagery analysis system such as binarization with two values(black and white), reversing and synthesizing two images, were used. Although imagery data of Band 4 and 5 were basically used in this procedure, using the data of Band 7 with Band 5 was more effective according to circumstances.

1. Introduction

Mangrove is a unique plant society as an important ecosystem distributed along the coastal sea and river mouth soaked in brackish water in the tropics and subtropics extensively. It is composed with many woody and several herb species, has supplied materials and stuff of the traditional use from house down for the local people, has cultivated coastal marine resources such as many kinds of crab, prawn, shrimp, small fish and so on, and further more has performed disaster preventive functions against the wind, waves and current from the sea and river. Although the management, control, working and operation methods as mangrove forestry had been established for the production of charcoal, firewood and thin log in some Southeast Asian countries, since the 1970s mangrove forest has been intensively cut for the chip production of pulp at each place in such countries. The cutover land has been diligently reforested, but it must be admitted that reforestation does not catch up with cutting. And in mangrove area, the change in land use has been proceeded on a very extensive scale than the disparity between cutting and reforestation of mangrove forest. The major changes are for digging and making fish ponds, prawn nurseries, reclamation for harbor facilities, industrial and residential sites.

In such situation the significance of mangrove ecosystem is reconsidered and many citizen's groups begin to reforest mangrove here and there. Administrative organs also regard management and control of mangrove areas as important for the sustainable forestry and conservation of the environment and start making efforts to grasp the present circumstances of mangrove forest and collect information on it for the establishment of a guideline on delicate management and control of it. But in many countries, it is not enough to collect and sum up the fundamental data such as distribution, area, species composition, tree height, trunk diameter, stand volume and so on because mangrove forest has been placed as the others. If the numerical values on mangrove forest in the world are asked, the distribution of species and total area should be had by fair means or foul, however it must be allowed that the source materials are derived from various survey methods and years ranged for the order of ten years.

In consideration of the situation mentioned above, many trials to extract mangrove areas using remote

Presented at the 16th Asian Conference on Remote Sensing in Nakhon Ratchasima, Thailand, November 20 - 24, 1995

sensing have been reported[6], and in most of the trials it was placed as one category among many categories for land use/cover. It generally corresponded with something to be desired and had produced some degree of accuracy. By reason of that necessity of detailed information on mangrove area will increase in future, the authors have investigated fundamental problems to link up with the detailed classification and estimation of resources. The effectiveness for some by band ratio of reflectance had been suggested to separate mangrove species in Okinawa based on the measurement of reflectance from crown layer by a photometer[5]. The significance was investigated on the distribution of dots for CCT count of TM data of Landsat 5 and by band ratio in a three dimensional space, and the possibility was suggested to classify mangrove species and the surroundings into more detailed categories[1,2,3]. In case of a trial to classify a mangrove area into some categories in a wide area including many categories, errors in classification had occurred like distributing mangrove in the mountain.

In this paper, mask procedure was proposed and tried as an effective method for the classification and expression on mangrove areas.The way of thinking and procedures were described paying our attention to the features of mangrove areas recognized in Band 4 and 5 of TM data of Landsat 5.

2. The way of thinking and procedures

Mangrove areas as a type of swamp occurs distinctively between the waters of the coastal sea and brackish water in the mouth of a river, and land not to be soaked in. This matter is markedly different from the other types of swamp and becomes a key to extract mangrove areas. From this it can be derived that the inside and outside of mangrove area is separately classified after extraction and definition of mangrove areas.

Mangrove areas are covered with many terns, fern and grasses. Land hardwood forest, maritime forest, swampy grass land, mud flat and waters are generally given as the neighboring categories with mangrove areas. In an image of Band 4, a mangrove area gives similar high reflectance to the other vegetation and has a clear boundary with large difference of CCT count between itself and the waters or mud flat. On Band 5 it has a boundary between itself and land area not to be soaked with a tide as it's forest floor is similarly soaked with a tide to mud flat. For two mangrove areas in the mouth of the Inderagiri River, Riau, Sumatera and the Nakama River, Iriomote, Okinawa, two images (digital values from 0 to 225 correspondence from black through gray to white) of Band 4 and 5 were shown in Fig.-1 with profiles of CCT count across a mangrove area. From the profiles, threshold can be easily designated for the binarization to make respective mask.

Through separate classifications of the inside and outside of mangrove areas, it becomes possible to make the error in the classification small and also to express mangrove areas effectively focusing our attention on them self. Mask and following procedures were described below.

1) Designation of the threshold value in Band 4 and binarization: image A (mangrove and land area to white of 255, waters to black of 0)
2) Designation of the threshold value in Band 5 and binarization: image B (land area to white of 255, mangrove area and waters to black of 0) -If there are many bare fields or rock exposures in a subject area, it is more effective to add the binarized image of Band 7 with a threshold value on mangrove areas to image B-
3) Subtraction of B from A: image C (the inside of mangrove area to white of 255, the outside to black of 0) -If there are remained white part shadows in the mountain and shallows, crests in the sea, it is effective to give them black of 0 using a software like painting.-
4) Reverse of image C: image D (the inside to white of 255, the outside to block of 0)
5) Subtraction of C from images of each band: imagery data set to classify the outside (the inside to black of 0, the outside to gray between 0 and 255)
6) Classification and three bands color composition of the outside: image E and F (the inside to black of 0)
7) Addition of D to images of each band: imagery data set to classify the inside (the outside to white of 255, the inside to gray between 0 and 255)
8) Classification of the inside: image G (the outside to black of 0 as the others)
9) Overlaying: image H and I (Classified the inside is separately overlaid to E or F classified and three bands color composition of the outside.)

Above mentioned mask and following procedures were shown as Fig.-2. This masking produced higher

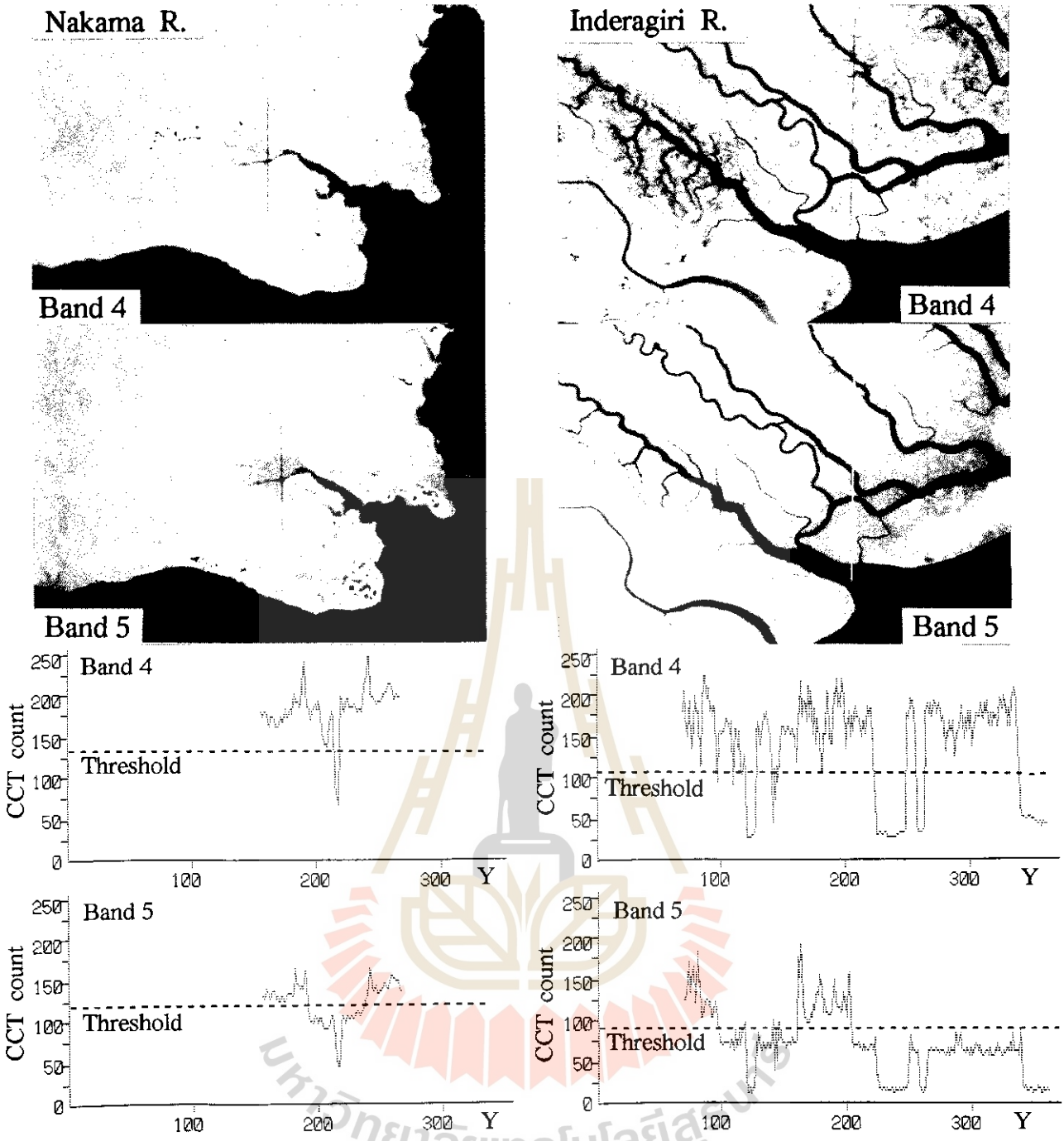

Fig.-1 Images and profiles of CCT count across a mangrove area of Band 4 and 5 for two mangrove areas in the mouth of Nakama River, Iriomote, Okinawa and the Inderagiri River, Riau, Sumatera

positional accuracy with the designation of appropriate threshold value than using a mouse or track ball on the CRT. Although a slightly similar method for updating land use data was reported, the NVI image and false color image were used to discriminate the waters and land or vegetation and non-vegetation area[4].

3. Practice of mask and following procedures

It is better to set some lines across mangrove areas in a image for designation of the threshold. Binarized images were saved as A from Band 4 and B from Band 5. In the case of masking for the data of Iriomote Island, it was effective to use Band 7 with Band 5 as there were many plowed farms, bare fields and rock exposures around mangrove areas. A painting software was used to give black of 0 to remained white parts without mangrove areas in the produced image by subtraction of B from A. The modified image was saved as a mask to cover the inside and outside of mangrove areas.

Imagery data of C was subtracted from the data of each band for the preparation of data set to classify the outside. Each data kept its own data in the outside and had 0 of black in the inside. Imagery data of D was added to the data of each band for the preparation of data set to classify the inside. Each data in this set kept its

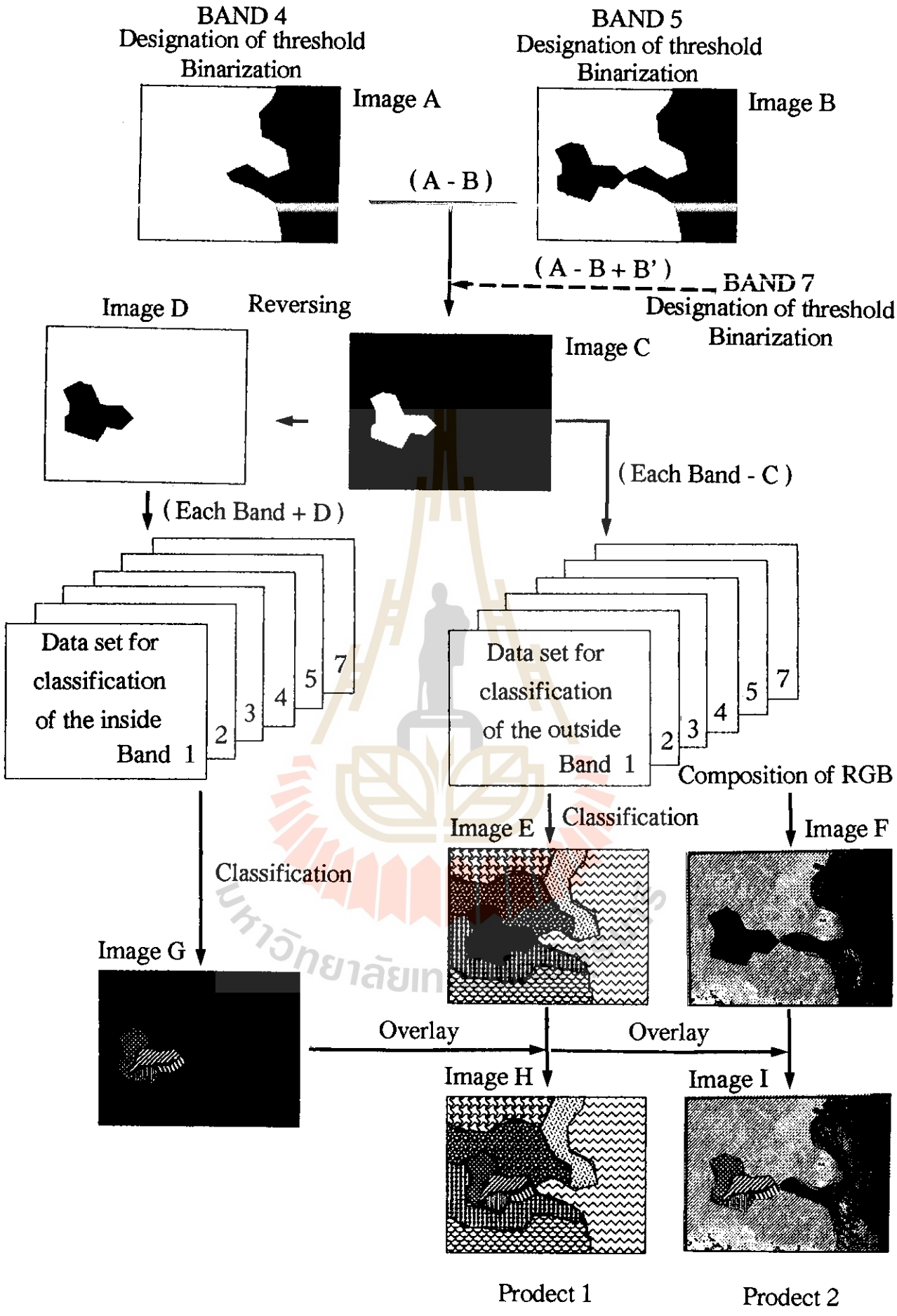

Fig.-2 Conception of Masking and following procedures

Image A

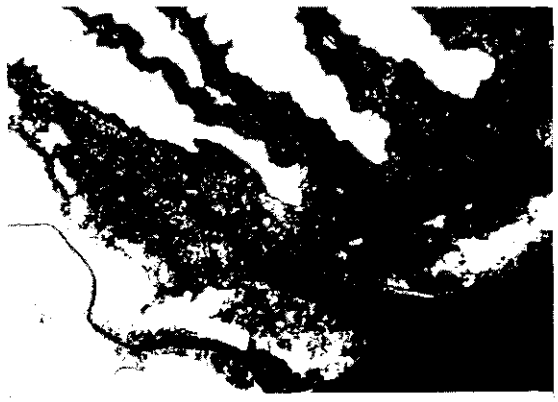

Image B

Image C

Image D

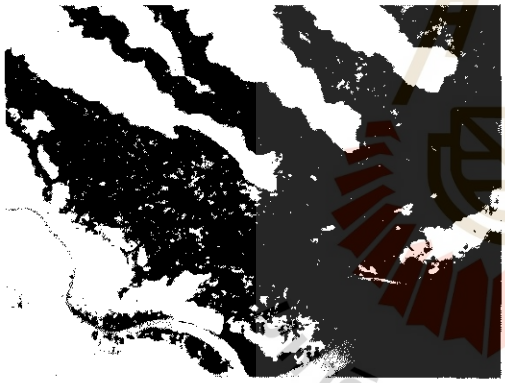

Imagery data of Band 4 for the outside

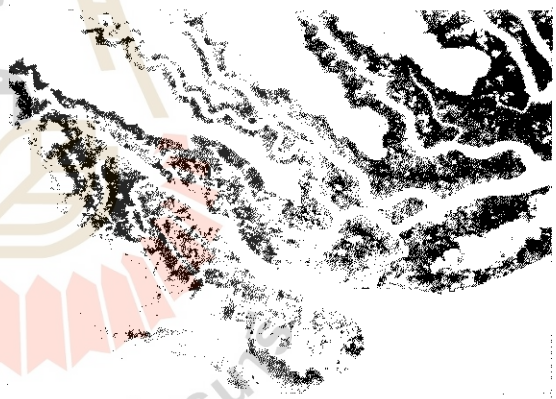

Imagery data of Band 4 for the inside

Imagery data of Band 5 for the outside

Imagery data of Band 5 for the inside

Photo.-1 Examples of images produced from masking and following procedures shown as Fig.1

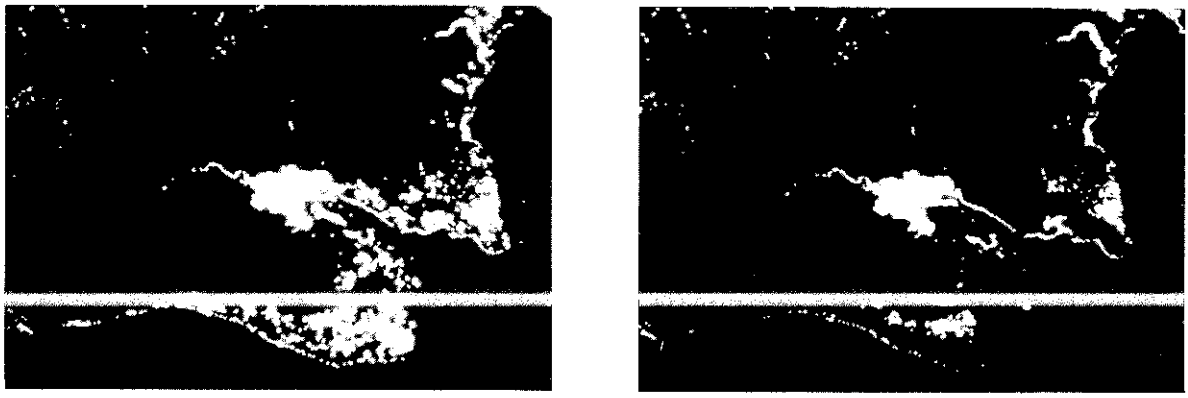

(A - B)　　(A - B + B')

Photo.-2 Comparison of Image C in Iriomote between (A - B) and (A - B + B')

own data in the inside and had 255 of white in the outside.

Mentioned process above was a mask procedure. The preparation was completed for separate classification of the outside and inside or three bands color composition of the outside. Binarized images in this mask procedure and examples in two data sets prepared for classification of the inside and outside were shown in Photo.-1, and two images were shown in Photo.2 to compare the effect using Band 7 with Band 5.

For classification of the outside, a fit classifier was applied to the prepared data set with image C and each band. Color images were composed with RGB corresponded to three bands within the set as true color, natural color or false color image. From these procedures, image E and F were produced. Classification of the inside also was similarly done to produce image G corresponding the outside to black of 0.

Finally G was overlaid to E to produce image H as a classification map and to F to show a classification of mangrove areas emphatically.

Mask and following procedures described above was effective for more detailed classification and clear expression of mangrove areas.

4. Conclusion

Mask procedure was proposed and tried as a preprocessing to classify mangrove areas detailedly paying our attention to the features in Band 4 and Band 5. By this procedure it became possible to classify mangrove areas without interference from each category giving similar spectral reflectance in the inside and outside. It produced to raise accuracy and clearness of classification of mangrove areas. A system packaged this way of thinking and procedures is expected to be effective for the establishment of the management and control methods of mangrove areas.

References

1) Dwi Setyono & K. Sato : Similarities between Mandah, Sumatera and Iriomote, Okinawa on the Distribution of TM data of Land sat 5 in the Multidimensional space for Mangrove and Surroundings, Proc. of the International Symposium on Vegetation Monitoring, 298-303,(1995)
2) Dwi Setyono & K. Sato : Structure of Thematic Mapper Data of LANDSAT 5 for mangrove Area in the River Mouth of Inderagiri, Riau, Sumatera,Proc. of the 15th ACRS, Vol.2,G-5-1-6,(1995)
3) Kohei Cho, H.Simoda ,T.Sakata &M.Yoshimura : Use of Vegetation Index of Satellite Data for Updating Land Use Data in Japan, Proc. of the International Symposium on Vegetation Monitoring, 267-274,(1995)
4) Sato, K., D. Setyono & S. E. Dah : Structure of Satellite Data for Mangrove Area in Okinawa (1) - Structure of TM Data of LAND SAT 5 for Mangrove Area in Iriomote Island -,Proc. of the 14th ACRS, E-3-1-6,(1993)
5) Sato, K., D.Setyono, O.D.Moraes & Hoshi, T.: Properties of Spectral Reflectance of Crown and Crown Structure of Mangrove Species in Okinawa, Proc. of PORSEC- 92, Vol.2,922-927,(1992)
6) S.Vibulsresth, B.Klankamsore, S.Ratanasermpong & C.Silapathong : Mangrove Forest Ecosystem and its Land Use Zoning by Remote Sensing, Proc. of the 7th ACRS, C-10-1-12,(1986)

RELATIONSHIP BETWEEN LAND COVER AND NOAA GVI IN THAILAND

Eiji KODANI *1, Haruo SAWADA *2

*1 Forestry and Forest Products Research Institute Shikoku Center
915 Asakuratei, Kochi-si, Kochi-ken, 780 JAPAN
E-mail : kodani@ffpri.affrc.go.jp

*2 Forestry and Forest Products Research Institute
1 Matunosato, Kukisaki-tyou, Inawasiro-gun, Ibaragi-ken, 305 JAPAN

ABSTRACT

In this study, effect of forest cover on NOAA Global vegetation Index(GVI) was discussed. Using climatic region map, Thailand was classified into 5 regions by humid months and elevation. In 5 climatic regions, correlation efficient and linear regression equation between forest area percentage and annual total GVI were calculated. Since gradient of all 5 equation are positive, annual total GVI increases with increasing forest area percentage in each climatic regions. Since intercept of 4 regression equation increases with increasing count of humid months, humid months affect annual total GVI not only forest land but also other land cover.

1. Introduction

Lately, growing demand for timber and agricultural expansion cause deforestation. Therefore, forest information is needed to assess them and remote sensing is hoped to provide this information. When using high resolution satellite data, for example, LANDSAT and SPOT, it is more difficult to observe land cover on country or continental scale than on regional scale, since monitoring land cover on larger scale make it more difficult to solve problems, for example, removing cloud, geometric correction and radiometric correction. By contrast to this, GVI data which are produced with meteorological satellite NOAA, are spatially continuous cloud free imagery, were corrected geometrically, and are corrected radiometrically*(1,2,3)*. These days, GVI data are published with CD-ROM and it is easy to handle data. In this study, relationship between GVI and forest cover was discussed.

2. Preparing data

GVI data were derived from "Global Ecosystems database" published by EPA/NOAA/NGDC. These GVI data are edited to monthly data. This CD-ROM include 69 month data from April 1985 to December 1990. For analysis 12 month GVI in one year were totaled up to annual total GVI(sigma GVI). To minimize fluctuation sigma GVI affected by climate fluctuation, sigma GVI was averaged from 1986 to 1990. Administrative division map on 1/2.5 million scale and climatic regions map on 1/4 million scale(Fig. 1) of Thailand which was published by Royal Thai Survey Department and forest cover map in 1985 on 1/4 million scale(Fig. 2)*(4)* were collected. Maps were digitized and converted to raster data. Forest cover map was digitized more finely than GVI mesh size and forest cover area percentage(Forest%) was calculated in each GVI mesh and projected on map. GVI and maps were managed with GRASS, GIS software on latitude longitude 1/6 degree mesh size. For analysis and plotting data, VisualSTAT(Statistica) was used.

3.1 Relationship between sigma GVI and forest cover

First, I discussed that forest cover affect sigma GVI in whole Thailand. When using LANDSAT imagery, Vegetation Index(VI) in forest cover is bigger than in other land cover. To reveal this trend about sigma GVI, with Forest% category as X axis and GVI as Y axis, data were plotted by not scatter plot but box plot(Fig. 3), since too many data prevent me from seeing diagram easily. This diagram shows that GVI increase with increasing Forest%. Correlation coefficient and linear regression equation between Forest% and sigma GVI was calculated(Table 1).

3.2 Relationship between sigma GVI and humid months

Second, I discussed that climate affect sigma GVI. In Thailand, rainfall affect vegetation activity and vegetation activity affect GVI. In other words, in dry season when rainfall is scanty, GVI is low, while in rainy season when rainfall is ample, GVI is high. Therefore, length of rainy season, or count of humid months affect sigma GVI.

In climatic regions map Thailand is classified into 4 climatic regions (i.e. A, B, C and D) by count of humid months. Climatic region A, B, C and D have 8-10, 6.5-8, 5.5-6.5 and 4.5-5.5 humid months, respectively. Climatic region A is named equatoropical climate and located in southern area or peninsula area of Thailand. Climatic region B, C and D is named tropical monsoon climate. Climatic region D is located in center of Korat plateau, and located around Kanchanaburi city and Nakhon Sawan city. Climatic region B and C surround climatic region A. Thailand is classified into 12 climatic regions, in detail. Since B5(mountainous with cool dry season in valleys) in these 12 climatic regions is located in higher land, rainfall effect on sigma GVI in B5 is different from effect in other 11 climatic regions. So for sigma GVI analysis, climatic region B is classified into two climatic regions, B5 and B except for B5.

To analyze effect of 5 climate categories, A, B except for B5, C, D and B5 on sigma GVI, data was plotted(Fig. 4). Fig. 4 shows that sigma GVI increases with increasing count of humid months except for B5.

3.3 Relationship between sigma GVI and forest cover in 5 climate regions

However, averaging Forest% in each climatic regions, A, B except for B5, C, D and B5 have 24%, 8%, 4%, 1 % and 42%, respectively. In 1985 forest is unevenly distributed. In other words, A and B5 climatic region have large forest cover, while B except for B5, C and D have small forest cover. Therefore, it is possible that since B except for B5, C and D have small forest cover, sigma GVI in these regions are low. Climatic region includes several types of land cover and affect GVI on whole land cover. Therefore, it is necessary to take account of humid months effect on sigma GVI, before analyzing Forest% effect on sigma GVI. In 5 climatic regions, or A, B except for B5, C, D and B5, correlation coefficient and linear regression equations between Forest% and sigma GVI were calculated(Table 1).

Table 1 shows that the more humid months, the more intercepts of 4 regression equations except B5. Intercept means sigma GVI in the case that there is no forest cover. In the other words, intercept is sigma GVI removing forest effect on GVI. Therefore, count of humid months affect sigma GVI. Table 1 shows that the higher Forest%, the higher sigma GVI since gradients in all regression equations are positive. Gradients of regression equation, or forest effect on GVI are different in 5 climatic regions, but form of regression equation in 5 regions are similar to form in whole Thailand.

3.4 Evaluation of regression equations

Hypothesis is defined, as follows.

H_0: $\rho=0$, H_1:$\rho\neq0$

(ρ: correlation coefficient of population, r: correlation coefficient of sample)

In the case that hypothesis H_0 is tested against hypothesis H1 at $\alpha=0.05$, in all equations H_0 is rejected. Therefore, it is false that Forest% doesn't correlated with sigma GVI. However, correlation coefficients r are small in A and B except for B5,.

In section 3.3 study, effect of forest cover on sigma GVI was discussed. Conversely, it was tested to estimate Forest% using sigma GVI for evaluating regression equations. Using regression equation of whole Thailand, Forest% was estimated and projected on map. This map is similar to Forest% map, roughly. However, estimated Forest% in climatic region A and B5 were higher than Forest%. Similarly, estimated Forest% in 5 climatic regions was calculated and projected. This map is more similar to Forest% map than the former map. Estimated Forest% in B5 were improved. However, in climatic region A and B except for B5, data where high Forest% data are have high estimated Forest% while some data where low Forest% data are have high estimated Forest%.

4. Discussion

Here, some reasons correlation coefficient is small were discussed. Roughly, reasons were classified into two, GVI error which occur when GVI data are produced, and other land covers except forest effect on GVI. The latter was discussed. Since GVI mesh area(about 18km*18km) is large, each GVI include several types of land cover. Each land cover has its own VI. To calculate VI accurately, it is necessary to take account of not only forest cover but also other land cover. But it is very difficult to collect several types of land cover map on country scale. Since in this study only forest cover map was took accounted with, it is possible other land cover affect sigma GVI.

Referencing land use by province of Thailand agricultural census in 1985*(5)*, in climatic region A, or southern part of Thailand 20% area is covered by land use item, or "under fruit tree and tree crops",

while other climatic regions have small area about this item. In case that VI in this item is more similar to VI in forest than VI in other items for example, paddy land, sigma GVI would increase and it would be difficult to recognize forest cover using sigma GVI. Besides climatic region A has long coast line. Since GVI is low in ocean, GVI in coast line is low. This would cause small GVI.

5. Conclusion

In this study, effect of forest cover on annual total GVI in 5 climatic regions and effect of humid months on annual total GVI were clarified.

For further study, it is better to collect forest and land cover map which are produced on larger scale and have more details category, and to use not only VI but also several channel of NOAA LAC or GAC data in order to obtain more details.

REFERENCES

(1) A.S.Belward, J.P.Malingreau, etc.(1991) Remote Sensing and Geographical Information Systems for Resource Management in Developing Countries, 169-187p, 253-278p, ECSC, EEC, EAEC, Brussels and Luxembourg.
(2) John, J.K.(1992),Global Ecosystems database User's Guide, National Oceanic and Atmospheric Administration(NOAA), Colorado.
(3) Katherine B. Kidwell(1990) Global Vegetation Index User's Guide 30 pp, NOAA, Washington. D.C.
(4) N, M.C., et al., (1991) The Conservation Atlas of Tropical Forests: Asia and the Pacific, 224-225p, Macmillian press Ltd., London and Basingstoke.
(5) Office of Agricultural Economics(1987), Agricultural Statistics of Thailand crop year 1986/87, etc., Bangkok.

Category	Regression Equation	r	n
Whole Land	Y = 0.017*X+3.17	0.562	1514
A	Y = 0.005*X+4.49	0.164	216
B except B5	Y = 0.007*X+3.67	0.215	177
C	Y = 0.021*X+3.35	0.375	401
D	Y = 0.029*X+3.11	0.314	224
B5	Y = 0.006*X+4.58	0.467	496

X(Forest%), Y(sigma GVI)

Table 1 Regression Equations

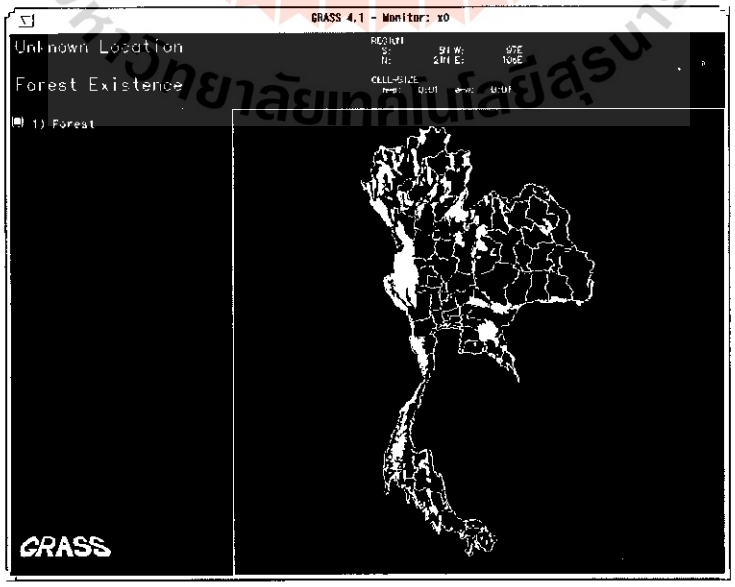

Fig. 1. Forest cover map

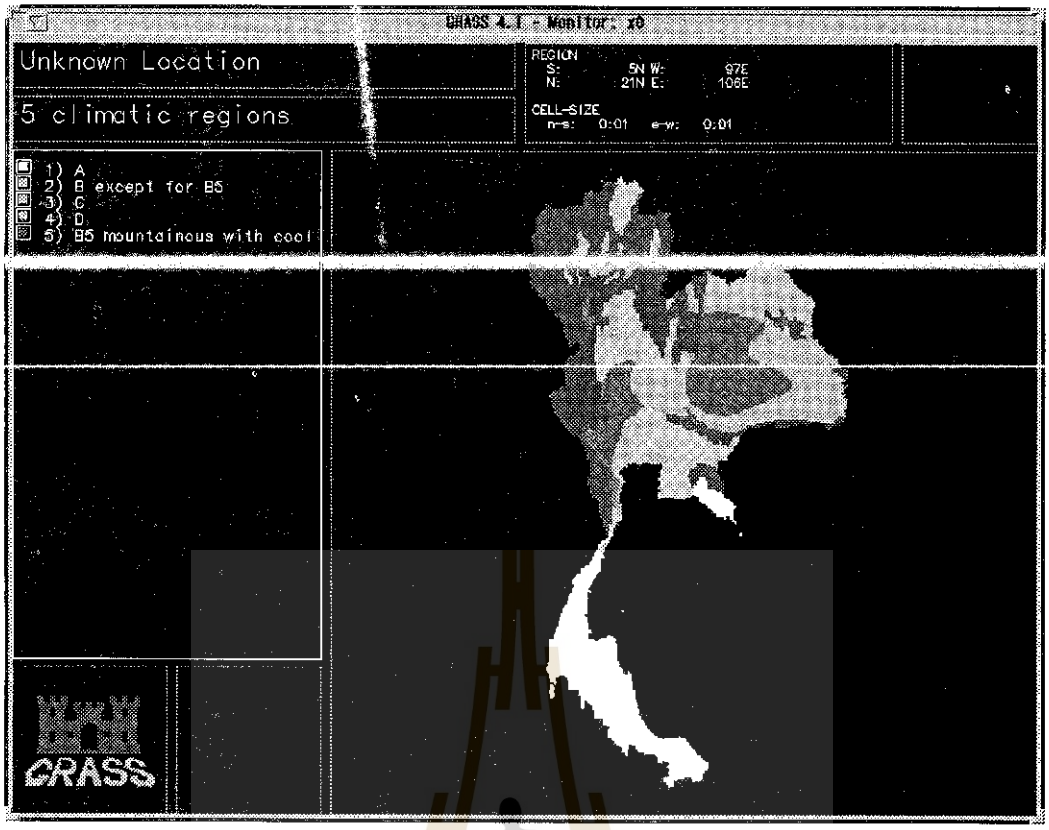

Fig. 2 Climatic region map

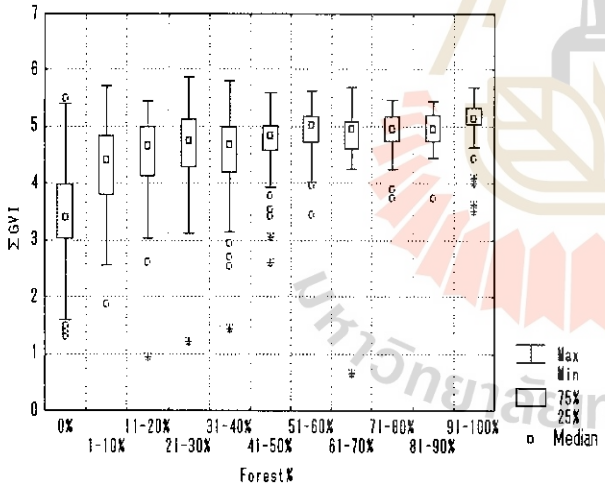

Fig. 3 Relationship between Forest% and sigma GVI

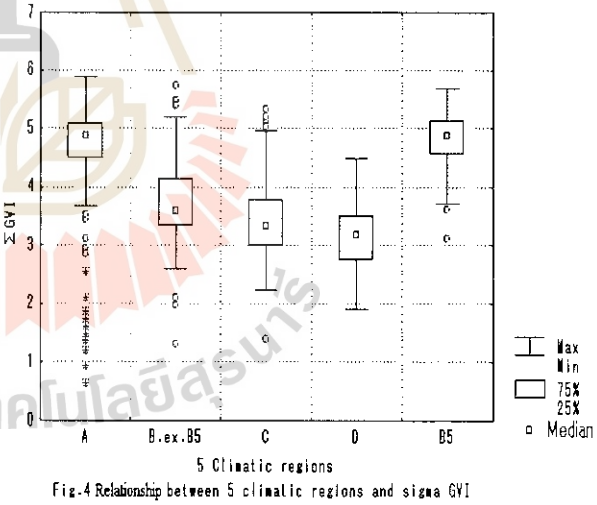

Fig.4 Relationship between 5 climatic regions and sigma GVI

DIFFERENCES OF SAR IMAGE BETWEEN JERS-1 AND ERS-1 TO LAND USE/LAND COVER INVESTIGATION

by

Anusorn Chantanaroj

Kenji Otsuka

Keisuka Katsuta

ABSTRACT

Since SAR data had been developed to use in remote sensing technology. Areas in South-West of Bangkok were selected to study the differences between JERS-1 and ERS-1 SAR images for land use/land cover application. It was observed that parameters influencing the backscatters were orientation of the object, incident angle and object height. Building oriented parallel to flight direction backscatter were very strong while object height which less than around 30 cm. would be very low . Angle of roof pitch was also one of the parameters influencing the RADAR backscatters.

INTRODUCTION

The joint research between the Geographical Survey Institute of Japan (GSI) and Department of Land Development of Thailand (DLD), funded by the Science and Technology Agency (STA) has been set up since 1992 to conduct researches on the development of remote sensing technology, using satellite data, particularly using ERS-1 and JERS-1 data in order to contribute environmental monitoring in tropical area. In 1993 project areas were carried out in Kanto Plain, Japan and Bangkok, Thailand to develop Manual of SAR Image Interpretation. In 1995, SAR images from JERS-1 and ERS-1 of the South-west of Bangkok were selected to study the differences between the two image data for land use/land cover application. Field verification was carried out in February 1995 and data analysis was done in GSI, Japan.

OUTLINES OF THE PROCEDURE

1. Collecting data
2. Specify area for field investigation
3. Field survey and get some information in the area
4. Discussion and report

METHODS OF IMAGE PROCESSING

1. Gray scale conversion from 16 bit to 8 bit data
2. Filtering
   - low-pass for noise removing
   - high-pass for image sharpening

RESULTS

JERS-1 SAR image acquired on 25 June 1992, path-row 127-277 and 127-278 resampling pitch 12.5 m, altitude 568 km, beam direction 35^{o}, frequency 1275 MHz (L band) and ERS-1 SAR image acquired on 10 August 1993, path-row 10684-3321 and 10684-3339, resampling pitch 12.5 m, altitude 785 km, beam direction 23^{o}, frequency 5.3 Ghz (C band), polarization VV, spatial resolution 30 m, swath 100 km were visually analyzed. Topographic maps on a scale of 1:50,000 and OPS image (1B 3G 2R) of JERS-1 of the same area were used in ground truth. From visual interpretation of SAR image and field observation, it was found that parameters which mainly influence differences of backscatters in SAR image from JERS-1 and ERS-1 are orientation of objects, vegetation height or object height and incidence angle.

Orientation of object is directly related to look direction. When the orientation of object is perpendicular to look direction, backscatters will be very strong. On the other hand backscatter will be very low when orientation of object is parallel to look direction.

Vegetation height or object height is one of the parameter which cause difference in backscatter. When object height is more than 30 cm backscatter in SAR image from ERS-1 will be strong while SAR image from JERS-1 will be very low backscatter. So weed and grass with 30 cm height can be observed by ERS-1 better than JERS-1. Incidence angle has an effect in urban and

built up land. In Thailand most of the angle of roof pitch are approximately 20°, backscatter to ERS-1 is stronger than JERS-1.

CONCLUSION AND RECOMMENDATION

There are tree main parameters influencing the backscatters from land use/land cover, they are orientation of object, vegetation height or object height and incidence angle. Urban area identification is easier ERS-1 SAR than JERS -1 image but some area it will be more clear from JERS-1 SAR image if object orientation is perpendicular to look direction. In agriculture land, backscatter will be stronger in ERS-1 image than JERS-1 SAR image, especially when vegetation height is less than 30 cm.

To use only SAR data to identify land use type, the result is not satisfied. To get best result, it is recommended to use SAR data together with other data from passive remote sensing system and also Geographic Information System.

ACKNOWLEDGMENTS

This project was funded by the Science and Technology Agency (STA). This support was greatly appreciated.

REFERENCES

Shunji Murai; Remote Sensing Note, JERS -1 1993

Rob Schuman; Microwave Remote Sensing, ESA, 1994.

B.N. Koopmans; Side looking Radar, ITC, 1991

Valairat Wanpiyarat; Synthetic Aperture Radar Image Interpretation annual Development Thailand Area, GSI 1994.

Wirat Thongma; Land use analysis by using remote sensing data, GSI 1993.

CHANGE DETECTION IN COASTAL ZONE BY REMOTE SENSING TECHNIQUE

by

Mrs.Valairat Wanpiyarat

Ms.Promchit Trakuldist

Mr.Boonrak Pattanakanok

Land Development Department, Ministry of Agriculture and Cooperatives, Thailand.

ABSTRACT

Because land use information was limited, therefore, the Landsat TM color composites, band 432 (RGB) acquired on May 29,1989, and band 453 (RGB) acquired on September 24, 1991, and September 10, 1992, were visually interpreted for land use changes detection in the coastal area of 340 km^2 at Amphoe Pak Panang, Nakhon Sri Thammarat province. The results of interpretation and field verification revealed that the increasing of shrimp farms , during the past three years, was up to 25.78 km^2 due to the encroachment of mangrove forest and land use change from paddy land to shrimp farming. Dispersed salt water, generated from shrimp farms, created soil salinity and water contamination to the nearby paddy fields, resulted in paddy abandonment. The total abandoned paddy field was found to be 17.80 km^2 The coconut and banana area increased about 9.84 km^2. Approximately 13.63 km^2 of the mangrove forest was destroyed and the highest depletion area, 9.72 km^2 ,was found between the year 1991 and 1992.

In addition, the Landsat TM images also showed that the coastal shore lines had been changed from year to year indicating the usefulness of satellite image for update mapping.

1. INTRODUCTION

The history of development of the Pak Phanang River Basin has long been more than 10 years. The first real development concept was created in 1980, with consideration of the Large-

Scale Project Section, the Project Planning Division, Royal Irrigation Development. Up to now, the serious problems in the Pak Phanang River Basin can be described as :

1. Shortage of fresh water for irrigation development and for domestic uses,
2. Salt water intrusion into the Pak Phanang River and tributaries which lasts about 9 months each year, causing shortages of fresh water into the lower Pak Phanang basin,
3. Conflicts of interest between rice farmers and marine shrimp farmers due to discharges of salt water from shrimp ponds into paddy fields, causing damages of rice fields along the coastline of the Gulf of Thailand, along the Pak Phanang River, and along the Khlong Cha Uad,
4. Annual flooding problems which usually occur in the period from November and December each year causing damages of houses, infrastructure, and agricultural areas of more than 1,248 km^2.

These serious problems have to be mitigated, and this is the reason why it is neccessary to develop the Pak Phanang River Basin. His Majesty the King, during his visits to Southern Thailand in 1992, gave the Royal Irrigation Department his concept of building salt water barrage at Ban Bung Pi, Tambon Hulong, Amphoe Pak Phanang, Nakhon Sri Thammarat province as well as a series of drainage canals in order to solve the above - mentioned problems.

In order to mitigate the conflicts between the rice farmers and the shrimp farmers in the area, land use zoning delineation between fresh water and saline water zone is very neccessary. Therefore, the Department of Land Development has carried out land use surveying, emphasizing on land use changes in the paddy area and the mangrove forest. Those existing land uses including the distribution of shrimp farms are basically required for creation of reasonable dividing line.

2. STUDY AREA AND OBJECTIVE

The study area is located between $8^0 15'$ to $8^0 30'$ N latitudes and $100^0 05'$ to $100^0 17'$ E longitudes covering about 340 km^2 in the Pak Phanang River Basin , eastern side of Nakhon Sri Thammarat province of the southern peninsula Thailand. Its physiography composes of bays, sandy beaches, river mouth, dunes, and tidal flat. The north side of the study area in the river mouth of the Pak Phanang River, is covered with mangrove forest while the rest mostly contains agricultural land (Figure 1).

Remote Sensing technology provides multiple, repetitive, and update physical information. For this research, the authors aim to apply remote sensing technology to monitor land cover and land use changes especially from mangrove forest and/or paddy to shrimp farm, and also estimate shrimp farming area in the study area.

3. METHODOLOGY

The methodology includes an analysis of temporal Landsat TM images, field verification, polygon overlay, and monitoring of land use changes.

An amount of three Landsat TM images, acquired on multidate between the year 1989 and 1992 and produced at scale 1 : 50,000, was visually interpreted for land cover / land use investigation. The qualitative comparison of land use changes was made during the period of these data.

To observe the circumstances, field verification was carried out in May 1992 and September 1993. In the field, land cover / land use, forest condition, soil and water condition were described and recorded.

To study land cover / land use changes, the multiple layers of previous interpretation maps were overlaid to create new polygons showing those changing areas. A number of changed polygons were examined and calculated for reporting.

4. RESULT AND DISCUSSION

Analysis of Land Cover / Land Use

Land use categories are distinguished on the color composite of Landsat TM band 234 and 354 (BGR), based on differences in color and texture. Those categories are recognized as : paddy, mixed fruit tree, shrimp farm, built up land, mangrove forest, marshland, and others. Paddy and mixed fruit tree are the major agricultural crops in the area. Both irrigated and non-irrigated paddy fields cover about 49 % of the total study area , 340 km^2. Mixed fruit trees area, ie; coconut, banana, and orange, were found to be approximately 7% in the year 1989. To identify the type of fruit trees from Landsat TM images without field checking is impossible. Active shrimp

farming areas, along the coast lines, along the Pak Phanang River, and in mangrove forest, are seen clearly from both combinations of Landsat TM. Dense mangrove forest can be recognized as bright red color with fine texture from the 234 combination and as peach color from the 354 combination. Amphoe Pak phanang is shown in bright blue color along both sides of the Pak Phanang River which flows downward from the river mouth to the south. The other land uses are marshland and abandoned paddy which can be identified by utilizing temporal data.

Land Use Change Analysis

An analysis of mechanisms of land use changes plays an important role in forcasting environmental changes. As the population increases, infrastructures develop, and economy blooms in the study area and its vicinity, these cause changes in the coastal environment and directly effect on the benefits of the farmers. Hence, we consider the factors of land use changes in the study area from the view point of human impact.

During the three years observed period, the major land use changes are as follow :

1. Changes from paddy to shrimp farming,
2. Changes from mangrove forest to shrimp farming,
3. Changes from paddy to abandoned paddy.

Figure 1 shows all of those changes from the year 1989 to 1992. Results from visual interpretation and field observation revealed that, during the year 1989 to 1991, paddy field had changed to be shrimp farm at the changing rate of 9.1 % and this change had slightly decreased to be 7.1 % during the year 1991 - 1992. Shrimp farming expanded dramatically, at the increasing rate of 116 % in the year 1991, from mangrove forest particularly in the north side of Amphoe Pak Phanang, to nearby paddy and to paddy along the coastal zone. The shrimp farming area was found to be 40.43 km^2 in the 1992 image while it was only 14.6 km^2 in 1989. Salt water, generated from shrimp farms, discharged into paddy fields causing soil salinity and water contamination. These problems had affected seriously to rice farmers by lowering rice yield to a very minimum, therefore, some of paddy fields were left abandon. The abandoned paddy area increased from 6.1 km^2 in the year 1989 to 17.89 km^2 in the year 1992. In the paddy fields and along stripped villages where were not affected by salt water, farmers planted fruit trees, coconut and banana, and this area rapidly increased approximately 9.84 km^2 within three years.

In spite of forest plantation at Laem Pak Phanang, mangrove deforestation still took place at the alarming rate due to shrimp farming. The destroyed mangrove forest area was found approximately 13.63 km^2 The highest depletion occurred between the year 1991 and 1992 with the rate of 8.62 % resulted in 9.72 km^2 loss.

In addition to the coastal land use changes, the extent of shore lines changes could be observed from the multi-temporal Landsat TM images. From the comparison among three images and information obtained from topographic maps, the findings could be summarized as follows :

1. The shore lines at the Pak Phanang River Mouth and along the Pak Phanang Bay advanced toward the sea due to forest plantation.

2. The north spit at Laem Talumphuk extended in a north - west direction to some extent (Figure 1).

5. CONCLUSION

Coastal land use changes can be monitored using overlay method of multi-temporal Landsat images. During the observed period of 1989,1991, and 1992, the major changes have been observed as changes from paddy and mangrove forest to shrimp farming as well as abandoned land. Rates of these changes are determined and total shrimp farming area is calculated. Shorelines movement is also detected from the study.

6. REFERENCE

1. F.A.O. 1982. Management and Utilization of Mangrove in Asia and Pacific Region. Environment Paper #3. Rome. F.A.O.
2. F.A.O. 1984. Mangrove forests in Asia Pacific Region : A Summary of Available Information. Bangkok. F.A.O.
3. Pheng, K.S. and Foo L.K. 1989. Detection of Land Use Changes Using Remote Sensing and GIS. Proceedings of the Tenth Asian Conference on Remote Sensing . November 23 - 29,1989. Kuala Lumpur, Malaysia.

a. May 29, 1989. Band 432

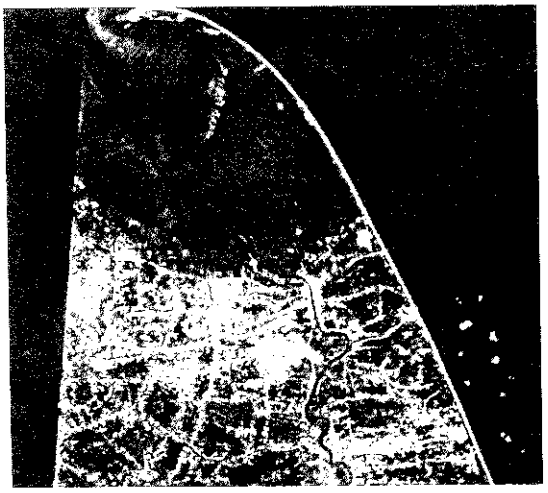

b. September 24, 1991. Band 453

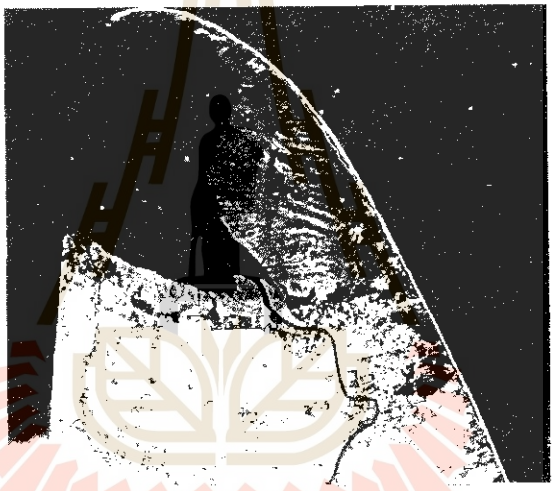

c. September 10, 1992. Band 453

Figure 1. Landsat images of the study area, acquiring on May 29,1989, September 24,1991, and September 10, 1992 respectively.

THE INTEGRATION OF REMOTE SENSING SYSTEM AND GIS FOR FOREST LAND USE PLANNING

Dr. Suwit Ongsomwang

Forest Resources Assessment Division
Forest Research Office, Royal Forest Department
Bangkok 10900. Thailand

ABSTRACT

In general, the applications of remote sensing to forestry in Thailand were mostly based on visual interpretation and the thematic data that were produced from the remote sensing data were still separated. The accuracy map acquired from the interpretation of aerial photographs at 1: 15,000 scale for forest and non-forest area in the past cannot be used as a base map for the interpretation of satellite imageries of scale 1: 250,000 at present. In fact, it leads to the inconsistency of the extraction data from Landsat imageries and also increases the time and cost for the ground truth survey. Actually, the integration of the thematic data with remote sensing data is limited because of using visual interpretation method. The main object of this study is to develop reliable method for integration of remote sensing system and the GIS for forest land use planning.

The method was developed by using the multistage remote sensing concept and the integration of remote sensing system and the GIS. In this study, Landsat images were used as the first stage for existing forest area classification. In the secondary stage, aerial photographs at the scale of 1: 15,000 were used for forest land use classification. In the third stage, ground verifications were conducted for collecting and generating the necessary information for forest land use planning. In addition, the geographic information databases that were designed for handling and processing spatial data of remote sensing and ancillary data were established under the exchangeable format of the image processing system and the GIS.

The main forest land types in the forest land use plan of the Ngao Demonstration Forest, Ngao District, Lampang Province are (1) non-forest area with no limiting conditions, (2) non-forest area with limiting conditions, (3) mining area, (4) community forestry area, (5) productive reforestation area, (6) productive forest area, (7) protective reforestation area and (8) protective forest area.

The results from this study shows that the integration of remote sensing and the GIS appears to have potential for providing the necessary information for forest land planing, particularly in classification of existing forest land uses and their status. In addition, forest land use planning which was conducted by using the GIS shows the new methodology to the manager and planner for making a forest land use plan.

1. INTRODUCTION

The application of remote sensing data in forestry in Thailand was mostly based on visual interpretation and the thematic data that were produced from the remote sensing data were still separated. The accuracy map that would be interpreted for forest and non-forest area in the past by using aerial photographs of scale 1: 15,000, for example, cannot be used as a basic map for the interpretation of satellite imageries of scale 1: 250,000 at present. In fact, it leads to the inconsistency of the extraction data from Landsat imageries and also increases the time and cost for the ground truth survey. Actually, the integration of the thematic data with remote sensing data is limited because of the visual interpretation. In addition an efficient geographic handling and processing system that transforms the thematic data into usable information does not exist.

At present the major tool for the geographic handling and processing system of the thematic data is the Geographic Information System (GIS). The GIS is a set of tools for collecting, storing, retrieving at will, transforming, and displaying spatial data from the real world for a particular purpose (**Burrough** 1986). The GIS evolved as a means of assembling and analyzing diverse data pertaining to specific geographic areas, using the spatial locations of the data as the basis for the information system (**Shelton and Estes** 1979). **Kalensky** (1992) stated that remote sensing and the GIS are closely related. They are complementary information technologies which are both needed and operationally used for natural resources mapping and inventories, natural disaster assessment and risk forecasting and for environmental monitoring. If they operated separately in institutes for management of natural resources, it would be harmful. It would result in costly duplication of various activities, training and some equipment and negatively affect the efficiency of project implementation. **Goodenough** (1988) also suggested that for the integration of remote sensing and the GIS, the remote sensing data must use the digital image analysis system.

The main objects of this study are to develop reliable method for integration of remote sensing system and GIS for forest land use planning.

2. STUDY AREA

Ngao Demonstration Forest area was chosen as the study area. The Ngao Demonstration Forest area extends over the headwaters of Ngao river in the north-west of Lampang province, Thailand down to its confluence with the Yom river on the Phrae province boundary, the boundaries being those of Ngao district. Most of the Ngao Demonstration Forest area that is in Ngao district, Lampang province lies between 18 °and 21.5 ' north, 99 ° and 45 ' east. The total area is about 1,751.59 sq. km.

3. METHODOLOGY

The basic concept for the development study method is employed from the "multi" remote sensing concept which was enunciated by **Colwell** (1975). Multistage remote sensing concept is used in this study. This concept encompassed the variety of remote sensing platforms and sensors that can be used in various combination, to acquire remote sensing data and also considered the processing, analysis and utilization methodologies available to practitioners in the field of remote sensing. In the multistage remote sensing approach, satellite data may be analyzed in conjunction with high and low altitude data, and ground observation. Each successive data source might provide more detailed information about geographical areas. Information extracted at any lower level of observation may then be extrapolated to higher levels of observation (**Lillesand and Kiefer** 1979). In addition, the geographic information databases that were designed for handling and processing spatial data of remote sensing and ancillary data were established under the exchangeable format of the image processing system and the GIS. **McFarland** (1982) stated that the establishment and maintenance of geographic databases in computer-readable form has great potential for supplying resource management information. To fulfill this methodology, a scheme of practical work on this study is shown in Figure 1.

4. RESULTS AND DISCUSSIONS

4. 1 Forest land utilization classification

Forest land utilization is classified by the normalized indexing operation of the four GIS images which represent the natural conditions and regulated conditions for forest land utilization in the study area. The areas and percentage of four input GIS images with their assessment and ranking for the normalized indexing operation are summarized in Table 1. The results of the normalized indexing operation are shown in Table 2. The results show that a relatively important value from 1 to 8 implies the suitability of forest land utilization from lowest to highest, respectively. In addition, the results also show the various alternatives in the classification. In this study, the determination of the three forest land utilization classes is a personal decision with the main objective of increasing the protective forest areas in the study area. The forest land utilization classification of the study area consists of unsuitability for forest area, suitability for productive forest area and suitability for protective forest area. They cover an area of 39,745.08 ha, 57,236.22 ha, and 78,178.14 ha, respectively. The results show that the proportion of the three forest land utilizations in the study area has been upgraded in comparison with the input GIS images.

4. 2 Combination of forest land utilization classification with a regulated forest utilization

In this study, the Temporary Cultivation Rights (STK) areas and mining concession areas GIS images, which represent the existing forest utilization by regulations in the study area, are combined with the forest land utilization classification by the maximum overlaying operation and the results are shown in Table 3. The results show that forest areas in the forest land utilization classification decreased from 135,414.36 ha to 133,404.84 ha after the combination existing forest utilization by regulations.

4. 3 Evaluation of the forest land utilization classification with the existing forest land use in 1989.

In this study, the existing forest land use in 1989 GIS image, which represents the social and economic factors affecting the natural resources in the study area, is combined with the forest land utilization classification with a regulated forest utilization GIS images by the unnormalized indexing operation. The evaluation of forest land utilization and existing forest land use 1989 are separately summarized as follows:

I. Unsuitability for forest area. The results show that existing forest areas which include the Mixed Deciduous forest, Dipterocarp Deciduous forest and productive reforestation areas overlap with the unsuitability for forest area. In fact, the existing forest areas cover an area of 15,991.92 ha or about 9.13 percent of the total study area. In the forest land use plan, the existing natural forest areas are assigned as the community forestry areas, while the existing productive reforestation areas are assigned as productive forest areas. In contrast, the existing non-forest area in the unsuitability for forest areas are assigned as the non-forest areas with no limiting conditions in the forest land use plan.

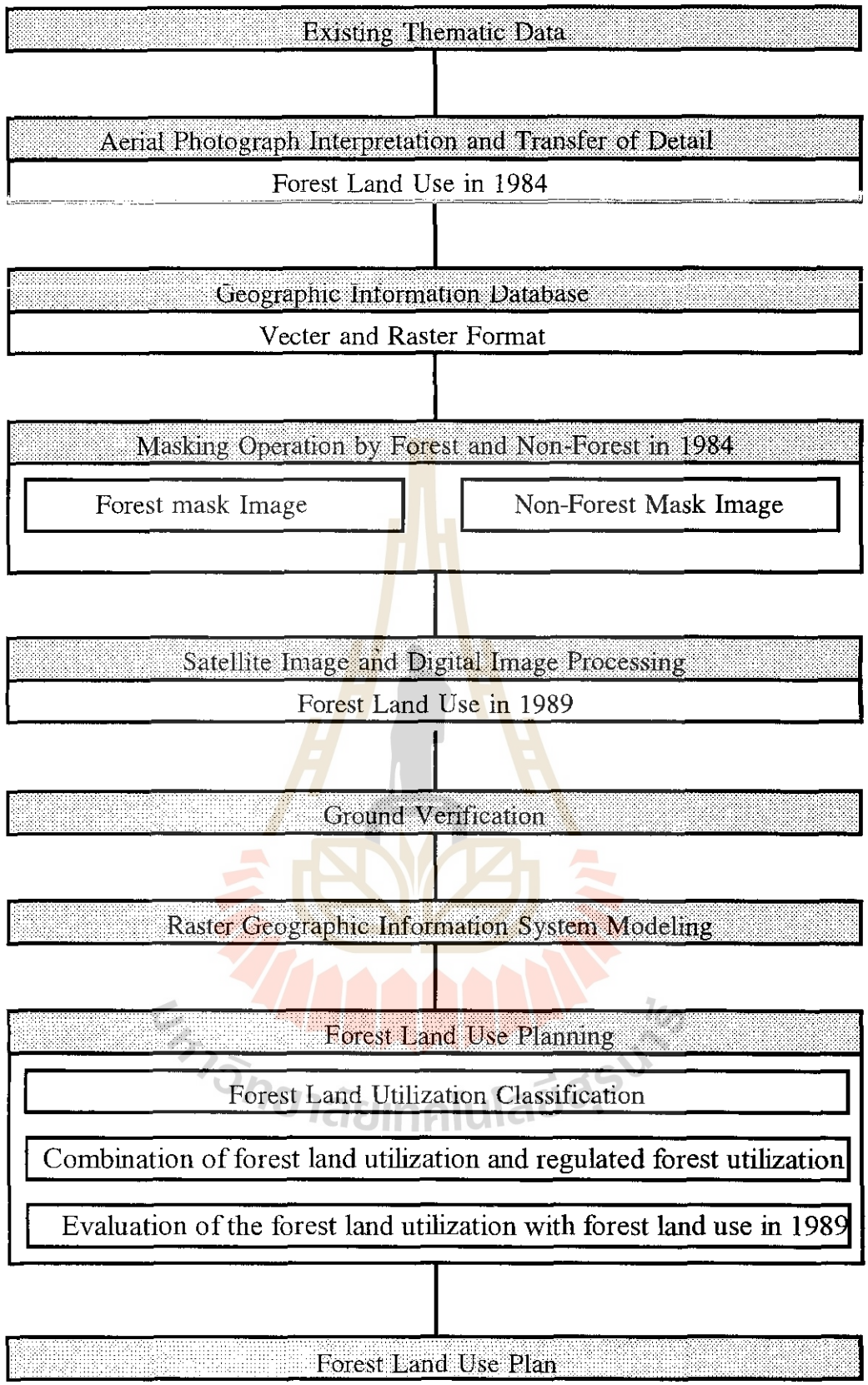

Figure 1 Schematic flowchart of the main tasks in this study.

Table 1 The area and percentage of the four input GIS images used in the forest utilization classification.

Watershed classification as forest land use capability by natural conditions				
No.	Class	Ranking	Area in ha	Percent
1	Unsuitability for forest area	1	55,008.36	31.41
2	Suitability for productive forest area	5	68,430.06	39.07
3	Suitability for protective forest area	10	51,721.02	29.52
3 units	Total		175,159.44	100.00
Soil classification as forest land use suitability by natural conditions				
No.	Class	Ranking	Area in ha	Percent
1	Unsuitability for forest area	1	47,408.85	27.07
2	Suitability for forest area	5	127,750.59	72.93
2 units	Total		175,159.44	100.00
National forest reserve as productive forest areas by regulated conditions				
No.	Class	Ranking	Area in ha	Percent
1	Unsuitability for forest area	1	12,176.19	6.95
2	Suitability for productive forest area	5	162,983.25	93.05
2 units	Total		175,159.44	100.00
Forest and national parks as protective forest areas by regulated conditions				
No.	Class	Ranking	Area in ha	Percent
1	Unsuitability for forest area	1	104,308.29	59.55
2	Suitability for protective forest area	10	70,851.15	40.45
2 units	Total		175,159.44	100.00

Table 2 The combination of four input GIS images by the normalized indexing operation.

No.	Value	Relative suitability for forest utilization	Area in ha	Percent
1	1	Very unsuitable for forest area	11,429.46	6.53
2	2	Unsuitability for forest area	28,315.62	16.17
3	3	Suitability for productive	27,154.62	15.50
4	4	Very suitable for productive forest	30,081.60	17.17
5	5	Suitability for protective forest	25,273.98	14.43
6	6	Moderate suitability for protective forest	16,396.02	9.36
7	7	Suitability for protective forest	157.41	0.09
8	8	Very suitable for protective forest	36,350.73	20.75
8 units	Total		175,159.44	100.00

Table 3 The combination of forest land utilization and existing forest utilization by regulations.

No.	Forest land utilization and existing forest utilization	Area in ha	Percent
1	Unsuitability for forest area	37,017.72	21.13
2	Suitability for production forest area	55,920.06	31.93
3	Suitability for protection forest area	77,484.78	44.24
4	Temporary Cultivation Rights (STK) areas	4,372.02	2.50
5	Mining concession areas	364.86	0.21
5 units	Total	175,159.44	100.00

II. Suitability for productive forest area. The results show that non-forest areas which consist of the settlement and built-up areas, agricultural areas, old clearing areas and mining areas overlap with the suitability for productive forest area. Areas of the existing non-forest are 7,648.56 ha. The main component of the existing non-forest areas is the old clearing area which covers an area of 7,348.14 ha or about 4.20 percent of the total study area. These areas are assigned as productive reforestation areas in the forest land use plan. In the meantime, the existing settlement and built up areas and agricultural areas are here assigned as non-forest areas with limiting conditions. In contrast, the existing forest areas in the suitability for productive forest area are assigned as productive forest areas in the forest land use plan.

III. Suitability for protective forest area. The same as with the suitability for productive forest area, the results show that the non-forest areas which consist of the agricultural areas and the old clearing areas exist in the suitability for protective forest area. The main component of the non-forest areas is the old clearing area which covers an area of

27,047.25 ha or about 15.44 percent of the total study area. These areas are assigned as protective reforestation in the forest land use plan. In the meantime, the existing settlement and agricultural areas are here assigned as non-forest areas with limiting conditions.

IV. Temporary Cultivation Rights (STK) area. The results show that existing forest areas overlap with the Temporary Cultivation Rights (STK) areas. This fact is contradicted with the principle of the Temporary Cultivation Rights projects which operate in the deteriorated forest land. In this study, all of the Temporary Cultivation Rights (STK) areas are assigned as non-forest areas with limiting conditions in the forest land use plan.

V. Mining concession area. The results shows that most of the active mining areas in 1989 overlap with the mining concession areas. The status of mining concession areas is unchanged in the forest land use plan.

4. 4 Forest land use plan

In this study, a forest land use plan is a possibility plan based on the evaluation of the relationship between the forest land utilization classification including the existing regulated forest utilization and the existing forest land use in 1989. In practice, the forest land use plan map is firstly produced by the recoding operation of the output from the unnormalized indexing operations and then a suggestion of the forest land utilization as the main content of the forest land use plan is given. The forest land utilization with suggestion in the forest land use plan are described as follows:

I. Non-forest area with no limiting conditions. The non-forest area with no limiting conditions includes the Temporary Cultivation Rights (STK) areas and the existing non-forest areas in 1989 which overlap with the unsuitability for forest area of the forest land utilization classification. It covers an area of 21,025.80 ha or about 12.00 percent of the total study area. In the execution of the plan, the existing old clearing areas from 1989 which were the main component in these areas should be promoted for the intensive agricultural utilization. In addition, the clarification of land rights and land reform for these areas are here suggested.

II. Non-forest area with limiting conditions. The non-forest area with limiting conditions includes the Temporary Cultivation Rights (STK) areas and the existing non-forest areas in 1989 which overlap with the suitability for productive and protective forest areas of the forest utilization classification. It covers an area of 4,888.17 ha or about 2.79 percent of the total study area. In the execution of the plan, the soil conservation protection measures and the clarification of land rights for these areas are required.

III. Mining area. The mining area is mining concession areas in the study area. It covers an area of 364.86 ha or about 0.21 percent of the total study area.

IV. Community forestry area. The community forestry area is the existing natural forest areas in 1989 which overlap with the unsuitability for forest area of the forest land utilization classification. In this study, the assignment of community forestry area is intended to decrease the activity of illegal tree cutting which occurs in the natural forest areas. In addition, this area can be considered as the buffer zone between the intensive productive or protective forest area. The community forestry area covers an area of 13,836.60 ha or about 7.90 percent of the total study area. This area should be divided into small areas for each Tambon (sub-district) in the execution of the plan. The management and utilization of the community forestry area are determined by the committee of the Tambon with the suggestion of the Royal Forest Department. Basically, trees in the existing Mixed Deciduous forest are suitable for timber utilization with the selection systems ,while trees in the existing Dipterocarp Deciduous forest are suitable for firewood production with the coppice systems.

V. Productive reforestation area. The productive reforestation area is the existing old clearing areas in 1989 which overlap with the suitability for productive forest area of the forest land utilization classification. It covers an area of 7,348.14 ha or about 4.20 percent of the total study area. The traditional planting system with Teak species is suggested in the execution of the plan.

VI. Productive forest area. The productive forest area consists of the existing natural forest and productive reforestation areas in 1989 which overlaps with the suitability for productive forest area of the forest land utilization classification. In addition, the existing productive reforestation areas in 1989 which overlap with the unsuitability for forest area of the forest land utilization classification is also included in this area. The productive forest area covers an area of 50,426.82 ha or about 28.79 percent of the total study area. This area has a main function of sustainable productive forest. In the execution of the plan, intensive forest inventory is required for the logging operation. In addition, the traditional selection system with a 30-years cutting cycle and a selection felling ratio of 60 percent for trees over girth limit (commercial trees) should be revised as the actual forest recovery forest situation. According to the forest inventory data in 1991 the number commercial trees in the natural forest is relatively low in all forest types and stratum. Furthermore, the termination of forest logging in the Mae Ngao demonstration forest management unit has proved to be the failure of the traditional selection system in the past. The clear cutting system in the small forest areas with a low gradient is here suggested. In practice, the traditional planting system is immediately operated after forest logging.

VII. Protective reforestation area. The protective reforestation area is the existing old clearing areas in 1989 which overlap with the suitability for protective forest area of the forest land utilization classification. The protective reforestation area covers an area of 27,047.25 ha or about 15.44 percent of the total study area. In the execution of the plan the traditional planting system with growing tree species is suggested for the old clearing areas without small trees from the natural succession. In contrast, enrichment planting systems are suggested for the old clearing areas with some trees from the natural succession. In practice, trees from natural succession in reforestation sites should be preserved and forest fire control is required.

VIII. Protective forest area. The protective forest area includes the existing natural forest areas and the protective reforestation in 1989 which overlap with the suitability for protective forest area of the forest land utilization classification. The protective forest area covers an area of 50,221.80 ha or about 28.67 percent of the total study area. In fact, this area has the main function of environment protection. In execution of the plan, tree felling is prohibited in this forest area.

5. CONCLUSION

In conclusion the integration of remote sensing and the GIS therefore appears to have potential for providing the necessary information for forest land use planning, in particular the existing forest areas and their status. In addition, forest land use planning can be conducted easily and effectively by using the GIS as a tool. However, the successful of the integration of remote sensing and the GIS for forest land use planning depends on the reliability of the existing information which are sources for the GIS, for example, reforestation map.

6. REFERENCE

Burrough, P. A. 1986. Principles of Geographic Information Systems for Land Resources Assessment. Oxford University Press, Oxford. 193 p.

Colwell, R. N. 1975. Introduction. In Manual of Remote Sensing, First Edition (Editor R. G. Reeves) American Society of Photogrammetry. Virginia: 1: 25.

Goodenough, D. G. 1988. Thematic Mapper and Spot Integration with a Geographic Information System. Photogrammetric Engineering and Remote Sensing, 54(2):167-176.

Kalensky. Z. D. 1992. FAO Remote Sensing Activities in Environmental Monitoring and Forest Cover Assessment in Developing Countries. Invited paper. ISPRS Commission VII, Session on Tropical Forest and Land Use Monitoring in Seventeenth Congress of the International Society for Photogrammetry and Remote Sensing, Washington, D. C., USA, 2-14 August 1992. 9 p.

Lillesand, T. M. and R. W. Kiefer. 1979. Remote Sensing and Image Interpretation. John Wiley&Sons. New York. 612 p

McFarland, W. D. 1982. Geographic Databases for Natural Resource. In Remote Sensing for Resource Management. (Edited by C. J. Johannsen and J. L. Sanders). Soil Conservation Society of America. Iowa: 41-50.

Shelton, R. L. and J. E. Estes, 1979. Integration of Remote Sensing and Geographic Information System. In Proceedings of the Thirteenth International Symposium on Remote Sensing of Environment, Volume 1: 675-692.

POSTER SESSION Q

AGRICULTURE / SOIL

Remote Sensing Data in relation to
The Ecological Indices of Tropical Monsoon Forest

Moe Myint and Tri. B. Suselo
Space Technology Application and Research
School of Environment, Resources and Development
Asian Institute of Technology
G.P.O Box 2754, Bangkok 10501
THAILAND

ABSTRACT

The Alaungdaw Kathapa National Park, in Myanmar represents different types of the tropical monsoon forest. Their ecological indices such as density, frequency, dominance of tree species, similarity and dissimilarity are important for the application of habitat classification and forest types classification.

These ecological indices are derived based on **the field samples** which are extracted from **the spatially defined and spectrally homogeneous samples** from the remote sensing data. The application of these indices to forest type mapping and habitat mapping was discussed.

Based on the ecological indices, **composition of dominant species** which determine the forest types was obtained. Therefore the field samples reflect not only the spectral homogeneity but also spatial and ecological definitions of forest types.

Habitats are the vegetational phenomenon. The absent, present, density, frequency and dominance **information of certain critical species for a particular animal or habitat** was obtained from the ecological indices. This information is very important for habitat mapping.

Study Area

Taungdwin reserved forest of the Alaungdaw Kathapa National Park, in Myanmar. The total area is 122,248 acres. The X-extent is between 94 degree 15 minutes to 94 degree 30 minutes and the Y-extent is 22 degree 15 minutes to 22 degree 45 minutes. The whole area was covered by the dry deciduous forest, moist deciduous forest, dry dipterocarp forest, hill evergreen forest and pine forest.

Objective

In order to derive the ecological indices of the tropical monsoon forest based on the spatially defined and spectrally homogeneous field samples derived from the SPOT multispectral data. The date of the data is 31st March 1994.

Rationale of the study

Plants typically occur together in repeating groups of associated plants. These groups are called communities and they are best described by the ecological indices such as density, frequency, dominance, relative density, relative frequency, relative dominance and important value of individual species within the community.
Plant communities can be considered sub-divisions of a vegetation cover. Whenever the cover shows more or less obvious spatial changes, one may distinguish a different community. These changes are caused by spatial changes in species composition, changes in spacing and height of plants, changes in growth form and life forms of plants or seasonal plant responses of other vegetation properties. Spatial changes in species composition are often obvious.

These spatial changes will influence the spectral response of the digital remotely sensed data. Spatially defined and spectrally homogeneous field samples (SSS) can be served to correlate the spectral responses and ecological indices of plant communities because SSS are derives based on the quantitative homogeneity of the spectral value in the objective way.

Methodology

Spatially defined and spectrally homogeneous field samples (SSS) were derived based on the spectral homogeneity of the individual band. These samples are contiguous group of pixels of four or five digital levels. These pixels are connected to each other to any direction and meet the area of minimum mapping unit. The standard deviation of each sample is less than 2 and approximately 1.7. Detail was discussed in the reference paper-1.

For the Band-1 (Green Band), minimum spectral value is 33 and maximum spectral value is 76. Digital numbers of pixels were grouped as spectral classes in such a way 33 to 38, 39 to 43, 44 to 48, 49 to 53, 54 to 58, 59 to 63, 64 to 68, 69 to 73 and *74 to 76* .
For the Band-2 (Red Band), minimum spectral value is 19 and maximum spectral value is 67. Digital numbers of pixels were grouped as spectral classes in such a way 19 to 23, 24 to 28, 29 to 33, 34 to 38, 39 to 43, 44 to 48, 49 to 53, *54 to 58*, *59 to 63* and *64 to 67*.
For the Band-3 (Near Infrared Band), minimum spectral value is 23 and maximum spectral value is 112. Digital numbers of pixels are grouped as spectral classes in such a way 23 to 28, 29 to 34, 35 to 40, 41 to 46, 47 to 52, **53 to 58**, 59 to 64, 65 to 70, 71 to 76, 77 to 82, 83 to 88, 89 to 94, 95 to 100, *100 to 105* and *105 to 106.*

Based on the field visit, the high lighted spectral classes represent the different kind of tropical monsoon forests. Based on the accessibility of walking distance, some SSSs that represent the different types of forests are selected. The (100m * 100m) filed samples were laid out on the ground for each selected SSS. Then the (25m * 25m) sub-sample plot were laid out within the 100m * 100m sample plot. Species name and diameter of all trees within the sample plot was recorded.

Ecological indices such as density, frequency, dominance, relative density, relative frequency, relative dominance and important value for each SSS were calculated. A sample result of ecological indices was illustrated. The detail result of ecological indices for each sample plot can be requested to the author. Most dominant species were reselected for each SSS. The 90% significant dominance level was applied.

Index of similarity and dissimilarity among samples based on the most dominant species by using MOTYKA similarity index for each SSS was derived. The results were illustrated .

X axis ordination and Y axis ordination was plotted. Some plots are combined according to the ecological similarity. The X-Y ordination graphs were illustrated..

Evaluation and Discussion

Ecological indices can be derived based on the SSSs which represent the certain plant community of particular spatial change that influence the response of digital remotely sensed data.

Pine forest (Plot-16) can be identified spectrally and ecologically . The total number of tree species found is 2. More than 90% of the area was dominant by pine trees. By the ecological parameter tables, it is very distinct ecologically from other types of forest Moreover, pine can be identified spectrally from other kind of forests. Therefore pine sample plot is not included for x-y ordination. The spectral range of pine forest in the study area is 89-94 and 95-100 in the near infrared band.

Hill evergreen forest (Plot-13) can be identified spectrally and ecologically. The total number of species found is 14. Dominant species according to the field samples and ecological indices are Quercus kingiana Craib. and Pinus merkusii Jungh. The spectral range is 77 to 82 and 83 to 88 in the near infrared band. There is some mixture between pine and hill evergreen forest.

Plot-8 is Dipterocarpus Tuberculatus dominant Dry Dipterocarp Forest. Plot-4 is Dipterocarpus Tuberculatus and Pentaceme Siamensis (Miq) Kurz. dominant Dry Dipterocarp Forest. Plot-14 is Pentaceme Siamensis (Miq) Kurz dominant Semi Dry Dipterocarp Forest. Plot-5 is transition zone between Dry Dipterocarp Forest and Dry Deciduous Forest because indicator species from both forest types was presented. The total number of species found are 18 for plot 8, 26 for plot 4, 28 for plot 5 and 27 for plot 14. Though different stages of Dry Dipterocarp Forest (Plot 4,5,8 and 14) can be identified ecologically by X-Y ordination, these stages cannot be identified by spectrally. Moreover, Dry Dipterocarp Forest(not stages) is spectrally mixed with the dry deciduous forest in the near infrared band. It was spectrally identified in the green band. The spectral range of dry dipterocarp forest is 49 to 53 in green band. Some dominant species according to the ecological indices are Dipterocarpus Tuberculatus and Pentaceme Siamensis (Miq).

Plot-1 and plot-2 represent the dry deciduous forest which can be identified spectrally and ecologically. The total number of species found for plot-1 is 34 and that for plot-2 is 34. Some dominant species are Tectona grandis Linn f., Acacia catechu Wild. , Millettia pendula Benth., Pterospermum semisagittatum Ham. , Homalium tomentosum Benth., Termanalia tomentosa W&A and Dillenia pentagyna based on the ecological indices. The spectral range is 53 to 58 and 59 to 64 in the near infrared band.

Plot-3 and plot-10 is semi evergreen type which is transition zone between evergreen forest and moist deciduous forest. This kind of forest can be found near to the streams and mixed with evergreen and deciduous species. The total number of species found in plot-3 is 50 and that for plot-10 is 47. This type can be identified from other communities by ecological x-y ordination. The dominant species are Homalium tomentosum Benth., Xylia dolabriformes Benth., Lagerstroemia villosa Wall., Xerospermum glabratum Radlk. , Lagerstroemia macrocapa wall. and Schleichera oleosa (Lour.) Merr. according to the ecological indices of the field samples. The spectral range of semi evergreen forest is 71 to 76 in the near infrared band.

Plot -7 and plot -11 is Lower Mixed Deciduous (LMD) forest which was found on more or less flat terrain and bamboo is scarcity. The total number of species found in the plot 7 is 26 and that for plot-11 is 20. Some dominant species are Tectona grandis Linn f., Termanalia tomentosa W&A., Xylia dolabriformes benth., Dillenia pentagyna Roxb., Mitragyna rotundifolia O.Ktze, Cereya arborea Roxb. and Haplophragma adenophyllum (Wall.) Dep. according to the ecological indices. Plot 6 and 15 is Moist Upper Mixed Deciduous Forest (MUMD). The total number of species found in the plot-6 is 28 and that for plot-15 is 10. Some dominant species are Xylia dolabriformes benth., Tectona grandis Linn f., Termanalia tomentosa W&A, Mitragyna rotundifolia O.ktze, Dillenia pentagyna Roxb., Diospyros montana Roxb., and Terminalia belerica Roxb. The MUMD and LMD can only be identified ecologically by X-Y ordination of index of dissimilarity based on relative density, but not by the relative dominance. MUMD and LMD cannot be identified spectrally. The spectral range is between 65 to 70 in the near infrared band. It is mixed with the semi evergreen forest. In the semi evergreen forest, the dominance of the deciduous species is higher than the evergreen species. Therefore, in the final forest type map, semi evergreen, MUMD and LMD are classified as Moist Deciduous Forest.

Based on the ecological indices, the information of certain critical species for a particular animal or habitat can be derived regardless of dominant or not.. For example, the presence of Quercus kingiana Craib. which present in the hill evergreen forest, indicates the habitat of Himalayan black bear (Selenarctos thibetanus) and the presence of Terminalia belerica Roxb. which present in the dry and moist mixed deciduous forests, indicates the habitat of barking deer (Munticaus muntiac). This information can be applied for habitat mapping of particular animal.

Recommendation

The species composition and the dominant species composition of a particular plant community which is important information for habitat and forest type classification can be derived from the ecological indices based on SSS.

By using the ecological indices and SSS, pine and hill evergreen can be identified without elevation model. Moreover, not only the forest types but also the species composition, dominancy and density information can be derived.

SSS can be used as field samples for ground truthing, primary data collection, forest inventory, mapping and ecological applications for biodiversity conservation by using remote sensing data.

According to the Mueller-Dombois and Heinz, there is no satisfactory objective method to select the sample which is uniform within the stand area, and the degree of plant-cover variation one considers integratable into a meaningful expression of average is still a matter of judgment. SSS can overcome the difficulty of the homogeneity of the judgment because these are selected based on the spectral homogeneity. However it has the technical limitation concern with the resolution of data and season of the data.

			Ecological Indices of Plot-16 Pine Forest				
Spp.Code	Density	R.Density	Frequency	R.frequency	Dominance	R.Dominance	I.Value
98	159	94.64286	4	57.142857	211823.797	97.408928	249.1946
76	9	5.357143	3	42.857143	5634.49658	2.59107	50.80536

			Ecological Indices of Plot-13 Hill Evergreen Forest				
Spp.Code	Density	R.Density	Frequency	R.Frequency	Dominance	R.Dominance	I.Value
5	14	6.422019	3	10.714286	27608.9512	13.4924	30.6287
76	95	43.57798	4	14.285714	53985.5234	26.382542	84.24624
98	89	40.82569	4	14.285714	113402.516	55.419422	110.5308

			Ecological Indices of Plot-3 Semi-Evergreen				
Spp.Code	Density	R.Density	Frequency	R.Frequency	Dominance	R.Dominance	I.Value
1	17	8.374384	4	4.347826	11908.7148	5.482237	18.20445
3	8	3.940887	3	3.26087	6614.47656	3.045008	10.24676
4	3	1.477833	3	3.26087	8584.16699	3.951765	8.690467
5	1	0.492611	1	1.086957	5281.0127	2.431141	4.010708
6	7	3.448276	3	3.26087	2511.02588	1.155963	7.865108
8	20	9.852217	4	4.347826	33303.0469	15.331225	29.53127
9	6	2.955665	3	3.26087	4869.59766	2.241744	8.458279
10	1	0.492611	1	1.086957	3257.32642	1.499527	3.079094
11	3	1.477833	2	2.173913	4015.04614	1.848347	5.500093
12	11	5.418719	3	3.26087	14846.9971	6.83489	15.51448
13	15	7.389163	4	4.347826	25442.4316	11.712552	23.44954
15	15	7.389163	3	3.26087	7501.19727	3.453214	14.10325
18	2	0.985222	2	2.173913	2425.30737	1.116503	4.275637
19	2	0.985222	1	1.086957	7731.64941	3.559304	5.631482
22	8	3.940887	2	2.173913	6471.1416	2.979023	9.093822
23	4	1.970443	3	3.26087	5707.65625	2.627548	7.858861
28	4	1.970443	3	3.26087	5630.31055	2.591942	7.823255
30	2	0.985222	2	2.173913	2473.87647	1.138862	4.297996
31	5	2.463054	2	2.173913	3431.88867	1.579887	6.216855
34	2	0.985222	2	2.173913	5584.25488	2.57074	5.729875
38	3	1.477833	3	3.26087	2135.00879	0.982862	5.721564
50	2	0.985222	1	1.086957	5295.74707	2.437924	4.510102
51	2	0.985222	1	1.086957	2419.53491	1.113845	3.186023
62	10	4.926108	1	1.086957	8208.45703	3.778805	9.791869
64	3	1.477833	1	1.086957	8336.59375	3.837793	6.402582
65	2	0.985222	1	1.086957	2219.44678	1.021734	3.093912

			Ecological Indices of Plot-1 DUMD				
Spp.Code	Density	R.Density	Frequency	R.frequency	Dominance	R.Dominance	I.Value
1	8	5.479452	4	6.666667	17990.016	7.312356	19.45847
2	2	1.369863	2	3.333333	4475.1084	1.818986	6.522182
3	7	4.79452	3	5	14286.633	5.807051	15.60157
4	39	26.71233	3	5	111082.55	45.15144	76.86377
7	21	14.38356	4	6.666667	17336.777	7.046835	28.09707
8	6	4.109589	3	5	9560.502	3.886033	12.99562
9	5	3.424658	3	5	6140.8584	2.496059	10.92072
10	3	2.054795	3	5	6054.1577	2.460818	9.515613
11	9	6.164383	4	6.666667	15755.813	6.404224	19.23528
16	11	7.534246	2	3.333333	14468.146	5.88083	16.74841
22	2	1.369863	1	1.666667	6516.4189	2.648712	5.685242

			Ecological Indices of Plot-6 MUMD				
Spp.Code	Density	R.density	Frequency	R.Frequency	Dominance	R.Dominance	I.Value
3	7	4.320988	4	7.017544	4613.582	2.124749	13.46328
4	14	8.641975	3	5.263158	42753.375	19.689734	33.59487
8	25	15.4321	4	7.017544	46364.641	21.352873	43.80251
9	9	5.555555	4	7.017544	19317.52	8.896533	21.46963
10	21	12.96296	3	5.263158	27517.773	12.673096	30.89922
11	5	3.08642	2	3.508772	3461.8984	1.59435	8.189542
22	1	0.617284	1	1.754386	2865.2559	1.319572	3.691241
23	7	4.320988	4	7.017544	11007.777	5.069546	16.40808
31	9	5.555555	3	5.263158	11191.317	5.154074	15.97279
33	34	20.98765	4	7.017544	24764.762	11.405217	39.41042
60	4	2.469136	2	3.508772	4128.2847	1.901249	7.879157
74	2	1.234568	2	3.508772	3735.4211	1.720319	6.463659

			Ecological Indices of Plot-8 Dry Dipterocarp Forest				
Spp.Code	Density	R.Density	Frequency	R.Frequency	Dominance	R.Dominance	I.Value
10	21	11.35135	4	9.090909	5708.23731	7.157618	27.59988
28	5	2.702703	3	6.818182	2414.01343	3.026957	12.54784
32	5	2.702703	3	6.818182	1497.05408	1.877172	11.39806
66	5	2.702703	3	6.818182	1470.35059	1.843688	11.36457
73	80	43.24324	4	9.090909	41544.2773	52.0928	104.427
75	5	2.702703	3	6.818182	1135.01709	1.42321	10.9441
86	20	10.81081	4	9.090909	9124.78809	11.441667	31.34339
87	20	10.81081	4	9.090909	10383.168	13.019562	32.92128

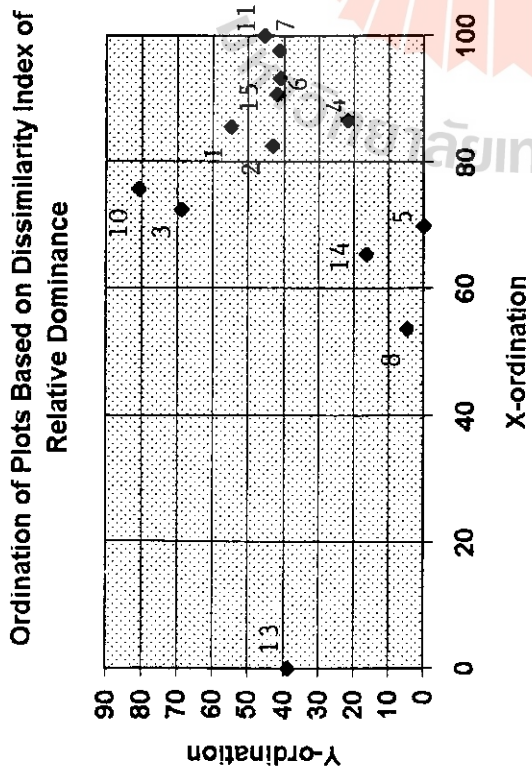

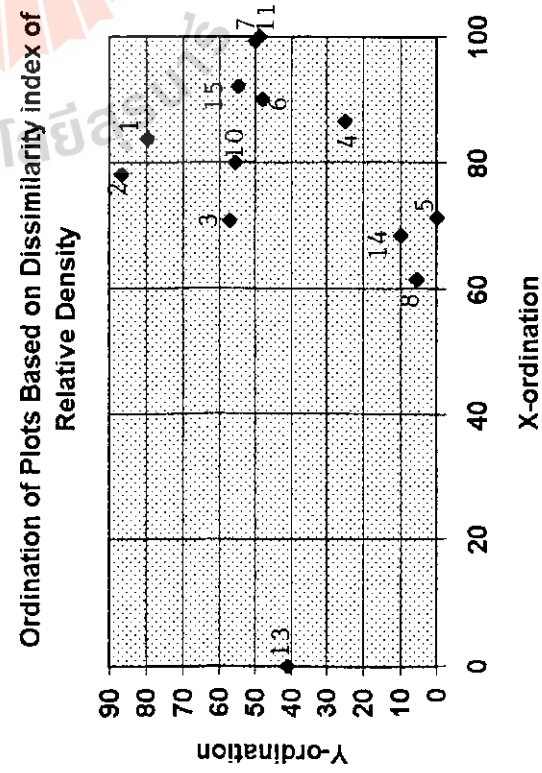

Matrix of Dissimilarity and Similarity Indices Based on Relative Density

Index Of Dissimilarity

		1	2	3	4	5	6	7	8	10	11	13	14	15
0	0	44.92754	74.16975	74.77477	91.36691	67.33067	55.78947	97.81022	72.97298	56.75676	100	92.34042	55.12195	
1	44.92754	0	68.25397	75.36945	86.87259	67.24138	66.16541	94.5098	63.1769	66.06498	100	87.96296	64.51613	
2	55.07246	31.74603	0	77.52809	83.90093	66.21622	78.78788	96.8652	39.58944	75.95308	99.5713	93.57143	92.8	
3	25.83026	24.63054	22.47191	0	49.63504	47.36842	50.17794	80	64.38356	52.05479	100	54.97836	51.24378	
4	25.22523	13.12741	16.09907	50.36496	0	72.93729	74.48071	48.46626	78.16092	72.9885	97.79614	43.55401	78.21011	
5	8.633094	32.75862	33.78378	52.63158	27.06271	0	42.58065	85.95318	62.61682	44.54829	100	80	58.26087	
6	32.66932	33.83459	21.21212	49.82206	25.51929	57.41935	0	87.38739	67.32394	11.54929	100	79.59184	37.12121	
7	44.21053	5.490196	3.134796	20	51.53374	14.04682	12.61261	0	86.04651	87.7907	100	67.49117	83.39921	
8	2.189781	27.02703	36.82311	60.41056	35.61644	21.83908	37.38318	32.67606	13.95349	0	63.38798	100	77.04918	73.81818
10	27.02703	43.24324	33.93502	24.04692	47.94521	27.01149	55.45171	88.45071	12.2093	36.61202	0	100	76.39343	39.63636
11	43.24324	0	0	0.428696	0	2.203857	0	0	0	0	0	0	97.5	100
13	0	7.659575	12.03704	6.428571	45.02165	56.44599	20	20.40816	32.50884	22.95082	23.60656	2.5	0	72.89719
14	7.659575	44.87805	35.48387	7.2	48.75622	21.78988	41.73913	62.87879	16.60079	26.18182	60.36364	0	27.1028	0
15	44.87805													

Index of Similarity

Matrix of Dissimilarity and Similarity Indices Based on Relative Dominance

Index of Dissimilarity

		1	2	3	4	5	6	7	8	10	11	13	14	15
0	0	55.74601	73.66776	71.32424	89.94767	64.52673	37.94738	96.15534	75.61961	53.75962	100	92.61137	47.2648	
1	44.25399	0	63.18672	70.07182	78.39352	55.94779	60.91435	94.72977	67.55039	59.20614	100	87.10497	59.28937	
2	26.33224	36.81328	0	73.52235	79.66874	64.77026	77.5965	95.79095	41.70974	70.42629	97.30088	90.54749	88.88591	
3	28.67576	29.92818	26.47766	0	45.39425	51.70603	53.93136	89.0102	71.18506	51.89436	100	55.75048	61.26719	
4	10.05233	21.60648	20.33126	54.60575	0	73.39594	78.37562	52.97025	80.79469	75.51478	98.48527	49.6869	82.53404	
5	35.47328	44.05221	35.22974	48.29397	26.60406	0	44.14673	95.84853	72.51323	36.46409	100	83.4571	50.77922	
6	62.05262	39.08566	22.40351	46.06865	21.62438	55.85327	0	96.44714	77.29008	21.86765	100	83.44898	35.46521	
7	3.844657	5.270228	4.209055	10.9898	47.02975	4.151468	3.552867	0	92.51732	96.25618	100	84.36725	94.33398	
8	24.38039	32.44962	58.29026	28.81494	19.20532	27.48677	22.70993	7.482678	0	69.7626	100	79.79105	81.03352	
10	46.24038	40.79387	29.5737	48.10564	24.48522	63.53591	78.13236	3.743821	30.2374	0	100	80.39465	43.11663	
11	46.24038	0	0	2.699121	0	1.514733	0	0	0	0	0	97.75789	100	
13	0	7.38863	12.89503	9.452518	44.24952	50.3131	16.5429	16.55102	15.63275	20.20895	19.60534	2.242112	0	79.04459
14	7.38863	52.7352	40.71063	11.11409	38.73281	17.46597	49.22078	65.53479	5.66602	18.96648	56.88337	0	20.95541	0
15	52.7352													

Index of Similarity

REFERENCES

1. MOE MYINT and JEAN PIERRE DELSOL (1995), Spatially Defined and Spectrally Homogeneous Samples from Remote Sensing Data, GIS AM FM ASIA '95.

2. KERMODE, C.W.D (1964), Some aspect of silviculture in Burma Forest, Forest Department, Burma.

3. DIETER MUELLER-DOMBOIS AND HEINZ ELLENBERG (1974), Aims and methods of Vegetation Ecology, John Willey & Sons.

4. D.M.STOMS and J.E.ESTES (1993), A remote sensing research argenda for mapping and monitoring biodiversity. Photogrammetric engineering & Remote Sensing, Vol.59, No.10, pp 1839-1860.

5. JOHN KOLTON (1993), Classification of satellite imagery in the development of Wildlife Habitat Types, Earth observation magazines, February 1993, pp 32-40.

Computer Assisted Monitoring of Vegetation Using Multi-resolution Satellite and Geospatial Data

Mr. Surat Lertlum *
Prof. Shunji Murai **
Email: {surat,smj}@cs.ait.ac.th

* Doctoral Student, Asian Institute of Technology
** Professor, Asian Institute of Technology

Abstract

The main purpose of this paper is to illustrate the outline of a new vegetation monitor methodology, especially tropical forest by using remote sensing and GIS.

The emphasis is on the usage of new technology in remote sensing and GIS to monitor, analyze, and predict the forest resource at regional level. First, a multi-resolution forest classification is proposed, by using low resolution remotely-sensed data (NOAA AVHRR LAC 1.1 km. resolution) as the main source of data for vegetation monitoring, and using high resolution remotely-sensed data (Landsat TM 30 m. resolution) as the ground correction data for each subregion. Next we illustrates the usage of objected-oriented data model to handle multi-resolution, multi-temporal integration problem.

1 Introduction

In this section, we introduce some general knowledge related to proposed multi-resolution tropical forest classification:

1.1 Main Data Source (NOAA AVHRR) :

The advantages of low resolution satellite data (NOAA AVHRR) data are :

- *Wide area coverage*
- *More frequency of obtaining input data*

The disadvantages of low resolution satellite data (NOAA AVHRR) data are :

- *Inaccurate classification of small area (less than 1.1 km^2).*
- *Inaccurate classification of subregion that vegetation may have different reflect characteristics.*

1.2 Vegetation Classification :

In general, vegetation classification methods using remotely-sensed data are :

- *Using NDVI (Normalized Difference Vegetation Index)*
- *Unsupervised Classification*
- *Supervised Classification*

1.3 Spatial Information System :

The current requirements for spatial information system are :

- Remote sensing stand point:
  - *Can handle multi-resolution data*
  - *Can handle multi-temporal data*
- GIS stand point:
  - *Can handle both raster and vector data*
  - *Can integrate raster and vector data*

2 Vegetation classification from satellite data utilizing thermal bands

In this section, we introduce a new methodology for vegetation classification from low resolution satellite data (NOAA AVHRR LAC 1.1 km.) utilizing thermal bands.

From the trend study on tested data, the relationship between forest area, data from each band, and normalized difference indices from selected bands, the result shows that forest land can be classified with the combination of 3 parameters:

1 NDVI = (band2-band1)/(band2+band1)
2 NR34 = (band3-band4)/(band3+band4)
3 NR42 = (band4-band2)/(band4+band2)

These parameters involve data from 4 bands, which include thermal infrared band (band 4) of NOAA AVHRR. The proposed classification method utilizes the use of thermal band by using natural characteristic of forest area that the temperature of forest area should lower than the surrounding. (Lertlum and Murai, 1994) (Figure 1 Decision tree for forest classification)

3 Vegetation classification from multi-resolution satellite data

Information derived from coarse spatial resolution sensors that have high temporal data acquisition rates (e.g. NOAA AVHRR) are required to accommodate the vast land area included in tropical surveys. Higher resolution sensors (MSS, TM, SPOT) are necessary tools to record the spectral and spatial detailed needed to link intensive ecological field of studied to the forest community and biome levels.

From previous section, a new methodology for vegetation classification from low resolution satellite data (NOAA AVHRR LAC 1.1 km.) utilizing thermal bands is introduced. In this section, we continue to apply similar methodology to high resolution satellite data (Landsat TM 30 m.).

For high resolution data (Landsat TM), the relationship between forest area and data from each band, normalized difference indices from selected bands shows that forest land can be classified with the combination of 2 parameters:

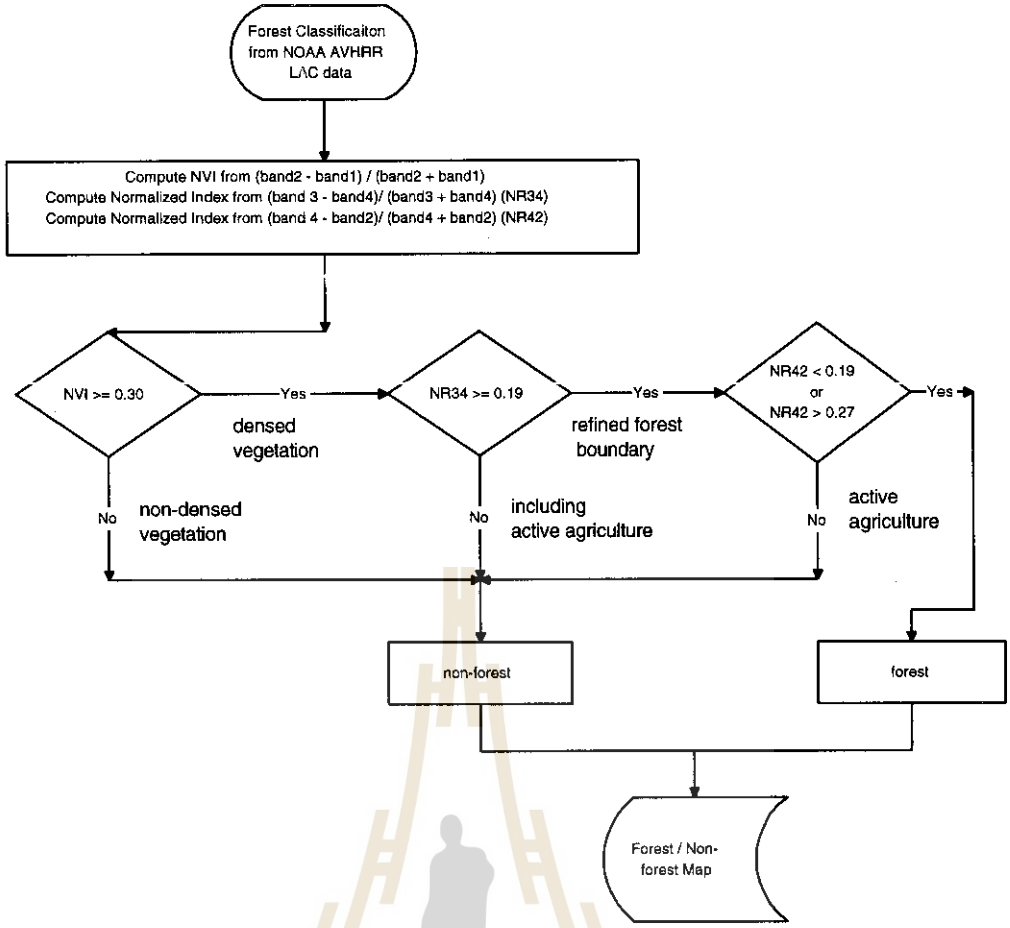

Figure 1 Decision tree for forest classification

1 NDVI (NVI) (Normalized Difference Vegetation Index)	***=***	***(band4-band2)/(band4+band2)***
2 NR64 (Normalized Difference Index between band 6 and band 4) =		***(band6-band4) /(band6+band4)***

Table 2 belows list the characteristics of NVI and NR64 for each type of area:

type of area	respond from NVI	respond from NR64
primary forest	**high**	**low**
secondary forest	**mid-range**	**mid-range**
plantation/high tree	**high**	**mid-range**
rice field	**low**	**low**
grass land/ rice field after harvest	**low**	**high**
water	**low**	**low**

Table 2 Characteristics of NVI and NR64 for each type of area

From the proposed forest classification methods for NOAA AVHRR and Landsat TM , we can integrated both of the classified results by using the result from Landsat TM classification to calibrate the result from NOAA AVHRR for each subregion as mentioned previously. The integration can be performed by the method of defining more precise threshold for NOAA AVHRR data using classified forest sample from Landsat TM for each subregion, that will be devided by ARID index (Figure 2 Forest classification framework)

4 Object-oriented data model for multi-resolution / multi-temporal remote sensing and GIS data

The object-oriented approach, a relatively new method in computing, is an attempt to improve modeling of the real world. Whereas previous modeling approaches were more record oriented, essentially too close to the computers, this new paradigm is a framework for generating models closer to real world features. The ideal would seem to be to provide an isomorphy, that is a direct correspondence, between real world entities and their computer representation. (LAURINI and THOMPSON, 1992)

In this section, an object-oriented data model for multi-resolution and multi-temporal remote sensing and GIS data sets is introduced. This data model can be used to solve the problem that is critical to relational spatial information system in handling complex data sets.

This data model is illustrated by classes and methods that can be used to integrate multiple data sets.

Proposed object-oriented data model for multi-resolution/multi-temporal remote sensing and GIS data is descripted by the following definition of classes and methods (Lertlum and Murai, 1995) :

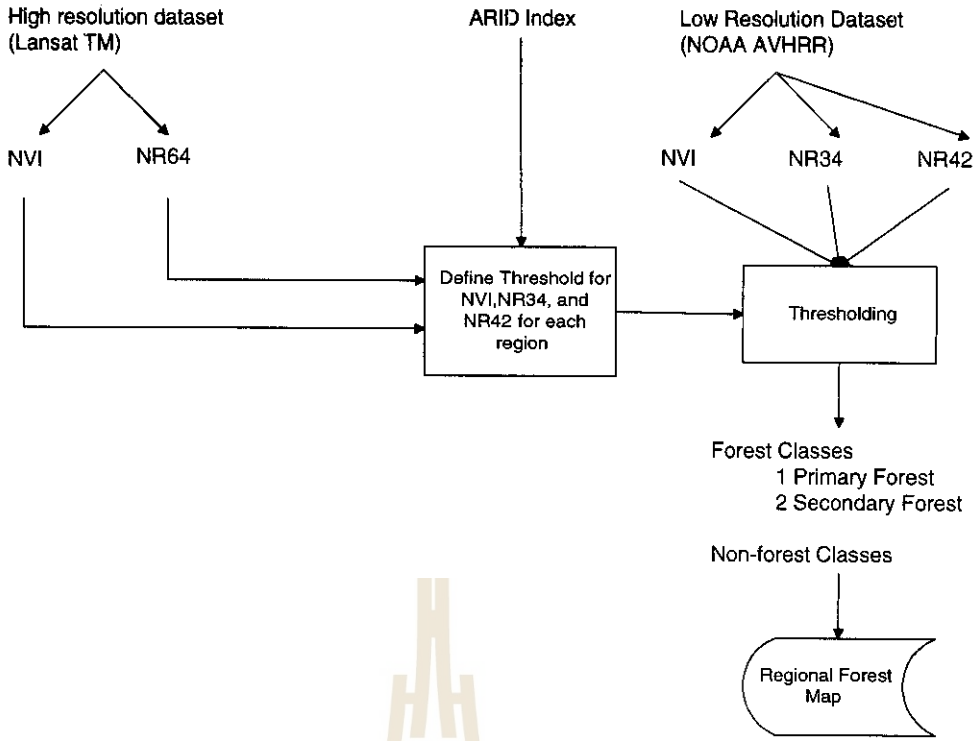

Figure 2 Multi-resolution forest classification framework

Classes

1 *Point Class* : to represent coordinate (x,y) for referencing purpose.

2 *Line Class* : to represent pair of coordinate (x,y) that can be used to define line object.

3 *Polygon Class* : to represent set of line obejct that can be used to define area by user.

4 *Pixel Class* : to represent smallest high resolution data object such as data from Landsat TM.

5 *Subarea Class* : to represent smallest standard resolution data object (NOAA AVHRR LAC 1.1 km)

6 *Area Class* : to represent smallest global data object such as NOAA AVHRR GAC or global data set such as Moisture Index, ARID index.

7 *Subregion Class* : to represent country as a data object which include data in both raster and vector formats.

8 *Region Class* : to represent multi-temporal region as a data object which also inherits properties from subregion class.

Methods

The following are general type of methods for classes defined above:

1 *Value reclassification* from real numbers, that is, interval or ratio scales, to ordered categories.

2 *Value substitutions*, such as averages, particular values like a maximum,

3 *Value creation* through combinations of values for different attributes via arithmetic operations, perhaps using advance statistical techniques.

4 *Value creation* through boolean logic combinations; via trigonometry or interpolation.

5 *Value assignment*, substituting values from one variable for another.

6 Those which involve a spatial property as well as non-spatial attributes.

7 *Integration* method between different resolution pixel (classes) of the same coverage.

In addition, at high level of abstraction (subclasss: *subregion, region*), additional selected types of operations are:

1 *Classification*: is a type of categorization of data object using spectral, spatial and temporal information.

2 *Change detection* : is the extraction of change between multi-date data object.

3 *Extraction of indices*: is the computation of a newly defined index, for example, the vegetation index from satellite data.

4 *Identification of specific features*: is the identification, for example, of disaster, lineament, archeological and other features.

5 Conclusion : Object-oriented implement of forest inventory at regional level

In order to monitor forest area in such a wide area as Southeast Asia Peninsula, high resolution dataset cannot easily be used for such a task because of the high volume of the data. Low resolution dataset such as data from NOAA AVHRR is a solution to such a task. A forest classification technique by using band 1, 2, 3, and 4 of NOAA AVHRR including thermal bands is proposed in this study for more precise tropical forest classification. In addition, the same methodology is applied to high resolution dataset (Landsat TM), the result of the classification with high resolution dataset can differentiate classes of forest.

Then we illustrates the use of objected-oriented data model to handle the integration problem of multi-resolution, multi-temporal data sets by defining an objected-oriented data model that can handle multi-resolution, multi-temporal remote sensing and GIS data sets. This data model consists of classes and methods that can be used to integrate multiple data sets.

The next step on this research study is to implement the spatial information system from the methodology and data model proposed in this paper.

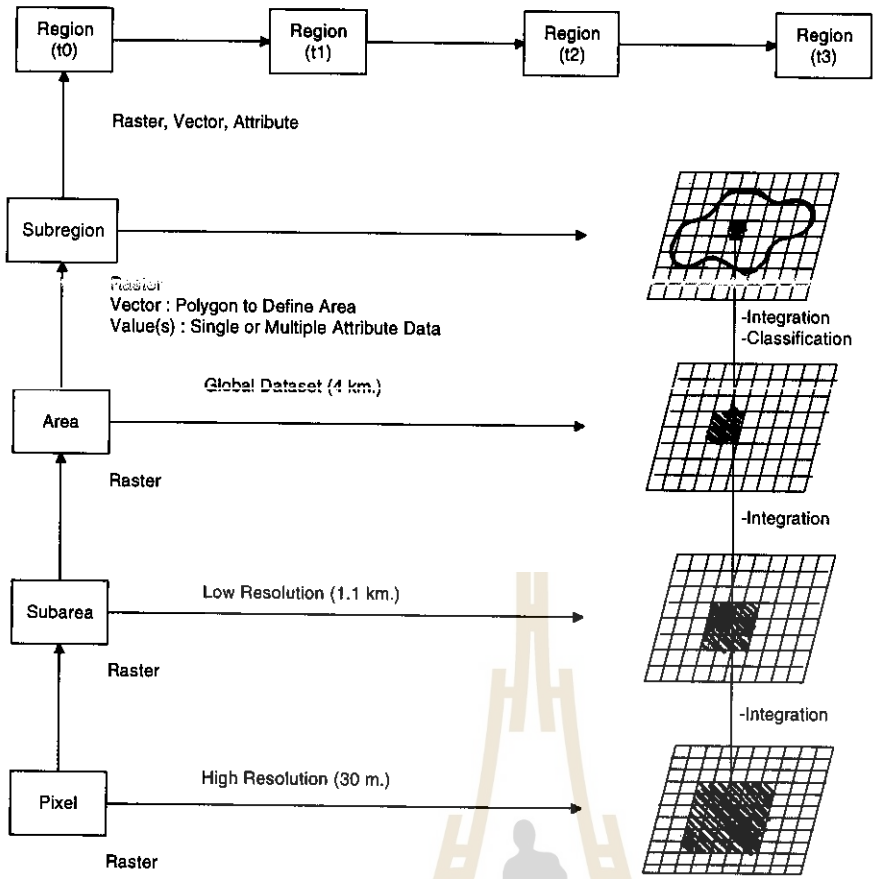

Figure 3 Object-Oriented Framework for Multi-resolution / Multi-Temporal Satellite Remote Sensing and GIS Data Sets

References

LAURINI, R., and THOMPSON, D.; *Fundamentals of Spatial Information Systems*, Academic Press, 1992, pp 644-646

LERTLUM, S., and MURAI, S.; *Forest Mapping with NOAA AVHRR Data : Case Study: Effect of Thermal and for Refining Forest Mapping*, Proceedings of the 15th Asian Conference on Remote Sensing, Nov 17-23,1994, Bangalore, India, pp E51-E56

LERTLUM, S., and MURAI, S.; *Object-Oriented Data Model for Multi-Resolution / Multi-Temporal Remote Sensing and GIS Data Sets*, Proceedings of the 2nd AM/FM Asia, Aug 17-23,1995, Bangkok, Thailand, pp E51-E56

LILLESAND, M., T, and KIEFER, W., R.; *Remote Sensing and Image Interpretation*, John Wiley and Sons,Republic of Singapore, 1987., pp 15-17, 566-567.

MILNE, P., MILTON, S., and SMITH, J., L. (1993); *Geographical Object-oriented Databases-a case study, Int. J. Geographical Information Systems*, 1993, Vol.7, No.1., pp39-55.

MURAI, S., (editor), *Applications of Remote Sensing in Asia and Oceania-Environment Change Monitoring*, Asian Association on Remote Sensing, 1991

MURAI, S., (editor), *Remote Sensing Note*, Japan Association on Remote Sensing, 1993

MURAI, S., *Special Course on Advanced Remote Sensing/GIS Technologies:Data Fusion of Multi-sensor Data*, AIT, Bangkok, Thailand, 1994.

PEUQUET, D., J. and DUAN, N., : *An Event-based Spatiotemporal Data Model (ESTDM) for Temporal analysis of Geographical Data, , Int. J. Geographical Information Systems*, 1994, Vol.9, No.1., pp7-24.

****

Presented to The 16th Asian Conference on Remote Sensing
20-24 November 1995
Suranaree university of Technology
Nakorn Ratchasima, Thailand

Simulating Agricultural Land Use Changes in Thailand

K.S.RAJAN, Ryosuke SHIBASAKI & Masataka TAKAGI
Murai-Shibasaki Lab, Institute of Industrial Science,
University of Tokyo, Tokyo, Japan

Abstract :

Land under agricultural land use/cover is a major component of the terrestrial ecosystem, which is always under the influence of human activities. The dramatic rise in population in the last century has led to an expansion of the land under agricultural uses. This expansion has been at the expense of other land covers, especially forest. In this paper, we describe the model and its development to estimate the changes in the agricultural land use/cover, by simulating the agricultural productivity for the entire Kingdom of Thailand, on a grid basis.

Introduction:

Land use/cover is continuously changing, both under the influence of humans and nature resulting in various kinds of impacts on the ecosystem. To understand the impacts on the ecosystem, we need to understand the mechanisms of the processes involved. The linkages between the human land management schemes and biophysical causes or drivers to land use/cover - are not sufficiently understood. This arises because of the complexity of dealing with the considerable variations in the drivers, and their consequences at the local, national, and regional levels.

The transformations in the land cover, occurring on the large scale will lead to large scale changes in the "global environment". These changes are complex and require different scales of analysis. The changes from forest to agricultural land uses have had tremendous impact from local to global scale, such as soil erosion, deterioration of water quality and carbon emissions. To understand this process of change, it is required to estimate the potential to support agriculture and the economic yield of each land unit, as these are the key factors in modeling the behaviour of land owners and developers. This paper focuses on the estimation of yields based on the climatic and ground

conditions, the productivities for different crops, and estimates the changes in the land use. The SPANS and ARC/INFO GIS packages were used for the data processing and analysis.

Data:

Different types of data, ranging from maps to statistical data were collected from a large number of sources, including the national organizations and government departments in Thailand. The spatial data were digitized and worksheets of non-spatial data was prepared. The data was then pre-processed as per our requirements for subsequent analysis using GIS.

Model Development:

The model simulates the distribution of agricultural land uses of the major crops based on the corresponding productivities and income. The overall model framework is shown in fig 1. The model consists of two sub-models - the agricultural productivity sub-model and the income estimation

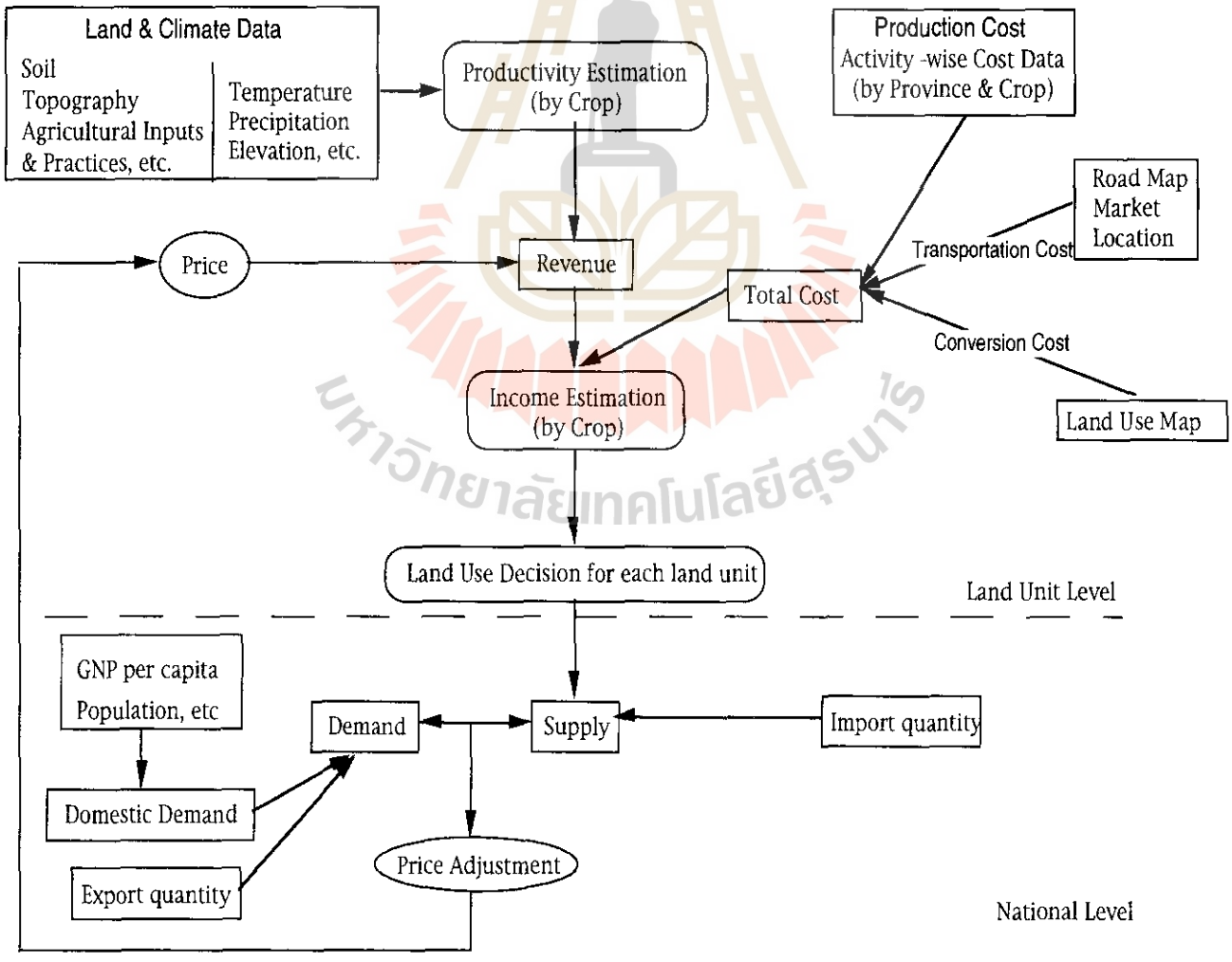

Fig 1. Overall model framework

sub-model, and a decision making module andthe model structure is sequential. The model calculations were carried out on a land unit basis (grid-based).

The agricultural productivity sub-model calculates the potential productivity of the land unit for the given conditions of soil, topography, water availability and climatic parameters. The distribution is initially calculated for the rain fed conditions and are then suitably modified for the availability of irrigation. The main assumption of this sub-model is that there is a strong linkage between the climate and crop distributions. (Leemans). The crop yield estimation is derived from the method developed by the FAO in its project on the agro-ecological zones (Anonymous 1978). The central concept of this approach is the growing period and the photosynthetic efficiency of the crops. The net biomass (Bn) is first calculated based on the aforesaid methodology. The final yield (By) is then calculated as follows:

$$By = Bn * Hi$$

where, Hi is the harvest index, defined as the fraction of the net biomass of the crop that is economically useful (e.g. grain in cereals, sugar in sugarcane, etc.).

The computations result in the climate based potential productivity distribution of the crops, assigning the values to each land unit. But to estimate actual potential production, soil characteristics are also of importance. Thus, the actual yield obtained in the above equation is modified based on the grid-specific soil conditions.

The income estimation sub-model estimates the income per land unit from the yield related revenue and its cost of production. The model also accounts for the initial cost incurred in land conversion from other uses to agricultural lands.

The final step in the simulation is the land use decision module, which uses the estimated income & the existing landuse in the land unit under consideration as its input to predict the land use. We use the 'Profit Maximization Principle' as the guiding principle in deciding the land use for a given land unit. As fluctuations in income over a short time-frame is quite natural, we prescribe a range of income, instead of a certain fixed value, to determine the shift. The land use decision is revised based on the price adjustment between the demand and supply for the various crops.

Results and Discussion:

In the estimation of the agricultural productivity, the value of the harvest index determines the economic yields of the respective crops. The

Crop	Product	Harvest Index	Average Index
Phaseolus Bean (inc. Mung Bean)	Grain	0.25 - 0.35	0.079
Soybean	Grain	0.30 - 0.40	0.151
Rice	Grain	0.25 - 0.35	0.259
Cassava	Tuber	0.50 - 0.60*	0.766
Maize	Grain	0.30 - 0.40	0.198
Sorghum	Grain	0.20 - 0.35	0.108

Table 1. Harvest Index of high yielding cultivars under rain fed conditions and the average harvest index of the calibrated values.

* Fresh Tuber at 35 percent dry weight

harvest index depends on a number of factors like the genetic potential of the crop - whether high yielding or low yielding and water regime - rainfed or irrigated. These are inherent to the crop variety in use and can be referred to as the unconstrained harvest yield index. But then, the level of agricultural inputs along with the soil conditions and topography also contribute to the harvest index at a given location, these can be referred to as the constraint factors. Then the harvest index (Hi) can be said to be a combination of the unconstrained yield index and the constraint factors. The harvest index ranges are given in the Table 1.

In the model simulation of the agricultural productivity, the harvest index has been first estimated and then calibrated. The village based point data for Rice and Cassava were obtained for the crop year 1990-91 and these values have been used to calibrate the harvest index of these crops. The yield values were calibrated for other major crops from the provincial values of the yield. The average harvest indexes for all crops and rice are also shown in Table 1.

Based on the calibrated harvest indexes obtained, we calculated the distribution of the yields for all the major crops and rice. Fig 2 shows the productivity distribution for rice. From these distributions of the productivities, were obtained the income distributions for three different cropping patterns, which was then compared with the land use patterns to determine the crop distribution. Fig 3. shows the distribution of the cropping patterns for the year of 1990.

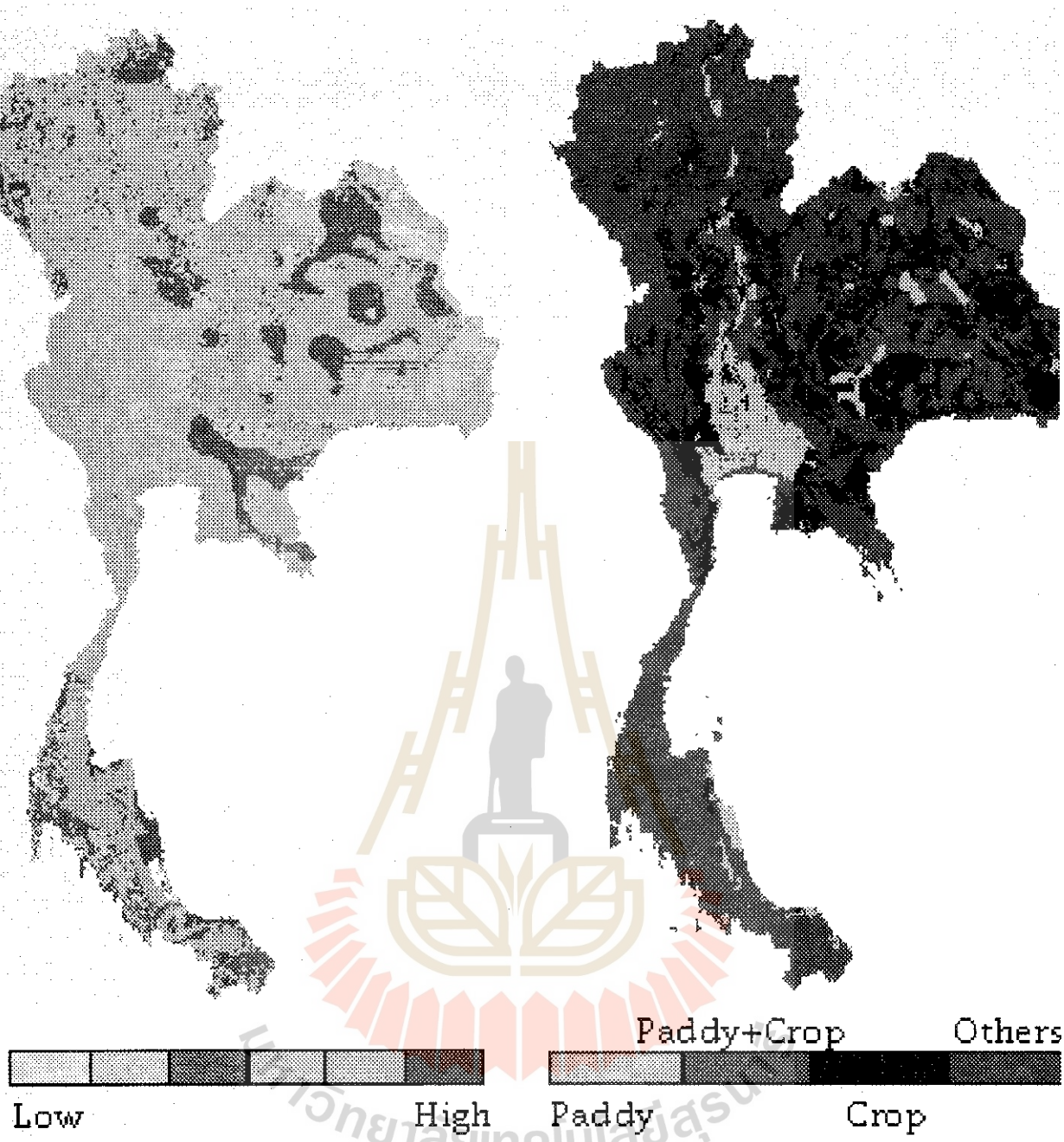

Fig 2. Productivity distribution of Rice **Fig 3.** Cropping Pattern in1990

Conclusion:

The climatic-based crop productivity estimation relations were formulated. The results show that the determination of the harvest index plays a significant role in such relations. As such, efforts must be made to suitably modify this factor to take into account the additional agricultural inputs such as fertiliser,etc to increase the yield. The quality of the datasets is of importance in these studies and so it is required to update the datasets to get a better understanding of the cropping patterns.

Reference:

1. Anonymous (1978), Report on the Agro-Ecological Zones Project. Food and Agricultural Organization of the United Nations, World Soil Resources Report 48, Rome.

2. Rik Leemans and A.M. Solomon : Modeling the Potential Change in Yield and Distribution of the Earth's Crops under a warmed Climate : Climate Research Vol.3, 1993

3. R. Leemans and G.J. van den Born : Determining the Potential Distribution of Vegettation,Crops and Agricultural Productivity : Water, Air and Soil Pollution Vol 76, 1994

4. Office of Agricultural Economics, Bangkok, Thailand : Agricultural Statistics of Thailand.

CAPABILITY OF REMOTE SENSING APPLICATION IN LANDUSE,LAND RESOURCES WITH USING TM DATA,GIS FACILITIES,IN PART OF IRAN

MAJID GHIASSI,MEHRDAD NEMATZADEH
REMOTE SENSING SPECIALIST
AGRICULTURAL STATISTIC AND INFO.
DEPT.(ASID)MINISTRY OF AGRICULTURE
TEHRAN IRAN.phone:9821-6122104
Fax:9821:650377

ABSTRACT

Capability of the landsat thematic mapper (TM)with high resolution,has now become much applicable to mapping,the various units of land resources,efficiently and accurately in a shorter period of time. During work described in this paper an attempt has been made to prepare various Landuse map by visual and digital interpretation of the TM data in conjunction with field check , covering an area about 68450 square km,in northern part of IRAN. In this project for interpretation,of the 9 quadrant from TM data, including visual interpretation,geometric correction,image enhancement,and classification,were applied to investigate , the total of 7 magor landuse levels, with their detailed sub-classes.
The GIS facilities also were applied to overlay and combine the results of visual and digital analysis.
The result of this project were the 1:100,000 scale landuse maps with the 30′ by 30′ geographic coordinates.

LOCATION OF AREA IN PHOTOMAP OF IRAN

1:INTRODUCTION

The thematic mapper(TM)data form landsat satellite have been utilized in Iran for the last few years to recognize and assess,land resources in various ways, proving their efficient performancs as a good tool,especially for landuse mapping and land deduction in general.
However the advent of the thematic mapper (TM)data with high resolution has made the mapping work facilitate better interpretation and analysis of the required object, as such,in this paper an attempt has been made to extract various information of crop land and land resources of Gilan region.

2:METHOD AND MATERIALS

To start with,the false color composit of the landsat TM,data inbands,2,3,4 and 4,5,7 in the month of june july 1989, 1990 1991 and 1993 at the average of1:100,000 scale,were selected ,the total image are 9 quadrants which cover the gilan province, an area about 68450 square km were chosen, for visual analysis as reflected through the image characteristics,during the month of july when the data were scanned,most of the cropsland were harvested , or in some part werenot devoid of crops, consequently , the radiant energy which produced the spectral signature mostly form the harvested surface,with communicated a good and usefull-idea to the interpreter that the various image characteristics recorded on the imagery were mainly due to the variation of crop land and soil color with the colors of exposed stones,and rocks, in forest region,and bare surface, the interpretative boundary become almost of crop land boundary in the region,all these interpretative units were correlated and compared with available data in hand ,finely a landuse uints were extract,after collection of ground truth,for compared interpretative units boundray with digital analysis units and available CCT tape,digitizing map also apply the GIS method,to overlay and combine together.

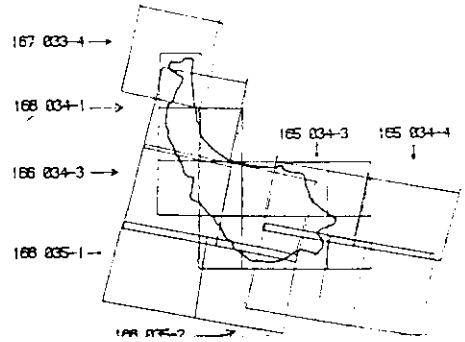

Location of study area in index of TM

3:VISUAL INTERPRETATION

The interpretation of the TM data was carred out in the Remote sensing Laboratory,

ASID on the basis of various image characteristics to occur in the area

MATERIAL

This porject was performed using map,satellite landsat(TM)data.

The MAP were:

Soil map classfication of study area 1:250000 scale

Geology map of area 1:250000

forest map of area 1:250000,

topography map of area 1:250000

Hydrology map of area 1:250000

Sensor	Date	Pixel	Scale
Landsat-TM	june1989	30x30	100000
image	june1990	30x30	100000
	july1991	30x30	100000
	jaunary1993	30x30	100000

Landsat-TM	Designation	Wavelength
CCT.july1993	1	0.45-0.52 um
	2	0.52-0.60 um
	3	0.63-0.69 um
	4	0.76-0.90 um
	5	1.55-1.75 um
	7	2.08-2.35 um

spectral bands of the sensor

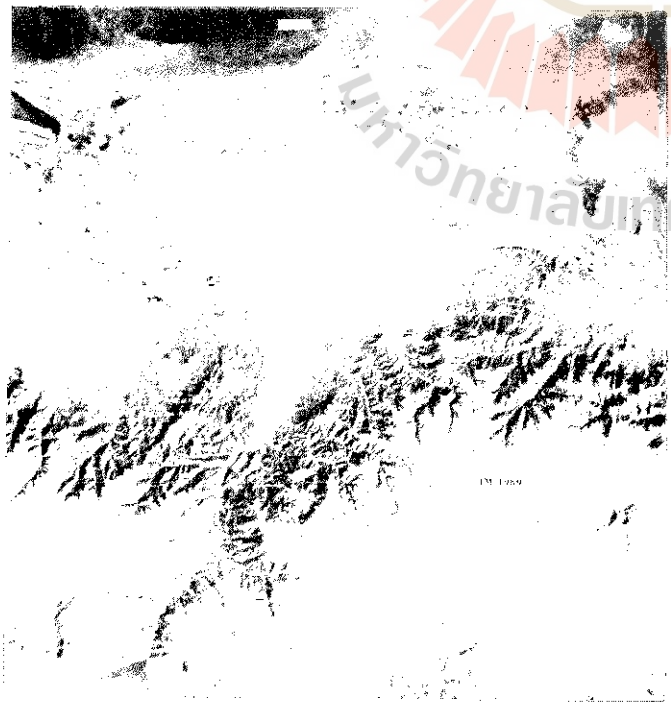

IMAGE OF STUDY AREA - 1989

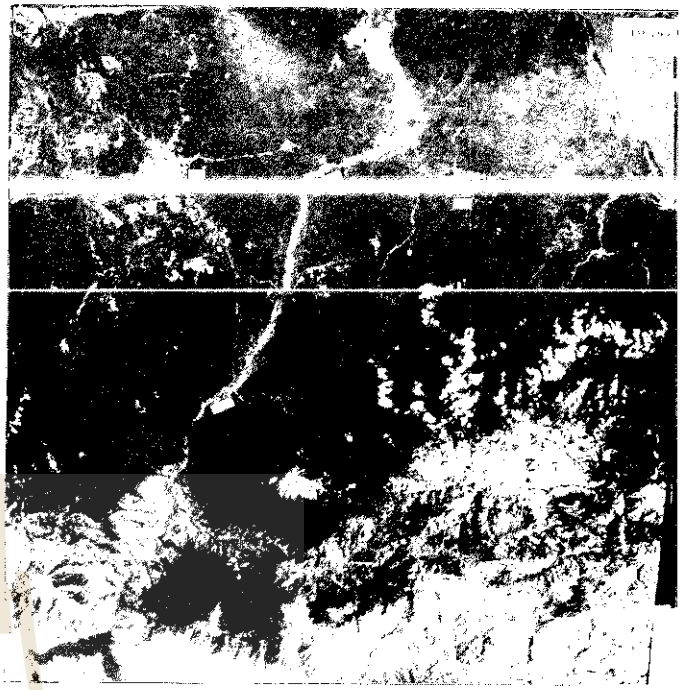

IMAGE OF STUDY AREA - 1991

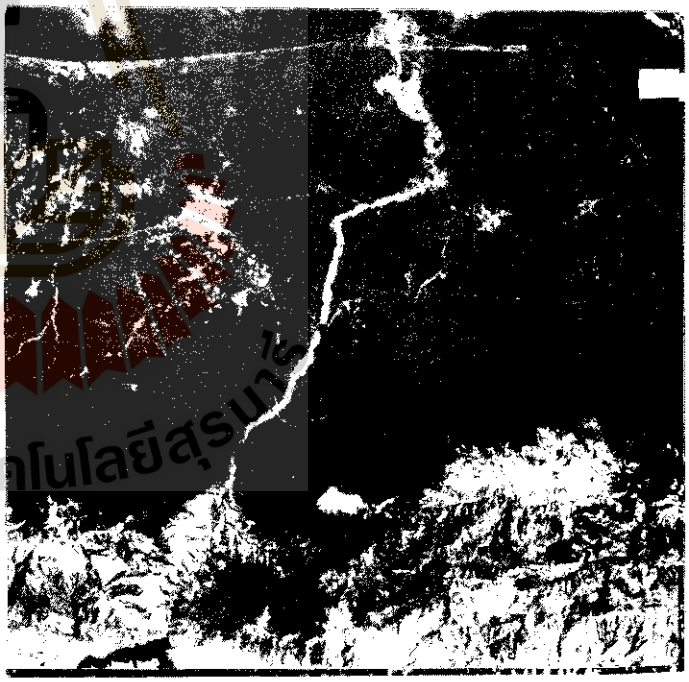

IMAGE OF STUDY AREA - 1989

3.1-FIELD WORK

With these recognition units ,a quick traverse was prepared, in the field to collect ground truth on landuse map, physiography ,for preparation of the maps corresponding to the landuse map,other scientist have also collaborated various natural resources.

4.DIGITAL IMAGE ANALYSIS

digital image processing is the numerical manipulation of digital image and includes preprocessing ,enhancement, and classification

4.1-Preprocessing:

In the initial processing of the raw data to collaboratethe image radiometry correction,geometric distortions,and remove noise.

4.2-Enhancement:

Image enhancement produces a new enhanced image, that is displaied on(CRT),this enhanced image may be easier to interpret than the original image in different ways, for example,more efficient use may be made of the orginal information.

4.3-GEOMETRIC CORRECTION

After processing raw data and apply projection properties of a map which is called geometric correction,a related technique were called registration,to utilizing of the coordinate system of one image to apply ofsame map or a second image of the same area,for example landsat TM image of a given area might be obtained for different dates and the user may wish to measure changes that have occured in period of time,the correction with two image of map, a map can be defined as a graphic representation on a plane surface of the earths' surface.

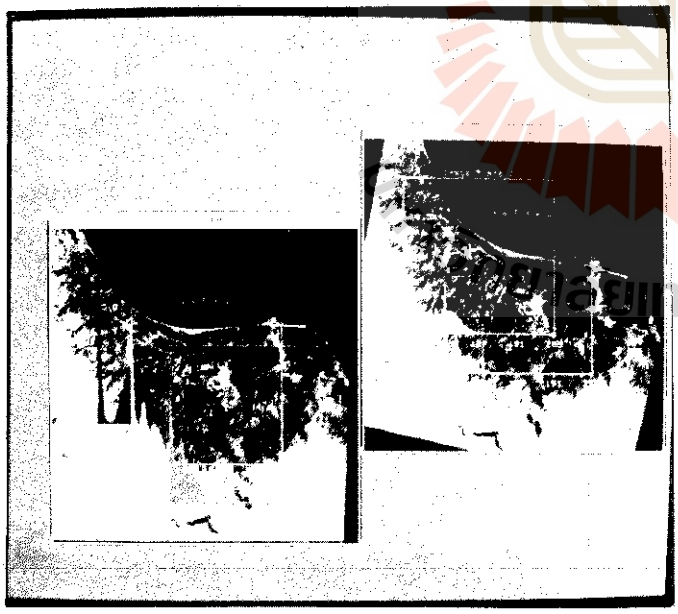

GEOMETRIC CORRECTION OF STUDY AREA

4.4-IMAGE CLASSIFICATION

For supervised training a representative area for each sample class must be located in the image ,it is important that the training area be a homogeneous sample of the respective class,but at the same time,the range of variability for class must be included,thus more than one training area,per class is often study area. aerial photography and existing maps are used to verify the training sites,if there is considerable within class variability, the selection of training sites can be laborious ,and it is impossible to be entirely certain that a comprehensive set of training samples for each class has been specified , sometimes in many cases it is impossible to obtain homogeneous sites,the problem is sparse vegetation, which complicates attempts to map both vegetation and soil,one technique for improving training data under these conditions is to clean the sites of outlying pixel,before developing the find class sigantures, the cleaning operation involves applying a histogram of scatterploting operation on the training data.until to apear interest classes,after the apear classes it is possible to designe pseudo-color image and transfers a pseudo color table segment stored on the database file, in this case to converte pseudo-color segment to transfer arc/view format was desigined to be developed all purpose standard for image interchange tiff file consist, of an image with a list of information tages describing the image,and then used GIS methodology,to converte the grid format of ARC/info,polygon type,the digital classification landuse units are overlay the GIS system.

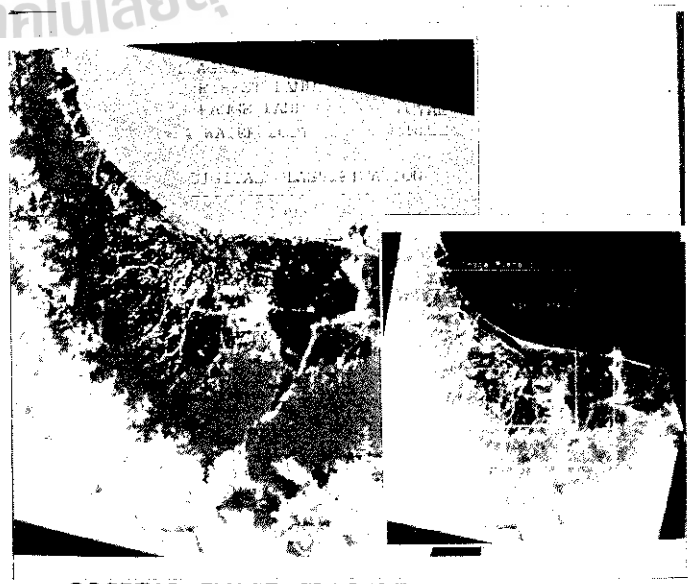

DIGITAL IMAGE CLASSIFICATION OF WHOLE GILAN REGION

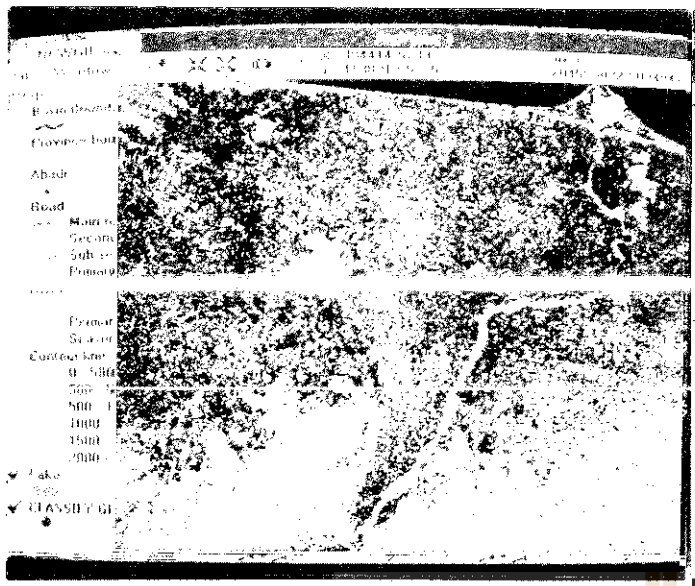

TRANSFER IMAGE CLASSIFICATION TO GIS

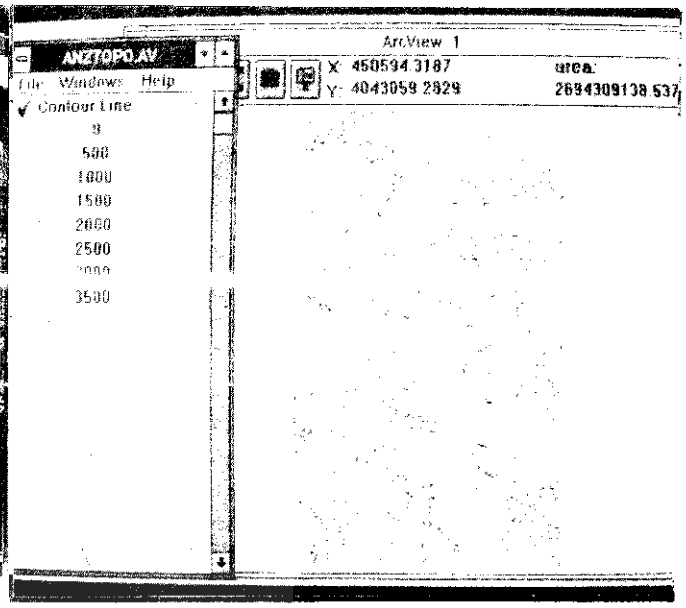

TOPOGRAPHY IMAGE OF TEST AREA

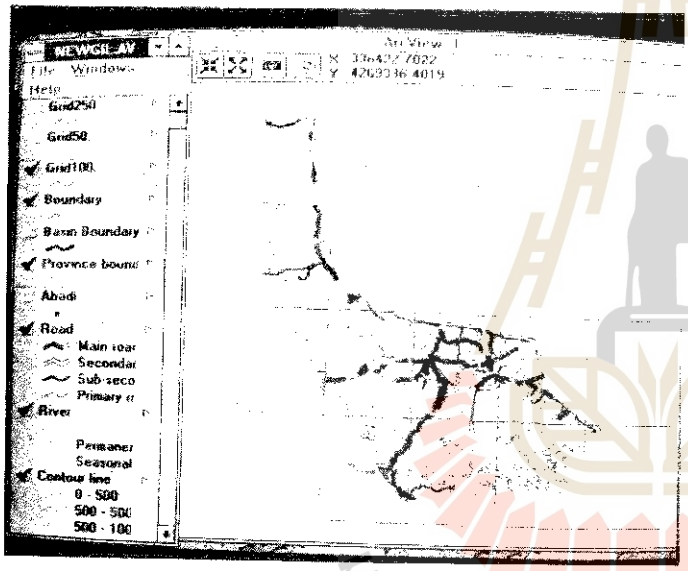

DRAINAGE PATTERN AND ROADS IN GIS

5.LANUSE MAP

It has already been stated that TM data were scanned in the june july 1989 1990 1991 and 1993,when the land surface in the region is most harvested or in some place was not hervested of crop,in this condition operation of map detailed information about landuse was recorded,while studing the forest unit and soil capability of the area ,all these information along with the new data from the survey of Iranian topo sheet to convention of different scale,and available data relating to various correlated image characteristics,were used to prepare the map,acoording landsat imagery,the index of TM data,with topo maps index of 1:100000 scale,gilan province recorded approximately 11 mapsheets was delineated.

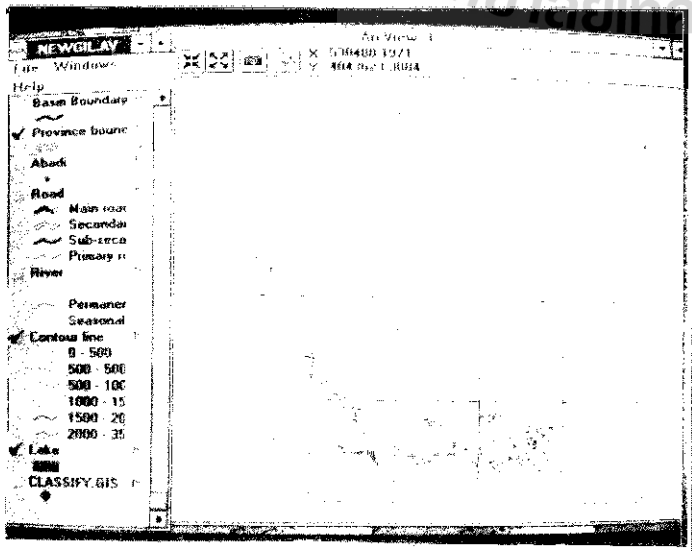

IMAGE OF TOPOGRAPHY PATTERN IN STUDY AREA

IMAGE OF LANDUSE CLASSIFICATION MAP

LANDUSE MAP LEGEND

IRRIGATED LAND
- -without limitation or low limitation 11
- - with limitation 12
- -nonirrigated land DF
- -orchard O
- -tea T
- -olive OL
- -mix with crop land and orhard 10
- -mix with orchard and crop land OI

FOREST LAND AND WOOD LAND
- -high density or medium density forest F1
- -low density forest F2
- -mixed forest and orchard FO

RANGE LAND
- -high density or medium density R1
- -low density range R2
- -mixed range and nonirrigated land RD

BARREN LAND
- -salty land without vegetation coverage SL1
- -sallty land with native vegetation SL2
- -sandy dume SD
- -bare land B

WET LAND
- -reed bed RB
- -swamp SW

SURFACE WATER
- -natural lake L
- - dam lake L1
- -permanent river Y
- -seasonal river -.-.-.
- -canal ======

URBAN BUILT-UP LAND
- -urban area U
- -constraction U1
- -airport
- -main road
- -secondary road
- -railway
- -international boundary
- -province boundary

ESTIMATION OF LANDUSE UNITS IN GILAN PROVINCE

LANDUSE UNITS	SHEET NUMBER									
	5766	5765	5764	5865	5864	5863	5964	5963	5962	5961
URBAN AREA AND BUILT-UP	1439	656	74	1427	5074	528	7905	204	3685	31	74
IRRIGATED FARMING	3853	16369	—	7827	33881	2725	90859	4926	40569	—	1312
MIXED-ORCHARD AND CROPLAND	4074	12014	33	5103	55055	4138	31153	13575	19596	11455	1328
OLIVE	—	—	—	—	—	7397	—	2191	—	—	—
TEA	—	—	—	—	8721	—	9366	—	19701	590	200
FOREST	72398	119213	45647	11588	98624	23583	62457	7527	24815	53876	6866
RANGE	16650	31738	11656	3505	8275	18743	2582	74965	2650	67344	—
DRY FARMING	—	43	—	—	—	10870	—	18374	—	11667	—
REED BED	—	—	—	690	9073	43	6214	—	3330	—	—
SWAMP	—	—	—	1030	3440	—	—	—	480	—	—
DAM LAKE	—	240	—	—	—	2300	40	90	—	—	—
POOL	120	8	—	105	976	—	2797	30	206	—	—
SANDY BEACHES	775	800	—	1210	187	895	7310	370	1920	—	200
BARE LAND	—	—	30	—	—	350	—	14801	—	310	—

PERCENTAGE OF LANDUSE UNITS IN GILAN PROVINCE

LANDUSE UNITS	URBAN AREA & BUILT-UP	FOREST	RANGE	IRRIGATED FARMING	DRY FARMING	TEA	OLIVE	MIXED-ORCHARD AND CROPLAND
AREA(ha)	29915	580345	238108	204222	40954	35578	9388	151936
PERCENTAGE	1.5	41.7	17.1	14.8	3	2.6	0.7	10.9
LANDUSE UNITS	SANDY BEACHES	DAM LAKE	POOL	BARE LAND	SWAMP	REED BED		* TOTAL AREA OF PROVINCE
AREA(ha)	13662	2670	4242	6380	4950	18350		1391368
PERCENTAGE	1	0.2	0.3	0.5	0.4	1.3		100

* TOTAL AREA OF GILAN PROVINCE INCLUDING FRONTAGE OF ROADS AND RIVERS

CONCLUSION :

Due to the wide spectral range of TM data, the better manipulation ability would be provided for analyst in the different stages of image processing. In the other hand, the sufficient number of TM spectral bands which causes more collection of ground features would be concerned to define the better detailed landuse units and consequently, the more detailed information would be extracted from relative landuse maps.

It is obvious that using the other kinds of satellite data (SPOT,COSMUS,...) combined with TM data and integration of visual and digital interpretation could provide the more useful and correct landuse maps.

Simulating forest degradation: Applying the Area Production Model in the Kali Konto area in East Java, Indonesia[1]

Alfred de Gier and Yousif Ali Hussin
International Institute for Aerospace Survey and Earth Sciences (ITC), Enschede, The Netherlands
E-mail: degier@itc.nl Fax: +31 53 874399

ABSTRACT

Forests cover large areas of the global land surface. For many developed and developing countries, they represent an important source for their economies. Due to the growing need for more agricultural land, more and more forests are under the risk of degradation and disappearance. To safeguard forests from extinction, alternative food production strategies need to be developed, while at the same time proper management of the forest resources is required. All this requires information on land use and its changes, and on the people who engage in these processes. This information is important to those who are responsible for forest and land use policy development, and to those engaged in land use planning and management.

The Area Production Model (APM) permits the simulation of future land use changes in response to *population growth*, *changes in gross domestic product*, and in *agricultural productivity*. The model was developed for the Food and Agriculture Organization (FAO) of the United Nations by Nilsson in 1984. The model is used for long-term scenario development and analysis. In its original form, the APM is numerical (and graphical) in data requirements and output. This paper shows that the Area Production Model can be used for the simulation of forest degradation in an area in East Java, Indonesia, using a combination of multitemporal aerial photograph, satellite and field data.

INTRODUCTION

Tropical deforestation is one of the major concerns today. Current deforestation rates are estimated to be about 15.4 million ha per year (FAO, 1994). However, forest degradation, as a result of unsustainable human activities, affects an even larger area of forest annually.

The importance of forests is well recognized by governments worldwide, as reflected in the "Forest principles" that were adopted by the UNCED conference in 1992. Foresters and all other land users and land use planners should therefore find ways to control, stop, and even reverse this process. Politicians are supposed to decide on and implement the required institutional measures. Given the speed of the process, two issues are clear: actions are needed without undue delay, and a sustainable effect of such actions can be expected only if the causes of the problem are tackled. The problem thus needs to be examined from a cause-effect point of view.

The major cause of forest destruction is the need for more agricultural land, which itself is largely a consequence of rapid population growth and rising economic expectations. This means that the major function of forest land is that of donor for agricultural land. In addition, the need for timber, fuelwood and cash also influence forest destruction. These

---

[1] To be presented at the 16th Asian Conference on Remote Sensing, Suranaree University of Technology, Nakhon Ratchasima, Thailand, 20-24 November 1995

causes should therefore be approached from a perspective of land and its products, and the increasing demands for it. Since, in principle, demand for more agricultural land (at least in part) could be met from non-forest land, not only forest land but also the agricultural lands in the area should be included. However, the need for more agricultural products not only can be met by bringing more land under cultivation, but also by increasing the productivity of existing agricultural land, i.e., by intensifying agricultural land use.

The development of the Area Production Model (APM) (FAO, 1986a) has been an important step in simulating land use changes, by varying the input variables. The APM is intended for simulation of long-term land use changes and the prediction of primary and secondary yields from agricultural and forest lands. One of the major features of the APM is its capability to simulate the future need for agricultural land. The model's demand and supply scenarios for agricultural products and land are generated primarily by the growth rates of population and GDP, and by changes in land productivity. The model is comprehensive, but does not have excessive data requirements.

The model uses three different agricultural classes:
- land for subsistence crops (used mainly for home consumption)
- land for market crops (produced mainly for the local markets)
- land for cash crops (destined primarily for markets outside the area).

An important aspect of the APM is the concept of land allocation. If demand for land in a particular class increases, transfers of land from another class to that one are generated by the model. Only when the donor class concerned is exhausted, land from another class is transferred, and so on. The sequence of the donor land use transfer classes is specified by the APM user. Forest land is commonly the last land donor.

The model has been tested in East Java, Indonesia and in Rachabury Province, Thailand (FAO, 1986a and 1986b) and in two parts of Peru (APODESA, 1989). In the three cases, tropical forest areas were included. The conclusions were that the model was adequate and sufficiently adaptable for extension as well as modification. The original FORTRAN version was later converted to LOTUS 123 (Williams (1987).

The APM requires numerical data input. Its output is in tabular and graphic form. Spatial data are neither required nor produced. The APM is therefore insensitive to the location where the need for more land exists, and to the location of the donor land use class from which land is to be transferred. This is considered a major limitation, because it is not possible to predict where the land for the specific classes will be needed, and where the land of the relevant donor class is located. Furthermore, a spatial model would allow to grade accessibility to potential donor land, by using friction coefficients. It could also simulate the locational effects of decisions that influence the need for land transfer.

De Gier and Hussin (1993) described how the spatial component was developed and succesfully linked to the model for the Kali Konto area in east Java, Indonesia. All spatial data used were in digital form. The results of this spatial implementation show the suitability of GIS for combining the spatial component and the numerical output from the APM.

Further enhancement of the spatial version was desired, to accomodate multi-temporal spatial data of transfer processes as they occur in reality. The outcome of this would then be used to calibrate the model, and would allow the determination of key operators. The test site was the Kali Konto area (Figure 1), a sub-watershed of the Kali Brantas watershed in East Java, Indonesia, for which multi-temporal data were available. The Kali Konto sub-watershed covers some 23,500 ha, of which about 15,685 ha are classified as forest land, owned by the state. The elevation varies between 620 m and 2650 m a.s.l. The existing forest consists of

natural stands and plantations which are mostly for protection and preservation. In 1991, the population of more than 100,000 people lived in villages outside the forest land (so-called village land). About 75 percent of them were small farmers and farm labourers. They crave land since they are unskilled for work other than in agriculture. About half of the labour force is unemployed or under-employed.

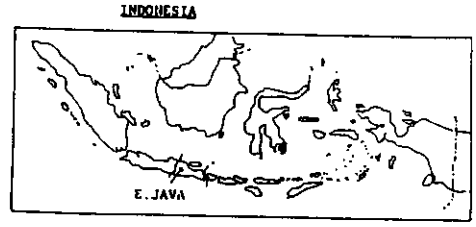

Figure 1 The location of the Kali Konto area

Wood is an important commodity in the rural areas. It is used as fuel in households and small industries, and as poles for housing. An unknown number of (mostly landless) people gain their income by illegal cutting and selling fuelwood from the nearby forests. This process has led to severe degradation of the natural forests in many parts.
According to Project Kali Konto (PKK, 1984), **forest** is defined as land that has a tree crown cover of more than 20 percent; **scrub** has a tree crown cover of 20 percent or less. The latter can include failed or abandoned plantations. In 1979, the proportion of scrub land was 18 percent.

Unlike forest lands outside Java, conversion of state forest lands to non-forestry purposes is not allowed by law. In the field, the state forest land boundary is separated from privately owned village land by clearly visible concrete boundary-posts. Land transfer from forest to agricultural land (as predicted by the APM) will in reality not occur: forest land remains forest land even if the forest cover changes.

There is very limited non-forest land available for transfer to agriculture land. The easiest way for the landless and the poor people in this area to satisfy their basic needs is to go to the forest, cut the trees, and sell them for timber or fuelwood. The income is used to buy food and other goods. This compensates their need for agricultural land, but at the same time causes degradation of the forests, and ultimately leads to scrub land. It follows that population growth in the Kali Konto area does not lead to new agricultural land, but to scrub land.

The main aim of this paper was to determine whether there is a relationship between the amount of new agricultural land as calculated by the APM over a given period of time and the actual increase in area of scrub land in the same period. If this relationship exists, the APM can help forest policy makers to anticipate future forest degradation, and to suggest timely action.

MATERIALS AND METHODS

To enhance the spatial component of the APM, the numerical results of the APM were used to define the spatial expansion of agricultural land over forest land on a year-by-year basis. Next these expansion areas were grouped in 10-year classes. Finally, the expansion was limited to a period of 50 years, the normal time horizon for APM.

The following data were available for the Kali Konto area: panchromatic aerial photographs, scale 1:20 000 of 1979; landuse map of village land and forest lands, based on the 1979 aerial photo interpretation; a Landsat MSS image of 1982; panchromatic aerial photographs, scale 1:20 000 of 1984; and field data of 1993. A TM image of 1989 was rejected because of cloud cover.

The boundaries of the cover types on the two land use maps mentioned above were digitized, resulting in digital land cover maps of 1979. Next, the types were grouped into the classes as required by the APM. The 1982 Landsat image was classified on the basis of bands 4,5 and 7, and a

supervised classification algorithm, using a maximum likelihood classifier. The result of the classification was filtered twice by applying a 3x3 median filter. The aerial photographs of August 1984 were interpreted and classified using the same classes of forest cover as in the 1979 data. The class boundaries were subsequently digitized. The forest cover map of 1993 was made using sketch mapping techniques. The same forest cover classes were identified and delineated during a field check with the help of an orthophoto mosaic and a forest plantation map of 1979. The class boundaries were then digitized.

From the local administrative and agricultural offices, data were collected on population and population growth, GDP and GDP growth, and agricultural production and production growth for the various crops concerned. Overlay techniques, using the ILWIS GIS, then permitted a multi-temporal analysis of land cover changes. The year 1979 was the base year from which all changes were monitored.

RESULTS AND DISCUSSION

Table 1 shows the presence of the following land categories in 1979 (groups of three classes each)

Table 1. Land cover/land use in 1979

APM category	Land use/land cover	ha
Agricultural land		5 756
Forest land, farm		1 577
Forest land, industrial		2 781
Forest land, environmental		12 898
Other land		1 266

After comparing the cover of the privately owned agricultural land and farm forest land (so-called village land) of 1979 and 1993, it was noted that hardly any change had occurred. It was also noted that it is very difficult to separate land use/land cover classes on village land, using the 1982 Landsat data. It was therefore assumed that within the village land no transfers took place (i.e., for the purpose of using the APM, all new agricultural land is supposed to come from forest land). Table 2 shows the changes in areal extent of the various land cover classes, and also the amount of agricultural land requirements as calculated by the APM (Hargyono, 1993).

Table 2. Summary of land cover area over 1979 - 1993

Class	Area (in ha) in year			
	1979	1982	1984	1993
Lake	319	- *)	319	319
Village land	6669	- *)	6669	6669
Built-up	906	- *)	906	906
Plantations	2939	1808	2883	2717
Natural forest	7171	7708	6382	6138
Scrub	5625	6162	6413	6823
Agricultural land required, according to APM	5757	6062	6275	6991

* not mapped

Figure 2 shows the relationship between the required area, as calculated by the APM, and the actually observed area of scrub. The

corresponding trend is approximated by the curve shown in Figure 3. This relationship indicates that the scrub area increases, as the need for agricultural land increases, but at a decreasing rate. More

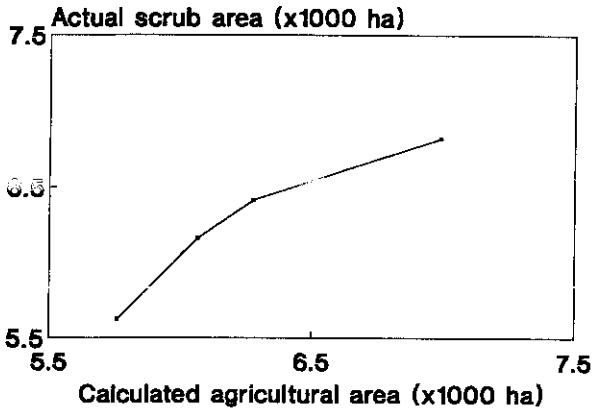

Figure 2 Relationship actual scrub area and APM-calculated agricultural area

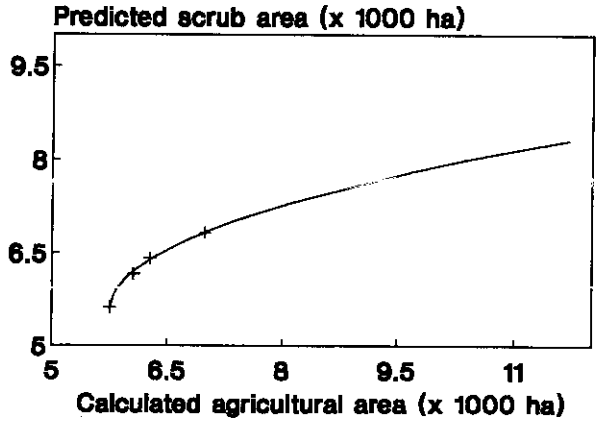

Figure 3 Predicted scrub area according to APM-calculated agricultural area

research is needed to explain the relationship, but it may be explained partly by the fact that an increasing part of the population finds employment in the towns just outside the study area. They would not require land for subsistence food.

The results as shown in Table 2 are numerical. The scrub areas, as they developed between 1979 and 1984, and between 1984 and 1993, are shown in Figures 4 and 5. These figures show two important aspects: (1) scrub areas develop mainly on the fringes of the forest, and (2) scrub areas do not develop uniformly along all these fringes. Comparing the two figures, a number of differences are clear: for the eastern village area the scrub edge at the northern boundary expanded almost uniformly between 1979 and 1984. Between 1984 and 1993, however, scrub expansion was confined mainly to the eastern part of the boundary. On the southern forest border of the same village area, scrub increase was more prominent in the eastern part of the border between 1979 and 1984, and in the western part between 1984 and 1993. It is also interesting that scrub increase was minimal along the borders of the western village area. In some places, scrub advanced into plantation forest areas between 1984 and 1993.

Figure 6 shows the results of the selective spatial expansion of the agricultural land into the forest land, as calculated by the APM.

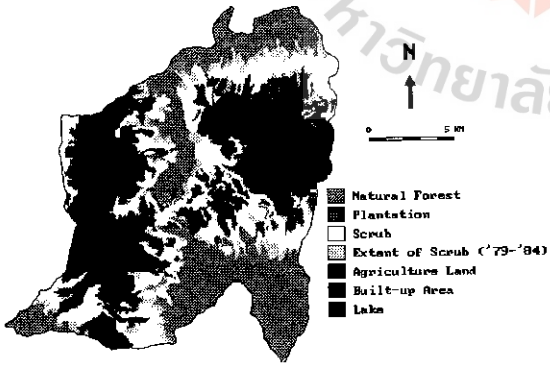

Figure 4 Scrub land increase 1979–1984

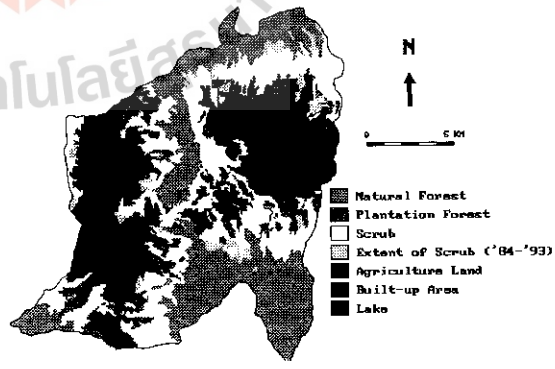

Figure 5 Scrub land increase 1984–1993

The calculated agricultural expansion is evenly distributed, according to the priorities set, and located just adjacent to the existing agricultural areas. In respect of expanse of agricultural area, the numerical and the spatial APM agree. Comparing Figure 6 with Figures 4 and 5, differences are apparent. The APM considers existing scrub land as forest land. These observations underscore the importance of spatial differentiation. One of the next steps in improving the APM

will be to simulate new scrub development outside the current scrub areas. Secondly, key factors that lead to the specific spatial patterns will be identified.

Conclusions

- The combination of multi-temporal data from aerial photographs, Landsat MSS and field observation permitted the monitoring of the advancement of scrub land, i.e. forest degradation, in the Kali Konto area between 1979 and 1993.
- Over the same period, the Area Production Model was used to calculate the additional area of agricultural land, required to satisfy the growing needs.
- A good relationship could be established between the observed scrub land increase, and the calculated agricultural area requirements.
- Spatial analysis of the locations were scrub expansion took place indicates the need for further enhancement of the spatial APM. This will permit the determination of key operators, that influence extent and location of future forest degradation.
- The presence of persistent cloud cover in the area points to radar imagery as a possibly better source of multi-date information.

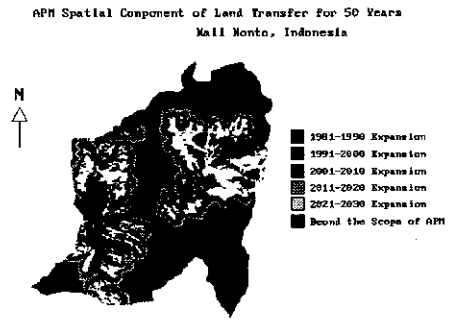

Figure 6 Agricultural expansion, according to APM 1980-2030

REFERENCES

APODESA (1989) El modelo de áreas de producción (APM) y su aplicación en la selva Peruana. Proyecto Apoyo a la Política de Desarrollo Regional. Apodesa, Lima, Peru

De Gier, A. and Y.A. Hussin (1993) Spatially resolved Area Production Model in Kali Konto, Indonesia. GIS/LIS '93 Proceedings, 2-4 November, Minneapolis. MN, USA. ASPRS, Bethseda, Maryland. pp. 157-169

FAO (1986a) Manual for using the Area Production Model (APM), Case Studies, Asia-Pacific Region. GCP/RAS/106/JPN. Field Document 12:2. 99 pp.

FAO (1986b) Users guide to Area Production Model, Asia-Pacific Region. GCP/RAS/106/JPN. Field Document 12:1. 65 pp.

FAO (1994) The State of Food and Agriculture 1994. FAO, Rome, Italy

Hargyono (1993) Occurrence and prediction of forest degradation. MSc. thesis. International Institute for Aerospace Survey and Earth Sciences (ITC), Enschede, The Netherlands

PKK (1984) Evaluation of forest land. Kali Konto Upper Watershed, East Java, Vol III. Natural Forest. Project Kali Konto, Malang, East Java, Indonesia.

Williams, D. H. (1987) LOTUS APM, version 1: a spreadsheet version of the Area Production Model 1. Asian seminar on forest planning, Kuantaun, Malaysia. 12 pp.

Simulating forest degradation: the application of a GIS-based Area Production Model in Kali Konto, East Java, Indonesia[2]

Alfred de Gier, Johan Bode and Yousif Ali Hussin
International Institute for Aerospace Survey and Earth Sciences (ITC),
Enschede, The Netherlands
E-mail: degier@itc.nl Fax: +31 53 874399

ABSTRACT

The spatial version of the Area Production Model (APM) would permit the simulation of future land use changes in response to changes in *population, gross domestic product,* and in *agricultural productivity.* Land transfers from forest to agriculture, for example, can be simulated in this way. The model was developed for the Food and Agriculture Organization (FAO) of the United Nations by Nilsson in 1984. The model is used for long-term scenario development and analysis. In the Kali Konto area forest degradation into scrub, takes the place of transfer of forest land to agriculture, due to strict law enforcement. The growing population sells the forest products and uses the proceeds to purchase food products. It was found earlier that a good relationship exists between the area of agricultural expansion, as calculated by the APM, and the actually observed area of degraded forest. Forest policy makers can thus use the APM to simulate the effect of changes in the above factors, and decide on appropriate actions.

Recently, an GIS-based APM was developed, by integrating it within the ILWIS-GIS. This permitted the inclusion and analysis of key operators, such as slope, distances, population pressure and population growth. This paper describes the results of the GIS-based APM in the Kali Konto area.

INTRODUCTION

One of the major functions of the Area Production Model (APM) is its capacity to simulate long-term land use changes, by varying several input variables, especially: *population and population growth, gross domestic product and its rate of change,* and *land use and the rates of change in agricultural productivity.* For a period of up to 50 years, the APM calculates the required primary yields from agricultural and forest lands and matches this by appropriate changes in agricultural land area. The model thus simulates the future need for agricultural land.

The model's demand and supply scenarios for agricultural products and land are generated primarily by the growth rates of population and GDP, and by changes in land productivity. The model is comprehensive, but does not have excessive data requirements. Its output in in the form of tables and graphs; it is thus a numerical model.

The model uses three different agricultural classes:
- land for subsistence crops (used mainly for home consumption)
- land for market crops (produced mainly for the local markets)
- land for cash crops (destined primarily for markets outside the area).

---

[2] To be presented at the 16th Asian Conference on Remote Sensing, Suranaree University of Technology, Nakhon Ratchasima, Thailand, 20-24 November 1995

The first class depends on population and population growth only; the latter two depend on GDP, being an expression of market forces.
An important aspect of the APM is the concept of land allocation. If demand for land in a particular agricultural class increases, transfers of land from another class to that class are generated by the model. Only, when the donor class concerned is exhausted, land from another class is transferred, and so on. In many areas of the world, the main land donor is forest land. In the APM, the category forest land is subdivided into three classes. More details on the APM can be found in FAO, 1986.

De Gier and Hussin (1993) linked a spatial component to the numerical APM. Recently an GIS-based version of the APM was developed, where its main components were integrated into the Integrated Land and Water Information System, ILWIS, a GIS with built-in processing capabilities for digital remote sensing images. It was developed by the ITC in The Netherlands. Hussin and Bode (1995) describe the structure of the GIS-based version.
This paper describes the experiences of the GIS-based version of the APM in the Kali Konto area in East Java, Indonesia.

In the Kali Konto area strict law enforcement prevents the state-owned forest land to be converted into agricultural land. The remaining land is already brought under agriculture or is used as housing land. The growing population is therefore facing a severe constraint to satisfy its demand for food and other basic needs, since agricultural expansion is not possible. It is felt that a growing number of landless people in particular, engage in illegal felling of trees and sell them for fuelwood and timber. The proceeds are then used to purchase food and other goods. As a result, the forest is then more and more degraded, finally reaching a state of scrub. Because the actual development of scrub is known from multitemporal data over the period 1979-1993, the overall aim of the research project is to identify the level to which the APM can be enhanced for properly simulating the ongoing forest degradation. Under the assumption that the landless people are mainly responsible for forest degradation, the class "land for subsistence crops" is determining in the APM. It follows that population figures and their rates of change are relevant, and not GDP.

This paper describes the results of applying the recently developed GIS-based Area Production Model to data of the Kali Konto area over the period 1979-1993, and compare the outcome with the real observations of scrub development over the same period.

METHOD

In an earlier paper, De Gier *et al* (1995) describe the performance of the spatial component that was linked to the APM, using multitemporal data for the period 1979-1993. The population growth was assumed to be the same for the entire area. One of the conclusions was that although the spatial component performs well in general, more precision in the specific locations of scrub development was desirable. For example, it was noted that scrub development did not develop uniformly along the fringes of the forest. It was hypothesized that these locations were not only dependent on the factors meantioned earlier (population, GDP, crop production, and their rates of change), but also on specific locational factors.

In the GIS-based model the so-called village land (*ie* the non-forest land) of Kali Konto, was first subdivided into indvidual villages, each one with its known area, population and population growth. In addition, the GIS-based model included six spatial factors: Slope percent, Distance from the village land, Priority of land transfer, Population density, Population growth. Each pixel was accordingly labelled. The underlying asumptions are that a larger slope percent means a slower forest degradation and a higher the friction value; a

greater distance results in a slower the forest degradation and a higher the friction value; a higher priority value (*ie* low priority!) means a slower forest degradation and a higher friction value; a higher population growth results in a faster forest degradation and a higher starter value; a higher population density means a faster forest degradation. It was assumed that one or more of these factors would explain most of the variation of the scrub land development. Contrary to the numerical APM, it was further assumed that different types of forest, such as plantation forest, protection forest, etc. could be degraded at the same time, as is normally observed.
In order to avoid unreasonably large values for the factor slope*distance, these values were reduced to within the range 1-10.

The demand for future agricultural (subsistence) land is calculated according to:

$$Na = Pa*(1+p/100)^n$$

where
Na demand for agricultural land in year n
Pa present amount of agricultural land
p growth percent of the population

The equivalent amount of degraded forest land or scrub (Ns) at year n is calculated according to (Hargyono, 1993):

$$Ns = 151.62*Na^{½} - 0.44*Na - 2989$$

where Na is defined as above.

RESULTS

To verify the outcome of the GIS-based APM, first a numerical comparison was made with the observed data from 1979 to 1993. Table 1 shows that the differences were 5% or less.

Table 1 Calculated scrub areas according to two APM models

Year	Scrub area numerical APM (ha)	Scrub area GIS-based APM (ha)	Difference (%)
1979	5756	5756	0.0
1984	6297	6140	-2.5
1989	6890	6550	5.0
1994	7102	6987	2.0

When comparing similar values for a period up to 50 years, differences do not exceed 7%. Unfortunately, no comparison was made for all years of which observed values existed. They were: 5757 ha (1979), 6062 ha (1982), 6275 ha (1984) and 6991 ha (1993). The data suggest that the GIS-based APM performs better than the numerical APM.

Next, the spatial data were inserted: a raster map of the villages was available. The population and population growth data for each village were obtained from Nibbering (1980) and Hargyono (1993). The year 1979 was the starting year. A detailed land cover map, based on an interpretation of panchromatic aerial photographs of 1979, scale 1:20 000, was available. A second land cover map, also based on airphoto interpretation, and using the same criteria as used for the 1979 map, was available for 1984. A map was constructed, showing the scrub developments that took place between 1979 and 1984.
Applying the GIS-based APM on the data, and comparing this with the number and location of the scrub pixels as they developed in reality

from 1979 to 1984, revealed that: forest plantations should be considered as absolute barriers (*ie* they hardly degrade), and new scrub develops from existing scrub land. Altogether, only 36% of the scrub pixels were spatially predicted correctly; numerically, as much as 77% of the pixels was classified correctly, highlighting the difficulties of spatial accuracy.

A further analysis was made with regards to which factor was the most determining one in scrub development. These factors were: Slope percent, PopulationDensity, PopulationGrowth, PriorityTransfer (of land), and the combined factors SlopeDistance (= slope*distance) and VillageFactor (population density*population growth). Two weights were used (0.1 and 10). The analysis refers to numerically and spatially correct number of pixels.
In decreasing order of importance, the following sequence of factors emerged: VillageFactor (36%), PriorityTransfer (31%), SlopeDistance (31%), Slope (30%), PopulationGrowth (29%) and PopulationDensity (29%). The percentages refer to the percentage of correctly classified pixels for the factor concerned, when setting the other factors at default. It was also found that a low weighing of the factors, *ie* 0.1 gave better results.

COMMENTARY

The study showed that better results were obtained when plantation forest was considered an absolute barrier, *ie* not degradable. However, field observations and multitemporal airphoto interpretation show that change into scrub can take place. It is not known, however, whether this is due to failed plantations, or to deliberate actions by people. Most of the forest plantations are located just inside the forest boundary, to serve as a barrier for forest penetration. Also, they are generally well protected by forest guards.

The numerical result of the GIS-based APM is satisfactory (77% correct), but the spatial accuracy is low, not exceeding 36%. To further increase this percentage, a further reduction of weighing should be tested, especially to the factors VillageFactor and SlopeDistance. Taking into consideration the location of roads and especially the tracks might further improve the model, because it is along such ways of access that people enter the forest, and transport the forest products. Many tracks can be seen on the 1:15 000 and 1:20 000 scale aerial photographs, but not on the current generation of satellite images. It is to be remarked that up to 1993 no cloudfree SPOT image was available.

Finally, the period of verification was from 1979 to 1984. Using a longer time period, eg from 1979 to 1993 for which verification data are available, might remove short-time variations, and yield a more accurate result.

REFERENCES

De Gier and Hussin (1993) Spatially Resolved Area Production Model in Kali Konto, Indonesia. Proceedings GIS/LIS '93, Annual Conference and exposition, Minnesota, USA, (1) pp. 157-169

FAO (1986) Users Guide to the Area Production Model, Special study on Forest Management, Afforestation and utilization of Forest resources in the developing regions, Field Document 12:1, Food and Agricultural Organization of the United Nations, Bangkok.

Hussin and Bode (1995) Simulating forest degradation: The Crystal Globe (a GIS-based operational Area Production Model in ILWIS Image Processing and GIS). Proceedings 16th Asian Conference on remote Sensing, Nakhon Ratchasima, Thailand (in press)

De Gier *et al* (1995) Simulating forest degradation: Applying the Area Production Model in the Kali Konto area in East Java, Indonesia. Proceedings 16th Asian Conference on remote Sensing, Nakhon Ratcha-sima, Thailand (in press)

Hargyono (1993) Occurrence and prediction of forest degradation, a case study of Upper Konto Watershed East Java Indonesia. Unpub MSc thesis, ITC, Enschede.

Nibbering (1980) Firewood trading and consumption in the Kali Konto Project Area, East Java – a socio-economic study in seven sample villages. Project Kali Konto, Malang, Indonesia

THE CRYSTAL GLOBE: A GIS-BASED OPERATIONAL AREA PRODUCTION MODEL[1]

Yousif Ali Hussin Johan Bode Alfred De Gier
The International Institute for Aerospace Survey and Earth Sciences (ITC)
7500 AA Enschede, The Netherlands
E-mail: HUSSIN@ITC.NL, DEGIER@ITC.NL
Fax: (31)(53)874-399

ABSTRACT

The Area Production Model (APM) is a simulation model of land use changes in response to growth population, gross domestic product and agriculture productivity. Given these factors, the model can predict the amount of land that will be transferred from forest to agriculture land use. APM was developed by order of the Food and Agriculture Organization (FAO) of the United Nation. This model was first written in fortran computer language and later implemented within LOTUS 123 spreadsheet software. APM is a numerical model, e.g. the data input in form of number such as tables and the output in forms of numbers such as tables or graphs. Earlier, the authors have resolved the model spatially and apply it to an area in East Java, Indonesia. This implementation include the land transfer part of the model. The above mentioned researchers used five different software packages to achieve the spatial implementation of APM. The objective of this research was to create an automated operational spatial APM in ILWIS (Integrated Land and Water Information System) image processing and GIS software. In most cases in countries like Indonesia and Thailand it is not possible to establish an agriculture field on a cleared forested land. Therefore, forest land will be change to scrub land. This new implementation of the model can be used for predicting forest degradation.

INTRODUCTION

As in ancient Biblical times, e.g. the history of King Saul and the female prophet of Endor (I Samuel 28 vss. 1-25), people always wanted to know what would happen in the future. One of the later developed methods to get knowledge of the future, people thought, was to look into a crystal globe and see clearly what would happen. Now a days, people have not changed in the curiosity for the future. They still want to know what will happen in the future. But what have changed is the materials and methods. In our time we would not use crystal globes to look in the future but we develop computer models which are able to predict the future based on regression curves. There are plenty of subjects useful for prediction. One of these subjects is the issue that the world scientists worry about and would like to know what will happen in the future, is tropical forest degradation. Forest degradation is defined as all biological, chemical and physical processes that result in loss of the productive potential of natural resources in areas that remain classified as forest (World Bank, 1991). The reasons of forest degradation are logging, human activities, animal grazing and natural factor (e.g. storms, lightening) (Palo et al., 1986). One of the computer programs which can predict the future land use and therefore predict forest degradation, is the Area Production Model (APM).

The development of the Area Production Model (APM) has been an important step in predicting land use changes. The APM is intended for simulation of long-term land use changes and the prediction of primary and secondary yields from agricultural and forest lands. Among other things, the model simulates the future need for agricultural land. The model's demand and supply scenarios for agricultural products and land are generated primarily by the growth rates of population and GDP, and by changes in land productivity. The model is comprehensive, but does not have excessive data requirements.

---

[1]To be presented at the 16th Asian Conference on Remote Sensing, Suranaree University of Technology, Nakhon Ratchasima, Thailand, 20-24 November 1995.

The model uses three different agricultural classes: land for subsistence crops (used mainly for home consumption), land for market crops (produced mainly for the local markets), and land for cash crops (destined primarily for markets outside the area).

An important aspect of the APM is the concept of land allocation. If demand for land in a particular class increases, transfers of land from another class to that one are generated by the model. When the donor class concerned is exhausted, land from another class is transferred. The sequence of the donor land use transfer classes is specified by the APM user. This sequence usually goes from currently under-utilized agricultural land, through the conversion of one category of agricultural land into another one, and finally to forest land.

The APM has been tested by FAO in East Java, Indonesia (FAO, 1986a and 1986b) and by FAO and USAID in two parts of Peru. In both cases tropical rainforest areas were included. The conclusions were that the model was adequate and sufficiently adaptable for extension as well as modification. Williams (1987) converted the original FORTRAN version to LOTUS 123. APM assumes that the forests are degraded mainly by human activities (expansion of the agriculture). Indicators which are used for predicting the future land use are the population growth and the growth of the gross domestic product (GDP) (FAO, 1986a). The APM requires only numerical data input. Its output is in tabular and graphic form. Spatial data are neither required nor produced. It is therefore insensitive to the location at which the need for more land exists and to the location of the donor land use class from which land is to be transferred. This is considered a major limitation, because it is not possible to predict where the land for the specific classes will be needed, and where the land of the relevant donor class is located. But if one would not only like to predict how much forest will be degraded but also where it will degraded, one have to take into account more factors than the numerical model takes (e.g. slope and distance). Furthermore, a spatial model would allow to grade accessibility to land, by using friction coefficients, and it could simulate the locational effects of decisions that influence the need for land transfer.

De Gier and Hussin (1993) described how the spatial component was developed and linked to the model for the Kali Konto area in east Java, Indonesia. All spatial data used were in digital form. The results of this spatial implementation show the suitability of GIS for combining the spatial component and the numerical output from the APM. The results also indicated that the spatial component of the APM significantly improved the model's behavior and interpretation capabilities. Later, Hussin et al., 1994 verified the results of spatial version by the numerical one and established the idea of predicting forest degradation using APM. While this paper can be considered as an step in the ongoing research of creating a computer model which will be able to predict spatially the forest degradation. It will gives ideas on how the model was transferred to GIS-ILWIS.

The objective of this research was to create an ILWIS-GIS spatial model which makes it possible to predict forest degradation using the principle ideas of APM in the numerical and spatial forms. The model will consist of two parts: Automation part, with the help of batch and text files for GIS-ILWIS, the process of forest degradation can be done more than once. This enables the user to quickly see the different results depending on different values of input factors. Second part is the forest degradation. The result of the model will be presented as a map. Depending on the idea of how forest degradation will occur, the contents of this map could/will differ. Four maps can be distinguished depending on the assumption about the idea of forest degradation made.

GENERAL APPROACH

In order to reach the research's aim a method was developed. The first step was to do manually the process of forest degradation in GIS-ILWIS. This derived information on which commands successively have to be given to create the desired map. Secondly these commands were written into a batch file in order to automate the process of forest degradation. The third step was to verify numerically and spatially the model on the reality.

In the first instance, spatial APM must be numerically verified. In the numerical APM the predicted surface of agricultural land depends on both the

population growth for subsistence crop and the GDP for the cash crops. But in spatial APM, the prediction of agricultural land only depends on the average population growth, in order to simplify the calculation. However, it must be verified in how far the prediction of agricultural land by using the numerical APM which approximates the prediction of agricultural land. Spatial verification means that we have to find the most correct data and make the best decisions in the spatial APM resulting in a spatial prediction of forest degradation which approximates as best the reality. The right data have to be found for the tables POPULATION, PRIORITY and YEAR.

Making the best decisions means that there has to be chosen whether the plantations are degradable or not and that there has to be chosen from where the forest degradation must start (the agricultural area, the existing scrub land or from both).

After the numerical and spatial verification, the spatial APM can be seen as most optimized for the situation on Kali Konto. Now it has been made possible to solve the research question: describing the impact of the input factors Slope, Distance, Population Growth, Population Pressure and Priority on the process of forest degradation in Kali Konto and classify the most important one(s).

The Area Production Model in LOTUS (Numerical APM)

The main idea behind the process of land use change is that land use classes (mainly forest) will transfer after each other at the benefit of the expanding agricultural land use class. The model assumes that the increasing demand for agricultural land is the most important factor for the land use changes. The agricultural development is assumed to be controlled by two parameters: First, the demand for new agricultural land differs according the types of crop (subsistence crops, market food crops and cash crops). Second, the production depends on the area cultivated and the productivity.

The next formulas are used to calculate for each crop type the demand for new land:

Demand for new land for subsistence crops = PRESENT AREA * $P_{(pop)}$ / $P_{(prod)}$
Demand for new land for market food crops = PRESENT AREA * $P_{(GDP)}$ / $P_{(prod)}$
Demand for new land for cash crops = PRESENT AREA * $P_{(GDP)}$ / $P_{(prod)}$

where:
$P_{(pop)}$ = Growth rate of population
$P_{(prod)}$ = Growth rate of the Gross Domestic Product
$P_{(GDP)}$ = Growth rate of the agricultural productivity

The numerical APM which run in LOTUS is working according to the following steps:

STEP 1. Choosing the option DATA to fill in the data for the specific region: this involved in:

The region: Starting year, total population, rural population, annual GDP/capita and the total land area.
The land use: The surfaces (ha) of the several land use classes.
Transfer: Choosing which land use classes will increase and which land use classes will decrease.
The priority: Making a ranking among the land use classes which are supposed to transfer (=decrease) Priority 1 means that this land use class will firstly be transferred into for example agriculture. The growth factors: Fill in for the next 10 years the growth factors of the rural and total population (P_{pop}), the Gross Domestic Product (P_{GDP}) and the agricultural productivity (P_{prod}) for the tree possible crops (subsistence, market and Cash).

STEP 2. Choosing the option CALCULATE. This causes a several results. The factors governing change in land use (P_{pop}, P_{GDP} and P_{prod}) are extrapolated for the next 50 years. The results are show in a table called table 1 and graph 1. With the help of these factors the totals in population, GDP and GDP/capita, are calculated and printed in a second table called table 2. With the help of the three formulas mentioned above, the known surfaces of the land uses (as mentioned in step 1) and the extrapolated values of the P_{pop}, P_{GDP} and P_{prod} ,it is possible to calculate the future area which has to be transferred which is = (subsistence area + market food area + cash crops area). The results are

printed in table 3 and graph 2. Now the total transfer land for every future year is known, it will be divided over the land use classes which are proper for transfer into agriculture. While the proper land use classes will transfer into agriculture one by one using the known priority for change by the division. The result is printed in table 4 and graph 3.

STEP 3. The final step is choosing the option results which makes it possible to print out the tables and the graphs. In this case the most interesting tables are table 1-4 and the most interesting graphs are the graphs 1-3 (FAO, 1986).

RESULTS AND DISCUSSIONS

The results of this research is a computer ILWIS batch file which includes all steps of the spatial APM. This model is based on the numerical model which was described earlier. This model was developed in GIS-ILWIS. In spite of the fact that the model is not difficult to use (e.g. it is fully automated), it is recommendable to get firstly knowledge of the assumptions of the model and how it is working.

Assumptions

Every model will be an approach of the reality. It cannot take into account every variable factor of life which does influence the process of the model e.g. forest degradation. Therefore, it is important to know the assumptions of a model. In this model the following assumptions were made:

1. The most important assumption is that in this model the forest classes do not degrade after each other as in numerical APM. It is assumed that the forest classes can be degraded at the same time. Every pixel gets a value depending on: slope, distance from agricultural/village land, priority for forest classes of the rural people, population density and population growth. None of these is extra weighted nor does have a primary key. These factors were chosen their data were available in raster maps.

2. It is assumed that each of these factors has the following influence: The steeper the slope the slower the forest degradation and the higher the friction value; The greater the distance the slower the forest degradation and the higher the friction value; The higher the priority value the slower the forest degradation and the higher the friction value. Note that the highest priority means the lowest priority value, the higher the population growth the faster the forest degradation and the higher the starter value. The higher the population density the faster the forest degradation and the higher the starter value.

3. It is not clear whether it has to be assumed or not that it is possible for plantation forest to degrade into scrub. It was argued that plantation forest could in practice only be thinned or harvested. While this is still not clear, it has been made possible for the user to decide whether he/she want to have the plantation forest as degradable forest or not. If it is decided that the plantations are not degradable, it means that the user has to make an absolute barrier of these land use classes which could easily be done by giving the plantations a negative value in the priority table.

4. In the first instance, preference was set on using the real values of the input factors: slope, distance, priority, population growth and population pressure. This would guarantee a proper relation among the values within an input factor. But taken into account all these, two arguments plead for reclassification of the values of every input factor between 1 and 10. First of all, using the real values of an input factor give a weighting among the input factors. For example, using the real values would give a high weighting to the map slope distance (values 1-18825) and a low weighting to the population growth (values 1-5). The second reason is that the real values of the input factors would, if you want to calculate the distances, result in values which exceed the maximum pixel value or the capacity of the computer.

5. Theoretically, forest degradation seems to start at the fringes of the scrub land. It is not clear whether the model is taking into account this theory. Therefore, it has been made possible for the user to chose whether forest degradation must start from the agricultural land or the existing scrub land or from both.

6. The process of forest degradation is simulated by creating a time-of-change-map. Firstly, this is done by calculating distances in a friction map in which each pixel has a weighting factor. This weighting factor includes the values of the DISTANCE, the SLOPE and the PRIORITY for change. This gives a direction to the forest degradation. Secondly, computing this map with the output of "population density (e.g. pressure) * population growth, creates the time-of-change-map.

7. It is assumed that the area of forest which will be degraded into scrub can be calculated in two steps. First, the future agricultural land is calculated with the help of the following formula:

$$N_a = B_a * (p/100)^n$$

where:
N_a = Total agricultural area in the future year (ha), B_a = Total begin agricultural area (ha)
p = Population growth (%), n = future years (years)

Second, the degraded area is calculated with the help of the following formula:

$$N_s = X1 * (N_a)^{1/2} - X2 * N_a - C$$

where:
N_s = Total scrub area in the future year (ha) N_a = Total agricultural area in the future (ha)
X1, X2, C = The coefficient of X1, X2, and the constant of the regression model between APM-predicted agricultural land and the real developed scrub land.

How is the new model working in ILWIS-GIS

The new spatial APM working according to the following steps:

STEP 1. The model uses four input maps: General, Slope distance, Forest and Villages; and three tables: Priority, Population, and Year; Two batch files: Program.bat and Program1.bat; Twelve text files: FORM0.txt up to FORM9.txt, The DOS command file: ASK.com.

STEP 2. Start ILWIS, then exit to Dos, change the directory to where the files of step 1 are loaded. The model will start by typing **PROGRAM** and then **[ENTER]**.

STEP 3. The Model comes up with the tables Population and Priority which can be altered by the user.
The table Population contains information about the number of people, the surface of agricultural land and the population growth for each village. In FORM0.txt the user (s) alternations, the pressure on land, the Vilfact (e.g. village population) for each village and the maximum Vilfact are automatically stored and/or calculated in table POPNEW.

The table Priority contains information about the people's priority for transfer of a forest class. In FORM1.txt the user's alternations and the maximum priority are automatically stored and/or calculated. It must be noticed that a forest class with a negative value for its priority will be considered as an absolute barrier and will therefore not degrade into scrub.

STEP 4. In ILWIS-MCalc Form2.txt the map STARTER is realized. Each village owns a part of the agricultural land. This village land is given an integer value between 1 and 10 based on the Vilfact values of table Population.
With the help of the Distances Module in ILWIS a Thiessen map Thies is created. In Thies, this Vilfact value of each village land is extrapolated into the non-agricultural land use classes.

STEP 5. The user have to chose whether the process of forest degradation will start from the agricultural land or the scrub land or from both the agricultural and scrub land using the files FORM4_1.txt, FORM4_2.txt and FORM4_3.txt

STEP 6. In ILWIS-MCalc Form4 x.txt the map FRICTION is realized. Each pixel of a non-agricultural land use class has an integer value between 1 and 10. This value is based on the slope, distance from the village land and the priority. With the help of the ILWIS Distances Module the time of change into scrub land has been made visible in the friction map. The time of change depends on the roughness (e.g. friction value) of the area.

STEP 7. In MAPOUT the time of change into scrub land has been weighted by the Vilfact of each village.

STEP 8. The Histogram (Mapo) of the pixel values is derived from mapout in Histogram Form6.txt.

STEP 9. The program comes up with table Year. The user has the possibility to change the begin area of agriculture, the percentage population growth and the future year for prediction. Based on these three values the total area of agricultural land for the future year is calculated (in Tabcalc Form7.txt), then transformed into a total needed area of scrub land and finally printed in table Newyear.

STEP 10. In ILWIS Tabcalc, the file Form8.txt, the total area of scrub land in the future year is translated into total needed pixels. If the cumulative number of pixels of table MAPO is lower than these needed pixels, then it will get a value of 23, otherwise it will get a value of 0. The result is printed in column (value) of table MAPON. The pixel groups with the value 23 will change into scrub land in the future. The other groups will not yet change.

STEP 11. Finally Map4 is constructed as follows: First, the pixels outside the area, the lake, the existed scrub land and the agricultural land use class will get the same value as the map Forest. Second, the pixel groups of table MAPO which has a value of 23 must be adjusted. These are the new developed scrub lands and will get a value of 23. Finally the rest pixels will also get the value of the map Forest.

REFERENCES

De Gier A. and Hussin Y.A., (1993) Spatially Resolved Area Production Model in Kali Konto, Indonesia, GIS/LIS '93, Annual Conference and exposition, 31 Oct. - 4 Nov., 1993, Minn, USA, Vol 1. 157-169 pp.

Hussin Y.A., A. de Gier and Hargyono (1994) Forest Cover Change Detection Analysis Using Remote Sensing: A test for the Spatially Resolved Area Production Model, Fifth European Conference and Exhibition on Geographic Information System, EGIS/MARI '94 Proceedings, Paris, France/Maroh, 29-April 1, 1994, Vol II 1825-1834 pp.

FAO, (1986) Manual for using the area production model (APM), Case Studies, Asia-Pacific Region. GCP/RAS/106/JPN. Field Document 12:2, May, 1986. 99 pp.

FAO, (1986) Users guide to area production model (APM), Asia-Pacific Region. GCP/RAS/106/JPN. Field Document 12:1, May, 1986. 65 pp.

Hargyono, (1993) Occurrence and prediction of forest degradation, a case study of Upper Konto Watershed East Java Indonesia,ITC, Enschede.

Palo,M., M. KANNINEN, G.MERY and A. SELBY. 1986. Forest-based socio-economic development and deforestation in developing countries: A feasibility study for a major research project. Proceedings of IUFRO World Congress, Ljubljana, Yugoslavia.

World Bank, 1991, A world Bank Policy Paper, The Forest Sector, The World Bank, Washington DC.

Williams, D. H., (1987) LOTUS APM, version 1: A spreadsheet version of the area production model 1. Asian seminar on forest planning, Kuantaun, Malaysia. November 5-7, 1987. 12 pp.

Identification and Mapping of Irrigated Vegetation using NDVI-Climatological Modeling

Ramesh S. Hooda and Dennis G. Dye
Global Engineering Laboratory,
Institute of Industrial Science,
The University of Tokyo,
Japan

Abstract

Distinguishing artificially managed vegetation (mainly agricultural crops and termed here as irrigated vegetation) from the natural vegetation is an important step in modeling and monitoring terrestrial primary production and carbon cycling through satellite remote sensing. Spectral indices such as the normalized difference vegetation index (NDVI) provide information about the vigor of the vegetation which in turn is influenced by climatic factors. Therefore, NDVI of the region is expected to have a relationship with the climatic parameters. NDVI values for irrigated vegetation (mainly agricultural crops), however, would show a less strong relationship to climatic factors compared to the natural vegetation which is totally dependent on climatic conditions. This differential behavior of the of the two types of vegetation can be exploited to identify and map the irrigated and non-irrigated vegetation zones. The irrigated vegetation pixels are screened out as outliers in the NDVI-climatological relationship. The present paper reports on work in progress in which we are examining the possibility of identifying irrigated vegetation based upon above relationship. NOAA AVHRR 10 day composite NDVI data with 8 km spatial resolution was used in combination with monthly average climatic data of the region for the study. The Indian territory having substantial mix of irrigated and natural vegetation, was chosen as the case study area.

1. Introduction

Biomass and productivity estimates from spectral data in the visible and near-infrared wavelengths originally used highly empirical relationships to assess the important biological variables of vegetation (Emori et. al. 1978). Recent work on this subject is more analytical and assumes that productivity results from photosynthesis through which a fraction of the incident solar energy that is intercepted by vegetation canopy is converted into biomass (Prince, 1991; Ruimy et. al. 1994). This involves decomposition of productivity into several independent variables such as incoming solar radiation, fraction of radiation absorbed and conversion efficiency of absorbed radiation into dry matter (ε).

A major challenge in the NPP estimation is finding representative values of ε for various vegetation types as it changes with the types of vegetation

and climatic conditions (Stockle and Kiniry, 1990). Estimating productivity based on vegetation indices, therefore, requires a land cover classification that distinguishes natural and irrigated vegetation (mainly agricultural crops) to account for differences in ε. In this paper we examine the potential of an NDVI-climatological modeling approach to distinguish natural and irrigated vegetation.

2. Background

The normalized difference vegetation index (NDVI) is calculated from surface reflectance in red (R) and near infra-red (NIR) regions obtained through sensors onboard many remote sensing satellites as

$$\frac{NIR - R}{NIR + R}$$

NDVI is an effective indicator of the amount of green vegetation present in an observed landscape. Goward et. al. (1985) showed that vegetation indices such as NDVI are related to net primary production (NPP, gm^{-2} $year^{-1}$). Kumar and Monteith (1981) showed that the fraction of photosynthetically active radiation (PAR) absorbed by the vegetation cover is related to the ratio of red reflectance (R) to near-infrared reflectance (NIR). Asrar et. al. (1984) subsequently related the NDVI to the fraction of PAR absorbed. These and related studies led to development of the "production efficiency model" (PEM). The simple form of the PEM is:

$$NPP = \varepsilon\Sigma(APAR) = \varepsilon\Sigma(NDVI * PAR)$$

where Σ(APAR) is the annual sum of APAR and ε is the PAR conversion efficiency (g MJ^{-1}). To account for differences in ε for different types of vegetation, first a classification among natural and managed vegetation is required.

Because climate influences the condition and growth of vegetation, the NDVI of a region may be expected to be related to the climatic variables of the region. The NDVI for artificially managed (irrigated) vegetation, however, should show a less strong relationship to the climatic factors compared to the natural vegetation which are entirely dependent on climatic conditions. This differential behavior of the of the two types of vegetation may be exploited to separate them. If NDVI is correlated with climatic variables that are known to influence plant growth, particularly temperature and rainfall, the pixels associated with irrigated vegetation can be separated as outliers. The values of these pixels then can be used in automated classification which distinguishes the irrigated vegetation from the natural vegetation.

3. Study Area

The study area consists of the Indian subcontinent and adjoining areas, which have a substantial mix of irrigated and natural vegetation. In India, the role of agro-ecosystem should be significant, since 45 percent of the geographical area of the country is under agriculture compared to 10-11 percent globally (Dhadwal et. al. 1994). Because the area has large deviations in climatic conditions and therefore, variety of vegetation, it provides a suitable study area in which to develop and evaluate our approach.

4. Methodology

Pathfinder AVHRR Land (PAL) 8 km data from NOAA 11 satellite was obtained from the Goddard Distributed Active Archive Center (DAAC), USA. The data for the year 1989 was selected for the study as it was a relatively normal year with respect to Indian monsoon which greatly influences vegetation growth and dynamics in the region. The NDVI is calculated from atmospherically corrected surface reflectance from the visible (0.58 - 0.68) and near infra-red (0.725 - 1.100) AVHRR channels. The 10 day composite NDVI data has been prepared by selecting the maximum NDVI value from the daily data during the 10 day period. This removes the effect of clouds to give a cloud free data set. A monthly average NDVI data was prepared by calculating the mean value for each pixel from the 10 day composite NDVI data set. As the area has different well defined growing seasons, as discussed later, seasonal average and total NDVI data sets were also prepared. These seasons include July to October (hot/humid monsoon season), November to March (dry winter season) and April to June (Summer season). Annual average and total NDVI of the area was also calculated.

The daily data on temperature and rainfall was obtained from Global Daily Summary for the years 1977-1991 produced by National climatic Data Center, USA. Mean monthly temperature and total monthly rainfall were calculated from the daily data from about 177 meteorological stations spread all over India. The average data values for the 15 years period were then calculated. The point-location data were subsequently interpolated to prepare average mean monthly temperature and average total monthly rainfall maps of the region. These data are analyzed vis-a-vis NDVI in different growing seasons.

5. Results and Discussions

The natural vegetation in the Indian peninsula has tropical dry deciduous and moist deciduous forests mainly in central and southern parts which shed their leaves in the autumn season. Therefore, the NDVI in these areas starts decreasing in November and again starts increasing in March. However, India also has some areas under tropical evergreen forests in the

northern Himalayas, north-eastern states and along western sea coast which show higher NDVI most of the year.

Fig.1. Average NDVI image of India during October, 1989.

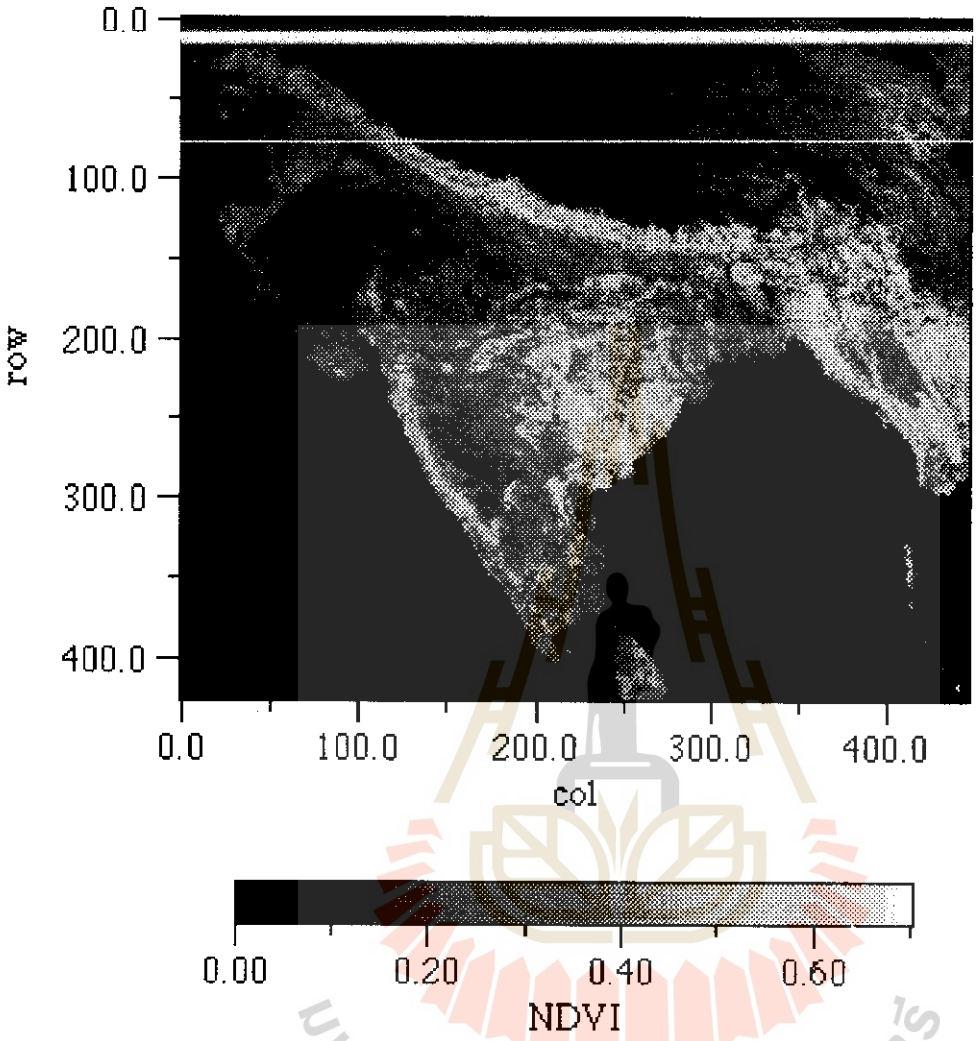

The northern Indo-Gangatic plains are the largest agricultural region in the area which has substantial irrigated agriculture. Besides this there are other agricultural areas scattered all over India having both dry land and irrigated agriculture. There are distinctively two agricultural cropping seasons locally called as Kharif and Rabi seasons. Kharif season begins in July and lasts in October. It is a hot and humid season characterized by heavy monsoonal rainfalls. Therefore, the NDVI in the area starts increasing with the sowing of Kharif crops in July and reaches its peak in the month of October (Fig. 1). Then it suddenly drops in November because of ripening and harvest of the agricultural crops. Rabi season extends from November to April which is dry and relatively cold particularly in the northern India. Therefore, NDVI again starts increasing in December indicating canopy development of the Rabi season crops. It reaches its peak in February/March (Fig. 2) and then suddenly drops in April because of yellowing and harvesting of the crops. The

season from April to June is relatively hot and dry and the agricultural fields remain almost vacant showing very low NDVI.

Fig. 2. Average NDVI of India during February, 1989.

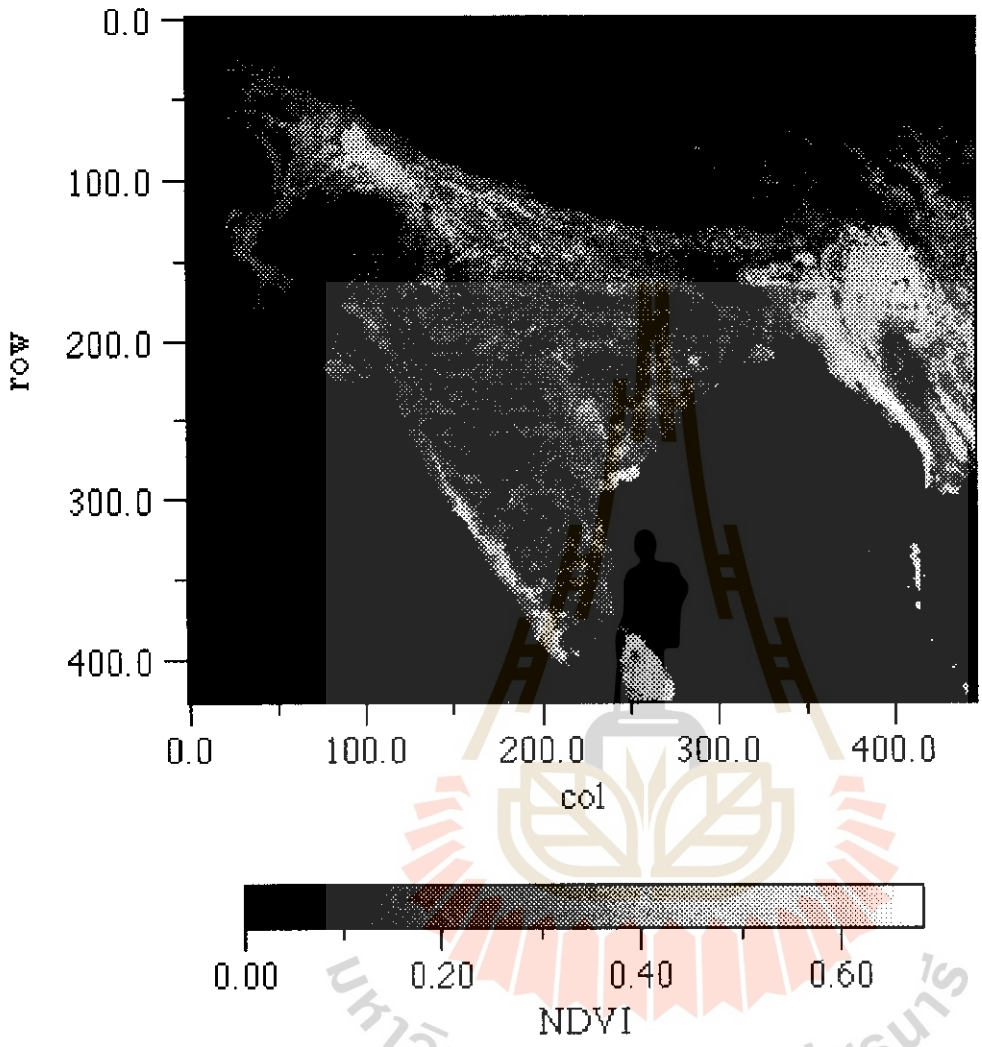

The average NDVI data for these three major seasons and annual average NDVI is being analyzed with the average monthly mean temperature and average monthly total rainfall. In our current work we are continuing to develop, test and refine the NDVI-climatilogical method which shows a promise for automated identification and mapping of irrigated vegetation.

References

Asrar, G., Fuchs, M., Kanemasu, E.T. and Hatfield, J.L. 1984. Estimating absorbed photosynthetic radiation and leaf area index from spectral reflectance in wheat. Agron. J., 76: 300-306.

Dadhwal, V.K., Shah, A.K and Vora, A.B. 1994. Carbon flow through Indian agroecosystem: A priliminary account. In Global Change Studies, Scientific

Report, ISRO-GBP-SR-42-94.

Emori, Y., Yasuda, Y., Yamamoto, H. and Isaka, I. (1978). Data acquisition and data base of spectral signature in Japan. In: Proc. Int. Symp. on Remote Sensing for Observation and Inventory of Earth Resources and the Endangered Environment, Freiburg (FRG), 2-8 July, 1978, 22(7/1):543-566.

Goward, S.N., Tucker, C.J. and Dye, D.G. 1985. North American vegetation patterns observed with the NOAA-7 Advaned Very High Resolution Radiometer. Vegetatio, 64: 3-14.

Kumar, M. and Monteith, J.L. 1981. Remote sensing of crop growth. In: H. Smith (ed.), Plants and the daylight spectrum. Academic press, London, pp. 133-144.

Price, S.D. 1991. A model of regional primary production for use with course resolution satellite data. Int. J. Remote Sensing, 12: 1313-1330.

Ruimy, A., Saugeir, B. and Dedieu, G. 1994. Methodology for estimation of terrestrial net primary production from remotely sensed data. J. Geophy. R., 99: 5263-5283.

Stockle, C.O. and Kiniry, J.R. 1990. Variability in crop radiation-use efficiency associated with vapor-pressure deficit. Field Crops Research, 25: 171-181.

FIELD PREDICTION AND POTENTIAL MONITORING OF CASSAVA PRODUCTION IN NAKHON RATCHASIMA[1]

A. Eiumnoh[2], R. P. Shrestha[2], S. Baimoung[3], P. Kesawapitak[4] and A. Noomhorm[2]

[2]*SERD, Asian Institute of Technology, G.P.O. Box 2754, Bangkok 10501*
[3]*Department of Meteorology, Bangkok 10260*
[4]*Department of Agriculture, Bangkok 10900*

ABSTRACT

The potential monitoring of cassava production in Nakhon Ratchasima province, Thailand was conducted using Remote Sensing (RS) and Geographic Information Systems (GIS) in integration. The soil units, topography and general landforms were digitized and grouped according to their surface texture, slope and elevation and types of land form respectively. The cassava productivity factors including soil moisture, drainage condition, effective soil depth, texture, organic matter content, base saturation, cation exchange capacity,. mineral reserve and fertility level were evaluated for land suitability classification. The soil, topography, landform and cassava productivity were analyzed for potential land productivity grouping. Landsat TM of 1995 was used to classify cassava area and to compare misclassified land uses with land use map of 1993. Land suitability evaluation for cassava was carried out to compare with existing cassava area. The NOAA-AVHRR data in 1993 and 1995 were used for monitoring purposes. It was found out that, however, remote sensing data are still having many limitations and constraints in monitoring of cassava production, integration of GIS and remote sensing can be exploited to have its fullest usefulness.

1.0 INTRODUCTION

There have been about 24 folds increase in the area of cassava cultivation in Thailand in the last three decades (Figure 1) to be Thailand as the major cassava producer in the region. This tremendous growth can be attributed to the unique capability of cassava for producing high biological and economic yield under marginal and low-input conditions and its flexible agronomic requirements. North-eastern region which is comparatively depressed than other regions of the country contributes about 60 percent of the total cassava production.

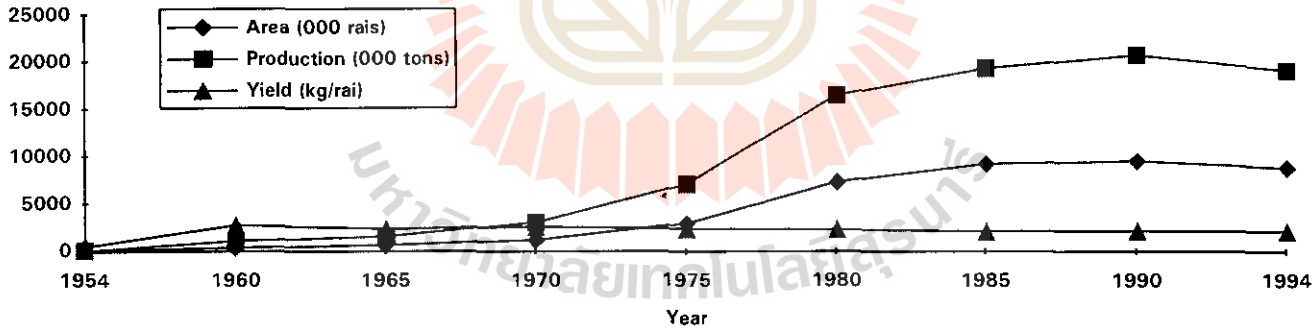

Figure 1. Cassava cultivation area, production and yield.
(Source: O.A.E. Agricultural Statistics, 1954/55 to 1993/94).

The popularity of cassava cultivation is attained due to both marginal land quality of North-east region and also high price fetching of cassava products in the past. Majority of cassava produced in the country is exported to EEC countries and less than 10 percent of it is used for domestic consumption. In the readjustment of EEC's policy to restrict cassava imports, as per 1980's agreement between Thailand and EEC, Thailand would limit the export to 5 million tons of pellets equivalent to 12 million tons of fresh roots (Titapiwatanakun, 1984). On the contrary, with the development of new high yielding varieties and expansion of cultivated area, the production trend remained increasing and is estimated to reach 17.57 million tons in the year 1996 (TTDI, 1995).

As the production is export oriented such limitations of the trade treaty would mean that excess of production has to be consumed within the country for which it has to be seriously reconsidered either opening domestic market consumption or limit

[1] Paper presented at the 16th Asian Conference on Remote Sensing, 20-24 November, 1995, Nakhon Ratchasima, Thailand.

the cassava production. In the lack of this, the country and its farmers will have to face the challenge of a great economic loss.

Monitoring of cassava production in Thailand have been traditionally relied on field information gathering. Application of advanced Remote Sensing and GIS has not gained popularity yet in this field. Moreover, cassava can be harvested for a longer period of time, its monitoring for production predictions becomes difficult. To cope these situations a study of three years duration has been started by Asian Institute of Technology to predict the cassava cultivation and production and suggest the suitable land for cassava cultivation. This paper, as part of the study, discusses the piece of work predicting the cassava production and suggest the land suitability for cassava in Nakhon Ratchasima.

2.0 THE STUDY AREA

Nakhon Ratchasima province is situated on Korat plateau of the North-east region of Thailand covering 12,811,162 rai (O.A.E., 1992). The climate is tropical Savannah with minimum and maximum temperature ranging from 14.1 to 39.5° C. The area receives an annual rainfall of 1,062.4 mm in an average annual rainy days of 104. Paddy is the principal crop on lowland and cassava on the upland followed by sugarcane and corn. This province is the largest among the cassava producer provinces in the country.

3.0 METHODOLOGY

The research methodology is presented in Figure 2 which employs the tools, such as, Remote Sensing, Geographic Information Systems (GIS) and field surveys. The basic source materials used were:

- Topo map (1:250,000), Royal Thai Survey Department, 1984.
- Land use map (1:250,000) O.A.E., 1993.
- Landsat TM hardcopy (1:250,000), February 1995.
- Soil Map (1:500,000), Soil Survey Division, 1982.
- Climate data
- Published and unpublished reports, documents, etc.

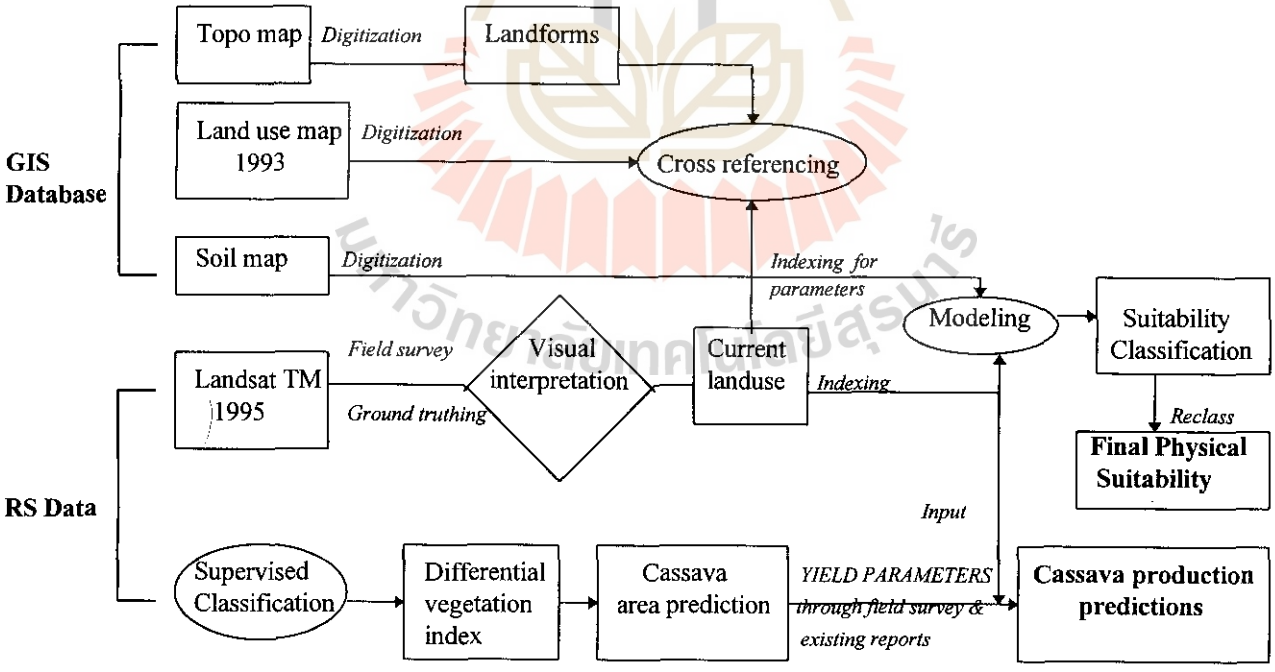

Figure 2. Conceptual framework of research methodology.

The soil units, topography and general landforms were digitized from different base maps to create the thematic coverages in vector based GIS (ARC/INFO). Landsat TM was visually interpreted for recent land use types. Existing database was used to predict the cassava yield. The cassava productivity factors including soil, moisture, drainage, effective soil depth, texture, organic matter, base saturation, cation exchange capacity, mineral reserve and fertility level were evaluated for land suitability classification employing limitation concept combined with parametric approach. Land use requirements were considered as given by LDD, 1992.

4.0 RESULTS AND DISCUSSION

4.1 Land Use

The land uses of Nakhon Ratchasima province interpreted from Landsat TM (1995) are presented in Table 1. In the province, Rice is the dominant land use types (42.31 percent of the total province area), which has been increased from what has been interpreted from the Topo map for paddy land (34.61 percent). The forest area of 17.72 % has been decreased to 15.48% in 1995. Cassava is the second to rice in areal extent followed by other upland crops.

Table 1. Land use and landforms of Nakhon Ratchasima.

Interpreted from Landsat TM, 1995		Interpreted from Topo Map	
Land Use	% of total area	Land forms	% of total area
Rice	42.31	Water body	0.42
Cassava	16.20	Low land (paddy)	34.61
Upland	14.61	Upland	47.25
Corn	0.72	Forest	17.72
Sugarcane	5.89		
Tree crops	0.02		
Rubber	0.01		
Other	0.15		
Orchard	1.99		
Shrub land	0.47		
Forest	15.48		
Grassland	0.30		
Urban	1.51		
Water	0.10		
Total area of the province - 12,811,162 rai (equivalent 2,049,786 ha)			

Existing cultivation of cassava are found on almost all types of soils. 37.3% of the total area under cassava are found to be cultivated on clayey upland soils followed by 33.9% on loamy upland, 10.3% on skeletal upland, 7.9% on sandy upland, 7.1% on associated soils, 2.1% on slope complex and 1.4% on cracking upland soils (Figure 3). It implies that cassava do not need specific physical requirement so far the land qualities is concerned. It is rather that the cultivation is largely governed by soil drainage condition and social and economic factors as well.

4.2 Land Suitability Classification for Cassava

In Nakhon Ratchasima province, as much as, 14.8 percent of land of the total provincial area was found to be most suitable for cassava cultivation (Figure 4). The area classified under moderately and marginally suitable were 16.73 and 4.09 percent, respectively. Nearly 2/3rd of the province (64.42 %) are found not suitable for cassava cultivation. Since the proportion of most suitable area is still less than the area being cultivated (16.2%), it articulates that not all the cassava area in the province yield good economic return. Most suitable area are presently under cassava and limited, at majority, to loamy upland and little to clayey upland soil types. Moderately suitable area falls under the sugarcane and other land under upland crops at present.

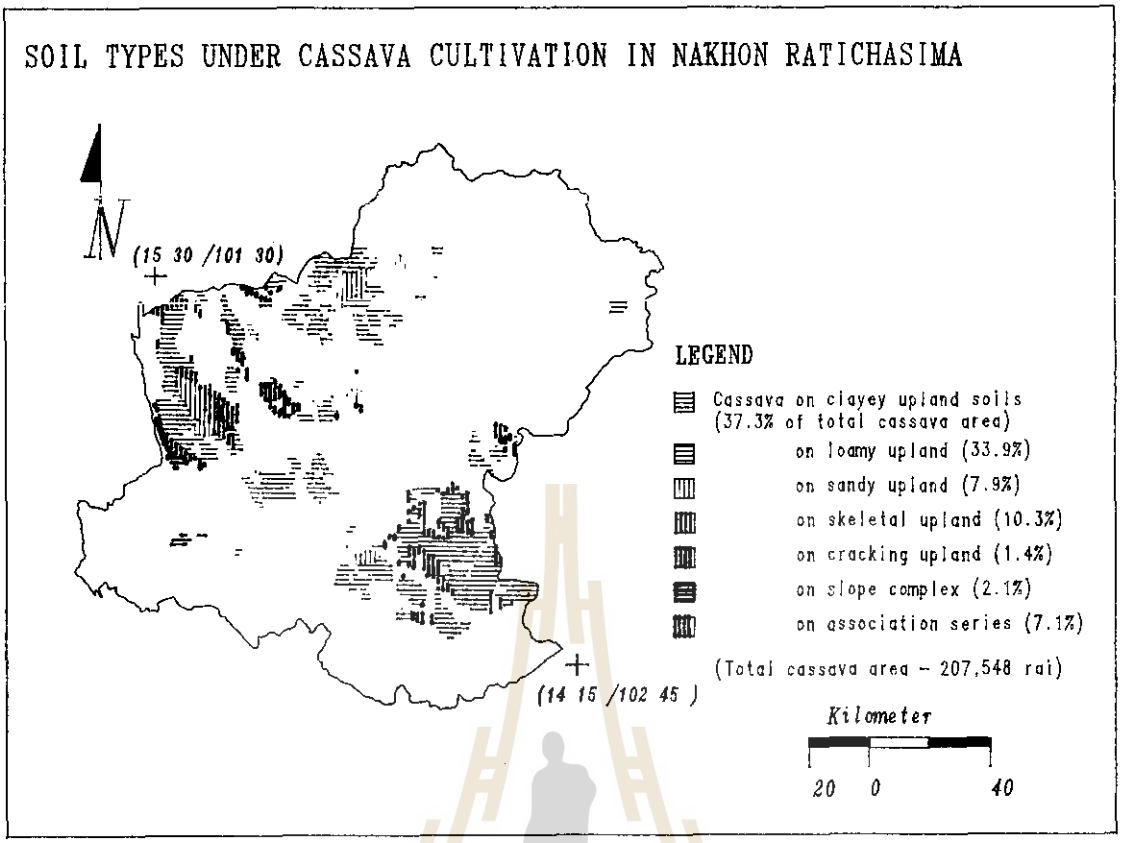

Figure 3. Soils types under cassava cultivation in Nakhon Ratchasima.

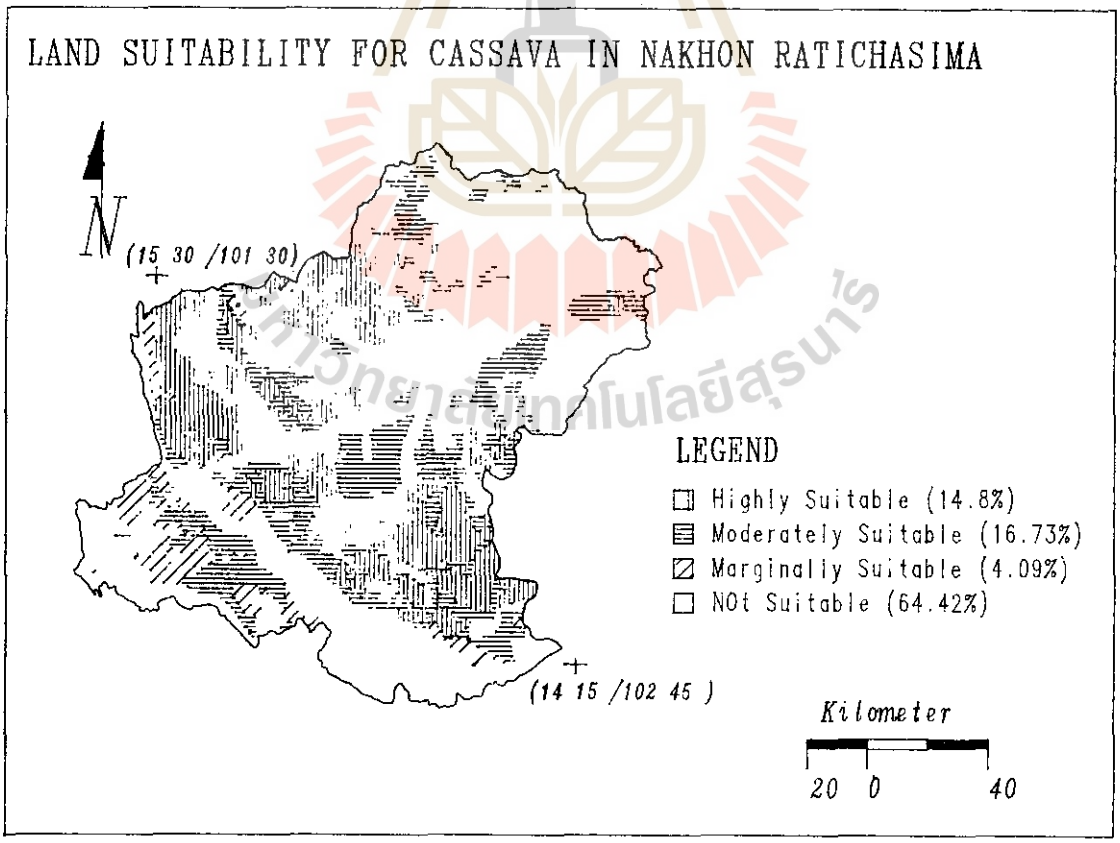

Figure 4. Land suitability for cassava in Nakhon Ratchasima.

4.3 Monitoring Cassava Cultivation and Field Prediction

4.3.1 Database Inconsistency

There are varied statistics reported for the area under cultivation of cassava and so are the productions (Table 2). Obviously, in the lack of reliable information, it is difficult to formulate sound policy planning whether it is the case of cassava production and trade or other aspects of planning. This differences might be basically due to the differences in methods used for monitoring purpose. In most cases, the monitoring does not employ the advanced tools like remote sensing for monitoring purpose but based on field surveys especially interview with the key informants or the farmers. In other case, land use maps are, however, prepared from interpretation of satellite data, selection of data and expertise largely dictates the level of accuracy and current information. Due to inadequate linkages in sharing the database and calibrating the database standards, database reported from various sources vary to a greater extent. In simple case to cross reference, the area derived from the digitized land use map is much higher than from other sources as shown in the table below.

Table 2. Cassava production in 1994 reported from different sources for Nakhon Ratchasima.

Crop	Area (rai)	% of province area	Yield (ton/rai)	Production ('000 tons)	Sources
Cassava	1,600,000	12.5	2.35	3,760	Thai Tapioca Dev. Institute
	1,905,306	14.9	2.20	4,191	O.A.E. Statistical reports
	3,228,939	25.2	-	-	Derived from Land use map, O.A.E., 1993
	2,075,408	16.2	2.20	4,565	Interpreted from Satellite data (LS_TM '95)

4.3.2 Remote Sensing Data Types

As the project area includes all the cassava growing provinces of Thailand, the study initially planned to use NOAA-AVHRR data (coarse resolution of 1.1 km) for monitoring purpose because of its temporal benefits and larger area coverage in relatively lower cost compared to that of Landsat_TM (high resolution of 30 m). To work with minimum data sets, besides costs matter it requires incomparably considerable data volumes and time while working with Landsat_TM for digital analysis. On the other hand, it was observed during the repeated field surveys that the size of the cassava fields are not only smaller than the required mapping units for the employed data (NOAA-AVHRR) in some part of the area but also it makes difficult to establish signatures for the training area in the satellite data because of their varied signatures representing different crop stages in the field. It is primarily due to the fact that cassava is such a crop that the harvesting season of this crop is not limited to particular period but rather prolonged depending upon the market situation. This means at a particular point of time, there could be various types of spectral signatures for cassava depending upon the crop's growth stages. Because of these reasons of crops versatility of the growth and to accommodate smaller field sizes, the area was cross referenced using currently acquired Landsat_TM.

5.0 SUMMARY

The study is a long term project which aims to predict the cassava production in Thailand at the national scale for the coming few consecutive years. However, with these arguments in this paper, it can be resolved that there is the need of establishing reliable database which can be achieved through the proper selection of the methods and data sets to be used. It also calls for the inter-agency linkages and coordination for the calibration of database. To cope the situation of ever increasing cultivation of cassava vis-à-vis export limitation it is important to monitor the cassava production in terms of areal extent and yield parameters. Land evaluation will not only suggest to get the better economic yield but also help abate the pace of land quality deterioration.

Remote Sensing data are the best means to monitor the cassava cultivation, however, there are limitations associated with the data types. Coarse resolution satellite data (NOAA-AVHRR) can successfully be utilized for monitoring at regional level, cross-referencing with high resolution data like Landsat_TM will give the reliable results. Similarly, GIS integration with remote sensing will help to a great deal for planning purpose.

REFERENCES

Cock, J. H. 1985. *Cassava: New Potential for a Neglected Crop*, Westview Press, Boulder and London.

F.A.O. 1983. *Guidelines: Land Evaluation for Rainfed Agriculture*. FAO Soil Bulletin No. 52, Rome.

L.D.D. 1992. *Quantitative Land Evaluation Manual for Economic Crops*, No. 2., Land Development Department, Bangkok.

O.A.E. 1992. *Agricultural Resources Map Interpreted from Satellite Data*, Volume 1, Office of Agricultural Economics, Bangkok (in Thai).

O.A.E. 1955 to 1994. *Agricultural Statistics of Thailand*, Crop year 1954/55 to 1993/94, Office of Agricultural Economics, Bangkok.

Titapiwatanakun, B. 1984. "Cassava in the Agricultural Economy of Thailand", In: *Cassava in Asia, its Potential and Research Development Needs,* CIAT/ESCAP-CGPRT Center.

T.T.D.I. 1995. *Annual Meeting Reports*, Thai Tapioca Development Institute, Bangkok.

IDENTIFICATION OF LANDUSE IN SONGKHLA LAKE FROM THE GLOBESAR DATA

DR.SUVIT VIBULSRESTH[1] DR.DARASRI DOWREANG[1] MISS SUPAPIS POLNGAM[1]
MR.WEERAPANT MUSIGASAN[2] MR.MARC D'LORIO[3]

[1]National Research Council of Thailand, 196 Phaholyothin Road, Chatuchak, Bangkok, 10900, Thailand Tel. 662-579-0345, Fax. 662-561-3035

[2]Prince of Songkhla University, Box 2, Kohong, Hat Yai, Songkhla, 90112, Thailand, Tel. 662-74-212895

[3]Canada Centre for Remote Sensing, 588 Booth Street, Ottawa, Ontario, K1A 0Y7, Canada, Tel. 613-947-1350, Fax. 613-947-1385, diorio@ccrs.emr.ca

ABSTRACT

As part of the GlobeSAR program, the simulated Radarsat data with fine resolution and standard mode products were generated from the SAR data which were acquired by the Canada Centre for Remote Sensing convair 580 aircraft with C-band and HH-VV polarizations. The data were taken in November 1993 covering Songkla lake and Thalae Luang area. During the data acquisition an extensive ground truth information was collected to support data analysis and interpretation.

The results showed that serveral land use classes could be identified and differentiated. These classes include shrimp farm and other aquaculture activities, rubber plantation, paddy field and urban area. Espectially the shrimp farm was clearly displayed on the single image. So there seems to be a potential for this data to be used as a tool for monitoring the expansion of shrimp farms. However, it was found difficult to separate mixed orchard from swamp forest area because of volume scattering from various sizes of canopy which made them appear very bright with coarse texture on the image for both cases. Future study will include the use of color composite of the radar data and Visible - Infrared data as well as another SAR data as could be more favourable for land use study than a single image.

1. INTRODUCTION

The Canada Center for Remote Sensing (CCRS) and the National Research Council of Thailand (NRCT) have coorperated under The GLOBESAR project since 1993. The purpose of this cooperation is to promote the application of radarsat data by inviting researchers from involved organizations who wish to conduct research using the radarsat data.

Under this project; 8 test sites were defined by researchers, each test site addresses the potentials of using radarsat image. TH4 is one of those test sites covering Songkhla lake and Thalae Luang area, Southern Thailand. On November 5, 1993, airborne radarsat image was acquired by The Canadian SAR Sensor System, on boarded convair 580 aircraft, which operated in C-band with HH and VV polarizations. During such time, the area was occupied by growing stage of paddy and on terrace, there were varieties of feature that ranged from bare soil prepared for rubber, young rubber, and productive rubber plantations.

2. PROJECT OBJECTIVES

To study how radarsat data can be used as inputs for development planning and monitoring of the project area

3. STUDY AREA

The study area covers most of Songkhla lake - Thalae Luang area. It lies approximately between latitude 6° 57′ - 8° 12′N and longitude 100° 12′ - 100 35′E. The area is 22 kilometers wide and 135 kilometers long. The physiography of the area can be described as follow : The eastern part is characterized as a coastal plain which consists of long stretches of sandy beach, broken only by major rivers, and followd by a series of parallel beach ridges. Between the beach barriers and the oldest series of beach ridges are the Lagoons. They are extremely shallow (2 meters in most places) and clearly undergoing rapid sedimentation, the western part is swamp. Sediments, are from the numerous short rivers that no longer have direct access to the sea.

The area is planted with coconuts, sugar palm, fruit trees and rubber plantation is contrast with paddy cultivation of the backswamp.

The climate is defined as northeast monsoon and southwest monsoon (see figure 1 : The study area)

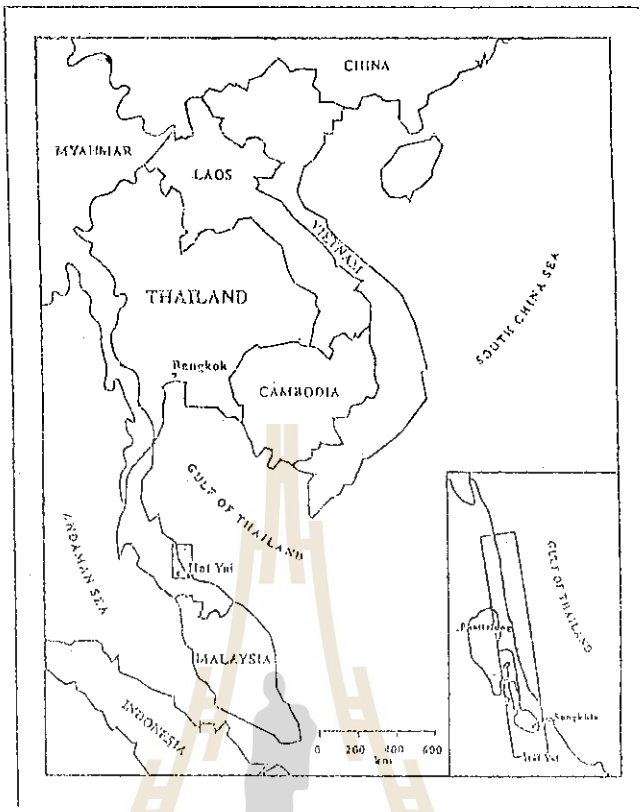

Figure 1 : Location of the study area, TH4

4. DATA ACQUISITION

4.1 Satellite data

Data Holdings

- The Airborne radarsat image, C-band, with was deployed by the CCRS convair - 580 aircraft at an altitude of 6 kilometers. The observation date was November 5, 1993, HH and VV polarizations, right look direction.
- Landsat-5 TM of path 128 row 55, acquired on September 10, 1992 and February 20, 1994.
- ERS-1 SAR C-band, VV polarization, acquired on October 11, 1993
- Spot 2 HRV of K 265, J 336, and K 265, J 335 (2 scenes) acquired on January 01, 1994 and September 03, 1993 respectively

Data required

- JERS-1 OPS and SAR data acquired in November 1993.

4.2 Field Information

Ground information collection was carried out during radar pass on November 5, 1993. The data collected from field observation include various ground objects and also personal interview with local farmers.

4.3 Topographic maps

Topographic maps at a scale 1:250,000 and 1:50,000 which were reprduced by the Royal Thai Survey Department

4.4 Thematic maps

Soil suitability map and existing land use map will be used for supporting image analysis

4.5 Other related research reports

5. METHODOLOGY

Image analysis will be done on a Meridian package software available at the Thailand Remote Sensing Center.

5.1 Image Pre-Processing

Geometric correction was done on the original data, the simulated radarsat image, by registering to a Universal Transverse Mercator (UTM) projection and resampling using a Nearest Neighbour technique to 6, 12. 5 and 18 meter square pixel sizes and then use this image as a reference image to which all data were registered.

Corresponding to the available satellite data, data analysis was conducted with two approaches. The first, the potential of airborne radarsat image was identified in term of object characteristics. Second, analysis of land use and land cover will be based on multisensor data of Visible-Infrared data and SAR data (see figure 2 : The processing flow chart)

In order to remove the speckle noise which mask the fine data. A standard filtering, 5 by 5 median filter was applied by using the Meridian system.

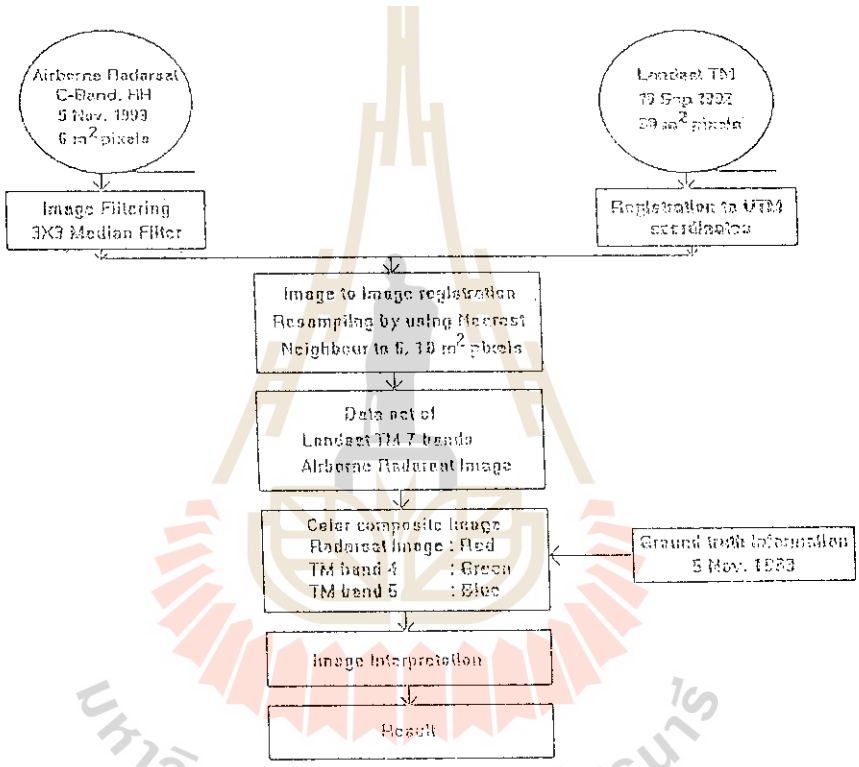

Figure 2 : Processing chart of muitlsenser study

6. RESULTS

The geocoded radar image is used here to illustrate the capability for detecting an object characteristics due to imaging system characteristic, and the differences in viewing geometry that appeared on the image in black and white tone. Black or dark tone signifies little or no return signal to the sensor while bright or white features indicate the higher return signal. The TH 4 image was categorized with regard to identification of tone, texture, pattern and association. Based on the project objective, 8 categories were delineated (see Figure 3). Table 1 illustrates a correlation between the object charateristics and their tone. But, the result indicate some confusion among a standing tree features such as swampy forest, mangrove forest, and mixed orchard. Because of a coarse surface roughness from vegetation canopies which are provide high return signals. Color composite of the radarsat and Visible - Infrared data as well as another SAR data were applied with expectation of landuse and land cover than use a single image. Figure 4 shows an example of the combination of SAR data and Landsat TM data. A satisfactory results were obtained with regard to the identification of color and another component. Swampy forest was clearly distinguished from mangrove forest (Figure 4;4a, 4b).

Figure 3 The airborne SAR C - band, HH polarization data

4a

4b

Figure 4 4a : Color composite of landsat TM data with band 4, 5 and 3 displayed in red, green and blue

4b : Color composite of SAR data, TM band 4 and TM band5 which were given in red, green and blue, sub area of Songkhla lake.

Feature key :

1 = Mangrove Forest

2 = Swampy Forest

7. CONCLUSION

This progress report describes how the airborne radarsat image could be used for identifying the object characteristics in Songkhla lake-Thalae Luang area. The first result from the identification of airborne radarsat image has provided an excellent demonstration of sensitivity of radar backscatter to the surface. The results are surface scattering from high vegetation canopies or coarse surface roughness is uniformly high backscatter such as sugar plam trees in rice field, bamboo poles for aquaculture and rubber trees while a surface scattering from low vegetation canopies or a smooth surface has no return signal or small scatters energy back to the sensor like rice field in early stage, aquatic plants on swamp area. Besides, surface roughness effect, moisture condition also show high backscatter in floating grass. However, a precision data registration and SAR data filtering should be carefully processed in order to retain the identification accuracy of data.

Table 1 Illustrates a correlation between the Object characteristics and their tone

No.	Description	Tone	Texture/Pattern	Remark
1.	Paddy with sugar Palm	bright	regular pattern with coarse texture	sugar palm trees are dominant feature, to act as corner reflector
2.	Rainfed paddy	dark	Rectangular pattern, fine texture	In November, paddy is in ealy stage, mostly cover with water
3.	Off-season paddy	bright	regular pattern, fine texture	In November,off-season paddy is in fully growth stage,
4.	Field preparation for rubber plantation	dark	regular pattern, fine texture	no return singnal
5.	Rubber plantation	white	Rectangular pattern, quite coarse texture	
6.	Floating grass	white	regular pattern	
7.	Shrimp farm	dark and surroundig white line	rectangular shape,	caused by reflectance from pond ridge, appearing white around the pond.
8.	Aquaculture	white spots	spot	high return singnal

8. REFERENCE

1. David S. Simonett, Manual of Remote Sensing, Second edition, Volume I, P 114 - 1158.

2. Le Toan, T., H. Laur, E. Mougin, and A. Lopes. 1989, Multitemporal and Dual-Polorization Observations of Agricultural Vegetation Covers by X-band SAR Image, "IEEE Trans- actions on Geoscience and Remote Sensing, Volume. 27 (6), PP. 709 - 718.

3. Musigasarn, W, S. Polngam, and C.Jee-Rajunya. 1994, GlobeSAR Input for Development Planning of Songkhla Lake Basin (TH4), Proceedings, GlobeSAR Southeast Asian Regional Workshop, Bangkok, Thailand.

4. Rob Schumann, SAR data for Cartographic Application, paper submit to training cource on ERS-1 & SPOT : A Complementary tool for Natural Resources Management, August 19-26, Bangkok

NATURAL RESOURCES AND LAND USE CHANGE OF PHUKET USING REMOTE SENSING

Surachai RATANASERMPONG
Jatuporn PORNPRASERTCHAI
Dararat DISBUNCHONG

Remote Sensing Division
National Research Council of Thailand
196 Phaholyothin Road, Chatuchak,
Bangkok 10900, Thailand.
Tel. 662-5790116, Fax. 662-5613035

.....

ABSTRACT

Satellite remote sensing data have been proven useful in assessing the natural resources and in monitoring the changes. Results that were obtained from the integrating of remote sensing and geographic information system have been used by policy makers to plan more effectively in natural resources management.

The natural resources assessment of Phuket island was performed by using the integration of visual and digital analysis of Landsat - TM data, recorded in 1987, 1990, 1992 and 1995. Based on the 1 : 50,000 topographic map, the three dimentional image of Phuket island was performed. Furthermore, using the method of overlaying , the natural resources change analysis during 1987, 1990, 1992 and 1995 was carried out on SPANS - GIS. Decreasing natural resources and increasing others land use patterns were identified, located and evaluated at various dates.

It was revealed that during 8 years (1987 - 1995) the mangrove forest has been deteriorated about 4 sq.km. or about 19 % caused by urban expansion, on shore mining, solid waste disposal area and particularly coastal aquaculture : shrimp farming. It was found that shrimp farming increases from 0.50 sq.km. to 10 sq.km., rubber plantation was also converted to shrimp farming and most of the ex-tin mining areas were transformed to golf courses or resorts.

INTRODUCTION

Phuket is the largest island of Thailand, located in the tropical zone between 7 deg. 28 min.and 8 deg. 13 min. N of the west coast of the southern part of Thailand in the Andaman Sea. The main island itself has an area of about 549 sq.km. and total area of the provinces , including nearly 30 small islets is about 543 sq.km.. Phuket is divided into 3 districts namely Muang, Thalang and Kathu and about 55 % is undulating -rolling topography and 36 % is mountainous areas which mostly located in the south (Figure 1). Land use of Phuket can be classified into 4 categories : agricultural land , forested land , urbanized area and others which cover 44.07 %, 7 %, 2.72 % and 45.58 % respectively.

With its luxuriant natural resources such as magnificent long white beaches, mangrove forest and others attractive scenery, Phuket is better known as a tourist paradise. It is a premier tourist destination in the region which average 500,000 visitors per year. As a consequence of the politic, economic and social pressures in the last decade, the natural resources of Phuket are subject to destruction or over exploitation for mainly tourism development. It thus has been realized that monitoring of natural resources is essential for sustainable development planning. This could be effectively done via remote sensing technique and its development as applied to land use changes study.

APPLICATION OF REMOTE SENSING AND GIS TO LAND USE CHANGE

Visual interpretation of Landsat - TM bands 4-5-3/R-G-B, recorded in 1787, 1990, 1992 and 1995 was carried out incooperate with colllected ground truth information. While supervised classification of Landsat - TM, recorded in 1995 was performed. Classified results were digitized to SPANS - GIS . Using the method of overlaying , the natural resources change analysis during 1987, 1990, 1992 and 1995 was conducted. So, decreaseing natural resources and increasing others land use were identified, located and evaluated at various dates. Futhermore, based on the contour line of the 1 : 50,000 topographic map, the three dimentional image of Landsat - TM recorded in 1995 of Phuket island was produced.

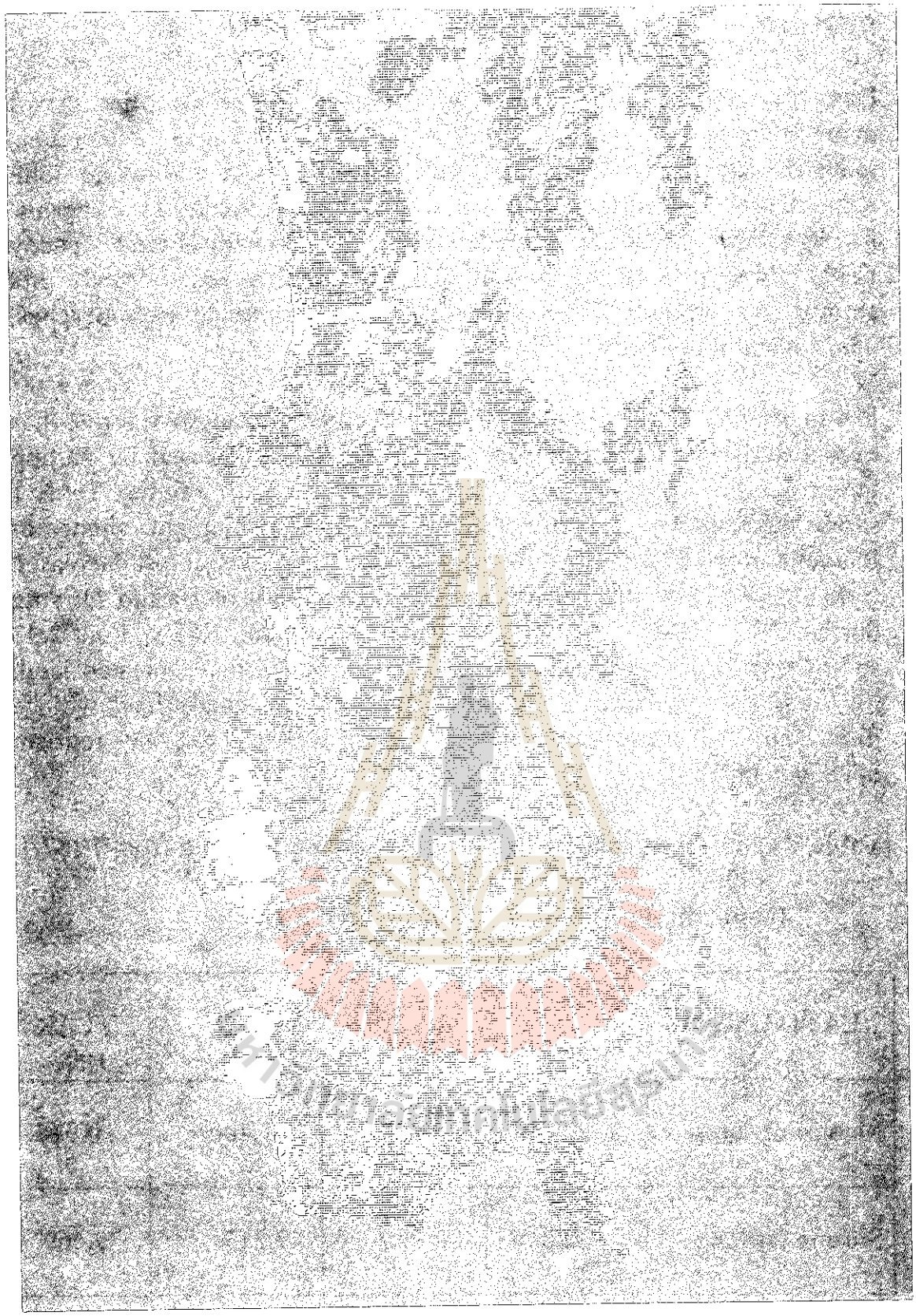

FIGURE 1 Pinatubo island from Landsat - TM band 4 recorded on March 20, 1993.

RESULTS

From the satellite images, land use of Phuket can be classified into 4 main categories (Figure 2) as follows : 1) built - up area : urban area, industrial area, habour, air port, golf courses, resort and waste solid disposal area. 2) forested land : inland forest, forest plantation, mangrove forest, swamp forest and degraded forest. 3) agricultural land : paddy field, rubber plantation, coconut plantation and mixed orchard and shrimp farming, and 4) miscellaneous : ex - tin mining area, beaches, mudflat and water body.

It was revealed that during 8 years (1987 - 1995) mangrove forest has been deteriorated about 4 sq.km. or about 19 % caused by shrimp farming, urban expansion, tourism development and tin mining. Table 1 shows the results of mangrove forest and shrimp farming area change of Phuket during 1897 to 1995. It was found that mangrove forest decreased from 21.55 sq.km. to 17.50 sq.km. The increasing of shrimp farming during 1987 - 1990 - 1992 - 1995 were 0.46 sq.km., 1.52 sq.km., 2.42 sq.km. and 10.35 respectively. It can be concluded that forested land, rubber plantation, coconut and mixed orchard and paddy land will be decreased and transformed to be urbanized area for the tourism deveopment.

Table 1 Changes of mangrove forest and shrimp farming from 1987 - 1995.
(unit : rai, 1 sq.km. = 625 rai).

LAND USE	YEAR 1987	YEAR 1990	YEAR 1992	YEAR 1995
Mangrove forest	13,468	12,287	11,400	10,918
Shrimp farming	288	950	1,513	6,469

FIGURE 2 PRESENT LAND USE MAP OF PHUKET

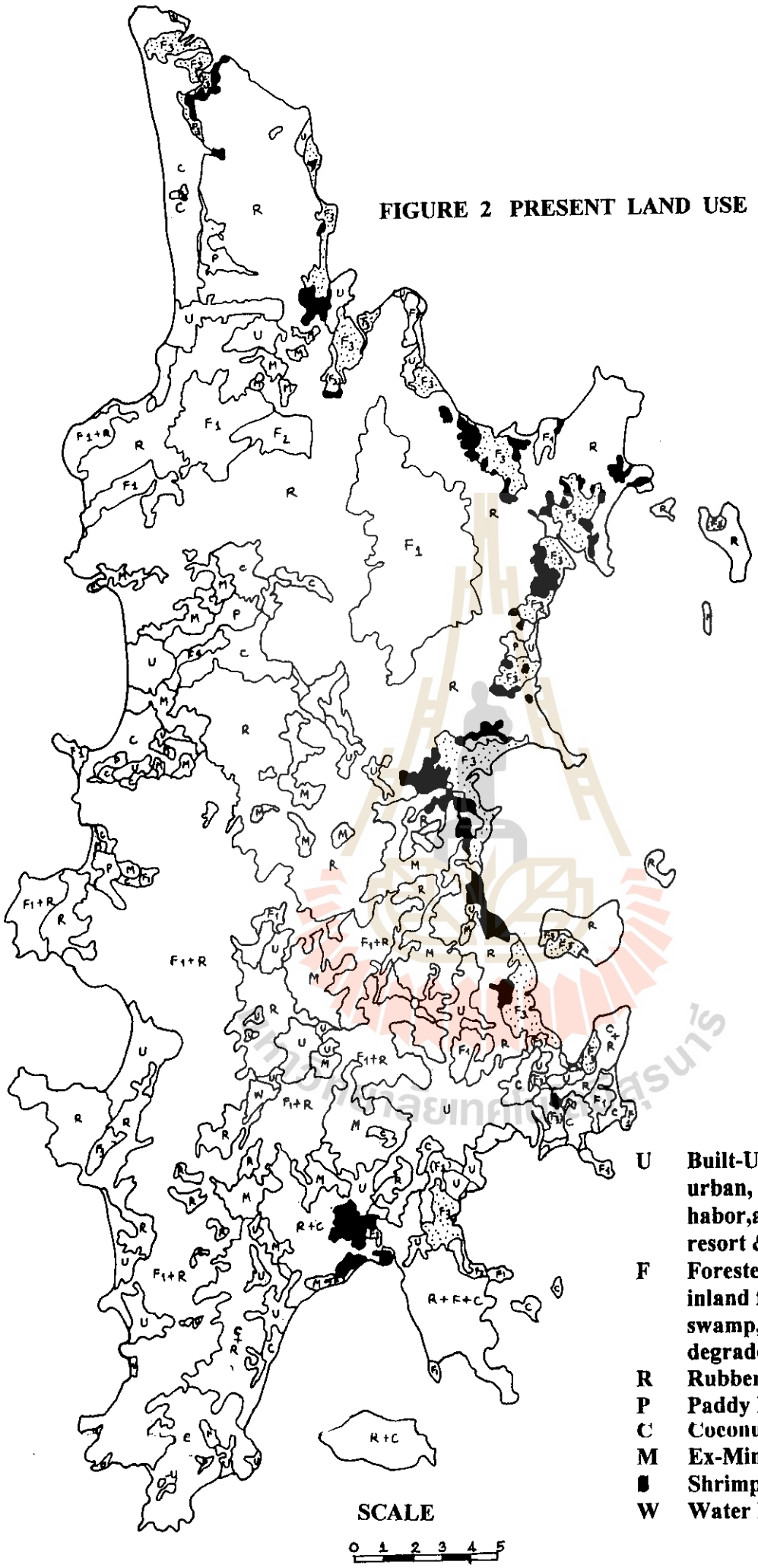

CONCLUSION

The study reveals that the multi-dates satellite images analysis yields an exellent result of natural resources and land use change. The Landsat - TM bands 4 - 5 - 3 / R - G - B, recorded during January through April , diffirentiates more classes of land use pattern than other combination. The preliminary results of the study can be used as a tool for natural resources management focusing on mangrove forest conservation and protection.

REFERENCE

Department of Land Development. 1991. Land Use Planning of Phuket. Bangkok (Thai Version). 94 p.

Office of Environmental Policy and Planning. 1995. Provincial State of the Coast Phuket. Bangkok (Thai Version).

Royal Forest Department. 1994. Forestry Statistices of Thailand. Bangkok. 130 p.

POSTER SESSION R

MAPPING FROM SPACE

USE OF SATELLITE IMAGERY FOR UPDATING TERRAIN INFORMATION IN TOPOGRAPHIC DATABASES

K. D. Parakum Shantha
Institute of Surveying & Mapping
Diyatalawa
Sri Lanka
Tel : 94-57-3016
Fax : 94-57-2004

ABSTRACT

Current terrain-information capturing procedures are mostly based on conventional photogrammetric methods. These procedures are slow and data acquisition is expensive. Developing countries cannot afford the time and cost required to capture terrain-information for updating topographic databases. However, with the increasing development of the remote sensing technology, the satellite data, has wide application potential in terrain-information production.

The main objective of this experiment was to investigation the use of SPOT imagery for updating terrain information in topographic databases. The study covers : Identifying the inherent characteristics of optical satellite images, Investigating a method for extraction of linear features (eg.,roads) in SPOT multispectral images using model based image analysis technique. The results shows that the feasibility of updating road network at 1 : 50 000 scale.

INTRODUCTION

The demand for timely and accurate geo-information has been increased for the management of the earth related disciplines. In response to this demand, geo-information are being producing in map form as well as in digital form. In most of the developing countries are now in a position to update the existing geo-information for the use of their development activities. Hence, the updating of this information should be less cost effective and less time consuming. The use of optical satellite imagery has this facility since its multi temporal and high resolution characteristics. With the use of SPOT multi spectral data, this study emphasis to update road network in topographic database. In this context, the study enable an opportunity to develop image understanding techniques to support the automated feature extraction of optical imagery that goes beyond the traditional extraction methods.

AUTOMATED FEATURE EXTRACTION

Automated feature extraction is performed by segmentation techniques. Segmentation is a process of generating image segments in which image elements having the same properties are merge together. According to the basic principle, the segmentation method can be divided into different categories, such as edge based segmentation, region based segmentation and segmentation in measurement space (spectral clustering).

In the edge based segmentation the goal is to find discontinuities in the image while region based segmentation is interested in the inner pixel of homogenous area, not the boundaries. Spectral clustering is based on the spectral values of the image pixel and it implies a grouping of pixel in a multispectral space. These three segmentation method can be considered as conventional procedures for image segmentation.

The new approach of image segmentation is segmentation with model based image analysis. Model based image analysis is based on the analysis of the image model that considers the recognition of objects by assuming a model for how real world features are represented in the image.

THE MODEL FOR IMAGE SEGMENTATION

The major point of interest is to detect linear features from SPOT MSS imagery. Linear features detection can be identified as a process for detection of the region heterogeneity in the image. Image heterogeneity can be measured considering local image coefficient variation. Therefore, the distribution of the reflectance values of homogeneous area has to be modeled and deviation from this model can be considered as heterogeneities.

The point source on the ground is seen on an image as a diffused circular region, due to the properties of the optical involved in imaging. A cross-section of the recorded or imaged intensity distribution of a single point source is shown in figure 1.0 and it can be seen to having a Gaussian-type distribution (Paul, 1987). The actual shape will depend upon the properties of the optical components of the system and the relative brightness of the point source. The distribution function shown in figure 1.0 is called the Point Spread Function (PSF) (Moik, 1980).

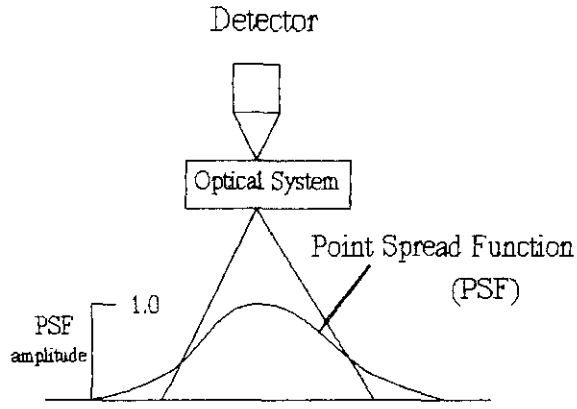

Figure 1.0 : Point Spread Function

With this criteria the model assumed that the variation of reflectance values of homogeneous areas can be described by a Gaussian function.

When a linear feature or point feature is inside the homogeneous area, the mean of the reflectance value within a window will be changed. Associated variance will be changed considerably with respect to the change of the mean value.

According to that, heterogeneity can be detected by considering the variation of the coefficient variation within a small window. It should be noted that for small window the statistics is not as valid as it is for large window. But large window do disappear small features.

PROCEDURES FOR TESTING THE MODEL

Two procedures are adopted to test the model.

Procedure (i) :

In this procedure, the variation of the reflectance value in a neighborhood around the center pixel of sub image is used to determine the homogeneity of an area. For that, the center pixel value is replaced by the variance of sub image. The existence of a heterogeneity is indicated by the higher value of the center pixel in the output image associated with the higher variance of the sub image.

The selected window size for sub image be small in order to find the significant variation of the variance due to thin

lines or points.

The algorithm is :

```
Begin
     For every (i,j) position on the original image Do
     Take the 3x3 surrounding sub image;
     Compute the variance of sub image;
     var-image (i,j)=variance of sub image;
End.
```

By slicing the variance-image at a certain threshold, only the heterogeneous areas (points, lines, edges) are detected.

The algorithm for the thresholding is :

```
Begin
     For every (i,j) position on the var-image Do
     If var-image (i,j) >= threshold;
     Then binary (i,j) = 1; (points, lines, edges)
     Else binary (i,j) = 0;
End.
```

Procedure (ii) :

It considers the rank order of a sub image (3x3). The presence of homogenous areas assume the rank 2 and rank 8 falling within the probability range of 5% and 95% in the Guassian distribution. Therefore, the range between rank 2 and rank 5 is equal to the that of rank 5 and rank 8. In the presence of heterogeneity, two ranges are not equal.

The algorithm is :

```
Begin
     For every (i,j) position on the original image Do
     Take the 3x3 surrounding sub image;
     Sort its 9 values into the array Rank;
     r2_image = Rank(2);
     r5_image = Rank(5);
     r8_image = Rank(8);
     r2_5_image = Rank(5) - Rank(2);
     r5_8_image = Rank(8) - Rank(5);
     Hetro_image = r2_5_image - r5_8_image;
     End.
```

CONCLUSION

This study compared extracted features with the information content of the map at 1 : 50 000 scale. This comparison shows that main roads and secondary roads can be detected successfully with SPOT multispectral images. However, resolution is important since it was not possible to identify tracks and unpaved roads with low resolution.

The experimental results shows positive indications for updating main roads and secondary roads in road network at 1 : 50 000 scale.

REFERENCES

Moik. J (1980). "Digital Processing of Remotely-Sensed Images", NASA special publication 431, Washinton DC.

Paul M. Mather (1987). "Computer Processing of Remotely-Sensed Images", John Wiley & sons, ISBN 0 471 90648 4,Chapter 2.

Parakum Shantha K. D. (1992). "Use of Radar Imagery for Updating Terrain Information in Topographic Databases", Dissertation, ITC, The Netherlands.

INTEGRATION OF REMOTE SENSING DATA WITH GIS TECHNOLOGY FOR THE ACCELERATION OF THE ACTIVITIES IN NATIONAL MAPPING AGENCIES

Shyamali Chithraleka Perera
Center for Remote Sensing
Survey Department
P.O.Box 506
colombo, Sri Lanka
Tel : 94-587988
Fax : 94-584532

K. D. Parakum Shantha
Institute of
Surveying & Mapping
Diyatalawa
Sri Lanka
Tel : 94-57-3016
Fax : 94-57-2004

ABSTRACT

As the world changes more rapidly, the demand for upto-date information for resource management, environment monitoring, planning are increasing exponentially. Mapping agencies must respond to the concerns of the public, and do so with increasing efficiency and effectiveness. Integration of Remote Sensing with GIS technology will significantly promoted the ability for addressing these concerns.

Despite a decade of effort to active completely automated integration process, authors identify a conceptual model that permits utilization of computers with Remote Sensing and GIS technology with human contextual analysis in order to support the National Mapping Agencies to acceleration their activities.

INTRODUCTION

The well-worn argument that geo-information is a pre-requisite for development. Most map makers absolve themselves from responsibility for the poor state of mapping with their territory. As the mapping will take several years to complete, it is clear that the National Survey and Mapping organization has to take initiatives to supply upto date geo-information for the users on their various requirements and expectations.

The integration of satellite data into a Geographic Information System (GIS) is one of the great idea that focus on the rapid acceptance of GIS technology in to the geo-information oriented applications in operational environments. Institutionalizing of the GIS and Remote Sensing process into everyday decision making has greater efficiency to overcome the problems identified in mapping at a National Mapping agency.

Hence, authors identified key issues of integration of Remote Sensing with GIS and the proposed structure perhaps most significant, however, is that the integrated approach leads to a new view of supplying geo-information rather than being static documents to completely recreated at periodic intervals.

INTEGRATION OF REMOTE SENSING WITH GIS

The volume of Remote Sensing is so large, its associated powerful image processing technology is used to manage geo-information with preprocessing analysis, accuracy assessment and information

distribution.

GIS are more and more being used for the storage and analysis of geo-referenced data and also it handles the linkages between spatial entities and their discrete attributes. GIS system have become accepted as a standard way of handling geographic data and performing analysis on those data for a number of earth related disciplines.

With the availability of high resolution satellite data and its processing technologies, integration of digital image analyzing systems with advance GIS systems permit compositing data sources as well as promoting a partnership between man and machine. Furthermore, a GIS when combine with upto date remote sensing data could assist in the automated interpretation, change detection and map revision processes. Satellite data offer repetitive, synoptic and accurate information of the earth's surface and as such offer the potential to monitor the dynamic changes with GIS.

However, one should bear in mind the integration will largely depend on the ability to understand and conceptualize the transition between one representation to another.

TECHNICAL IMPEDIMENTS TO INTEGRATION

Geographic phenomena do not occur with a specific data structure. Obviously certain types of objects are well represented in a raster data structure (eg., elevation, soil type) while others more appropriately represented as vectors (eg.,boundaries, point information). Consequently, it can be significant strength for a GIS to incorporate advantages of both data types. New commercial systems designed expressly around data integration are also emerged. However, the full potential of integrate GIS with remote sensing will not be realized unless we overcome the dichotomy of data structures for GIS and remote sensing (Ehlers, 1991). Data accuracy and system communications are other major issues that discussed under problems related in integration.

DATA STRUCTURES

The major problem is caused by the different in the structures used to acquire and store data. Remote Sensing detectors produce raster digital information directly then the raster processing of these data seems "natural". GIS systems typically used the vector data structure.

In a model of geo-information extraction from raster imagery, at lower level processed raster data can be used to extract and manipulate at pattern recognition in middle level. At the highest level with the knowledge based information, models the predictive description of the "imaged" object. Hence, at the middle and the highest level the image information can be stored as vectors or objects than gray values, thus facilitating the integration approach. Additionally, the data structures that used for computer vision, quadtrees and other tessellation are also possible data structures to manipulate remote sensing data (Samet.,1984).

Presently, the common used approach dealing with this problem is data conversion eventhough the raster to vector conversion leads to a loss of accuracy of information.

DATA ACCURACY

The classification accuracy, mapping accuracy and spatial resolution are main data accuracy problem which have to considered when integrating Remote Sensing data with GIS. The problem of classification accuracy present a major difficulty in the integration. Researchers has been suggested to improve Remote Sensing image classification accuracy by referencing the information already available in GIS's.

A data processing system must assess levels of data accuracy and associate the level with the data it provides. Based on the assessment a user can understand how reliable the data are and determine how being to use them.

Different methods are used in Remote Sensing and GIS's for data accuracy assessment. The method are incompatible with each other. Remote Sensing data analyzing mainly uses the error matrix method which provide global accuracy information while GIS operators use error model which provide more local accuracy information. But up to now no effective approach has been reported which facilitate the flow of accuracy information between Remote Sensing image analysis system and GIS's (Fangin Wang., 1991).

SYSTEM COMMUNICATION

In the communication between Remote Sensing system and GIS, spatial and non spatial data must be transferred in an integration fashion. Facilitating the communication have been mainly made on query/reasoning languages and communication procedures. This method developed usually include the steps of language conversion, query optimization and data translation. Even so mismatch is unavoidable and the communication is still expensive (Fangin Wang, 1991).

ISSUE OF NEW INTEGRATED GIS DESIGN

In the technological and institutional side, potential and problems have been mentioned. The proposed structure (figure 1.0) is to accelerate the activities in a national mapping agencies and this integrated approach permits exploitation of multiple data sources and provides accelerated mapping capabilities.

It is possible to input vector data as well as raster format data to above proposed integrated data base model.

Existing analogue form maps can be convert to digital form by manual digitizing or scanning. The digital photogrammetric and digital form field survey data can connected to the databases directly. In this case user can get digital form map as well as analogue form maps. The advantage of use of Remote Sensing data is updating all topographic maps and thematic maps within a short time period. Hence, always possible to supply correct information to user. Further more, this data base can provide not only map information but also statistics and reports.

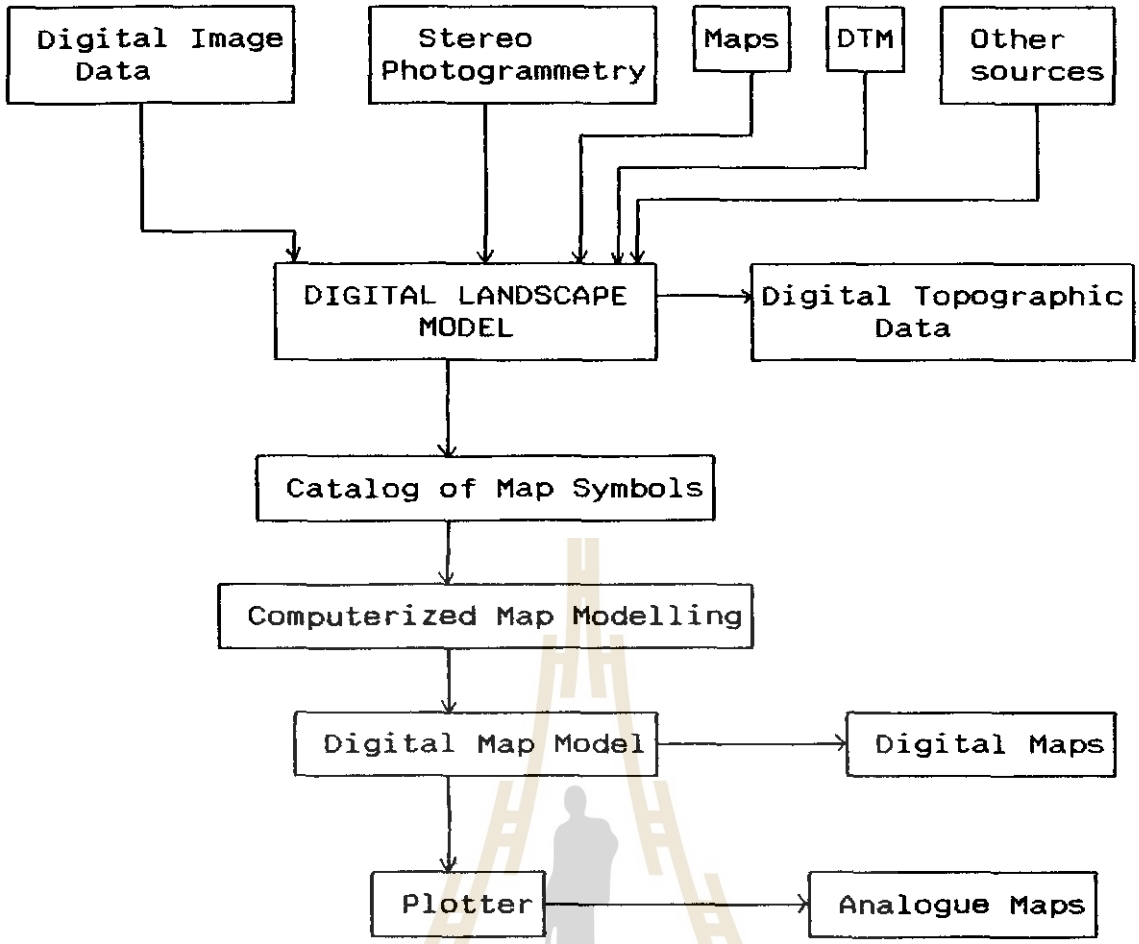

Figure 1.0 : Integrated GIS System

Since the capability thus exist to implementation the proposed structure, Survey and Mapping organizations should examine the major obstacals which have been encountered to date. The impact of automation on the need of software system architecture, hardware system architecture and education and training to be recognized.

SOFTWARE SYSTEM ARCHITECTURE

Software system architecture means this "Organizational Context" within which all the software modules, programs etc. perform certain tasks and communicate with each other and data stores. It reflects the processes or group of processes defined in the logical architecture.

The software should be selected which has capability for data capture by manual digitizing or scanning, Remote Sensing data on tape and digital form field survey data. Attribute data should be able to enter from alpha-numeric terminals.

Database management system interface should be capable of providing search/query facility to access graphical display from the database to satisfy a certain search criteria to display certain map elements and also in the opposite direction to access the database from graphical display to textural attribute information about certain map elements and generate a report about them. Also it should have possibility for

editing and utility programs to improve the quality of graphical data. Specially there should be image processing system to process and classify Remote Sensing data.

Software system should be able to give out put in paper plot either as verification plot to check the data quality or precision final plots from graphical out put and attribute data in report form. Also it should be possible to out put digital map sheet on tape as back-up tapes.

HARDWARE SYSTEM ARCHITECTURE

The hardware system should be chosen to match the system capability requirements to perform the task imposed by the logical model and the performance requirements necessary for the software system capabilities.

EDUCATION AND TRAINING

To implement the database model have to give training to persons with necessary and innovative skills to manage the transition from existing analogue to digital technologies and to decide how conventional and new processes can best be integrated to optimally serve user needs.

CONCLUSION

Integration of Remote Sensing and GIS technologies will significantly promoted the ability to handle geo-information. It is possible to obtain high benefits in producing and updating maps with proposed system. It has facilities to do repetitive task without complaining, sort things fast, draw and store points, lines or area fastly and retrieving of geo-information rapidly. Thus the new system leads to geo-information which are accurate and reliable in rather short time for decision making.

But some times it takes the same time to do a job the first time whether using a computer or by hand. The difference is on the second or third time around, repeating the process with only a few changes to make a new map.

REFERENCES

Fangju Wang, " Integrating GIS's and Remote Sensing Image Analysis Systems by Unifying Knowledge Representation Schemes", IEEE Transactions on Geo Science and Remote Sensing, 1991.

Manfred Ehlers, "Remote Sensing and Geo Information Systems : Towards Integrated Spatial Information Processing", IEEE Transactions on Geo Science and Remote Sensing, 1990.

Manfred Ehlers, Geoffry Edwards, Yvan Bedard,"Integration of Remote Sensing with Geographic Information System : A necessary evolution", International Journal of Photogrammetry and Remote Sensing, 1990.

John Leatheradle,"New Strategies for Funding Mapping and Land Information System", Conference of Common Wealth Surveyors, 1991.

Samet H.,"The Quadtree and Related Hierarchical Data Structures", ACM Comput. Surveys, vol.16, 1984.

Block Adjustment Method for Mosaicing a Large Number of Satellite Image Data

Koki Iwao , Ryosuke SHIBASAKI and Masataka TAKAGI
Institute of Industrial Science,
The University of Tokyo.
7-22, Roppongi, Minato-ku, Tokyo 106, JAPAN
E-mail iwao@shunji.iis.u-tokyo.ac.jp
Tel. +81-3-3402-6231 ext.2563
Fax. +81-3-3479-2762

Abstract

This paper focused on the development of geometric correction method for mosaicing a large number of satellite data under the auspices of Land Use/Cover Change Study of South-East Asia(LUCS-ASIA).

In this project, we have to geometrically correct more than one thousand Satellite(Mainly Landsat TM & MSS, MOS-1 MESSER) scenes for three different years, i.e. 1970's, 1980's and 1990's of South-East Asian region. If these images are geo-corded separately one by one, geometric distortions are likely to occur between different images. And it is not always easy to find enough GCPs in every scene. This makes the mosaicing of images labor-depending.

In this paper, we propose a method to adjust geometric errors over all images at one time borrowing the idea of block adjustment in photogrammetry. Even if we can not find enough GCP points to one scene, we can adjust geometric errors over all images with the information of tie points between images.

1.Background and Objectives of the Study

Land use changes are becoming an important component for environmental studies at all levels - local, regional and global levels especially in South-East Asian regions. For a proper and complete understanding of the changes that are taking place in land use and their effects on the local, regional and global scales, we need to have a quality database of the landuses - both past and present, to help us in analyzing the changes on the time scale.

The Land Use/Cover Change Study of South-East Asia(LUCS-ASIA) was taken up with an aim to develop uniform and standard time-series database of the land uses by a core group among universities/National Institute of environmental Studies (NIES) in Japan under the cooperation with research institutes

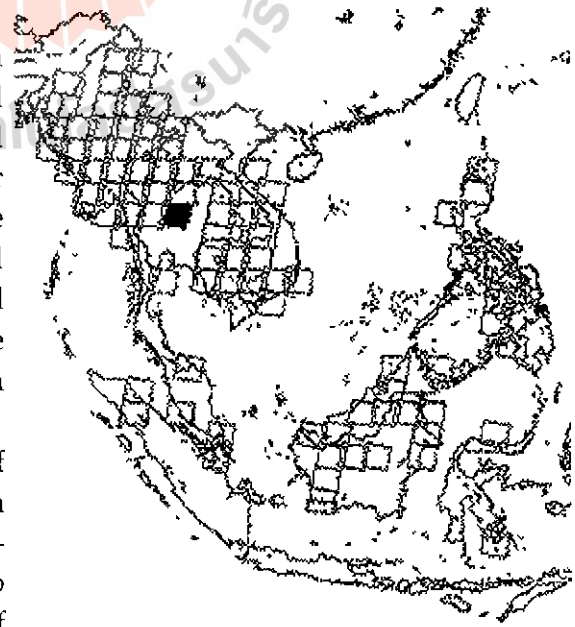

Fig.1 Map Illustrating the 100 Landsat Scenes

/universities and governmental organizations in South-East Asian countries.

In this project,we have three main aims i.e.

1. To generate time series mosaicing images around South-East Asia
2. To generate land use/cover time-series data set using satellite data
3. To develop comprehensive GIS database

Up to now,we already got more than 100-Landsat TM images for 1990's(Fig.1) and more than 400 MOS-1(MSSR) images of this area.

Here we focused on the method for mosaicing such a large number of data.

2.Methodology

So as to locate GCP's, we have to identify correspondence between feature points in images and those in topographic-maps such as DCW and World Data Bank. But there are so many images where typical geographic features such as river branch points and coastal lines which employs tie-points(TP) to conjugate neighboring images and conduct geo-cording of all images simultaneously. Even if we can get enough number of GCP data, these distribution may be so biased. We propose*"Block adjustment method"* for mosaicing large number of data. Even if we can not find enough GCP points and these distributions are not so much homogeneous, we can adjust geometric errors over all images. The process of the Block adjustment method for mosaicing large number of data are introduced in Fig 2.

We can divide this process for four stages.

2.1) Measuring GCP and Tie points for each Images

In this stage, we identify and measure coordinate values of GCP (image coordinate data and map coordinate data) and tie points (Image coordinate data) for each images. We use World Data Bank (coast and river data) to determine the map coordinate information for GCP.

2.2) Checking the Number and Distribution of GCP for each images

We use Pseudo Affine transform formula for geometric correction.

$$x=a_1uv+a_2u+a_3v+a_4,\ y=a_5uv+a_6u+a_7v+a_8$$

We need more than four GCP's to determine the parameters in this formula. And GCP points should be homogeneous. The number of GCP and these distribution have to be checked to avoid extreme bias in GCP / TP distribution over all images.

2.3) Setting the initial value of transform parameters for block adjustment and detecting / eliminating gross errors

After checking the number and distribution of GCP points,

This stage also consists of four steps.

2.3.1) Calculate unknown transform parameters of "AA class" images (number of GCP≧7) only from GCP

2.3.2) Compute map coordinate values of TP in AA class images

2.3.3) Replace TP with GCP in images overlapping / neighboring AA class images.

2.3.4) Calculate unknown transform parameters for the neighboring images (GCP<7)

By using the information of "geo-located" tie points, we can propagate initial geo-location of individual images from AA class image to neighboring "lower class" images.

If any gross errors may be detected through these steps, we can evaluate the original image of GCP / TP.

2.4) Adjust geometric errors over all images with the information of tie points between images

By using initial values of the transfer parameters of each images, geometric errors over all images are adjusted borrowing the idea of block adjustment in photogrametry to

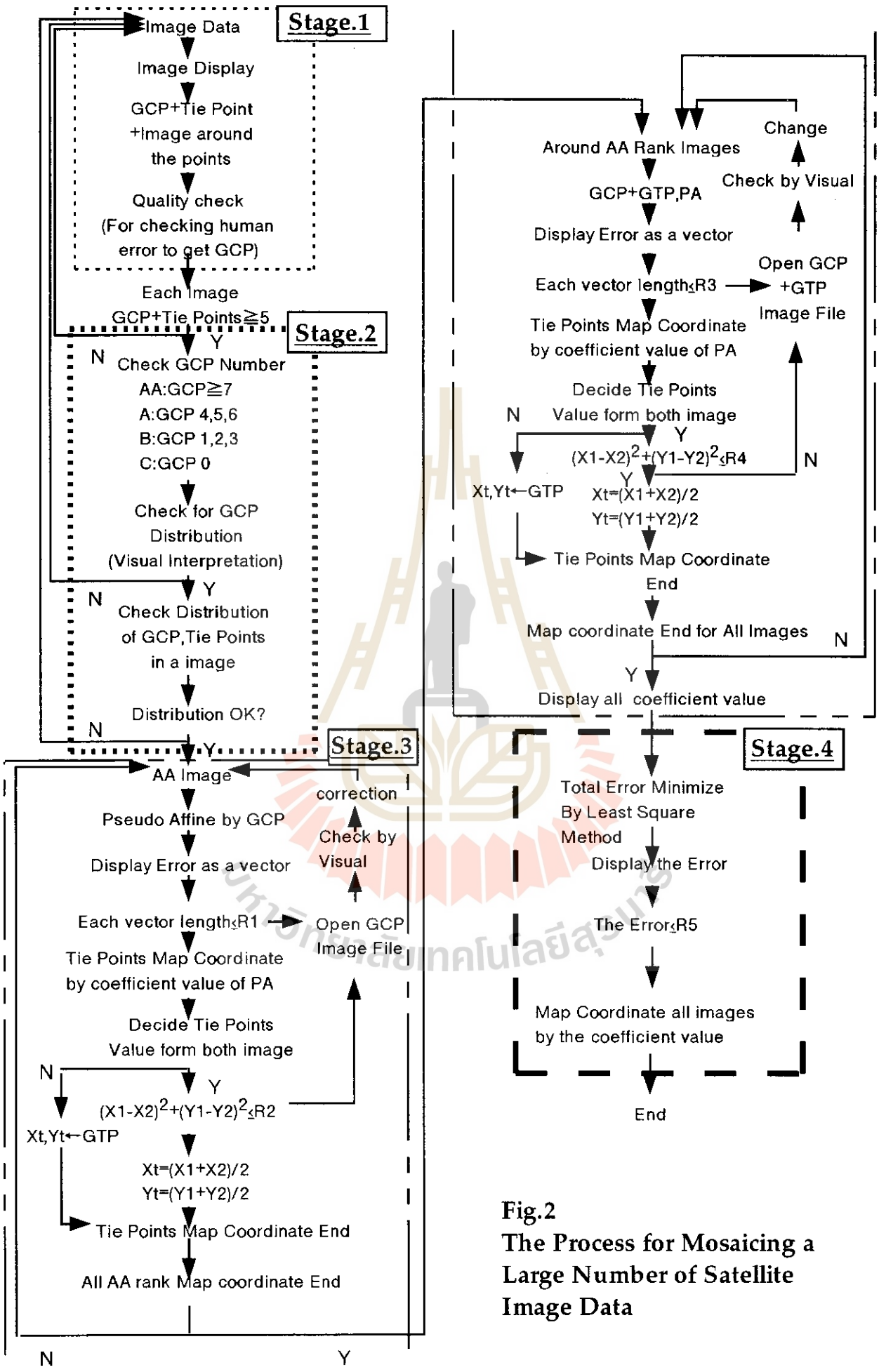

Fig.2
The Process for Mosaicing a Large Number of Satellite Image Data

compute accurate values of the transform parameters.

3. Experiment

The block adjustment method is being applied to MOS-1 MESSER images. The results will be present in the Conference.

4.Future Works

Automated identification / measurement of GCP's and TP's as to minimize human labour in GCP /TP measurement, we need to develop automated processing for identifying / measuring GCP's and TP's. For GCP identificate / measurements, feature-based matching will be employed while template matching techniques of image are applied to TP measurement.

References

[1] JARS,Remote Sensing Note, Nihon Printing Co.,Tokyo,1993 pp.178 - 179

[2] Ryosuke Shibasaki, Masataka Takagi and Koki Iwao (1995), "Land Use Change Study of South East Asia(LUCS-ASIA)", Proceedings of the International Symposium on Vesitation Monitoring International Archives of Photogrammetry and Remote Sensing, Chiba, Japan, pp.199 - 205

[3] K.S.Rajan, Koki Iwao,Ryosuke Shibasaki & Masataka Takagi (1994), " Semi-Automated Classification System for Landsat Pathfinder Project", Proceedings of the 15th Asian Conference on Remote Sensing, Bangalore, India, vol.2 pp.L-6-1 - L-6-4

A STUDY OF ECOSYSTEM DEVELOPMENT ALONG CORAMANTAL COAST OF TAMIL NADU USING REMOTE SENSING TECHNIQUES

M.Manivel, B.Manikiam,* D.Kumaran Raju, J.Moses Edwin

SCHOOL OF EARTH SCIENCES, BHARATHIDASAN UNIVERSITY

* NNRMS, ISRO HEADQUARTERS, BANGALORE

ABSTRACT

The extensive Coastal Zone of Tamil Nadu remained unexplored until the advent of aerial photography and satellite remote sensing. Recently acquired date from IRS-I and NOAA satellites have helped in better understanding of the ecosystems of the coastal zone. The seasonal effects and the movement of currents along the east coast could be detected and monitored using multidate satellite imageries. The growth of spits along such bck waters and creeks of Tamil Nadu coast could be associated with the sediment dispersal pattern near the estuarine mouths. Remote sensing plays a vital role in mapping of these features seasonally and in identifying sites for construction of jetties at appropriate places to avoid excessive sedimentation. Also, the sea surface temperature derived from the NOAA data is being operationally used to derive information on potential fishing zones for the benefit of the fisherman.

1.0 Introduction

India has an extensive coastline of nearly 7,527 kms. and vast exclusive economic zone (EEZ). It contributes about 46% of total exploitable living resources of Indian Ocean. The State of Tamil Nadu is blessed with 950 kms. long. coastline with Pulicat Lake in the north and Kanyakumari in the south. The advent of modern technology of remote sensing has attracted the geo-scientists for detailed studies of the coastline and associated features. It has opened up new vistas in the exploration of oceanic resources also. A perspective plan for all round development of coastal areas through intensive agriculture, fishing activities and industrial development needs detailed information on coastal zone. The multidate satellite data has been found to be of immense help in studying the growth along the coast and its effects on the Biotic Environment. With the availability of sea surface temperature from NOAA data fishery potential zones along the coast could be delineated during monsoon and non-monsoon periods thus aiding the fisherman. The remote sensing technology has also been successfully used in India and particularly in Tamil Nadu to map the probable areas for brackish water farming in Pulicat and Ennore regions (Durariraj, 1988). The backwaters and creeks along these areas from potential areas for developing fishing

grounds along Tamil Nadu Coast. The heavy sedimentation due to the seasonal effects and oceanic currents could also be mapped using remote sensing techniques.

2.0 Coastal Zone Geomorphology

The coastal zone geomorphology is a major parameter controlling coastal zone environment. The landforms are generally fluvial landforms like deltas, palaeochannels and the marine landforms like backwaters, creeks, beach ridges, etc. The analysis of multidate satellite data shows changes in the coastal geomorphic features due to implact of monsoon rains and tidal actions (Fig.1). The movement of littoral currents along the coast are found to modify the coast at some places especially near the mouth of backwaters and creeks and cause lagoonal environment which affects the brackish water formations all through the cycle of a year (Ramasamy 1991)

3.0 Backwater Environment

The backwaters along the east coast of Tamil Nadu are very dynamic during the seasonal cycle. Analysis of Landsat Thematic Mapper data of April 1983 has shown that the Pulicat backwaters remain closed due to the constantly forming spit and its south eastern cornder motion (Fig-2a) during nine months in a year and hence it is almost under lagoonal environment during that period. The study of littoral currents along east-coast shows that they move in clockwise direction during these months and such littoral currents move all along the east coast. During the three months of north-east monsoon period, it moves in anticlockwise direction (Sambasiva Rao, 1987).

The movement of littoral currents are responsible for deposition and erosion along east coast and also for the growth of such spits near the mouth of backwaters such as Pulicat lake. Such spits growing near the mouth are developed due to the northerly moving littoral currents which keep on dumping the sediments during its nine months of northerly movement from January to September (Fig.1). But during the NE monsoon period (October, November, December), the littoral currents move southerly and change such growth of the spits resulting in free of sea water inside Pulicat lake as observed during the monsoon period. The cycle of rebuilding of spits once again starts after the NE monsoon is over. Similar phenomenon is observed in the Kalveli chains of backwaters (Fig.2b).

4.0 Creek Environment

The creeks are comparatively less along Tamil Nadu coast and the analysis of Landsat and Thematic Mapper data of April 1983 and December 1983 shows that the creeks are dynamically changing due to the seasonal variations (Fig.3). The study of Ennore and Kovalam creeks are also dynamically changing during the southwest monsoon and suffer excessive sedimentation during this period.

5.0 Conclusions

It has been found that multidate satellite data analysis could provide detailed information on the coastal zone/acquatic environment. The remote sensing provides an ideal tool

for monitoring of backwaters and creeks and for siting of Jetties at appropriate places. The already existing Jetties near Kalpakkam and Madras harbour causes excessive sedimentation near the Kovalam creeks and Ennore creeks so, the two proposed Jetties one near Mahabalipuram and another near Kasikovilkuppam will deflect the littoral current and will cause erosion near the mouth of creeks and promote regular inflow and outflow of sea water. In the Pulicat backwater, the mouth is silted much and construction of Jetties below the mouth or breaking the sand bunds by construction of break waters to destroy the deposited sand during the non monsoon period will ensure regular flow of sea water as backwaters.

The Indian marine fish catch in the past ten years has fluctuated between 1.444 to 1.779 million tonnes and as much as 90% of this catch is realised from the continental shelf area. The fish catch can be improved through efforts in the deeper oceanic areas and through aquaculture development in coastal areas. Remote sensing can play a vital role in both these areas. The SST charts being generated from NOAA-AVHRR data analysis provides information on potential zones for fishing. The coastal landuse maps generated from satellite data are found to assist in site selection for aquaculture development.

References

Durariraj. S., (1988). Application of remote data for Coastal Zone Mapping - A case study of the part of east coast of Tamil Nadu, M.Tech. Thesis, Anna University, Madras, p.138.

Parulekar, A.H., S.N.Harkantra and Z.A. Ansari, 1982. Indian J.Mar.Sci., 11, pp.107-114.

Ramasamy, S.M.,D.Kumaran Raju, T.Balasubramanian, S.Prabhu, (1991). Remote sensing and coastal environment of Tamil Nadu, presented in ISRS Symp. on Remote Sensing and Environment at Anna University, Madras (In Press).

Sambasiva Rao, M., (1987). Influence of coastal process along with the modern delta front of Godavari in Andhra Pradesh, Jour. Geol. Society of India, Vo.29, pp.399-404.

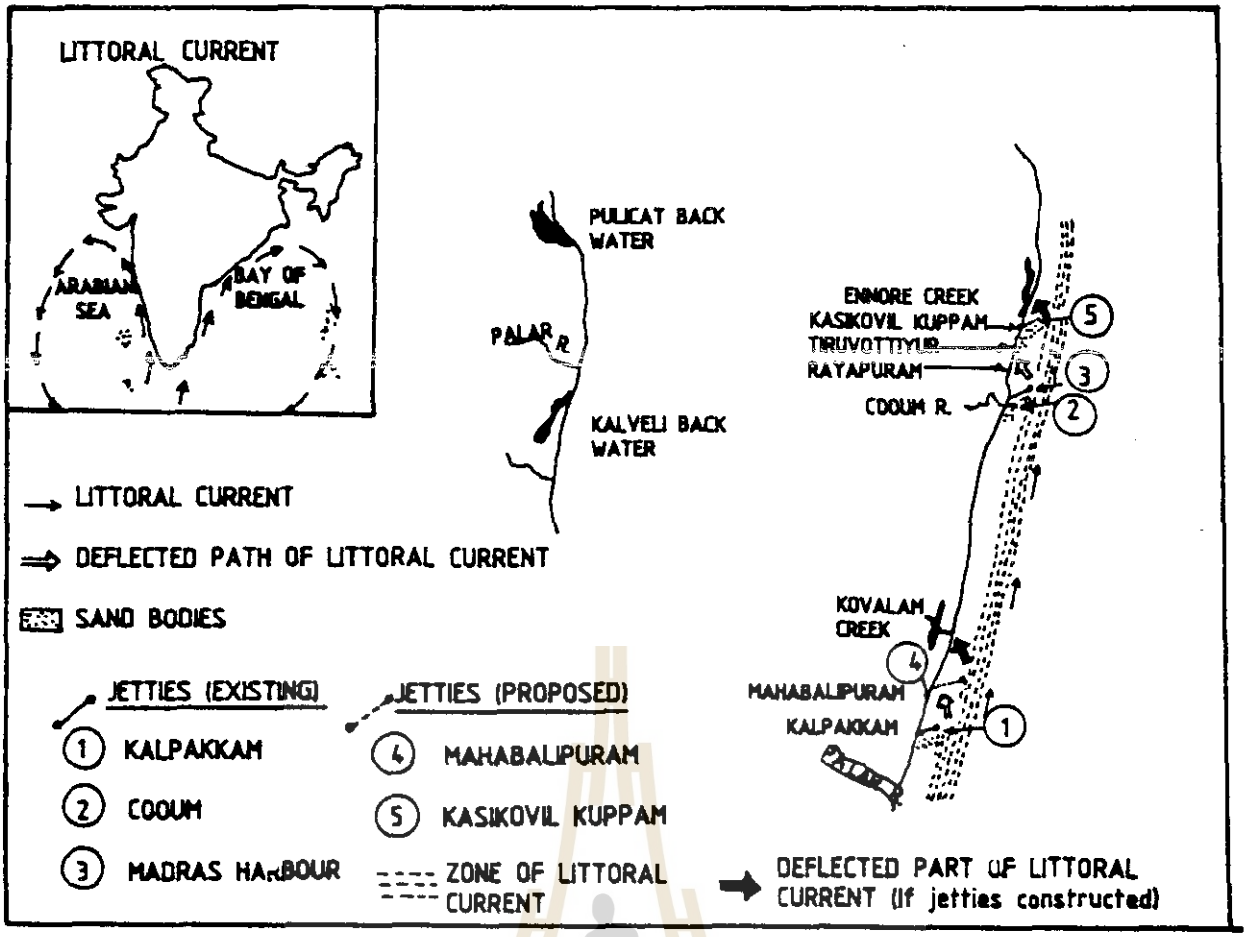

Fig. 1 : Erosion along Tamilnadu coast

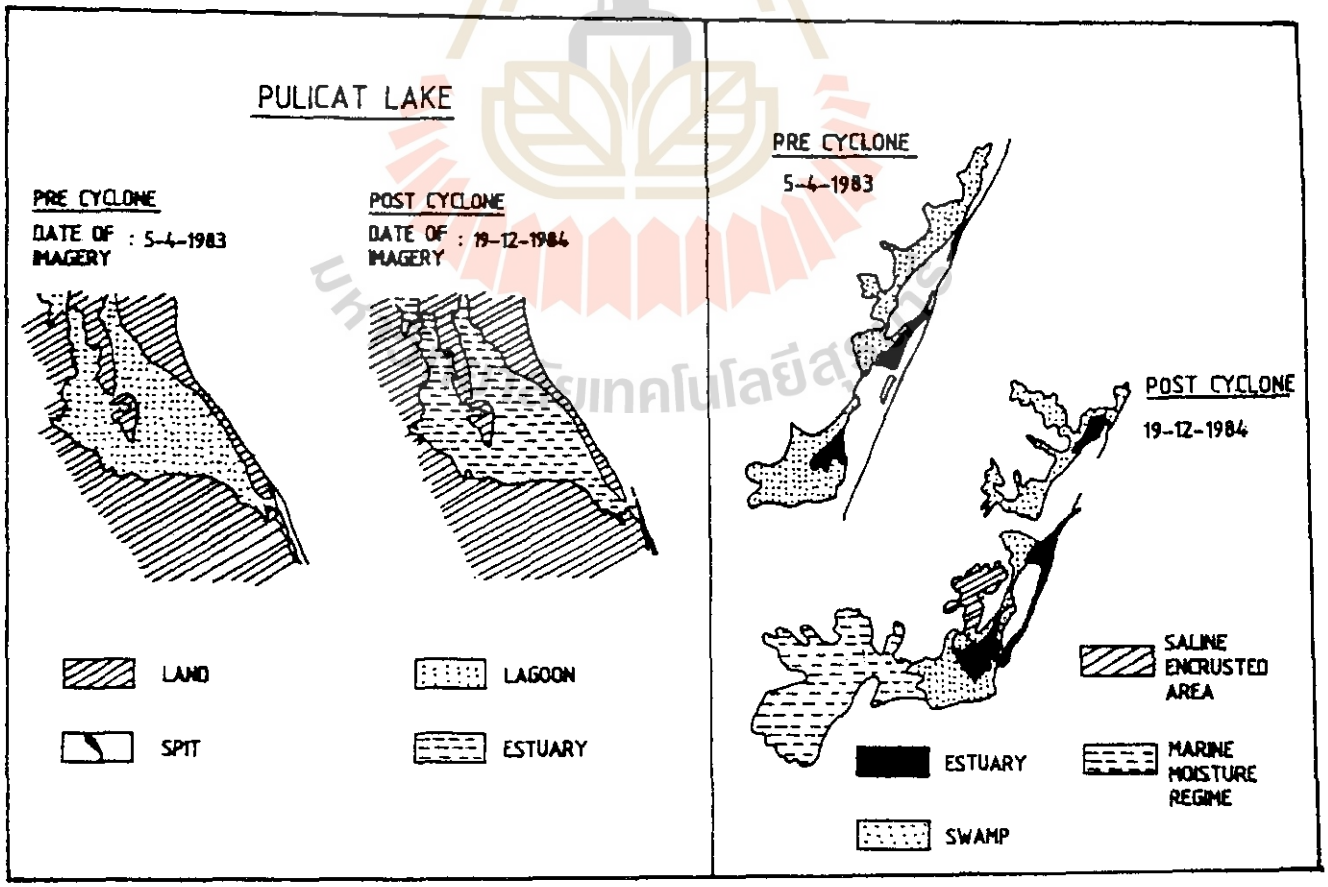

Fig. 2(a) : Spit destruction and estuary formation

Fig. 2(b) : Estuary reactivation (Kalveli area)

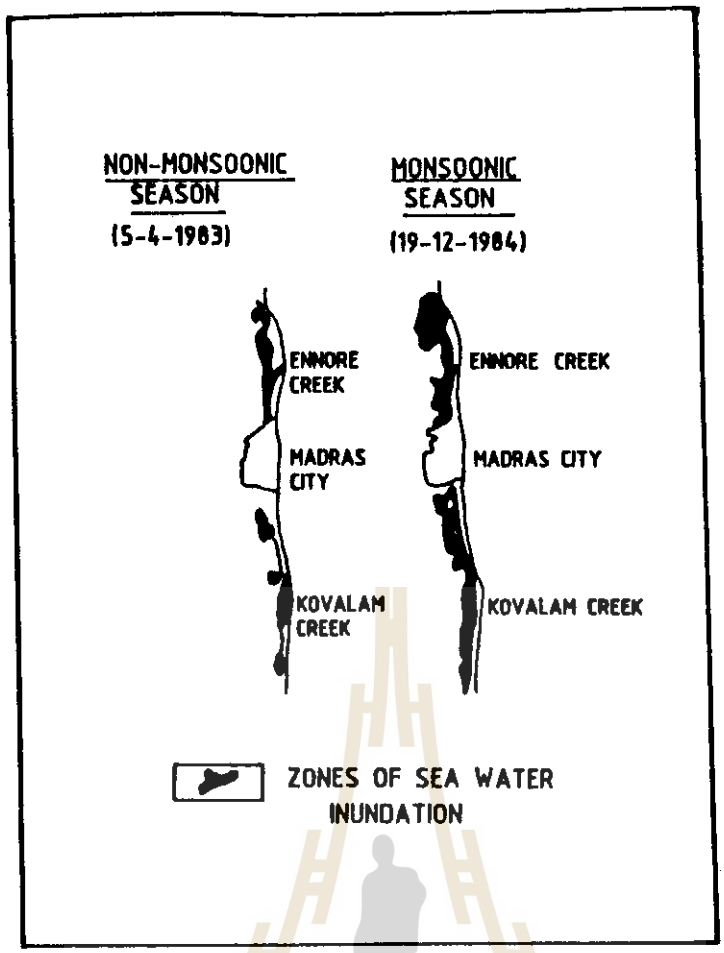

Fig. 3 : Creek dynamics in Tamilnadu

AN ASSESSMENT OF SEDIMENTARY ENVIRONMENT USING IRS-IA DATA: A CASE STUDY IN THE LOWER HOOGHLY ESTUARY, EAST COAST OF INDIA

SYRIAC SEBASTIAN AND AMITAVA GHOSAL

Society of Management Science and Applied Cybernetics
C/o International Management Institute
B10/30-31, Qutab Institutional Area
New Delhi - 110 016
INDIA.

ABSTRACT

The present study has been carried out to classify bottom sediment characteristics of Lower Hooghly estury using IRS-IA (LISS-II) digital data in combination with field measurements in concurrence with the IRS-IA overpass. The effect of water depth and bottom sediment on reflectance were also studied by analysis of variance. From the study, it is found that bottom sediment has got significant effect on reflectance. Sandy bottom had the highest mean radiometric reflectance than sandy silt and muddy sand. Mean reflectance for sandy silt and muddy sand did not differ significantly, although both of these bottom types were significantly lower in mean percent reflectance than sandy bottom. Hence, for the accurate estimation of suspended load in the water column, the effect of these factors should be considered.

INTRODUCTION

Knowledge of bathymetry and bottom sediment type in the coastal sedimentary environment is necessary, because different bottom types commonly exhibit great difference in reflectance. These differences can result incorrect determination of suspended load, and it is necessary to separate or stratify radiometric data into bottom type classes. The strength of the relation between reflectance and concentration of Suspended Sediment Concentration depend on sediment type (Novo Emon et al, 1989). Hence, an accurate estimation of suspended load in the coastal environment is possible by subtracting the effect of bottom sediment on reflectance. It is important for coastal planners and scientists to know the areal extent of various bottom sediment types for managing and assessing ecosystem that are changing due to human impacts. Lyzenga et al (1979) carried out mapping for the evaluation of bottom features under variable depth of water. Discrimination of bottom sediment types for coastal region of the northern Dominican Republic were conducted by Luczkovich et al (1993).

In an estuary, the nature and type of bottom sediment vary from place to place. So, an assessment of estuarine sedimentary environment using remote sensing will provide a better knowledge on the bathymetry and bottom features, which in turn expected to be helpful for an accurate estimation of suspended load in the coastal sedimentary environment. The objective of the present study is to understand the effect of bathymetry and bottom sediment type on the reflectance and to classify the bottom type in the Lower Hooghly estuary, east coast of India.

STUDY AREA

The Hooghly estuary located in the east coast of India, drains the major river complex Bhagirathy-Hooghly. Geographically, the estuary is confined by latitude 21° 50′ and 22°15′ and longitude 87°45′ and 88°15′, derives most of its upland supply of sediments from the Ganga during the south-west monsoon season. As far as the Hooghly estuary is concerned, the sediment distribution pattern is a typical one, as it is located at the mouth of the major river systems of the world, the Ganges. The sediment discharge along with the river run off into the head of the bay of Bengal follows a seasonal pattern under the tropical climate. The region also experiences high tidal range and strong waves and alongshore flow under the influence of monsoon wind. The offshore region of the estuary extends to a distance of 50 miles south of Sagar. The Calcutta Port is situated 230 Km inland from the open sea of Bay of Bengal, on the Hooghly river. The Hooghly estuary is highly dynamic in terms of suspended load, erosion and deposition resulting problems of safe and assured navigation throughout the year.

METHODOLOGY

The sea truth collection was taken in accordance with the IRS-IA overpass in the zones corresponds to 138/45 path and row and 18/53 path and row respectively. The sampling stations are indicated in the figure-1. Total 15 stations extending over an area around Nayachara Island were selected for Sea Truth collection. The Syledis System (SR-3) is used for fixing the sampling stations in the present study.

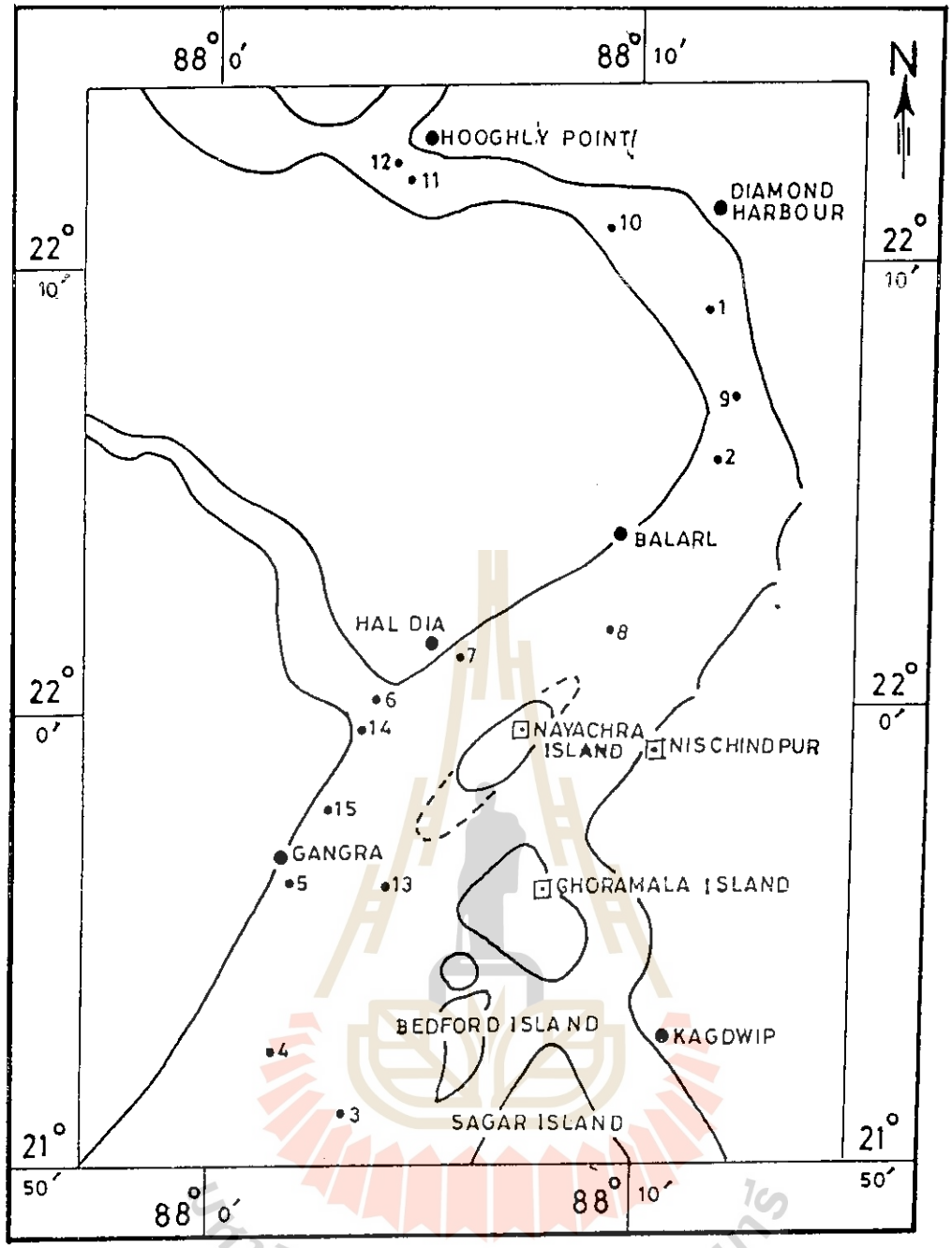

SCALE = 1 : 30,000

Fig. 1 STUDY AREA & SAMPLE LOCATION

Radiometric measurements were made using Exotech Radiometer (041-Optomech Engineers). Reference readings for radiometer were taken with reference to barium Sulphate plate. The radiometer readings were corrected by plotting time versus radiance graph.

RESULTS AND DISCUSSION

The textural characteristics of the sediments are given in the table-1. The prodominant type of sediment in the estuary is sand followed by sandy silt and muddy sand. It is seen that river inflow and tidal transport mechanism are effective in carrying the coarse grained sediments to the estuarine area (George et al, 1993). The abundance of sand near river inlet and towards north may be due to the input of river distributary, the main source of Hooghly.

The radiometric reflectance and digital numbers (IRS-LISS-II) for different bottom types under variable depth is given in the table-2.

BOTTOM TYPE CLASSIFICATION

Sediments were collected from different parts of the estuary in order to know the bottom sediment type and its effects on reflectance with respect to water depth. Fifteen sediment samples were collected from different depth level varying from 0 to 11.2 meters. From the sediment texture analysis, the samples fall under the category sand, sandy silt and muddy sand. In order to study the effect of water depth and bottom type on reflectance, radiances were measured for certain exposed portion of the land (islands) which are exposed at low tide and submerged in high tide condition. Readings were taken for different bottom types under variable depth. From the study it is found that as the depth increases, the reflectance decreases. For the sandy bottom sediment, Bank-4, Band-3 and Band-1 shows an inverse relation with depth ($r = -0.50, -0.50$ and -0.59 respectively). For the sandy silt bottom sediment, Band-4 and Band-1 various inversly with water depth. For muddy sand the Band-1,2 and 3 varies inversly with water depth. However, for precise quantitative assessment of the percentage cover, sufficient number of sediment samples from the study area is essential over varying tidal situations.

TABLE - 1 : TEXTURE OF THE SEDIMENTS

S.N.	STATION	SAND (%)	SILT (%)	CLAY (%)	NOMENCLATURE
1.	S1	95.00	5.00	0.00	Sand
2.	S2	97.00	2.80	0.00	Sand
3.	S3	95.20	1.40	3.40	Sand
4.	S4	94.00	5.40	0.60	Sand
5.	S5	96.00	4.00	0.00	Sand
6.	S6	48.00	42.00	10.00	Sandy Silt
7.	S7	45.20	47.40	7.40	Sandy Silt
8.	S8	46.00	47.00	7.00	Sandy Silt
9.	S9	86.00	14.00	0.00	Sandy Silt
10.	S10	36.00	47.00	17.00	Sandy Silt
11.	S11	72.00	14.00	14.00	Muddy Sand
12.	S12	36.00	27.00	37.00	Muddy Sand
13.	S13	6.00	77.00	17.00	Muddy Sand
14.	S14	38.00	29.00	37.00	Muddy Sand
15.	S15	42.00	32.00	24.00	Muddy Sand

EFFECT OF DEPTH

The sample site occured in water depth ranging from 0 to 11.2 meters. The difference among the mean depth of the bottom types is given in table-2. Although less than 22% of the total radiation was explained by water depth (Luczkovich et al, 1993), radiance was declined with increasing depth in all bands, except Band-1,2 and 3 for muddy sand bottom type. Linear regression analysis carried out for each band with radiometric reflectance. Variation in radiance seemed to decline with increasing depth for all bands, which may reflect turbulent nature of shallow water, where wave action could influence radiance value greatly (Luczkovich et al, 1993).

EFFECT OF BOTTOM TYPE

Sand bottom had the highest mean radiometric reflectance than sandy silt and muddy sand (table-3). However, bottom type explained less than 30% of total variance in the reflectance for all bands (Luczkovich et al, 1993). Mean reflectance for sandy silt and muddy sand did not differ significantly, although both of these bottom types were significantly lower in mean percent reflectance than sandy bottom type. Analysis of variance is carried out for three bottom type and reflectance for the Band-1,2,3 and 4. Significant differance is noticed among bottom type and mean percent reflectance (F_{36}= 12.12, F_{26}= 10.66). From the study it is found that bottom sediment type have the influance on reflectance.

TABLE-2 : DATA SET USED FOR THE ANALYSIS OF VARIANCE, BOTTOM TYPE, DEPTH IN METERS AND IRS-DIGITAL NUMBER FOR BAND-1,2,3 & 4.

STA. NO.	BOTTOM TYPE	DEPTH	RADIOMETRIC REFLECTANCE				: DN VALUES (IRS-LISS-II)			
			BAND-1	BAND-2	BAND-3	BAND-4	: BAND-1	BAND-2	BAND-3	BAND-4
S1	Sand	0.00	26.90	30.23	31.03	39.23	42	28	29	18
S2	Sand	0.14	13.51	15.78	16.12	9.90	39	25	26	21
S3	Sand	1.15	13.19	14.30	14.03	10.00	38	24	25	30
S4	Sand	2.40	12.60	13.22	18.00	9.92	36	24	25	29
S5	Sand	6.60	10.35	14.38	12.42	7.48	41	27	30	23
S6	Sandy Silt	0.00	13.78	18.19	19.70	24.91	37	24	25	23
S7	Sandy Silt	1.00	11.84	15.24	13.88	8.64	39	27	28	19
S8	Sandy Silt	6.00	11.56	15.40	15.73	12.12	38	27	29	22
S9	Sandy Silt	7.60	11.86	16.87	16.43	7.42	39	26	27	24
S10	Sandy Silt	8.60	11.40	15.99	15.47	9.48	40	25	27	25
S11	Muddy Sand	0.00	10.35	13.67	13.68	10.00	37	24	24	32
S12	Muddy Sand	1.80	9.18	12.05	11.86	15.88	37	28	29	19
S13	Muddy Sand	8.60	10.04	14.17	15.47	9.58	37	24	23	32
S14	Muddy Sand	8.90	10.65	15.69	14.75	10.85	38	23	24	26
S15	Muddy Sand	9.90	9.94	13.83	14.42	7.69	40	27	29	18

TABLE - 3 : MEAN DEPTHS, MEAN REFLECTANCE AND MEAN DN VALUES FOR IRS BY BOTTOM TYPE GROUP

BOTTOM TYPE	DEPTH	RADIOMETRIC REFLECTANCE				: DN VALUES (IRS-LISS-II)			
		BAND-1	BAND-2	BAND-3	BAND-4	: BAND-1	BAND-2	BAND-3	BAND-4
Sand	1.93	15.31	17.58	16.92	15.21	39	26	27	26
Sandy Silt	4.83	12.08	16.33	16.24	12.51	39	26	27	23
Muddy Sand	5.84	10.09	13.88	14.03	10.80	38	25	26	29

CONCLUSION

It is found that bottom sediment type and water depth has a significant role on reflectance. From the present study, it is concluded that satellite remote sensing can be used for bottom sediment discrimination, by considering the effect of bottom type and water depth on reflectance.

ACKNOWLEDGEMENT

This study forms the part of the training programme in the CPMR Division of the Indian Institute of Remote Sensing. The auther is thankful to Head, IIRS for the facilities provided.

REFERENCES

George Roy, Syriac Sebastian and Damodaran K.T. (1993). Granulometric Studies on the modern sediments of Ettikulam Lagoon, West Coast of India. Ind. J. Marine Science. Vol.22, pp. 28-32.

Luczkovich J. J, Thomas W.W, Jeffrey L.M and Richard W S (1993). Discrimination of Coral Reefs, Seagrass Meadows and Sand Bottom types from Space: A Dominican Republic case study. Photogrametric Engineering and Remote Sensing, Vol.59, No.3, pp. 2151-2159.

Lyzenga D.R, Shuchman R.A and Aruone R.A (1979). Evaluation of an algorithm for mapping bottom features under variable depth of water. Proceedings of the Thirteenth International Syposium on Remote Sensing of Environment. Ann Arbor, Michigan, 23-27 April, 1979, pp. 1767-1780.

Novo E.M.M, Hanson J.D and Curran P.J (1989). The effect of sediment type on the relationship between reflectance and suspended sediment concentration. Int. J. Remote Sensing, Vol. 10, pp. 1283-1289.

THE EFFECTIVE USE OF THERMAL IMAGES FOR THE PRESERVATION OF WEATHERED RELICS

Y. Yamano and K. Saito
Asia Air Survey, Co., Ltd.
13-16, Tamura-cho, Atsugi-shi,
Kanagawa-ken, 243, Japan

Tel : +081-462-22-1002
Fax : +081-462-22-1281
E-mail : KFH02140@niftyserve.or.jp

ABSTRACT

As a new method for the preservation technique of weathered stone relics, the effectiveness of thermal infrared images have been confirmed.

Because the weathering area is distinguished from the other normal area by the difference of the surface temperature change pattern, it is possible to extract the parts deteriorated due to weathering by using thermal images. This method also have characteristics that are indirect, non-destructive and two-dimensional measurements, which are very important for valuable cultural assets.

In this paper, authors introduce two examples which was carried out under the different observation condition. One is the observation for stone relics carved in a cliff. This thermal environment is directly affected by sunbeams. The other is the case of the indoor observation. The target stone exists in the house where the range of the temperature change is smaller than outside.

The subtraction operation between two images that were acquired at different time in a day has been examined in the both case. It has been shown that thermo-anomalous parts were emphasized by these subtracted images and the distribution of weathered parts were consequently enabled to map.

1. INTRODUCTION

A new technique using thermal infrared video images has been examined for the test of soil mechanics of weathered stone relics. Characteristics of this technique are to measure by non-touch and non-destructively for the target. Many stone relics are generally made of tuff in Japan. They have been weathered for a long time. For the preservation of weathered relics, the measurement using thermal images has been adopted as a satisfactory technique.

The estimation of weathering condition by the direct looking to the object and by the hitting test of the schmidt hammer has been done until now. These means need to approach and to touch the target. It is a very clear that they are not available to apply to the very high and unclimbable place. As the direct looking depends on personal technique, it includes much subjectivity. Although the hitting test brings the information of the stone strength to us, this method is not able to display the two-dimensional distribution of the weathering area.

On the other hand, the thermal video camera can take the far and dangerous place, because it is able to zoom in. Moreover, thermal images are able to map the two-dimensional distribution for weathering phenomena.

2. METHODS

2-1 The surface temperature change in a weathering area

The surface temperature change is affected by the surface or inner condition of the object. The area that is covered by splittings show larger thermal change than the normal area. The surface temperature rises with the

atmospheric temperature increasing. In the normal area, the heat can be transmitted efficiently into the object. The flaking area makes difficult to transmit the heat toward inside. On the other hand, the area including the standing water in cracks shows usually lower temperature than the normal area in the daytime. The water temperature is not easy to be influenced by the atmospheric temperature due to its heat capacity, therefore the standing water interrupts the heat conduction into the object. These concepts are shown in Figure.1.

2-2 Thermal infrared video

Thermal infrared video used in this study has the wave length range from 8,000 nm to 13,000 nm. This range decrease the influence of the reflection from the object and it is most efficient among the thermal range (Figure.2).

Performance of the thermal video is indicated in Table.1. It has three thermal range modes. The L-range that is able to measure from -40 °C to 160 °C was employed in this study. Also it has five scanning time modes. In this study, the 9.6 seconds scanning time mode was used. After the measurement, thermal data were saved into the SCSI hard disk or 3.5 inch floppy disks. One image size is 512 columns by 240 lines and one pixel has 12 bits.

2-3 Content of the method

The flow of this method is indicated in Figure.3. The content of each flow elements is described as follows.

(1) Acquisition of thermal image data

Thermal images were taken two or four times in a day. In the case of two times, thermal images were taken on the early morning and the afternoon. The early morning temperature is the lowest in a day, and it becomes higher in the just before noon or afternoon. If thermo-anomalous areas are included in the target, the characteristic change of the surface temperature will appear between two images.

Four images were taken in the early morning, the before noon, the afternoon and the night. The surface temperature rises from the early morning to the noon and falls from the noon to the night. The difference of two morning thermal images taken in the early morning and in the before noon indicates the thermal condition of the target at the time of temperature rising. The thermal condition at the time of temperature falling are shown by the difference of evening images that are acquired in the afternoon and night.

(2) Geometric correction

The geometric correction was carried out to correct each image.

(3) Subtractive operation of thermal images

In order to get the difference of the surface temperature, one thermal image is subtracted from the image taken at another time. In the case of using two images, the image of higher surface temperature (just before noon or afternoon image) is subtracted by lower (early morning image). The case of using four images get two subtractive images. One is the morning image that the before noon data is subtracted by the early morning data. The other is the evening image that the afternoon data is subtracted by the night data.

(4) Level slice of thermal images

Subtracted images are sliced by the degree of the temperature change and they are classified. In this study, the interval of temperature slice is about 0.25 °C at the time of temperature rising and about 0.10 °C at the time of temperature falling.

(5) Addition of thermal images

When four images are used, two images operated the level slice, that is, the morning and evening image are added to emphasize the surface temperature change.

(6) Estimation of the weathering area

The thermal condition of the anomalous area is different from the normal area. The reason is shown as follows.

The case of larger temperature change :

(a) The surface of the target is covered by different materials like splittings.

(b) There are cavities in the target.

The case of smaller temperature change :

(a) The cavity of the target includes the standing water.

(b) The water is welling up from cracks.

(7) Mapping

Thermo-anomalous parts are extracted and the weathering distribution are mapped.

3. ANALYSIS AND RESULTS

3-1 Relieves of Kiyomizu cliff-surface stone Buddha in Kagoshima-ken

The target cliff area extends for 20 meters high and 400 meters long. About two hundreds of relieves were carved on the cliff surface from the thirteen to the nineteen century. Relieves that are called "three Sanskrit words" and "the five-storied pagoda" are selected in this study. They are carved outdoors and directly affected by sunbeams. The surface temperature change gives the difference of about twenty degrees centigrade in winter. Table.2 shows environmental parameters at the time of data acquisition.

(1) The case of "three Sanskrit words"

Thermal images of "three Sanskrit words" were taken from the opposite side of the river far from about 80 meters. This cliff has an irregular surface. The relief was carved at about 13 meters high.

The subtracted thermal image is shown in Photo.1 and the weathering distribution map is shown in Figure.4 as the reference. This map was made by the photo interpretation and the site survey. Large temperature change areas on the upper cliff face to the southwest, because the surface that faces to the south or the west rises the temperature in the afternoon. Photo.1 and Figure.4 show that the flaking and covering splittings areas indicates larger change than another areas in the upper area of the cliff. The lower side of the cliff is hidden by trees except the center of the lower area. In this center area, the large change area is flaking and is covered by splittings.

(2) The case of "the five-storied pagoda"

"The five-storied pagoda" is carved on the stone of 10 meters high. This relief faces to the east. The surface of the relief makes the shade after the noon. The subtracted thermal image and the distribution map are shown in Photo.2 and Figure.5 each other. The surface temperature change was smaller than the case of "three Sanskrit words". As small river flows near the relief, the stone carved the relief is apt to be percolated by the ground water. However the lower area of the relief indicates large temperature change than the upper. This lower side corresponds to the area that is covered by splittings and flaking area.

3-2 The relief of "Moto-machi stone Buddha" in Oita-ken

The relief of "Moto-machi stone Buddha" was carved in the eleven century. The relief is inside of the shrine and is not affected by sunbeams. As the inner air temperature change are not large, the surface temperature change of relieves are smaller than the case of "three Sanskrit words" in Kiyomizu. Table.3 shows environmental parameters at the observation time.

The relief is weathered by the flaking and the deposition of the chloride. The water condition in the relief relates to the deposition. The chloride deposits with the evaporation activity from the surface of the relief.

As four images were used in this case, the method of the addition operation was carried out for the analysis of the relief. The added image and the distribution map of the weathering are shown in Photo.3 and Figure.6 each other. The left earlobe, the jaw and the right bosom show the large surface temperature change. There are the weathered or repaired area. The area from the jaw to the lower lip will be in danger of flaking off in the near future. The nose and the cuff of the right hand show the large difference of the temperature change, because projections and edges of the object rise the surface temperature in a daytime. Although these areas do not indicate the weathering, they may be weathered in future.

4. CONCLUSION

It was confirmed that the method by using thermal infrared video images was effective for the preservation of the weathered stone relics. Advantages of this method are as follows.

(a) The target is not destructed by this method.

(b) It can display an untouchable place like a high cliff.

(c) The weathering condition is able to be objectively estimated.

(d) It is possible to map the two-dimensional distribution of the weathering.

Notices of this method are indicated as follows.

(a) Thermal images are affected by meteorological environments.

(b) Edges or projections of the object tend to change the surface temperature largely.

To relax the effect of (a), it is necessary that images are taken in a same day as possible. On the case of (b), it is better that the surface form is checked when thermal images are taken, and the preliminaly study is done before the analysis.

ACKNOWLEDGMENTS

The authors are grateful to Prof. Nishida for the useful advice. Sigeyuki Tohyama and Ryuichiro Egawa always gave helpful comments during this analysis.

REFERENCES

1) Saito, K. and Y. Yamano(1995), The Use of Thermal Images for the Preservation of Relieves of Buddha on a cliff, Journal of the Japan Society of Photogrammetry and Remote Sensing, vol.34 no.1, pp.2-3.

2) Inoue, M. , J. Kanmura, K. Saito, Y. Yamano, S. Tohyama and K. Nishida(1995), An Examination on Weathering Condition Analysis of Cliff-surface Stone Buddha Images by Using Thermal Infrared Sensor, Reports of the Symposium of Preservation Techniques for Historic Sites, International Society for Soil Mechanics and Foundation Engineering, pp.47-52.

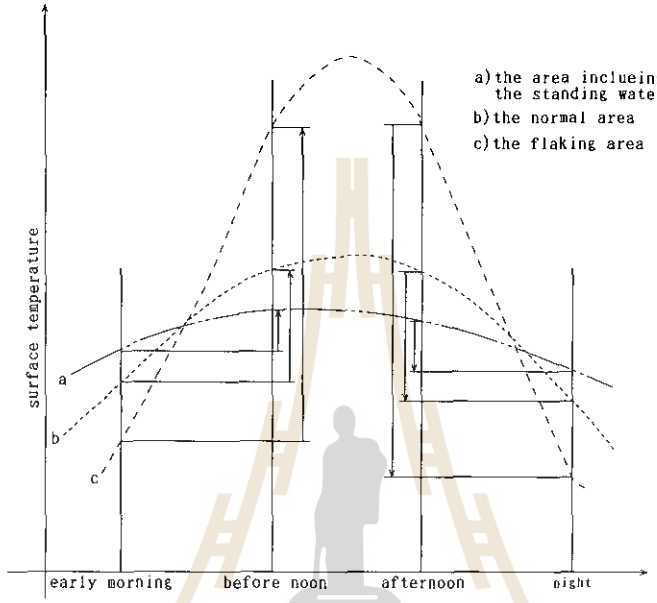

Figure.1 The surface temperature change in a day

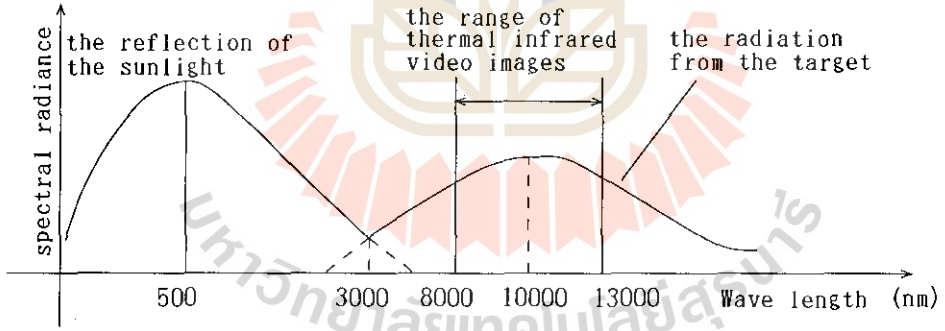

Figure.2 The wave length of the thermal video

Table.1 Performances of the thermal video

Items	Data	
Measurement range (℃)	L range	-40 - 160
	M range	100 - 500
	H range	400 - 2000
Resolving power (℃)	0.05 (at 30 ℃ of black body)	
Angle of visibility(°)	30(H) x 28(V)	
Wave length (nm)	L range	8000 - 13000
	M range	8000 - 13000
	H range	8000 - 13000
Sensor	HgCdTe Stirling Cooler Type	
Scanning time (s)	0.08, 0.15, 0.30, 0.60, 2.40, 9.60	
Display pixel numbers	512(H) x 480(V)	
Capacity of memory	512 x 480 x 16 bits x4 memory	
Data recording mode	MS-DOS	512 x 240 x 12 bits 5 images per a disk
	N88 basic	256 x 230 x 8 bits 15 images per a disk

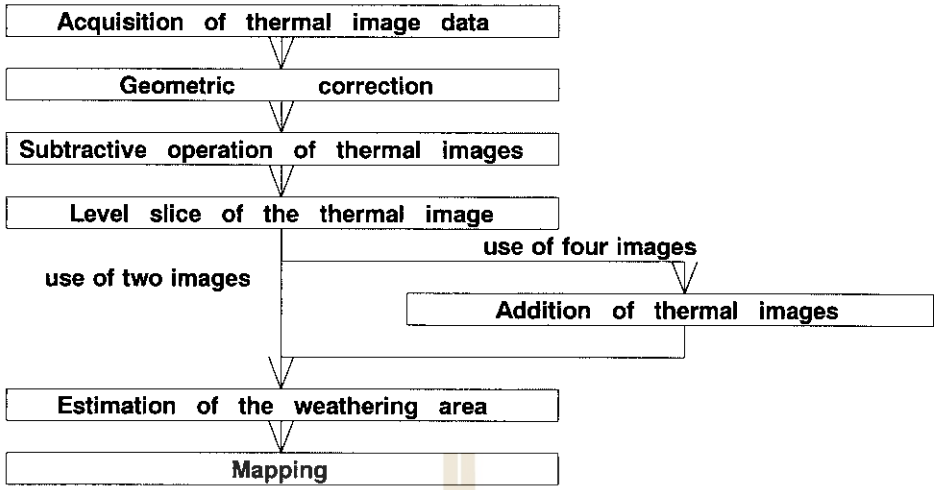

Figure.3 The flow chart of this method

Table.2 Environmental parameters at the time of data acquisition in Kiyomizu

	three Sanskrit words		the five-storied pagoda	
Date	1994.02.02			
Thermal video	JTG-4230			
Distance (m)	80		10	
Time	7:15	11:39	8:55	14:30
Air temperature (℃)	8.5	11.3	9.0	11.1
Humidity (%)	68	62	58	55

Photo.1 The subtracted image of "three Sanskrit words"

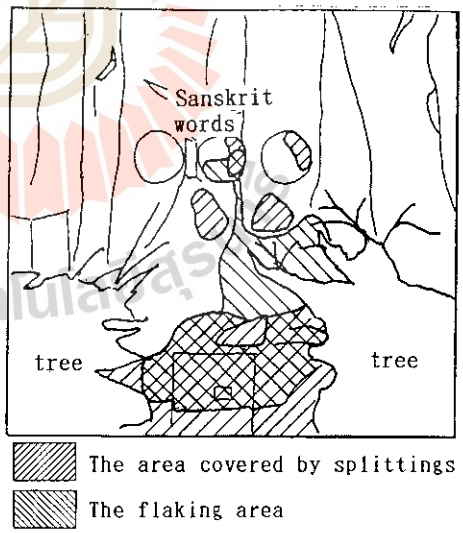

Figure.4 The weathering distribution map of "three Sanskrit words"

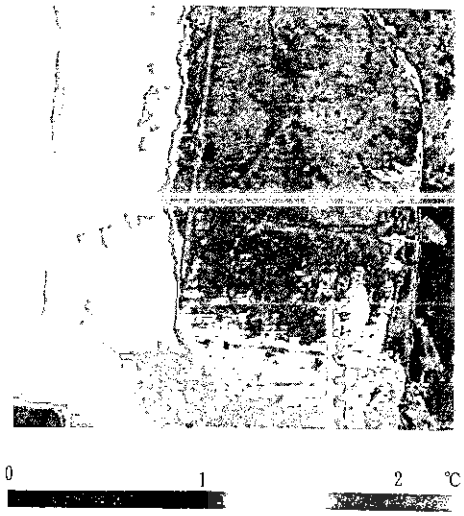

Photo.2 The subtracted image of "the five-storied pagoda"

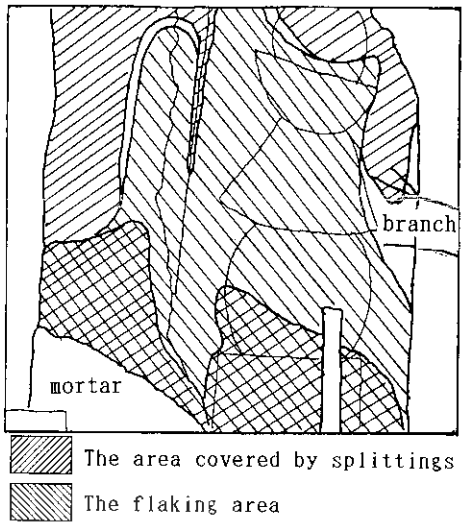

Figure.5 The weathering distribution map of "the five-storied pagoda"

Table.3 Environmental parameters at the observation time in Moto-machi

	the relief of Buddha			
Date	1995.02.16			
Thermal video	JTG-5700			
Distance (m)	3			
Time	6:24	10:13	14:37	19:20
Air temperature (℃)	2.1	9.5	10.7	8.1
Humidity (%)	73	50	45	60

Photo.3 The added image of "Moto-machi stone Buddha "

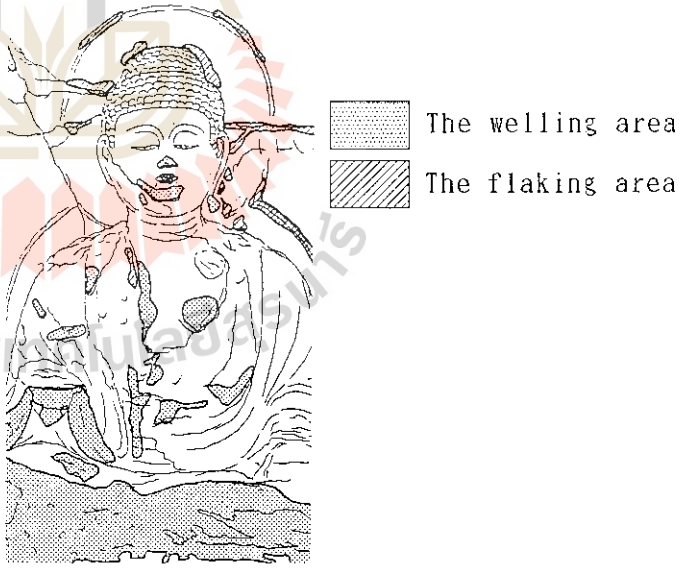

Figure.6 The weathering distribution map of "Moto-machi stone Buddha"

MODELING FOR GLOBAL LAND DEGRADATION USING REMOTE SENSING AND GIS

Krishna Pahari, Shunji Murai
Space Technology Applications and Research Program
School of Environment, Resources and Development,
Asian Institute of Technology, GPO Box 2754, Bangkok 10501, Thailand

ABSTRACT

Land degradation or desertification has become one of the most pressing environmental problems in the world today. This paper is an attempt to highlight the use of GIS and remote sensing for the assessment of global land degradation. The research is based on a combination of climatic modelling, mainly based on rainfall and temperature data, and the physical process modelling, based on the analysis of land degradation mechanics, for which land use is an important contributing factor. Some preliminary findings of the research are also presented.

1. General Background

Land degradation is the reduction of land resource potential which can be manifested in various forms such as soil degradation (waer erosion, wind erosion or chemical degradation), degradation of vegetation or degradation of rangeland. Desertification may be considered as the land degradation in the arid, semi-arid and dry subhumid areas due to natural or anthropogenic factors.

Although the land degradation is one of the most pressing environmental problems at the global level, the systematic study of global land degradation or desertification is emerging only recently. The technology of Remote Sensing together with global GIS is providing new possibility for a more scientific analysis of this problem.

2. The Research Methodology

In this research, the extent and nature of desertification is being studied by using two approaches, namely climatic modeling based mainly on rainfall and temperature data, and the physical or bio-process modeling in which remote sensing data play an important input.

2.1 Climatic model

This mainly consists of modeling for aridity and moisture indices calculated on the basis of temperature and rainfall data from many points around the globe and then interoplated to the areal data. The various indices considered are the following:

i. Moisture Index

This index is calculated by:

Moisture Index = Annual Rainfall/PET,

where, PET is the potential evapotranspiration, which can be estimated by using either Thornthwaite method, Holdridge method or others. So far, the PET data produced by Ahn and Tateishi has been used for calculating this index.

ii. Martonne's Aridity Index

This is given by:

$$AI = \frac{P}{T+10}$$

where, P = annual precipitation (mm),
T = sum of monthly mean temperature of those months with monthly mean temperature greater than 0, divided by 12.

On the basis of the values of this index, different areas can be classified into various zones.

iii. Aridity Index revised by Murai and Honda

The index used by Murai and Honda(1991) is slightly revised from the Martonne's index, with additional distinction between ordinary forest and tropical forest.

The range of values for different aridity classes in this method is given in Table 1. Figure 1 illustrates the steps involved in modeling aridity zones.

Table 1 Aridity indices for different classes

Class	Martonne AI	Revised AI(Murai and Honda)
Desert	<=5	<=5
Semi-desert	5-10	5-10
Grass land	10-30	10-20
Forest	>30	20-40
Tropical forest (annual ave temp>24° C)	---	>40

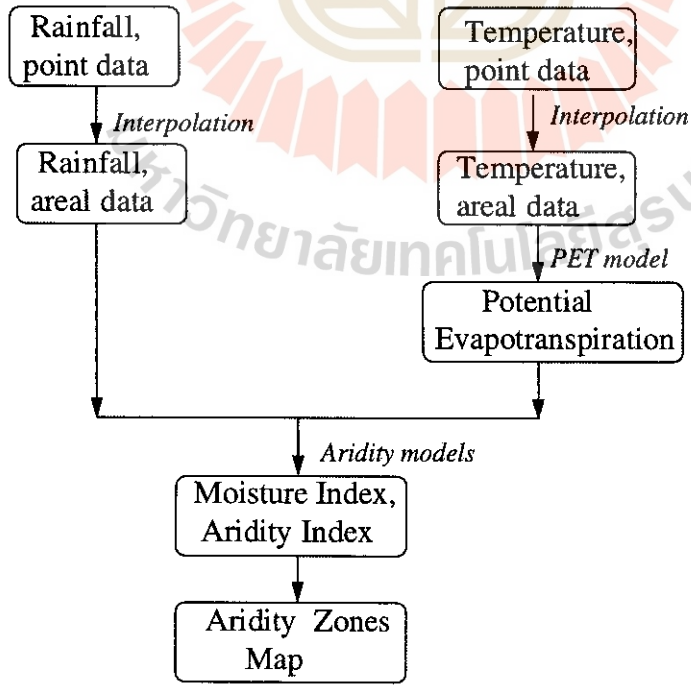

Fig 1. Flow chart of methodology for climatic modeling of aridity zones

2.2 Physical and bio process model

Besides the climatic model, the physical processes of land degradation such as water and wind erosion can also be modelled by using the remote sensing data in combination with other data such as rainfall, elevation, wind and soil types. Since land use/cover is a major factor contributing to such processes, the remotely sensed data, particularly, NOAA GVI data, can be specially useful for such studies.

i. Water erosion

Water erosion is a function of land use/cover, rainfall, topography and soil characteristics. However, due to the scale factor, it is necessary to make some generalizations in case of global study. For example, to relate the topography for land degradation, instead of calculating the slope in absolute values, some topographic roughness factor may be more appropriate. Fig 4.2 illustrates the procedure for analysis of water erosion.

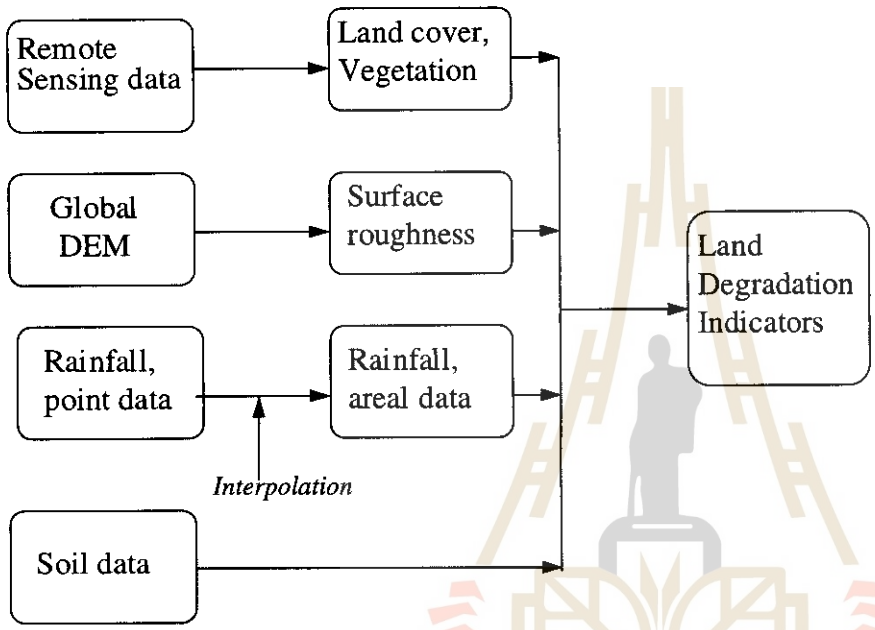

Fig 4.2 Flow chart of methodology for analysis of water erosion.

ii. Wind erosion

Wind erosion is a function of speed and direction of wind, land use/cover and the soil properties. Some inference about wind conditions can also be made from the duration of dry period based on the rainfall data.

iii. Net primary productivity

Since vegetation degradation is one form of desertification, the net primary productivity can also be taken as an indicator of the land degradation. It has been shown by various authors (such as Box and Bai 1993) that NOAA GVI data have good correlationship with the primary productivity.

3. Preliminary Results and Discussion

So far, preliminary results from the climatic modeling have been produced. The results of Aridity zoning and the moisture index have been represented in Tables 1 and 2 respectively.

The results of the aridity zoning indicate the forest area of about 42% based on the climatic data. But the actual amount of forest is less than this, approximately 33% of the total area, as found by some authors (Murai and Honda 1991) by using remote sensing for mapping actual vegetation. This can be considered as an indication of deforestation from the natural forest cover for the given climatic conditions to other land use type.

Table 1 Areas under different Aridity zones

Sr No	Aridity Zone	AI	Percent area
1	Desert	<= 5	7.34
2	Semi-desert	5 - 10	5.94
3	Grass land	10 - 30	31.47
4	Forest	> 30	41.96
5	Cold	-	13.29

Table 2 Areas under different zones based on Moisture Index

Sr No	Zone	MI	Percent area
1	Hyperarid	< 0.05	2.45
2	Arid	0.05 - 0.20	8.39
3	Semi-arid	0.20 - 0.50	14.69
4	Dry subhumid	0.50 - 0.65	6.99
5	Humid	> 0.65	54.90
6	Cold	-	12.59

The moisture index (Table 2) values show the smaller area of Hyperarid and arid zones and larger area of humid zones compared to the results of the desertification atlas (UNEP 1992). The reason may be related to the different method used for calculating the potential evapotranspiration. The PET used here is taken from the global PET dataset produced by Ahn and Tateishi at 0.5° resolution.

Figure 3: Aridity zoning based on Martonne's Aridty Index

4. Conclusions and Further Research

The research based on climatic model so far has demonstrated the usefulness of GIS for classifying the globe into different aridity and moisture index zones, which are important indicators of desertification. More work is underway to demonstrate the applicability of remote sensing and GIS for land degradation studies at the global level. Further research is being continued in the following way:

- Developing models for physical processes of land degradation such as water and wind erosion.
- Linking the climatic model with the physical process model.
- Linking local, regional and global level studies of land degradation

References

Box, E.O. and X. Bai (1993): "A Satellite Based World Map of Current Terrestrial Net Primary Productivity" in Seisan-Kenkyu (monthly journal of IIS, Univ. of Tokyo), Vol.45, No.9

Murai, S. and Y. Honda (1991): "World Vegetation Map from NOAA GVI Data" in S. Murai (ed), Applications of Remote Sensing in Asia and Oceania, AARS.

United Nations Environment Program(1992): World Atlas of Desertification

Variation of Surface Currents Offshore from Rayong Rivermouth from NRCT Buoy Data in 1994

Absornsuda Siripong, Supichai Tangjaitrong

Sirichai Dharmvanij,Chaiyong Yuangthong

and Pakorn Purimatikant

Marine Science Department, Faculty of Science

Chulalongkorn University, Bangkok 10330, Thailand.

Presented at **the 16th Asian Conference on Remote Sensing,**

20-24 Nov.1995, at Suranaree University of Technology,Nakhon Ratchasima,Thailand.

Abstract.

The monthly current rose data at 3 metre depth,Lat.12 ^{0}29'42"N,Long.101 ^{0}14'16"E. in 1994 from the TOBIS buoy, under the SEAWATCH program of the National Research Council of Thailand, at the offshore of the Rayong Rivermouth were analysed with the mean wind data to study the pattern of wind-driven currents. In North monsoon, from October to January,the sea currents mainly flow to 300 ^{0} from North with the mean speed of 10.65 cm/sec. In South monsoon season, from February to May, the currents principally flow to 120 ^{0} from North, with the mean speed of 11.775 cm/sec. During the Southwest monsoon season, from June to September, the principal currents flow to 90 ^{0} (to East), with the mean speed of 12.10 cm/sec.

Introduction The continuous current data in the sea are important especially for the study on transport of energy and matter, among others. The data from the ship are only discrete and not continuous for a long term study. The National Research Council of Thailand moored 7 buoys in the Gulf of Thailand under the SEAWATCH program.

Data and Method of Study. One of the TOBIS buoy of NRCT by the OCEANOR was moored offshore of the Rayong Rivermouth at the Lat.12 ^{0}29 '42"N,Long.101 ^{0}14'16"E. The current data at 3 metre depth under the sea surface in 1994 were plotted per month by the software ORKAN to show the current rose method.The data were missing in January, June, July and December 1994. From the climatological datafor 1981 to 1994 by the Meteorological Department, at Rayong, Lat.12 ^{0}38'N,Long.101 ^{0}21'E. were used to study the wind direction and velocity. The sea current data are related to the wind regime to study the variation of surface wind-driven currents here.

Results. Table 1 is the wind speed and direction at each month average from 1981 to 1994 at Rayong station. the Northerly winds blow during October to January, the Southerly winds blow during February to May, and the Southwesterly winds blow during June to September.

Table 1. Wind speed and direction to at Rayong from 1981 to 1994.

(Data from Meteorological Department).

Wind (Knots)	**Jan**	**Feb**	**Mar**	**Apr**	**May**	**Jun**	**Jul**	**Aug**	**Sep**	**Oct**	**Nov**	**Dec**
Mean speed	3.10	4.60	5.10	4.50	5.60	8.60	8.00	8.70	4.60	2.90	2.90	3.20
Prevailing	**N**	**S**	**S**	**S**	**S**	**SW**	**SW**	**SW**	**SW**	**N**	**N**	**N**
Max.speed	24	33	30	35	40	45	50	40	35	35	24	24

February 1994 (Southerly wind),Fig.1, the principal surface currents flow to 300^{0} from North, and second maxima to 120^{0} with the mean speed of 12.5 cm/s.This month is the transition period from Northerly wind to Southerly wind.

March 1994(Southerly wind),Fig.2, the principal surface currents flow to 300^{0} and the second maxima to 120^{0}, with the mean speed of 12.0 cm/s.

April 1994 (Southerly wind),Fig.3, the surface sea currents mainly flow to 300^{0} and the second maxima to 120^{0}, with the mean speed of 11.5 cm/s.

May 1994(Southerly wind),Fig.4, the principal surface currents flow to 300 ^{0} and the second maxima to 120 ^{0}, with the mean speed of 11.1 cm/s

August 1994(Southwesterly wind),Fig.5, the principal surface currents flow to 90 ^{0}(to North), and the slower currents flow to 330 ^{0}, with the mean speed of 12.3 cm/s.

September 1994(Southwesterly winds),Fig.6, the principal surface currents flow to 90^{0} and the second maxima to 300 ^{0}, with the mean speed of 11.9 cm/s.

October 1994(Northerly wind),Fig.7, the principal surface currents flow to 300^{0}, and the smaller maxima to 90 ^{0}, with the mean speed of 12.9 cm/s. This month is the transition period from Southwest monsoon to North monsoon season.

November 1994 (Northerly wind),Fig.8, the principal surface currents flow to 300 ^{0} and second maxima to 120 ^{0}, with the mean speed of 8.4 cm/s.

Summary. From the mean wind data(1981-1994) at Rayong,Lat.12 ^{0}38 'N,Long.101 ^{0}21'E, the Northerly winds blow from October to January, the Southerly winds blow from February to May, and the southwesterly winds blow from June to September. During North monsoon season (Nov.1994), the principal sea surface currents flow to 300 ^{0}(from N) and second maxima to 120 ^{0} with the mean speed of 8.4 cm/s. During the South monsoon season (March to May), the principal sea surface currents flow to 300 ^{0} and second maxima to 120 ^{0}, with the mean speed of 11.53 cm/s. During the Southwest monsoon season (August to September), the principal sea surface currents flow to 90 ^{0}(to N), and the second maxima to 330 ^{0}(August) and 300 ^{0}(September), with the mean speed of 12.10 cm/s. In the transition period from N to S monsoon(February), the principal currents flow to 300 ^{0}, and the second maxima to 120 ^{0}, with the mean speed of 12.5 cm/s. In the transition period from S to SW monsoon, actually in June, but there is no data in June and July. In the transition period from SW to N monsoon (October),

the principal currents flow to 300 ^{0} and smaller second maxima to 90 ^{0}(N), with the mean speed of 12.9 cm/s.

Acknowledgements

The authors would like to appreciate the kind assistance of Dr.Darasri Daorueng,Dr.Pithan Singsanae and Ms.Chinoros Booncherm(SEAWATCH THAILAND,NRCT) for sending the current data from the buoys and Mr.Wattana Kanbua(Meteorological Department) for sending the meteorological data at Rayong.

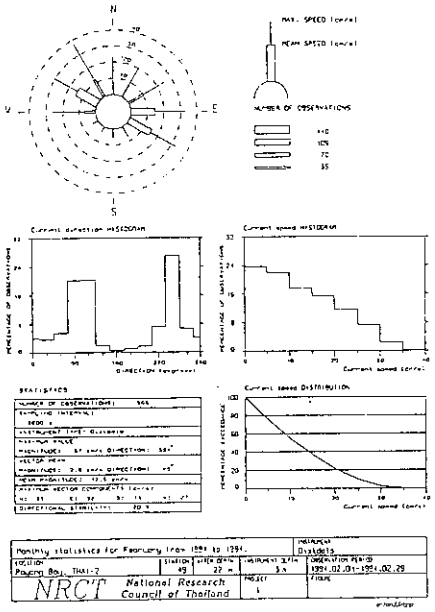

Fig.1.

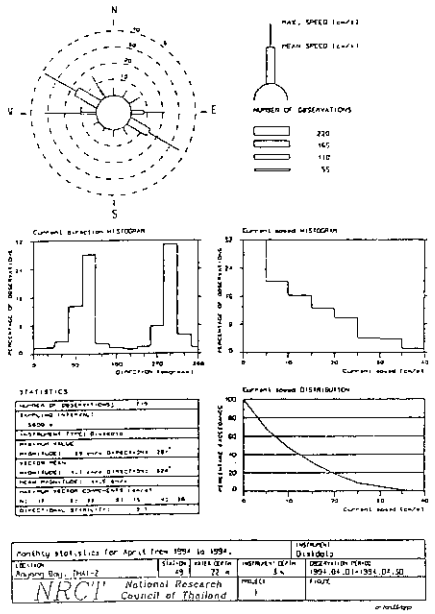

Fig.3.

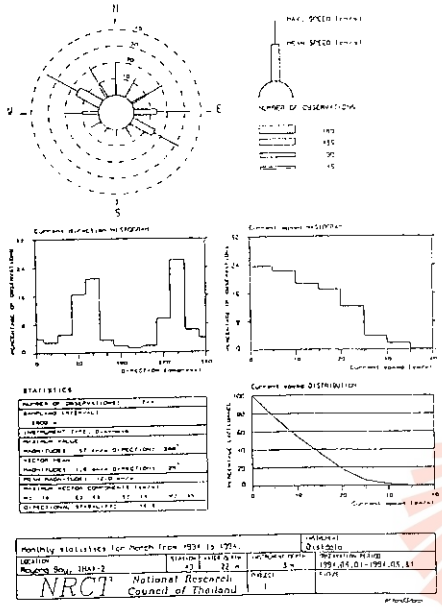

Fig.2.

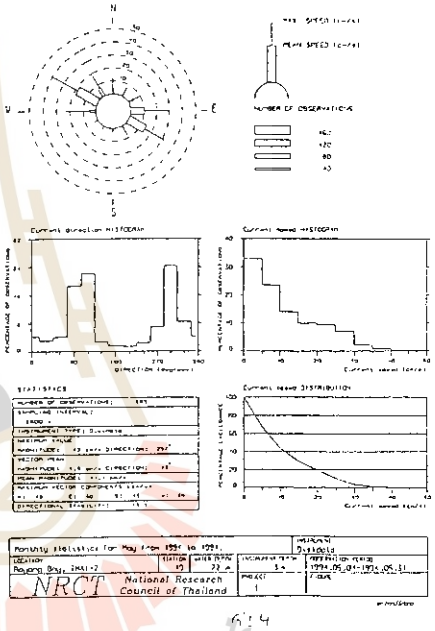

Fig.4.

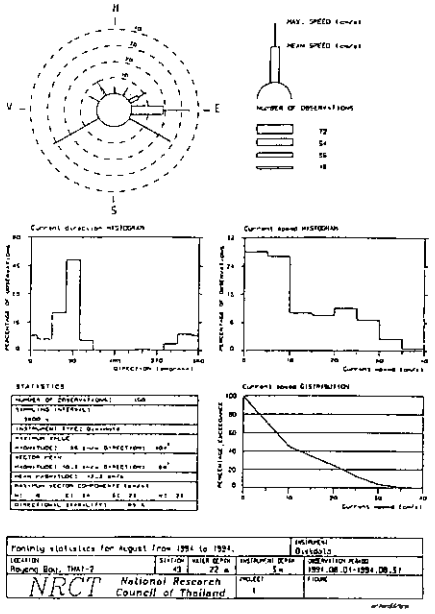

Fig.5.

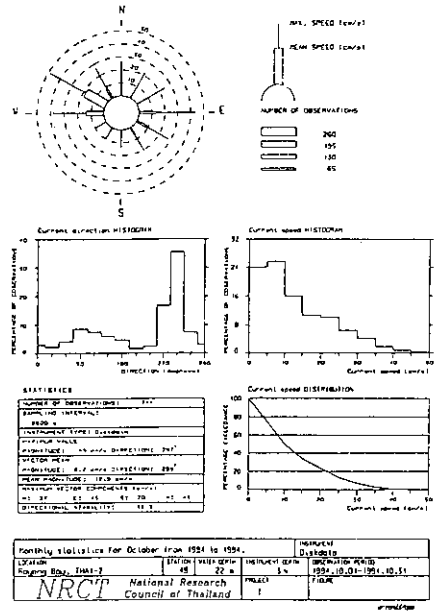

Fig.7.

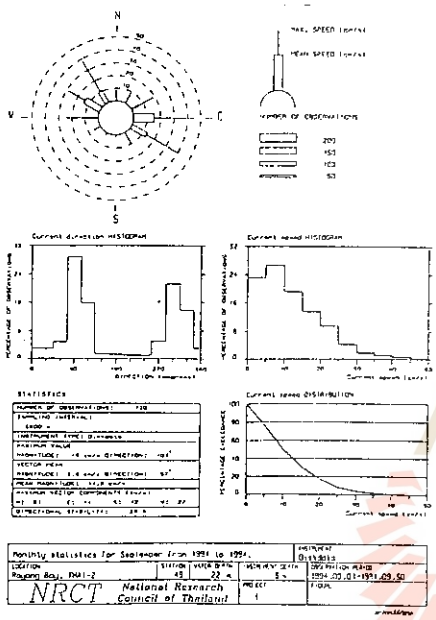

Fig.6.

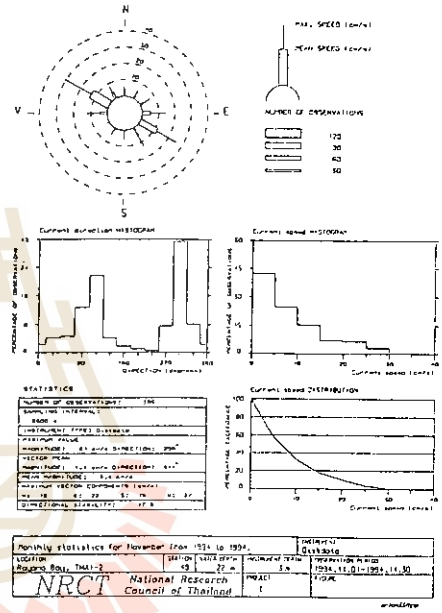

Fig.8.

Digital Classification of LANDSAT TM for Land Cover Mapping of the Pa Wang Phloeng-Muang Khom-Lam Narai National Forest Reserve, Lop Buri Province, Thailand

Kaew Nualchawee and Lilita Bacareza

Asian Institute of Technology (AIT), Bangkok, Thailand

INTRODUCTION

The objective of the study was to come up with a land cover map of the Pa Wang Phloeng-Muang Khom-Lam Narai National Forest Reserve using various computer-assisted classification of Landsat digital data taken on 18 July 1993 with reference data from 26 January 1994, and to determine practical remote sensing approaches for high classification accuracy results. The demonstration of the stages and final results of the study are presented with focus on the major steps that were employed:

1. Geometric correction of the image
2. Pre-classification processing
   a. Enhancement for reference purpose
   b. Training sample selection and evaluation
3. Digital classification proper
   a Supervised approach
   b. Unsupervised approach
   c. Modified clustering approach

BACKGROUND

Related Past Studies

In a related study of the area done by Kasetsart University in 1984, manual analysis of aerial photographs of scale of 1:15,000 (date 18 November 1983) was performed to identify extent of land cover and land use within the forest reserve. Recently, the Prcticum research Team of the Natural resources Program of AIT conducted another study using Landsat Thematic Mapper (TM) digital data to demonstrate the usefulness of satellite remote sensing in yielding information for land cover changes from 1983 to 1994 in the absence of aerial photographs (Practicum Research Study, 1994). Information derived from the two studies served as input to the present study.

The Study Area

The study area is a part of Khok Charoen District, Lop Buri Province in the upper Central region of Thailand, specifically located in the Yang rak Subdistrict at latitude 15 degree 15 minutes to 15 degrees 27 minutes North and longituds 100 degrees 52 minutes to 101 degrees East.

The average annual rainfall from 1983 to 1994 was 1,054 mm to 1,324 mm, with the rainy season lasting from May to October leaving November to April a distinctly dry season. Average temperature over the past eleven years was 27.8 degrees Celcius.

The elevation level in the area varies from 80 m to 560 m above mean sea level, with more than 40% of the land area having a slope gradient of 0-2%, while 4.7% has slope gradient of 40%

Vegetation is a mixture of fruit and forest trees, such as Swietenia spp., Bauhinia spp., Terminalia spp., and other leguminous trees. Eucalyptus and Casuarina plantations abound, while the mountains and hills or upland vegetation are dominated by reproduction of salings of Dipterocarpacaea, Myrtaceae and Leguminosae (Practicum research Study, 1994).

METHODOLOGY

Selection of the remotely-sensed Data

There was no past experience over the study area as to what season would be best for discrimination of major vegetation cover, etc. The selection of the remotely-sensed data was mainly depended on the availability of the most recent high quality and cloud-free satellite image. In summary, the following images were selected and used for the study:

Type of image	Date of acquisition	Some characteristics
Landsat TM	18 July 1993	* 30x30m spatial resolution
		* .45-12.5 micron wavelength
Landsat TM	26 January 1993	* used only as reference data

The Image Analysis System Used

The digital analysis was performed at the Remote sensing Laboratory (RSL) at AIT, using the ERDAS Image Processing, PC-based System, and CCT was used for data input. The following steps were taken during this study:

Geometric Correction of the Image

A first order polynomial transformation and resampling with nearest neighbor algorithm was used to spatially geo-reference the Landsat image to UTM map projection system. Ground control points identifiable at road intersections in reference to topographic maps (1:50,000) and those obtained from field visits through the Global Positioning System (GPS) were used. A root mean square error of 1 pixel (30m) was accepted for the correction process using a total of 8 Ground Control Points (GCPs).

Image Enhancement

The contrast stretch image enhancement was applied to the original image to be used as reference for the interpretation of the raw data. For the study, however, the histogram-equalized stretch was used.

Identification of the different Resource Classes

Based on the field visits to the study area conducted from February to May 1994 and adopting the US Geological Survey classification (Anderson, 1976), land cover classes to be mapped were defined, and a classification scheme for the digital analysis was determined. Brief descriptions of the categories are presented as follows.

Table 1. Resource classes used for digital analysis of the study area.

	Level I	Level II
1.	Agricultural Land	Newly planted cropland
		Older cropland
		Paddy fields
		Tree plantations (orchards)
2.	Rangeland	Bushes
		Shrubs
		Bareland
		Grass land/Pasture land
3.	Forest land	Forest
		Mixed vegetation
4.	Water	Water bodies

In this study, the two basic approaches to training set selection were used, namely, supervised and unsupervised approaches. These two approaches, however, are not always satisfactory for various conditions of environment and variations in cover types, etc. Therefore, additional to the two approaches mentioned, the third approach was also considered, wherein both supervised and unsupervised methods were taken into consideration. It involves applying first, a clustering algorithm to the data (the unsupervised way) to define spectral clusters, the results of which can then be manipulated by the analyst for further analysis and training-set determination (the supervised way). Past tests have shown that this "modified (controlled) clustering approach" was judged best because it resulted in savings of man-hours and computer time, as well as having the highest classification accuracy (Fleming, et al., 1975; Rohde, et al., 1977, 1978; Pettinger, 1982). These studies have concluded that the modified clustering approach was best suited when the area are spectrally complex due to variation in vegetation cover and terrain.

RESULTS AND DISCUSSIONS

The Supervised Classification Approach

A total of 10 resource classes were identified based on the supervised classification scheme. Table 2 below show the area and percentage distribution of each resource class.

Table2. Resource Classes from Supervised Classification.

	Resource Class	Area (in hectares)	%
1.	Paddy fields	1,447.38	18.83
2.	Cropland	893.94	11.62
3.	Tree plantations	514.50	7.09
4.	Bareland	235.26	3.06
5.	Grassland	915.12	11.91
6.	Shrubs	259.83	3.38
7.	Bushland	989.28	12.87
8.	Forest	1,449.54	18.86
9.	Mixed vegetation	936.00	12.18
10.	Water bodies	14.49	0.19

	Total	7,684.74	

The Unsupervised Classification Approach

In the unsupervised classification approach, spectrally separable classes are first determined and

their informational utility is then defined. Clustering algorithms are used to determine the natural spectral groupings present in a data set. The basic premise is that values within a given cover type should come close together in measurement of space, whereas data in different classes should also be well separated (lillesand and Kiefer, 1987).

For this study, the sequential method for clustering was employed, and the classification results, based on the final 12 resource classes are shown in Table 3 below. The Table shows the spectral classes represented from the clustering method for unsupevised classification and its corresponding area-wise distribution.

Table 3. Representations of the Spectral Classes from Unsupervised Clustering.

	Resource Class	Area (in hectares)	%
1.	Paddy fields	1,171.53	15.24
2.	Newly-planted cropland	504.18	5.56
3.	Older cropland	239.22	3.11
4.	Tree plantations	542.52	7.06
5.	Bareland (upland)	301.23	3.92
6.	Bareland (lowland)	347.85	4.53
7.	Grassland	654.93	8.52
8.	Shrubs	382.41	4.98
9.	Bushland	993.87	12.93
10.	Forest	1,363.23	17.74
11.	Water bodies	20.16	0.26
12.	Mixed vegetation	1,163.61	15.14

	Total	7,681.74	

The Modified Clustering Classification Approach

This approach, commonly termed *hybrid* classification, involves elements of both unsupervised and supervised analysis. A hybrid classifier is one which incorporates two or more decision rules (Mather, 1987) such as the independent clustering of the pixels (unsupervised method) which are then subject to analysis for spectral separability and normality (supervised method). Five training areas were statistically clustered into 100 spectrally separate clusters and an evaluation of the statistics of the signatures derived from each cluster was performed. The final classification using Maximum likelihood classifier shows the results in the Table 4 which presents the area distribution and percentage of various resource classes that have been identified.

Table 4. Area Distribution Derived from the Modified Clustering Approach.

	Resource class	Area (in hectares)	%
1.	Paddy fields	1,538.82	20.02
2.	Newly-planted cropland	675.99	8.80
3.	Older cropland	228.15	2.97
4.	Tree plantations	533.16	6.94
5.	Bareland	651.78	8.48
6.	Grassland	602.64	7.84
7.	Shrubs	410.31	5.34
8.	Bushland	871.56	11.34
9.	Forest	1,069.20	13.91
10.	Water bodies	15.48	0.20
11.	Mixed vegetation	1,087.65	11.15

	Total	7,684.74	

Classification Performance for the Three Classification Approaches

To evaluate the results of the classifications and to verify the degree to which the land cover maps derived would meet users' needs, classification accuracy assessment was done through machine-assisted procedure. One basic constraint in the study is the lack of in-depth ground truth data for the study area and thus accuracy assessment is based mainly on spectral analysis of the digital data. The derivation of accuracy figures are based on the following definitions:

Overall accuracy = # of correctly classified areas/total # of areas

Procedure accuracy = Total # of correct areas in each resource class

---

Total # of reference areas in each resource class

User accuracy = Total # of correct areas in each resource class

---

Total # of classified areas in each resource class

Using the above reasoning, the following figures compare the performance of the three approaches:

	Supervised approach	Unsupervised	Modified Clustering
Overall Classification Accuracy	80%	85.7%	90.9%

CONCLUSIONS

Where areas are characterized by topographic and vegetation complexity as in the case of the Pa wang Phloeng-Muang Khom-Lam Narai National Forest Reserve, an effective method for the classification process suited for the environment results in a significant improvement in identification of various individual cover types. Among the different approaches to classification, the study shows that the modified clustering approach to classification is the best technique to employ since it allows for a high degree of interaction between the analyst and the machine, thereby complementing the inadequacies of either party. The difficulty in derivating signatures is efficiently executed through the methodology of hybrid classification, at lesser processing time. The analyst on the one hand, is also given the opportunity to "control" which signatures best qualify to represent a certain resource class considering the fact that he or she holds the reference data from which to base the final decision for classification. The results of the study also show that the modified clustering approach gives the highest overall classification accuracy of 90.9% for level II resource class.

The capability of ERDAS for man-machine interactionalso facilitates the various steps in digital analysis and the use of Landsat TM data for vegetation mapping has produced reasonableaccuracy results. Its main limitation however, is the presence of cloud cover in the image, which constrains the interpretation of some areas. It is therefore recommend that further studies on the area with use of remote sensing data be realized in conjunction wth the use of radar digital data whose capabilities allow the user to 'see' through the clouds (aschbacher, 1991).

ACKNOWLEDGEMENTS

The authors are grateful for the advice and assistance given by many people involved, especially Mr. Yian Kwan Ang, Manager of the Remote Sensing Laboratory (RSL), Mr. Than Naing, and Mr. Quang, Instrumentation Engineer and System Analyst, respectively. Also sincere thanks are due to Mr. Moe Myint, a doctoral candidate of the STAR Program of AIT.

REFERENCES

Anderson, J. R., et al. 1976. A Land Use and Land CoverClassification System for Use with Remote Sensing Data. U. S. Geological Survey Professional Paper 964. U. S. Gov. Printing Office, Washington, D. C.

Aschbacher, J. 1991. Application of Microwave remote Sensing for Tropical Forest Management. Paper Presented at the "International Workshop on Conservation and Sustainable Development" 22-26 April 1991, Khao Yai, Thailand.

COMPARISON OF DIFFERENT SENSORS AND ANALYSIS TECHNIQUES FOR TROPICAL MANGROVE FOREST MAPPING

J. Aschbacher[1*], P. Tiangco[2], C. P. Giri[3], R. S. Ofren[3], D. R. Paudyal[2], Y. K. Ang[2],

[1]European Commission, Joint Research Centre, IRSA, TP441, I-21020 Ispra (VA), Italy;
Tel: +39-332-785968, Fax: +39-332-785461, E-mail: josef.aschbacher@jrc.it

[2]Asian Institute of Technology (AIT), SERD-RSL, GPO Box 2754, Bangkok 10501, Thailand

[3]UNEP/EAP-AP, c/o AIT, GPO Box 2754, Bangkok 10501, Thailand

ABSTRACT

The objective of this study is to compare different remote sensing sensors and analysis techniques for the purpose of mangrove mapping. A study area in Southern Thailand of approximately 40 x 30 km size was selected. A systematic assessment of strengths and limitations of data taken from different sensors, namely Landsat TM, Spot HRV, MOS MESSR, JERS-1 SAR and ERS-1 SAR, was carried out. The results of the investigation show that optical remote sensing data is highly suitable for mapping mangrove forests and can discriminate reasonably well four mangrove forest classes, namely *homogeneous rhizophora, homogeneous nypa, mixed dense* and *mixed open mangrove forest.* The classification accuracy is approximately 87%. The use of radar data alone resulted in a significantly lower classification accuracy, but on the other hand provided additional information related to the *age distribution of rhizophora stands.*

INTRODUCTION

A mangrove forest is a salt tolerant forest ecosystem of the inter-tidal regions along the coastlines. It is predominantly a tropical evergreen forest comprising trees and shrubs. Although the mangrove forest is characterised by very low floristic diversity it is considered as one of the most productive ecosystems. In the past years, mangrove forests have been severely threatened by over-exploitation and, more recently, conversion of mangrove forests into shrimp ponds. Other factors of mangrove degradation are related to mining activities, establishment of industrial estates, coastal development and agricultural land expansion programmes. The environmental impact is irreversible and mostly severe with changes occurring within a few months. The need for updated and continuous information is evident for a sound management approach.

Currently, monitoring is widely based on visual interpretation of aerial photography or optical satellite imagery. The latter is hampered by frequent cloud coverage along the tropical coastlines. This study will introduce radar imagery and digitally based analysis methods.

* The work presented in this paper was carried out within the framework of a research project sponsored by the Austrian Academy of Sciences (AAS), with support from the European Space Agency (ESA), the National Research Council of Thailand (NRCT), the Thai Royal Forestry Department (RFD), the Asian Institute of Technology (AIT), and the United Nations Environment Program (UNEP). The Austrian Association for Development & Co-operation (ADC) supported the administration of the project.

OBJECTIVES

The main objective of this study is to systematically compare different remote sensing sensor types for the purpose of mangrove monitoring. Data of common optical and radar sensors shall be compared, and a suitable methodology developed. Recommendations shall be made regarding the best approach for the use of remote sensing for mangrove mapping and monitoring.

STUDY AREA AND DATA BASIS

Study Area

A study area of approximately 30 x 40 km size was selected in Phangnga Bay, Southwest Thailand. The centre co-ordinates are 98.5 deg E, 8.4 deg N. The topography is generally flat, with a few single mountain cliffs reaching out from the Andaman Sea, or the land surface. The flat topography causes a very large tidal range with extended mud flats. The soil in the mangrove area comprises clayey and silty sediments, they are alkaline in nature and generally moderately fertile and high in organic matter. The climate is humid tropical with seasonal monsoon rainfall from April to September and around December [1,2].

The mangrove types observed in the study area are homogeneous stands of *Nypa palms* and *Rhizophora*, as well as *mixed mangrove forests* of varying density. Selective logging by the local people and tin mining activities are the main reason for deforestation, which is done in a reasonably controlled fashion. No conversion from mangrove forests into fishponds is observed in the study area.

Data Basis

The satellite images available for this study are listed in Table 1.

Table 1: Satellite data available for data analysis.

Sensor	Acquisition date	Spatial resolution
Spot HRV	22-Mar-92	20 m
Landsat TM	20-Apr-93	30 m
MOS-1 MESSR	22-Feb-89	50 m
JERS-1 SAR	8-Sep-92	18 m (3 looks)
ERS-1 SAR	16-Jul-92, 20-Aug-92, 29-Oct-92	25 x 30 m (3 looks)

Among the three optical images only the Spot data are practically cloud-free, while the Landsat and MOS images show scattered clouds over the mangrove study area. No recent image with less cloud cover could be obtained of this region. The ERS-1 radar images were available in 8-bit only, as processed by the Indian receiving station. Data calibration was carried out according to [3]. The JERS-1 SAR data

were available in standard 16-bit format. The Spot and multi-temporal ERS-1 images are shown in Fig. 1a and 1b, respectively.

The interpretation of remote sensing data was supported by extensive ground measurements taken concurrently with ERS-1 overflights as well as topographic maps, soil maps, meteorological and tidal information and a digital elevation map.

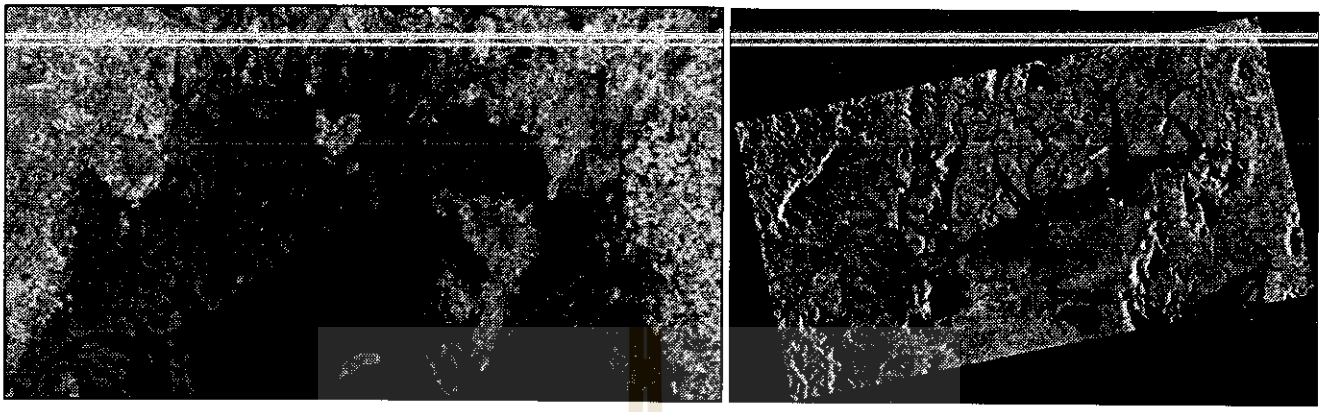

Figure 1: Mangrove study area of Phangnga Bay (Thailand), as shown in (a-left) Spot HRV imagery and (b-right) multi-temporal ERS-1 SAR imagery *(image copyrights: SpotImage, ESA).*

DATA ANALYSIS

Systematic investigations were carried out to identify the strengths and limitations of various sensors and sensor combinations as well as different analysis techniques. In particular, the analysis steps shown in Table 2 were performed [4].

The centre piece of the study is the systematic comparison of the five different digital classification methods shown as ID 7a-e in Table 2. Digital classifications were carried out based on both, single data sources such as Spot, Landsat or ERS-1, as well as combinations of different sensors such as Spot & ERS-1. Training sample selection for the maximum likelihood classification was based on detailed ground surveys carried out at different times of the year.

Table 2: Different analysis steps performed within the current study (from [5]).

ID	Analysis Methodology	Data Source
1	Visual interpretation	individually: Landsat, Spot, MOS, ERS-1, JERS-1
2	Image rectification	all images rectified to UTM proj.
3	Speckle filtering (Gamma MAP)	ERS-1, JERS-1
4	Texture analysis (variance, homogeneous contrast, dissimilarity)	all ERS-1 images
5	image stratification (GIS based)	Spot, Landsat, ERS-1, JERS-1
6	Spectral/temporal signature analysis	Spot, Landsat, Spot & ERS-1, Landsat & ERS-1, ERS-1 & JERS-1, mERS-1
7a	Digital image classification	SPOT

7b 7c 7d 7e		Landsat ERS-1 & Spot ERS-1 & JERS-1 multi-temporal ERS-1
8	Integration of GIS for classification enhancement	as 7
9	Classification accuracy assessment	as 7

RESULTS

The overall classification accuracies based on data from the various sensors showed that the highest accuracy is achieved combining ERS-1 and Spot imagery. The overall accuracy was 87.3% considering the following six classes: *homogeneous rhizophora, homogeneous nypa, mixed open mangrove forest, mixed dense mangrove forest, water*, and *rubber plantations*. The classification accuracy based on radar data alone was significantly lower and reached 52.1% for combined ERS-1 & JERS-1 image data, which was also similar as for ERS-1 data alone. For comparison, the classification based on the Landsat image showed a relatively low accuracy of 68.6%, which can partly be attributed to some misclassifications due to cloud cover. The Spot image, for comparison, was practically cloud-free and resulted in a classification accuracy of 84.8% [1, 5].

Generally, radar backscattering coefficients are higher for multi-storied, uneven aged mixed forest as compared to more homogeneous stands. Also, clear-cut areas, twigs, stumps and other debris give strong backscattering signatures in both ERS-1 and JERS-1 SAR images. This phenomenon has great potential for the monitoring of mangrove deforestation [1,4].

Table 3: Error matrix for the classification of mangrove types based on ERS-1 & Spot images (from [5]).

Class	Omission (%)	Commission (%)	Map accuracy (%)
Rhizophora	11.1	15.6	76.9
Nypa palms	9.7	12.9	80.0
Mixed dense	22.4	10.0	71.4
Mixed open	26.7	33.3	55.0
Rubber	8.9	13.3	80.4
Water	0.0	0.0	100.0

Taking the example of the combined ERS-1 & Spot classification, the error matrix for the classification of mangrove types is shown in Table 3. If the four mangrove types are considered as one class ("mangroves") and a discrimination with the other non-mangrove classes such as rubber, water, dense forest, built-up areas and other land-cover is performed, the user's and producer's classification accuracy is 92.1 and 89.7%, respectively, for mangroves versus non-mangrove classes. The classified image is shown in Figure 2.

An independent test of the different classification procedures shown in Table 2 (ID 7a-e) was carried out on a different study area, located 50 km south of the area shown in Fig. 1. The results were very similar

to the ones reported above, with overall accuracies of 83.8%, 48.0% and 72.9% for the Spot & ERS-1, ERS-1 & JERS-1 and Landsat based classifications, respectively [1, 5].

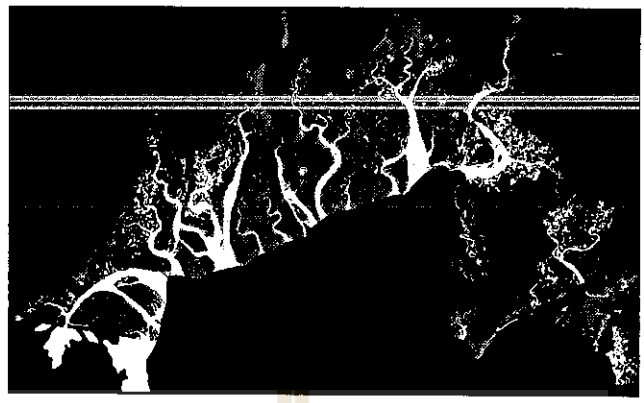

Figure 2: Classified land-cover map based on images of Spot and ERS-1 (from [1]). Legend: Rhizophora (green), nypa (yellow), mixed open mangroves (orange), mixed dense mangroves (brown), rubber (red), water (blue).

CONCLUSIONS AND RECOMMENDATIONS

Based on the study of different sensors and analysis techniques of mangrove forests at a study area in Thailand, the following conclusions can be drawn:

1. The use of cloud-free optical data is most suitable for the discrimination of mangrove from non-mangrove areas.
2. The best discrimination, also between different mangrove types, was achieved when both data sources, optical (Spot) and radar (ERS) data, were combined.
3. At least four mangrove classes can be identified using optical data, namely *homogeneous rhizophora*, *homogeneous nypa*, *mixed dense* and *mixed open mangrove forest*.
4. The inclusion of radar data gives additional information on the approximate age of rhizophora stands, the presence of clear-cut areas or abandoned paddy fields. Multi-storied, uneven-aged mixed forest has a higher radar backscattering compared to more homogeneous stands. Clear-cut areas where tree trunks, twigs, stumps and other debris are still left on the ground give a strong radar backscattering signal.
5. For the use of radar data the use of multi-temporal imagery is crucial, as is the selection of acquisition dates. Changes are occurring mainly in the non-mangrove areas.
6. The inclusion of GIS-based data such as topographic information, or soil information increases the mapping accuracy.

For tasks similar to the one carried out within this study, and if available resources allow, it is recommended to use an integrated approach which includes the use of optical and radar data together with GIS based information.

REFERENCES

[1] J. Aschbacher, C. P. Giri, R. S. Ofren, P. N. Tiangco, J-P. Delsol, T. B. Suselo, S. Vibulsresth, and T. Charuppat, "Tropical Mangrove Vegetation Mapping Using Advanced Remote Sensing And GIS Technology"; Final Report, Asian Institute of Technology, 1994, 90 pp.

[2] S. Aksornkoae, "Ecology and Management of Mangroves", IUCN Publ., Bangkok, Thailand, 1993.

[3] D. R. Paudyal and J. Aschbacher "ERS-1 SAR data calibration at the Indian National Remote Sensing Agency"; Asia-Pacific Remote Sensing Journal, Vol. 6, No. 2, Jan. 1994, pp. 117-120.

[4] J. Aschbacher, R. Ofren, J-P. Delsol, T. B. Suselo, S. Vibulsresth and T. Charuppat, "An Integrated Comparative Approach to Mangrove Vegetation Mapping using Advanced Remote Sensing and GIS Technologies: Preliminary Results"; J. Hydrobiologica, Vol. 295, nos. 1-3, Kluwer Academic Press, Jan. 1995, pp. 285-294.

[5] J. Aschbacher, C. P. Giri, R. S. Ofren, P. Tiangco, D. R. Paudyal: "*Comparison of different sensors and analysis techniques for tropical mangrove forest mapping";* Proc. IGARSS '95, 10-14 July 1995, Firenze/Italy; pp. 2109-2111.

ACKNOWLEDGEMENT

The authors wish to warmly thank the staff of the Remote Sensing Laboratory of the Asian Institute of Technology for their continued and tireless support of the current work. In particular, the support of Mrs. Zhang, Ms. Srisa-ang and Mr. Shankar is acknowledged. Thanks are also given to Mr. Apan and Mrs. Bevis who supported the initial phase of the project.

POSTER SESSION S

WATER / MARINE

A SOBEL EDGE DETECTOR DIGITAL FILTER STRUCTURE AND ITS DISTRIBUTED ARITHMETIC IMPLEMENTATION

Kobchai Dejhan, Fusak Cheevasuvit, Somjin Thongplew, Soontorn Oraintara

Faculty of Engineering, King Mongkut's Institute of Technology Ladkrabang

Ladkrabang, Bangkok 10520, Thailand

Tel : 66-2-326 9967, 66-2-326 9081, Fax : 66-2-326 9086, 66-2-326 9965

Narong Arjrith

Faculty of Engineering, Srinakharinwirot University

Bangkhen, Bangkok 10220, Thailand

Tel : 66-2-972 9652, 66-2-521 1005, 66-2-521 1108 ext 474

Ekachai Prommas

Faculty of Engineering, Kasembundit University

Patanakarn Road, Bangkok 10250, Thailand

Tel : 66-2-321 6930-39 ext 212

ABSTRACT

Edge detection is an important step in most image segmentation techniques. It can identify the areas of an image where larges change in intensity occur. These changes are associated with the physical boundary or edge in the scene from which the image is derived. The ultimate object in segmentation is to develope a contiguous set of pixels forming a closed contour around each object of interest in the image with more heuristic rules-based algorithms which track boundaries and link edges to form whole contours. Sobel edge detection method based on Sobel operators has the advantage of emphasizing the central part of the edge. Each direction of Sobel operator is applied to an image, then two new images are created. One image shows the vertical response and the other shows the horizontal response. The purpose is to determine the existance and location of edges in a picture. Two images is combined into a single one. Distributed arithmetic (DA) is used in digital signal and image processing instead of the encountered form of computation such as sum of products. DA is an extreme computational efficiences and exploited in circuit design form. This paper proposes an implementation of 2-dimensional digital image filter for low pass filter and Sobel edge detector. The method of DA in this paper is a transformation of transfer function by using look-up table.

Presented at the 16th Asian Conference on Remote Sensing, at Suranaree University of Technology, Nakhon Ratchasima, Thailand.

THEORY

The distributed arithmetic (DA) is a bit serial computational operation by forming an inner product (or dot product) of a pair of vectors in a single direct step. The method is to distribute all of the number into binary digit in order to process the signal in the form of digital circuit. The use of DA will be high efficiency in the case of sum of multiplication equation. The DA technique is faster than standard microprocessor when used the same clock rate [2,3]. DA uses look-up table to multiplie the input signal with the coefficients which are stored in memory unit.

Consider the calculation of the following sum of products : [1]

$$Y = \sum_{k=1}^{K} A_k X_k \tag{1}$$

The A_k are fixed coefficients, and X_k are the input data words. If X_k is a 2's-complement binary number scaled such that $|X_k| < 1$, then the expression of each X_k can be shown as

$$X_k = -b_{k0} + \sum_{n=1}^{N-1} b_{kn} 2^{-n} \tag{2}$$

where the b_{kn} are the bits, 0 or 1, b_{k0} is the sign bit,

$b_{k,N-1,}$ is the least significant bit (LSB), and N is number of bit per input data.

The equation can be obtained :

$$Y = \sum_{k=1}^{K} A_k [-b_{k0} + \sum_{n=1}^{N-1} b_{kn} 2^{-n}] \tag{3}$$

Rearrange the equation, thus

$$Y = \sum_{k=1}^{N-1} [\sum_{k=1}^{K} A_k b_{kn}] 2^{-n} + \sum_{k=1}^{K} A_k (-b_{k0}) \tag{4}$$

Distribute the equation :

$$\begin{aligned} Y = & -2^0 (b_{10} A_1 + b_{20} A_2 + b_{30} A_3 + \ldots + b_{k0} A_k) \\ & + 2^1 (b_{11} A_1 + b_{21} A_2 + b_{31} A_3 + \ldots + b_{k1} A_k) \\ & \ldots\ldots\ldots\ldots\ldots\ldots\ldots\ldots\ldots\ldots\ldots\ldots \\ & \vdots \\ & + 2^{-(N-1)} (b_{1,N-1} A_1 + b_{2,N-1} A_2 + \ldots + b_{k,N-1} A_k) \end{aligned} \tag{5}$$

The equation (5) is distributed arithmetic form, consider the factor $\sum_{k=1}^{K} A_k b_{kn}$

and suppose that it is equal to Y'. Then, the equation is shown as

$$Y = \sum_{k=1}^{N-1} [Y'] 2^{-n} + \sum_{k=1}^{K} A_k (-b_{k0}) \tag{6}$$

The b_{kn} are the bits, 0 or 1. Thus, Y' should be possible 2^K values and these values will be calculated and pass to store in ROM as in Table 1. The input data will be used to be ROM address. The final results will be stored in accumulator [5,6] and obtain the output Y. Fig.1 shows the distributed arithmetic structure [1] of the type 1 BAAT (one-bit-at-a-time) for equation (1).

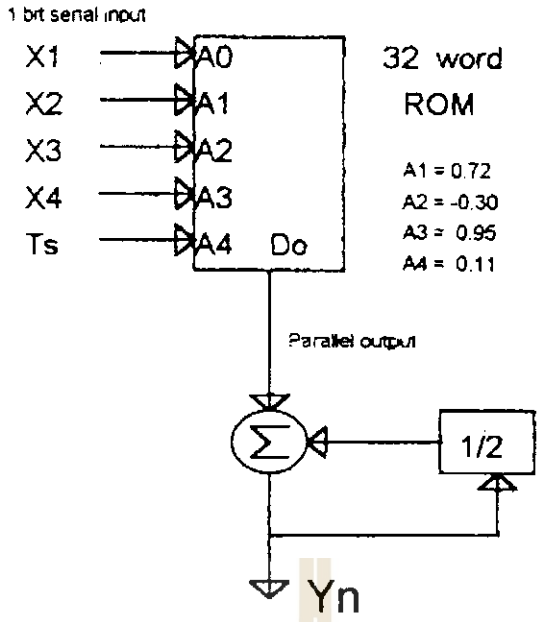

Fig.1 DA Structure of type 1 BAAT for equation (1)

$1 \leq n \leq N-1$					
Input Code					32-Word
T_S	b_{1n}	b_{2n}	b_{3n}	b_{4n}	Memory Content
0	0	0	0	0	0
0	0	0	0	1	A4 = 0.11
0	0	0	1	0	A3 = 0.95
0	0	0	1	1	A3+A4 =1.06
0	0	1	0	0	A2 = -0.30
0	0	1	0	1	A2+A4 = -0.19
0	0	1	1	0	A2+A3 = 0.65
0	0	1	1	1	A2+A3+A4 = 0.75
0	1	0	0	0	A1 = 0.72
0	1	0	0	1	A1+A4 = 0.83
0	1	0	1	0	A1+A3 = 1.67
0	1	0	1	1	A1+A3+A4 = 1.78
0	1	1	0	0	A1+A2 = 0.42
0	1	1	0	1	A1+A2+A4 = 0.53
0	1	1	1	0	A1+A2+A3 = 1.37
0	1	1	1	1	A1+A2+A3+A4 = 1.48

Table 1 Stored data in ROM [1]

An application of DA can be used with two-dimensional signal processing, for example the digital filter [10]. Therefore, the linear differential equation of two-dimensional second order recursive digital filter [5]. has a general form as :

$$Y_{m,n} = \sum_{k=0}^{2}\sum_{l=0}^{2} a_{k,l} X_{m-k,n-l} - \sum_{i=0}^{2}\sum_{j=0}^{2} b_{i,j} Y_{m-i,n-j} \qquad (7)$$

The $X_{m,n}$ and $Y_{m,n}$ are output data of system, respectively. The $a_{k,l}$ and $b_{i,j}$ are fixed coefficients of filtering, its values are between ±1 of 2's-complement for B bit resolution including 1 sign bit.

DESIGN TECHNIQUE

The system consists of the digital image data calculation circuit and the imagery data delay line. The processes of imagery data for obtaining the new image (edge detection, contrast of image) depend on impulse response by using mask over imagery data and move it to every position of picture. All of data will be multiplied with the results and sum together. Therefore, the new digital image data will be obtained.

1/16

1	2	1
2	4	2
1	2	1

(Smooth filter)

0	-1	0
-1	5	-1
0	1	0

(High-pass filter)

-1	0	1
-1	0	1
-1	0	1

(Vertical edge detection)

1	1	1
0	0	0
-1	-1	-1

(Horizontal edge detection)

The picture processing using DA uses the signal sequence X(m,n) to rearrange. All of 9 data sequence will pass to process by using look-up table which stored the data of low-pass filter, high-pass filter of edge detector. The input data are in parallel and the are converted into serial, DA will increase the processing speed better than the old method [2,3]. The digital image data delay line can be used by serial shift register to shift the data.

SOBEL EDGE DETECTOR

Sobel edge detector gets better the contour of object in image. The edge detection process is shown in Fig.2. The experiment uses the process as shown in Fig.3. DA converts the three sets of data (smooth filter, horizontal edge detector and vertical edge detector) as the method shown in Table 2.

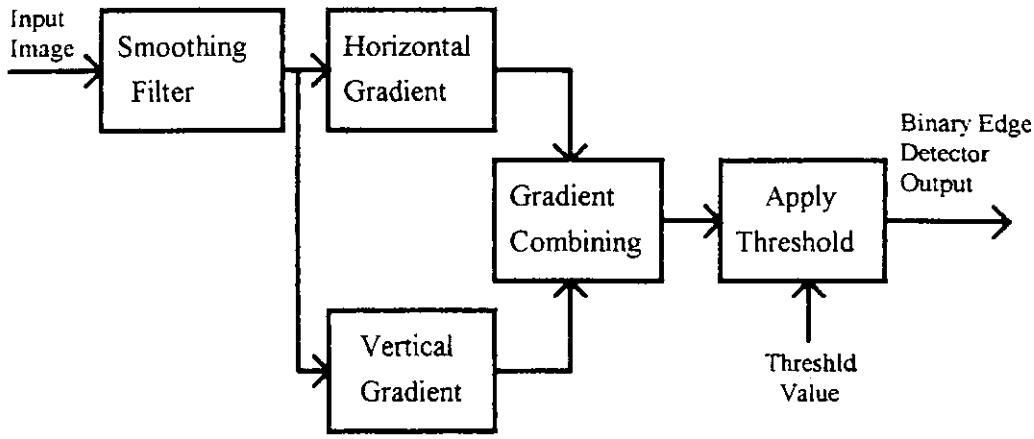

Fig.2 Edge detection diagram

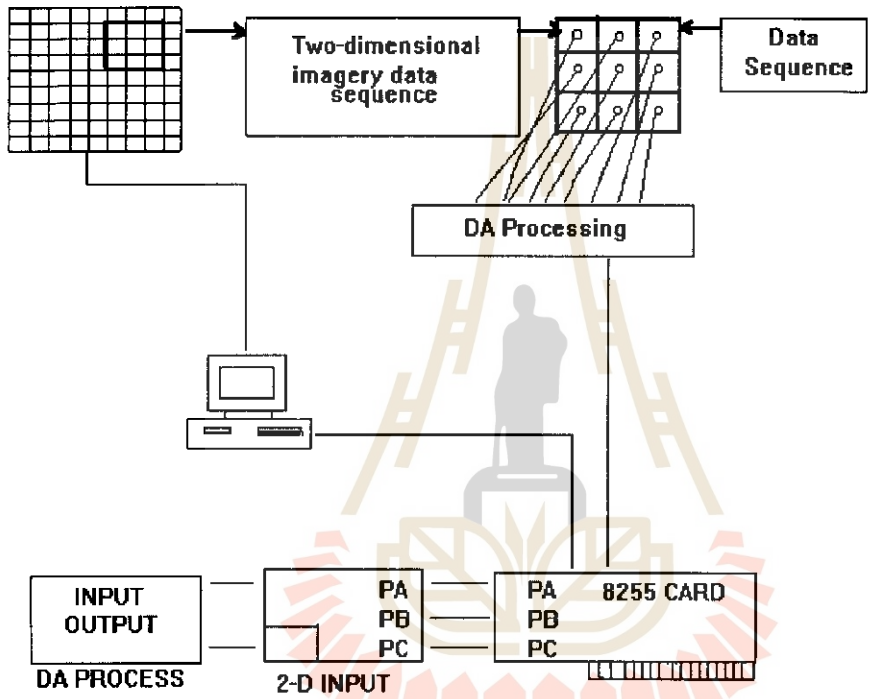

Fig.3 Picture data processing based on DA

The hardware [7,8] can process only each digital image data and then arrange the vertical edge and horizontal edge data together by using software [9]. The increase of hardware can be done and will increase the processing speed and more convenient [4].

A	B	C
D	E	F
G	H	I

a	b	c	d	e	f	g	h	i	Y=aA+bB+cC+dD+eE+fF+gF+hH+iI
0	0	0	0	0	0	0	0	0	Y=0
0	0	0	0	0	0	0	0	1	Y=I
0	0	0	0	0	0	0	1	0	Y=H
0	0	0	0	0	0	0	1	1	Y=H+I
0	0	0	0	0	0	1	0	0	Y=G
0	0	0	0	0	0	1	0	1	Y=G+1
:									:
:									:
0	0	1	0	1	0	1	0	0	Y=C+E+G
0	0	1	0	1	0	1	0	1	Y=C+E+G+I
0	0	1	0	1	0	1	1	0	Y=C+E+G+H
0	0	1	0	1	0	1	1	1	Y=C+E+G+H+I
:									:
:									:
1	1	1	1	1	1	1	0	0	Y=A+B+C+D+E+F+G
1	1	1	1	1	1	1	0	1	Y=A+B+C+D+E+F+G+I
1	1	1	1	1	1	1	1	0	Y=A+B+C+D+E+F+G+H
1	1	1	1	1	1	1	1	1	Y=A+B+C+D+E+F+G+H+I

Table 2 Stored data in ROM

RESULTS

The analytic digital image data and the effect of Sobel edge detector can be compared together as shown in Fig.4.

Analytic digital image data

Effect of Sobel edge detection

Analytic digital image data

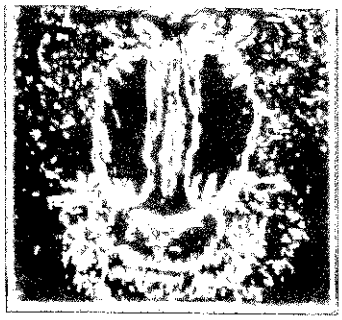

Effect of Sobel edge detection

Fig.4 Comparison of analytic data and effects of Sobel edge detector

CONCLUSION

The application of DA is used to apply for image processing and it can be implemented in easily form. This technique will be useful to construct the system that can use with picture of image processing.

REFERENCES

[1] S.A. White, "Applications of distributed arithmetic," IEEE ASSP Mag., vol.6, no.3, pp.4-19, July 1989.

[2] A. Peled and B. Liu, "A new hardware realization of digital filter," IEEE Trans. ASSP, vol.ASSP-22, pp.456-462, Dec. 1974.

[3] A. Peled and B. Liu, "Digital signal processing," John Wiley & Sons, pp.212-226, 1976.

[4] D.F. Elliott, "Handbook of digital signal processing," Academic Press, pp.964-972, 1987.

[5] H. Jaggernaught and A.N. Venetsanopoulos, "Real-time image processing through distributed arithmetic", IEEE Trans. Circuit and Systems, vol.1 pp.393-397, May 1983.

[6] C.F.N. Cowan, S.G. Smith and J.H. Elliott, "A digital adaptive filter using a memory accumulator architecture," IEEE Trans. ASSP, vol.ASSP-31, June 1983.

[7] K-S. Lin, "Digital signal processing," Texas Instrument Series, Prentice Hall, pp.F2-F9, 1988.

[8] C.E. Sporck, "F 100 K ECL logic databook," National Semiconductor, pp.(3)199-(3)205, 1990.

[9] P.M. Embree and B. Kimble, "C language algorithm for digital signal processing," Prentice Hall, pp.393-400, 1991.

[10] J.S. Lim, "Two-dimensional signal and image processing," Prentice Hall, pp.476-487, 1990.

Digital Image Data Recovery from Printed Image

by

F. Cheevasuvit*, K. Dejhan*, V. Tipsuwanporn*, S. Wongkham* and A. Somboonkaew**

*Faculty of Engineering, King Mongkut's Institute of Technology Ladkrabang,

Bangkok 10520, Thailand.

**Mahanakorn University of Technology, Bangkok 10530, Thailand.

Abstract

Sometime, the raw data of selected image cannot be provided by the producer. Therefore, the digital image data must be reproduced from the available information especially a printed image. To accomplish this task, a scanning device is used. However, for the printing reason, some undesired texture is appeared in the printed image. This kind of texture will result a specified Fourier spectrum, so it can be removed by using filter function in the frequency domain. Hence, the digital data of desired image scene is recovered.

1. Introduction

Nowadays, the advances in technology of electronics cause the decrement in price of personal computer (PC) and also the scanning device. Accordingly, the small organizations can purchase by their own budget, especially the remote local department such as forestry department, irregation department and agriculture department etc.. All these remote local organizations need to use the remote sensing data for resource management or for some special applications. Sometime they want to process a new data of selected satellite image and seemingly the producer cannot provide the data to the requested organization in time. However, if the remote organization already has a selected satellite image in hand but in another form such as printed image on paper. The satellite data can be reproduced in digital data form by using a scanning device and PC of the organization. However, for the printing reason, some undesired texture will be presented in the printed image. This kind of texture have a specified Fourier spectrum, and it can be eliminated by using some kind of filter function which will described in the following paragraph.

2. Reproduction of digital image data from printed image

To response the immediately desired to use of a digital satellite data from an available printed image, a scanning device and PC are used. The interested image is scanned by using some solfware program to converse the printed image into the digital image data and store in the PC memory. Nevertheless, for some printing reason, it will appear an undesired texture which can be shown as an instance in Fig. 1 and 2. Fig. 1 (a) and 2(a) are some printed images. While the Fig. 1(b) and 2(b) are some part of images which are enlarged to show clearly the existance of texture.

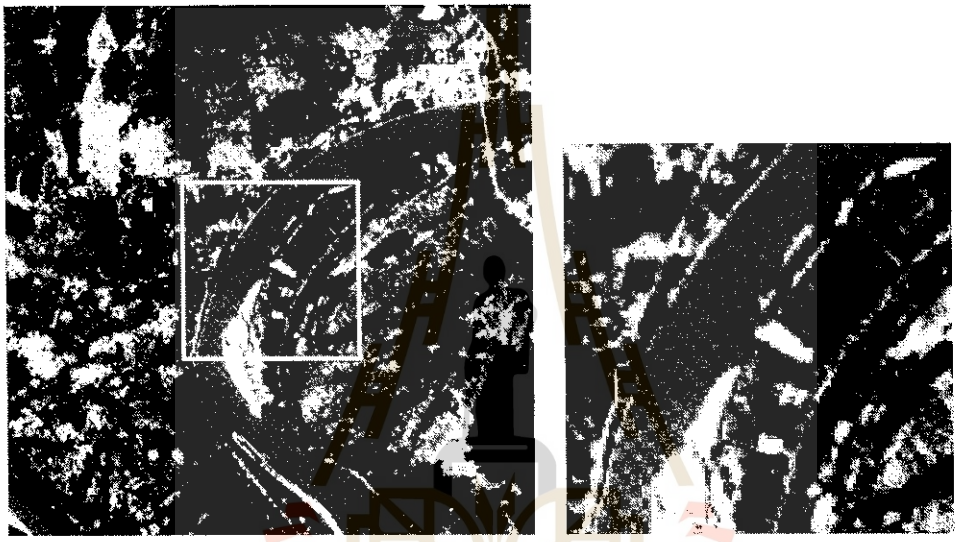

(a) Whole printed image. (b) Enlargement of some part.

Fig.1 Printed image of satellite data.

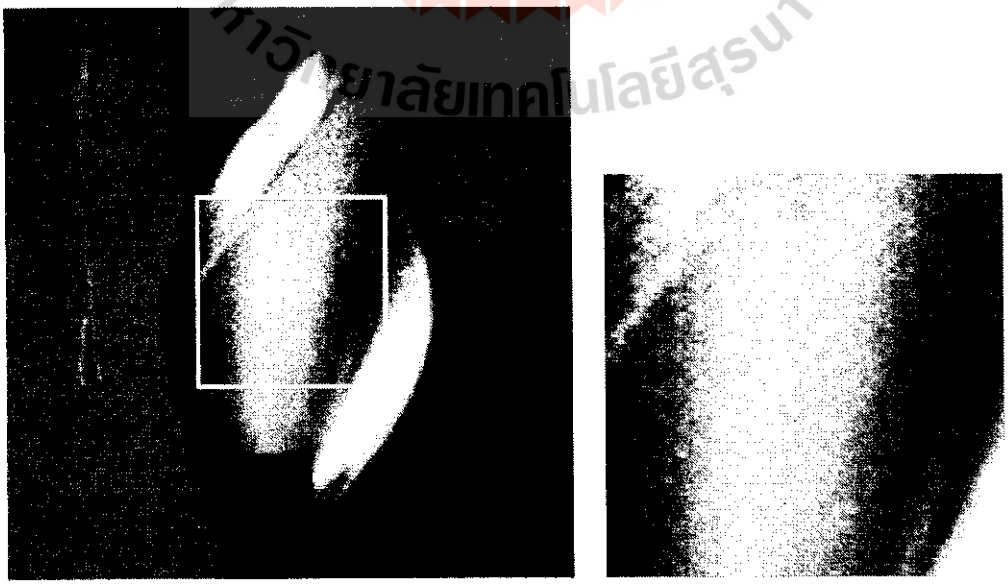

(a) Whole printed image. (b) Enlargement of some part.

Fig.2 Printed image of drilling machine.

The undesired texture is distributed over the whole image with the same structure which is considered as periodic noise. This periodic noise is unable to exclude by simple template matching method [1]. Anyway this kind of noise can be eliminate by using filter function in frequency domain. Fourier transform is applied to the noisy image in order to obtain the spectrum of the interested image. The center of the Fourier transform array is the average brightness value. The spectrum away from the center depicts the proportion of increasing spartial frequency component. Generally the spectrum of undesired texture will be located in the high frequency portion. Hence, the filter is applied to eliminate the high frequency spectrum corresponded to the undesired texture. Consequently, the digital data of interested image is obtained.

3. Experimental and result

The image Fig. 1(a) is obtain by scanning the printed image and store in the memory of PC. Enlargement a part of Fig. 1(a) is shown in Fig. 1(b). It is cleared that there exists some undesired texture in the scanned image. Hence, to reproduce a complete digital image, this kind of texture must be removed. Here, the Fourier transform is applied to the scanned image to obtain its spectrum which is shown in Fig. 3. The undesired texture or periodic noise is easy found in high frequency portion of the spectrum. A filter function of Fig. 4, which defined certain bands for rejecting the specified frequencies of undesire texture, is applied to the image spectrum. The filtered spectrum is shown in Fig. 5. The resulting image shown in Fig. 6 is achieved by appling inverse Fourier transform to the spectrum of Fig. 5. The Fig. 6 shows the periodic noise free image.

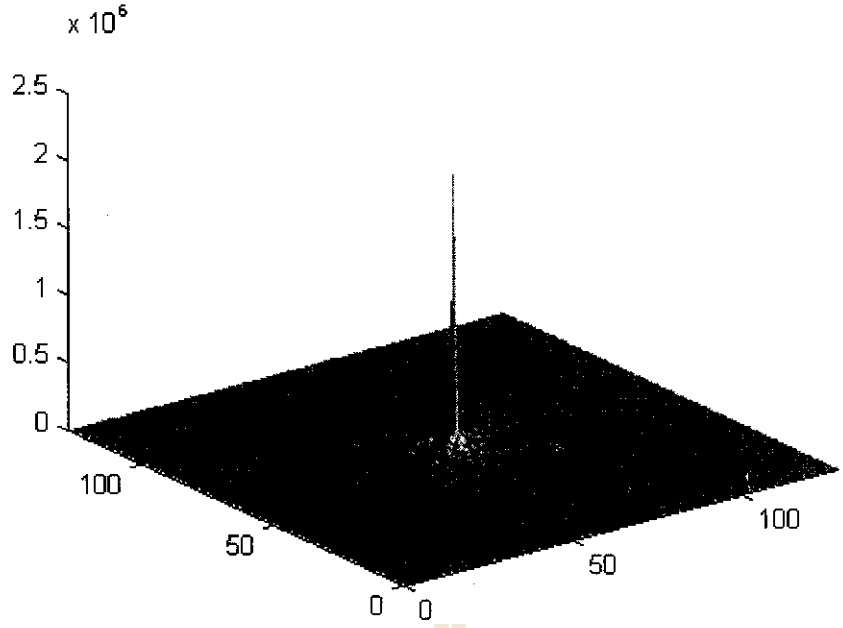

Fig. 3 Spectrum of image in Fig. 1(a) obtained by using Fourier transform.

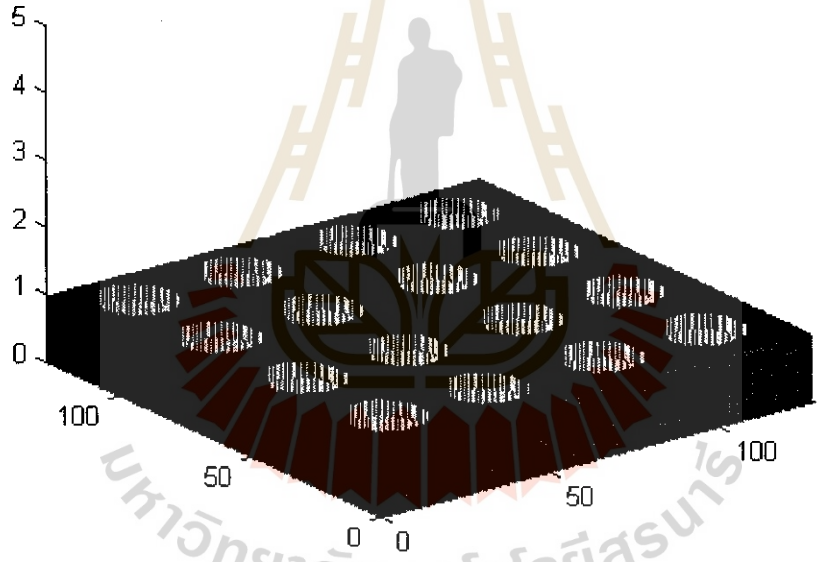

Fig. 4 Specified filter function to remove the spectrum of undesired texture is high frequency portion.

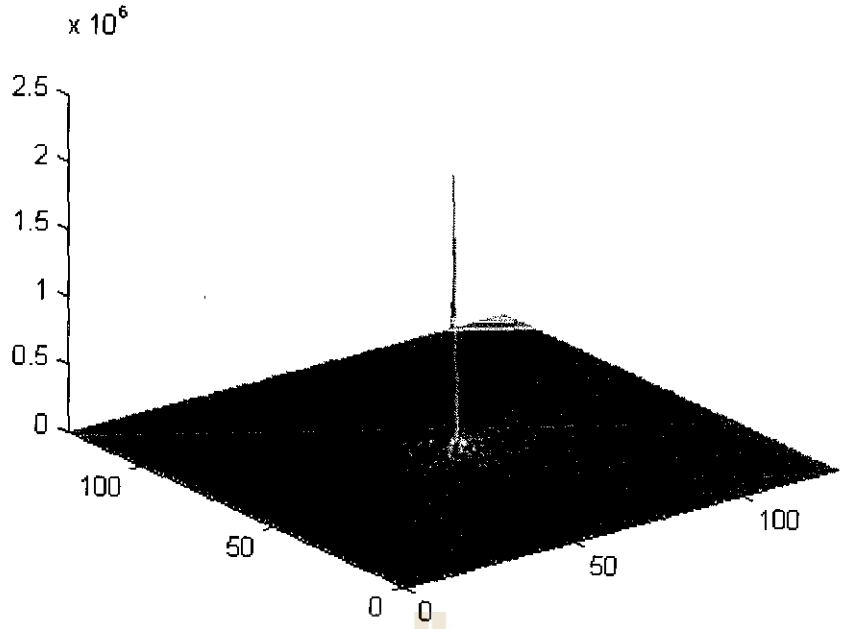

Fig. 5 Filtered spectrum.

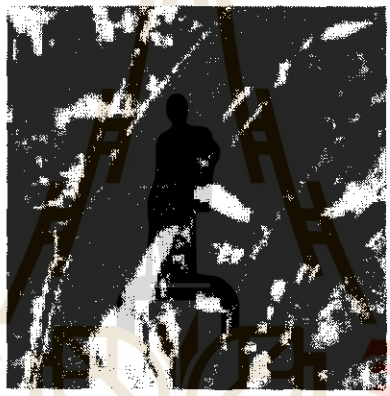

Fig. 6 Resultant of digital image data obtained by the inverse Fourier transform of filtered spectrum.

4. Conclusion

This paper presents a method of image data recovery from printed image by using scanning device and PC. The scanned image is stored to be digital form. However, for some printing reason, the scanned image is consisted of undesired texture or periodic noise. This kind of noise effects a specified frequencies spectrum. Then, some filter function can be applied to remove the undesired texture. The result of digital data image is accomplished by applying the inverse Fourier transform to the filtered spectrum. Hence, the digital image data can be recovered from the printed image.

5. Acknowledgement

The authors wish to thank the staff of Thailand Remote Sensing Center for providing monthly TRSC Newsletter.

6. Reference

[1] J.A. Richards, "Remote Sensing Digital Image Analysis: An Introduction," Springer-Verlag, Berlin, 1986.

[2] S.P. Banks, "Signal Processing, Image Processing and Pattern Recognition," Prentice Hall, New York, 1990.

[3] J.C. Russ, "The Image Processing Handbook," 2nd Edition, IEEE Press, 1994.

[4] M.A. Sid-Ahmed, "Image Processing : Theory, Algorithm and Architectures," McGraw-Hill Books Co., 1995.

[5] P.M. Embree and B. Kimble, "C Language Algorithms for Digital Signal Processing," Prentice Hall, New York, 1991.

A NEW AND EFFICIENT TRANSFORM FOR SIGNAL PROCESSING BASED ON GABOR DISCRETE COSINE TRANSFORM

V.K.SINGH, A.S. MANJUNATH
NATIONAL REMOTE SENSING AGENCY, HYDERABAD, INDIA

ABSTRACT

Gabor transform is very useful for remote sensing applications. Since the Gabor elementary functions are not mutually orthogonal, its implementation is time consuming. The computational speed can be improved by using a modified transform, Gabor Discrete Cosine Transform (DCT), because of a real valued transform. The Gabor DCT was implemented for the purpose of image data compression for browse application in remote sensing area. Since this application needs time valued processing of the remotely sensed data, the speed achieved in implementation of Gabor DCT was not satisfactory. To achieve a higher throughput a new transform which is variant of the basic Gabor DCT has been developed. The paper discusses the new algorithm and implementation methodology. A matrix multiplication based method for computing new transform for any discrete signal is proposed in the paper. The results of compression on remote sensing images by both techniques are presented. The paper describes the new algorithm and implementation methodology.

1 INTRODUCTION

Remote sensing has been an efficient and useful technique for the monitoring and management of natural resources. Remote sensing involves acquisition, processing, analysis and archival of images acquired from airborne/spaceborne platform. The Gabor Transform has been found to be very useful for image analysis and compression tasks. Implementation of Gabor transform is very complicated and time consuming because the Gabor elementary functions are a set of overlapping functions and not mutually orthogonal. An important property of Gabor elementary functions is their achievement of the theoretical lower bound of joint un-certainty in the two conjoint domains, space and frequency [1]. They achieve the maximum possible joint resolution in the conjoint visual space and spatial frequency domain. Furthermore experimental results show that the receptive field of the mammalian visual cortex can be very well represented using 2-D Gabor elementary functions. Some properties of the visual system, such as spatial localization, orientation selectivity and spatial frequency selectivity can also be modeled in terms of these functions [3]. Another important reason that encourages the user of Gabor functions is that it has been shown that the Gabor decomposition reduces the low-order entropy of the data [3]. This means that, like DCT, the Gabor transform has the beneficial property of decorrelation. Therefore when the Gabor transform is used for image compression, in which the properties of the visual system can be incorporated into an image coding scheme, a high data compression ratio may be achieved.

Derivation of key formulae of Gabor representation is usually facilitated by relationships taken from Fourier and Zak transform theory. Several of these fundamental formulas can be obtained directly using Bessel's equality [5]. Complete discrete 2-D Gabor transforms for image analysis and compression was described by J. G. Daugman [3]. Numerical implementation of the generalized Gabor expansions and synthesis was described by J. Wexler et al [4].

A very fast and easily implemented method was proposed by T.Ebrahimi and M. Kunt [6] for the computation of the weighting factors of the Gabor decomposition. A modified Gabor transform referred to as the Gabor DCT was proposed by Wang and Yan [8]. An adaptive Gabor DCT was also proposed by H. Wang and H. Yan [2]. An FFT based gradient descent approach for fast implementation of the discrete 2-D Gabor transform was described by V. Srinivas et al [7].

Based on Gabor DCT, a new and efficient transform is proposed in this paper for discrete signal processing. The implementation of this transform and the results of both (Gabor DCT and New Transform) the transforms have been discussed. The weighting factors [6] are extracted by simple multiplication between a matrix and the vector data. Images are reconstructed by multiplying the matrix of the transform functions and vector of the weighting factors. The advantage of this transform is that, similar to Gabor DCT, the transformed coefficients of this new transform have more compact energy distribution than those of the Gabor transform coefficient [1] and in addition, the computation speed of this transform is much higher than that of the Gabor DCT.

2 IMPLEMENTATION OF THE NEW TRANSFORM

2.1 THE 1-D TRANSFORM

The one dimensional (1-D) discrete Gabor DCT elementary function [8] may be expressed as :

$$gd(x) = \exp\{-\pi\alpha^2 (x - x_0)^2\} \times \cos\{\pi u_0 (x - x_0 + \delta x\} \quad (1)$$

where x_0 represents a sample in the space domain, u_0 represents a sample in the spatial frequency domain and δx is spatial offset of the frequency modulation function. The Gabor DCT is calculated within area of support (defined by α) of Gaussian function, where x_0 corresponds to the centre of a Gaussian function.

Since the exponential and cosine functions are inter-related, a study was carried over in this regard and the Gabor DCT in (1) was modified and a new transform has been developed as :

$$gd(x) = \cos\{\pi\alpha^2 (x - x_0)^2\} \times \cos\{\pi u_0 (x - x_0 + \delta x\} \quad (2)$$

Expansion of a discrete signal F(x) in terms of elementary functions of this new transform can be expressed as :

$$F(x) = \sum_{k=0}^{n-1} gd_k(x)\, x_k \quad (3)$$

where x_k are transform expansions. The above expression can be described in matrix notation [6] as :

$$F = G.X \quad (4)$$

where

$$F = \begin{vmatrix} f(0) \\ f(1) \\ . \\ . \\ f(N-1) \end{vmatrix} \qquad X = \begin{vmatrix} x(0) \\ x(1) \\ . \\ . \\ x(n-1) \end{vmatrix} \quad (5)$$

$$G = \begin{vmatrix} gd_0(0) & gd_1(0) & \ldots\ldots & gd_{n-1}(0) \\ gd_0(1) & gd_1(1) & \ldots\ldots & gd_{n-1}(1) \\ | & . & & | \\ | & . & & | \\ | & . & & | \\ gd_0(N-1) & gd_1(N-1) & \ldots\ldots & gd_{n-1}(N-1) \end{vmatrix} \quad (6)$$

Solution of (4) can be found analytically [6] as :

$$X = A.F \quad (7)$$

where

$$A = (G^T.G)^{-1}.G^T \quad (8)$$

The original signal f(x), specified, say, at N points, is divided into block of dimension p, with centres located at $\{x_m\} = \{mp\}$ for blocks m. The elementary functions, whose widths are determined by Gaussian envelop parameter in (3), are defined over a 2p spatial cell. A complete set of elementary functions of transform is defined for each block m by varying the spatial frequencies $\{u_r\} = \{r/2p\}$, corresponding to the 2p spatial cell. The parameter r takes on even integer values, r = 0, 2, 4 .... 2p-2, because the block size is p. The centre of each elementary function coincides with that of a block and (2) can now be rewritten as :

$$gd_{mr} = \cos\{\pi\alpha^2(x - mp)^2\} \; x \; \cos[\pi r(x - mp + \delta x) / 2p \quad (9)$$

Each elementary function $gd_{m,r}$ is now uniquely determined by the integer m and r representing the spatial centre and frequency parameter respectively [7]. We obtain N/p distinct values for m.

2.2 THE 2-D TRANSFORM

In case of two dimensional (2-D) discrete Transform, the expansion of a 2-D discrete signal (for example an image) F(x,y) may be represented as :

$$F(x,y) = \sum_{k_1=0}^{n_1-1} \sum_{k_2=0}^{n_2-1} gd_{k1,k2}(x,y) \; x_{k1,k2} \quad (10)$$

where $x_{k1,k2}$ are 2-D Transform expansions. Elementary functions $gd_{k1,k2}(x,y)$ are separable. They may be written as :

$$gd_{k1,k2}(x,y) = gd_{k1}(x).gd_{k2}(y) \quad (11)$$

Here the Eq.(11) can be rewritten in matrix form as [6] :

$$F = G.X.G^T \quad (12)$$

where

$$F = \begin{vmatrix} f(0,0) & \ldots. & f(0,N-1) \\ | & & | \\ | & & | \\ | & & | \\ f(N-1) & \ldots. & f(N-1,N-1) \end{vmatrix}$$

$$X = \begin{vmatrix} x(0,0) & \ldots. & x(0,n_2-1) \\ | & \ldots. & | \\ | & \ldots. & | \\ | & \ldots. & | \\ x(n_1-1) & \ldots. & x(n_1-1,n_2-1) \end{vmatrix} \quad (13)$$

and G is same expansion matrix as described by Eq.(6).

Solution of (10) can be found analytically [6] as :

$$X = A.F.A^T \quad (14)$$

where

$$A = (G^T.G)^{-1}.G^T \quad (15)$$

3 RESULTS AND DISCUSSIONS

Image compression is needed for browse application on remotely sensed data at NRSA, India. For this purpose, it was found that Gabor DCT is a suitable technique and the necessary software was developed to implement the same. After a comprehensive study to improve computational speed another useful variant Gabor DCT which we call here New Transform has been developed. Software for implementation of the New Transform has also been developed as already described. The software is developed in 'C' on Unix platform(SUN workstation) and performances of both the transforms have been measured. The software computes number of transform expansions based on same Mean Square Error(MSE) for both the transforms and then each expansion is coded in 8 bits. Both the techniques were applied to picture and remotely sensed data of different sizes viz 256x256, 512x512 and 1k x 1k pixels. Performance measurement is made on the basis of MSE, compression ratio and computational speed. The MSE is computed between original and reconstructed images. Fig.(1) shows the original image whereas Figs.(2) & (3) show the reconstructed images using Gabor DCT and New Transform techniques respectively.

At NRSA, several images of different sizes were compressed using both the techniques viz Gabor DCT and New Transform and our observations are shown in Table(1) and Table(2). It is observed from both the tables that for the same MSE the New Transform gives better compression ratio and the same time takes lesser time for computation. Quality of the compressed image depends upon number of transform expansions stored for that image. If number of transform expansions increases, quality of compressed image also increases i.e. MSE is reduced but the execution increases.

Table(1) : Observations with Gabor DCT

Sl. No.	MSE	Compression Ratio(bits/pixel)	Execution Time(in sec.)	Image Size
1	5.28	0.5	7.9	256x256
2	9.08	0.5	75.6	512x512
3	9.53	0.5	681.4	k x 1k
4	10.11	0.25	3.3	256x256
5	17.65	0.25	29.0	512x512
6	19.02	0.25	276.7	1k x 1k

Table(2) : Observations with New-Transform

Sl. No.	MSE	Compression Ratio(bits/pixel)	Execution Time(in sec.)	Image Size
1	5.28	0.4	7.7	256x256
2	9.08	0.4	72.8	512x512
3	9.53	0.4	632.4	1k x 1k
4	10.11	0.25	3.2	256x256
5	17.65	0.25	28.1	512x512
6	19.02	0.25	240.6	1k x 1k

4 CONCLUSIONS

Gabor DCT and New Transform have been applied on 2-D discrete signals, such as remotely sensed images, and performances of both have been examined. It has been found that the computational speed achieved here for implementing this New non-orthogonal transform is quite satisfactory and it is suitable for various applications, such as image analysis, segmentation and compression, in remote sensing . It is observed that performance of New Transform is much better than the Gabor DCT. Since, like the Gabor DCT, transform coefficients of New Transform have a more compact energy distribution, a better image compression result can be achieved. The 2-D New Transform is also useful for image analysis and segmentation because, it also extracts locally windowed 2-D spectral information concerning form and texture without sacrificing information about 2-D location or more global spatial relationships.

REFERENCES

[1] Hang Wang, Hong Yan, " Efficient image coding method based on adaptive Gabor discrete cosine transforms ", *Journal of Electronic Imaging*, January 1993, Vol.2, No.1, pp.38-43.

[2] H. Wang and H. Yan, " Adaptive Gabor discrete cosine transform for image compression ", *Electronics Letters*, Aug. 1992, Vol.28, No.18, pp.1755-1756.

[3] John G. Daugman, " Complete discrete 2-D Gabors transforms by neural networks for image analysis and compression ", *IEEE Trans. on ASSP*, Vol.36, No.7, July 1988, pp.1169-1179.

[4] J. Wexler and S. Raz, " Discrete Gabor expansion ", *Signal Processing*, Vol.21, No.3, Nov.1990, pp.207-220.

[5] Richard H. Orr, " Derivation of Gabor transform relations using Bessel's equality ", *Signal Processing*, Vol.30, No.2, January 1993, pp.257-262.

[6] Touradj Ebrahimi, Murat Kunt, "Image compression by Gabor expansion", *Optical Engineering*, July 1991, Vol.30, No.7, pp.873-880.

[7] V. Srinivasan, P. Bhatia and S. H. Ong, "A fast implementation of the discrete 2-D Gabor transform", *Signal Processing*, Vol.31, No.2, March 1993, pp.229-233.

[8] Wang H. and Yan H., " Efficient implementation of Gabor transform for image compression ", *Electronics letters*, 1992, Vol.21, No.9, pp.870-871.

Fig.(1) ORIGINAL IMAGE

Fig.(2) RECONSTRUCTED IMAGE USING GABOR DCT
COMPRESSION RATE:0.25 BITS/PIXEL

Fig.(3) RECONSTRUCTED IMAGE USING NEW TRANSFORM
COMPRESSION RATE:0.20 BITS/PIXEL

Effect of Atmospheric Correction on Satellite Image Data by Lowtran Model

Kiyoshi Torii*, Tomoyuki Mase and Takashi Hoshi*****

*Dept. of Agric. Eng. Kyoto Univ, Kyoto, Japan
**Ministry of Agric., Forestry & Fisheries, Tokyo, Japan
***Dept. of Comp. & Information Sci., Ibaragi Univ, Hitachi, Japan
Fax (Int'l+81)+773-64-3617, E-Mail cxk02755@niftyserve.or.jp

Abstract

Remote sensing technique is one of the most expected tools to be used in environmental measurements. However, distortions and noises contained in satellite images become serious impediments for quantitative analysis.
In the present study, we used Lowtran Model to eliminate atmospheric effects with respect to thermal infrared, visible and near infrared bands due to technical differences and examined the result.
Data used in the study are Landsat 5 TM data on Chaophraya plain, Thailand, and Kojima bay, Okayama Pref., Japan. We obtained interesting data derived from the difference in atmosphere in the tropics and temperate zone.

1. Introduction

Accuracy in earth survey by satellites has been raised with the advancement in space technology and measurement techniques and objects of the survey have also been variegated. Observations of vegetation, soil water, chlorophyll content and earth surface temperature are included in the related fields. With the progress, programs for satellite data analysis has also been developed and excellent soft wears such as Arc/Info, IDRISI and ERDAS have become popular. Analytical method has shifted from visual and qualitative ones at the beginning to quantitative one utilizing observed radiance intensity. However, satellite data contains not a little errors and noises and they form a great hindrance in quantitative analysis. These errors and noises are roughly classified into 3 categories; noises derived from ability of a sensor, geometrical distortions, and atmospheric effects. Here, we discuss about elimination of atmospheric effects, which is the main theme of correction.

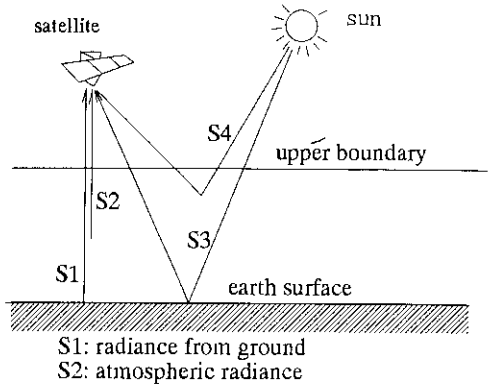

Fig. 1 Incxident radiatio to satellite senser.

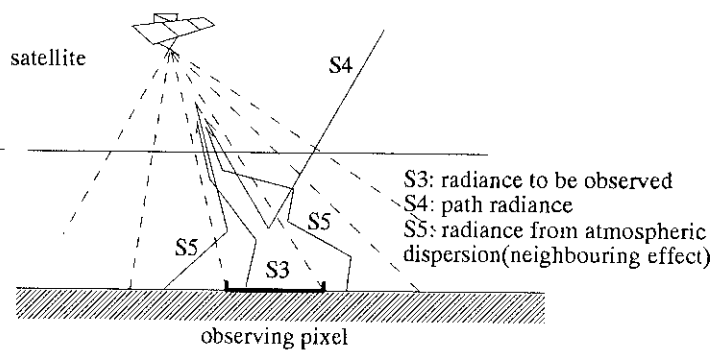

Fig. 2 In the case of visible, and near-infrared band.

Presented at the 16th Asian Conference on Remote Sensing , Suranaree University of Technology, Nakhon Ratchasima, Thailand, November 20-24, 1995

2. Concepts of atmospheric correction

Radiation entering a sensor is classified as in Fig. 1. Atmospheric correction is the processing to eliminate S2 and S4 leaving S1 and S2 which are the objects of observation as well as to eliminate S5 in Fig. 2 contaminating from the vicinities of the observed pixels. However, techniques for atmospheric correction have not been established and many studies are still going on at present. A general formula for transmission of radiation in a multiple atmospheric model is as follows,

$$I_\nu(\tau_1,\mu,\phi) = \varepsilon_{earth\nu}B_\nu(T_{earth})e^{-(\tau_1/\mu)} + \int_\tau^{\tau_1}\varepsilon_{air\nu}B_\nu(T_{air})e^{-t/\mu}\frac{dt}{\mu} + \int_\tau^{\tau_1}\left[\frac{a_\nu}{4\pi}\int_0^{2\pi}\int_{-1}^{1}P_\nu(\mu,\phi;\mu',\phi')I_\nu(\tau,\mu',\phi')d\mu'd\phi'\right]e^{-t/\mu}\frac{dt}{\mu} \quad \cdots\cdots(1)$$

where I_ν: spectral radiance in frequency range ν, ν: optical thickness, μ: cosine of the zenith angle, ϕ: azimuth, ε_{earth}: emission rate of the ground, ε_{air}: emission rate of the medium, B_ν: Planck function, $B_\nu = \dfrac{2h\nu^3}{c^2\exp(h\nu/kT)-1}$, h: Planck constant, ν: frequency, c: velocity of light, k: Boltzmann constant, T_{air}: temperature of the medium, T_{earth}: temperature of the ground, a_ν: albedo of the primary scattering of the medium, and P_ν: probability function of the scattering angle. The left hand side of the equation is the radiance observed by a satellite $(\tau_1 = 0)$, the first term of the right hand side is the surface radiation, the second term is the atmospheric radiation and the third term is the scattered light including that by the earth surface. Optical thickness, τ, is the integrate of the volumetric dispersion coefficient, K_ν, from the upper boundary of the atmosphere ($z=\infty$) to the altitude z and is defined as follows,

$$\tau = \int_z^\infty K_\nu dz \quad \cdots\cdots(2)$$

To solve the equation (1), parameters including atmospheric temperature and optical thickness (scattering coefficient) are needed. Formerly, these parameters were decided on the basis of the actual measurement values obtained from a radiosonde in the vicinity of the site of analysis or correlation in observation intensities in multiple bands. However, in recent years, excellent atmospheric models such as LOWTRAN and FASCODE have been published facilitating easy access to these parameters. In the present study, we used LOWTRAN 7 as an atmospheric model in our calculation. LOWTRAN 7 is a program source written in FORTRAN and, in a simple case, it can provide optical thickness, atmospheric temperature and altitude distribution of aerosol content in each model selected from Table 1.

Table 1 Standard input parameters in LOWTRAN 7

Parameters related to temperature humidity, gaseous concentration	Parameters related to aerosol		
Tropical type	No aerosol	Summer type	Stratospheric type
Midlatitude summer type	Rural type (23 km visual range)	Winter type	Aged volcanic type
Midlatitude winter type	Rural type (5 km visual range)		Fresh volcanic type
Subarctic summer type	Marine type		
Subarctic winter type	Urban type		
1976 U.S. standard type	Tropospheric type		
User definition	Fog type		
	Desert type		
	User definition		

The image data used in the present study is the one observed by LANDSAT-Thematic Mapper (TM) and it has 7 bands ranging from visual to thermal infrared wavelengths (0.45-12.5 μm). The parameters used in Equation (1) differ greatly depending on the wavelength and the method of atmospheric correction differs accordingly. In the present study, we discuss about atmospheric corrections in 2 wavelength zones, visual and near infrared zone and thermal infrared zones.

2.1 Data correction in thermal infrared zone

LANDSAT-TM consists of 7 channels and only one channel is designated to the thermal infrared zone (10.4μm-12.5μm). Calculation for correction of thermal infrared band data concerns with accurate calculation of the earth surface temperature. While the model equations to convert the observed values to the surface temperature have been published by NASA, etc., they are either uniform totally ignoring longitude and atmospheric effects of the observation site or localized concerning specific data. So, in the present study, we modified the correction technique to be applicable to all sorts of atmospheric models using LOWTRAN 7. In the thermal infrared zone, dispersion and reflection by atmosphere or earth surface can be ignored and, therefore, radiation laws can be simplified greatly. In other words, upward radiance, I_{obs}, from the earth surface ($\tau = \tau_1$) to the satellite ($\tau = 0$) is expressed by the following equation obtained by multiplying each term of Equation (1) by the satellite response function, R_ν, and integrating it by the instantaneous angle of view and frequency,

$$I_{obs} = \int_{\phi_1}^{\phi_2}\int_{\mu_1}^{\mu_2}\int_{\nu_1}^{\nu_2} R_\nu\left[\varepsilon_{earth\nu}B_\nu(T_{earth})e^{-(\tau_1/\mu)} + \int_0^{\tau_1}\varepsilon_{air\nu}B_\nu(T_{air})e^{-t/\mu}/\mu dt\right]d\nu d\mu d\phi \quad \cdots\cdots(3)$$

In the equation, $\mu_1\,\mu_2$: the range of instantaneous field of view and $\nu_1\,\nu_2$: the range of frequencies observed by the satellite. In the calculation, atmosphere up to 100-km altitude was horizontally divided into 32 uniform layers and the atmospheric temperature and optical thickness determined by LOWTRAN 7 as well as the response function of the sensor were substituted into Equation (3). Then, T_{earth} was changed in the temperature range corresponding to the atmospheric model and the observed radiance, I_{obs}, was determined. While LOWTRAN presents a mean data of a long period including fine and rainy weather, observation by the thermal infrared remote sensing is limited to fine weather and, therefore, humidity which is an important factor in the present problem becomes excessive in comparison to that of the atmosphere at the time of observation. Because of this, only humidity was modified to the respective winter types in the mid latitude and subarctic summer models in the present study. The maximum input radiance of the sensor was set as $I_{\max} = B_\nu(340.)$ and the minimum input radiance as $I_{\min} = B_\nu(200.)$ and the digital output value, D, is recorded as follows,

$$D = \frac{255}{I_{\max} - I_{\min}}(I_{obs} - I_{\min}) \quad \cdots\cdots(4)$$

By the above equation, the supplied satellite data, D, and the ground temperature, T_{earth}, are correlated as follows. Here, aerosol models were all designated to the rural model (5 km visual range).

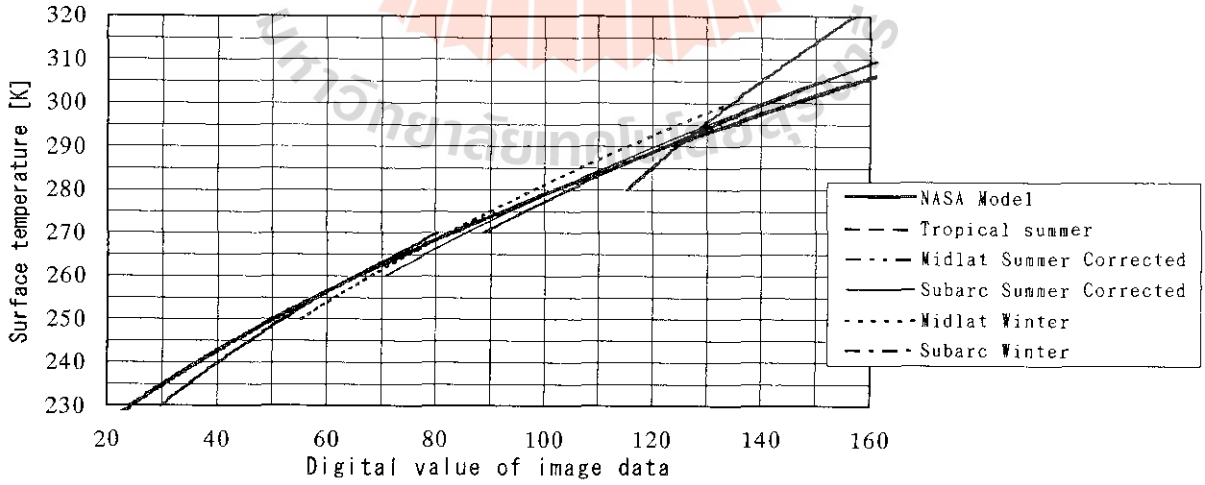

Fig. 3 Correlation between quantitized radiance and surface temperature

The ratio of atmospheric radiation included in the observed radiance, I_{obs}, becomes as Fig. 4 The temperature of the observed radiance, T_{obs}, of Fig. 4 is defined by $B_\nu(T_{obs}) = I_{obs}$

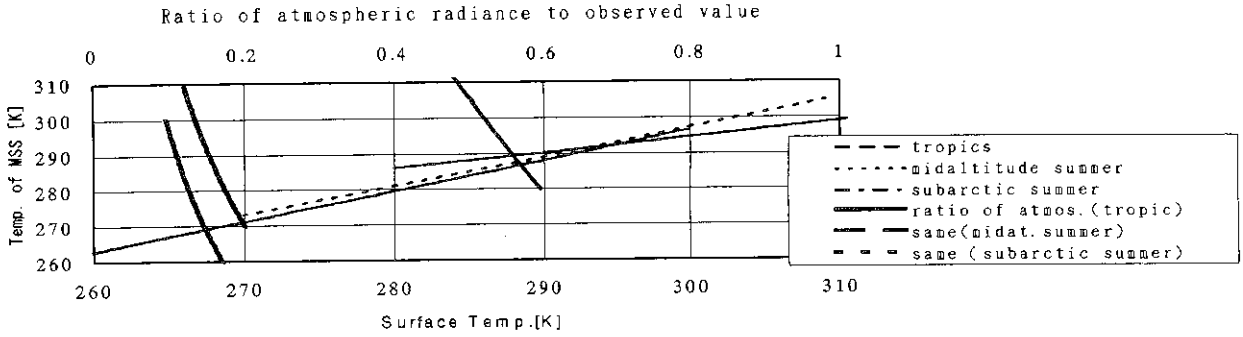

Fig. 4 The ratio of atmospheric radiance to observed value

2.2 Correction of visible and near infrared data

In LANDSAT-TM, 4 channels are designated to the visual range and 2 channels to the infrared range. In these wavelength ranges, Planck function is negligible and, therefore, $B_\nu(T) = 0$, we only have to consider the third term of the right hand side of Equation (1). As in Fig. 2, dispersed light and reflected light are dealt with as the light entrance paths. It is necessary to eliminate S4 and S5 to extract the objective S3. S4 is considered as being constant in the horizontal direction but S5 increases as it approaches to the observation pixel. If the point (X,Y) of the ground coordinates is observed, introduction of a filter $a(x,y)$ gives the observed radiance, I_{obs},

$$I_{obs}(X,Y) = \int_\phi\int_\mu\int_\nu R_\nu\left[\int_x\int_y a(x,y)I_{earth}(X+x,Y+y)dxdy + I4\mu\right]d\nu d\mu d\phi \quad \cdots\cdots(5)$$

assuming that S5 is dependent only on the distance from the observation pixel and $I_{obs}(X,Y)$ can be expressed as a sum of the convolution of S3 by the filter $a(x,y)$ and S4. As path radiance, S4, is calculable by LOWTRAN, reflection intensity at the ground site (X,Y), $I_{earth}(X,Y)$, can be extracted by reverse conversion regarding the filter $a(x,y)$ as a point spread function provided that it is known. In the present study, $a(x,y)$ was determined by the simulation wherein numerous photons were allowed to enter into the atmospheric models. The ground surface was regarded as Lambertian surface and the reflection flux as constant.

Essentially, we should let photons enter from far up in the atmosphere and count those entering the focusing surface of the sensor through dispersion and reflection but it is difficult to let a sufficient number of photons enter the focusing surface of a few mm^2 of the area present at 700 km altitude above the ground. Thus, we let the photons enter a random point within the observation pixel on the upper boundary of the atmosphere from the satellite and determined the number of photons arriving at the ground (X,Y) to decide the filter $a(x,y)$.

Free journey, L, is the distance to the point where a photon collides with next particle and is defined by the following equation using the uniform-distribution random numbers from 0 to 1, $ran(\alpha)$,

$$\tau(L) = -\log\{ran(\alpha)\} \quad \cdots\cdots(6)$$

As for scattering angle, θ, $ran(\alpha)$ was generated after a number, n (n=200, in the present study), of θ_k satisfying the following equation were prepared using the probability function $P(\theta)$ for the scattering angle, θ.

$$\int_{\theta_k}^{\theta_{k+1}} P(\theta)d\theta = \int_0^\pi P(\theta)d\theta \Big/ n \quad \cdots\cdots(7)$$

Then, θ_k satisfying the following equation was adopted.

$$k/n \le ran(\alpha) \le (k+1)/n \quad \cdots\cdots(8)$$

The azimuth of scattering, ϕ, was set $\phi = 2\pi ran(\alpha)$ assuming isotropy. $P(\theta)$ differs greatly depending on whether the collided particle is air molecule or aerosol. It follows Rayleigh's scattering law if the photon collides with a fine air molecule,

$$P(\theta) = 3\{1+\cos^2(\theta)\}/16\pi \quad \cdots\cdots(9)$$

but it follows Mie scattering if collision with a larger aerosol takes place. We used built-in $P(\theta)$

in LOWTRAN related to individual aerosols for calculation. Whether the collided particle was an air molecule or aerosol was judged by generating $ran(\alpha)$ using the ratio between the dissipation coefficient due to air molecular scattering within the layer and that due to aerosol scattering. Convergence of the solution was decided by diving the earth surface into pixels and finding the convergence of the maximum value in the rate of change of the photons $N(X,Y)$ reaching the cell (X,Y). Then, filter $a(x,y)$ can be obtained according to the following equation,

$$a(x,y) = \frac{N(x,y)}{\left(N_{total} - N_{escape}\right)} \quad \text{.....(10)}$$

Figs. 5 and 6 show the examples of the filter $a(x,y)$. The center of the mesh is the observation pixel, the cell division is 30x30 [m] on the basis of the satellite specificity and the value unit is %.

Tropical marine winter type								
0.03	0.04	0.05	0.06	0.07	0.06	0.05	0.04	0.03
0.04	0.06	0.08	0.1	0.11	0.1	0.08	0.06	0.04
0.05	0.08	0.14	0.22	0.27	0.22	0.14	0.08	0.05
0.06	0.1	0.22	0.6	1.27	0.6	0.22	0.1	0.06
0.07	0.11	0.27	1.27	70.8	1.27	0.27	0.11	0.07
0.06	0.1	0.22	0.6	1.27	0.6	0.22	0.1	0.06
0.05	0.08	0.14	0.22	0.27	0.22	0.14	0.08	0.05
0.04	0.06	0.08	0.1	0.11	0.1	0.08	0.06	0.04
0.03	0.04	0.05	0.06	0.07	0.06	0.05	0.04	0.03

Fig. 5 Point spread function (Bangkok)

Corrected midaltitude, marine summer type CHANNEL1								
0.04	0.05	0.05	0.07	0.07	0.07	0.05	0.05	0.04
0.05	0.06	0.08	0.11	0.12	0.11	0.08	0.06	0.05
0.05	0.08	0.13	0.21	0.26	0.21	0.13	0.08	0.05
0.07	0.11	0.21	0.52	1.03	0.52	0.21	0.11	0.07
0.07	0.12	0.26	1.03	67.2	1.03	0.26	0.12	0.07
0.07	0.11	0.21	0.52	1.03	0.52	0.21	0.11	0.07
0.05	0.08	0.13	0.21	0.26	0.21	0.13	0.08	0.05
0.05	0.06	0.08	0.11	0.12	0.11	0.08	0.06	0.05
0.04	0.05	0.05	0.07	0.07	0.07	0.05	0.05	0.04

Fig. 6 Point spread function (Okayama south)

3. Prospects

We attempted correction of satellite data using atmospheric models and found that it would be necessary to confirm accuracy of the atmospheric models themselves or to modify the problem of selecting atmospheric models. In the present study in which visual infrared data was corrected using an inverse filter, accuracy in the periphery of the data drops due to the assumption of periodicity of the data. As for the filter, it is strongly dependent on the scanning angle and its effect is detected in a sensor with an extremely small scanning angle such as LANDSAT-TM. Therefore, it is necessary to adopt a filter considering the scanning angle at a point distant from that right under the satellite. Modification of these points facilitates elimination of principal distortions and noises included in the satellite data. Reliability of the analytical result is expected to improve greatly through this correction even though the analytical process thereafter is left to the commercial software.

4.Concluding remark

In the present study, we applied LOWTRAN model to satellite image data which was divided into thermal images and visual infrared images. In the thermal images, the values did not differ much from those predicted from the conventional NASA model in the mid latitude region including Japan but a rise of about 5℃ was predicted in the tropics. Although it is difficult to give a conclusive judgment as we have not conducted the ground survey, application of the NASA model to the tropics seems to require careful consideration.

In the visual infrared region, we could introduce filters corresponding to the respective bands as shown in Figs. 5 and 6. A considerable amount of calculation is needed to apply these filters to enormous image data and carry out analysis and we are in the stage of examining how to introduce routine program. Thus, although we have not assessed the program with numerical ground, it seems to be modified greatly on the basis of visual judgment, especially in the regions including water zone.

The original code of LOWTRAN 7 was supplied directly from GPOS/L.W.Abreu, U.S.Department of the Air force, Simulation Branch, Optical Environment Division, Phillips Laboratory (AFSC) as a medium of MT. The majority of calculations in the present study were conducted under the development project of Kyoto University Center. Landsat 5 TM data was provided by NASDA (National Space Development Agency of Japan) and NRCT (National Research Council of Thailand) at special prices. We express our thanks to whom it may concern.

5. References

1) Kneizys, F.X., et.al.: Atmospheric Transmittance/Radiance: computer code LOWTRAN6 AFGL-TR-83-0187 (1983).
2) Kneizys, F.X., et.al.: Users Guide to LOWTRAN7, AFGL-TR-88-0177, ERP, #1010 (1988).
3) Tanba, S., et.al.: Proceedings of 2nd meeting of Earth Environment Monitoring from Space, Institute of Industrial Science, Univ. of Tokyo, 1994
4) Marchuk, G.I., et.al.: The Monte Carlo Methods in Atmospheric Optics. Springer-Verlag, Berlin (1980).
5) Markham, B.I. and Barker, J.L.: Spectral Characterization of the LANDSAT Thematic Mapper sensors. NASA Conference Publication 2355, vol. II, Part I (1983).
6) Takagi, M., et.al.: Image Analysis Handbook. University of Tokyo Publication (1991).
7) Japan Society of Photogrammetry and Remote Sensing : Techniques and practice of thermal infrared remote sensing. Kashima Publication (1985).

A Massively Parallel Implementation of an Image Classifier

[1]P.A. Caccetta, [2]N.A. Campbell and [1]G.A. West

[1]School of Computing, Curtin University of Technology
peterc,geoff@cs.curtin.edu.au

[2]CSIRO Division of Mathematics and Statistics
normc@per.dms.csiro.au

September 18, 1995

Abstract

This paper describes the parallel implementation of a classifier based on maximum likelihood classification with pixel neighbourhood modifications. This is used for remotely sensed data which are large in comparison to other forms of 2D spatial data. The computational complexity of the algorithm restricts its use and has lead to an implementation on a SIMD processor namely the DECmpp. Issues addressed in the paper include: the ease of porting of the serial algorithm to a parallel machine and the resulting improvement in throughput due to the increased speed of computation.

1 Introduction

Maximum likelihood classification (MLC) has a long history as a tool for the interpretation of remotely sensed data. The technique is used in isolation [12] or in conjunction with other methods [9]. The algorithm is computationally expensive which is exacerbated by the large datasets that are typical of remote sensing e.g 2048×2048 pixels in size with 6 bands of 8-bit data. For this reason implementing this form of classifier on a massively parallel machine is desirable. The important issues are the ease with which it can be done and the increase in computational performance over typically available serial machines.

The MLC technique takes the raw data and transforms them into an image composed of labels defined by the user. Labels are often called *classes* and the resulting image a *classified* image. In essence, MLC involves allocating a pixel to a class for which it shows greatest affinity. Classes are modelled by multivariate distributions whose parameters are estimated from representative samples of the class. The multivariate distributions are then used to assesss which class an individual pixel is most likely to belong.

This paper considers the problem of processing the remotely sensed data once the class models have been obtained (that is the classifier has already been *trained*). In the following processing based on multivariant distributions will be referred to as *spectral processing.*

Spectral processing tends to produce images that have a certain amount of noise. In the current context, noise is when a pixel's data vector has affinity for a class other than its *true* class i.e. an error in classification. Noise can be the result of a pixel sample containing more than one cover class, in which case the pixel is referred to as a *mixed* pixel, or the result of errors of omission and commision present in the classification process. A typical result of noise is that a pixel is classified as belonging to a class not in agreement with its general surroundings e.g. a single pixel of lupins in a paddock of wheat. Neighbourhood techniques are incorporated into the classification procedure to reduce the effects of noise by taking account of neighbouring pixel classifications to aid the classification of the current pixel. Processing based upon neighbouring information will be referred to as *spatial* processing. The overall algorithm iteratively performs spectral and spatial processing to produce a classified image, and for large images becomes computationally expensive.

This paper outlines issues that were addressed during the porting an existing serial-based version of the algorithm to a DECmpp massively parallel processor, and discusses the computational advantages in doing so. The original serial code was written in FORTRAN 77 and based on a SUN platform. The target machine was a DECmpp 12000 comprising 2048 processors. Parallel code was created using DEC MPFORTRAN version 2.1.46 as opposed to the more efficient parallel C language (MPL) because the code was already in FORTRAN.

The remainder of this paper is divided as follows. Section 2 describes the architecture of the processor which governs the porting process. The classification algorithm is described in Section 3. Section 4 describes how parallelism is exploited in the algorithm. Section 5 discusses issues that arose with respect to the port to the DECmpp. Finally Section 6 discusses the computational performance and improvement in the execution time.

2 The DECmpp Massively Parallel Processor

The DECmpp 12000 is a parallel processor based on a single instruction multiple data (SIMD) architecture [11]. It is a modern implementation of ideas originally developed on the CLIP series of machines [5, 6], and the original MPP [1]. These were characterised by having many simple processors with a small amount of local memory and 4 or 8 way connectivity with their neighbouring processors. They are highly suited to operations that operate on single data elements or small neighbourhoods e.g. 3×3. These operations are very common in image processing and analysis algorithms such as distance transforms [4] and skeletonisation [8]. It consists of a front end workstation (FE) and a backend parallel processing unit called the Data Parallel Unit (DPU). The DPU has two components: the processor array consisting of many Processing Elements (PEs) and the Array Control Unit (ACU) which controls the PE array and performs operations on singular data.

Each PE in the array consists of a simple 4-bit ALU, a floating point co-processor and memory that is local to the PE. The PEs are arranged in a grid which incorporates specialised hardware for inter-PE communications. The hardware allows efficient communications between a PE and its immediate 8-connected neighbouring PEs, that is if a PE is located at position (i, j) on the grid, then efficient communications exists with the PEs located at $(i-1, j)$, $(i+1, j)$, $(i-1, j-1)$, $(i-1, j+1)$, $(i, j+1)$, $(i, j-1)$, $(i+1, j+1)$ and $(i+1, j-1)$. This form of communication is implemented in hardware and is referred to as the X-net. The connectivity is arranged as a toroid in which the top row of the array is connected to the bottom row, and the left column of the array is connected to the right column. This allows efficient raster shift communication to be used.

Two programming languages exist for the DECmpp: (1) MPFORTRAN which is based on FORTRAN 77 with extensions from VAX FORTRAN and the FORTRAN 90 ANSI standard, and (2) MPL which is based on ANSI C, and like MPFORTRAN has parallel constructs for handling arrays and I/O. In this application code utilising each language was written, with the image I/O code written in MPL as MPFORTRAN 2.1.46 did not support reads on byte data and the rest written in MPFORTRAN.

MPFORTRAN provides high level constructs for handling array operations, where ideally each PE performs the processing for one element of the array. When an array has dimensions larger than the dimensions of the PE grid, then the array is mapped to the grid such that a PE may process more than one element. The process of mapping an array which is larger that the PE array is called *virtualisation*. Performing virtualisation efficiently for arrays of different sizes is a complex problem. For MPL virtualisation has be addressed by the programmer whereas MPFORTRAN automatically handles virtualisation.

The DECmpp used was configured with 2048 PEs arranged on a 32×64 grid. Each PE had 64k of local RAM and the DPU hardware is scalable to 64k PEs.

3 The Classification Algorithm

This section provides an overview of the classifiaction algorithm, and is based on previous work [10, 3, 2]. In the following, it is assumed that an input image is available and the class means and covariance matrices for each class have been estimated during training.

3.1 Spectral Processing and Typicality Probabilities

Assuming multivariate Gaussian densities for k classes and an image composed of m spectral bands, this corresponds to calculating, for each class k, the density function $f_k(\underline{x}_m, \bar{\underline{x}}_k, \underline{V}_k)$ defined as:

$$f_k(\underline{x}_m, \bar{\underline{x}}_k, \underline{V}_k) = (2\pi)^{-m/2}|\underline{V}_k|^{-1/2}e^{-1/2D^2_{k,m}} \quad (1)$$

$$D^2_{k,m} = (\underline{x}_m - \bar{\underline{x}}_k)^T \underline{V}_k^{-1}(\underline{x}_m - \bar{\underline{x}}_k) \quad (2)$$

where $\bar{\underline{x}}_k$ is the vector of sample means, $\underline{V}_k$ is the sample covariance matrix, $\underline{x}_m$ is the pixel data vector and $D^2_{k,m}$ is the squared Mahalanobis distance for vector $\underline{x}_m$ and class k.

The density function $f_k(\underline{x}_m, \bar{\underline{x}}_k, \underline{V}_k)$ is also used to calculate *typicality probabilities*. These probabilities consider each class in isolation, and are used to judge whether a pixel conforms to the class statistics. If it does not, it is labelled as being *atypical*. For more details see [3]:

3.2 Spatial Processing

Neighbouring pixel class labels produced from the previous stage are used to influence the local prior probability of the pixel in the current iteration. For a pixel located at image position (i, j), the neighbourhoods considered are

$$N_1 = \{(i-1, j), (i+1, j), (i, j-1), i, j+1)\} \quad (3)$$

and

$$N_2 = N_1 \cup \{(i-1, j-1), (i+1, j-1), (i-1, j+1), (i+1, j+1)\} \quad (4)$$

where N_1 is referred to as a *first-order neighbourhood* and N_2 a *second-order neighbourhood*. The distinction is necessary because the distance between first-order neighbours is 1.0 and the remaining neighbours is $\sqrt{2}$. This difference is taken into account in the algorithm.

A count n_k of neighbour class labels is made (that is, there are n_k neighbours having class label C_k) and the probability of the pixel belonging to class k given neighbourhood N is calculated by:

$$P(C_k|L_N) = A^{-1}e^{0.5(\alpha_k + \beta_k n_k)} \quad (5)$$

where L_N denotes the labelling of pixels in N, α_k and β_k are user controlled parameters, and A is a normalising constant.

Hence the probability of a class label is increased as a function of n_k. If n_k is large then the probability will increase and visa versa for a low value of n_k. The constant A is used to keep the sum of the probabilities for all classes equal to 1. The parameters α_k and β_k are used to *tune* the system.

3.3 Posterior Probabilities

Results from sections 3.1 and 3.2 are combined to form the posterior probabilities of class membership. The values are calculated as:

$$P(C_k|\underline{x}_m, L_N) = \frac{f_k(\underline{x}_m, \bar{\underline{x}}_k, \underline{V}_k)P(C_k|L_N)}{\sum_z f_z(\underline{x}_m, \bar{\underline{x}}_z, \underline{V}_z)P(C_z|L_N)} \quad (6)$$

If super-classes are specified (a class that is made up of two or more classes), then the posterior probability for a pixel belonging to each super-class is evaluated by simply adding the probabilities for all its member classes.

4 Algorithm Pseudo Code and Complexity

The pseudo code for the critical section of the serial code implementation is shown below. The loop I controls the number of iterations, L is the number of image lines, P is the number of image pixels per line, N is the number of image bands and C is the number of classes. The functionality of the pseudo code functions correspond to the appropriate descriptions given in section 3.1.

```
INITIALISATION()
for all I {
    for all L {
        for all P {
            if (I !=  first) then for all classes SPATIAL_PROCESSING()
            for all classes SPECTRAL_PROCESSING()
            if (I == last) then for all classes TYPICALITY()
            for all classes POSTERIOR_PROBABIITIES()
            for all super classes AGREGATE_POSTERIORS()
        }
    }
}
```

The complexity of the calculation is O[ILPCN^2]. Of the functions in the critical loop, SPECTRAL_PROCESSING() has the highest order, being proportional to N^2.

5 Exploiting Parallelism—Mapping Data to Processors

From the algorithm complexity equation it is observed that a number of variables affect the computation time. Typically, the total number of pixels LP in the image is the dominating factor, being several orders of magnitude greater than that of the number of PEs. All other variables have dimension less than that of the number of processors available, hence parallelism in pixel processing was used.

The volume of data typically processed precludes loading the entire image into the DPU and hence sections of the image must be processed separately. Further, band-interleaved by line (BIL) data format was specified for input and output files making lines of image data a convenient partition. As the dimension of an image line are of the same order as that of the number of PEs i.e. 2048, it was convienient to spread the pixels of the line across the PE grid, with one pixel (and corresponding calculation) per PE. The pixel iteration loop in the serial code thus became redundant.

Spectral processing does not impose any constraints on the relative orientation of pixels on the PE grid and as such data could be mapped to the grid in any fashion. The determining factors for choosing an image line to PE grid mapping was the requirements of spatial processing and efficient I/O routines. Considering only spatial processing, it would seem natural to locate a pixel at grid position (i, j) with neighbours at locations as defined for N_1 or N_2 and make use of the X-net operations that explicitly represent these directions.

The I/O mapping from BIL format to this scheme would be complicated and, as a consequence, suffer inefficiencies such as unnecessary file seeks. Further, I/O is potentially more time consuming than spatial processing so it was given greater importance.

Pixels are mapped in a raster scan fashion across the PE grid, such that the grid can be considered a one-dimensional array of processors. This is similar to the scheme adopted for CLIP4S [7] in which a small rectangular array was rejected and replaced by an array 512×4 which scans down an image row by row. When the image row is larger than the number of processors, *virtualisation* occurs. The virtualisation used is the MPFORTRAN one-dimensional array default—*cut and stack*. That is, if N is the number of processors and m is a non-negative integer, pixel $mN + i$ maps to PE i. All data dealing with an image pixel were mapped in this way.

A simple scheme using three rotating buffers was used for spatial processing. Each buffer contains one line of class labels produced from the previous iteration. Given this scheme, a PE stores locally its own label and the labels of its north and south neighbours. Labels of other neighbours are assessed by comunicating with the left and right PE, which corresponds to a PE grid raster shift operation which is efficiently handled by X-net communications.

	Iteration 1	Iteration 2	Iteration 3	Total Time
Serial Time T1 (sec)	5099	6010	15255	26364
Parallel Time T2 (sec)	325	360	594	1279
Ratio T1/T2	16	17	26	21

Table 1: Classification times for the processing stages.

6 Computational Performance

A test area of Landsat TM data was processed on the DECmpp and on a SUN SPARC II workstation and the computation times recorded in table 1. The dataset consisted of 2170 lines with 2048 pixels per line and 6 bands per pixel. Spectral signatures for 106 classes were used which were grouped into 5 super-classes.

From the tables a number of observations can be made:

- On average the parallel implementation was 21 times faster than the serial version.
- The first iteration is the least time consuming as the only calculation performed is SPECTRAL_PROCESSING(). In fact, in all but the last iteration only the exponent of equation 2 is calculated.
- Comparing iterations 1 and 2, SPATIAL_PROCESSING() is not that expensive in terms of computation time, and comparing this difference with the total time for iteration 3, the computation time for SPATIAL_PROCESSING is insignificant.
- The final iteration is the most expensive accounting for almost half (46%) of the entire computation time.

Time profiling of the parallel code revealed computation time was: 45% front end (FE), 50% DPU and 5% FE-DPU communication. Function profiles revealed that SPECTRAL _ PROCESSING() accounted for 50%, TYPICALITY() 10% and SPATIAL _PROCESSING() 3%, I/O was insignificant and the remaining 37% was spent by the FE servicing the DPU. Function profiles suggested that of the 45% total time consumed by the FE, most of it (37/45) was actually used to set up communications in some form or other with the back end (BE), which, once set up, FE to BE communication acounted for 5% of the total time.

The time spent by the FE servicing the DPU is an artifact of the MPFORTRAN compiler, which places scalar operations on the FE which then have to be communicated to the DPU (this includes indexes to arrays). This extra time could be eliminated by an MPL version of the code which can perform scalar operations on the ACU, thus avoiding costly FE to DPU communications. However this would incur much more code development time.

7 Conclusions

This paper has decribed the porting of a heavily used classification algorithm to a SIMD machine to enable higher throughput. The DEC MPFORTRAN compiler provided a convenient means for creating a massively parallel version of the existing FORTRAN 77 coded algorithm. Because of the implicit nature of the MPFORTRAN parallel constructs, the DEC MPPE debugging environment provided an invaluable tool for code development as it allowed easy tracing of DPU arrays and array mappings.

The algorithm was well suited to a SIMD architecture as it used pixel-based as well as local pixel neighbourhood operations. Hence considerable computational improvements would be expected over a serial implementation. Testing has shown a computational advantage of 21 times over that of a SUN SPARC II. As with all high-level languages, there are limitations revealed when implementing one particular algorithm. Analysis of the performance of the MPFORTRAN compiler reveals that the performance of the parallel code is front-end CPU bound. This can be improved by implementation of the critical routines in C using the DEC MPL compiler.

8 Acknowledgements

This work was supported by a grant from the DEC External Research Programme which funded P.A. Caccetta and the DECmpp. Further funding and the data were supplied by the CSIRO Division of Mathematics and Statistics.

References

[1] K. E. Batcher. Design of a massively parallel processor. *IEEE Transactions on Computers*, C-29(9):836–840, September 1980.

[2] J. E. Besag. On the statistical analysis of dirty pictures (with discussion). *Journal Royal Statistical Society Series B*, 48:259–302, 1986.

[3] N. A. Campbell. some aspects of allocation and descimination. *Multivariate Statistical Methods in Physical Anthropology*, pages 177–192, 1984.

[4] S. Campbell and G. A. W. West. Parallel implementation of salience distance transforms. In *Proceedings of PART-95, Perth, Western Australia*, 1995.

[5] T. J. Fountain. CLIP4: A progress report. In M. J. B. Duff and S. Levialdi, editors, *Languages and Architectures for Image Processing*, pages 283–291. Academic Press, London, 1981.

[6] T. J. Fountain. The development of the CLIP7 image processing system. *Pattern Recognition Letters*, 1:331–339, 1983.

[7] T. J. Fountain, M. Postranecky, and G. K. Shaw. The CLIP4S system. *Pattern Recognition Letters*, 5:71–79, 1987.

[8] C. J. Hilditch. Linear skeletons from square cupboards. In *Machine Intelligence IV*. Edinburgh University Press, Edinburgh, 1969.

[9] L.L.F Janssen and H. Middelkoop. Knowledge-based crop classification os a landsat thematic mapper image. *International Journal of Remote Sensing*, 13:2827–2837, 1992.

[10] H. T. Kiiveri and N. A. Campbell. Allocation of remotely sensed data using markov models for image data and pixel labels. *Australian Journal of Statistics*, 34(3):361–374, 1992.

[11] J. B. Rosenberg and J. D. Betcher. Mapping massive SIMD parallelism onto vector architectures for simulation. *Software—Practice and Experience*, 19(8):739–756, 1989.

[12] J .F. Wallace and G. A. Wheaton. Spectral discrimination and mapping of land degredation in western australia's agricultural region. In *5th Australiasian Remote Sensing Conference, Perth Western Australia*, pages 1066–1073, 1990.

DEVELOPMENT OF A STEREOSCOPIC IMAGE PROCESSING SOFTWARE

Nobuhiko Mori
Earth Remote Sensing Data Analysis Center (ERSDAC)
Forefront Tower, 3−12−1, Kachidoki, Chuo−ku, Tokyo 104, Japan

Abstract

A digital stereoscopic image processing software has been developed on a personal computer (PC) system. The system was originally developed as a digital photogrametric system, and had a special three dimensional(3D)display module which could display stereoscopic drawings together with stereoscopic images. The stereoscopic drawings were used as a tool of man−machine interface. For instance, stereoscopic points on stereoscopic images were used to inform the positions of some stereo conjugate points to computer, and to correct the results of computer stereo matching. The functions of the stereoscopic image processing software which have been developed on this system are mostly similar to those of an ordinary two dimensional image processing software. Using the software, images can be processed, overlaid and changed into stereoscopic images. Further more, this system has a special ability to draw stereoscopic graphics on stereoscopic images, and this stereoscopic graphics can be used as a tool of man−machine interface. This ability has been taken over from the digital photogrametric system. This software can be used widely where geographical information is necessary. As an application example, stereoscopic images which can be used in earth resource exploration field have been made using this software, and presented here.

1. Introduction

Topographic information is very important in many application fields, such as earth resource exploration, route selection (road, pipeline, etc.), dam construction and wide area development. However, it is very hard to get topographic information on digital systems because usually they have only two dimensional display. Some digital photogrametric system have 3D display, but no sufficient image processing software attached. In this work, a stereoscopic image processing software has been developed on a PC system with 3D display. This system was originally developed as a digital photogrametric system, but now the ability of a digital stereoscopic image processing system is developed.

This system has a special 3D display module, which has an ability to display stereoscopic drawings together with stereoscopic images. Figure 1 shows the function of the 3D display module. In figure 1, stereoscopic drawings are memorized in Video Random Access Memories (VRAM), and stereoscopic images are in Frame Memories. Left image and drawing, and right image and drawing are overlaid respectively and displayed on a display one by one alternately. Observer can get a stereoscopic view by using liquid crystal shutter glasses,which are synchronized with the display. By using this module, this system get a special ability as man−machine interface.

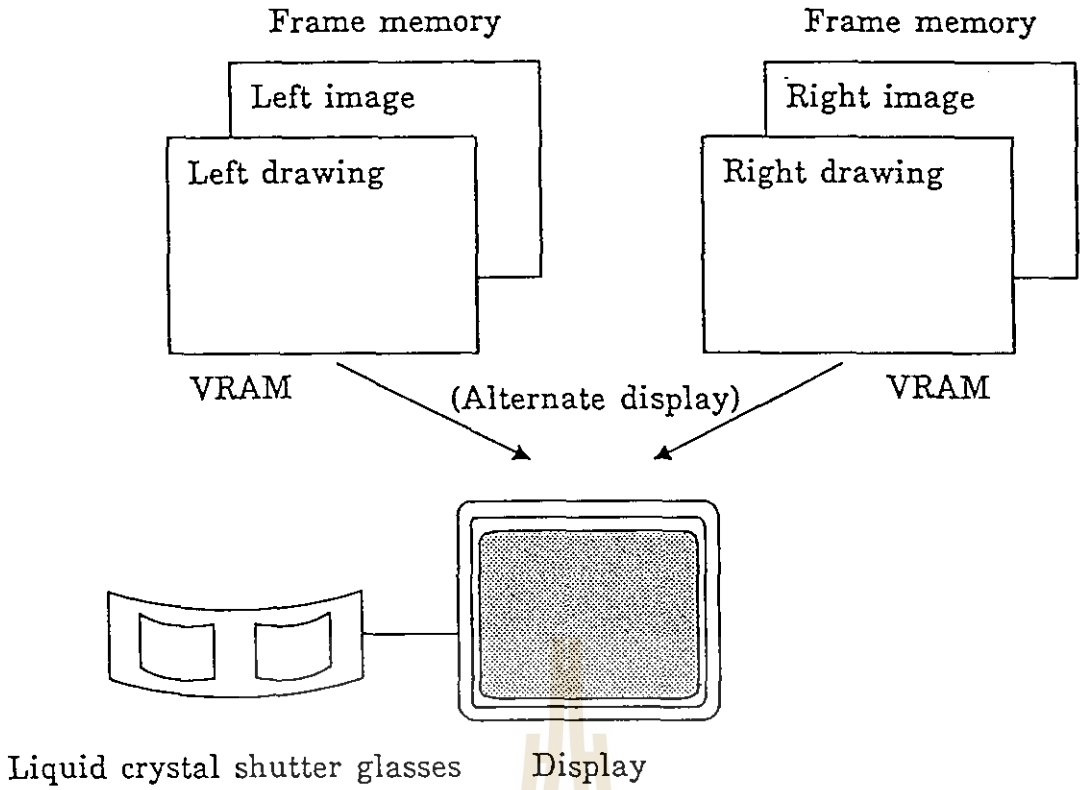

Figure 1 The function of the 3D display module

2. Man–machine interface in DEM extraction from digital stereoscopic images

Generally speaking, image recognition is very difficult for a computer because there are too many informations in images to be analysed. It is also true in the case of stereo matching, which is one technique to determine stereo conjugate points automatically with digital photogrametric systems. Now the errors of stereo matching are very serious problem for automatical DEM extraction , because it is impossible to get rid of them completely by present computer techniques. Many methods are already proposed, but they all need to be improved. It seems that the best way is to get human help at appropriate stages. In order to get human help, man–machine interface (3D display module) is necessary. In automatical stereo matching, man–machine interface can be used to reduce matching errors at two stages, before and after the stereo matching.

Before the stereo matching, some stereo conjugate points can be informed to a computer by using the man–machine interface. Photo 1 is one example. In this case, 25 stereo conjugate points were informed to the computer, which were determined manually by using 3D display module. Because this module can display stereoscopic images together with stereoscopic drawings of points,the hight of the points can be easily ajusted to the hight of earth surface of images by using a mouse device.

Photo 2 is another example.In this case,stereo conjugate lines were informed to the computer. These lines were drawn one by one along the earth surface of images with a mouse looking at the 3D image through liquid crystal shutter glasses. The sequence to draw these lines are as follows.

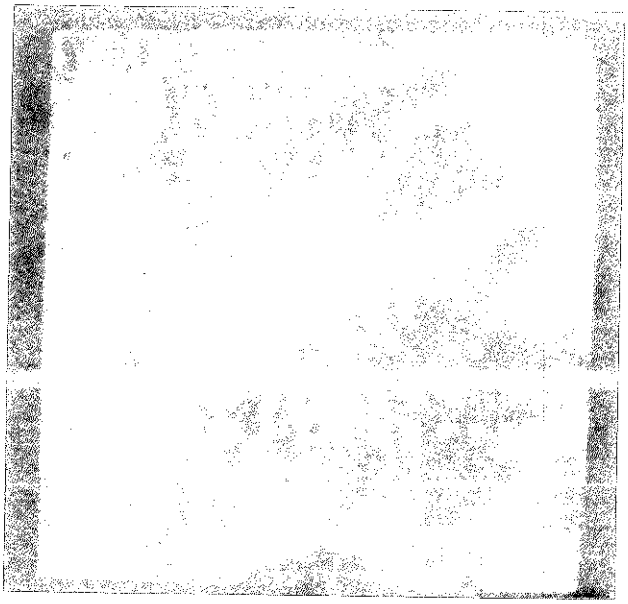

Photo 1 Manually determined stereo conjugate points

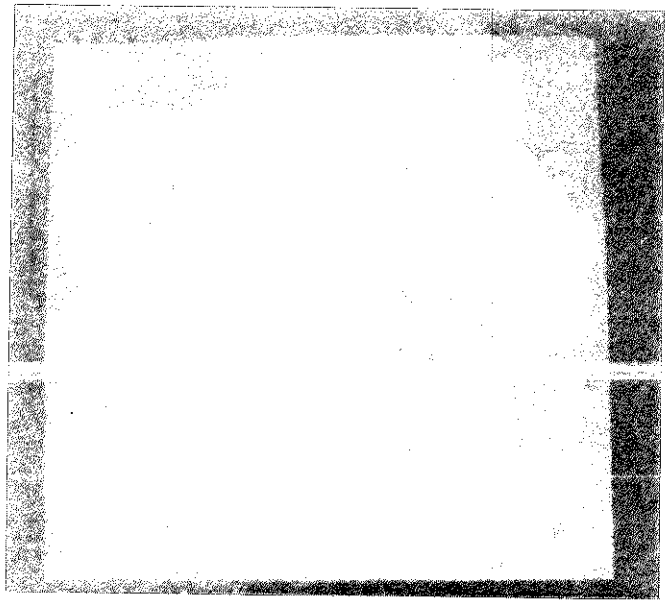

Photo 2 Manually drawn stereopair lines

1)First draw one line of stereopair along a valley or a ridge in one (left or right) image.
2)Next draw the second line just on the line mentioned above in the other image.
3)Repeat these two kinds of drawings.

These lines are very useful for automatical stereo matching because the accuracy of stereo matching is usually bad at valleys and ridges when a small area correlation method is used.

After the stereo matching, the errors of automatically determined stereo conjugate points can be corrected by using the man–machine interface. Photo 3 is a simultaneous display of stereoscopic images and stereo conjugate points determined automatically. When observed through liquid crystal shutter glasses , correct points are positioned on the surface of a model of a mountain and error points are positioned in the air or under the ground. These error points can be corrected by the mouse easily. In the photo, a pair of big cross marks indicate the points under correcting.

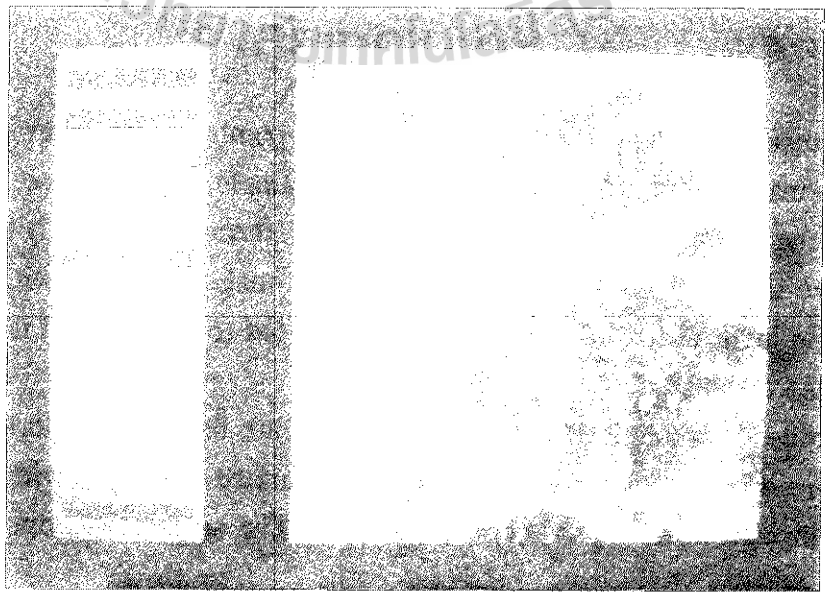

Photo 3 Simultanious display of stereoscopic images and stereo conjugate points

3. Development of a general purpose stereoscopic image processing software

A stereoscopic image processing system is very useful in such field that needs topographic information, especially when it has man–machine interface function mentioned above. Since there are now scarcely any stereoscopic image processing systems which have these abilities, it has been planed to develop such a system. Because there was a digital photogrametric system which was already developed using a general purpose personal computer with 3D display, it was selected to develop some general purpose stereoscopic image processing programs on this system. The programs were developed on the OS of the personal computer, MS–DOS. The functions of the programs developed on this system were as follows: enlargement and reduction, brightness enhancement, affin transformation, calculation between images, cutting out and displaying a part of a big image, etc.. A program which produce stereoscopic images from a digital orthoimage using DEM is also developed.

Photo 4 and 5 show the example of enlargement. Photo 4 is an alternative display of stereoscopic images,and the operator can get a stereoscopic view through liguid crystal shutter glasses.

A square in the photo, the size of which is determined from the rate of enlargement, is overlayed on one of the stereoscopic images. The operator can move the square in the stereoscopic view with a mouse, and can select the place to enlarge. Photo 5 is the enlarged image of the place selected in photo 4, and the operator also can get a stereoscopic view by looking at the images in photo 5.

Photo 4 Selection of the place to enlarge by a square

Photo 5 Enlarged image of the selected place

A 3D graphic program, which can draw stereoscopic points, lines, circles, etc., has also been developed to serve a tool of man--machine interface to the system using the two dimensional graphic programs provided in the OS, MS-DOS. Photo 1 is an example of writing stereoscopic points on stereoscopic images. Photo 2 is another example of writing stereoscopic lines on stereoscopic images. In this case, stereopair lines are written one by one. Photo 6 is another example of drawing stereoscopic lines. In this case, stereopair lines can be writen at one time, but the hight of the line in the 3D image can not be changed. This mode can be used to draw contour lines.

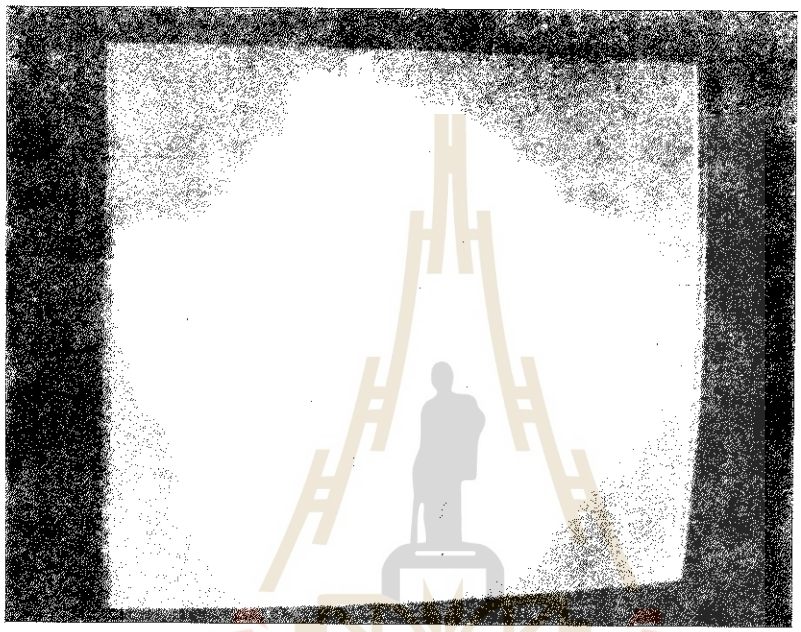

Photo 6 Drawing stereopair lines at one time

4. An example of the utilization of stereoscopic image processing

This stereoscopic image processing software can be used in many fields,such as earth resource exploration, route selection, dam construction, wide area development, etc.. The experiments of the utilization of this software have already been done in some fields. Photo 7 is an application example in the field of earth resource exploration. In the photo 7, broken lines are faults, filled dots are hot springs and small marks like eyes are veins. These informations were written on a orthoimage using the calculation program developed in this system, and then transformed to stereoscopic images. The B/H ratio of these stereoscopic images is 0.5, which is the most suitable value in this case. Looking at these stereoscopic images with liquid crystal shutter glasses, observers can get a precise topographic information together with images and other important informations, can draw dots and lines on these stereoscopic images to indicate the results of image analysis.

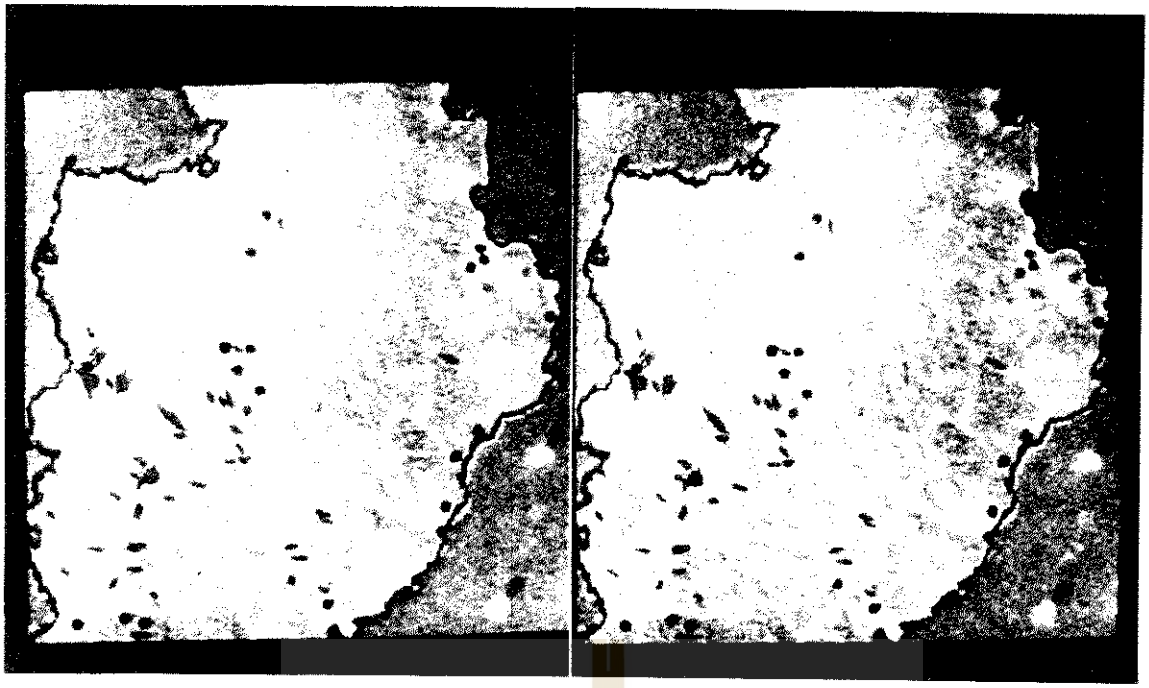

Photo 7 An example of stereoscopic image processing

5. Conclusion

A stereoscopic image processing software has been developed on a PC system which was originally developed as a digital photogrametric system. The system has a special 3D display module which has an ability to display stereoscopic drawings together with stereoscopic images.

Besides usual image processing programs, the functions of which are similar to ordinary ones in a two dimensional image processing system, a 3D graphic program has also been developed. The latter one can be used to draw stereoscopic points, lines, etc., on stereoscopic images. By using this system, many informations about stereoscopic images can be informed from operator to computer. This system has a powerful man–machine interface ability. The usefulness of this ability has been explained in this paper in the field of digital photogrametry and earth resource exploration. This system has high application potential in many fields.

Finally I would like to express my appreciation to the members of Murai laboratory in Tokyo university and NEC corporation for their contributions to this research.

[Reference]

1.M.Boulianne,P.A.Gagnon,J.P.Agnard,C.Nolette;Large Scale Map Revision Using a PC–Based Videoplotter;ISPRS Com.4,Tsukuba,May,1990,pp.273–279

2.N.Mori,S.Murai,X.Bai;Development of a New Method Attaching Precise Topographic Information to GIS by Using 3D Display;ACRS,China,Nov.,1990,pp.H·2·4·1–H2·4·6

3.N.Mori,T.Tagawa,S.Murai,S.Ito;DTM Extraction and Its Application Using a Digital Stereoscopic Image Processing System with 3D Display;ACRS ,Singapore,Nov.,1991,pp.p·8·1–p·8·6

4.N.Mori, S.Masuda, S.Murai ; Development of a PC–Based Digital Photogrametric System ; ISPRS,Washington,Aug.,1992,B2–2,pp.319–322

Classification Methodology for Land Cover Mapping Using Global Monthly 8-Km AVHRR Data

Wen Cheng-gang and Ryutaro Tateishi

Center for Environmental Remote Sensing (CEReS)
Chiba University,1-33 Yayoi-cho,Inage-ku
Chiba 263 Japan
FAX: +81-43-290-3857
Email: wen@rsirc.cr.chiba-u.ac.jp

Abstract

For the purpose of land cover classification of the global area, phenological information and temperature information were used by NDVI and Channel 4 of NOAA/NASA Pathfinder AVHRR Land Cover DATA Set. Phenological information includes onset of greenness, duration of greenness, green peak, total NDVI and a result of cluster analysis of 12 monthly NDVI. These feature images were used in order to identify ground truth data from existing maps .

Introduction

Phenological differences among vegetation types, reflected in temporal variation in the Normalized Difference Vegetation Index (NDVI) derived from satellite data have been used to classify land cover of Asia. The objective of this research is to examine and illustrate the value of NOAA AVHRR data for the investigation of vegetation phenology. Specially, we are concerned with the depiction of the land cover of very large areas over time. Phenology is generally accepted as including not only the timing of recurring biological events but also their causes, especially with regard to meteorological phenomena.

Data Sources

10-days composites of NOAA/NASA Pathfinder Land Data Set with8Km resolution were used in this study, and is georegistered to GOOD map projection. The size of the data are 5004 rows by 2168 columns.

Composite method

In one month, three 10-days composite data sets are included. The data sets

consist of NDVI, CLAVR flag, QC flag, Scan Angle, Solar Zenith, Relative Azimuth, Ch1 Reflectance, Ch2 reflectance, Ch3 Btemp, Ch4 Btemp, Ch5 Btemp and Day of Year . In order to remove noise and cloud, the monthly composite data were produced by the maximum composite method as follow:

(1) If a 10-days composite NDVI value of a pixel in one month is larger than 0.656, this value is eliminated as a noise.

(2) If there are one or two or three 10-days composite NDVI value of a pixel in one month corresponding with no-cloud status are below than 0.656, the average of these NDVI values is assigned to a monthly NDVI value. The average of coincident 10-days composite channel 4 values is also calculated as a monthly channel 4 value.

(3) If there is no 10-days composite data corresponding with no-cloud status but there are one or two or three 10-days composite data with mixed cloud status of a pixel in one month, the maximum NDVI value below than 0.656 is chosen as a monthly NDVI value. The coincident 10-days composite channel 4 value is also chosen as a monthly channel 4 value.

(4) If there is no 10-days composite data corresponding with no-cloud or mixed status of a pixel in one month, the maximum NDVI value below than 0.656 is chosen as the monthly NDVI value. but if all 10-days composite NDVI value are larger than 0.656, the minimum NDVI value is chosen. The coincident 10-days composite channel 4 is also chosen as a monthly channel 4 value.

The NDVI is defined by the equation as followed:

$$NDVI = (ch2 - ch1) / (ch2 + ch1)$$

where ch1 represents value from the visible channel (0.58 - 0.68 μm) and ch2 represents value from near-infrared channel (0.725 - 1.1 μm). The NDVI is then scaled to Binary NDVI by following equation :

$$Binary\ NDVI = (NDVI / 0.008) + 128$$

the range of Binary NDVI value is from 3 to 253.

Image Classification

Land cover classification is carried out by analyzing monthly NDVI composite

spanning the January to December 1990 period. Through visual interpretation, an NDVI threshold of 0.2 was selected to separate much vegetation and less/no vegetation lands. The threshold was determined by comparison of the strata to available maps and imagery from different countries and regions in Asia and Oceania.

An unsupervised clustering algorithm was used to define 78 phenological classes using 12 monthly NDVI data sets.

Land Cover Characterization

Using the 12 monthly NDVI data sets, the following phenological feature images were developed ,

(1) Onset of Greenness -- The month in which the NDVI value first rose above the threshold.

(2) Period of Greenness -- The number of month when the NDVI reached or exceeded the threshold value.

(3) Peak of Greenness -- The month in which maximum NDVI occurred.

(4) Total NDVI -- The means of monthly NDVI through 1990.

These images were derived through analysis of individual class NDVI statistics produced from the 12 monthly NDVI composites. Interpretation of temporal NDVI means led to the identification of the four interpretive images. The four factors are strongly related to the phenologic cycle of vegetation. The month in which the NDVI increases dramatically corresponds to the time of emergence of green vegetation at beginning of the growing season. The month of maximum NDVI reflects the time of maximum photosynthetic activity. The time that the NDVI exceeds a certain threshold value is similar to the length of growing season. The average of NDVI through one year generally reflects total photosynthetic activity or net primary productivity.

Summary and Conclusions

The previous examples of imagery about phenology in demonstrate that the AVHRR system provides us with a tool with which we can monitor the seasonal dynamics of world's vegetation at a very broad range of scales. Through the daily coverage of the AVHRR system combined with temporal compositing of NDVI we can obtain essentially cloud-free imagery for the entire land surface of the Earth on a regular and timely basis. The NDVI has been shown to be related to greenness activity and as such provides a useful means by which to monitor vegetation phenology.

Although this paper has only presented the role of 8Km coarse resolution data for vegetation monitoring, authors believe that AVHRR system should be used in conjunction with high-resolution sensors and systematic ground data collection to

NDVI90_CLUSTERING
1 3
4-5
6-9
10-13
14-15
16-18
19 22
23-24
25-30
31
32-34
35-38
SEA
39-41
42-46
47-51
52-57
58-61
62-68
69-70
71-72
73 74
75
76
77-78

provide the means for better management of the Earth's resources.

In conclusion, we believe that the science and society community now has a new important source of data to provide quantitative information on the vegetation of our planet to answer questions which have been unanswerable due to the lack of spatially comprehensive and reliable data.

References

Thomas R. Loveland, James W. Merchant, Donald O. Ohlen, Jesslyn F. Brown, 1991, Development of a Land-Cover Characteristics Database for the Conterminous U.S., Photogrammetric Engineering & Remote Sensing.

Ryutaro Tateishi and Wen Cheng-Gang, 1994, Land Cover Database of Asia

Land Use/ Land Cover Change Detection In the Chiang Mai Area Using Landsat TM

Somporn Sangawongse
Department of Geography and Environmental Science,
Monash University, Clayton, Victoria 3168, Australia

ABSTRACT

The rapid growth of Chiang Mai city in Northern Thailand has resulted in much change in land use and land cover over time. Some changes occurred very rapidly and have had an adverse effect on the environment, and therefore there is a necessity to monitor these changes on a regular basis. The use of multi-temporal Landsat TM imagery for monitoring land cover change has proven to be the best tool in this study. Suitable change detection techniques were developed for the Chiang Mai area by taking into account its physical and cultural conditions, thereby optimising use of information in the land cover maps. Results showed that forested areas have decreased by about 29% during 1988 to 1991, while agricultural lands and built-up areas have increased by about 5% and 26% respectively. The image processing system used in this study was microBRIAN.

1 INTRODUCTION

Chiang Mai, the second largest city in Thailand, is located approximately 700 kilometers to the north of Bangkok. Its surroundings are experiencing much change in land use and land cover. Due to the rapid growth of population and the expansion of commerce and industry at the present time, urban and suburban/industrial land is sharply increasing. The expansion of the city has resulted not only in the depletion of natural resources, but the deterioration of the environment (Surarerks, 1992). Agriculturally productive land and forest lands have been converted into residential and other uses. Evidence of the rate of change is found in time series of Landsat TM imagery and can be documented using various change detection techniques. This paper reports on the application of remote sensing techniques to map land use/land cover patterns as well as to detect areas of change using dry season image data of the Chiang Mai area as an example.

2 THE STUDY AREA

Chiang Mai city and its surroundings was selected for this study. The study site lies approximately between 18° 40′ and 19° 00′ N latitude and between 98° 55′ and 99° 10′E longitude (Figure 1). It encompasses the administrative districts of Mae Rim, Muang, Hang Dong, Saraphi, Sansai, Sankamphaeng and Doi Saket. The size of the study area corresponds to the 1002 by 1236 pixels of the Landsat TM image subscene which covers four 1:50000 scale topographic mapsheets (4746I-II and 4846III-IV) of the Royal Thai Survey Department (1969). The total area accounts for about 111,460 Ha.

3 METHODOLOGY

Landsat- 5 TM digital data, path/row 131/47, of February 9, 1988, and February 17, 1991 were employed in this study. This data set was supplied by the Thailand Remote Sensing Center (TRSC), National Research Council of Thailand. Criteria to the selection of the multi-temporal Landsat data set involved assessment of cloud cover percentage , time of acquisition, and sensor type so that change detection scope was optimized.

In order to obtain the maximum information from Landsat TM used for image processing for land use/land cover change study, the selection of optimum Landsat TM bands is necessary. There are many different ways to select the optimum bands, such as the use of entropy criterion (Chen et al., 1986), calculation of transformed divergence between classes (Swain & Davis, 1978; Mausel et al., 1990), optimum index factor (OIF)(Chavez, et al.,1984) ; analysis of variance and covariance of the image scene (Sheffield, 1985) and

[1] Presented at the 16th Asian Conference on Remote Sensing, at Suranaree University of Technology, November 20-24, 1995.

image differencing of a suitable band, and Principal Components Analysis (PCA) of bands (Horler and Ahern, 1986 ; Byrne et al., 1980). In this study, the selection of TM bands was based on PCA and an OIF technique. PCA is regarded as one of the most effective ways to reduce the redundant information (of highly correlated bands) contained in Landsat TM data, while retaining the useful information. The OIF offers the optimum combination of triplet bands by order, based on the standard deviation and the coefficient correlation of the image statistics (ILWIS User's Manual 1993). Procedures followed the application of PCA and OIF have been extensively detailed in Sangawongse (1995).

To ensure overlay precision for change detection purposes, a geometric rectification was conducted (on microBRIAN version 3.01-PC based software) using image-to-map and image-to-image techinques. More detailed descriptions regarding geometric rectification and resampling can be seen in Sangawongse (1995).

Various change detection techniques were applied on both TM images individually. The change detection techniques used here have been developed to take into account the physical and cultural conditions within the study area, as well as the characteristics of any change detection algorithms that are appropriate to the image data (Jensen, 1981). Two major approaches were found to be best suited to the study area in terms of either ground conditions and the algorithms used. These approaches are: 1) change detection based on two-date classification; and 2) change detection based on image ratioing.

3.1 Change detection based on two-date classification

This method has been developed from a number of previous studies (Ahmad, 1992; Monkolsawat and Thirangoon 1990; Wara-Aswapatti, 1990; Singh, 1986). Using this method, both actual and temporal changes in land use/land cover between different dates can be detected.

In order to extract the maximum information on land use/land cover in the study area, classification using the best band combinations of Landsat TM imagery was emphasized. As the classified images were to be used as inputs for change detection analysis later, they had to be classified as accurately as possible. Monkolsawat and Thirangoon(1990) and Ahmad (1992) have pointed out that the accuracy of the output image is greatly dependent upon the accuracy of the input images used for a classification.

Classification procedures were applied on each Landsat TM scene separately by using the supervised classification method. For Landsat TM scene 1988, some possible combinations (as indicated by OIF) such as 2,3,4 and 3,4,5 were chosen for the supervised classification using minimum distance to means, and maximum likelihood classifiers. The supervised classification technique is preferred, because the data of the study area is available and the author has a prior knowledge of the study area.

There are 24 training areas (2030 samples) used for the supervised classification of this image. These training areas were delineated from a false color composite image generated from two combinations (2,3, 4 and 3,4,5). Training areas represent a wide range of land use and land cover within the study area, e.g. forests, agricultural field and orchards. To avoid misclassification, these training areas must be as homogeneous as possible. Ancillary data such as soil map and vegetation map were considered during the selection of training areas in order to obtain the greatest accuracy of the classification results (Hutchinson, 1982).

For Landsat TM scene 1991, it was found that the visibility of this scene is not clear due to atmospheric effects such as haze and the increased air pollution in the city mainly caused by increased number of motor vehicles. In order to remove/reduce atmospheric effects, Normalized Difference Vegetation Index (NDVI) image was considered as another channel of information for extracting land use and land cover patterns from this scene.

Some possible combinations of different bands together with NDVI were tested at different times in order to obtain the best result . In the end, the combination of all bands was chosen for the classification of the 1988 scene , whereas the combination of 2, 3, 4, 5 and NDVI was applied to the 1991 Landsat scene . The inclusion of NDVI as another channel in this classification has offered considerable benefit, not only for extracting the maximum information on vegetation, but also for eliminating the shadowing effects caused by topography and sun angle (Holben and Justice, 1980).

Twenty five training areas (1458 samples) were used for classifying this image into 15 different classes using a maximum likelihood classifier. These training areas were also chosen from the same band combinations as the 1988 one.

Actual change can be obtained by a direct comparison between classification result from one date with that from the other date. Temporal changes that have occurred between the two dates can be measured by performing a change matrix (Howarth and Wickware, 1981). The change matrix was created in three stages: (1) to combine the classification channels of two Landsat scenes together; (2) to calculate changes between two dates using an appropriate formula; and (3) to crosstabulate two image channels as a means of portraying pixels in the classified images into a matrix (CSIRO and MPA, 1993). The change image was created by using the following formula: (Jupp 1993-pers.comm)

$$ij = ci + (cj - 1) * N2$$

where i is the number of elements in the matrix by row;
j is the number of elements in the matrix by column;
ci provides the rows and has N1 levels (i =1.....N1);
cj provides the columns and has N2 levels (j =1.....N2);
N1 and N2 are the number of levels in the rows and columns respectively.

The output image was rescaled into the range of 1 to 225 (15 * 15 matrix) digital values, which can be painted to enhance where changes occur. These values contain the number of pixels that have been changed from February 1988 to February 1991.

3.2 Change detection based on image ratioing

This technique has been successfully applied by many authors for the study of land use/land cover change (e.g. Howarth & Wickware, 1981 and Howarth & Boasson, 1983). Because of its simplicity and efficacy, it was selected as one of the techniques for examining changes in the study area.

In this study, band 3 (visible red) from the February 9, 1988 scene was divided by band 3 from the February 17,1991 on a pixel-by-pixel basis. Band 3 for Landsat TM (similar to Landsat MSS band 5) which has band width between 0.63-0.69 micrometer was chosen because it is useful for discriminating between many plant species as well as for determining soil boundary, geological boundary delineation and cultural features (Howarth and Boasson, 1983).

Also, bands 4 from both Landsat TM scenes, which have similar wavelength to Landsat MSS band 7 were ratioed in the same manner as bands 3.

Areas of change in the study area can be enhanced by producing a False Colour Composite (FCC) image (Howarth and Wickware 1981). The FCC image can be created by two ways: (1) assigning band 3 ratio to the red gun, band 4 ratio to the green and blue guns respectively and (2) assigning TM 3 or TM 4 of date one on the red gun, TM 3 or TM4 of date 2 on the green gun and either ratioed 3 or 4 image on the blue gun for examining localized change.

5 RESULTS AND DISCUSSION

5.1 Results obtained from two-date classification for change detection

Land use/land cover in the 1988 and 1991 image scenes was classified into 15 categories equally. The accuracy assesment was conducted for both classified data (Congalton, 1991) to obtain an overall accuracy level of 82% and 85% for the 1988 and 1991 respectively. The land use/land cover statistics derived by a direct comparison between the two classified image data are represented in Table 1. It was found that the use of some possible combinations for classifying the 1988 image did not provide a satisfactory result as indicated by difference between the classified image and the ground data. For example, the 234 band combination did not provide accurate information on built-up areas. A paddy field to the south-west of the Chiang Mai international airport was mis-classified as belonging to a high density built-up area. Nor did it provide good enhancement on water bodies. For this reason, the overall TM bands (except the thermal band) was chosen for extracting information on land use from the 1988 scene so that, regardless of data handling problem, all information contained in these original bands would be assessed. Another reason is that this data has a good quality in terms of stability and is less subject to noise (Jupp, 1994-personal communication).

Classification of the 1991 Landsat TM scene using the combination of bands 1-5 and 7 to give correspondence to the 1988 image yielded poor results. In particular, some shadows in the mountains were misclassified as belonging to water bodies.

The change image constructed by performing change matrix yielded 225 possible land cover changes in the study area (see Table 2). In Table 2, the number of unchanged pixels are represented by values along the diagonal of the matrix, while the number of changed pixels are represented by values off the diagonal. It was found that 350398 pixels (31536 ha) had not changed, while the number of changed pixels totaled 888074 (79927 ha). Only 14 major changes were considered meaningful in the comparison to the ground truth information, so that they were maintained in the change map as shown in Figure 2.

The biggest change was found from dipterocarp forest to low density built-up areas, which accounts for about 10422 hectares. In a descending order, the changing from dry paddy field to low density built-up areas accounts for about 7537 ha; change from dipterocarp forest to vacant land use accounts for 6996 ha; change from dipterocarp forest to dry paddy field accounts for about 5205 ha, and change from dipterocarp forest to mixed field crops accounts for about 4127 ha (see Table 3).

5.2 Change results obtained from the ratio image

The result of applying this technique shows that changes have occurred between 1988 and 1991. Based on the false color composite image created by combination of bands 3 from two dates, and its ratio (Figure 3), green and blue colors obviously highlight areas of change, especially from dry paddy field to development land (mostly construction sites) and from dipterocarp forest to vacant land use. The prominent change areas are the green valley resort in Mae Rim district, the Mae Kwang dam in Doi Saket district and the housing estate near Hang Dong district, which clearly appears green.

Areas of no change appear deep red, for example, hill evergreen forest at Doi Suthep (Suthep Mountain), cropland in Sansai district, and soya beans cultivation in Hang Dong district.

A false color composite image created by combinations of bands 4 from two dates and its ratio does not give a satisfactory result compared with the first combination, therefore it is not acceptable.

6 CONCLUSIONS AND RECOMMENDATIONS

The application of any change detection technique may be unsuccessful if users do not have enough knowledge about its characteristics in relation to the conditions over the area of study. Generally, the use of more than one technique is preferred by many researchers, because they can compare the results derived , and finally select the best ones for their project.

The technique of change detection based on two-date classification has been found to be less restricted in terms of the algorithms used when compared with other change detection techniques. For example, the use of image differencing requires that the geometry of an image must be known as accurately as possible (about a quarter to half a pixel), otherwise substantial errors in change detection will occur.

Close phenological correspondence between the images is also required, in order to reduce errors in change detection. However, change detection based on two-date classification requires good results from a classification .

The most important factors that should be taken into account when performing change detection, as recommended by Jensen (1981), have involved the familiarity with the study area, the quality of the data set, and the characteristics of change detection algorithms.

It may be concluded that the use of Landsat TM for mapping land use/land cover change in the Chiang Mai area provided a satisfactory result if the appropriate techniques were used in data analysis. However, the research work on land use/land cover should be conducted on a regular interval, so that the information can be updated through time.

This research is further investigating the use of GIS data and sequential air photos of the test area as another means of studying land use/land cover change. The large scale of the air photographs allows comparatively accurate interpretation of the relevant land cover boundaries, and these can be recorded in the digital spatial data base through use of a Digital Elevation Model (DEM) (Salamanca Software Pty Ltd, 1992). Thus it can be demonstrated that older as well as more modern elements of the national

information infrastructure can be used to augment and to test the change detection results.

7. ACKNOWLEDGMENTS

I wish to acknowledge the Thailand Remote Sensing Center for providing the Lansat data for this research project. Thanks are given to resource persons, from both Thailand and Australia e.g. Prof. Vanpen Surarerks (Dept. of Geography, Chiang Mai University, Dr. David Jupp (CSIRO, Division of Water Resources, Canberra, Australia) for their useful suggestions and recommendations on my work. My appreciations also go to my supervisors, A/Prof Jim Peterson and A/Prof. Paul Bishop for thier assistance and encouragements throughout my research period.

8. REFERENCES

Ahmad, W. (1992). "The Use of Remotely Sensed Data in the Context of a GIS for Monitoring Temporal Changes in a Forested Region of Australia", Asian Pacific Remote Sensing Journal, Vol. 5, No.1, pp. 133-143.

Byrne, G. F., P. F. Crapper and K. K. Mayo (1980). "Monitoring Land Cover Change by Principal Components Analysis of Multi temporal Landsat Data", Remote Sensing of Environment, Vol.10, pp. 175-184.

Chavez, P. S., C. Guptill, and J. A. Bowell (1984). "Image Processing techniques for Thematic Mapper Data", Technical Papers, 50th Annual meeting of the American Society of Photogrammetry, Vol. 2, pp. 728-42.

Chen, S. C., Batista, G. T. & Tardin, A. T. (1986). "Landsat TM band combinations for crop discrimination", Symposium on Remote Sensing for resources Development and Environmental Management, Enschede, August.

Congalton, R. G. (1991). "A review of assessing the accuracy of classifications of remotely sensed data", Remote Sensing of Environment, Vol. 37, pp. 35-46.

CSIRO and MPA (1993). microBRIAN Application Notes. MPA Communications and CSIRO Australia.

Holben, B. N. and Justice, C. (1980). "The topographic effects on spectral response from nadir pointing sensors", Photogrammetric Engineering and Remote Sensing, Vol. 46(9), pp. 1191-1200.

Horler, D. N. H. and F. J. Ahern (1986), "Forestry Information Content of Thematic Mapper Data", International Journal of Remote Sensing, Vol.7/3, pp. 405-428.

Howarth, P. J. and Wickware, G. M. (1981). "Procedure for Change-detecting Using Landsat Digital Data". International Journal of Remote Sensing, Vol. 4, pp. 129-148.

Howarth, P. J. and Boasson, E. (1983). "Landsat Digital Enhancements for Change-detection in Urban Environment". Remote Sensing of Environment, Vol. 13. pp. 149-160.

Hutchinson, C. F. (1982). "Technique for Combining Landsat and Ancillary Data for Digital Classification Improvement". Photogrammetric Engineering and Remote Sensing, Vol. 48/1, pp. 123-130.

ILWIS User's Manual (1993). International Institute for Aerospace Survey and arth Science, Enschede, the Netherlands.

Jensen, J. R. (1981). "Urban Change Detection Mapping Using Landsat Digital Data". The American Cartographer, Vol. 8/2, pp. 127-147.

Jupp, D. L. B. (1993, 1994 and 1995). CSIRO, Division of Water Resources, Canberra ACT, Australia, personal communication.

Mausel, P. W., Kramber, W. J. and Lee, J. K. (1990). "Optimum Band Selection for Supervised Classification of Multi spectral Data", Photogrammetric Engineering and Remote Sensing, Vol. 56(1), pp. 55-60.

Monkolsawat, C. and Thirangoon, P. (1990). "Land Cover Change Detection Using Digital Analysis of Remotely Sensed Satellite Data: A Methodological Study". Remote Sensing, Soil and Water Management in North east Thailand, Technical Report Series.

Royal Thai Survey Department (1969). Topographic maps of the Chiang Mai area 4746I-II; 4846III-IV), scale 1:50000.

Salamanca Software Pty Ltd (1992). PHOTOGIS Users Guide. Hobart, Australia.

Sangawongse, S. (1993). 'Land Use Change in the Chiang Mai Area From Two-date Classification Analysis on Landsat TM Imagery: A Preliminary Results. Paper presented at the third International Conference and Exhibition on Computer-Aided Technologies, Queen Sirikit National Convention Centre.

Singh, A (1986). "Change Detection in the Tropical Forest Environment of North eastern India Using Landsat", Remote Sensing and Tropical Land Management (M. J. Eden and J. T. Pary eds), John Wiley & Son, Chichester, pp. 237-254.

Surarerks, V. (1992). "Land Use Change in Thailand and Its Impacts on Environmental Change", Proceedings of Asean Symposium on Global Environmental Change, Tokyo,1-2 December 1992, Centre for Global Environmental Research, National Institute for Environmental Studies Environmental Agency of Japan.

Swain, P. H. and Davis, S. M. (1978). Remote Sensing: The Quantitative Aproach, New York: McGraw-Hill.

Wara-Aswapatti, P. (1991). "Image processing technique for urban and rural land use monitoring in northern Thailand". Journal of Thai Geosciences. Vol. 1. pp. 59-63.

Wickware, G. M. and Howarth, P. J. (1981). "Change Detection in the Peace-Athabasca Delta Using Digital Landsat Data". Remote Sensing of Environment, Vol. 11/9, pp. 9-25.

A Development of DEM Generation System

Jaeyeon LEE, Kiyonari FUKUE, Haruhisa SHIMODA
and Toshibumi SAKATA

Tokai University Research and Information Center
2-28-4 Tomigaya, Shibuya-ku, Tokyo 151, Japan
TEL +81-3-3481-0611 FAX +81-3-3481-0610

ABSTRACT

A DEM generation system which generates DEM from topographic map is reported. In the developed system, a new restoration algorithm which uses adjoining relationship between contour lines is adopted. By using the new algorithm, throughput of the system is improved quite largely(5 to 24 times compared to surveyed methods). Also by using contour/grid conversion algorithm which utilizes Euclidean distance transformation, DEM of good quality can be generated.

1. Introduction

DEM(Digital Elevation Model) is seriously needed from various fields of science, practical applications, environmental researches and/or natural disaster analysis. However, the available DEM is so scarce compared to the necessity. Generally, DEM is generated from the topographic map by recognizing the contour on the map and convert it to grid data using contour/grid conversion algorithm. However, the process is very costly, and there are many cases where the quality of acquired DEM is not satisfactory.

This paper is to report the newly developed DEM generation system which provides an integrated functionality for the process of generating DEM from the topographic map. In the developed system, restoration of extracted contour image which had been the most time-consuming task in the flow, is automated. Also, the system provides new contour/grid conversion functionality which can generate DEM of quite good quality. Further, the system is implemented on Microsoft Windows NT Operating System which supports wide variety of computing environments including personal computers and workstations.

In this paper, the configuration of the system and the algorithms for restoration and contour/grid conversion is described. Also, the evaluation results will be presented.

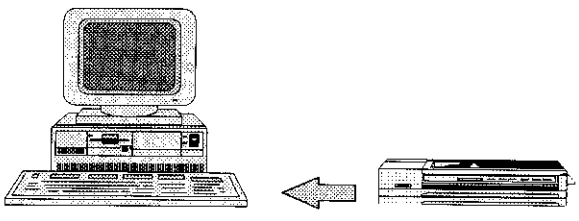

Fig. 1 Hardware Configuration of the System

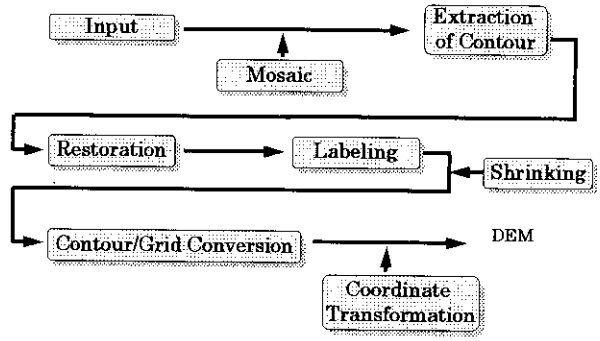

Fig. 2 Processing Flow of the System

2. System Configuration

The configuration of the developed system is very simple and no special hardware is included as shown in Fig.1. The system operates on the personal computer and uses color scanner for scanning topographic map.

Fig. 2 is the processing flow of the system. A scanned topographic map is imported via input module and mosaiced if necessary. In mosaic module, multiple pages of the topographic map is merged so as not to make gap between pages by converting the coordinate system of the topographic map to latitude-longitude coordinate system.

In the next step, contour is extracted from the map by using the color and line width parameter. Actually, a neural network whose input is R, G, B components of each pixel is used for color extraction and Kasvand filter is applied to the result of neural network for thin line extraction.

Even though the contour extraction module showed good performance, there still exist quite large number of cut lines in the extracted contour image. To restore them, the contour image is processed by restoration module(the detail of the restoration algorithm will be described later). After restoration, labeling module assigns respective elevation for each contour lines by interactive operation with human.

Up to labeling, the resolution of the image is quite high(approximately 300dpi). However, the original data, topographic map has not so high accuracy. Therefore, it is meaningless to conserve so high resolution to Contour/Grid conversion process. Shrinking module shrinks the image conserving the connectivity of the contours.

By applying Contour/Grid conversion algorithm(the detail of the algorithm will be described later), DEM is generated and finally the data is converted to coordination system of user specification.

3. Restoration of Contour Image

Beside of contour lines, topographic map includes many symbols, characters and various kinds of lines, which make the image very complex. Generally, it is inevitable that extracted contour image contains a large number of cut lines(hence, ending points). This is why restoration process is required. However, because of the complexity of the contour image, it is very difficult to restore the cut lines. Even though there has been reported many algorithms for this problem, those algorithms had achieved only limited success and seldom used in the field.

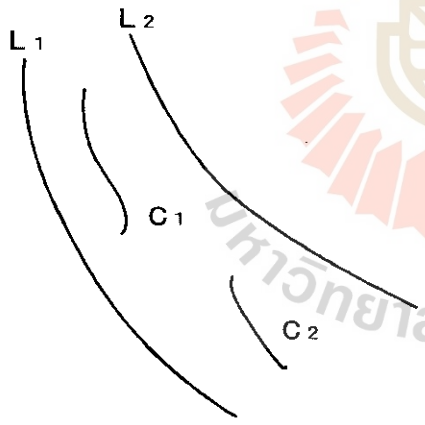

Fig.3 Basic Idea for the Restoration Algorithm

In the previously reported algorithms, only local relationships between ending points are used for the restoration. In the developed system, a new restoration algorithm utilizing adjoining relation is proposed[1]. Adjoining relation has global characteristics and is able to recognize the structure of the contour image. Fig.3 shows the basic idea of the adopted restoration algorithm. That is, if both of the contour C_1 and C_2 is adjoined with L_1 and L_2, then C_1 and C_2 should be the contours of same height and need to be connected.

With consideration of the above idea, the proposed restoration algorithm restores the

Table 1. Experimental Result

	Contour Image	After 1st Stage	Finale Result
Number of Endings	130 (100%)	62 (48%)	8 (6%)

contour image in two stage operations. In the first stage, the traditional restoration method which uses local relationships between ending points is applied. By this processing, a short and simple cut lines can be restored. And in the second stage, the adjoining relationship is applied to the contour image for more efficient restoration.

The experimental result is shown in Table 1. At the time of extraction, there had been 130 ending points in the image. After the first stage processing, it is lessened to 62, about half of the ending point is eliminated. In traditional restoration algorithms, the processing is terminated at this point, and the remaining ending points should be restored by human operator.

On the contrary, in the proposed method, a second stage processing is applied, and the number of ending points is lessened to 8, that is, only 6% of the original ending points remains.

4. Contour/Grid Conversion

Contour/Grid conversion is a so extensively researched topic and there has been reported a lot of algorithms for this problem. However, the available algorithms often generates peculiar grid data which contains unnatural linear incontinuities as shown in Fig. 4.

In general, contour/grid conversion process consists of the two sub-operations. That is, searching for the standard points for the interpolation and interpolation itself. Among the two sub-operations, the later is straight-forward and not so much problem. Mainly the former is thought to be the cause of the

Fig.4 Quality Problem of the Previously Proposed Algorithms

(a) searching for standard points

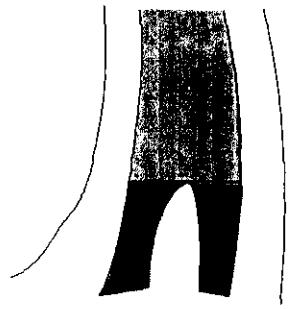

(b) interpolated result

Fig. 5 Cause of Incontinuity

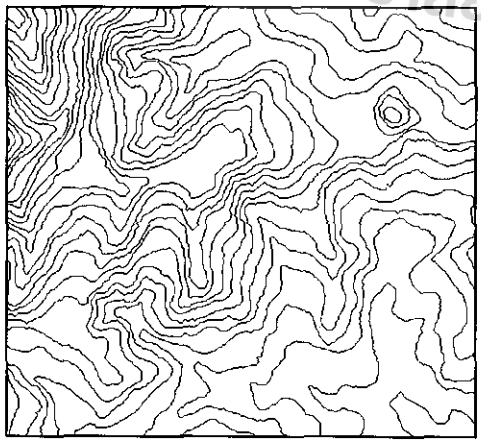

(a) Original Contour Image

(b) Resulted DEM

Fig.6 Experimental Result

peculiar results. For example, Fig.5 shows a well-known contour/grid conversion algorithm, in which a contour map is scanned, and the detected contours are interpolated by a spline curve. As shown in the figure, the standard points for interpolation abruptly changed at the scan point indexed by an arrow mark, which results in the incontinuity of the grid data as shown in (b) of the figure.

Table 2 Comparison on the Throughput

	Surveyed Methods			Developed
	A	B	C	System
Contour Recognition	32.0	92.0	200.0	3.5
Labeling	4.0	8.0	5.0	3.0
Contour/Grid Conversion	4.0	0.5	2.0	2.0
Sum	40.0	100.5	207.0	8.5

In the developed system, a new contour/grid conversion algorithm which do not require the searching for the standard points for interpolation is adopted. In the proposed algorithm, instead of searching process, contour itself is propagated to the region by Euclidean Distance Transformation. As a result of the transformation, the distance to the contour from every to-be-interpolated points is automatically obtained[2].

Fig.6 (a) is the experimental contour image, and Fig.6 (b) is the result generated by adopted algorithm. The incontinuities scattered in Fig. 4 is not shown in the result and the quality of the DEM is quite satisfactory.

5. Evaluation

To evaluate the performance of the developed system, a throughput which is defined as a time to generate DEM from a topographic map is measured(a 1:25,000 topographic map published by Japanese Geographical Survey Institute is used). Also, throughput of the methods which are adopted by the organizations who generates DEM from topographic map is surveyed for the comparison.

Table 2 is the result. Because the flows of the surveyed methods vary, each operation steps are grouped into contour recognition(includes contour extraction and restoration), labeling, and contour/grid conversion. As shown in the table, totally 40 to 207 hours for 1 page of topographic map. On the contrary, in the developed system, only 8.5 hours were necessary.

6. Conclusion

Even though there exist wide need for DEM, it has been very difficult to satisfy them because of lack of efficient DEM generation technology. In this paper, a new DEM generation system is reported.

In the developed system, a new restoration algorithm is adopted, which resulted in 5 to 24 times improvement of throughput. Also, by using a contour/grid conversion algorithm which uses Euclidean distance transformation, DEM of satisfactory quality could be generated.

[References]

1) Lee, Fukue, Shimoda, Sakata, "Restoration of Contour Image by Using Adjoining Property", Journal of the Japan Society of Photogrammetry and Remote Sensing, Vol.34, No. 2, pp45-53, 1995.

2) Lee, Fukue, Shimoda, Sakata, "A Contour/Grid Conversion Method by Using Euclidean Distance Transformation", Journal of the Japan Society of Photogrammetry and Remote Sensing, Vol.33, No. 6, pp26-34, 1994.

Developmet of highspeed programmable formatter for earth observation satellite downlink data formatting

Hideyo Yokotsuka* Toshibumi Sakata* Haruhisa Shimoda*
Shinichi Sobue** Mineo Sekiguchi***

* Tokai University Research and Information Center
** National Space Development Agency of Japan
*** Remote Sensing Technology Center of Japan

Abstract: Formatting process of earth observation satellite downlink data is usually performed with custom made hardware which designed for one satellite or a sensor. In this paper we introduce a high speed programmable formatter system which is able to process many kinds of satellite downlink data without changing the hardware.

1. Introduction

The various sensor data acquired with earth observation satellites are transmit to ground receiving stations. The sensor data and multiplexed with telemetry using special format called downlink format.

The transfer rate of the down link data to ground receiving station exceeds to 100Mbps,and the quantity of the downlink data per reception exceeds to several GB.Generally, this downlink data is processed through two step as follows.In the first step, the data is record in High Density Digital Tape(HDDT) in real time using High speed Digital Data Recorder (HDDR).In the second step, the downlink data is reproduced from HDDT, sensor data is extracted/divided into each scene unit, and output to certain medium for computer peripheral equipment. Generally, "The format processing of downlink data" corresponds to the second step. In order to perform format processing a large quantity of down link data ,in high transfer to rate. most of the processing systems are consist of customized computer for certain sensor or satellite.

However, in the near future lunch of various kinds of multi sensor satellite such as ADEOS are planned.If we make hardware for each sensor for

format processing, it the system , and operation becomes very complicated. It also causes degradation of reliability of the format processing system. This is a very big problem. We have developed a programmable formatter which solved these problems.The hardware dependency was reduced and made multiusable,highspeed processing was realized.

2. Hardware formatter

Fig.1 Shows the block diagram of MOS-1 MESSR formatter as a typical example of synchronizer. The figure shows that the important processing parts such as synchronization of minor frame, synchronization of major frame and serial to parallel conversion,are done by hardware. It is not only in case of MOS-1 MESSR formatter system, but also in the other sensor formatters. Each formatter hardware are not so different from others. But there is no interchangeability between each formatter at all. It is because we designed speed priority to cope with a large quantity of data .In each system, hardware are customized to realize high speed processing.

3. Investigation of downlink data format of earth observation satellite

Fig.2 Shows the downlink data format of MOS-1 MESSR/VTIR and Fig.3 Shows the downlink data format of JERS-1 OPS as typical examples.
Through for our investigation of many satellite downlink data format we have found that the way to specify recording start location of sensor data from minor frame sync pattern is same.*(1),*(2)

If we make a circuit which is able to take synchronization for minor frame of any kind of patterns, we can process all downlink format. Paying attention to this facts,we have developed a new formatter system with low hardware dependency.

4. Programmable formatter system

It is a very important point in formatter system to keep high efficiency of processing speed when serial data is reproduced from HDDR.However,if the ratio of hardware processing too high the multiusability drops.By our system, processing by the hardware is only limited to detection of minor frame and addition the time code for format processing as shown on Fig.4.This system is allows to take synchronization by only setting a parameter in programmable

sync hardware for various minor frame patterns.It adapts to many downlink data format without changing the hardware.Processing difference due to types of sensor or satellites are solved by a software on a WS with high speed and high multiusability.

5. Analysis and result

We used the downlink data of MOS-1 MESSR/VTIR for analyzing the performances of the programmable formatter.Fig.5 shows the processing time result compared with the hardware formatter currently used at our ground station.But, due to the from a difference of the system structure , we could not use the same output equipment for analysis. So,we measured time of the main processing, and the write time to CCT is not included.And both were equal as a result of having done format processing.The processing time of the programmable formatter was a tenth times faster than the previous hardware formatter.This result proves the high speed performance of the programmable formatter.

6. Summary

Recently it is becoming necessary to process downlink data of earth observation satellites at ground receiving station if distribute it to end users in timely manner.More over,in order to adjust to various satellite programs construction of flexible data reception & processing system with has become important.It was the aim of our study to develop the high speed programmable formatter to cope with such actual situation.The sensor data used in this experiment was of MESSR of MOS-1.We are planing to perform the quantitative analysis of the programmable formatter in this with other sensor data and intend to upgrade of the system.

7.References

*(1)JERS-1 SAR/ AMI IMAGE MOS-1 DATA USERS HANDBOOK
National Space Development Agency of Japan ,Earth observation center
2nd.edition (HE93065A) April,1995

*(2)JERS-1 OPS data format instrucrion
National Space Development Agency of Japan ,Earth observation center
2nd.edition (HE93064A) April,1995

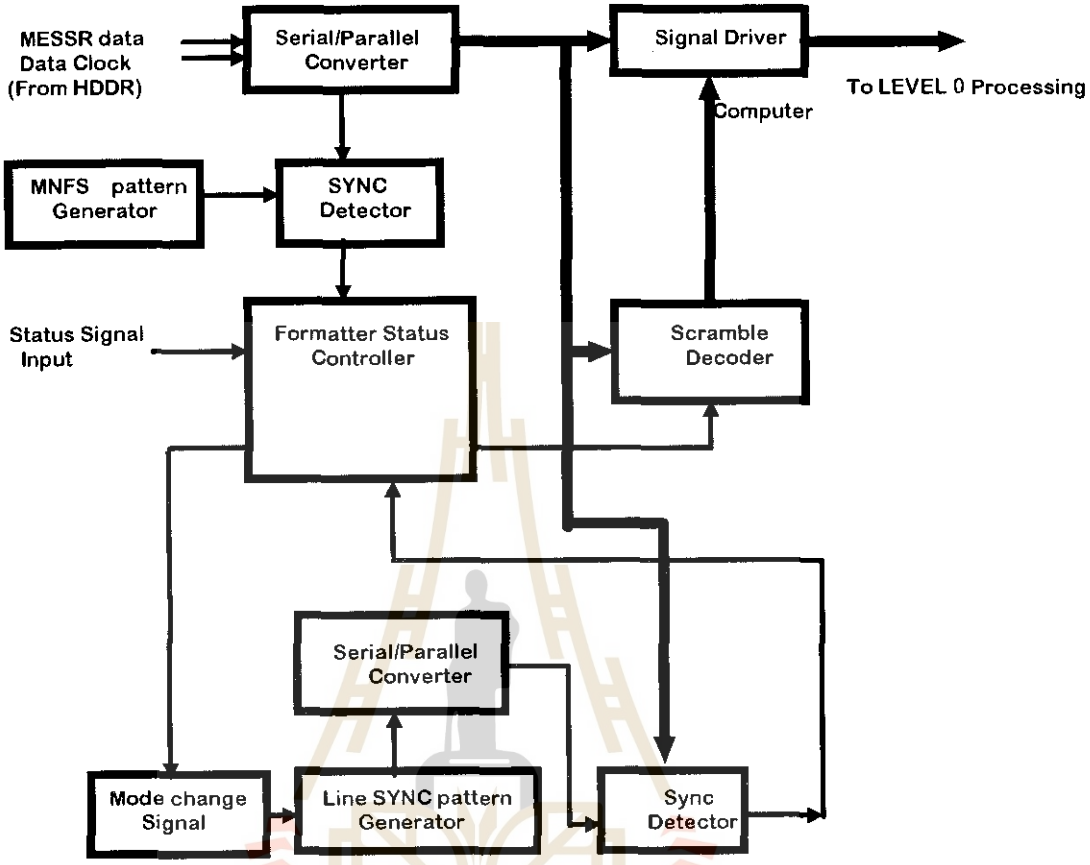

Fig.1 : Block diagram of MOS-1 MESSR hardware synchronizer. Each block is made by discrete device.

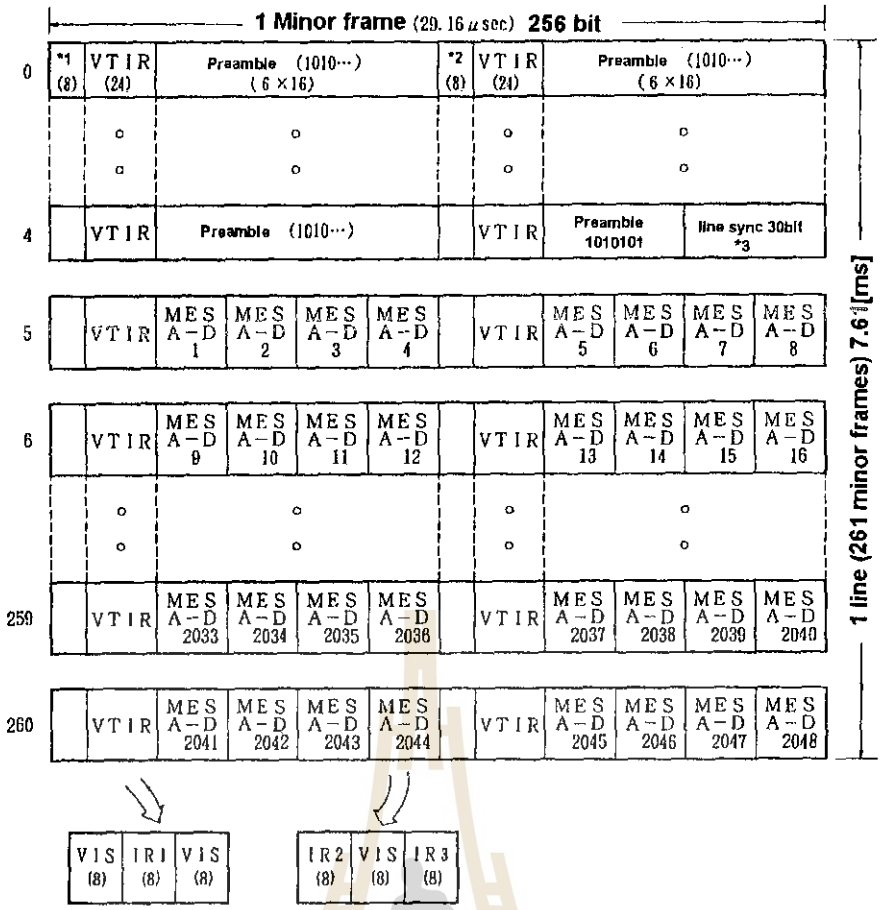

*1:MNFS Minor Frame sync pattern signal 7bits (1011000) + TLM signal 1bit

*2:$\overline{\text{MNFS}}$ Minor Frame sync pattern signal 7bits (reversed) 0100111 + TLM signal 1bit

*3:Line sync pattern code (30bits) 11111010 ,11110011, 0110100 ,000000

Fig.2 : Downlink data format of MOS-1 MESSR/VTIR

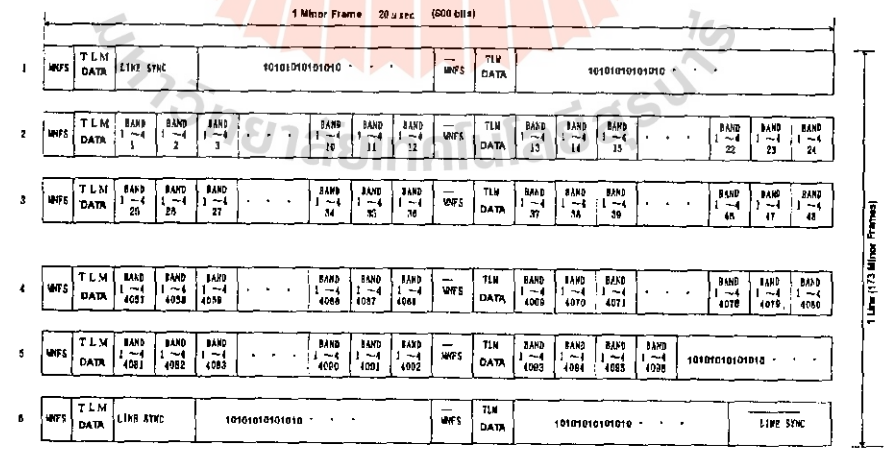

MNFS (MiNor Frame Sync) Code : 101101 11000 (11bits)

$\overline{\text{MNFS}}$ (MiNor Frame Sync) Code : 101101 11000 (11bits)

LINE SYNC Code : 111110 10111 001100 110100 000000 (30bits)

$\overline{\text{LINE SYNC}}$ Code : 000001 01000 110011 001011 111111 (30bits)

Fig.3 : Downlink data format of JERS-1 OPS

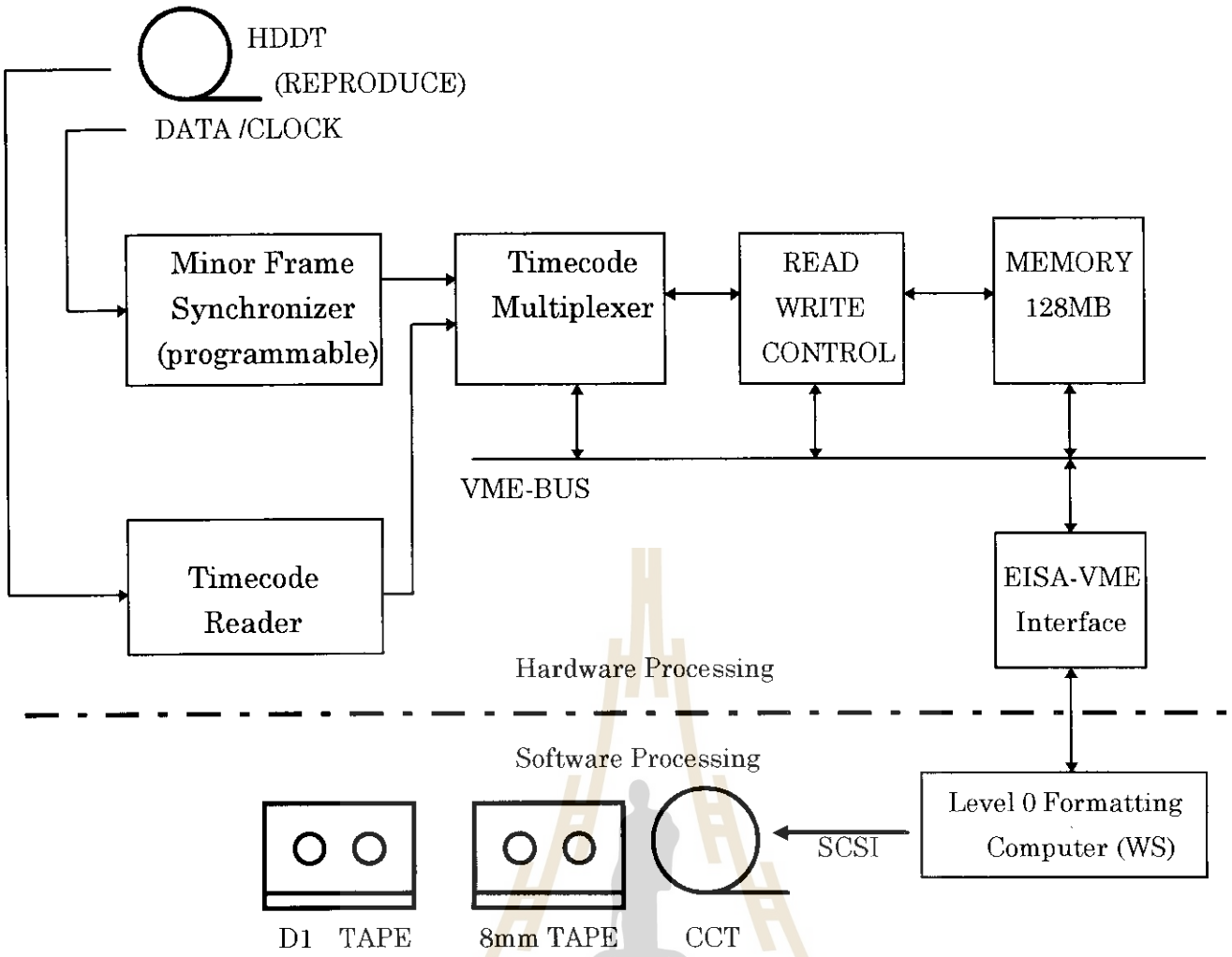

Fig.4 : Block diagram of the programmable formatter system

	Hardware Formatter System	Programmable Formatter System
Control Computer	MS-175	HP9000 / 755
Processing Time [S]	About 600	About 60

Fig.5 : Result of Processing Time of MOS-1 MESSR LEVEL 0 Processing at one scene.

THAI REMOTE SENSING SATELLITE SYSTEM

Dr. Suvit VIBULSRESTH

Waraporn SUCHAICHIT

The National Research Council of Thailand (NRCT)

196 Phaholyothin Road , Chatuchak

Bangkok 10900, Thailand

Tel. 662-5790116 Fax. 662-5613035

ABSTRACT

In October 1994, the Ministry of Science, Technology and Environment (MOSTE) concluded a Memorandum of Understanding (MOU) with the Canadian Space Agency for cooperation in space technology and applications. An earth observation smallsat mission, as the first cooperative mission under the MOU recently received the Thai Government approval. MOSTE, through its technical authority in the National Research Council of Thailand (NRCT) will own and operate the satellite system. This will be the first satellite to operate in an orbit dedicated to the equatorial regions. The first operational mission will extend the information available to both scientific and operational users and will augment data currently available from the Landsat series of spacecraft. This paper will present an overall system concept for the Smallsat Program, which will operate over its 5 years lift span.

1. System Overview

The purpose of the system is the provision of regularly updated multispectral image data on an operational basis. Output from the system will take the form of image data products which can be distributed to users who will apply the data, either directly or after further processing, to the management of resources.

2. System Architecture

The essentilal elements of the Thai Remote Sensing Satellite System are :

1. the Ground Segment
2. the Space Segment
3. the Launch Segment

2.1 System Description and Performance

2.1.1 Overall System Description

The performance parameters of the Thai Remote Sensing Satellite System are summarized in the following tables.

TABLE 2.1.1-1 Mission Performance

Parameter	Value
Mission Life	5 years
Orbit Type	73 orbits/5 days Multi-sun-syschronous
Orbital Period	97 minutes
Orbit Inclination	28 degrees
Orbital Altitude	600 km
Coverage Repeat	Every 5 days
Illumination Repeat	49 days
Command Uplink	S-Band: 2 kbps
Telemetry Downlink	S-Band: Direct 2/4 kbps Playback 32/128 kbps
Data Downlink	X-Band: < 85 Mbps

TABLE 2.1.1-2 Temporal Performance

Parameter	Value
Revisit Time	Twice every 5 days
Accessibility Region	29.6°N to 29.6°S
Maximum Imaging Capability	10 minutes/orbits
Useable opportunities per year	63

TABLE 2.1.1-3 Spatial Performance

Parameter	Value
Swath Width	185 km imaged swath which is selectable within a 275 km accessibility region.
Across Track Resolution	30 m (nadir)
Along Track Resolution	30 m (madir)
Geometric Distortion	< 1/2 pixel
Band to Band Registration	< 1 pixel
Image Locations	< 5 km

TABLE 2.1.1-4 Spectral Performance

Parameter	Value
Spectral Bandwidths:	
Blue	0.45 to 0.52 μm ±.01
Green	0.52 to 0.60 μm ±.01
Red	0.63 to 0.69 μm ±.01
NIR	0.76 to 0.90 μm±.01

2.2 Ground Segment

The Ground Segment comprises two main system:

(1.) the Mission Control Center (MCC)

(2.) the Data Processing Facility (DPF)

(2.2.1) the Mission Control Centre (MCC) :

The role of the Mission Control Centre (MCC) is to accept user requests for image data, plan the operations of the satellite, control, coordinate and execute the planned operations, track end-to-end operations, and monitor data quality. The MCC has the authority required for day-to-day mission operations and control, and the responsibility for ensuring that the mission objectives are satisfied. The MCC undertakes and coordinates implementation of the overall mission by monitoring, directing and controlling all mission aspects and resources.

(2.2.2) the Data Processing Facility (DPF)

The system is capable of processing raw satellite data, received by the X-Band Data Reception station, into high quality image products in either film or CCT formats. The products produced are geocoded and georeferenced and presented in the form of 185 km x 185 km images.

2.3 Space Segment

The Space Segment comprises a Spacecraft bus and an instrument.

(2.3.1) The Spacecraft Bus

The Spacecraft structure is a modular configuration comprises Bus and Propulsion moduls. The Spacecraft protects against "credible" single point failures by using full redundancy, space qualified hardware, cross-strapping, and backup modes. The propulsion subsystem uses monopropellant hydrazine. The Telemetry,Tracking & Control subsystem includes a Digital Storage Unit, which may be hosted in the Integrated Avionics Processor for storage of housekeeping data and S-Band transponders for command uplink and housekeeping data downlink. The power subsystem implementation consists of a deployable, non-articulated solar array for primary power operating in conjunction with a nickel hydrogen (NiH_2)

battery for energy storage with a redundant cell. The thermal subsystem combines both passive and active elements to maintain the spacecraft temperatures within acceptance limits during normal operation, and within survival limits during emergency modes. The Attitude Determination and Control Subsystem is a zero net momentum implementation using magnetorquers and reeaction wheels as actuators, and sun sensors, horizon scanners, and magnetometers as sensors. The thrusters are used to control orbit maneuvers.

(2.3.2) Instrument

The instrument mounted on the Spacecraft Bus, contains a Visible and Near Infrared (VIS/NIR) pushbroom camera. A data formatter configures the image data for relay to the ground station via the X-Band downlink

2.4 Launch Segment

The launch segment comprises the launch element, the Low Earth Orbit Phase network, and launch services.

The launch element comprises a Pegasus XL launch vehicle, an on-board monopropellant system, and the required propellant. The necessary launch support equipment for integration, handling, shipping and launch operations is also part of the element. The selected launch element meets all of the specified requirements and is consistent with the standard proven procedures of the Pegasus launch system and the Eastern Test Range.

3. Conclusion

Thai Remote Sensing Satellite System will be launched in the next few years, which will not only benefit Thailand but would also provide new opportunity for international collaboration.

ANALYSIS OF MULTI-TEMPORAL SAR IMAGES

by

RASAMEE SUWANWERAKAMTORN
NATIONAL RESEARCH COUNCIL OF THAILAND
and
SHOJI TAKEUCHI
REMOTE SENSING TECHNOLOGY CENTER OF JAPAN

Abstract

As a result of its cloud penetrating capability, the JERS-1 SAR data have provided a unique temporal data set for observation of land use / land cover change in Thailand where the cloud coverage is a severe limitaton. Three different dates of SAR data acquired on March 16, April 29 and September 08, 1993 were used to monitor land cover change in the Central Plain of Thailand.

Unsupervised classification was applied for clustering of the SAR backscatter which has been pre-processed including fittering and calibration.

The result showed that multi-temporal JERS-1 SAR data include the information about seasonal change of land cover in the study area where paddy field is dominant. The difference in backscatter in paddy field is related to the stage of rice or the height of rice. However, there are other factors affecting SAR backscatter in paddy field (i.e. water content / soil moisture and surface roughness) between March and April images. The clearer land cover type is riparian trees although they appear bright as the built-up area. Nevertheless there is a high potential to use the multi-temporal SAR data to detect the land cover change especially to monitor the different stages of rice.

1.Introduction

The synthetic aperture radar (SAR) data by Japanese Earth Resources Satellite 1, JERS-1, are expected to be used effectively for the purpose of monitoring of land use/land cover condition in the tropical regions since the optical sensor data are difficult to obtain in timely maner due to cloud conditions while the SAR data can be obtained repetitively in any weather condition because of its cloud penetration capability. Therefore with the collaboration between the National Research Council of Thailand and Remote Sensing Technology Center of Japan under the support of the Special Coordination Fund of the Science and Technology Agency of Japan, the preliminary analysis of multi-temporal SAR data has been carried out for the Central plain of Thailand where the cloud coverage is a severe limitation.

2. Objectives

- To investigate the possibility of land cover classification using multi-temporal SAR images.
- To investigate the relationship between the seasonal changes of SAR backscatter and actual land cover types.

3. Study Area

The study area is located between latitudes 14° 18′ and 14° 38′ and between longitudes 100° 02′ and 100° 37′ , covering some part of Ayutthaya, Ang-Thong and Suphan Buri; the Central Plain of Thailand (Fig. 1). The main rivers in the area are the Chao Phraya and the Suphan Buri river. The terrain is mostly flat and formed by deposition of sediment from the Chao Phraya river and other tributaries. The mean elavation of the Flood plain is about 11 meters above mean sea level (MSL). The main land use is paddy field.

4. Methodology

4.1 Data Used

- Three different JERS-1 SAR data acquired on March 16, April 29 and October 8, 1993 (Fig. 2) in the middle of dry season, the end of dry season and the middle of rainy season, respertively, were used to monitor land cover change of the study area.
- JERS-1 OPS data acquired on February 07,1993 and Landsat TM data acquired on the same day of SAR data (April 29, 1993) were used as supporting and verifying.

Paper presented at 16th Asian Conference on Remote Sensing, 20-24 November, 1995, Suranaree University of Technology, Nakhon Ratchasima, Thailand.

- Ground observations were taken on March 18, April 29 and September 26,1995 (the same period of SAR data).

4.2 SAR Data Analysis

The procedures of digital SAR data analysis (shown in Fig. 3) are as follows:

4.2.1 Pre-processing

- The 12.5 m x 12.5 m resolution of SAR data were reduced to 25 m X 25m before filtering
- Map fiter was employed to remove the speckle noise.
- The filtered images were co-registered with each other as well as with digital geomorphological map in order to orient the geometry of the study area.
- SAR data calibration was conducted by the Normalized Radar Cross Section (NRCS) which can be derived from the SAR level 2.1 product using the calibration coefficient given by National Space Development Agency of Japan as shown in Table 1.

$$NRCS = 20 \log_{10} (I) + CF \text{ [dB]} \qquad \text{(Takeuchi,1995)}$$

where I = Value of each pixel, which can be expressed from 0 to 2^{15} -1

CF = Calibration coefficient (-68.5 for all SAR data)

Table 1 Conversion Factor

CF (dB)	Reception date	Processed data
- 68.5	Until end of April 92, Sept. 1/92, Since Sept. 18/92	Since Feb 15/93
-70.0	(same as above)	Until Feb 14/93
- 66.42	Between May 1/92 and Sept. 17/92 Except Sept. 1/92	Since Feb 15/93

Source : Shimada ,1993.

- Calibrated images were converted from NRCS in dB to 8 bit to obtain 256 values of intensity by the equation as shown below.

$$Xc = 5 \times (NRCS + 30 \text{ dB}) \qquad \text{(Takeuchi,1995)}$$

where Xc = Digital count

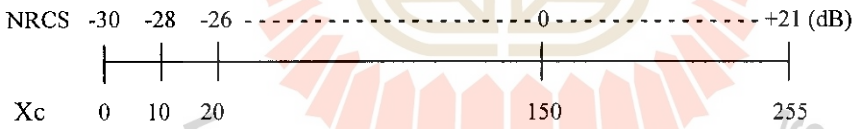

- Principal component tranformation was applied to reduce the spectral redundancy of 3 SAR images. The combination image of 1st component (R), 2nd component (G) and 3rd component (B) is shown in Fig. 4.

4.2.2 Classification

Cluster analysis was employed to identify land cover type of the study area using 3 component images. Eight classes of land cover type were designed for clustering and classified by Maximum Likelihood classifier. The results of land cover classification are shown in Table 2 and Fig. 5.

5. Results

The multi-temporal of 3 SAR images showed the interesting changing pattern in two kinds of paddy field . Fig. 6 illustrates the different backscatter of main land cover type in the study area. The change for paddy-1 is seen mainly in the central part of the images (Fig. 2). It was confirmed by ground survey that the area was almost covered by dry bare soil with no vegetation during March to April. This area is known as a rainfed paddy field where rice is planted in the rainy season. These facts suggest a possibility that the increase of the SAR backscatter from March/April to September is caused by the increase of vegetation cover. The change in paddy-2 is found mainly in the right side of the images. Almost of the area could be identifed as bare soil wherever the brightness of color is different among the locations during March to April (evidenced by Landsat TM acquired on April 29,1993 ; the same day as SAR data and ground survey on April 29,1995). These suggest that the increasing of the backscatter from March to April was not caused by the change of vegetation coverage but by the change of soil moisture content condition and surface roughness (since the late of April is the season for land reclamation of the paddy fields) as well.

Digital multi-temporal SAR data analysis which provided a lot of different backscatter using cluster analysis gives a good result of land cover types (Table 2 and Fig. 5).

Table 5 Land cover classification result obtained from 3 different SAR images.

No.	Categories	Land cover type (Based on ground observation , JERS-1 OPS and Landsat TM data)		
		Middle of March	Late April	Early September
1	Rainfed paddy field (Paddy-1)	Bare soil	Bare soil	Paddy field
2	Riparian trees (Mixed orchards)	Riparian trees (Mixed orchards)	Riparian trees (Mixed orchards)	Riparian trees (Mixed orchards)
3	Second paddy field	Second paddy field	Bare soil	Paddy field (Early stage)
4	River/Prepared land	River/Bare soil	River/Bare soil	River/Prepared land (for rice cultivation)
5	Built-up/Urban area	Built-up/Urban area	Built-up/Urban area	Built-up/Urban area
6	Rainfed paddy field/ Second paddy field (Paddy-2)	Second paddy field/ Moist bare soil	Second paddy field / Moist bare soil	Paddy field
7	Prepared land	Bare soil	Bare soil	Prepared land
8	Second paddy field/ Prepared land	Second paddy field	Bare soil	Prepared land

6. Conclusion

The result showed that multi temporal JERS-1 SAR data include the information about seasonal change of land cover in the study area where paddy field is dominant. The difference in backscatter in paddy field is related to the stage of rice or the height of rice. However, there are other factor affecting SAR backscatter in paddy field (i.e. water content / soil moisture and surface roughness) between March and April images. The clearer land cover type is riparian trees although they appear bright as the built-up area. Nevertheless there is a high potential to use the multi-temporal SAR data to detect the land cover change especially to monitor the different stages of rice. The cluster analysis using multi-temporal SAR images can be applied for discriminating the change of land cover types.

7. References

Takeuchi S. and Suwanwerakamtorn R. ,1995, Analysis of the Influence of Land Cover Condition on SAR Backscatter Using Simultaneous SAR and TM Data, Journal of the Japan Society of Photogrammetry and Remote Sensing , Vol.34, No.5.

Takeuchi S.,1995, A Method of Secondary Correction for SAR Standard Product (Japanese), Journal of the Japan Society of Photogrammetry and Remote Sensing , Vol.34, No.2, pp 54-64.

Shimada M. , 1993, Image Quality of SAR/OPS, JERS-1 Newsletter, No.1, October,1993.

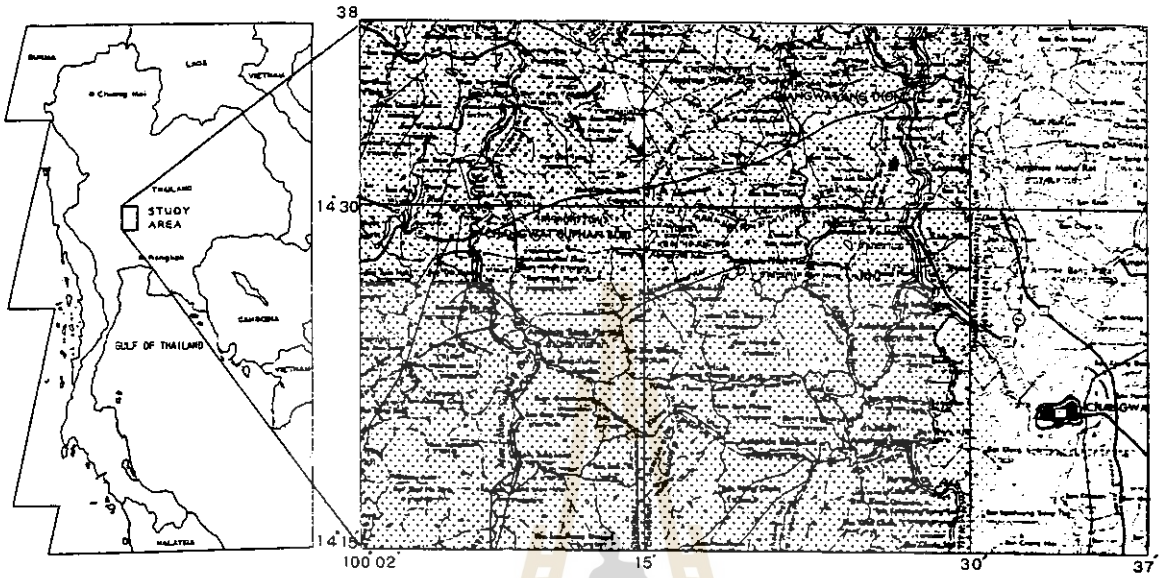

Fig. 1 The lacation of study area.

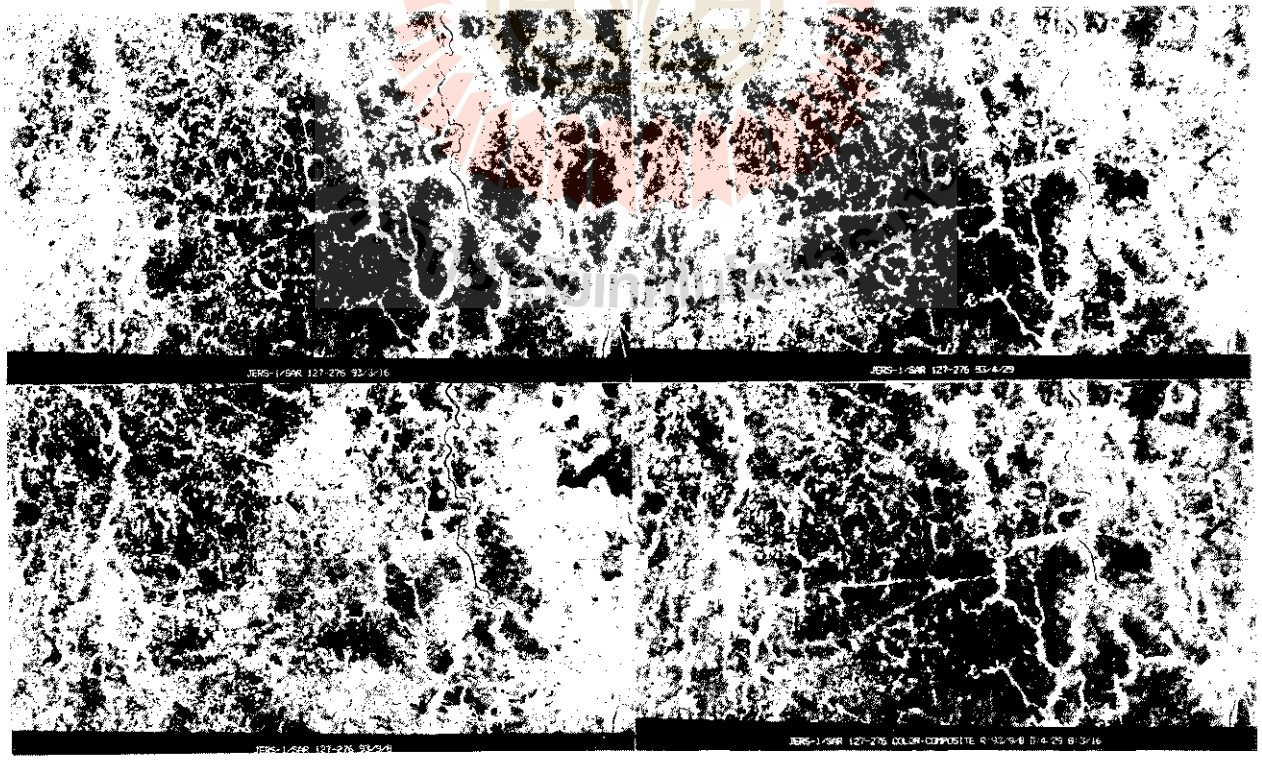

Fig. 2 Muti-temporal SAR images of the Central Plain of Thailand acquired on March 16, April 29, and September 08,1993.

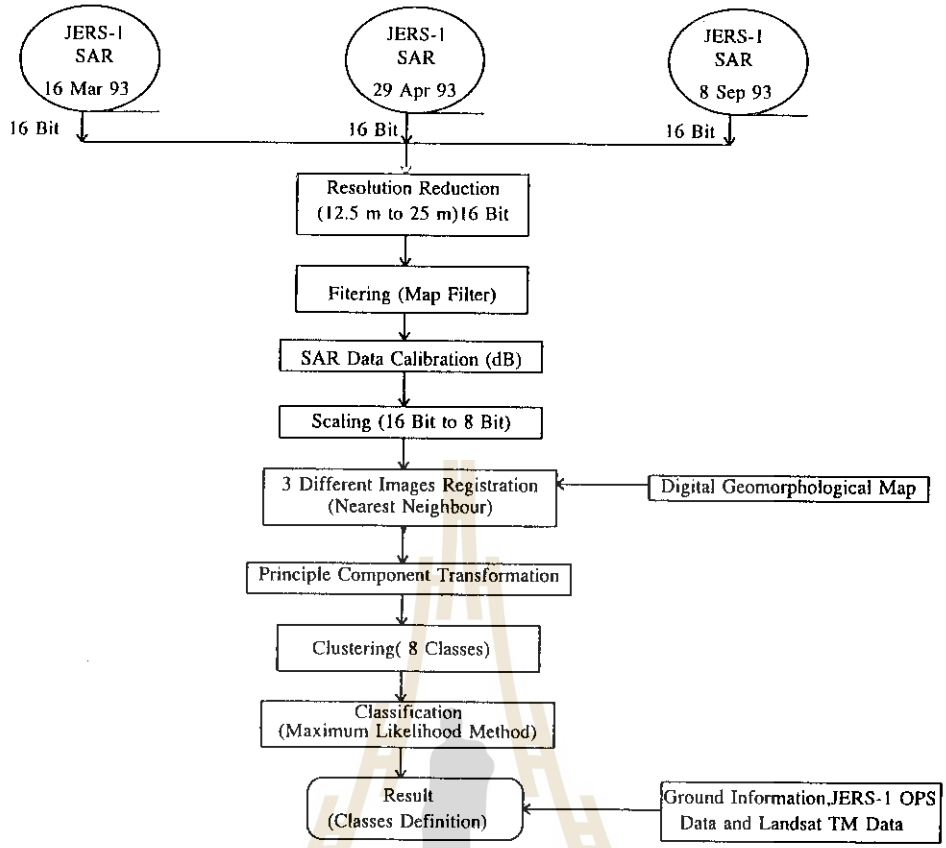

Fig. 3 Procedures

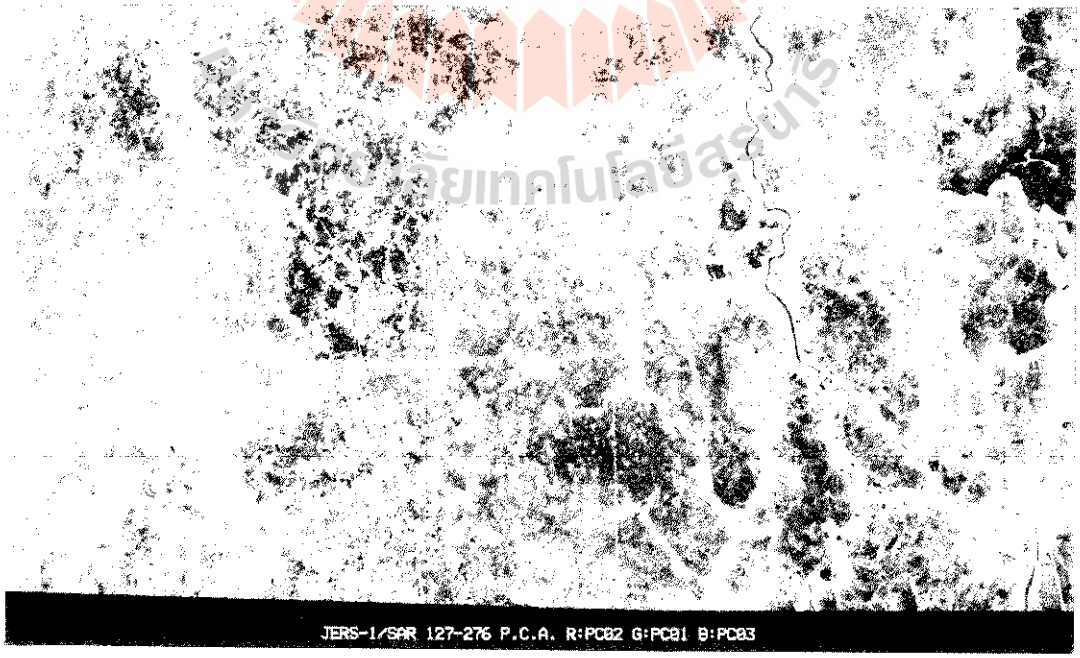

Fig. 4 False color composite of 1st coponent (Red), 2nd component (Green) and 3rd component (Blue) of 3 SAR images acquired on March, April and September .

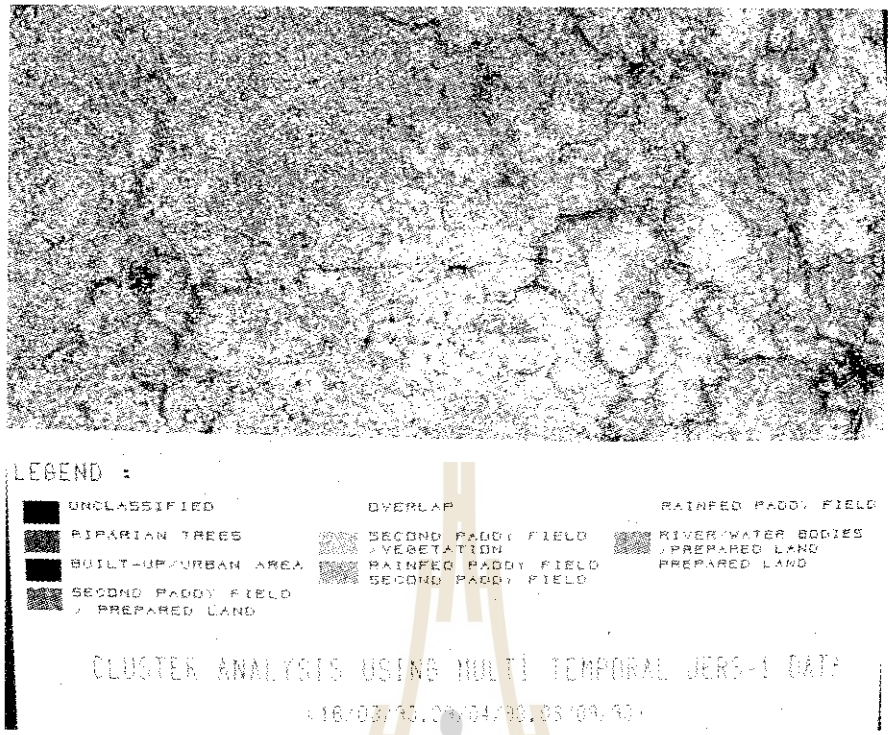

Fig. 5 Land cover classification result by cluster analysis based on 3 principal components of 3 SAR images.

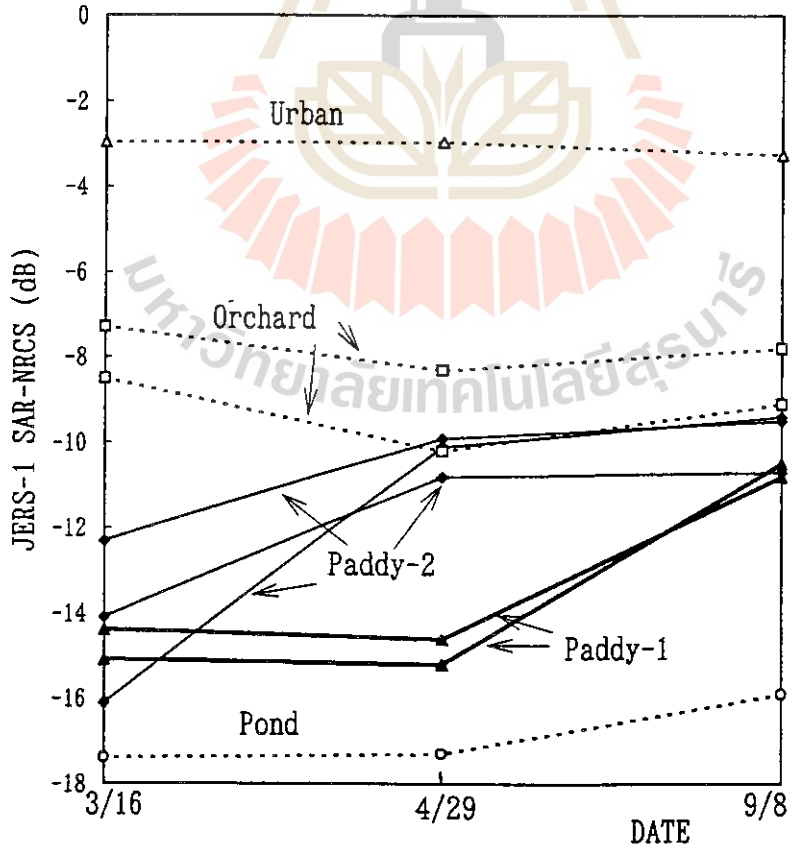

Fig. 6 Typical seasonal change of the SAR backscatter (after Takeuchi and Suwanwerakamtorn,1995).

WORK SHOP

EDUCATION & TRAINING

A new program in AIT: Space Technology: Applications and Research

Jean-Pierre Delsol
Associate Professor
-
School of Environment, Resources and Development
-
Asian Institute of Technology
(AIT)
Bangkok, Thailand
-

Abstract

The Asian Institute of Technology (AIT) has a long history in training and education to serve the Asia and Pacific region in many fields and many disciplines.

In the last decade AIT entered into the training and education in the field of Remote Sensing which followed by Geographic Information Systems (GIS) a few years later. Since the establishment of the AIT's Asian Regional Remote Sensing Training Center (ARRSTC) in 1979 various degree and non-degree courses were offered to many students, mainly from Asia as well as from other parts of the world in smaller number.

The new "Space Technology: Applications and Research" program is keeping pace with the the recent Ministerial's declaration on space applications for Asia and the Pacific (Beijing 23 September 1994). Continuously observed by a large number of Earth remote sensing's Satellites (Landsat TM, SPOT 2&3, ERS 1&2, JERS 1, IRS1, NOAA, MOS...) the region records an important flow of data. Receiving stations - seven actually functionning in the region and two others planned- provide data every day. A huge number of users (geographers, cartographers, decisions makers, planners, geologists, soil scientists, hydrologists, foresters, urbanists, agronomists ....) become more and more numerous and are, day after day, deeply concerned by the applications of satellite data in their respective fields of action.

The "STAR Program" will encompasses two technically oriented field of study namely: "Remote Sensing and Geoinformatic Science" and in 1997 "Photogrammetry and Computer Assisted Cartography". The third FOS focussed on Natural Resources Planning and Management. These two first FoS intend to give to the students basic concepts, theories, and principles, in Remote Sensing and GIS and necessary skills to apply Remote Sensing technologies for monitoring resource systems and information processing techniques for creating sustainable societal systems.

In support of this, a Remote Sensing Laboratory (visual, digital and photographic sub-laboratories) and a Geographical Information System Center (GAC), as well as internationally recognized Faculty and Staff members, are the main components to conduct and transmit education and research activities in "Space Technology: Applications and Research" for degree of Masters of Science (MSc) and Ph.D.
A brief description of corresponding two technical FOS as well as existing facilities and Faculty and Staff is made in this presentation.

Keywords: Training, Education, Remote Sensing, Geographic Information Systems, Geoinformation Technology, Asian Institute of Technology.

1. INTRODUCTION

The Asian Institute of Technology (**AIT**), founded in 1959 as SEATO (South East Asia Treaty Organization) Graduate School of Engineering, is an autonomous, non-profit international post-graduate technological institution located 42 kilometers on Paholyothin highway, north of Bangkok, Thailand.

The Asian Institute of Technology's mandate is to provide the necessary and relevant training and education to the new generation of the Asia and Pacific region.

Educational programs are in four broad academic disciplines: the classical civil engineering subjects, natural resource technologies, planning, and management.

The programs of study in AIT lead to the degrees of Master or Doctor, or to the award of the Institute's Diploma or Certificate.

The Institute has 1,100 students from 30 countries and an equally diverse faculty and research staff of over 200. The Institute operates on a term basis (4 months), whom intakes are in January, May, and September for various programs of study.

The Asian Institute of Technology has 4 different schools in which similar programs of study are operated, namely, School of Advanced Technology, School of Civil Engineering, School of Environment, Resources and Development, and School of Management.
Space Technology Applications and Research (STAR) Program is among other programs within the **School of Environment, Resources and Development.**

2. THE SPACE TECHNOLOGY APPLICATIONS AND RESEARCH (STAR) PROGRAM

The Space Technology Applications and Research (STAR) Program is among one of the programs teached in the School of Environment, Resources and Development (SERD) and is focussed on addressing problems using remote sensing technics, Geographical Information System and Systems analysis.

This program has been built gradually from the Environmental Remote Sensing and Geo-information for Development introduced at AIT in January 1993 under the former "Natural Resources Program (NRP)".

2.1. Rationale

Since 1972, year of the launching of the first earth's observation satellite, fabulous progress have been accomplished in term of sensors as well as in term of satellite products and digital image processing systems.

The development of Geographical Information System has lead to a complete integration of thematic maps and satellite data. These tools are now widely disseminated and are components of a rationale, technical and scientifical approaches for a sustainable development of renewable and non-renewable resources.

The STAR is keeping pace with the international trends in development and the recent Ministerial's declaration on space applications for Asia and the Pacific (Beijing 23 September 1994).

This region is continuously observed by a large number of Earth's remote sensing Satellites. The flow of data transmitted to the receiving stations - seven actually functionning in the region and two others planned- is increasing every day and the potential number of users become more and more numerous.

A large community of scientists, geographers, cartographers, decisions makers, planners, geologists, soil scientists, hydrologists, foresters, urbanists, geographers, agronomists is deeply concerned by the applications of satellite data in their respective fields of action and the "STAR" program intend to give them basic concepts, theories, and principles, etc. in a wide variety of environments.

The STAR Program, attempts to prepare students to apply remote sensing technologies for monitoring resource systems and apply system analysis and information processing techniques to use monitored data for creating sustainable societal systems.

The STAR conducts master's degree and doctoral programmes which encompass coursework, learning laboratory and research studies.

2.2. The STAR Program

The STAR Program will offer in January 1996 the degrees of Masters of Science (MSc) and Doctor of Philosophy (D.Phil) in Space Technology, with subdivisions according to Field of Study & specialisation.

The programme comprises three FOS whom two are clearly technically oriented. This paper describes these two fields. These are: "Remote Sensing and Geoinformatic Science", and "Photogrammetry & Computer assisted Cartography" which will be implemented for intake in January 1997.

2.2.1. Remote sensing field and Geoinformatic Science field of study

This field includes the following subjects within its syllabus:

* Principles of Remote Sensing
* Digital Image Processing (including algorithm development
* Microwave Remote Sensing
* Advanced Remote Sensing (3 D, GPS,..)
* Principles of Dynamic systems
* Principles of Geoinformatics
* Statistics in Geoinformatics
* Spatial data handling
* GIS Database design
* Automated data capture
* Applications

2.2.2. Photogrammetry & Computer Assisted Cartography field of study

This second field of study will include, in January 1997 intake, the following subjects in its syllabus:

* Digital photogrammetry
* Digital Terrain Models
* Automated Mapping
* Cartographic Information Processing
* Applications

Fields of study are designed to offer combined tuition in both Technology and Applications, although permitting students to choose the balance between the 2 which most interest them.

First term and part of the second would require tuition in the required technology for the chosen Field, with specialisations (technology or applications or crossover) establishing themselves partially in the second term and significantly in the third.

After the third term of classes in their master degree study, students can select to do thesis (two terms) or reseach study (one term) which then require to take one more course work option.

2.3. Facilities and Equipments

To support academic courses and conduct different workshops, a Remote Sensing Laboratory and a Geographical Information System Center (GAC) are providing the following facilities and equipments:

2.3.1. Remote Sensing Laboratory

A) The Digital Analysis Laboratory

The digital Analysis Laboratory is composed of three rooms dedicated to academic support to the Students.

* Geographic Information Systems room: 12m x 8m sized room in which 11 PC with 9 (A3 size) digitizers and 2 (topo map size) digitizers, GIS software ARC/INFO & IDRISI installed and connected to LAN system, 2 Plotters (for Master Student).

* Image Processing Room: 12m x 8m sized room in which 15 PC with 5 image display monitors, image processing software ERDAS, ENVI, EASI/PACE, ER MAPPER installed, connected to LAN system; (for Master students and Training).

* Project Room: 12m x 8m sized with 10 PC, 1 ink-jet printer, CCT reader, 1 SUN station SPARC 10 (with 3 X-Terminals) with ARC/INFO (station version, 6.0) and ERDAS (station version, IMAGINE 8.1, ENVI, ER MAPPER, PLANETES) installed, 1 SUN Station SPARC 2, LAN server etc. (for Ph. D. students and project research).

B) The Visual Laboratory

The visual laboratory encompasses ProCom II W 208 A image interpretation and map transfer equipment, 3 ARC/INFO Station, 1 Plotter, 1 CANON Colour Laser Copier, GPSs, 15 mirrors stereoscopes, 1 Digitral aoto scaler, data archives in the form of: images and films, air photos, topographic maps, soil maps, landuse maps, slides, video tapes....

C) The Photographic Laboratory

This laboratory encompasses a film processor for Black and White and Color

2.3.2. Geographical Information System Center (GAC)

The GAC will conduct specialized training courses/workshops in GIS Applications. These training/workshops are designed to give indepth treatment into specific techniques of specific topics to enable resource scientists and technicians to know more of how to apply these techniques.

Others courses, related to basics of Remote Sensing, Applied Remote Sensing and Digital Image Procesing of Remotely Sensed Data, which were offered under the former program, will be still organised according to needs and demands.

Located in a room sized 7m x 5m, the GAC is equiped with:

- 10 PCs 486
- 10 Digitizers, 10 Hardware keys. LAN server
- 10 ARC/INFO & IDRISI
- 2 Plotters

In 1996, a same number of PCs 486 (10) with the same and extra softwares, and one plotter will be installed in order to conduct 3 regular international Training courses of a duration of 3-6 weeks. These trainings will take place in December, April and August.

At least in 1997, 2 SUN stations with 15 terminals linked to LAN sever will complete the installation of the GAC.

2.4. Faculty/Staff

Faculty and Staff has been provided needed faculties coming actually from Japan, France, Thailand, United Kingdom, Phillipines, Malaysia, China, Vietnam, Burma, and Nepal.

2.5. Students and Scholarships

Students waited in STAR for January will come from: Nepal, India, Pakistan, Sri-Lanka, Bengla-desh, Myanmar, Thailand, People's Republic of China, Vietnam, Malaysia, and Philippines.

Scholarships for this program are offered by Japan, France and Thailand. Special agreement to obtain remote sensing data at a raisonnable price have been offered by the National Research Council of Thailand (NRCT). Memorandum of Understanding (M.O.U.), concerning training of the Staff, donation of Microwave data and optical data, have been signed between the STAR program and the University of Munich and RADARSAT Company of Canada. Exchanges and fructuous relations are on the way with International Space University (ISU) and the International Institute for Aerospace Survey and Earth Sciences (ITC).

Remote Sensing and GIS Education in IRAN

Ramin Rahimi Djafari,
National cartographic centre of IRAN(NCC),
P.O.Box 13185-1684 Tehran-IRAN
Tel: ++98212521906, Fax: ++98216001971
E-Mail: ncc iran@irearn.bitnet

Abstract

Nowadays the increasing need for different applications of GIS and remote sensing techniques in third-world and developing countries, is obviously an evident matter. In IRAN due to existence of abundant natural resources, and the necessity for planning and managing those resources for effective use and because of the rapid development of the country, the need for those applications is severely sensed . To use GIS and remote sensing techniques effectively and scientifically, existence of academic education in different levels to fulfil required educated personnel as well as to teach users are necessary.

In this paper different universities in IRAN that have taken some action to instruct these sciences, and educational lacks about those topics will be stated. Also other organisations and companies (Governmental or in private section) that have some rule in teaching these fields to different applicants are mentioned along with different activities of each one. There will also be an indication to difficulties and ambiguities in using GIS and remote sensing techniques and some solutions will be offered for them.

National cartographic centre of IRAN (NCC) has done some important activities and practices including:

To train graduated staff in post-graduate levels at well-known institutes in the world, organising scientific courses in GIS and remote sensing for peoples from other organisations and private individuals and also some other different activities that will be mentioned in this paper.

Introduction:

In the Islamic republic of IRAN after Islamic revolution victory, The rate of country's development increased and notwithstanding all difficulties due to imposed war, it continued rapidly and especially after finishing the war, this rate enhanced much more so that today our country is developing in all constructional, economical, cultural and social matters. On the other hand to make necessary planning for optimum use of natural resources, having sufficient and accurate geographic information about country's situation is very critical. Nowadays with existing advanced technology, the best way of acquiring this information is to establish GIS'es and to use satellite remote sensing data.

While the precedent of using these technologies in developed countries are about one quarter of a century, but in third-world countries are just one decade that importance of these techniques has been sensed. In developing IRAN although before revolution some activities had been done to receive and use of satellite data, but it was just in past few years that importance of using GIS and remote sensing techniques have been severely sensed and serious work has been started. The problem is that in advanced countries, there is an agreement between teaching technology and it's applications; but usually in developing countries' technology arrives without any teaching and training before that, which makes a lot of financial or technical problems.

In IRAN acquaintance with these technologies and their wide range of applications has been occurring since ten years ago via international conferences and seminars, visits, magazines and papers. A few years ago when importance of using these techniques for country's development was sensed, there was no academic or classic or even private teaching and training programs about these topics and there were only a few of dispersed specialists in the country. In that situation different organisations started to import and struggled to use these technologies somehow and in different ways.but because of the lack of necessary specialists in different levels, this process of importing has been facing with abundant difficulties.

In this paper different activities of universities or other organisations to solve those problems, along with some proposes and solutions that should be done and the vast amount of academic requirements of the country, will be stated.

Actions of universities:

In IRAN after revolution and in past decade, higher education has been developed so much and variety of fields of study and number of students has been increased in graduate and post-graduate levels. But in despite of this increasing rate from day to day, still we do not have GIS and remote sensing fields of study in graduate levels, while the trained manpower requirements are growing day by day.
At present there are only a few lectures related to these sciences that are teaching in some fields of studies in graduate levels that are mentioned here.

In IRAN in the field of surveying engineering there is a lecture in the last year of graduate Level, students can study one course about photography from space and remote sensing although this is not an obligatory course and usually those who is more interested to photogrammetry than geodesy, pass this course. In this course student become familiar with concepts and techniques of photography from space and different kinds of films along with elementary principles of remote sensing and photo interpretation. This course is offering in four months with two hours per week teaching program. Therefore only half of the graduated students in surveying engineering have some brief acquaintance to these sciences. Interested persons should make individual studies to become more familiar with these topics. But about GIS, there is not any academic course in any field of study in graduate levels. Only it has been agreed to put an experimental lecture of two hours per week on GIS for the last year of surveying engineering in one university in TEHRAN and in case of successfulness, it should be taught for all of the students of surveying engineering.
It is said that contents of most famous books on GIS will be taught in this course.
In post-graduate levels, an important action has been done by one university that its aim is to train and provide teachers for other universities(TARBIAT-E MODARRES university). This university established a MSc course in remote sensing in 1993, with co-operation of Iranian remote sensing centre. Each year ten graduated students can start this course. In this course they study scientific principles and techniques of remote sensing widely and also principles of GIS. Successful students will have MSc degree in remote sensing and they can teach in universities and satisfy country's requirements for researchers about these sciences. Until now this has been the only action in post-graduate levels in our country. It should also be said that students of MSc course in photogrammetry are becoming a little bit familiar with remote sensing. Activities of National cartographic centre(NCC) about these subjects will be explained in detail.
Therefore you can see that educational lacks and vacuums in different levels of these topics are so serious that mentioned actions are not satisfactory.

Activities of other organisations and companies:

Constructive and economical plans in IRAN have widely increased in recent years and country's development is becoming very fast. With existence of high velocity global communications and acquaintance of ministries and organisations with wide range of applications and usefulness of GIS and remote sensing techniques, they have been encouraged to use them and each have taken some action to buy necessary equipment and to establish GIS 'es and use of remote sensing products. But these actions were very scattered and with different aims. Some of these organisations have prepared brief training programs for their personnel. Iranian remote sensing centre is the governmental centre to receive, use and distribution of satellite data that is related to ministry of communications. Until now the most important educational activity of this centre has been some co-operation with " TARBIAT-E-MODARRES" university to establish a MSc course in remote sensing. This centre has three branches in 3 provinces and there is a short course about " principles and techniques of remote sensing and applications of satellite data" for the personnel of those branches.
A remote sensing group has been formed since ten years ago in Iranian geological survey(IGS). Their objectives are to use satellite images for geological map updating, mine explorations, geotechnique surveys and making geomorphologic maps. This group has good equipment and they have done useful activities, but they didn't have important educational programs.
Other organisation which is dealing with geographical information is "geographic organisation of armed forces"which is related to army. The duty of this organisation is to satisfy military requirements for maps and other geographic information. If army needs for some special GIS, this organisation should make that It has also a section for remote sensing Because in IRAN urban development is occurring

very fast, city information systems or LIS'es are very necessary and useful. In this direction, TEHRAN municipality has established a GIS for TEHRAN that has been very useful for rural application. In some ministries they have started with research activities to become familiar with these techniques in more basic way; For example in ministry of power, they have tried to make a research committee on GIS to analyse the requirements and determine characteristics of theirs required systems.
In private section the most important activities are to imitate representative companies from famous foreign companies to import their products but in one or two private companies, some useful actions have been done to use satellite data for national objectives. One company has made the image map of IRAN at scale 1/1000000 with SPOT data and this is the first time that private section is doing this job.

Activities of national cartographic centre(NCC):

National cartographic centre of IRAN(NCC) was established in 1953 as a lower part of ministryof plans and budgets. NCC and geographic organisation of armed forces were merged in 1972. NCC started to make topographic maps at scale 1/25000 in 1979, but this task was stopped because of the war. Real production of these maps was started in 1990 with help of united nations. At present these maps are being produced in a totally digital way. NCC is responsible for implementation of all national mapping programs and Islamic parliament has given the national GIS program to NCC that it's operational carry out has seriously been begun since last year. Basic maps of this national GIS are 1/25000 digital maps produced at NCC. Most important objectives of GIS department of NCC are: To educate and research about GIS, making national topographic database, making national GIS at scale 1/1000000 and to propagate GIS culture in the country.
The most important action that has been done to meet the trained manpower requirements was to send graduated specialists abroad to famous international institutes like ITC (The Netherlands) to study in post-graduate courses. AT present there are about 25 peoples at NCC that have studied in ITC on Photogrammetry, GIS, remote sensing and cartography and they have post-graduate diploma or MSc degree. Considering this NCC has some co-operation with universities for educational programs or conducting them. Now most of them are teaching new techniques of photogrammetry, GIS and remote sensing in universities. Other important activity of NCC is to carry on short educational courses for specialist personnel of other organisations and interested individuals to teach general principles and techniques of GIS and remote sensing. These classes have been started last year and during them theoretical principles and operational techniques of GIS & remote sensing which are needed for various applications of different organisations, is explained. People who pass these courses can effectively use these techniques for special requirements and applications of their organisations.

Ambiguities, difficulties and solutions:

Although GIS and remote sensing techniques are widely used in developed countries for various applications and these sciences are rapidly expanding, but sometimes there are still some doubts and myths to use them even among specialists of other scientific fields. Perhaps this is because of their insufficient and incorrect understanding about these techniques and their fields of applications.
Nowadays with convincing answers to those ambiguities, the doubts are becoming lesser day by day, fields and correct methods to apply those techniques are becoming more clear and more specialists are finding proper use of the technology as the best tool for their constructive, natural or environmental planning problems. In developing countries like IRAN, main difficulties in GIS and remote sensing education that has been existed and partly existing is:
-Computer equipment has been expensive and necessary maintenance was a complex task for educational institutes and sufficient numbers of computers have not been available.
-Correct using of complex GIS and remote sensing software was difficult especially for those who have a little experiment on computers and their mother tongue is not English.
-Satellite imagery was expensive and it has been difficult to obtain them.
-Importance of using satellite imagery and GIS'es for development was not clear for governmental decision makers, and because of this it has been very difficult to justify training courses on these topics.
It has been more or less these difficulties or similar problems that caused retardation and sensible educational lacks about these topics in countrie such as IRAN. Fortunately computer equipment is gradually becoming less expensive and different specialists more familiar with GIS& remote sensing softwares;Satellite imagery are becoming available with reasonable prices, Therefore decision makers are understanding that they can and they should use new technologies for planning& development

affairs. Therefore they are recognising the necessity for serious care about educational problems. In IRAN we need two kinds of specialists:

1) Researchers who can develop new methods and expand applications and to teach in universities as professors.

2) Technicians who can apply proved techniques in special operational problems.

Considering rapid development of the country and recognising wide range of applications of these techniques and to remove educational lacks to reach to an independence situation in training and using them, it is foresighted that specialist man power requirements in different levels in next ten years shall be as following:

Level -----> Years	Graduated from high school (with technical training)	Technician level	Graduated level	Graduated level	PHD level
1996	500	250	100	40	10
2000	700	350	200	60	20
2005	900	450	300	80	35

Table 1) Foresighted manpower requirements in different levels on GIS and remote sensing in next ten years in IRAN.(Numbers are in persons).

To attain above aims and predicted trained manpower requirements as above table, we should establish non-existing required educational curriculum and GIS and remote sensing subjects should be included in all academic levels from elementary school to highest levels of university in a proper way. With this action, not only we can educate required specialists but also the public will have some general knowledge about basis of these sciences. In each of the educational levels there should be some subjects suitable for that level and age.

In elementary school following subjects can be included : General figure of the earth, ability to take pictures of this globe from sky and outline of aerial photographs. In geography lectures of secondary school we can teach : Stereoscopic vision of aerial photographs and concept of scale of images.

In geography lectures of first two years of high school, principles of aerial photography, electromagnetic radiation and spectrum and also spectral behaviour of different objects on earth's surface, can be taught. An introduction to different sensors, various formats of data in computers, concept of resolution in satellite images, an introduction to atmospheric effects, general concept of GIS and using different layers of data for GIS analyses along with computer operations and field works, can be included in last years of high school.

In establishing proposed curriculum as above table, care should be made that graduated persons should have abilities suitable to country's requirements.

In the technician curriculum, half of the course should be covered with teaching necessary theories and in the rest students should do different operational projects

During the graduate level, all of the proved general sciences and theories about that topic should be taught and students should accomplish a good project in the last year.

In the master of science course, students should have ability to develop and expand related techniques in some special subject and they should also teach with full domination in the related lower levels.

I believe that with two plans, in 5 years and 10 years, we can become quite independent about specialist manpower requirements and university teachers in GIS and remote sensing. Of course to attain this aim we should take maximum advantage of existing specialists and scientists and also in the first 5 years, we should send abroad some specialists to study in MSc and PHD levels at good universities in other countries.

The most important necessary background for successfulness in graduate level on GIS is high skills in mapping sciences and map reading, computer analyses, database management and computerised cartography . Therefore the major part of lectures in graduate level on GIS should be : Surveying, cartography, computer, software and databases. It is also better that half of the MSc students in GIS, have licentiate's degree in surveying or GIS and the rest with degrees in mathematics and computer.

In the graduate level on remote sensing, successfulness depends on having good abilities in maps, map reading, photogrammetry, computer and optics and also basics of Electronics and electromagnetic waves. Then in the curriculum there should be serious emphasis on physics. It shall be better that half

of the MSc students in remote sensing had been graduated in photogrammetry or remote sensing and the rest in physics.
I believe that graduated people in geography can not be successful in MSc courses on GIS or remote sensing, because they do not have necessary knowledge about physics, computer and surveying.
In this way, all necessary curriculum shall be established in a consistent and suitable manner, which will satisfy country's requirements in all different levels.

Conclusion:

Nowadays the correct way of advancement in all of the scientific fields is quite clear and proved and it needs for serious struggle and effort. About GIS and remote sensing techniques, considering requirements of developing IRAN to these sciences and on the other hand serious mentioned deficits and lacks, an obvious necessity for effort and advancement on these fields is sensed. Therefore we should apply all our possibilities and capabilities and we should make earnest effort to establish mentioned curriculum and promotion of related scientific culture across the country. Time is priceless and this should be done as fast as possible. With this action we can reach to required necessary level in ten years. To do so we should take advantage of experiments of advanced countries and also there is good readiness to present our experiments for other developing nations. There is a proverb that says: If your horizon is one year, plant rice; If your horizon is ten years, plant trees; And if it is 100 years educate your children. Only with serious and planned effort, we can reach to that high level in these sciences which is really decent and suitable for our nation and our country.

References:

Bhan, S. K. And Dutt, C.B.S. (1991) "Remote sensing training opportunities", J. Current sciences. Vol.61, Nos. 3&4, pp 278-281.

Chandrasekhar, M.G. (1994) " Remote sensing and GIS for planning and development" Proc. 15Th ACRS, Nov. 1994, Bangalore, India.

Chandrasekhar, M.G. (1994) "Remote sensing for sustainable development" special UN workshop on remote sensing for rural development held at Graz, Austria. on Sept. 12, 1994.

Gupta,A.K., V. Jayaraman and M.G. Chandrasekhar,(1994)." Strategies for the introduction of remote sensing in the educational curriculum in India" Proc. 15Th ACRS, Nov.1994, Bangalore, India.

Gupta, A.K., Ganesha raj,K. and Chandrasekhar, M.G. (1992)" Perspective approach in remote sensing training " Proc. 13Th ACRS, Oct.1992, Ulaan baator, Mangolia.

Kurt T. Rudah and Sally E. Goldin, (1994)." The impact of new technologies on remote sensing education" Proc. 15Th ACRS, Nov. 1994, Bangalore, India.

Hamid,J.R. And Ahmad, N (1991) " Education and training future surveyors" proc. 4Th south east Asian survey congress, Kuala Lumpur.

PE&RS (1993) " The NCGIA core curriculum in remote sensing" Photogrammetric engineering and remote sensing vol 59 No. 6 June 1993

" Recent development in remote sensing and GIS" in remote sensing newsletter Vol. 11, No.2 , Oct. 1993.

Voute. C. (1983) " Education and training in remote sensing for resource development " ITC Journal 1983-1, PP 34-41.

GEOGRAPHIC INFORMATION ANALYSIS : A CASE STUDY AS AN AID TO TEACHING

R. SUDARSHANA, S. SEBASTIAN,* AND S.K. BHAN

Indian Institute of Remote Sensing, 4, Kalidas Road, Dehradun - 248 001, INDIA.

ABSTRACT

A Digital Elevation Model (DEM) was created for a small geographic area on the personal computer subsequent to digitising the elevation from a map of 1:1000 scale. The DEM was transformed into a raster of single band image and several overlays of utilities and features were created as boundary files to be covered on the DEM. Several combination of the overlay considerations have been analysed and presented. In addition, case was taken to manage the datafiles in a way that suits the needs of imparting training in Geographic Information System (GIS). Several tutorial schedules that could be adopted for teaching are suggested and it is hoped that the emulation of this example would came a long way in the transfer of a technology which is fast emerging and is calling for attention.

* Society of Management Science and Applied Cybernetics.
C/o International Management Institute
B10/30-31, Qutab Institutional Area,
New Delhi - 110 016, INDIA.

INTRODUCTION

Development of spatial resources require an in-depth analysis of the existing units within a definitive geographic boundary in terms of location, quality and quantity. Further, the interrelationships of these units in providing useful solutions to the problems of space and resource use are of immense importance in explains the optimal behaviour of geographic features. In the conventional scientific education, this situation is simulated by studying various academic disciplines initially and considering a multidisciplinary condition at the decision making level. But in the recent time technology has enabled us to consider the features as segregated layers of information which may be computed in various ways to indicate natural processes. The later ability is termed popularly as geographic information systems (GIS) suggesting an arrangement of systems analysis of various information, processing compatible geographic identity.

Hence, the term 'geographic information analysis' broadly includes the capability of compiling, formating, storing, manipulating and retrieving information of defined geographic enclosures for the benefit of optional development of spatial resources. In the present context too, it has been envisaged to collect and collate diverse information in the ambit of their geography.

Moreover, realising the need of evolving case studies as an aid in teaching, the example has been organised into a set of modules of information and suggestions on how to develop curricular schedules around them are provided. The case study has already been adopted as a teaching aid and is found to be of interest amongst scientific workers.

DATA SYNTHESIS AND ANALYSIS

FEATURES OF STUDY AREA :

The study was conducted for the campus of Indian Institute of Remote Sensing (IIRS), Dehradun which covers an area of about 20.9 acres. This small parcel of land is a segregated geographic entity in the sense that most of it forms a plateau which is surrounded by sharp slopes and deep valleys on three sides. Out of the 20.9 acres, nearly half lies on slope and valleys for the purpose of study, same portions of surrounding area were also included and the total range of altitude in the area was from 665.5 m to 699.5 m above chart Datum.

COMPILATION OF BASIC DATA AND GENERATION OF DIGITAL ELEVATION MODEL (DEM)

Basic source of data was the recently prepared map of campus region in the scale of 1:1000. A close grid was overlaid on the map and 982 points were sampled from grid intersections for elevation data. This intense sampling at very close interval provided a very real representation of the terrain of the region. The X, Y (map co-ordinates) and Z (elevation) data from all the 982 points were arranged in a LOTUS-spread sheet format and further subjected to interpolation on a personal computer using the following model.

$$Z(x_j) = \frac{\sum_{i=1}^{n} Z(x_i)\, d_{ij}^{-2}}{\sum_{i=1}^{n} d_{ij}^{-2}}$$

where,

Z = elevation in meters

X_j = points at which surface is to be interpolate

d_{ij} = distance from the reference point to the point to be interpolated.

The above model follows the logic of weighted moving average or inverse squared distance weighting (Burrough, 1990) based on the argument that observations located close together tend to be more alike than observations spaced further apart. For the interpolation, a size of 250 (x) and 210 (y) was considered with a search radius of 20.6155281 and 10 nearest points. The inherent cell size was 0.177 meters in both x and y directions. The resultant grid raster was of the size of 52,500 elements and it seemed as the DEM for IIRS campus region. A contour plot of this DEM is shown as Fig. 1 and a perspective surface plot is given as Fig. 2.

IMAGE GENERATION FROM DEM

The grid raster of interpolated DEM was reorganised and formated into a raster image of 210 lines and 250 columns. The image became akin to a single band satellite image and was provided with a header information on cell size, latitude centre, projection etc. enabling it to accept polygon overlays later. This DEM image was monitored on Image Display Analysis (IDA), (FEWS, 1989) on a personal computer. The image header details are provided in Table 1, while the image of DEM is shown in Fig. 3.

GENERATION OF OVERLAYS AND PERSPECTIVE VIEWING

The formation of the image of DEM of IIRS campus with a header providing definitive geographic position of each pixel opened up the possibility of overlaying feature boundaries within the image frame. Making use of this, a number of boundary files were created on the grid with the help of sources like engineering drawings and field work. The overlay files had a very simple structure of co-ordinate listing. The overlays were lines and polygons, depending on the feature and one line header for each vector was maintained. This header consisted of two values, the first being the vector attribute and the second being vector size in terms of number of points. The overlays could be called one after the other and superimposed on image of DEM on IDA. The simple structure of image and its overlays provided possibility of considering the features in various combinations. The layouts of various overlays in combination are given in Figs. 4 to 9. Further, the vectors of landuse were also generated containing information on lawns, groves, gardens etc. and a choropleth formation of each feature vector provided a comprehensive layout as shown in Fig. 10. Once the choropleth images were developed, several choropleths were pooled in one file and the whole was overlaid on the DEM in perspective using IDRISI on personal computer. This perspective is given as Fig. 10. The percent occupation of each vector in the campus is also shown in Table 2.

DATABASE AS A TRAINING AID

The database of the IIRS campus has been created with a very simple structure as stated earlier in view of its proposed use as an effective tool in training activities. While learning GIS at conceptual and technical levels, this example is hoped to serve a multi-disciplinary clientele. Before appraising of the tutorial pattern that may be followed with the help of database, it would be appropriate to list the overlays that were created, as follows :

OVERLAYS	BASIC IMAGE
1. Buildings	1. Digital Elevation Model
2. Roads	
3. Fence	
4. Water supply	
5. Power supply overhead	
6. Power supply underground	
7. Vegetation	
8. Land morphology	
9. Telephone line	
10. Sewer lines	

Several tutorials could be developed around this database in order to derive various thematic objectives. While the combinations could be many, a few important suggestion as schedule are given in Table 3.

CONCLUSION

In all, system analyses such as this have a definite advantage over the conventional means of data synthesis in view of resource development and optimal planning. In the contemporary context, use of these case studies for imparting training in an organised way is also of utmost importance. The basic inherent advantage of databases like this is that the format is simple and may be created, maintained and augmented at case on a variety of hardware platforms. Being raster in format and changing over to vector only for overlaying, is a definite advantage in view of personal computers that are largely available. Moreover, the database when used as a training aid fulfills the needs of technology transfer and every step of database augmentation would result in updation of tutorial schedules in a way similar to curricular updation. Hence, the scope of experiments such as this is wide and diverse.

REFERENCES

Burrough, P.A., 1990. Principles of geographical information systems for land resources assessment. Oxford science publ., Oxford, U.K. pp. 194.

FEWS, 1989. Image Display and Analysis. Price, Williams and Associates inc., U.S.A. pp. 42.

Table 1 : Header Information of DTM image

Title : IMAGE OF THE DTM OF INDIAN INSTITUTE OF REMOTE SENSING

Image type code	0	Generic
Projection	3	Platee Carre
Height	210	
Width	250	
Lat-center	19.50000	
Long-center	26.00000	
X-center	125.00000	
V-center	105.00000	
DX	0.1760000000	
DY	0.1761904762	

Table 2 : Areas of feature polygons

FEATURE POLYGON	NO. OF PIXELS	AREA			PROPORTION	
		in sq.ft	in sq.ft	in acres	% of Plateau	% of Total
Offices	1401	36823.37	3420.99	0.8453	8.21	4.04
Residences	599	15743.90	1462.65	0.3614	3.51	1.73
Hostels	396	10408.32	966.96	0.2389	2.32	1.14
Lawns	811	21316.03	1980.32	0.4893	4.75	2.34
Groves	617	16217.00	1506.60	0.3722	3.62	1.78
Plantations	415	10907.71	1013.35	0.2504	2.43	1.20
Kitchen Gardens	671	17636.32	1638.46	0.4048	3.93	1.94
Gardens	537	14114.31	1311.26	0.3240	3.15	1.55
Roads	530	13930.33	1294.16	0.3197	3.10	1.53
Total Landuse	5977	157097.29	14594.75	3.61	35.02	17.25
Total campus on Plateau	17070	448668.00	41682.54	10.3	---	49.28
on Ravines	17567	461736.00	42896.60	10.6	---	50.72
Grand Tot.	34637	910404.00	84579.14	20.9	---	100.00

Table 3 : Suggested Tutorial Schedules for Database of IIRS Campus

THEME CONCEPT		OVERLAYS AND OUTPUT	
OBJECTIVE	SOLUTION	GRAPHIC OVERLAYS	NUMERIC OUTPUT
Layout map	Combination of permanent features	Fence,buildings,roads vegetation	Polygon areas
Utility map	Indication of supply network with destination	Fence,buildings,water supply, power supply, telephone sewer	length of cables, length of water,pipelines,length of sewer lines
Underground utilities	Projection of earth work	Fence,buildings,water supply network, sewer lines, power cables	Length of trenches Redundancy analysis
Probable water pollution	Indication of sewer proximity to water supply line	Fence,buildings,water supply sewer lines	Number of crossings, distances at grid positions, Length of proximal areas
Vegetation map	Combination of all vegetation classes	Fence, Vegetation	Areas of polygons
Development of green areas	Indication of possible areas for lawn, grove etc. development	Fence,buildings,roads vegetation, water supply	Available areas proximal to water supply
Space for new buildings	Exploration of DEM for suitable areas	Fence,buildings,roads vegetation, DEM	Position and areas of available flat zones, proximity analysis with power water,sewer lines
Soil conservation	Observation of landslide and erosion prone areas	Fence, DEM	Slope positions,Euclidean distance to gradient ratio Total erosion prone area
Local Area Network (LAN) of computers	Exploration of optimal path for cable laying between	DEM, buildings, power supply, telephone	Positions to avoid power supply crossing, Positions to avoid slopes shortest cable distance costing of earth work.

WORK SHOP

SPATIAL INFORMATION PROCESSING

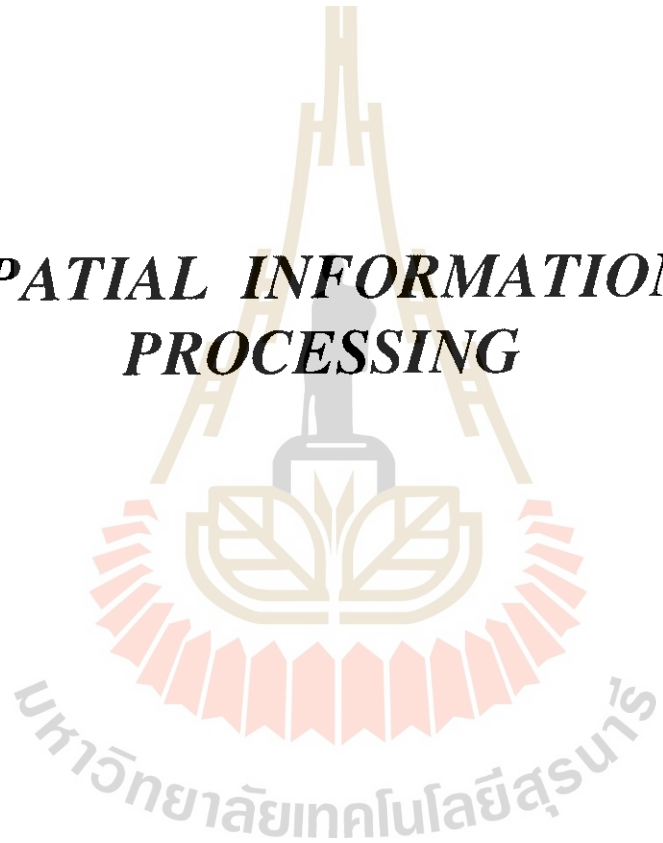

GA OPTIMIZATION TECHNIQUE ON SPATIO-TEMPORAL INTERPOLATION FOR DYNAMIC GIS

Shaobo HUANG* and Ryosuke SHIBASAKI**

ABSTRACT

Generating cross-sectional data of arbitrary time slice is a basic function to support temporal operations such as time-series analysis and integration of dynamic models in Global GIS environment. To generate time slice data, it is necessary to interpolate/integrate existing global data with different temporal coverage and spatial resolution. Although interpolate/ integrate methods have been developed for continuous variable data, there are only very primitive interpolation methods such as nearest neighbour interpolation considered about class variable data. Here we proposed a spatio-temporal interpolation scheme for pixel-based class variable data under the framework of optimization of likelihood. To optimize the likelihood of spatio-temporal data, a Genetic-Algorithm/Hill-Climbing model (GA/HC), which combined genetic-algorithm and Hill-climbing method together to increase the efficiency and quality of optimization, was developed. In GA/HC, a direct coding method and new reproduction and crossover operators are proposed for 3D spatio-temporal data. The evaluation function of GA/HC is defined in the respect to the effect of neighbouring spatial-temporal relations on the class change. Through several testing experiments, it showed that GA/HC can be a good spatio-temporal interpolation.

KEYWORDS

Spatio-temporal Interpolation, Class Variable data, Optimization, Genetic Algorithm, Hill-Climbing

1. BACKGROUND AND OBJECTIVE OF THE STUDY

Temporal or dynamic analysis of spatial data are needed in various fields such as environmental systems analysis. One of the most fundamental problems which users are facing is the difficulties in generating spatio-temporal filed of quality data for analysis through an interpolation or integration of observational data. In several fields, to improve reliability of spatio-temporal interpolation/ extrapolation in generating quality data, models and/or equations describing an underlying mechanism and structure is integrated with observational data. By integrating observational data and models describing underlying mechanisms and structures of object-phenomenon with a GIS, we can provide a GIS-based environment which allow dynamic update of spatio-temporal field of data whenever a new observational data and an improvement of models are given. If computational speed for integration is fast enough, we can store only observational data and can estimate data at any locations based on the requests.

Integration methods for data and models have been mainly developed for continuous variables in meteorology and oceanography such as temperature and precipitation. For categorized or class variables such as land use types, there is only very primitive interpolation methods such as nearest neighbor interpolation and so forth. In this paper, the authors propose a integration methods of models and class data from multi-sources under the framework of optimization of likelihood of spatio-temporal events. For optimizing the likelihood, genetic algorithm (GA) is modified by combining GA with classical "Hill climbing" method. Experimental results demonstrate that GA can be successfully applied to the integration.

2. GENETIC ALGORITHM(GA) AND CLASS VARIABLE INTERPOLATION

2.1 Introduction of Genetic Algorithm (GA)

Genetic algorithms are developed by John Holland and his colleagues as an approach to optimization which requires efficient and effective search in natural and artificial systems. They are search algorithms based on the mechanism of natural selection and evolution of natural genetics. They combine survival of the fittest among string structures with a structured but randomized gene exchange to form a search algorithms with some of innovative flair of human search (D.E.Goldberg, 1989).

Genetic algorithms are computationally simple and powerful in their search without restrictive

* **Shaobo HUANG** : **Center for Environmental Remote Sensing, Chiba University, JAPAN**
shaobo@rsirc.cr.chiba-u.ac.jp
** **Ryosuke SHIBASAKI** : **Institute of Industrial Science, University of Tokyo, JAPAN**
shiba@shunji.iis.u-tokyo.ac.jp

assumptions about search spaces. In a simple genetic algorithm, five basic aspects should be considered: the representation or coding of problem, the initialization of population, the definition of evaluation function, the definition of genetic operators, and the determination of parameters.

2.2 Optimization Scheme for Class Variable Interpolation

Most natural properties may vary continuously. However, the observation that describe these properties and which form the data bases of GISs are usually fragmentary. Ever where a complete cover of information exists, for instance from the satellite images, we still often need to resample because there are too many data to handle or analyze in any reasonable time. Because the properties are continuous that values in sites are close together in space are more likely to be similar than those further from one another, i.e., they depend on one another in a statistical sense. This important feature of spatial data provides the rationale for interpolation (M.A.Olover, 1990).

Spatial-temporal data can be divided into two types: continuous variables data and class variables data. R.Shibasaki et al.(1993) proposed a Kriging-based integrating/interpolation method for continuous variable data and an interpolation method for class variable data based on the estimation of time of changes according to "class boundary distance". But for the class variable data, the method of the time-of-change estimation seems not to work well, because complex temporal and spatial relations among classes around a pixel greatly affect class variation at this pixel and make it difficult to estimate the time of change at the pixel. In fact, interpolation problem of class variable data is a hardest combinatorial optimization problem in spatial and temporal dimensions.

In this research, we go to integrate observational class data with behavioral/structural models/rules to make robust and reliable spatio-temporal interpolation of class variables. Since searching for the most likely spatio-temporal field of class data is typical combinatorial optimization problem, we introduce the genetic algorithm as a optimization scheme for class variable data to get optimized interpolated time-slice data. To estimate the most likely spatio-temporal field of class data, we maximize the likelihood of estimated spatio-temporal field. The likelihood is computed based on both the fitness to observational data and that to behavioral/structural models/rules. The fitness to observational data is determined from the accuracy and resolution of observational data, while the fitness to behavioral/structural models/rules is computed as the combined likelihood(probability) of transitional events under the assumption that all transitions follow probabilistically the behavioral/structural models/rules.

3. APPLICATION OF GENETIC ALGORITHM FOR INTEGRATING BEHAVIORAL MODELS AND OBSERVATIONAL DATA TO CLASS VARIABLE INTERPOLATION

3.1 3D Representation of an Individual (coding)

In the research, two dimensional spatial and one dimensional temporal space was considered to compose a 3D spatio-temporal space as shown in **Figure.1**, in which horizontal surface is used to represent 2D space and vertical dimension is used to represent temporal dimension. A three dimensional array is defined to represent the individual.

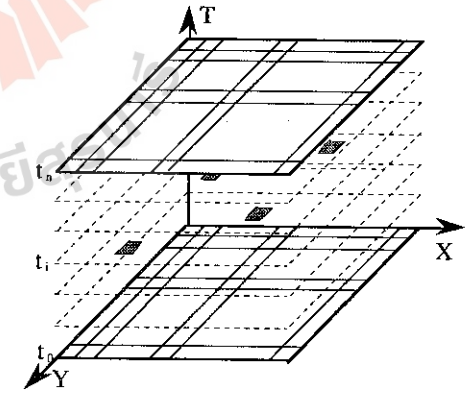

Figure.1 Representation of Individual

3.2 Initialization of Population

An initial population for a genetic algorithm is usually chosen at random; one random trial is made to produce each individual. All members of initial population are chosen automatically by same procedure so that the expected value of each member of initial population is same. In addition we use cubes of 1*1*1, 2*2*2 and 3*3*3 pixels as the initial unit for the initialization of population to increase the efficiency of algorithm.

3.3 Definition of Individual's Fitness

3.3.1 Spatio-temporal Behavioral Models/Rules of Class Variable Data

It should be noted that any types of behavioral/structural models/rules can be used for the GA-based interpolation if they can determine the probability of every possible behavior/transition of class variables. In class variable data, the possible changes of a class at one pixel is basically defined by the probability of the changes from one class to another. One of the simplest example is a Markov chain, where transitional probability is determined only by the previous class. In addition the probability also can be affected by

combination of classes in the neighborhood. In this study, we assume the transitional probability is determined by the combination of classes in the neighborhood. And landuse data with five classes is used as test data.

The spatial and temporal relations affect the transitional probability in three ways as shown in the **Figure.2**. The first is so-called the spatial continuity, which is based on the assumption that the same class data tends to continue in spatial dimension. Therefore, the effects of the spatial relation happen just within the same time-slice data. Second one is called temporal continuity. This is an extension of spatial continuity to temporal domain. The third aspect is expansion-contraction relations based on the assumption that some class data has high possibility to expand its area at next time-slice, while others tend to contract. The temporal change in the pixel with un-contractible class type will be determined by the pixel's class itself. And the temporal landuse change in the pixel with contractible type will be determined by class of the pixel and classes of its expandable neighborhood.

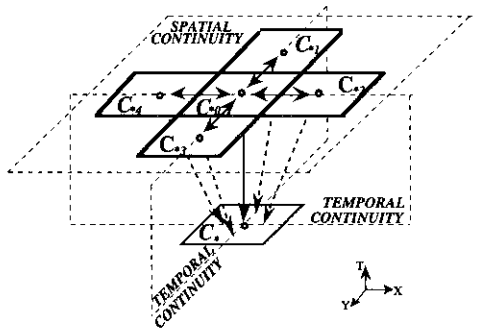

Figure.2 3D Spatial-Temporal Relation of Pixel-based Class Variable Data

3.3.2. Calculation of Individual's Fitness

Individual's fitness has two parts: behavioral fitness and observational fitness. Behavioral fitness is defined as combined probability of change events of class variables when these changes follow probabilistic behavioral models or rules. Observational fitness can be defined as combined probability that the observational class values occur under probabilistic functions of observational errors / uncertainties. By multiplying behavioral fitness and observational fitness, overall fitness can be computed. To integrate behavioral/structural models and observational data, the overall fitness have to be optimized. In this paper, we omit the observational fitness just for simplification of simulation.

Figure.3 shows possible class change in spatio-temporal space. Let define $P_{TC}(C_{*0}, C_*)$ as the probability of class change from class C_{*0} to class C_* by temporal continuity under the effect of expansion-contraction within C_{*0}'s neighbourhood and $P_{SC}(C_{*0} \sim C_*)$ as the probability of class change by spatial continuity. If it is assumed that $P_{TC}(C_{*0}, C_*)$ and $P_{SC}(C_{*0} \sim C_*)$ are independent, we can compute behavioral fitness of each individual according to following formula:

$$\underset{\text{(behavioral fitness)}}{\text{FITNESS}} = \prod_{P=1}^{N_P} \{ \prod_{T=1}^{N_T} P_V (C_{P,T}, C_{P,T+1}) \} = \prod_{P=1}^{N_P} \{ \prod_{T=1}^{N_T} P_{TC} (C_1, C_*)\, P_{SC} (C_1, C_2, C_3) \}$$

where N_P : is the pixel number,
N_T : is the temporal slice number,
$C_{P,T}$: is the landuse class of the cell on the Pth pixel at the T time slice;

For the class change probability with spatial continuity, $P_{SC}(C_{*0} \sim C_*)$, we set values according to following five neighboring pixel's statues along the spatial dimension, which form a set of behavioral rules: 1) If classes in all 5 pixels are equal; 2) If classes in 4 pixels including middle pixel are equal; 3) If classes in 3 pixels including middle pixel are equal; 4) If classes in 2 pixels including middle pixel are equal; 5) If all classes in 5 pixels are unequal.

As respect to class change by temporal continuity under the effect of expansion-contraction, all

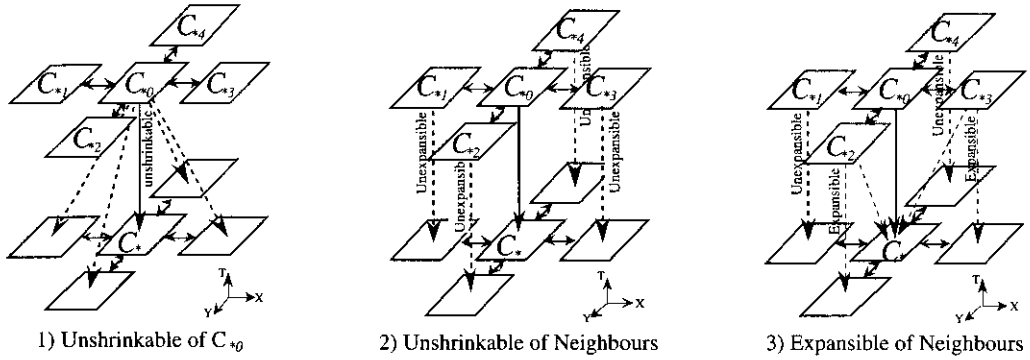

1) Unshrinkable of C_{*0} 2) Unshrinkable of Neighbours 3) Expansible of Neighbours

Figure.3 Possible Class Change in 3D Spatio-temporal Space

C_{*0}'s neighbours \ C_{*0}	unshrinkable	shrinkable
unexpansible	Markov chain	Markov chain
expansible	Markov chain	Markov chain + Invasion

Table.1 Pattern of Class Change by Temporal Continuity under Expansion & Contraction

Value of Invasion C_{*i1}	Value of Invasion C_{*i2}	C_{*i1} $P_M(C_{*0}, C_{*i1})$	C_{*i2} $P_M(C_{*0}, C_{*i2})$	$C_{*i1} = C_{*i2}$ $P_M(C_{*0}, C_{*i1})$	Others $P_M(C_{*0}, C_*)$
Yes ($\alpha_{C_{*i1}}$)	Yes ($\alpha_{C_{*i2}}$)	0	0	Invasion	0
Yes ($\alpha_{C_{*i1}}$)	No ($1-\alpha_{C_{*i2}}$)	Invasion	0	Invasion	0
No ($1-\alpha_{C_{*i1}}$)	Yes ($\alpha_{C_{*i2}}$)	0	Invasion	Invasion	0
No ($1-\alpha_{C_{*i1}}$)	No ($1-\alpha_{C_{*i2}}$)	Markov Chain	Markov Chain	Markov Chain	Markov Chain

Notice: 1> Supposed C_{*i1} and C_{*i2} are expansible (i1, i2 = 1 – 4) ;
2> $\alpha_{C_{*i1}}$ and $\alpha_{C_{*i2}}$ are defined as expansion speed of C_{*i1} and C_{*i2} ;

Table.2 Behaviors of Class Change

possible patterns of class change are listed in **Table.1**. From this table, we can determine the probability of class changes by temporal continuity under the effect of expansion-contraction, $P_{TC}(C_1, C_*)$, based on the probability of class changes in Markov chain $P_M(C_{*0}, C_*)$, and the expansion speeds if the invasion of neighbouring pixels is happened. All behaviors of class change under the effect of expansion-contradiction can be deduced from the table like **Table.2**.

3.4 Definition of Operators

3.4.1 Reproduction

Reproduction is a process in which individual strings are copied according to their objective function values or the fitness values. Copying strings according to their fitness values means that strings with a higher value have a higher probability of contributing one or more offspring in the next generation(**Figure.4**). This operators, realizing an artificial version of natural selection, a Darwinian survival of the fittest among string creatures.

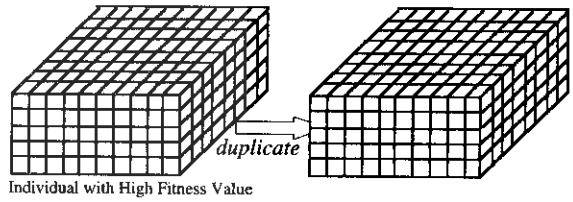

Figure.4 Reproduction of Individual

There are several proposals for selecting survival individuals. The most basic scheme are called the roulette wheel scheme, the deterministic sampling and the elitist scheme. In order to efficiently find the best solution in search space, in our search, we proposed the selection scheme based on the combination of the deterministic sampling and the elitist scheme. The selected survival possibility in next generation of each individual is calculated as in the deterministic sampling. And the best individual is kept into the next generation as in the elite scheme.

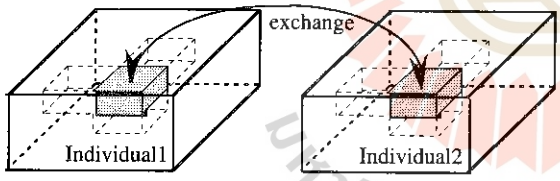

Figure.5 Crossover of Individuals

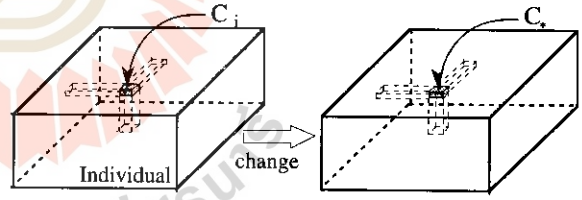

Figure.6 Mutation of One Individual

3.4.2 Crossover

Crossover operator first randomly mates newly reproduced individuals in the mating pool. Then it randomly locates a window with random size for a pair of individuals. Finally, the contents of individuals within the window are swapped to create new individuals (**Figure.5**).

3.4.3 Mutation

Mutation operator plays a secondary role in the simple GA. It occasionally alters the value in a individual position (**Figure.6**).

4. IMPROVEMENT OF THE SEARCH IN GENETIC ALGORITHMS

4.1 Hill-Climbing method to improve the efficiency of genetic algorithm

Searching a complex space of problem resolutions often involves a trade-off between two apparently conflicting objectives: exploiting the best solutions currently available and robustly exploring the space(Lashon Booker, GA&SA). Generic algorithms have been toured as a class general purpose search strategies that strike a reasonable balance between exploration and exploitation. The power of these algorithms is derived from a very simple heuristic assumption: that the best solutions will be found in regions of the search space containing relatively high proportions of good solutions. The problem is that, if the complex space of problem resolutions become larger and larger, the population size and the generation

size have to be increased at same time. The efficiency of GA is one of obstacles to apply GA in reality.

Hill climbing is a good example of a search strategy that exploits the best among known possibilities for finding an improved solution. Although Hill-Climbing strategies is easy to trap in one of local maxima more far away from the optimal solution, it is a very good search strategy that exploits the best among known possibilities for finding an improved solution. So in our research we try to combine the Hill-Climbing strategy with GA.

4.2 Maintenance of Population Diversity

Despite the demonstrated advantages of GAs and high performance of most implementations, it still fails to live up to the high expectations engendered by the theory. The problem is that, any implementation uses a finite population or set of sample points. Estimates based on finite samples inevitably have a sample error associated with them. Repeated iterations of algorithm compound the sample error and lead to search trajectories much different from those theoretically predicted. The most serious phenomenon is the premature convergence.

The premature convergence is caused by early emergence of an individual that is better than the others in the population, although far form optimal. Copies of this structure may quickly dominate the population. Search continues then but is concentrated in the vicinity of this structure and may miss much better solutions elsewhere in the search space.

To avoid the premature convergence, one has to maintain population diversity or to reduce the different of best fitness with others. Although, to reduce the reproduction number can not eliminate the premature convergence, it can be used as a simple way to reduce the rapid convergence. Therefore, in our research, we limited the duplicated number of individuals within two. It means that if individual's expected duplicated number is larger than two, we will force it to equal two. To do so, the premature convergence speed can be reduced.

5. EXPERIMENT

The test program of GA/HC for spatio-temporal interpolation of pixel based landuse data was coded with C language and was run on SPARC/station2. Several simple landuse class variable data had been used to test program. For the test data, only two dimensional spatio-temporal data is shown here. The test data size of individual had been defined with 20pixels*6time-slices. The first and last time-slice in the individual were supposed to be sampled data and all middle time-slices were unsampled data which needed to estimate through interpolation processing. In these experiments, we set the generation size of GA/HC to 2000, which was large enough to get stable results. The probability of crossover operation was defined as 0.7, while the probability of mutation operation was relative small in natural population, so that we used 0.01 as the probability of mutation. **Figure.7** is one of experiment results of GA/HC, in which the individual has largest fitness value.

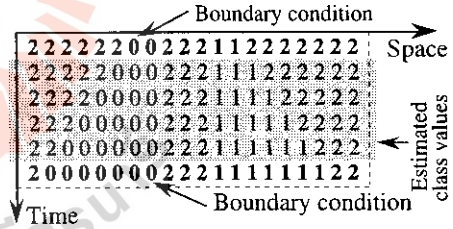

Figure.7 Result of GA/HC

Figure.8 shows the comparison of several experiment results. From this figure, we can find that the larger the population size is, the faster the stable result can be obtained, and the closer the stable result tend to best solution. **Figure.9** is a comparison of GA/HC with GA for spatio-temporal interpolation of landuse class variable data. It shows GA/HC has much higher efficiency than GA for spatio-temporal interpolation.

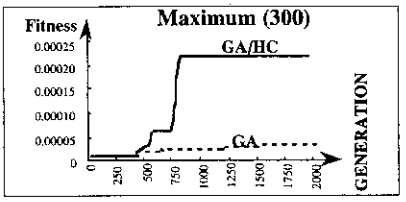

Figure.8 Comparison of GA with GA/HC

When observed location of class '0' in the first time slice and the last time slice are overlapping spatially, the Interpolation result naturally connect class '0' together, as shown in **Figure.10**, forming a band of class '0'. On the other hand, if class '0' is not overlapping spatially, the most likely interpolation result do not connect class '0' together

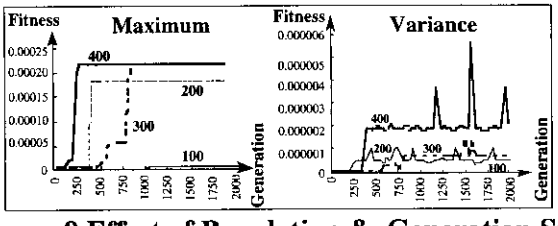

Figure.9 Effect of Population & Generation Size

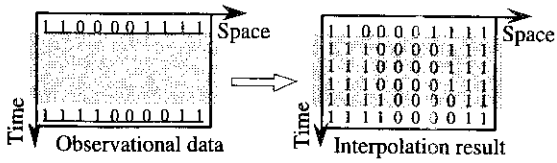

Figure.10 Interpolation Result in Overlapping Case

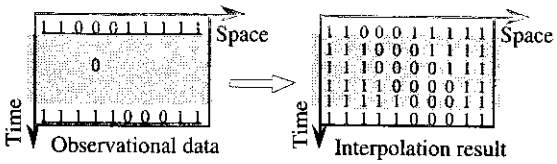

Figure.12 Interpolation Result with Additional Observational Data

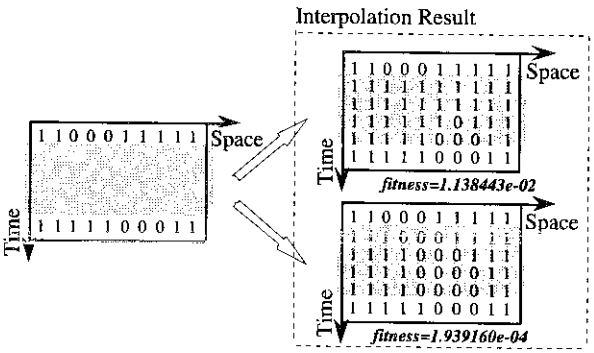

Figure.11 Interpolation Results in Unoverlapping Case

as in **Figure.11**, while the case forming a band of class '0' apparently have lower likelihood, though it looks natural. In **Figure.12**, another observational data is given at the middle. In this case, the most likely spatio-temporal pattern of class changes has a band of class '0'. It means that the interpolation methods integrating observational data and behavioral models can update the most likely results dynamically whenever new observational data are given.

6. CONCLUSION AND FUTURE PROSPECTS

In this study, Genetic-Algorithm/Hill-Climbing was proposed as a spatio-temporal interpolation scheme for pixel based class variable data which allows integration with observational data and behavioral/ structural models/rules. Test experiments can be summarized as following:

1) GA/HC can be very rigorous because it can generate the most likely spatio-temporal distribution of class variables under observational data and a behavioral model;

2) Hill-Climbing method can be effective method to greatly improve the efficiency of GA;

Although the GA/HC authors proposed can be a good scheme for spatio-temporal interpolation, it just a first attempt to apply GA in the field of spatio-temporal interpolation. We will extend GA/HC for Large Size of Class Variable Data, to reduce the speed of premature convergence and get higher efficiency of GA/HC.

[1] Bramlette, M.F. (1991): **Initialization, Mutation and Selection Methods in Genetic Algorithms for Function Optimization**, Proc. of the 4th. Conf. on GA, R.K.Belew and L.B.Booker (Editors), July, 1991, pp.100-107.

[2] Burrough, P.A. (1986): **Methods of Spatial Interpolation**, Principle of GIS for Land Resource Assessment, Monographic on Soil and Research Survey, No.12, 1989, pp.147-166.

[3] Davis, L. (1987) : **Genetic Algorithms and Simulated Annealing**, Pitman Publishing, 128 Long Acre, London WC2E 9AN, 1987.

[4] Davis, T.E., J.C.Principe (1991) : **A Simulated Annealing Like Convergence Theory for the Simple Genetic Algorithm**, Proc. of the 4th Conf. on GA, R.K.Belew & L.B.Booker (Editors), July,1991,pp.174-181.

[5] Eshelman, L.J. and J.D.Schaffer (1991): **Preventing Premature Convergence in Genetic Algorithms by Preventing Incest**, Proc. of the 4th. Conf. on GA, R.K.Belew and L.B.Booker (Editors), July, 1991, pp.115-122.

[6] Goldberg, D.E. (1989) : **GENETIC ALOGRITHMS in Search, Optimization and Machine Learning**, Addison-Wesley Publishing Company, Inc., 1989.

[7] Gold, C.M.(1989): **Surface interpolation, spatial adjacency and GIS**, Three Dimensional Applications in Geographic Information System, Edited by J.Raper, Taylor & Francis Ltd., 1989, pp.22-35.

[8] Huang, S.B. and R.Shibasaki(1995): **Development of Genetic Algorithm /Hill-climbing Method for Spatio-temporal Interpolation**, The 6th Symposium on Funtional Image Inf. System, IIS, Univ. of Tokyo, Apr. 1995, pp.81-86.

[9] Shibasaki,R., T.Ito and Y.Honda (1993): **Integration of Remote Sensing and Ground Observation Data for Developing Global GIS**, Proc. of SEIKEN Symposium, Vol.12, Aug. 1993, pp.263-277.

Contour Line Interpolation by using Buffering Method

Masataka TAKAGI and Ryousuke SHIBASAKI
Institute of Industrial Science,
The University of Tokyo.
7-22, Roppongi, Minato-ku, Tokyo 106, JAPAN
E-mail mural1@shunji.iis.u-tokyo.ac.jp
Tel. +81-3-3402-6231
Fax. +81-3-3479-2762

Abstract

For regional DEM (Digital Elevation Model) generation, an interpolation method becomes very helpful. We developed new reliable interpolation method which based on an intermediate contour line generation. The intermediate contour line can be drawn by using a buffering method. The buffering is a very popular technique in GIS (Geological Information System), which can be calculated distance from any points, vectors or polygons.

This paper presents a methodology of buffering method. And the results were compared with existing methods. Items for comparison are elevation, inclination, aspect and undulation. The developed method gave the best results in all items.

Moreover, a relationship between a contour interval and an accuracy of generated DEM was concluded. The results showed a ratio of pixels of contour line in the whole raster map image must be more than 20%.

1. Introduction

Nowadays, there are many kinds of DEM (Digital Elevation Model) generation methods such as a stereo-matching from aerial photograph or satellite image, an interferemetry from stereo SAR data and an interpolation of topographic maps. For regional DEM or continental DEM generation, the interpolation method using small scale contour maps becomes very helpful. However, almost existing methods of the interpolation are intended for large scale contour maps. Small scale contour maps have some problems which a form of contour line is often much different from the neighbor contour line, and contour line information is very few in low land area.

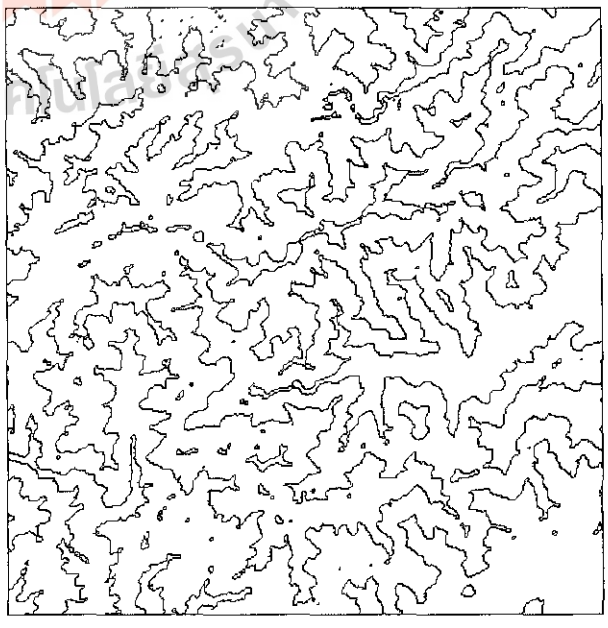

Figure 1 Contour line map

An objective DEM in this study is raster type. Usually, interpolation of contour line is calculated pixel by pixel. The most popular method of the interpolation is using a profile which include target pixel for elevation extraction. In this paper, this method is called *"profile method"*. An elevation of the target pixel can be estimated by curve fitting from

crossing points of contour line along the profile. Linear equation, polynomial equation, second order equation or Spline function is used as curve fitting equation. Figure 2 shows a shaded image of generated DEM from a test contour line map (Figure 1). A contour line interval was spread purposely in order to see reliability of the result. Spline function was used for curve fitting. In this image, there are many radiated noises which are along calculated profile. Searching the most suitable direction of profile is difficult in this method.

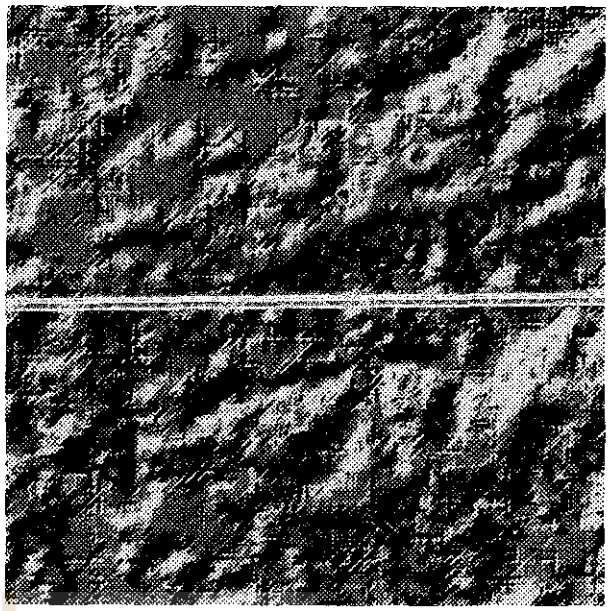

Figure 2 Shaded DEM from Profile method

Another popular method of the interpolation is using a window which a target pixel is located on the center. In this paper, this method is called *"window method"*. Consisted pixels of contour lines in the window are used as random points. An elevation of the target pixel can be estimated by weighted mean calculation. Figure 3 shows a shaded image of generated DEM from the same contour line map (Figure 1). In this image, there are steep slope along the contour lines. And other area become flat. In this method, definition of weight and window size is difficult. And in case of complex form contour line, a detail can't be represented.

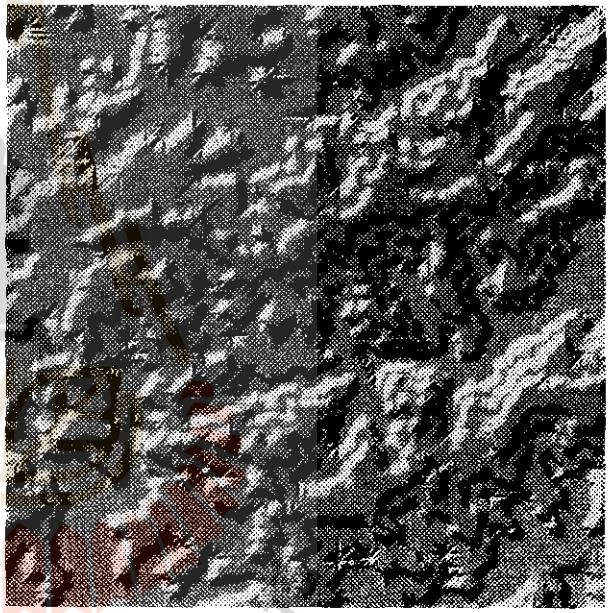

Figure 3 Shaded DEM from Window method

Therefore, more reliable method of the interpolation should be developed when rough contour line map is used. We attempted to develop a new method using buffering which is one of GIS techniques. In this paper, this method is called *"buffering method"*. This paper presents the methodology of interpolation using buffering. And the results will be compared with existing methods. Items for comparison are elevation, inclination, aspect and undulation. Finally, a relationship between contour interval and an accuracy of generated DEM will be concluded.

2. Methodology

The buffering method is not calculate elevation at every pixel, which is based on an intermediate contour line generation. The intermediate contour line can be drawn by using buffering image. Buffering can represent distance from any points, vectors or polygons. In raster type data, distance is set to each pixel as an attribute. If we have 100m and 200m contour line in the image, the distance from each contour line can be set to whole pixels (Figure 4). For example, gray level represents distance from contour line. Therefore, the intermediate contour line is located on same distance from each contour line. Figure 4 shows general idea of intermediate contour line generation. Same distance

points from each contour line compose intermediate contour line. On the other hand, we have another easy process to draw intermediate contour line. It is based on making fat contour line. Every contour line is made fat by one pixel at a same time until whole pixels are fill with contour line value. Then, boundaries of the contour line become intermediate contour line. After that, new intermediate contour line can be drawn from previous intermediate contour line and original contour line. By iteration of this process, intermediate contour line should be drawn until whole pixels are fill with contour line.

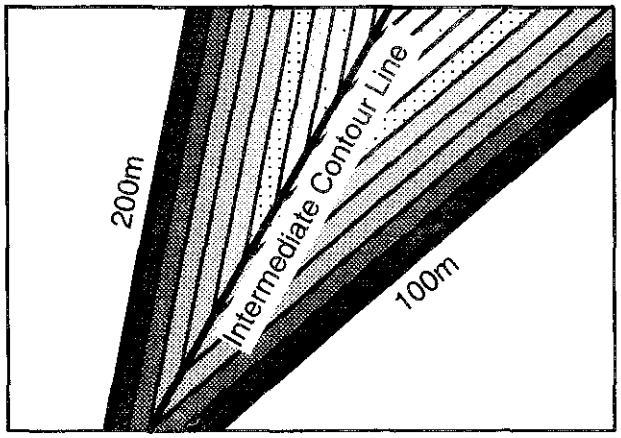

Figure 4 General idea of intermediate contour line generation

By the way, the intermediate contour line generation can be applied in case of enclosed area with different contour line. Other area which enclosed with same contour line must be calculated by different method. Such area is corresponded to valley or ridge area. A buffering can also apply in such area. Figure 5 shows general idea of buffering result in enclosed area with 200m contour line. The buffering result can be seen like contour line itself. Therefore, same elevation can be given to same buffering pixels. In this method, the most important thing is definition of extreme value in the enclosed area. An undulation curve was used for extreme value estimation in this study. An undulation curve is expressed a relationship between radius from top of a mountain and the undulation which means difference between minimum elevation and maximum elevation. It is represented one of the topographical feature. If geological structure is homogeneity, the undulation curve becomes almost same with neighbor mountains. So, when acreage of enclosed area could be calculated, maximum elevation can be estimated. Moreover the enclosed area must be judged ridge or valley. Usually, when around contour line of the enclosed area is higher, the area is estimated valley. When around contour line is lower, the area is estimated ridge reversely. If there are some exceptions, some attributes layer must be attached to the contour image.

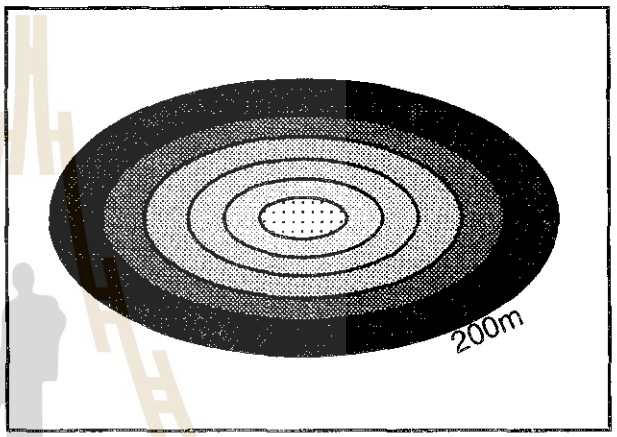

Figure 5 General idea of buffering results

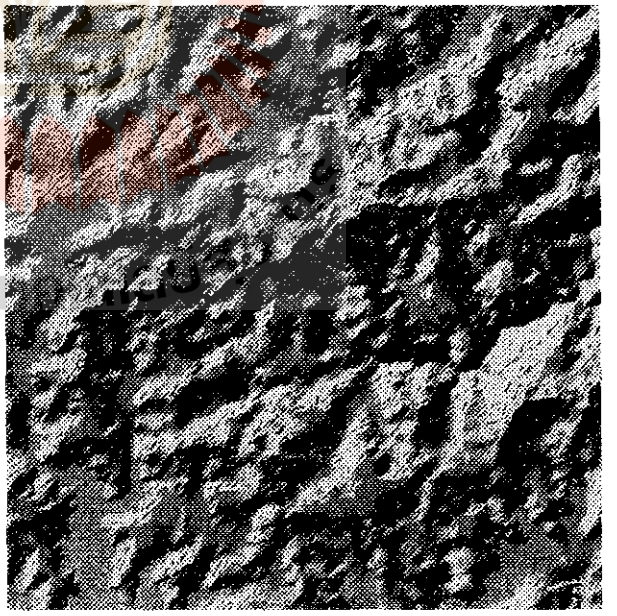

Figure 6 Shaded DEM from Buffering method

A complete DEM can be generated from combination of previous two interpolated

DEMs. This method doesn't need searching profile or definition of calculation window size. So, this will be more reliable method. Figure 6 shows shaded image of generated DEM by this method. In this figure, there are no noisy area.

3. Evaluations of Buffering Method

Evaluations of buffering method were carried out by comparison with existing methods which are profile method and window method. And effects of contour line interval on DEM accuracy were concluded. Items for evaluation is not only elevation but also topographical feature such as slope gradient and slope aspect.

Verification data were generated from 5m grid DEM which were generated by profile method with the linear equation from 1:25000 topographical maps. The 5m grid DEM were resampled to 50m grid size by taking the average in order to make suitable DEM for verification. Moreover, slope gradient data and slope aspect data were generated from the verification DEM. 100m, 200m, 300m and 400m interval contour line maps were created from the verification DEM. From those contour line maps, DEMs were generated by using each interpolation method.

3.1 Elevation Accuracy

An index of elevation accuracy is used percentages of correct pixels. In case of elevation evaluation, correct pixel means difference with verification DEM indicates inside of 20m. Figure 7 shows relationship between contour line interval and correct percentage in each method. In this figure, accuracy has tendency to drop with increasing contour interval. And buffering method is always located the highest accuracy in all contour intervals. Though window method shows almost same accuracy with buffering method in 100m contour interval, the accuracy becomes 10% less in other contour intervals. Profile method shows the worst results, because radiated noises influence to accuracy.

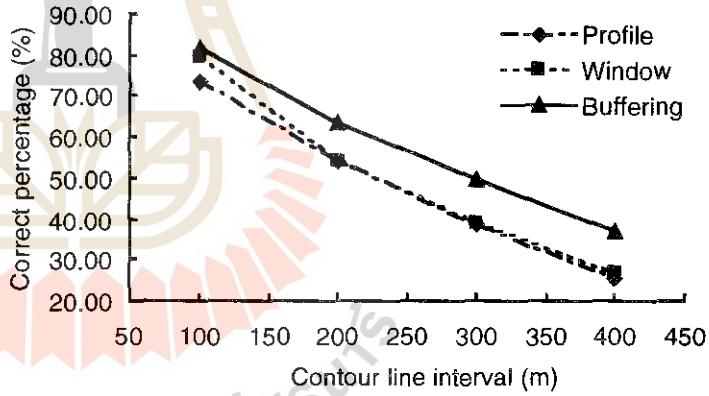

Figure 7 Relationship between contour line interval and correct percentage of elevation

3.2 Slope Gradient Accuracy

A slope gradient can be expressed from DEM, which is one of the most important items for topographical analysis. In this study, the slope gradient means maximum inclination angle at one target pixel. An index of slope gradient accuracy is also used percentages of correct pixels. In case of slope gradient accuracy, correct pixel means difference with verification slope gradient data indicates inside of 20 degree. Figure 8 shows relationship between contour line interval and correct percentage in each method. Buffering method is always located the highest accuracy in all contour intervals. Though profile method shows almost same accuracy with buffering method in 100m contour interval, the accuracy

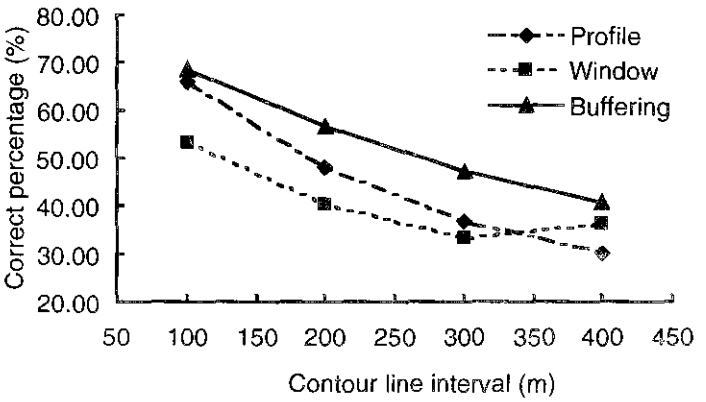

Figure 8 Relationship between contour line interval and correct percentage of slope gradient

becomes 10% less in other contour intervals. The window method shows the worst results, because steep slope along contour line influenced to accuracy.

3.3 Slope Aspect Accuracy

A slope aspect can be expressed from DEM, which is one of the most important items for topographical analysis. In this study, the slope aspect shows along the maximum inclination angle at one target pixel. An index of slope aspect accuracy is also used percentages of correct pixels. In case of slope gradient accuracy, correct pixel means difference with verification slope gradient data indicates inside of 45 degree. Figure 9 shows relationship between contour line interval and correct percentage in each method. The correct percentage shows very lower than elevation or slope gradient, which is indicated less than 68%. However, buffering method is almost located the highest accuracy in all contour intervals.

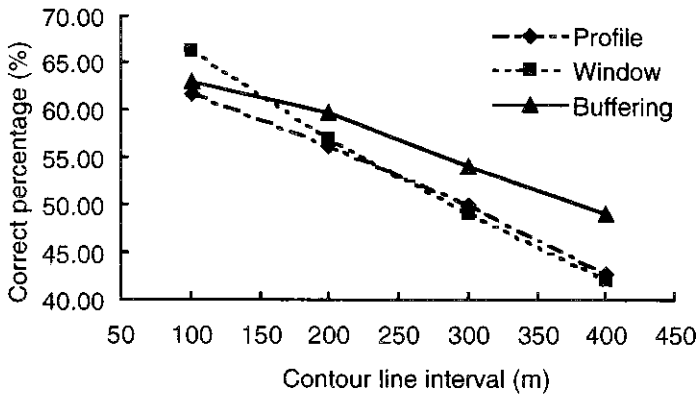

Figure 9 Relationship between contour line interval and correct percentage of slope aspect

4. Conclusions

In this study, buffering method was developed for small scale maps. The developed method was compared with existing methods on elevation, slope gradient and slope aspect. In all items, the buffering method showed very good results.

Existing method had some problems in one items of topographical features. For example, profile method has much error in elevation value, because there are many errors along calculated profile. Window method has much error in slope gradient, because there are many errors along contour lines. Anyhow, existing methods didn't show good results in case of wide contour intervals.

A contour line interval influenced accuracy of DEM. When contour line interval becomes over 300m, a correct percentage becomes less than 50%. A percentage of pixels which are consisted contour line is about 10% in case of 300m contour interval. Moreover, in case of 100m contour interval, the percentage becomes 30%. Therefore, 20% contour line information on whole map are required for reliable DEM generation.

In this paper, calculation speed was not evaluated. Actually, buffering method spends much time in comparison with existing two methods. However, if we need high accuracy DEMs, it will not be so serious problem. And computer is progressing rapidly.

References

[1] Sukit Viseshsin and Shunji Murai (1990), "Automated Height Information Extraction from Existing Topographic Map", International Archives of Photogrammetry and Remote Sensing, Vol.28 Part 4, pp.338 - 346

[2] Kiyonari Fukue, Yousuke Kuroda, Haruhisa Shimoda and Toshibumi Sakata (1990), " Simple DEM Generation Method from a Contour Image", International Archives of Photogrammetry and Remote Sensing, Vol.28 Part 4, pp.347 - 355

[3] F. Ackermann (1994), " Digital Elevation Models - Techniques and Application, Quality Standards, Development", International Archives of Photogrammetry and Remote Sensing, Vol.30 Part 4, pp.421 - 432

COMPARISON OF THE CERTAINTIES IN A GIS

D.Amarsaikhan, M.Ganzorig

Informatics & RS Centre, Mongolian Academy of Sciences
av.Enkhtaivan-54B, Ulaanbaatar-51, Mongolia

ABSTRACT

At present there are many techniques for land cover mapping using RS data. The results of various parametric and non-parametric classifications with different certainties (qualities) are put to a GIS and used in decision making. The most commonly used algorithms are the parametric and non-parametric (eg, k-nearest neighbour) maximum likelihood classifiers against which other classification algorithms are compared. Various authors have used the Dempster-Shafer theory of evidence for the land cover discrimination and argued that the result is better than the result of the standard maximum likelihood classification. The aim of the study is to compare these methods. For the comparision, two different natural regions have been selected.

1. INTRODUCTION

The linkage between RS and GIS can be made automatically by the use of some pattern recognition techniques and manually by a visual interpretation. Over the years, researchers have developed various techniques to improve the classification results. The results of the existing classification techniques containing various certainties can be put into a GIS or directly used in some decision making. The processing steps of RS data to be used in a decision making process is shown in Figure 1. When the result of an image classification is used to update a layer of a GIS or in a decision making process the requirements proposed by Mulder et al. (1990) and Amarsaikhan et al. (1992) should be met. Traditionally, the parametric maximum likelihood classification incorporating a priori probabilities or ancillary data is considered as one of the most efficient methods for the spectral classification. However, it has many limitations; for instance, in practice it is rare that the reflectance values have a multivariate normal distribution (Ince 1987, Mulder et al. 1990). A number of authors (eg, Srinivasan and Richards 1990, Bronsveld et al. 1992) used the theory of evidence in the classification process and judged that the result is better than the result of the standard maximum likelihood classification. However, assumptions made in the Dempster theory are weaker than those made in the maximum likelihood classification, because it uses some assumptions (eg, $A \cap B$) used in fuzzy logic schemes. These techniques have been tested in two different natural regions. The results showed that by the use of the same technique, different results can be expected according to the context of the area.

2. THE TEST SITES AND MATERIALS

2.1. The first target area selected was in the central part of

Mongolia, near Ulaanbaatar city and has various natural diversities. In this area, the boundaries between the object classes are hardly distiguishable, and it is not easy to choose the satisfactory training samples. In this area soil, vegetation and water classes were selected.

2.1.1. For this area, a Landsat TM image of 1990 has been selected. In the maximum likelihood classification bands 2, 3, 4 and in the classification which uses the theory of evidence bands 3 and 4 were used, respectively. A landuse map was produced using a knowledge of a specialist who worked for a long time in the study area.

2.2. The second test area was selected in the south eastern part of the country. The area is related to the steppe zone and during the summer time the land in this region is mainly covered by grass. For our study, we selected a part where vegetation, soil and solonchak are clearly separable from each other. In this area soil, vegetation and solonchak classes were selected.

2.2.1. For the image classification, 3 bands (green, red and NIR) of MSK-4 data converted to a digital format were used. The data were resampled to a spatial resolution of 30 meters. The band selection and a landuse map production in the area have the same procedures as mentioned above (see section 2.1.1).
In both cases, the training samples (total of 180 to 240 pixels for each class) were selected avoiding multimodel and asymmetric distributions.

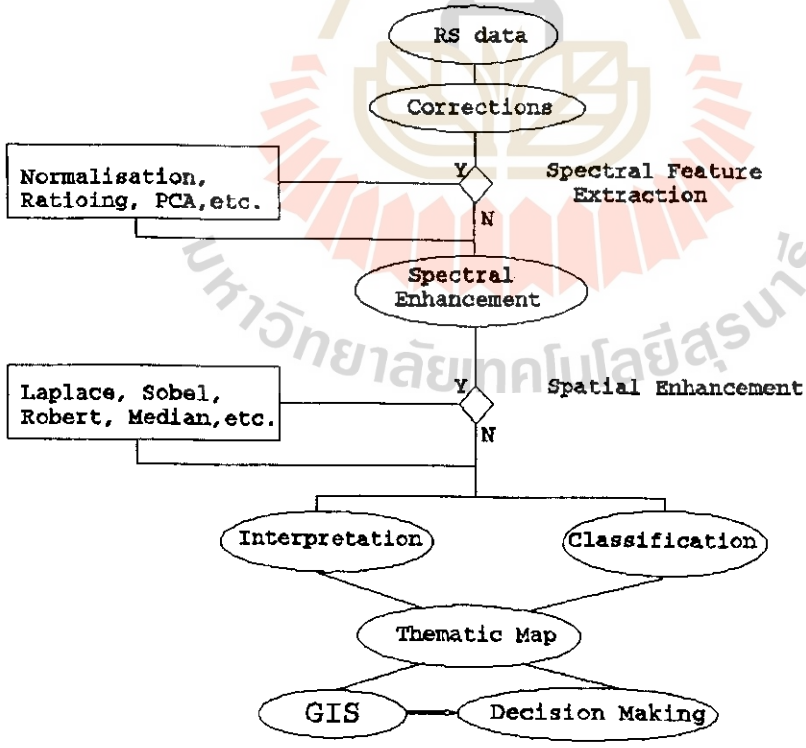

Figure 1. Processing Steps of RS Data to Update A GIS

3. THE METHODS AND RESULTS

3.1. The idea of the Dempster-Shafer theory is to break down large datasets into components for each of which the probability judgements are made. Description and application of the theory in RS can be found in Srinivasan et al. (1990) and Brnsveld et al. (1992). In the theory, the beliefs are combined according to the Dempster's rule of combination, which is expressed as follows:

$$Bel = Bel1 \oplus Bel2$$

Under this rule, the mass committed to a subset A under Bel is

$$m(A) = \frac{\sum_{A_i \cap B_j = A} m_1(A_i)\, m_2(B_j)}{1 - \sum_{A_i \cap B_i = \phi} m_1(A_i)\, m_2(B_j)}$$

In the theory belief is non-additive, Bel(A)+Bel(¬A) # 1
where Bel(¬A) is belief against A.
Ignorance = 1-{Bel(A)+Bel(¬A)}
Plausibility(A) = 1-Bel(¬A)

In the Dempster's rule the belief functions must be independent and must refer to the same frame of discernment(Θ). As discussed in Srinivasan et al. (1990) a direct application of the theory is complicated because all labels within the frame of discernment have to be compared with each other. To make a practical use some restrictions should be made. In our study, we used the following restrictions made in Bronsveld et al. (1992).

Bel (Θ) is assumed to be always 0.9.
Only the belief against a particular label is expressed, consequently only the plausibility of each label can be calculated. By expressing only belief against a label the need to compare all possible combinations of the labels is not necessary. The final label for a pixel is classified after all the evidence is used according to the following rules: The label is picked then the label with the least belief against that label is chosen, if two or more labels have the same amount of minimum belief against them, one of them is chosen. According to the rules, both test sides were classified and the overall classification accuracies were 88.14% for the first area and 84.16% for the second area, respectively.

3.2. To perform maximum likelihood classification for each image, the training samples were selected through thorough analysis. The pixels representing the interested classes were selected from different places of the images and then merged. The overall classification accuracy for the first area was 82.02% and for the second area it was 86.19%.

4. CONCLUSIONS

In this study, we compared one of the widely used classification techniques with the latest developed technique. As seen from the analysis, the traditional technique gives more accurate result in case of homogeneous area. This means, using the same technique different results can be expected according to the context of the area.

REFERENCES

1. Amarsaikhan, D., Gorte, B., 1992, Knowledge-based Approach to Update Landuse Layer of an Operational GIS, Proceedings of ACRS, Ulaanbaatar, Mongolia.

2. Amarsaikhan, D., Ganzorig, M., 1994, Modification of the Prior Probabilities in the Maximum Likelihood Classification, Proceedings of ACRS, Bangalore, India.

3. Bronsveld, K., and Kostwinder, H., 1992, Improving a Landuse Map using GIS and RS, International Symp. RS and Space '92, Hat Yai, Thailand.

4. Ince, F., 1987, Maximum Likelihood Classification, Optimal or Problematic? A Comparison with the Nearest Neighbour Classification, International Journal of RS, Vol.8, No.12, 1829-1839.

5. Mulder, N.J., and Middelkoop, H., 1990, Parametric Versus Non-Parametric Maximum Likelihood Classification, Proceedings of ISPRS Symposium, Wuhan, China.

6. Srinivasan, A., and Richards, J.A., 1990, Knowledge Based Techniques for Multi-source Classification, International Journal of Remote Sensing.

Plan of the Construction of GIS for Northeast Thailand

Yasuharu YAMADA※, Mitsuo SUZUKI※,
Wapakorn AMORNDHAM※※, Somsak SUKJARN※※※

Japan International Research Center for Agricultural Sciences(JIRCAS)※
1-2 Ohwashi, Tsukuba, Ibaraki, 305 JAPAN
Agricultural Development Research Center in Northeast Thailand(ADRC) ※※
Moe Din Daeng, Khon Kaen 40000, THAILAND
Soil Survey and Land Classification Division, Land Development Department(LDD) ※※※
Moe Din Daeng, Khon Kaen 40000, THAILAND

Abstract

JIRCAS has a started comprehensive study on sustainable agricultural systems with Thai agricultural organizations in the northeast Thailand from this year. Agriculture of the region is faced with diverse problems associated with environmental degradation. It will be very important to evaluate the potential agricultural productivity to design suitable agricultural landuse system in this region. We reviewed 3 papers to construct a GIS to create maps by using GIS and a remote sensing technique.

1 Introduction

Two years ago, JIRCAS (formally Tropical Agricultural Research Center) has established to extend internatinally collaborating research activities. The activities includes;

- Evaluation and improvement of agriculture-forestry-animal husbandry-fisheries combined farming systems in the Mekong Delta(Vietnam)
- **Comprehensive study on sustainable agricultural system in Northeast Thailand**
- Productivity and Sustainable Utilization of Brackish Water Mangrove Ecosystems(Malaysia)
- (China)
- (Planning : Brazil)

2 Outline of the plan of comprehensive study on sustainable agricultural system in Northeast Thailand by JIRCAS

Background: Agriculture of Northeast Thailand is faced with diverse problems associated with environmental degradation such as rapid deforestation. Typical soils are low in fertility and in the water

holding capacity. Soil degradation has been accelerated by the continuous cultivation of field crops, and areas resulted in increased unproductive dry land. Soil salinity is also an increasing problem in many areas of the region. The annual rainfall is extremely erratic and unpredictable. Under such disadvantageous conditions, the productivity is very low level. If the current agricultural production systems continued in this region, the sustainability of farming system could not be maintained. This may come an increased social unstability. These conditions of the poor agricultural productivity accelerate the increase of rural-to-urban migration.

Northeast Thailand is one of the major target areas of the agricultural development. The development of a sound sustainable agricultural systems is urgently needed for Northeast Thailand. Such studies will contribute to the agricultural development of other developing countries which have common environmental and agricultural problems. This project is expected to pave a way for an establishment of international collaborative research on sustainable agricultural development in environmentally vulnerable areas in the tropics.

Objective: This project aims to develop sustainable farming systems in environmentally vulnerable areas in Thailand by identifying agricultural technologies of crop and livestock production which are readily transferable to local farmers.

More specific objectives of this project are : 1) to evaluate environmental and biological resources in the area and to develop more effective uses of those resources, 2) to develop sustainable cropping systems in lowland and upland areas with emphasis placed on soil and water conservation and to develop postharvest technologies for local agricultural products, and 3) to improve livestock production technologies with locally available feed resources to promote mixed farming systems.

Project Implementation: (tentative outline)

1. Inventory and evaluation of agro-environmental and agro-biological resources
   1) Agro-environmental resources: climatic factors, water and soil resources
   2) Agro-biological resources: crops, livestock, and microorganisms
   3) Possibilities of more effective uses of existing resources
   4) Systematization of regional information (GIS)
2. Development of sustainable agricultural systems
   1) Intensive paddy cropping systems with tank irrigation
   2) Sustainable upland farming systems with crop rotation
3. Improvement of livestock production with locally available feed resources
   1) Forage crop management
   2) Livestock production with local feed resources
   3) Sustainable mixed farming systems
4. Development of postharvest technologies for local agricultural products
   1) Postharvest technologies to minimize postharvest losses
   2) Quality improvement and food processing
5. Economic evaluation of mixed, multiple-cropping agricultural systems
   1) Management evaluation of farming systems with tank irrigation
   2) Evaluation of various types of mixed farming

3) Economic evaluation of regional agriculture

Following institute will participate into collaboration in our project:

Thailand: Department of Agriculture (DOA), Department of Livestock Development (DLD), Agricultural Development Research Center in Northeast (ADRC), Khon Kaen University (KKU), Department of Land Development (LDD), [Asian Institute of Technology (AIT), Kasetsart University(KU)].

Japan: National Agriculture Research Center (NARC), National Institute of Agrobiological Resources (NIAR), National Institute of Animal Industry (NIAI), National Grassland Research Institute (NGRI), National Research Institute of Agricultural Engineering (NRIAE), National Research Institute of Agricultural Economics (NRIAE), National Food Research Institute (NFRI).

Duration: 7 years from April 1995 to March 2001

3 Previous studies using GIS and Remote sensing in Thailand

Following 3 papers are the previous studies related to our plan. The authors found out some helpful points for a future plan.

"Utilization of the Geographical Information System in North-East Thailand"

GIS is a useful method for evaluating land suitability and yield prediction based on information concerning land resources such as soil, topography, climate, land use and so on. The objectives of this investigation are to develop a geographical database for Northeast Thailand using PAMAP (GIS installed at ADRC) to evaluate the suitability of paddy rice production of the Kohn Kaen Province.

Basemaps were prepared to digitize it at a scale of 1/250,000, namely maps showing soil classification, soil salinity, landuse, boundaries, rivers and roads.

By selecting the factors related to cultivation and rating, an equation indicating for suitability for paddy rice was developed. Selected factors were consolidated layer, soil texture, permeability, nutrient status, salinity, slope topography and rockiness. Based on the limitation of cultivation for paddy rice, these factors were classified into five ranks (Table.1; rank of limitation is P-1 < P-5) and overlaid to generate polygons with suitability.

A suitability map of paddy rice (Fig.5; rank of suitability is S-1 > S-5) was made as a result of their evaluation. Suitable land (S-1 and S-2) was found to be limited in Kohn Kaen Province. The major problems of unsuitable areas (S-4 and S-5) were slope topography, permeability and salinity. In these areas, it is necessary to shift to other crop production and to adopt some techniques for improvement. These way were in evaluating the sustainable rice production; Approach 1 consists of generating polygons by overlaying some related layers. This approach was utilized in this study. Approach 2 and Approach 3 are ways to evaluate based on the ranking of estimated yields. In Approach 2, yield estimation models are made based on cultivation experiments. Models with Approach 3, statistical methods are used to survey data which yield criterion variables and environmental features are analyzed as predictor variables. Therefore, many sampling points are needed for this Approach.

Table.1 Limitation of soil in 5 suitabitily level for paddy rice

Limition	P-I	P-	P-III	P-IV	P-V	DATA SOURCE
Consolidated Layer : C	none	none	between 25-50 cm	between 15-25 cm.	deeper than 15 cm.	SOIL MAP
Texture : T	C SC SiC CL SiCL	L SCL SiL	SL	S LS SI		SOIL MAP
Organic Layer : O	none	none	none	found in surface ,thick 20-40 c	found in surface ,thick > 40 c	none in NE.
Gravels : G	none	none	gravel	gravel	gravel	SOIL MAP
Permeability : P			medium	repid		SOIL MAP
Nutrient Status : N		low	low	low	low	SOIL MAP
Jarosite : J	none	none	in 40-100 cm. dept	in < 40 cm. depth or pH < 4		none in NE.
Salinity : X	class 6	class 6	class 4	class 3	class 1,2	SALIN SOIL MAP
Risk of Water shortage : W		slightly risk	moderatly risk	very risk	too risk, plant can't survive in cropping season	RAIN FALL DATA
Topography of Slope : T	flat	flat	flat-undulating	undulating,undulating-rolling	undulating-hilly , rolling , rolling-hilly , hilly , hilly-steep , steep	SOIL MAP
Rockiness or Stoness : R					RL	SOIL MAP
Flood Hazard : F		occur 1-3 t 10 years	ocuur 4-6 times in	occur 7-9 times in 10 years	occur every year	none in NE.

Figure.1

SOIL TEXTURE BOUNDARIES
KHONKAEN PROVINCE

Figure.2

PERMEABILITY BOUNDARIES
KHONKAEN PROVINCE

Figure.3

SOIL SALINITY
KHONKAEN PROVINCE

Figure.4

TOPOGRAPHY BOUNDARIES
KHONKAEN PROVINCE

Figure.5

SUITABILITY MAP
KHONKAEN PROVINCE

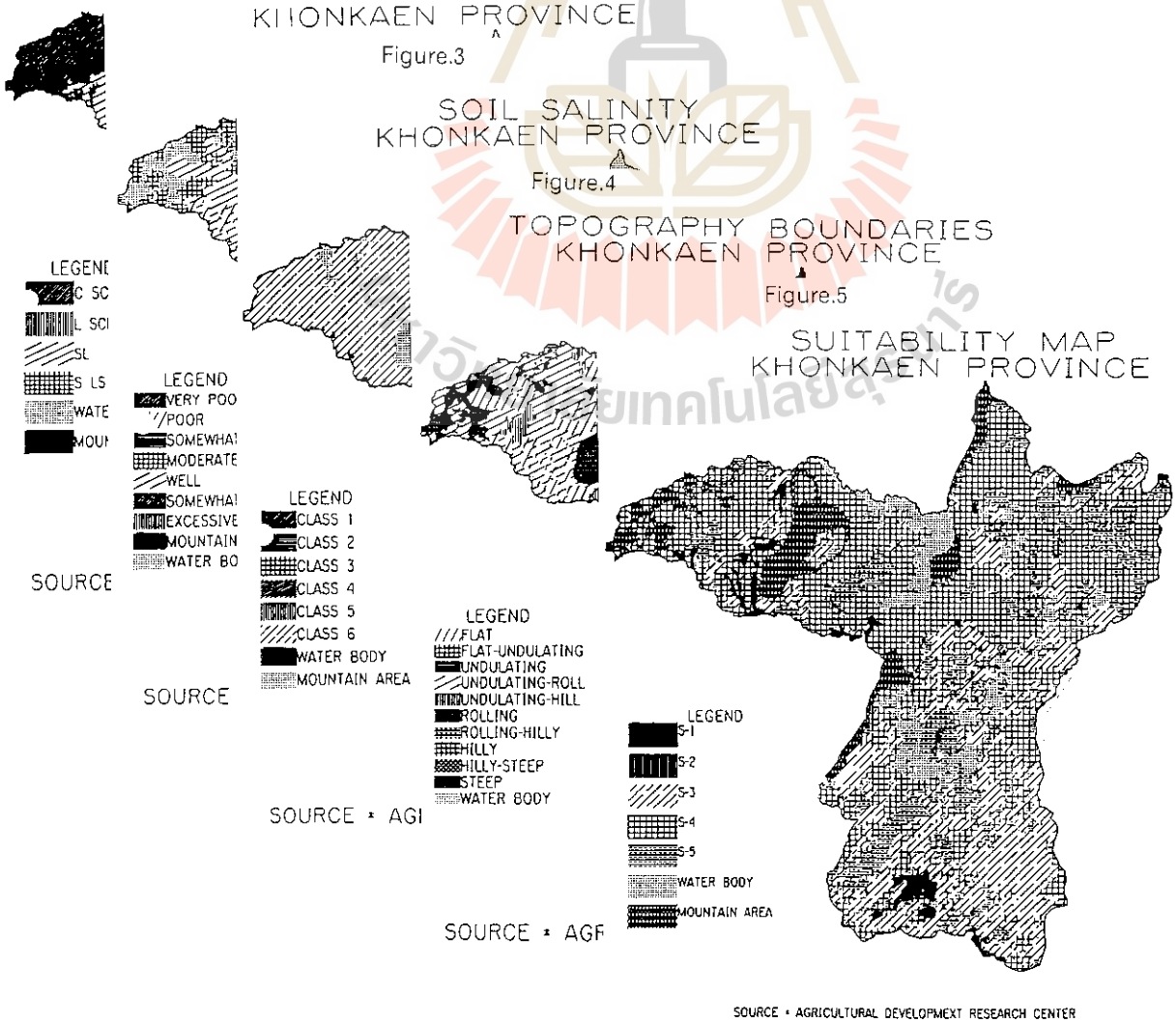

"Agricultural landuse classification using remote sensing and Geographic information in the Central Plain of Thailand"

Geographic Information System (GIS) has many advantages such as overlay between map data and remote sensing data, buffering, network analysis, etc. As agricultural landuse spread out on a plane, the management of various information about agriculture is easy and efficient in case of dealing with plane. YAMADA submitted a sample analysis using minute topography information in the Central Plain of Thailand. The obtained results were combined with the results from remote sensing analysis using LANDSAT data.

His final result of analysis shows (1) The drainage of farm land on the natural levee after rainy season is very good and vegetation exists even in dry season; the landuse maybe is orchard. (2) At the area, where the inundation has relatively short stay, in the Central Plain of the production area of floating rice, the harvest is earlier than the other places: To reap rice is over at the beginning of the dry season. The gradation of the hight of topographical features just agrees with the amount of biomass estimated by the vegetation index (VI) calculated from LANDSAT TM and MSS data when to reap rice. (3) At the western part of the Central Plain, the region is not flooded except for extraordinary inundation. Sugarcane is widely cultivated in the area.

"Land Evaluation for Agricultural Productivity in North-East Thailand Using Landsat TM Data and Geographic Information"

In the north-east Thailand, there are many paddy fields and other annual crop fields. The size of farmland is not so large as that of the Central Plain. There is a big problem of soil salification which caused by the unbalance of precipitation and evapo-transpiration. It is one of primary target to detect the salt damaged areas using satellite data.

An agricultural landuse classification for using Landsat TM data in this region collected in a dry season and a wet season is proposed by Dr. SAITO et al. He proposed a map of potential agricultural productivity.

(1) Landuse map Landuse map is made from the changes in Landsat images of rainy season and dry season. After that, the extraction of salinization area, paddy field and upland field is held from the map. **(2) Normalized vegetation index (NVI) map** NVI is calculated by the following expression.

$NVI = \{(B4-B3) / (B4+B3)\} \times 100 + 127$

Average and difference NVI maps were computed with dry season and wet season data. VCR, KVI are proposed and similar average/deference maps are made.

(3) Digital soil fertility map and digital topography map Those maps are digitized from soil map and topography map.

After preparation **(1)** to **(3)**, each map is weighted and overlaid by evaluation of paddy field and upland field suitability on GIS. The map of potential agricultural productivity is created. In this report, to weight the maps is experiencely done by researcher.

Findings:

In Northeast Thailand, both precipitation and soil salinity are considered major restriction factor for agriculture.

GIS is useful as a mapping system and a database management system, but the development or construction of these digital information system has several problems such as accuracy, format, data entry, data management and data transference to other GIS software at other organization.

Remote sensing is a useful method to obtain real time information about land cover change; The data exchange between remotely sensed data and GIS data will play important role.

4 Future plan and conclusions

(1) Construction of geographical database of land resource information in Northeast Thailand is at the preliminatry stage. For example, soil maps, salinity distribution maps, soil erosion maps, some kinds of landuse maps, etc are demanded.

(2) We plan to create a potential agricultural productivity map and a suitable agricultural landuse evaluation map from the existing information.

GIS system is very powerful and useful tool for recognizing agricultural landuse. It will be convenient that geographic data such as topography, soil map, etc. and ground truth data are managed by GIS. Furthermore, there is a good possibility that satellite remote sensing data can update to geographic information data. Because satelite data can obtain periodically.

There are several problems of how to weight maps theoretically and quantitatively, how to verify the potential productivity map.

It will require stable organization to conduct data entry, management for land resource information and to upgrade GIS data.

Acknowledgments:

The report of "Utilization of the Geographical Information System" was the work of Dr. Kenji Matsumori (National Institute for Agro-Environmental Sciences in Japan), Dr. Wapakorn Amorndham (ADRC) and Dr. Somsak Sukjarn (Land Development Department in Thailand), operated by Japan International Cooperation Agency (JICA) cooperative research project with ADRC.

The report of "Land Evaluation of Agricultural Productivity in Thailand using Remote sensing Techniques" is one of the results of the joint research project on the enhancement and application of the remote sensing technique between ASEAN countries and Japan supported by Science and Technology Agency (STA) of Japan. Dr. Genya Saito, Dr. Tsuyoshi Akiyama, Mr. Yasuharu Yamada, Mr. Yoshiki Yamagata and Mr. Nobuyuki Mino are joint researchers for Japanese side; Mr. Pongpit Piyaponse and Ms. Ekkanit Hansakdi are Thailand side researchers.

References:

Genya Saito, Yasuharu Yamada, Yoshiki Yamagata, Tsuyoshi Akiyama, Michio Shibayama, Shinsuke Mirinaga, "Evaluation of Agricultural Productivity in Thailand using Remote sensing techniques", Technical Report of Joint Research on the Enhancement and Application of the Remote Sensing Technology with Asian Countries and Japan, 119-141, 1991.

Genya Saito, Tsuyoshi Akiyama, Yasuharu Yamada, Nobuyuki Mino, "Evaluation of potential agricultural productivity using LANDSAT TM and GIS in Northeast Thailand", Journal of the Japanese Agricultural Systems Society, **10**, 1, 1-10, 1994. (in Japanese)

Kenji Matsumori, Wapakorn Amorndham, Somsak Sukjarn, "Utilization of the Geographical Information System", Report of Short Term Expert of Japan International Cooperative Agency (JICA), 1995

Yasuharu Yamada, "Agricultural landuse classification using remote sensing and Geographic Information in the Central Plain of Thailand ", Proceedings of the annual meeting of Japanese Society of Irrigation Drainage and Reclamation Engineering, 18-19, 1991 (in Japanese)

WORKING GROUP

GIS FOR EDUCATION

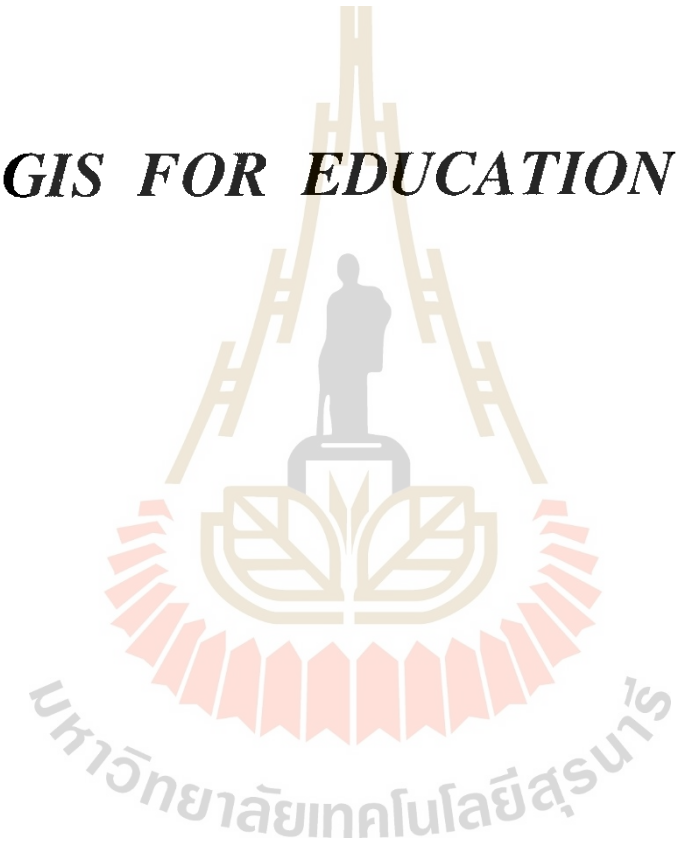

Working Group Meeting: GIS for Education

November 23, Thursday 1995
16:00 - 17:30
Room A

Co-Chaired by Dr. R. Shibasaki and Dr. K. Cho (Japan)

1. Introduction

In order to improve the educational environment of GIS, the establishment of two Working Groups on GIS were approved by General Conference of AARS on 21 November, 1994 Bangalore, India. Following this approval, The first official meeting on the two working groups will be held at the 16th ACRS. Participation of those who are interested in any items described below are most welcome. ***Come on and join us!***

(a) Working Group on GIS Text Book

Chairman : Dr. Ryosuke Shibasaki
Institute of Industrial Science
University of Tokyo, Japan
7-22-1 Roppongi, Minato-ku,Tokyo 106 JAPAN Phone:+81-3-3402-6231 ext.2590
Fax:+81-3-5411-0441
e-mail:shiba@shunji.iis.u-tokyo.ac.jp

Terms of Reference

* To edit a systematically structured text book on GIS in 1995.
* To publish the book in 1996 with refree process.
* To integrate theory and application, remote sensing and GIS and education and operational aspect in the book.
* To introduce successful GIS applications in Asian Region in cooperation of AARS members and WG members.
* To collaborate with the Working Group on GIS software for educational purpose with respect to computer assisted teaching of GIS theory and applications.

(b) Working Group on GIS Software for Educational Purpose

Chairman : Dr. Kohei Cho
Research & Information Center
Tokai University, Japan

2-28-4, Tomigaya, Shibuya-ku, Tokyo 151 JAPAN Phone: +81-3-3481-0611
Fax: +81-3-3481-0610
e-mail: kcho@keyaki.cc.u-tokai.ac.jp

Terms of Reference

* To review the existing public domain GIS software.
* To develop or compile GIS software including theory and applications for educational purpose in 1995 or 1996.
* To collaborate AARS members and GIS related institutions with respect to educational software package.
* To collect GIS dataset and teaching materials for educational purpose.
* To Cooperate with the Working Group on GIS text book with respect to computer assisted teaching.

2. Agenda

The following items will be discussed at the meeting on free discussion basis. If you have any particular item for discussion, please contact one of the chairmen in advance to the meeting.

(a) Membership nomination
(b) Concept of Integrating GIS text book and software (c) Configuration of GIS text book / software (d) Materials of GIS applications
(e) Datasets for GIS training
(f) Media for publication
(g) Schedule for publication

MONITORING OF FOREST STAND CONDITION IN THAILAND
- TROPICAL SEASONAL FOREST -

Haruo Sawada, Hideki Saito
Forestry and Forest Products Research Institute, Japan
P.O.Box 16, Tsukuba-Norin, Ibaraki, 305 Japan

Thongchai Charuppat, Jirawan Charuppat, Suwit Ongsomwant
Royal Forestry Department, Thailand

Surachai Ratanasermpong, Chaowalit Silapathong
National Research Council of Thailand

ABSTRACT

This study aims to find and develop practical methodology on digital processing of satellite remote sensing data and other geographical information for observing and monitoring tropical seasonal forest area.

Around the Doi Intanon, Chiang Mai, was selected as one of the study areas to develop forest type classification method and to delineate forest area affected by shifting cultivation.

The main methodologies of the study are (1) to make a forest type map of Chiang Mai study area based on the normalized difference vegetation index (NDVI) derived from satellite remote sensing data, and (2) to establish the field check system for comparing ground measurements with the processed remote sensing data. The results are as follows: (1) The shifting zone between evergreen forests and deciduous forests in 700m and 800m was found by the four Landsat images and checked by the field survey. (2) A field survey system was established among the researchers concerned to the project. The video system was found useful for recording field survey plot.

1. INTRODUCTION

IUFRO (International Union of Forestry Organization) published the "International Guideline for Forest Monitoring" in 1994. The basic forest types which have been used by FAO for the "Forest Resources Assessment(1990)" are introduced in the Guideline as the minimum requirement for global monitoring in order to contribute international activities in forestry community.

Based on the idea of this Guideline, we could classify forests into several types in Thailand. The main forest types in Thailand are evergreen forest, mixed forest and deciduous forest, and

plantation and mangrove forest are found at specific areas. In northern Thailand, DDF (Dry Dipterocarp Forest) are dominant in low altitude and evergreen trees are dominant at high altitude. MDF (Mixed Deciduous Forest) stands at the transitional zone of these two forest types. Phenological changes of forests correspond to the rainfall and the components of forest (forest stand condition) and it is clearly observed in DDF and MDF stands.

Satellite remote sensing technology are considered effective for monitoring these phenological aspects. The periodicity of observation is one of the main important characteristics of Satellite remote sensing. NOAA, Landsat, SPOT, MOS and JERS are main satellites from which we can get earth observation images regularly.

The remote sensing community has used Normalized Difference Vegetation Index (NDVI) of NOAA AVHRR data to monitor global vegetation conditions (Goward et al. 1991; Spanner et al. 1990; Tucker and Choudhury 1987). The index is sensitive to the quantity of active photosynthesizing biomass on the landscape (Burgan and Hartford 1993). Geographers have used NDVI data to develop a map that portrays vegetation patterns across the United States (Loveland et al. 1991).

This study aims to find and develop practical methodology on digital processing of satellite remote sensing data and other geographical information for observing and monitoring seasonal changes of tropical forest, which correspond to forest stand conditions.

Chiang Mai district were selected for this study. Forest development by shifting cultivation is widely being executed in Chiang Mai and multi-temporal TM data are considered useful to classify the forest types and to detect cultivation activity.

2. METHODOLOGY

(1) NDVI images of Landsat TM

The Landsat series polar-orbiting satellites with TM (thematic Mapper) sensor and other satellite, such as SPOT and MOS, provide frequent observations of Earth's surface. These remote sensing data have been received at the ground receiving station since 1986 in Thailand.

The NDVI is the deference of near-infrared and visible red reflectance values normalized over total reflectance of the two channels.

$$NDVI = \frac{Near\_IR(TM.Channel\_4)-Red(TM.Channel\_3)}{Near\_IR(TM.Channel\_4)+Red(TM.Channel\_3)}$$

This equation produces NDVI values in the ranges of -1.0 to 1.0, where negative values generally represent clouds, water and other non-vegetated surfaces, and positive values represent vegetated surfaces. The NDVI relates to photosynthetic activity of living plants. The higher the NDVI value, the more "green" the cover type (Deering et al.), That is, the NDVI increases as the quantity of green biomass increases (Burgan and Hartford, 1993).

To interpret the NDVI values for field use, we have devised methods to convert the NDVI data into more easily understandable representations of vegetation greenness as is used for AVHRR (Burgan

and Hartford, 1993). These are called "visual greenness" and "relative greenness".

Visual greenness (VG) indicates how green each pixel is in relation to a standard reference such as a highly green and densely vegetated evergreen forest. It is calculated as:

VG = NDV / V_dens

where

NDV = observed NDVI value, V_dens = NDVI value of densely vegetated evergreen forest

An image is produced that portrays vegetation greenness as we would expect to see it if we were flying over the landscape. In this context, normally deforiaged, sparsely vegetated area will look cured compared to fully vegetated area such as the evergreen forest.

Because the visual greenness image may indicate rather limited changes over time, a second measure of vegetation greenness is useful. Relative greenness (RG) is also a percentage value, but it expresses how green each pixel currently is in relation to the range of greenness observations for that pixel among the data collected. It is calculated as:

RG = (NDV - ND_min) / (ND_max - ND_min)

where

NDV = observed NDVI value

ND_min = minimum NDVI value observed historically for that pixel

ND_max = maximum NDVI value observed historically for that pixel

Historical maximum and minimum NDVI maps for the study area are necessary to be produced by searching all the TM NDVI values of collected data and saving the largest and smallest values observed for each pixel. Pixels affected by clouds and noises are excluded. These NDVI values are then composed into maximum and minimum maps and used with current NDVI maps to perform the visual and the relative greenness calculations.

(2) Forest Type Classification and Shifting Cultivation in Chiang Mai

Typical forest types are tropical seasonal forests in Chiang Mai Province. The highest mountain in Thailand, Doi Intanon, is located at the west side of the study site. Four Landsat TM data of the same dry season, 31 Dec. 1990, 17 Feb. 1991, 5 March 1991 and 21 March 1991 (Path-Row:131-47), were selected and geometrically corrected to be overlaid with each other using several ground control points obtained on UTM maps.

The forest type classification was executed using the normalized differential vegetation index (NDVI) images derived from the four Landsat TM data by the following formula.

NDVI = (TM4 - TM3) / (TM4 + TM3)
where TM3 and TM4 indicate the Channel 3 and the Channel 4 of Landsat TM, respectively.

The steps of the analysis are as follows;
a. The minimum value is subtracted from each channel data separately to reduce atmospheric effect before calculating the NDVI.

b. The clustering analysis is applied to make forest cover map based on the NDVIs. The NDVI values are considered to be correspond to terrestrial (forest) condition and vegetation cover types in each image.
c. After the clustering, the vegetation type of each cluster is checked with existing vegetation maps, aerial photography and ground survey.
d. Digital elevation data are also collected by digitizing a present map and overlaid on TM data to analyze the correlation between the classification result and elevation that indicates some environmental condition, especially, such as temperature and water availability to vegetation.

Digital elevation data were extracted from an existing map with the scale on 1:50,000. The contour lines of every 100 meters of the map were input into a GIS system and elevation of each pixel correspond to TM data was generated.

(3) Field check system

Field checks were conducted to compare the results of clustering analysis and to check changes of forest types according to the elevation and shifting cultivation activities and land conditions in forest area.

Especially, the relations between forest types and terrestrial condition was the one of the main concerns in Chiang Mai study area. We compared the classification maps derived from the clustering method using satellite NDVI images with elevation and slope direction data.

A GPS (Global Positioning System), a Polaroid camera , a video camera with fisheye lens, a rotator system for the video camera and a field note were used for the field survey.

3. RESULT

(1) Forest type mapping

Four sequential LANDSAT TM images of a dry season, from December 1990 to February 1991, were used. Then NDVI images were created by these satellite data (fig.1) on which radiometric corrections have been performed as explained before. A classification map was created based on the changes of these NVI values and the clustering method. As a result, sixteen clusters were generated and were merged into six vegetation classes that correspond to deciduous forest, two mixed forests, evergreen forest, upland agricultural land and paddy field.

Comparing this result with elevation data, the shifting zone between evergreen forests and deciduous forests was clearly appeared. Evergreen forests dominate above 800m and deciduous forests dominate below 700 m sea level.

By the satellite image interpretation, it was easily identified that the shifting cultivation was carried out only in ever green forest area, which are dominant upland area in Chiang Mai .

(2) Field check system

Original image and classification map were printed with the scale of 1/50,000. Road and terrain condition were checked based on the

topographic maps with the same scale. Using these information, field check points were selected beforehand and the field survey was executed at the each selected point.

The procedure at the field was as follows;
- get position with GPS
- note the position on video and the field note
- note the direction on Polaroid
- rotate the video camera with 180 degrees or 360 degree
- note on the field note (an example is shown in Figure 5)
- In forest: put the video upward with fisheye lens and keep walking slowly along a straight line for more than 10 meters

4. DISCUSSION

Although, the classification result clearly delineates evergreen forests, deciduous forests and paddy fields using the TM NDVI data, image interpretation technique was needed for separating agricultural lands from mixed forests. The shifting zone between evergreen forests and deciduous forests in 700m and 800m is checked by the field survey, which support the analysis method using remote sensing data. Other researchers who checked on the ground at the same area, Chiang Mai Province, reported almost the same information *(Miyawaki, 1989)*.

The field surveys were successfully executed by the help of counterparts. We found that the video system is useful. One of the problems is that the NTSC system is used in Japan and PAL system is used in Thailand. Although we have some problems on using the video systems, the system is very convenient and easy to handle. Measuring the crown density on video system will be developed in the laboratory almost as same as on a photo prints.

5. REFERENCE

(1)Burgan, R. E. and R. A. Hartford, 1993, Monitoring Vegetation Greenness With Satellite Data, USDA Forest Service 14p
(2)Deering, D. W., J. W. Rouse, R. H. Haas, J. A. Schall, 1975, Measuring foriage production of grazing units from Landsat MSS, Proceedings of 10th International Symposium on Remote Sensing of the Environment, ERIM, 1169-1174
(3)Goward, S .N., B. Markham, D. G. Dye, W. Dulaney, J. Yang, 1990, Normalized difference vegetation index measurements from the advanced very high resolution radiometer, Remote Sensing of the Environment, 35:257-277
(4)Loveland, T. R., J. W. Merchant, D. O. Ohlen, J. F. Brown, 1991, Development of land-cover characteristics database for the conterminous U. S., Photogram- metric Engineering and Remote Sensing, 57(11):1453-1463
(5)Miyawaki, A., 1989, Vegetation and agriculture in South-East Asia, pp. 31-55, Diversity of Tropical Forest
(6)Spanner, M. A., L/L/ Pierce, S. W. Running, D. L. Peterson, 1990, The seasonality of AVHRR data of temperate coniferous forests: relationship with leaf area index, Remote Sensing of the Environment, 33:97-112
(7)Tucker C. J. and B. Choudhury, 1987, Satellite remote sensing of drought conditions. Remote Sensing of the Environment, 23:243-251

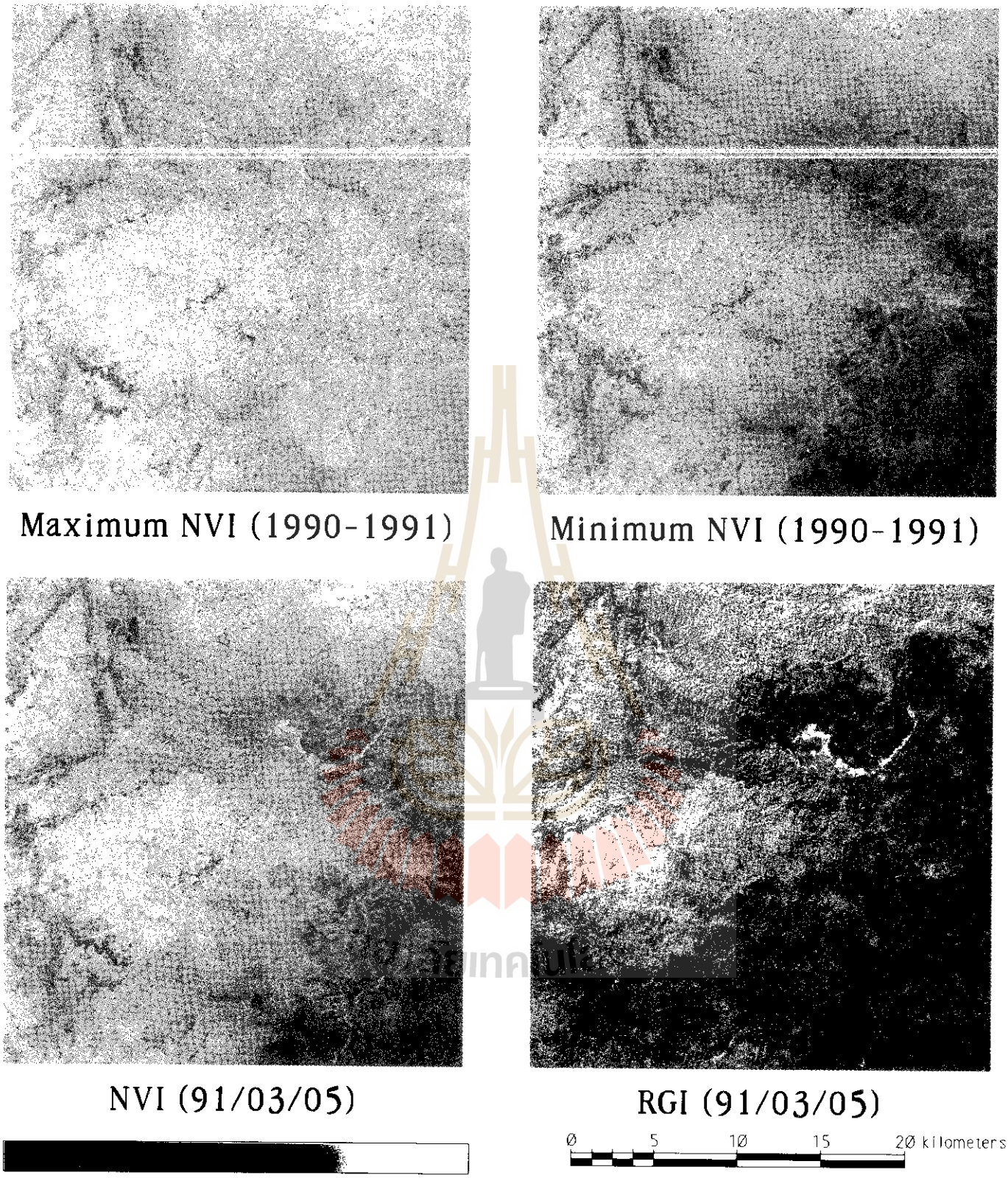

Figure 1. Image set for calculating Relative Greenness

AUTOMATION OF ROAD EXTRACTION FROM SPACE AND AERIAL IMAGES

Armin Gruen
Haihong Li

Institute of Geodesy and Photogrammetry
Swiss Federal Institute of Technology
ETH-Hoenggerberg
CH-8093 Zurich
Switzerland

ABSTRACT

This paper deals with the automation of monoscopic extraction of linear features, in particular roads, from space or aerial images. The objective is to devise a digital photogrammetry strategy for the automation of object extraction and precise measurement during GIS data acquisition in order to facilitate and speed-up the GIS generation and updating processes. The proposed techniques can be either used in a monoplotting mode (combining one image with the underlying DTM) or in a multi-image mode. We will focus here on the first option.

We present some of the results which we obtained with various model-based feature extraction techniques, e.g. dynamic programming, and LSB-snakes (Least Squares B-spline snakes). In these model-driven feature extraction schemes a road is represented by a generic model with various photometric and geometric properties. We will briefly report about the mathematical approaches for optimization and estimation that have been used and address also the implementation and application aspects.

1. INTRODUCTION

Of all parts in the process of GIS data generation from aerial photographs and satellite images, the actual mapping phase is one of the most time consuming and expensive. Research is therefore increasingly focusing on the development of efficient methods to extract topographical features like houses and roads from digital images. As fully automatic methods for mapping are still far out of reach, semi-automatic methods for feature extraction that interact with a human operator are considered to be a good compromise, combining the mensuration speed and accuracy of a computer algorithm with the interpretation skills of the operator.

This paper deals with road extraction, a semi-automatic monoplotting approach to extract road networks from digital images for GIS data capture, where the identification task is performed manually on a single image, while a special automatic digital module performs the high precision road tracking. More specifically, a human operator is used to identify a road from an on-screen display of a digital image, selects the particular class this road belongs to and provides some very few seed points coarsely distributed. It is done through activation of a mouse in a convenient interactive graphics-image user interface. Subsequently, with these seed points as approximation of the position and shape, the road will be extracted automatically. These techniques can be either used in a monoplotting mode (combining one image with the underlying DTM) or in a multi-image mode.

The next section provides an overview of our sequence of algorithms as it runs in monoplotting mode. Section 3 outlines the mathematical representation and implementation of our model driven road extraction algorithms. Section 4 presents some experimental results. Finally, some

conclusions will be given in section 5.

2. THE CONCEPT OF SEMI-AUTOMATIC ROAD EXTRACTION

A semi-automatic scheme for the extraction of road networks from digital images is shown in Figure 1. Its central procedure is a model driven feature extraction algorithm based on either dynamic programming or LSB-snakes (Least Squares B-spline snakes).

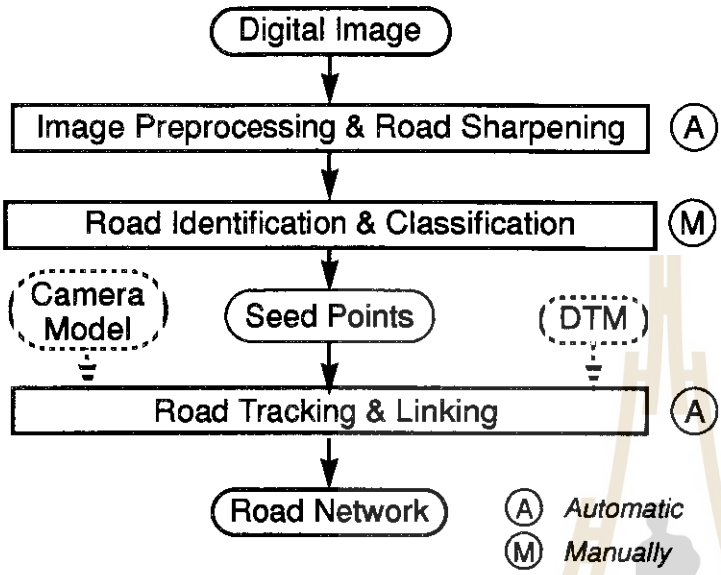

Fig. 1: A semi-automatic road extraction scheme.

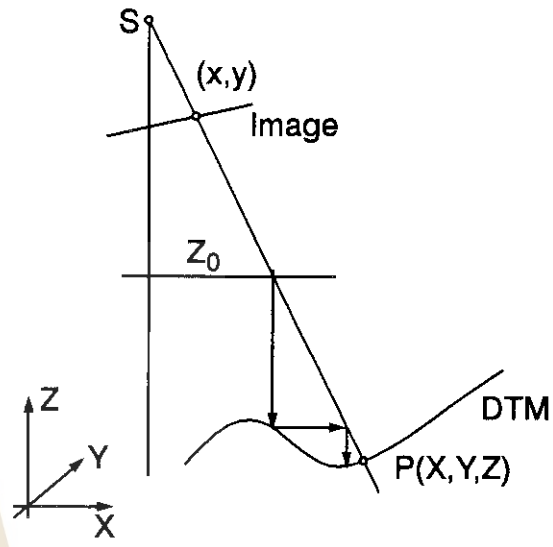

Fig. 2: 3-D interpolation within the DTM.

In the current implementation, image preprocessing and road sharpening are performed by two separate programs. The Wallis filter is used for preprocessing to enhance the image and facilitate the subsequent road extraction process by locally forcing the gray value mean and especially contrast (dynamic range) to fit certain target values (Baltsavias, 1991). After the Wallis filtering, wavelet transform is applied to the image to emphasize features of interest, while suppressing other details (Gruen, Li, 1994). The semi-automatic road extraction runs in a monoplotting mode, in which a single preprocessed image is displayed in a convenient interactive graphics-image user interface. The road identification and classification are performed by the human operator. After some very few seed points have been given by the operator, through activation of a mouse on the displayed image, the road will be extracted automatically and precisely by a model driven feature extraction algorithm whose details will be given in the next sections. The algorithm derives either image coordinates (x, y) or orthoimage coordinates (X, Y), or space coordinates (X, Y, Z) of the roads, whereby the Z-component comes from real-time interpolation within an underlying DTM. If an orthophoto is used this is simply done by a bi-linear interpolation. Otherwise, a camera model or projection equation is applied, as illustrated in Figure 2, in an iteration procedure for the computation of (X, Y) coordinates and interpolation of the Z-component.

3. MODEL DRIVEN OPTIMIZATION FOR FEATURE EXTRACTION

Model driven optimization, or fitting models to photometry (Suetens et al. 1992), is one of the classic approaches to feature extraction from digital images. In its basic form an objective function is defined as a metric or similarity measure of fitness between the model of the feature to be extracted and the image data and an algorithm is used to perform the optimization, finding the maxima or minima of the objective function. There are many different optimization and

estimation techniques used for feature extraction, for instance, least square template matching (Gruen, Stallmann, 1991), dynamic programming (Gruen, Li, 1994), active contour models (Kass et al. 1988, Fua, Leclerc, 1990, Trinder, Li, 1995), edge relaxation, graph searching and so on. The general procedure consists of the following three basic elements:

1. A generic or specific object model to describe the geometric and photometric appearance of the object of interest in the digital image.

2. An objective function to measure the fitness between the object model and the image data.

3. An algorithm to evaluate the objective function and perform the optimization or estimation.

The effectiveness of the method depends strongly on the appropriateness of the modelling primitives that are searched for. If well-known object models are available, they can be described by a limited number of photometric and geometric constraints.

In large scale aerial images the details of a road surface are clearly evident, so that a linear element can be decomposed into detectable primitives and a precisely specified road model could be defined with the exact knowledge of roads. In contrast, satellite images contain a tremendous number of objects which, however, are imaged at a very small scale. In this case, road extraction is usually viewed as linear feature extraction. Instead of the application of a precise object model, which is difficult to realize with small scale images, a generic model which consists of a set of photometric and geometric constraints on road characteristics such as smoothness, curvature and homogeneity is used.

A road is a well-defined object. Its characteristics can be classified in five groups: photometric, geometric, topological, functional and contextual characteristics (Vosselman, Knecht, 1995). In our semi-automatic road extraction scheme the high level knowledge, which requires quite some intelligence for the image interpretation process, is used by the human operator to identify and classify the road networks. The generic road model involved in the model driven road extraction algorithms consists of some photometric and geometric characteristics (Gruen, Li, 1994, 1995). Examples are:

- a road surface often has a good contrast to its adjacent areas,
- a road surface usually is homogeneous (at least in a certain portion of the image),
- a road is a continuous and narrow region or linear feature,
- a road is smooth and does in general not have small wiggles,
- the local curvature of a road has an upper bound,
- the width of a road or road segment does not change significantly.

These properties can be mathematically formulated and discretized by a merit function and an inequality constraint in the form of

$$E = \sum E(p_i, p_{i+1}) = \text{Maximum}, \tag{3.1}$$

$$C_i = |\alpha_i - \alpha_{i+1}| < T_1. \tag{3.2}$$

This multistage optimization problem is efficiently solved by dynamic programming through the time-delayed algorithm (Gruen, Li, 1994). Its advantages stem from its efficiency in handling long curves, robustness in the presence of noise and ability to bridge gaps.

For the LSB-snakes algorithm, we suppose a road can be approximated by a cubic spline as

$$x(s) = \sum_{i=0}^{n} N_i(s) X_i, \tag{3.3a}$$

$$y(s) = \sum_{i=0}^{n} N_i(s) Y_i, \tag{3.3b}$$

where X_i and Y_i are the parameters of the cubic spline in x and y direction respectively. In terms of spline concept, they form the coordinates of the control polygon of the curve. $N_i(s)$ is the normalized $4th$ order B-spline between knots S_i and S_{i+4}.

Thus road extraction can be treated here as the problem of estimation of the parameters X_i and Y_i of the spline. In least squares notation we use three types of observations, the region of the image and its photometric features as the observations of the photometric part of the road model, the seed point locations and the initial curve formed by these seed points as the geometric model. A further development of these observation equations will result in the normal equations used for the estimation of the parameters as

$$N_x \Delta X + L_x = 0, \tag{3.4a}$$

$$N_y \Delta Y + L_y = 0. \tag{3.4b}$$

In a semi-automatic feature extraction scheme, the human operator initially places some seed points near the image structure of interest. With these seed points, the approximations X^0 and Y^0 of parameters X and Y, an initial curve and the matrices N_x, N_y, and vectors L_x, L_y can be calculated. The iterations are stopped if each element of the solution vectors ΔX and ΔY falls below a threshold (for details see Gruen, Li, 1995).

With B-splines as the approximation of snakes and least squares estimation of the parameters we have the advantages of local support, continuity control and especially quality control.

4. EXPERIMENTAL RESULTS

The model driven optimization strategies for semi-automatic road extraction described in this paper have been successfully implemented at our Institute on a digital workstation under X-Windows and OSF/Motif and tested on a number of real images. In this section, some typical examples will be given.

Figure 3a shows a portion of a preprocessed SPOT panchromatic image of Moudon, Switzerland. The seed points provided by the operator along the road which is to be extracted are marked by black discs. The white rectangles denote potential problematic areas, i. e. gaps due to the road going through forest areas. The road extracted by dynamic programming is shown in Figure 3b in black. Obviously the algorithm bridges gaps in a robust manner.

Figure 3c focuses on another portion from the same SPOT image. At this time, the problematic areas marked with white rectangles are intersections with other roads and a passage through an urban area, which might cause ambiguities and erroneous changes of direction. The result of Figure 3d shows that no problems are encountered in this case.

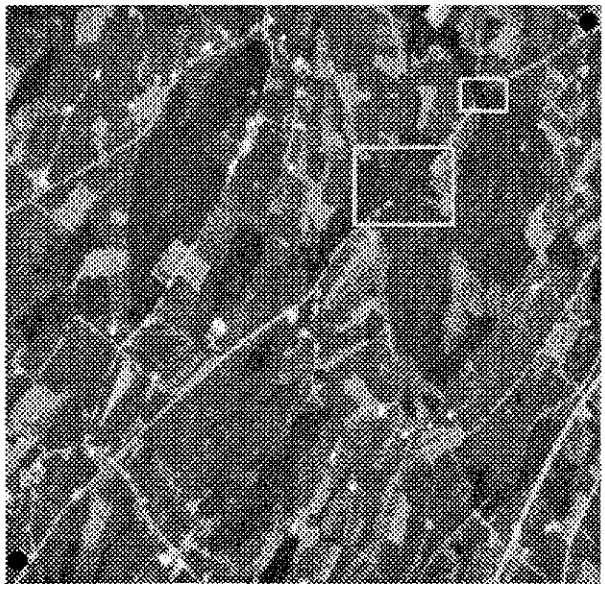

Fig. 3a: A portion of a SPOT panchromatic image with seed points and potential problematic areas.

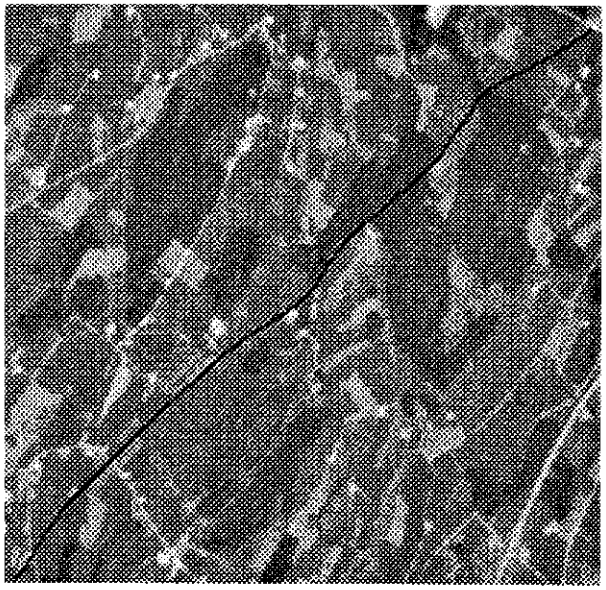

Fig. 3b: The road extracted by dynamic programming.

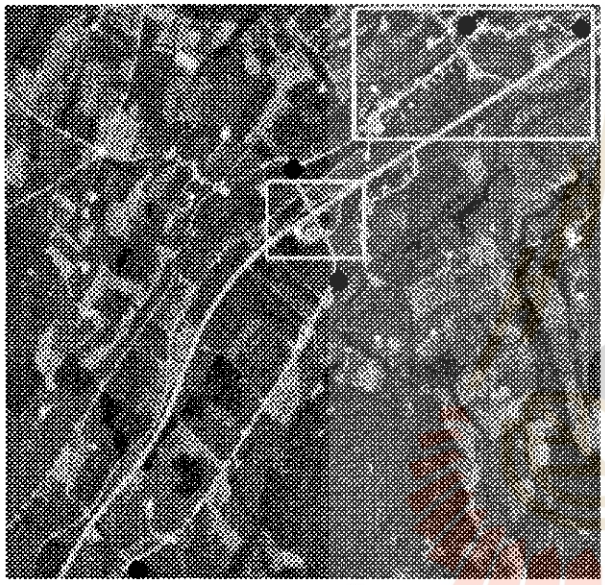

Fig. 3c: A portion of a SPOT panchromatic image with seed points and potential problematic areas.

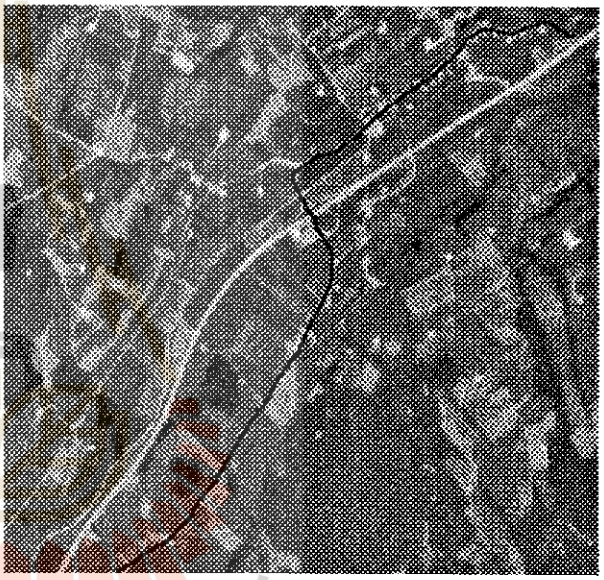

Fig. 3d: The road extracted by dynamic programming.

Figure 4a is a portion of a larger scale aerial image of Avenches, Switzerland. Roads in this image have different widths and are disturbed by buildings, trees, cars and other objects. The LSB-snakes algorithm is applied to this image. The extracted roads are shown in Figure 4b. The snake does not follow the center line of the roads in all cases because of disturbing vehicles. This kind of required high level knowledge is impossible to integrate into the objective function or energy of snakes. For this case, a special high level processing or postprocessing procedure should be developed.

Additional experiments with other images verified the efficiency and good accuracy performance of the technique.

Fig. 4a: A portion of an aerial image with seed points.

Fig. 4b: Roads extracted with LSB-snakes.

5. CONCLUSIONS

The semi-automatic object extraction strategies presented here can be used for monoplotting on a digital photogrammetric station. A human operator is required to identify a road and give a few start points coarsely distributed. Such use of a human operator within a system is considered optimal because humans perform the identification task flawlessly and almost effortlessly. The precise road extraction, which experience shows to be a time-consuming and error-prone part of photogrammetric data collection, is performed fully automatically and fast. It is possible to include in these optimization and extraction procedures the given camera models, such that we obtain a multi-image and fully 3-D geometrically constrained approach.

The technique can be extended and customized through the use of other specific photometric and geometric properties to extract various other types of objects. Roads on large scale images have many details and are disturbed by other objects. For this case, a postprocessing procedure based on high level knowledge should be developed.

6. REFERENCES

1. E. P. Baltsavias, "*Multiphoto geometrically constrained matching*". Mitteilungen Nr. 49, Institute of Geodesy and Photogrammetry, ETH Zurich, 1991.
2. P. Fua and Y. Leclerc, "*Model driven edge detection*", Machine Vision and Applications, Vol. 3, pp. 45-56, 1990.
3. A. Gruen and H. Li, "*Semi-automatic road extraction by dynamic programming*", International Archives of Photogrammetry and Remote Sensing, Vol. 30, Part 3/1, pp. 324-332, 1994.
4. A. Gruen and H. Li, *"Semi-automatic road extraction as a model driven optimization procedure"*, SPIE Proceedings, St. Petersburg-Great Lakes Conference on Digital Photogrammetry and Remote Sensing'95, 1995
5. A. Gruen and D. Stallmann, *"High accuracy edge matching with an extension of the MPGC-matching algorithm"*, SPIE Proceedings, Industrial Vision Metrology, Vol. 1526, pp. 42-45, 1991.
6. M. Kass, A. Witkin and D. Terzopoulos, "*Snakes: Active contour models*", International Journal of Computer Vision, Vol. 1(4), pp. 321-331, 1988.
7. P. Suetens, P. Fua and A. J. Hanson, "*Computational strategies for object recognition*", ACM Computing Surveys, Vol. 24, No. 1, pp. 5-61, 1992.
8. J. Trinder and H. Li, "*Semi-automatic feature extraction by snakes*", Automatic Extraction of Man-Made Objects from Aerial and Space Images, Birkhaeuser Verlag, pp. 95-104, 1995.
9. G. Vosselman and J. de Knecht, "Road tracing by profile matching and Kalman filtering", Automatic Extraction of Man-Made Objects from Aerial and Space Images, Birkhaeuser Verlag, pp. 265-274, 1995.